

## **The function and origin of the CD4+ T cell in the classical Hodgkin lymphoma microenvironment**

Greaves, Paul

The copyright of this thesis rests with the author and no quotation from it or information derived from it may be published without the prior written consent of the author

For additional information about this publication click this link.

<http://qmro.qmul.ac.uk/jspui/handle/123456789/2965>

Information about this research object was correct at the time of download; we occasionally make corrections to records, please therefore check the published record when citing. For more information contact [scholarlycommunications@qmul.ac.uk](mailto:scholarlycommunications@qmul.ac.uk)

**The function and origin of the CD<sub>4</sub><sup>+</sup> T  
cell in the classical Hodgkin lymphoma  
microenvironment**

Paul Greaves

A thesis submitted for the degree of  
Doctor of Philosophy at the University of London

Centre for Haemato-Oncology  
Barts Cancer Institute  
Charterhouse Square  
London

## Abstract

Classical Hodgkin lymphoma (CHL) is a germinal centre B cell malignancy where the bulk of the tumour comprises a non-clonal immune infiltrate enriched for CD4<sup>+</sup> T cells. The role of these cells in the pathophysiology of CHL is poorly understood. Biomarkers predictive of clinical outcome in CHL are limited. This thesis examines microenvironment biomarkers with the goal of identifying the 10-20% of patients who are not cured by conventional therapy, and also investigates the function of the CD4<sup>+</sup> T cell in CHL.

The prognostic power of FOXP<sub>3</sub>, a marker of regulatory T cells, CD68, a macrophage marker and CD20, a B cell marker, is validated in a new patient cohort and for the first time CD68 and FOXP<sub>3</sub> are combined in a statistically robust scoring system. The data presented challenge the assumption that the microenvironment is Th<sub>2</sub>-polarised or senescent and demonstrates relative over-expression of T-BET, a Th<sub>1</sub> marker and under-expression of PD<sub>1</sub>, a marker of senescence/exhaustion, with little evidence for Th<sub>2</sub> marker expression. A cytokine-enriched *in vitro* culture system was developed demonstrating superior proliferation and longevity of CHL-derived T cells compared to non-malignant tissue-derived controls. These cells sustain expression of markers associated with proliferation and longevity (e.g. CD27, CD28) and remain functional (express cytokines) for many weeks. A panel of CD4<sup>+</sup> T cell-specific markers was determined capable of differentiating CHL-derived from non-malignant or non-Hodgkin lymphoma-derived CD4<sup>+</sup> T cells, in which markers of central memory (CD62L and CCR7) and early activation (CD69) are over-represented and markers of senescence (CD57 and PD<sub>1</sub>) are under-represented. Cytokine profiles were found to resemble Th<sub>1</sub> (expression of IL<sub>2</sub>, IFN- $\gamma$  and TNF $\alpha$  expression) rather than Th<sub>2</sub> (IL<sub>4</sub>, IL<sub>13</sub>, IL<sub>21</sub>, IL<sub>10</sub> and IL<sub>6</sub>) responses.

The data presented confirm a new prognostic biomarker signature and show a Th<sub>1</sub> rather than Th<sub>2</sub>-dominated microenvironment enriched for cytokine-secreting functional effector CD4<sup>+</sup> T cells and long-lived, proliferative cells resembling central memory cells rather than hypoproliferative, anergic, non-functional T cells.

## Acknowledgements

There are many people within the Centre for Haemato-oncology, Bart's Cancer Institute, and Bart's hospital who have made this work possible and made my time at Charterhouse Square a genuine pleasure. I can mention only a few in person.

Thank you to Tom Baker and his family for their tireless efforts in fundraising, which entirely supported this research. My primary supervisor, John Gribben who conceived of this project, gave me the freedom and autonomy to pursue it as I chose and has always promoted and supported me. David Taussig and Maria Calaminici for their supervision, expertise and critique, and Abigail Lee for the inspiration and validation.

Particular thanks are due to Andrew Clear and Andrew Owen for constructing the tissue microarray and for their exceptional technical ability and guidance in immunohistochemistry and image analysis. To Jenny Dunne and Lauren Wallis for instruction and company in the tissue culture suite, Farideh Miraki-Moud, Tim Farren and Guglielmo Rosignoli for patient, expert demonstration of flow cytometry, Sameena Iqbal whose relentless pursuit of tissue is unrivalled, Janet Matthews and Andy Wilson for database management and record turnarounds in data analysis, Milensu Shanyinde for meticulous and transparent data analysis, Lynn Haddon and Carol Jennings for running a tight ship against all the odds, Rita Coutinho, Fabienne McClanahan and Csaba Bödör who showed me what genuine, open, enthusiastic collaboration is all about, Rob Petty for invaluable lessons in scientific scepticism and dry humour, Simon Hallam for understanding how it all works, and Tom Butler whose impeccable logic and adjacent chair were indispensable to my sanity. And to all my friends and colleagues in the big office and the small office.

Finally to my mentors and friends in haemato-oncology - Jane Stevens for pushing me in the right direction and looking after me, Joost de Vos whose pragmatism, common sense and dedication to teaching and service make him the model physician, and particularly Andrew Lister, for insisting that I do the right thing and always prioritising a patient-centred, clinical service above all else.

For my sister, Clare, who has always been there for me.

# Table of Contents

<b>ABSTRACT.....</b>	<b>2</b>
<b>TABLE OF CONTENTS.....</b>	<b>4</b>
<b>1. INTRODUCTION &amp; OBJECTIVES.....</b>	<b>15</b>
<b>1.1 CLASSICAL HODGKIN LYMPHOMA: CLINICAL BACKGROUND.....</b>	<b>15</b>
<b>1.2 THE MALIGNANT CELL IN CHL.....</b>	<b>16</b>
1.2.1 THE HRS CELL IS DERIVED FROM A GERMINAL CENTRE B CELL .....	16
1.2.2 SURVIVAL PATHWAYS IN CHL AND THE ROLE OF EBV .....	17
<b>1.3 CANCER AND IMMUNITY .....</b>	<b>18</b>
<b>1.4 CD4+ T CELLS IN CHL.....</b>	<b>19</b>
1.4.1 THE UNIQUE INFLAMMATORY MICROENVIRONMENT OF CHL.....	19
1.4.2 THE COMPLEX ROLE OF THE CD4+ T CELL IN THE CHL MICROENVIRONMENT .....	19
1.4.3 CD4+ CYTOKINES AND CHEMOKINES IN CHL.....	20
<b>1.5 NORMAL B CELLS REQUIRE T CELL HELP FOR SURVIVAL.....</b>	<b>21</b>
1.5.1 COGNATE AND NON-COGNATE T/B CELL INTERACTIONS.....	22
1.5.2 MOLECULAR MECHANISMS OF T CELL HELP .....	22
1.5.3 T CELL / B CELL INTERACTIONS IN THE LYMPH NODE .....	25
<b>1.6 THE NATURE OF THE CD4+ T CELL IN THE CHL MICROENVIRONMENT.....</b>	<b>28</b>
1.6.1 HETEROGENEITY OF CD4+ T CELLS: PHENOTYPE AND FUNCTION.....	28
1.6.2 METHODOLOGICAL PROBLEMS IN DETERMINING A FUNCTIONAL CD4+ T CELL SUBSET.....	28
1.6.3 EFFECTOR T CELL AND MEMORY T CELLS .....	29
1.6.4 THE PARADIGM SUBSETS: TH1 AND TH2.....	30
1.6.5 A CONTROVERSIAL SUBSET: THE REGULATORY T CELL (TREG).....	34
1.6.6 A PROFESSIONAL GCB CELL-HELPING T CELL: T FOLLICULAR HELPER.....	39
1.6.7 CONCLUSIONS: DEFINING A T HELPER CELL SUBSET .....	46
<b>1.7 CURRENT UNDERSTANDING OF CD4+ T CELLS IN THE CHL MICROENVIRONMENT .....</b>	<b>46</b>
1.7.1 EVIDENCE FOR A TH2-DOMINATED INFILTRATE.....	46
1.7.2 EVIDENCE FOR AN ANERGIC, SUPPRESSIVE CD4+ T CELL INFILTRATE .....	48
<b>1.8 CHALLENGES IN STUDYING THE FUNCTION OF THE MICROENVIRONMENT IN CHL .....</b>	<b>50</b>
1.8.1 FUNCTIONAL STUDIES .....	50
1.8.2 IN VITRO CULTURE SYSTEMS.....	50

1.8.3 IN VIVO CULTURE SYSTEMS .....	52
<b>1.9 DESCRIPTIVE AND CORRELATIVE STUDIES OF THE CHL MICROENVIRONMENT .....</b>	<b>53</b>
1.9.1 THE FUNCTION / PROGNOSIS FALLACY .....	53
1.9.2 IMMUNOHISTOCHEMICAL PROFILING OF T CELLS IN THE CHL MICROENVIRONMENT .....	54
1.9.3 GENE EXPRESSION PROFILING OF THE CHL MICROENVIRONMENT .....	59
<b>1.10 AIMS AND OBJECTIVES .....</b>	<b>68</b>
<b><u>2. MATERIALS AND METHODS .....</u></b>	<b><u>70</u></b>
<b>2.1 PATIENT SAMPLES .....</b>	<b>70</b>
2.1.1: FORMALIN-FIXED PARAFFIN-EMBEDDED TISSUE.....	70
2.1.2: FROZEN SINGLE CELL SUSPENSIONS (SCSS).....	70
<b>2.2 IMMUNOHISTOCHEMISTRY .....</b>	<b>71</b>
2.2.1 TISSUE MICROARRAY CONSTRUCTION.....	71
2.2.2 PRINCIPLES OF IMMUNOHISTOCHEMISTRY .....	74
2.2.3 BATCH IMMUNOHISTOCHEMISTRY USING THE DAKO AUTOSTAINER SYSTEM.....	75
2.2.4 PRIMARY ANTIBODIES FOR IMMUNOHISTOCHEMISTRY.....	76
2.2.5 PROTOCOL FOR IMMUNOHISTOCHEMISTRY STAINING USING AUTOSTAINER .....	76
2.2.6 SLIDE ANALYSIS, IMMUNOHISTOCHEMISTRY SCORING AND CELL COUNTING .....	78
<b>2.3 MULTICOLOUR FLOW CYTOMETRY .....</b>	<b>82</b>
2.3.1 PRINCIPLES.....	82
2.3.2 FLUOROCHROMES AND STAINING PROTOCOLS .....	85
2.3.3 SURFACE MARKER STAINING .....	87
2.3.4 INTRACELLULAR MARKER STAINING .....	87
2.3.5 CYTOKINE AND SECRETED PROTEIN STAINING .....	87
2.3.6 VIABILITY .....	88
2.3.7 NON-SPECIFIC FLUOROCHROME-CONJUGATE BINDING-BLOCKING STEP.....	89
2.3.8 PROTOCOL FOR STAINING; (CHAPTERS 6&7; 96 WELL PLATE METHOD) .....	89
2.3.9 THRESHOLD GATING STRATEGY: SELECTION OF CONTROL POPULATIONS .....	97
2.3.10 DATA ACQUISITION AND ANALYSIS .....	100
<b>2.4 OTHER STATISTICAL ANALYSIS .....</b>	<b>113</b>
2.4.1 COMPARISON OF MEANS AND MEDIANS OF POOLED SAMPLES.....	113
2.4.2 MULTIVARIATE ANALYSIS USING THE COX PROPORTIONAL HAZARDS MODEL .....	113

**3. FOXP3, CD68 AND CD20 EXPRESSION IN THE CLASSICAL HODGKIN LYMPHOMA MICROENVIRONMENT ARE PREDICTIVE OF PROGNOSIS..... 115**

**3.1 INTRODUCTION ..... 115**  
**3.2 OBJECTIVES ..... 116**  
**3.3 METHODS ..... 117**  
3.3.1 PATIENTS ..... 117  
3.3.2 TMA/IHC AND IHC ..... 120  
3.3.3 MICROSCOPE SLIDE SCANNING, IMAGE ANALYSIS AND CELL COUNTING ..... 122  
3.3.4 STATISTICAL ANALYSIS ..... 125  
**3.4 RESULTS..... 127**  
3.4.1 CATEGORICAL DATA ANALYSIS ..... 127  
3.4.1.4 PROGNOSTIC SIGNIFICANCE OF CD20 EXPRESSION ..... 133  
3.4.2 CONTINUOUS DATA ANALYSIS ..... 136  
**3.5 DISCUSSION ..... 138**  
**3.6 SUMMARY AND FURTHER WORK..... 139**

**4. T-BET, GATA3, PD1 AND PD-L1 EXPRESSION IN THE CLASSICAL HODGKIN LYMPHOMA MICROENVIRONMENT ..... 142**

**4.1 INTRODUCTION ..... 142**  
4.1.1 TH1 AND TH2 IN MALIGNANCY ..... 143  
4.1.2 TH1 AND T-BET ..... 144  
4.1.3 TH2 AND GATA3 ..... 145  
4.1.4 IMMUNOSUPPRESSION AND PD1 ..... 146  
**4.2 OBJECTIVES ..... 149**  
**4.3 MATERIALS AND METHODS ..... 149**  
4.3.1 PATIENT SAMPLES, TMA CONSTRUCTION AND STAINING METHODOLOGY ..... 149  
4.3.2 STATISTICAL ANALYSIS ..... 150  
**4.4 RESULTS..... 151**  
4.4.1 T-BET EXPRESSION IN THE MICROENVIRONMENT ..... 151  
4.4.2 GATA3 EXPRESSION IN THE MICROENVIRONMENT ..... 160  
4.4.3 PD1 EXPRESSION IN THE MICROENVIRONMENT ..... 163  
4.4.4 PD-L1 EXPRESSION IN THE MICROENVIRONMENT ..... 167  
**4.5 DISCUSSION ..... 169**

4.5.1 LIMITATIONS OF IHC .....	169
4.5.2 LIMITATIONS OF TMA.....	170
4.5.3 TH1 AND TH2 .....	170
4.5.4 PD1 AND PD-L1 .....	172
<b>4.6 SUMMARY AND FURTHER WORK.....</b>	<b>172</b>

**5. A CULTURE SYSTEM TO SUSTAIN PRIMARY TISSUE-DERIVED HRS CELLS AND TUMOUR-INFILTRATING CD4+ T CELLS..... 174**

<b>5.1 INTRODUCTION .....</b>	<b>174</b>
5.1.1 CLINICAL TRIALS WITHOUT IN VITRO OR IN VIVO MODELS .....	174
5.1.2 MAINTAINING THE HRS CELL INDIRECTLY USING T CELL SUPPORTING CYTOKINES .....	175
<b>5.2 AIMS AND OBJECTIVES.....</b>	<b>176</b>
<b>5.3 MATERIALS AND METHODS .....</b>	<b>177</b>
5.3.1 SINGLE CELL SUSPENSIONS .....	177
5.3.2 MULTICOLOUR FLOW CYTOMETRY FOR IDENTIFICATION OF HRS CELL POPULATION .....	178
5.3.3 CULTURE OF SINGLE CELL SUSPENSIONS DERIVED FROM LYMPHOID TISSUE .....	179
5.3.4 STATISTICAL ANALYSIS .....	188
<b>5.4 RESULTS.....</b>	<b>190</b>
5.4.1 FLOW CYTOMETRY OF SINGLE CELL SUSPENSIONS.....	190
5.4.2 CULTURE OF SCS DERIVED CELLS .....	197
<b>5.5 DISCUSSION .....</b>	<b>203</b>
<b>5.6 SUMMARY AND FURTHER WORK.....</b>	<b>206</b>

**6. FLUORESCENCE IMMUNOPHENOTYPING TO FUNCTIONALLY CHARACTERISE AND DISCRIMINATE CHL-INFILTRATING CD4+ T CELLS FROM OTHER LYMPH NODE-INFILTRATING CD4+ T CELLS..... 208**

<b>6.1 INTRODUCTION .....</b>	<b>208</b>
<b>6.2 AIMS AND OBJECTIVES.....</b>	<b>208</b>
6.2.1 SELECTION OF ANTIGENS FOR T CELL PANEL.....	209
<b>6.3 MATERIALS AND METHODS .....</b>	<b>209</b>
6.3.1 SINGLE CELL SUSPENSIONS .....	209
6.3.2 SELECTION OF FLUOROCHROMES AND ANTIBODIES .....	209
6.3.3 FLOW CYTOMETRIC ANALYSIS, DATA ACQUISITION, COMPENSATION AND GATING.....	213
6.3.4 STATISTICAL ANALYSIS .....	213
<b>6.4 RESULTS.....</b>	<b>214</b>
6.4.1 RAW FLOW CYTOMETRY DATA.....	214



6.4.2 SUMMARY OF FLOW CYTOMETRY FINDINGS .....	241
<b>6.5 DISCUSSION .....</b>	<b>249</b>
6.5.1 LIMITATIONS OF INTERPRETATION .....	249
6.5.2 CONDITION-DEFINING CD3+CD4+ T CELL SUBSETS .....	252
6.5.3 A CD3+CD4+ SIGNATURE FOR CHL WITH POTENTIAL CLINICAL APPLICATION .....	263
<b>6.6 SUMMARY AND FURTHER WORK.....</b>	<b>264</b>
<b><u>7. FLUORESCENCE IMMUNOPHENOTYPING TO CHARACTERISE CHL-DERIVED</u></b>	
<b><u>PROLIFERATIVE CD4+ T CELLS .....</u></b>	<b><u>267</u></b>
<b>7.1 INTRODUCTION .....</b>	<b>267</b>
<b>7.2 AIMS AND OBJECTIVES.....</b>	<b>268</b>
<b>7.3 MATERIALS AND METHODS .....</b>	<b>268</b>
7.3.1 SINGLE CELL SUSPENSIONS .....	268
7.3.2 FREEZING METHODOLOGY.....	268
7.3.3 SELECTION OF FLUOROCROMES AND ANTIBODIES .....	269
7.3.4 FLOW CYTOMETRIC ANALYSIS, DATA ACQUISITION, COMPENSATION AND GATING.....	269
7.3.5 STATISTICAL ANALYSIS .....	270
<b>7.4 RESULTS.....</b>	<b>271</b>
7.4.1 LIMITATIONS OF METHOD AND DATA INTERPRETATION.....	271
7.4.2 INDIVIDUAL MARKER ANALYSIS, ANOVA AND PAIRWISE COMPARISONS.....	271
7.4.3 DISCRIMINATORY MARKERS IN PROLIFERATING CELLS .....	292
<b>7.5 DISCUSSION .....</b>	<b>293</b>
7.5.1 LIMITATIONS OF THIS EXPERIMENT .....	293
7.5.2 MARKERS OF ACTIVATION .....	293
7.5.3 THE SIGNIFICANCE OF CHEMOKINE RECEPTORS IN THE EXPANDING CULTURES.....	295
7.5.4 THE SIGNIFICANCE OF TH2 CYTOKINES IN THE EXPANDING CULTURE .....	296
7.5.5 THE INFLUENCE OF A SUPPRESSOR/REGULATORY T CELL IN THE EXPANDING CULTURES .....	296
7.5.6 MARKERS OF LONGEVITY AND SENESCENCE .....	296
7.5.7 A DISTINCTIVE PHENOTYPE FOR THE PROLIFERATING CHL-DERIVED CD4+ T CELL? .....	297
<b>7.6 SUMMARY AND FURTHER WORK.....</b>	<b>299</b>

<b>8. DISCUSSION .....</b>	<b>301</b>
<b>8.1 A MODEL FOR THE CHL PATHOGENESIS BASED ON THE CD4+ T CELL INFILTRATE .....</b>	<b>301</b>
8.1.1 THE CHL MICROENVIRONMENT SEQUESTERS NAÏVE AND MEMORY T CELLS FROM THE PHYSIOLOGICAL LYMPHOID POOL.....	301
8.1.2 THE IMMUNE INFILTRATE IS AN INDICATOR OF IMMUNOLOGICAL HEALTH OF THE HOST HENCE PREDICTING OUTCOME.....	303
8.1.3 SEQUESTRATION OF THE CENTRAL MEMORY COMPARTMENT LEADS TO PROFOUND CELL- MEDIATED IMMUNE DEFECT .....	303
<b>8.2 POTENTIAL CLINICAL TRANSLATION OF THIS WORK.....</b>	<b>304</b>
8.2.1 A CLINICALLY APPLICABLE PROGNOSTIC SCORE MAY BE DERIVED BASED ONLY ON THE EXPRESSION OF FOXP3 AND CD68 AT DIAGNOSIS. ....	304
8.2.2 CHL CAN BE DISCRIMINATED FROM NORMAL AND OTHER MALIGNANT TISSUE BASED ONLY ON THE PHENOTYPE OF THE NON-MALIGNANT CD4+ CELL.....	305
8.2.3 APPROPRIATE T CELL TRAFFICKING IS ESSENTIAL TO ANTI-CHL-IMMUNITY .....	305
<b>8.3 TH2 POLARISED CELLS ARE NOT AN IMPORTANT PART OF THE MICROENVIRONMENT .....</b>	<b>306</b>
<b>8.4 HYPOPROLIFERATION, ANERGY AND SENESCENCE ARE NOT CHARACTERISTIC OF THE MICROENVIRONMENT CD4+ T CELL.....</b>	<b>306</b>
<b>8.5 SUMMARY .....</b>	<b>307</b>
<b><u>CHAPTER 9: REFERENCES.....</u></b>	<b><u>308</u></b>

## Tables

<b>Table 1.1:</b> Expression of selected TNFRSF and IGRSF with their ligands.....	24
<b>Table 2.1:</b> Reagents used for the Polymer/HRP method of IHC.....	78
<b>Table 2.2</b> Reagents Used for Staining Protocol.....	90
<b>Table 2.3:</b> Final laser / filter and PMT voltages .....	102
<b>Table 2.4.</b> Compensation algorithm applied for Cocktail 1 analysis .....	112
<b>Table 3.1:</b> Patient characteristics for the entire arrayed cohort .....	118
<b>Table 3.2:</b> Primary Antibodies or in-situ hybridization probes used for the experiment .....	121
<b>Table 3.3:</b> Probability values generated from the Cox regression analysis .....	137
<b>Table 3.4:</b> Improvement in prognostic model incorporating FOXP3.....	138
<b>Table 4.1:</b> Optimal antibody dilutions and suppliers .....	150
<b>Table 4.2:</b> Summary of results of Kaplan Meier analysis .....	158
<b>Table 4.3:</b> Summary of differential expression of T-BET in HRS nuclei.....	159
<b>Table 5.1</b> Samples established in culture using the optimised cytokine enrichment systems .....	177
<b>Table 5.2:</b> Antibody panel to examine T cell, B cell and monocyte/macrophage lineage.....	178
<b>Table 5.3:</b> Lymphocyte culture media enrichment reagents .....	179
<b>Table 5.4:</b> Cytokines used for cell culture .....	179
<b>Table 5.5:</b> Scoring system for individual wells using visual inspection .....	185
<b>Table 5.6:</b> Composition of all viable cells at baseline.....	192
<b>Table 5.7:</b> Summary of composition of viable cells at baseline by tissue of origin.....	192
<b>Table 5.8:</b> Few cells, or none at all appeared in the proposed HRS gate .....	195
<b>Table 6.1:</b> Justification for selection of antigens for use in CD4+ characterising panel.....	210
<b>Table 6.2:</b> Details of fluorochromes for CD4+ T cell typing experiment.....	211
<b>Table 6.3:</b> Summary of cocktails and major antigen class for analysis within each cocktail.....	213
<b>Table 6.4:</b> Expression of Cocktail 1 markers (TNFRSF/IGSF) .....	219
<b>Table 6.5:</b> Expression of Cocktail 2 markers (Chemokine Receptors).....	220
<b>Table 6.6:</b> Expression of Cocktail 3 naïve / homing T cell markers .....	223
<b>Table 6.7:</b> Expression of Cocktail 3b immunosuppressive/senescence T cell markers. ....	227
<b>Table 6.8:</b> Expression of Cocktail 5 IL2/IL4 receptor components .....	230
<b>Table 6.9:</b> Expression of Cocktail 5 CD45 isotype.....	233
<b>Table 6.10:</b> Expression of Cocktail 4 Th1/inflammatory cytokines. ....	236
<b>Table 6.11:</b> Expression of Cocktail 4 Th2/suppressor cytokine .....	237
<b>Table 6.12:</b> Most heterogeneously expressed CD4+ T cell markers .....	243
<b>Table 6.13:</b> Most discriminatory CD4+ T cell markers.....	245
<b>Table 6.14:</b> CHL score-defining markers demonstrating a classification system.....	249
<b>Table 7.1:</b> Samples used for the experiment described in Chapter 7.....	269

## Figures

<b>Figure 2.1:</b> Tissue microarray construction.....	72
<b>Figure 2.2:</b> Example microarray slide .....	73
<b>Figure 2.3:</b> Primary Antibody -- Horseradish peroxidase – DAB method of IHC .....	75
<b>Figure 2.4:</b> Grid superimposed in Adobe Photoshop from selected x20 region of tissue .....	80
<b>Figure 2.5:</b> Cut-point uncorrected probability distribution figures.....	83
<b>Figure 2.6:</b> Illustration of 96 well plate staining technique.....	86
<b>Figure 2.7:</b> Final stage of 96 well plate staining technique .....	86
<b>Figure 2.8:</b> Threshold determination for gating: The problem of compensation.....	97
<b>Figure 2.9:</b> Compensation step 1: using beads. ....	98
<b>Figure 2.10:</b> Threshold determination for gating: The internal control .....	100
<b>Figure 2.11:</b> Gating strategy for analysis of SCS at baselin.....	103
<b>Figure 2.12a:</b> Compensation step 1: using beads, pre-compensation.....	106
<b>Figure 2.12b:</b> Compensation step 1: using beads, post-compensation. ....	107
<b>Figure 2.13a:</b> Compensation step 2: sample by sample (pre-compensation).....	109
<b>Figure 2.13b:</b> Compensation step 2: sample by sample (post-compensation) .....	110
<b>Figure 2.13c:</b> Compensation step 2: sample by sample Importance of gating out DAPI.....	111
<b>Figure 3.1:</b> Kaplan Meier curves showing OS of all patients treated at Bart's.....	119
<b>Figure 3.2:</b> Kaplan Meier curves showing PFS of all patients treated at Bart's.....	120
<b>Figure 3.3:</b> A: In order to discriminate follicular and non-follicular CD20+ cells .....	123
<b>Figure 3.4:</b> Example TMA cores to demonstrate quality control of samples.....	124
<b>Figure 3.5:</b> Mean expression of CD68, CD20 and FOXP3 by EBV expression .....	127
<b>Figure 3.6:</b> Variability of expression of CD68 between patients.....	128
<b>Figure 3.7:</b> Level of expression of CD68 was associated with survival outcom .....	128
<b>Figure 3.8:</b> Heterogeneity of T cell infiltration between patients.....	129
<b>Figure 3.9:</b> Heterogeneity of CD3 (top) and CD 8 (bottom) expression .....	130
<b>Figure 3.10:</b> CD3 (top left) and CD8 (top right) optimal cut-point probability matrices s.....	131
<b>Figure 3.11:</b> Variability of expression of FOXP3 between patients .....	132
<b>Figure 3.12:</b> Level of expression of FOXP3 was associated with survival outcome .....	132
<b>Figure 3.13:</b> Variability of expression of CD20 between patients.....	133
<b>Figure 3.14:</b> Level of expression of CD20 was associated with survival outcom .....	133
<b>Figure 3.15:</b> FOXP3 and CD68 expression show no correlation in CHL.....	134
<b>Figure 3.16:</b> Illustration of method of assigning a combined FOXP3/CD68 score.....	135
<b>Figure 3.17:</b> The combined FOXP3/CD68 score discriminates prognostic groups .....	135
<b>Figure 3.18:</b> Applying a logarithmic transformation suitable for subsequent analysis. ....	136
<b>Figure 4.1:</b> HRS cells were positive for T-BET in the majority of cases .....	151
<b>Figure 4.2:</b> Expression of T-BET in TMA control tonsil.....	152
<b>Figure 4.3:</b> Expression of FOXP3 in TMA control tonsil .....	153

---

<b>Figure 4.5:</b> T-BET expression was widely heterogeneous between patients.....	156
<b>Figure 4.6:</b> T-BET expression was significantly greater in EBV+ cases.....	156
<b>Figure 4.7:</b> Survival Curves stratified by expression of T-BET .....	158
<b>Figure 4.8:</b> Expression of T-BET in HRS cell did not stratify patients by prognosis .....	159
<b>Figure 4.9a-d:</b> GATA3 staining difficulties and observations: .....	160
<b>Figure 4.10:</b> PD1 expression virtually absent in most CHL cases .....	164
<b>Figure 4.11:</b> Heterogeneity of expression of PD1 .....	165
<b>Figure 4.12:</b> In CHL only a minority of microenvironment cells express PD1.....	166
<b>Figure 4.13:</b> PD1 expression was associated with outcome.....	167
<b>Figure 4.14:</b> PD-L1 staining is heterogeneous between samples but difficult to quantify. ....	168
<b>Figure 4.15:</b> Tonsillar PD-L1 staining reveals differential staining between follicle and T-zone....	169
<b>Figure 5.1:</b> Cytokine Optimisation Pilot.....	181
<b>Figure 5.2:</b> Cell number estimation by occupancy of x10 objective field .....	182
<b>Figure 5.3:</b> Documentation of viable wells at each media change and formula application .....	186
<b>Figure 5.4:</b> Gating strategy for analysis of SCS at baseline. ....	189
<b>Figure 5.5:</b> Viability of all SCS-derived cells at baseline .....	191
<b>Figure 5.6:</b> Representative FACS plots derived from each sample .....	193
<b>Figure 5.7:</b> Lymphoid subset composition of SCS at baseline.....	194
<b>Figure 5.8:</b> Composition of SCS at baseline.....	194
<b>Figure 5.9:</b> Gating strategy for analysis of identification of putative HRS population .....	196
<b>Figure 5.10:</b> Composition of example cultures at day 60.....	198
<b>Figure 5.11:</b> IL2&IL4-enriched culture conditions were longer lived.....	199
<b>Figure 5.12:</b> Longevity of T cell cultures influenced by node of origin.....	199
<b>Figure 5.13:</b> Differences in proliferation in IL2-only and IL2&IL4-enriched conditions.....	200
<b>Figure 5.14:</b> Relative proliferation of IL2&4-enriched culture systems.....	201
<b>Figure 5.15:</b> Mean relative proliferation of IL2&4-enriched culture systems by tissue of origin ....	202
<b>Figure 6.1a:</b> Cocktail 1 Analysis: TNFRSF and IGSF member expression. ....	216
<b>Figure 6.1b:</b> Cocktail 1 Analysis: TNFRSF and IGSF member expression. : Summary .....	217
<b>Figure 6.2a:</b> CD69 analysis: Representative FACS plots .....	218
<b>Figure 6.2b:</b> CD69 Analysis: CD69 is significantly under-expressed.....	218
<b>Figure 6.3a:</b> Cocktail 2 Analysis: Chemokine receptor expression. ....	221
<b>Figure 6.3b:</b> Cocktail 2 Analysis: Chemokine receptor expression: Summary. ....	222
<b>Figure 6.4a:</b> Cocktail 3a Analysis: Naïve T cell / T cell homing markers. ....	224
<b>Figure 6.4b:</b> Cocktail 3a Analysis: Naïve T cell / T cell homing markers: Summary .....	225
<b>Figure 6.5a:</b> Cocktail 3b Analysis: Immunosuppressor markers.....	226
<b>Figure 6.5b:</b> Cocktail 3b Analysis: Immunosuppressor markers: Summary.....	228
<b>Figure 6.6a:</b> CD57 expression.....	229
<b>Figure 6.6b:</b> CD57 Analysis: Summary .....	229
<b>Figure 6.7a:</b> Cocktail 5 Analysis: IL2 and IL4 receptor expression .....	231

---

<b>Figure 6.7b:</b> Cocktail 5 Analysis: IL2 and IL4 receptor expression. Summary .....	232
<b>Figure 6.8a:</b> Cocktail 7 analysis: CD45 isotype. ....	234
<b>Figure 6.8b:</b> Cocktail 7 Analysis: CD45 isotype. Summary 1.....	235
<b>Figure 6.8c:</b> Cocktail 7 Analysis: CD45 isotype. Summary 2.....	235
<b>Figure 6.9a:</b> Cocktail 4 Analysis: Th1 / inflammatory cytokines.....	238
<b>Figure 6.9b:</b> Cocktail 8 Analysis: Th2/T suppressor cytokines. ....	239
<b>Figure 6.10:</b> Overall Cytokine expression profile. ....	240
<b>Figure 6.11:</b> A second unsupervised hierarchical clustering analysis .....	241
<b>Figure 6.12:</b> Unsupervised hierarchical clustering using derived two major clusters .....	242
<b>Figure 6.13:</b> Markers expressed in >5% of CHL-derived CD4+ T cells.....	244
<b>Figure 6.14a:</b> Markers whose mean expression was significantly different in CHL .....	246
<b>Figure 6.14b:</b> Further markers whose mean expression was significantly different in CHL .....	247
<b>Figure 6.15:</b> CD4+ T cell-expressed markers demonstrating the least variability.....	248
<b>Figure 7.1:</b> Loss of CD8 cells and CD45 isotype change with time.....	273
<b>Figure 7.2:</b> Gain of expression of TNFRSF and IGSF members by CD4+ T cells with time .....	275
<b>Figure 7.3:</b> Loss of expression of TNFRSF and IGSF members by CD4+ T cells with time .....	276
<b>Figure 7.4:</b> Variance of expression of IL4Ra and CGC on proliferating CD4+ T cells with time .....	279
<b>Figure 7.5:</b> Variance of expression of CD25 and CD69 on proliferating CD4+ T cells with time .....	280
<b>Figure 7.6:</b> Variance of expression of node homing molecules on CD4+ T cells with time.....	281
<b>Figure 7.7:</b> Variance of markers of persistence and senescence on CD4+ T cells with time.....	283
<b>Figure 7.8:</b> Variance of markers of immunosuppression on CD4+ T cells with time.....	284
<b>Figure 7.9:</b> Variance of Th1 cytokine expression on proliferating CD4+ T cells with time.....	287
<b>Figure 7.10:</b> Variance of Th2 cytokine expression on proliferating CD4+ T cells with time.....	288
<b>Figure 7.11:</b> Variance of Th1 / Tfh associated chemokine receptors on CD4+ T cells with time .....	290
<b>Figure 7.12:</b> Variance of Th2 / Treg associated chemokine receptors on CD4+ T cells with time .....	291
<b>Figure 7.13:</b> Hierarchical clustering fails to differentiate groups by tissue of origin.....	292

# CHAPTER ONE:

## Introduction & Objectives

## 1. Introduction & Objectives

### 1.1 Classical Hodgkin Lymphoma: Clinical Background

Classical Hodgkin lymphoma (CHL) is a cancer arising from the transformation of a germinal centre B (GCB) lymphocyte leading to a progressive accumulation of malignant cells (Hodgkin and Reed Sternberg - HRS cells) within a dense inflammatory and fibrotic microenvironment<sup>1</sup>. The disease often arises within a cervical lymph node, initially spreading through contiguous lymph nodes<sup>2</sup> and eventually involving extranodal sites, commonly liver, lung and bone marrow, although presentation at advanced stage often occurs<sup>3</sup>. It is rare, occurring in 2/100,000 population per year in Europe and the US<sup>4</sup>, rarer still in non-white ethnic groups and in the developing world<sup>5</sup>, but in ethnic and geographical areas of highest prevalence it is the second commonest cancer of young adults, with a second peak of incidence in the elderly<sup>6</sup>.

Without treatment, progression is inevitable and death from bulky lymphadenopathy, cachexia, organ failure and infection follows within months or a few years<sup>7, 8</sup>. The disease carries an excellent prognosis for most patients, with long-term remission following conventional chemotherapy or radiotherapy-based protocols greater than 80% but there remains a subset of patients whose disease is refractory to all conventional therapy<sup>9-12</sup>. Novel therapies with agents active in other haematological malignancies (targeted immunotherapy, immunomodulators, epigenetic manipulations and intracellular signalling pathway antagonists) have met with limited success in disease refractory to conventional treatment<sup>13</sup>, although novel therapeutics research is challenging for a disease which is in the most part curable and where conventional therapy-refractory patients are heavily pretreated. The curable nature of the disease has also generated a large cohort of long-term survivors many of whom suffer the late effects of treatments that were probably excessively toxic: cardiovascular, endocrine and secondary malignancies<sup>14, 15</sup>, providing further impetus for tailored therapy development: reducing toxicity for the 'favourable risk' patients, and maintaining treatment intensity in the 'unfavourable risk' patients. Identifying these patients early remains elusive, with current pre-treatment prognostic scoring



systems<sup>16</sup> making little impact on therapeutic decisions beyond stratifying by early and advanced stage disease<sup>17</sup>. A better understand of the molecular biology of the disease is essential to identify clinically applicable predictive factors and in novel therapeutics development.

Nodular lymphocyte predominant Hodgkin lymphoma (NLPHL) is a histologically and clinically similar disease<sup>18</sup> arising from a transformed GCB cell comprising the minority of tumour predominantly composed of reactive immune cells<sup>19</sup>. However despite superficial similarities, its distinct immunohistochemical and genetic signature, along with differences in natural history and epidemiology<sup>20</sup> mean this distinct entity requires a separate functional analysis.

## **1.2 The Malignant Cell in CHL**

### **1.2.1 The HRS cell is derived from a germinal centre B cell**

Microdissection of the histologically distinct HRS cell from primary tissue to a degree of purity sufficient for subsequent genetic analysis provided the first definitive evidence that the malignancy was derived from a germinal centre B cell (GCB)<sup>21</sup>. The cells possess clonal immunoglobulin gene rearrangements with evidence of somatic hypermutation, and some have undergone class switching confirming entry into a germinal centre (GC) reaction. However the cells do not express immunoglobulin due either to destructive somatic mutation (in around 25%) or modification of the B cell genetic<sup>22</sup> or epigenetic program<sup>23</sup> preventing expression of an otherwise functional gene. Loss of the normal B cell phenotype is a defining feature of this malignancy<sup>24</sup>. It remains unclear how this cell is then rescued from the normal stringent surface immunoglobulin expression-dependent, apoptosis-driven selection pressures of the GC. While anti-apoptotic factors may have been initiated within the malignant cell itself through genetic mutation, the malignant cell remains dependent upon its microenvironment: *ex vivo* maintenance of the disease has proved difficult (see below) and the malignant cell is always found *in vivo* to be embedded in a characteristic microenvironment. Hence, the malignant cell's survival is at least as dependent on extracellular signals as from endogenous signals arising from its own mutated genome.

### **1.2.2 Survival Pathways in CHL and the role of EBV**

CHL, a GCB-cell derived malignancy, shares survival mechanisms common to normal B cells and other B cell-derived malignancies, despite loss of much of its B cell-defining phenotype. Many of these pathways require T cell help.

Apoptosis pathway regulators frequently dysregulated in other haematological malignancies, such as FAS, caspase 8, caspase 10, FADD, BAD, ATM and BCL2, are rarely seen in CHL (reviewed in Kuppers 2009<sup>25</sup>), although MDM2 gains may be present in 60%<sup>26</sup> and TP53 mutated in 10%<sup>27, 28</sup>. However, components of the paradigm antiapoptotic pathways of normal lymphocyte physiology and lymphoid malignancy: nuclear factor- $\kappa$  light chain enhancer of activated B cells (NF- $\kappa$ B) and Janus-associated kinase / signal transducer and activator of transcription (JAK/STAT), are frequently dysregulated in HRS cells. REL (the core NF- $\kappa$ B subunit) shows genetic gains and amplifications in half of CHL cases<sup>29</sup>, and abnormalities of NF- $\kappa$ B IA<sup>30</sup>, NF- $\kappa$ B IE<sup>31</sup>, TNFAIP and BCL3<sup>32</sup> are seen in 10-40%. Jak2<sup>33</sup> and SOCS1<sup>34</sup>, central components of JAK/STAT signalling are mutated in around 40% of cases. None are pathognomonic or even seen in the majority of cases. Clearly many survival pathways are at work.

The commonest of the known viral immortalisers of B cells is Epstein Barr Virus (EBV) which has a well-established association with CHL and is a prime candidate for the initial cellular rescue mechanism. Only a limited selection of EBV gene products are expressed including EBNA1 (Epstein Barr Nuclear Antigen 1), LMP1 (Latent Membrane Protein 1) and LMP2a. LMP1 appears to be the most potent B cell survival factor of those expressed in the HRS cell. The mechanism of LMP1-mediated growth was elucidated in parallel with a physiological B cell survival mechanism: CD40/CD40-ligand (CD40-L) in a tetracycline-conditional LMP-1 gene expression system<sup>35</sup>. Tetracycline-activated LMP1 and CD40-L stimulated pathways showed mutual redundancy but no synergism in supporting B cell proliferation. Activation of either pathway leads to increased NF- $\kappa$ B to DNA-binding activity. However EBV is only found in 40% of CHL cases, predominantly HIV-associated disease and in the developing world and so cannot be the key survival factor in most cases of CHL.

### 1.3 Cancer and Immunity

The immune system has an integral role in tumour suppression and development. Systemic immunodeficiency and localised chronic inflammation both predispose to malignancy. The tumour immune surveillance model has now gained wide acceptance and current work focuses not only on mechanisms by which the tumour escapes detection and effective destruction, but also means by which a tumour may subvert the immune infiltrate to provide a supportive environment rich in growth factors and survival signals, and insulated from an effective immune response. Despite being derived from self, tumours aberrantly express antigen thus providing targets for immune cell recognition, first demonstrated in mouse sarcoma models where suppression of a sarcoma's growth was facilitated by exposing the mouse before transplant to syngeneic sarcoma cells<sup>36</sup>. Identity of the effector mechanism responsible was demonstrated to be largely T cell-mediated when it was found that lymph node isolates but not serum could suppress in vitro growth of similar explanted cells<sup>37</sup>, and antigen-specific<sup>38</sup>, with the first tumour-associated antigen recognised by cytotoxic T cells identified in a human melanoma cell line<sup>39</sup>.

Since a T cell-mediated immune response is integral to suppressing early malignancy, any clinically progressive tumour must escape immune control. Many mechanisms by which this is achieved have been proposed, both tumour-mediated (such as reduced immunogenic antigen presentation), or host immune response suppression-mediated (reviewed in Dunn 2002<sup>40</sup>). A T cell-mediated immunity defect has been observed in CHL for 50 years<sup>41, 42</sup>, which may persist beyond treatment<sup>43</sup> but the mechanistic basis for this remains obscure and the relationship between tumour-infiltrating T lymphocytes (TILs) and the HRS cell is poorly understood. A growing body of evidence in solid malignancy has implicated subversion of another key immune effector – the macrophage – changing its phenotype such that its ability to eradicate malignant cells is suppressed while it develops tumour supportive functions, through mechanisms of stromal augmentation aiding malignancy growth, stromal disruption facilitating metastasis, and angiogenesis promotion<sup>44</sup>. Understanding the relationship between lymphoid tumours and the immune system is complicated by the fact that the malignant cell itself represents a subverted component of that immune system.

## **1.4 CD4+ T cells in CHL**

### **1.4.1 The unique inflammatory microenvironment of CHL**

CHL is unique amongst the lymphomas in that the bulk of the infiltrate comprises not the malignant cell, a morphologically distinct, large, complex, multinucleated cell known as the Hodgkin-Reed-Sternberg cell but also inflammatory cells including macrophages, neutrophils, eosinophils, fibroblasts, plasma cells, mast cells, and lymphocytes<sup>1</sup> the most dominant component of which are T cells. These cells are not antigen restricted or tumour specific<sup>45</sup>. The T cells in the tumour microenvironment probably have an essential role in supporting the malignant cell's growth.

### **1.4.2 The complex role of the CD4+ T cell in the CHL microenvironment**

Most nucleated cells in the HRS microenvironment are CD4+, showing upregulation of early markers of activation including co-stimulatory CD28, (Poppema 1995, unpublished observation, personal communication) lymphoid tissue homing CD62L<sup>46</sup>, and the 'effector' isotype of CD45: CD45RO<sup>47</sup>. It is likely that these microenvironmental T cells are playing disparate roles in tumour suppression and progression, some representing the remnants and ongoing subversion of the initial GC reaction that enabled an antigen experienced B cell to thrive despite failure of its immunoglobulin-expressing apparatus. Others will have been attracted passively through expression of chemokine receptors or adhesion molecules and trapped by chemotactic stimuli, perhaps not providing any direct support or anti-tumour activity, but only tumour bulk or displacement of appropriate anti-tumour response. Other cells, including macrophages and CD8+ cytotoxic T cells along with activated proinflammatory Th1 cells may have appropriately recognised the malignant cell as a viable target, and been rendered incompetent by being crowded out by passively accumulated and HRS-supporting cells, or with their active function immobilised by immunosuppressive cytokines or lymphocytes. Other CD4+ cells may have recognised an inappropriate immune response and be discharging their regulatory function (again ineffectively) in an attempt to inactivate it. The remainder of the microenvironment: macrophage, dendritic cell, eosinophil, plasma cell, neutrophil, lymphoid and stromal form part of this interactive network, with tumour supportive, inflammatory, immunomodulatory, structural and passive roles.

### **1.4.3 CD4+ Cytokines and Chemokines in CHL**

There is evidence to suggest that IL4 stimulates the growth of HRS derived cell lines<sup>48</sup> with some IL4-encoding mRNA expressed in the reactive tumour microenvironment of biopsy material<sup>49</sup>, and HRS-derived cell lines strongly express IL-4 receptor<sup>50</sup>, although contradictory evidence exists<sup>51-53</sup> and there are limitations to analysis of cytokine function in non-vital fixed tissue. IL13 is more widely expressed in primary samples and HRS cell lines<sup>54-56</sup> and seems to be a distinctive property of CHL compared to NLPHL and another histologically similar malignancy T cell-rich B cell lymphoma (TCRBCL)<sup>54</sup> with IL13R expressed in most CHL cell lines and primary tissue<sup>55, 56</sup>. Exogenous IL13 fails to augment cell line growth, but growth is inhibited by antibody-mediated IL13 receptor blockade<sup>54-56</sup>. This highlights a Th2-like autocrine growth pathway (see 1.6.4) which may well be important *in vivo*, but cell line based models will always be limited by their absolute independence of the microenvironment, and hence underestimate the importance of microenvironment-derived supportive factors. IL5 and IL6, two further Th2-associated B cell-augmenting cytokines failed to show biological activity on HRS derived cell lines<sup>54</sup>, although both cytokines and their receptors have been found in some cell lines and primary material<sup>51, 57-59</sup>.

Whether as passive bystanders, ineffective antagonists, or essential promoters of HRS cell growth and survival, T cells must be attracted into the malignant microenvironment. HRS cells secrete abundant cytokines and chemokines, integral as autocrine survival signals and in forming the distinctive microenvironment (reviewed in Skinnider 2002)<sup>60</sup>. Serial gene expression analysis identified TARC/CCL17 (thymus activation-regulated chemokine) mRNA in a CHL cell line (L428) at strikingly high frequency<sup>61</sup> but not in NLPHL, NHL and EBV-transformed B cell lines, and confirmed its expression in a number of other CHL derived cell lines and patient derived material. Binding assays had already established the receptor for this chemokine: CCR4<sup>62</sup>. TARC/CCR4 interactions may be central to recruiting specific functional T cell subsets in CHL. The importance of soluble TARC, and specificity for Hodgkin disease is becoming more apparent since it is almost universally present at increased levels in the serum newly diagnosed patients, rapidly reduces following chemotherapy and may be an early prognostic marker of tumour sensitivity<sup>63</sup> and a tumour-specific target for chemo-immunotherapy<sup>64</sup>. MDC/CCL22 (macrophage-derived cytokine), a second ligand for CCR4 is also expressed in CHL tissue<sup>65</sup> along with other functional subset-

specific T cell-recruiting chemokines. These include RANTES/CCL5<sup>66</sup> (Regulated on Activation, Normal T cell Expressed and Secreted) whose receptor CCR3 is over-expressed on Th2 cells<sup>67</sup> and eosinophils<sup>68</sup>, MIP3A/CCL20<sup>69</sup> (macrophage inflammatory protein-3) and its receptor CCR6, over-expressed in memory and regulatory T cells<sup>70</sup>, and MIP1A/CCL3<sup>71</sup> and its receptors CCR1&5, over-expressed in Th1-biased responses<sup>72</sup>. It is possible that reciprocal attraction of HRS cell towards the T cell zone occurs in addition to T cell attraction towards HRS. As will be described in the discussion of normal germinal centre B cell / T cell interactions, upregulation of CCR7 by activated follicular B cells leads to movement towards the T cell zone and hence encounter with cognate T cells for support. CCR7 is up-regulated in CHL cell lines and strongly expressed by the malignant cell in CHL, but not in NPLHL.<sup>73</sup>

### **1.5 Normal B cells require T cell help for survival**

It has long been established that normal B lymphocyte survival requires interactions with the morphologically similar yet functionally and phenotypically distinct T lymphocyte. Seminal work showed that thoracic duct-derived cells synergise with bone marrow-derived cells to augment antibody production following infusion into irradiated syngeneic recipients<sup>74</sup>. A combination of secreted and cell surface mediated factors are required. Murine antigen-specific responses were found to be augmented by supplementing with activated T cell-derived soluble factors<sup>75</sup> although only with large excess of antigen, otherwise the T cell itself or at least T cell-derived cell membrane<sup>76</sup> needed to be available. In fact, the T cell could itself entirely replace antigen as activating stimulus<sup>77</sup>. The T and B cells require a 'priming' step to allow this interaction: naïve T cells were found to be ineffective and only activated T cells capable of delivering the necessary signals to allow *in vitro* antibody production<sup>78, 79</sup> while *in vitro* stimulation of B cells using surface Ig cross linking at concentrations too low to induce proliferation, leads to upregulation of cell-surface expressed factors essential to B cell function: IL4 receptor<sup>80</sup>, IL2 receptor<sup>81</sup>, Major Histocompatibility Complex (MHC) class II<sup>82</sup>, and other co-stimulatory molecules such as B7 (CD80/86)<sup>83</sup> and adhesion molecules<sup>84</sup>. Priming lowers the threshold for mutual interaction. T cells in the CHL microenvironment show evidence of priming, while the HRS cell expresses many markers of primed B cells, despite loss of most B cell defining features.

### **1.5.1 Cognate and non-cognate T/B cell interactions**

Normal B/T interactions require mutual activation by antigen presented in the context of compatible MHC complexes: early studies demonstrated superior T cell help in syngeneic over allogeneic systems<sup>74</sup> and, following characterisation of the MHC<sup>85</sup> dependence of this help on the MHC<sup>86-88</sup>. T cell activation requires antigen presented in the context of the MHC<sup>89</sup> while B cells encounter their cognate antibody via surface expressed immunoglobulin (B cell receptor). Immunoglobulin (IG)-bound antigen is internalised, degraded, assembled with MHC class II molecules, and presented as multiple epitopes capable of interacting with various cognate T cell receptors (TCR) thus facilitating cooperative action. These epitope-specific T cells then go on to provide the reciprocally activating signal to the B cell. The requirements of such a model are of extreme specificity: colocalisation of B and T cells recognising the same antigen, the former primed and demonstrating APC function, the latter primed to discharge helper functions, and both primed to migrate to optimize chance of encounter.

*In vitro* models have shown that such cognate antigen dependency may not be absolute since cocktails of activated T cell derived cytokines are able to stimulate some short-lived B cell proliferation without any antigen or B cell receptor engagement<sup>90</sup>. Activated murine T cell lines characterised as Th<sub>1</sub> or Th<sub>2</sub> (see also 1.6.4) by their particular cytokine expression profiles<sup>91</sup> promote allogeneic B cell activation<sup>92</sup>, with Th<sub>2</sub> cell lines providing the most efficacious support. Finally, MHC class II knock out mouse B cells still respond to activated T cell lines, as measured by DNA synthesis, immunoglobulin secretion, intracellular calcium flux and PI<sub>3</sub>-kinase signalling pathway activation<sup>93</sup>. Hence appropriately activated T cells producing sufficient survival factors may provide 'bystander' help: a physiological mechanism of recruiting additional T cells into an inflammatory reaction, and a mechanism which may be subverted by the HRS cell to promote its own survival.

### **1.5.2 Molecular Mechanisms of T cell help**

CD40 was recognised as an early candidate for T cell derived B cell help. Initially discovered as an activation-associated B cell surface specific molecule, designated Bp50<sup>84</sup>, a monoclonal antibody was developed which was found to augment B cell proliferation<sup>94</sup>, and its ligand (CD154, CD40-L) was confirmed in the T cell

transcriptional repertoire by several groups: Armitage et al 1992<sup>95</sup> cloned the ligand from a cDNA library derived from a murine thymoma cell line with high soluble CD40 binding capacity while Noelle et al 1992<sup>96</sup> confirmed function in B cell proliferation and IgE class switch by transfecting a cell line with the same clone. It was subsequently demonstrated in humans<sup>97</sup>.

CD28 (Tp44) was discovered during screening for B/T cell discriminating proteins, and found to be involved in TCR independent activation in antibody binding experiments<sup>98</sup>. Its ligands are structural homologues of the immunoglobulin superfamily, known collectively as 'B7'. B7-1/BB-1/CD80 was first discovered as a B cell activation marker<sup>99, 100</sup>, later as the ligand of CD28 through cell-adhesion experiments using a CD28 over-expressing CHO line<sup>101</sup>, and finally as the costimulator of anti-CD3 activated T cells, in which it induces IL2 secretion and proliferation<sup>102</sup>. A further CD28 binding, B cell expressed molecule, B7-2/CD86 was identified later<sup>103, 104</sup> and a potent and essential co-stimulatory mechanism defining one interaction between B and T cell became clear. Other immune cells, particularly activated, antigen presenting DCs and macrophages express these co-stimulatory molecules, further strengthening the evidence for their role in immune activation.

The confirmation of a pro-survival role for CD28 and CD40 implicated other structurally related molecules of the immunoglobulin (IGSF) and TNF receptor superfamilies (TNFRSF) respectively. Once primed by cognate antigen the T cell up-regulates numerous cell surface molecules capable of delivering necessary survival, proliferation and differentiation signals to the B cell, and the B cell provides signals in return. Exploration of the unique surface repertoire of activated T cells revealed a structural homologue of CD28 with apparent potent stimulatory activity (ICOS)<sup>105</sup>. Its ligand, CD275 (B7-H2), was discovered through homology with B7-1, B7-2 and B7-H1, and found expressed on DCs<sup>106</sup> and B cells<sup>107</sup>. Its essential role in B/T interaction, particularly in the GC was revealed by failure of affinity maturation, class switching and GC formation in deficient mice<sup>108, 109</sup>.

The spectrum of known TNFRSF members and ligand pairs with key stimulatory roles has grown and includes CD40 and its ligand (CD40-L/CD154), CD30 (first discovered in CHL derived cell lines) and its ligand (CD30-L/CD153), OX40 (CD134) and its ligand



(OX40-L/gp34), CD27 and its ligand (CD27-L/CD70) and 4-1BB (CD137) and its ligand (CD137-L). Immunoglobulin superfamily members include CD28 and its ligands B7-1/B7-2 (CD80/86) and ICOS (CD278) and its ligand (ICOS-L/ B7-H2/CD275). Related, but potentially suppressive molecule pairs have also been discovered. Many of these cell surface factors are found expressed in the HRS cell and their ligands within the T cell-dominated immune microenvironment (Table 1.1). Hence, despite lacking BCR and down-regulation of MHC class II, the B cell derived HRS expresses a range of activated B cell-associated surface molecules, with surrounding cells possessing appropriate molecules capable of ligating and hence signalling downstream to survival pathways.

MOLECULE	CD	Family	R/L	Expression	Evidence	Ref
<i>4-1BB</i>	<i>137</i>	<i>TNF</i>	<i>R</i>	<i>N/A</i>	<i>N/A</i>	<i>N/A</i>
<i>B7-H4</i>	<i>276</i>	<i>IG</i>	<i>L</i>	<i>N/A</i>	<i>N/A</i>	<i>N/A</i>
<b>B7.1</b>	<b>80</b>	<b>IG</b>	<b>L</b>	<b>HRS</b>	<b>Prot</b>	<sup>110</sup>
<b>B7.2</b>	<b>86</b>	<b>IG</b>	<b>L</b>	<b>HRS</b>	<b>Prot</b>	<sup>110</sup>
<i>BTLA</i>	<i>272</i>	<i>IG</i>	<i>R</i>	<i>N/A</i>	<i>N/A</i>	<i>N/A</i>
<i>CD27</i>	<i>27</i>	<i>TNF</i>	<i>R</i>	<i>N/A</i>	<i>N/A</i>	<i>N/A</i>
<b>CD27-L/Ki-24</b>	<b>70</b>	<b>TNF</b>	<b>L</b>	<b>HRS</b>	<b>Prot</b>	<sup>111</sup>
<b>CD28</b>	<b>28</b>	<b>IG</b>	<b>R</b>	<b>T</b>	<b>Prot</b>	*
<b>CD30</b>	<b>30</b>	<b>TNF</b>	<b>R</b>	<b>HRS</b>	<b>Prot</b>	<sup>112</sup>
<i>CD30L CD153</i>	<i>153</i>	<i>TNF</i>	<i>L</i>	<i>N/A</i>	<i>N/A</i>	<i>N/A</i>
<b>CD40</b>	<b>40</b>	<b>TNF</b>	<b>R</b>	<b>HRS</b>	<b>Prot</b>	<sup>113</sup>
<i>CD40L CD154</i>	<i>154</i>	<i>TNF</i>	<i>L</i>	<i>N/A</i>	<i>N/A</i>	<i>N/A</i>
<i>CD95-L/FAS-L</i>	<i>178</i>	<i>TNF</i>	<i>L</i>	<i>N/A</i>	<i>N/A</i>	<i>N/A</i>
<b>CTLA4</b>	<b>152</b>	<b>IG</b>	<b>R</b>	<b>T</b>	<b>RNA</b>	<sup>114</sup>
<b>FAS</b>	<b>95</b>	<b>TNF</b>	<b>R</b>	<b>HRS</b>	<b>Protein</b>	<sup>115</sup>
<b>HVEM</b>	<b>258</b>	<b>IG</b>	<b>L</b>	<i>N/A</i>	<b>DNA</b>	<sup>116</sup>
<b>ICOS</b>	<b>278</b>	<b>IG</b>	<b>R</b>	<b>T</b>	<b>RNA</b>	<sup>114</sup>
<i>ICOS-L/B7-H2</i>	<i>275</i>	<i>IG</i>	<i>L</i>	<i>N/A</i>	<i>N/A</i>	<i>N/A</i>
<b>OX40</b>	<b>134</b>	<b>TNF</b>	<b>R</b>	<b>T</b>	<b>RNA</b>	<sup>114</sup>
<b>OX40L</b>	<b>252</b>	<b>TNF</b>	<b>L</b>	<b>HRS</b>	<b>Protein</b>	<sup>117</sup>
<b>PD-L1/B7-H1</b>	<b>274</b>	<b>IG</b>	<b>L</b>	<b>HRS</b>	<b>Protein</b>	<sup>118</sup>
<b>PD-L2/B7-DC</b>	<b>273</b>	<b>IG</b>	<b>L</b>	<b>HRS</b>	<b>Protein</b>	<sup>118</sup>
<b>PD1</b>	<b>279</b>	<b>IG</b>	<b>R</b>	<b>T</b>	<b>Protein</b>	<sup>118</sup>
<b>RANK</b>	<b>265</b>	<b>TNF</b>	<b>R</b>	<b>HRS</b>	<b>Protein</b>	<sup>119</sup>
<b>RANK-L</b>	<b>254</b>	<b>TNF</b>	<b>L</b>	<b>HRS</b>	<b>Protein</b>	<sup>119</sup>

**Table 1.1:** Expression of selected TNFRSF and IGRSF with their ligands important in B/T cell interactions and evidence for their expression in CHL. **Bold:** expression data exists, *Italics:* theoretical only or no evidence of expression; Key: **CD:** cluster of differentiation designation; **IG:** Immunoglobulin Receptor Superfamily and ligands; **TNF:** TNFRSF and ligands; **HRS:** Expressed in HRS of primary CHL tissue or cell line; **R:** Receptor; **L:** Ligand; **T:** Expressed in microenvironment T cells of primary CHL tissue; **DNA:** CGH evidence of mutation in responsible genes only; **RNA:** PCR-based mRNA over-expression data only; **Protein:** Protein up-regulated by Western blot, IHC or Flow cytometry. \*Sibrand Poppema et al; Unpublished: personal communication.

### **1.5.3 T cell / B cell interactions in the lymph node**

#### **1.5.3.1 The lymph node is a lymphocyte and antigen concentrator**

As sophistication of microscopic imaging techniques has improved, so too has the understanding of the anatomy of B/T cell interactions. Lymph node architecture may be defined in terms of clearly distinct B and T cell zones. B cells form discrete aggregates - primary follicles, within which can sometimes be found further B cell aggregates with interspersed T cells - GCs (GCs), comprising a peripheral dark zone of tight packed cells, and a central light zone. The follicles are embedded in a cortex dominated by T cells and the structure circumscribed by a capsule penetrated by endothelium lined organs - the sinuses. Macrophages, dendritic cells (DCs), follicular dendritic cells (FDCs), and terminally differentiated plasma cells are found distributed in these various compartments. Assumptions of function can be surmised from this structural arrangement: antigen delivered through the sinuses in tissue fluid draining the regional anatomy, both free and contained within phagocytes (macrophages and dendritic cells) or complexed with antibody, passing through the nodal structure and encountering B and T cells. B and T cells are themselves in constant circulation throughout the body, homing preferentially to lymph nodes in which foreign antigens are being processed. This is achieved by regulation of adhesion molecules, chemokines and cytokines. For T cells, CD62L and CCR7 are essential, preferentially expressed by antigen-naïve T cells or by rapidly responding central memory cells. Their ligands are expressed by the high endothelial vessels permitting entry to the lymph nodes, and the stromal cells of the paracortical T cell zones respectively, ensuring a concentration of lymphocytes and antigen to maximise opportunity for cognate encounter<sup>120</sup>.

#### **1.5.3.2 B cell/T cell interactions in the paracortex and the germinal centre**

Interaction between B and T cells was proposed to originate in the T cell zones. However more sophisticated work has shown the junction of B and T cell zones is a more likely candidate for initial T cell dependent B cell activity<sup>121</sup>. Garside and colleagues (1998)<sup>122</sup> infused BALB/c mice with syngeneic T cells receptor-restricted to recognise a chicken ovalbumin peptide (cOVA), along with B cells restricted to recognise hen egg white lysosome (HEL). The mice were then challenged with a peptide construct consisting of cOVA fused with HEL (cOVA-HEL) and lymph nodes examined at various time points, stained to show localisation of cOVA specific T cells

and HEL specific B cells. B and T cell populations initially migrated to primary follicles and cortex T cell zone respectively. Following cOVA-HEL challenge T cells clustered and proliferated within the paracortex, and B cells migrated towards the T cell zone-abutting periphery of their follicles. Subsequently, T cells approached and formed close associations with B cells, which had proliferated. The cognate T cell dependence of B cell proliferation was confirmed by the fact that challenging with turkey ovalbumin (tOVA)-HEL conjugate peptide in combination with unconjugated cOVA antigen led to T cell proliferation and clustering (response to cOVA antigen), with HEL-specific B cells present in the node. However, since these were only capable of presenting tOVA and unable to interact with non-cognate cOVA-specific T cells, they failed to migrate or proliferate. This finding confirmed that the initial T cell engagement with antibody and activation can occur independently of a B cell: initial antibody presentation to T cell was by some other cell existing within the T cell zone. It also confirmed the necessity of cognate interaction with T cell for subsequent B cell proliferation and confirmed the location for initial T/B interaction. B cell expansion was blocked with anti-CD40-ligand, confirming this molecule's key role in the initial interaction. Further evidence for the cognate nature of this interaction was inferred from the fact that most B cells in the cOVA-conjugate challenged mouse lymph nodes were engaged with cOVA specific T cells, while with non-cognate challenge with tOVA-HEL and cOVA antigen showed far less T/B engagement. Time-course IHC has revealed some molecular mechanisms behind these migration findings. Antigen engaged B cells up-regulate CCR7<sup>123</sup>, receptor for T zone expressed CCL19 and CCL21<sup>124</sup>, while downregulating CXCR5, responsible for follicle localization via CXCL13 interactions<sup>125</sup>. CCL19/21 knock out models show impaired migration, CCR7 over-expression (by retroviral gene transfer) will induce antigen-unexposed B cells to migrate to the T zone, while CXCL13 over-expression traps B cells within their primary follicles<sup>123</sup>.

### 1.5.3.3 The T cell confers a GC selection pressure by selective B cell help

Affinity of antibody increases with time of exposure to antigen<sup>126</sup>. The mechanism behind this phenomenon emerged when sequencing of the B cell immunoglobulin gene revealed a physiological process of mutation was at work, termed somatic hypermutation<sup>127</sup>. The lymph node compartment in which this phenomenon arises was confirmed by demonstrating that plasma cells in extra-follicular foci show less

hypermutation than in GCB cells<sup>128</sup>, with overrepresentation of amino acid replacing, rather than silent mutations implying a selection bias towards mutations conferring B cell receptor conformation and hence antigen affinity changes. A mechanism favouring B cells synthesizing antibody with greater affinity for antigen with deletion of those with lesser affinity suggests a mechanism requiring constant exposure to a selection pressure, namely competition for antigen<sup>129</sup>. Selection pressure and cell cycling probably occurs continuously as the B cell traffics around the GC until eventually triggering a terminal differentiation program and GC exit to migrate elsewhere as plasma cell or memory B cell<sup>130</sup>. The selection pressure was presumed initially to be a function of competition for immune complex derived from soluble antigen, displayed on FDC and determined by strength of association and hence signalling through the B cell receptor (Reviewed in MacLennan 1994<sup>131</sup>). This has been contested by data showing that soluble immunoglobulin deficient mice are still able to form GCs<sup>132</sup> and that long-lived associations with FDCs have not been seen in real-time imaging studies: B cells seem to traffic freely between compartments<sup>133</sup>. Another selection pressure is being exerted, and this appears to arise from competition for T cell help in the GC. Fixed tissue analysis shows the GC light zone is rich in T cells<sup>122, 134</sup> with dynamic fluorescence microscopic studies showing constant, brief interactions between T and B cells. Notably, in contrast to the interaction at initial activation between B and T cells in the paracortical zone, where B cells synapse so robustly that they are able to migrate with T cell in tow<sup>135</sup>, most interactions in the light zone appear to be brief: less than five minutes, too brief for a productive conjugate in which help-conferring cell-cell signalling can occur<sup>136</sup>. CD40 signalling is essential for B cell survival in the GC<sup>137</sup>, but T cells available to provide this CD40-L-mediated help are outnumbered up to twenty to one in the GC and only a small proportion of GCB cells show evidence of CD40 signalling as evidenced by downstream cREL expression<sup>138</sup>. Hence for a B cell to receive help from T cells it must out-compete the surrounding cells: presumably through differential strength of binding cognate antigen. The GC T cells themselves may be relatively hyporesponsive to activation with altered expression of help-conferring molecules. The GC T cell may even be a phenotypically distinct subtype in itself.

## **1.6 The nature of the CD4<sup>+</sup> T cell in the CHL microenvironment**

Most conclusions regarding the nature of the T cell infiltrate in CHL are based on limited evidence and oversimplification, while functionally defining a human CD4<sup>+</sup> T cell is challenging and often artificial being based on *in vitro* and murine *in vivo* experimental models.

### **1.6.1 Heterogeneity of CD4<sup>+</sup> T cells: Phenotype and Function**

The heterogeneity of T cells has become clear as scientific methods have become more sophisticated; however while there is little controversy that they represent a morphological homogenous, long-lived, proliferative, mobile population of cells, each possessing a unique surface receptor (TCR) with stringent specificity for a limited number of amino acid sequences presented within the MHC, the eventual outcome of interaction of the activated cell with its targets is enormously diverse. This complexity distinguishes it from a morphologically similar cell (the naïve B cell) with similarly fastidious receptor/ligand demands but whose terminally differentiated function, whether immediately following activation and expansion, or after a long period of 'primed' senescence (memory) is quite simply to secrete vast quantities of antibody. Non-phagocytic cell-mediated cytotoxicity was determined to be the key effector function of another group of apparently similar cells which express CD8, the cytotoxic T cell<sup>139</sup>. The function of CD4<sup>+</sup> T cells have been based on studies of artificially discriminated populations of cells. The immunoglobulin synthesis-helping, but not secretory capacity which originally discriminated T helper cells from B cells is only one of many roles for this cell defined by expression of TCR, CD3 and CD4.

### **1.6.2 Methodological problems in determining a functional CD4<sup>+</sup> T cell subset**

The mechanism of polarisation and relative flexibility of CD4<sup>+</sup> T cell phenotype commitment has yet to be fully understood and requires multiple layers of regulation, from microenvironmental and APC presented cytokines, TCR stimulation strength<sup>140</sup> and TCR-independent 'alternative pathway' activation mechanisms<sup>141</sup>, to differential activation of intracellular signalling pathways, such as Notch<sup>142</sup> as well as epigenetic changes of gene accessibility. Interspecies as well as *in vivo/in vitro* differences have demonstrated the complexity of these mechanisms and the need for caution in interpreting and taking forward these findings. Studies of cellular function, preferably *in vivo* are the most robust and practical method of defining a T cell subset and should always remain the gold standard of phenotype definition.

Chromosomal packaging and accessibility (epigenetics), gene and consequent protein expression with attendant layers of regulatory mechanisms (genetics), signalling pathways and intra/extracellular communication (proteomics) influence the nature of a cell, and the consequence of these interactions leads to functional physiology and dysfunctional pathology. Scientific reductionism is increasingly accessible. An individual cell or cell population may be defined genetically by its nucleic acid sequence, epigenome, composition of transcribed and translated products, through high resolution whole genome sequencing, chip-based gene expression, RNA expression and methylation/acetylation profiling. Interdependently activated and inactivated intracellular and surface expressed proteins may be determined through techniques ranging from Western blotting to mass spectroscopic proteomics, phosphoproteomics and single cell multi-parameter flow cytometry. However emergent function can often only be inferred. Even with contemporary computational network analysis the significance of vast arrays of data and application to physiological models can be overwhelmingly complex, leading to inappropriate *post-hoc* analysis, selectivity of data interpretation and erroneous conclusions. Data generated from inevitably heterogeneous populations of cells may swamp the detail of functionally more important cells concealed in a mass of less important cells. Even studies based on samples highly enriched for the cells of interest rely on over-simplistic, surrogate markers for that cell. Functional assays of these purported subsets are considered a gold standard in understanding any biological system. But functional validation can only be performed using a model system amenable to interrogation by the scientific technology available. In the case of modelling human biological systems, ethical necessity means that *ex vivo* and animal models must be resorted to. The validity of these systems can only be inferred by successful applications of pharmacological experiments in man, with the further complexity of enormous interpersonal physiological variability.

### **1.6.3 Effector T cell and Memory T cells**

The capacity to recognise antigen with a greater efficiency and discharge function with greater potency on subsequent exposure is the cornerstone of adaptive immunity. This depends upon the existence of a long lived memory component of the adaptive immune system with fine-tuned antigen specificity and capacity to more efficiently proliferate and function in response to a subsequent pathogenic challenge than their

naïve equivalent (reviewed in Berard & Tough 2002<sup>143</sup>) while being maintained at a low level for many years, up to the lifetime of the organism. In contrast, effector cells tend to devote their entire replicative and synthetic apparatus to the discharge of their pathogen-destroying function, with the majority arising in response to antigen challenge rapidly dying<sup>144</sup>. Hence the 'memory' compartment is functionally and phenotypically distinct. Memory compartments exist for each component of adaptive immunity: B cell, cytotoxic T cell and 'helper' T cell. The latter, with its widely varied and poorly understood repertoire of potential effector function is likely the most complex.

Models of the memory compartment have largely arisen from observations in the CD8+ compartment. Memory compartments are defined by expression of CD45 isotype (with CD45RA being truncated predominantly to CD45RO in the effector and effector memory cell compartments and re-expressed as CD45RA in some long-lived memory cells) along with tissue homing molecules particularly node-homing CD62L, paracortical T cell zone-homing CCR7<sup>145</sup> and survival-promoting cytokine receptors particularly CD127 – the IL7 receptor. The accumulated evidence supports a model whereby a naïve T cell although committed to either CD8 or CD4 lineage, is uncommitted to memory or effector fate until after antigen exposure<sup>146</sup>. The functional bias of the memory T cell component towards priming for future encounter rather than discharge of immediate function makes it a less feasible candidate for a HRS/T cell interacting subset. However, the cytokine rich microenvironment may well attract these cells passively into the involved lymph node tissue.

### **1.6.4 The Paradigm Subsets: Th<sub>1</sub> and Th<sub>2</sub>**

#### **1.6.4.1 Functional Definitions of Th<sub>1</sub> and Th<sub>2</sub>**

The earliest T helper dichotomies, defined as Th<sub>1</sub> and Th<sub>2</sub>, were based on physical separation properties (degree of binding nylon wool) and relative ability to render B cell help in antibody synthesis<sup>147</sup>. These properties were entirely artificial and functionally unhelpful, arising from differential expression of MHC class II (then known as Ia antigen) by T cells, conferring possible antigen presenting function, a property that remains poorly understood today<sup>148</sup>. The most enduring and physiologically applicable discriminator of Th<sub>1</sub> and Th<sub>2</sub> function remains that described by Mosmann and Coffman in a more biologically applicable system<sup>149</sup>. The supernatant derived from the murine Th<sub>1</sub>-defined cell line LB2-1 was found to support

the growth of an IL2-dependent cell line HT2 more robustly than that from a murine Th2-defined cell line MB2-1. On addition of an IL2 blocking antibody, all of the supportive activity of the Th1 cell line was lost, while the Th2 cell line retained its activity, implying the existence of a less efficacious, but distinct Th2 growth factor (defined as T-cell growth factor 2: TCGF2). Conversely, MB2-1 ('Th2') preferentially supported the growth of a mast cell line (the activity being defined as mast cell growth factor 2: MCGF2). MB2-1 was also found to be superior to LB2-1 in enhancement of B cell line immunoglobulin secretion (B cell growth factor 1: BCGF1). Finally, IFN- $\gamma$  suppressed the growth of the NFS60 cell line: a cytokine known to be synthesized by LB2-1 ('Th1'), and not by MB2-1.

These bioassays were applied to an extended panel of cell lines. Fortuitously, and by a mechanism still not understood, the biological function-discrimination coincided with the relative nylon wool adherence capacity of the Th subtypes. Western blotting confirmed that the 'Th1' cell lines produced IFN- $\gamma$ , unlike Th2, and on SDS-PAGE fluorography the Th2 cells showed a distinctive band in the 16kd region, absent in Th1 cells: a candidate for the mysterious TCGF2/BCGF1. These fundamental experiments, while purely *in vitro* assays, generated a robust basis for the Th1/2 dichotomy. The identity of the key secreted effectors of Th1 and Th2 function had been discovered: IFN- $\gamma$  and IL2 defining the Th1 subtype, and Th2 being defined by secretion of TCGF2/MCGF2/BCGF1-secretion, now known to be the same factor, IL4<sup>150</sup>. While huge advances in understanding the mechanism of differentiation into these subsets from naïve T cell have been made in the 25 years since these observations, these defining features remain the functional readout of Th1 vs Th2 activity: IFN- $\gamma$ /IL2 vs IL4/B cell help. *In vitro* polarisation protocols were established for Th2<sup>151-153</sup> and, with the identification and cloning of IL12<sup>154, 155</sup> for Th1<sup>153</sup>. These experiments confirmed this polarisation was true in man as well as mouse. An *in vivo* model already existed that replicated this *in vitro* dichotomy. It had been observed that susceptibility to *Leishmaniasis* varied greatly between inbred mouse strains, in that some strains (e.g. C57BL/6) cleared infection effectively whereas others (e.g. BALB/c) invariably succumbed<sup>156</sup>. Athymic mice rapidly developed fulminant infection despite the mechanism of pathogen clearance being confined to macrophages, of non-thymic origin. A cooperation between T-cells and macrophages was proposed that was effective in some immunocompetent mouse strains, but ineffective in others. The



model was supported by lymphocyte transfer experiments from both allogeneic *Leishmania*-'healer' mice, and syngeneic 'non-healer' mice whose lymphocytes had been pre-activated using concanavalin-A. Under these conditions, recipient macrophages were effective in pathogen clearance. These differences implied a heterogeneity of T cell helper activity, and building on their *in vitro* work Coffman's group went on to demonstrate increased IFN- $\gamma$  and reduced IL4-coding mRNA in lymph nodes and spleen in C57BL/6 compared to BALB/c mice<sup>157</sup>. The fact that the difference arose from the differential T cell populations was confirmed when Th1 or Th2 cell lines were derived from otherwise susceptible BALB/c mice by limiting dilution and mice reconstituted with one or other<sup>158</sup>. Th1 reconstituted mice were now able to clear the infection. Th2 reconstituted mice succumbed more rapidly than the unmanipulated BALB/c mouse. Not only was the *in vitro* differential shown functionally but mutual inhibition confirmed, as well as demonstration of the capacity for one population to dominate an immune response in a genetically identical animal.

#### 1.6.4.2 Th1/Th2 defined by intracellular protein expression

Advances in intracellular signal transduction studies revealed several receptor mediated protein phosphorylation cascades as candidate molecular mediators of lymphocyte polarization. STAT3 and 4 were found associated with Th1 polarisation<sup>159</sup> while STAT5 associated with Th2<sup>160</sup>, and their necessity was proven with knockout mouse models<sup>161, 162</sup>. A 'master transcription factor (TF)' lying behind more global gene, protein, signal transduction and effector mechanism expression is an attractive proposition for subset discrimination. Differential gene expression profiling comparing Th1 with Th2 based on cDNA library representational difference analysis (cDNA RDA) and subsequent functional antisense gene expression knockdown experiments revealed Gata3 as a fundamental Th2 TF<sup>163</sup>, with T-bet required for a Th1 response<sup>164</sup>. However, specificity of these TFs, murine/human physiological differences as well as stability of expression and plasticity of phenotype continues to limit their application in functional subset definition.

#### 1.6.4.3 Th1/Th2 defined by surface protein expression

Cellular function is defined by the spectrum of cytokines, chemokines, and surface molecule interactions exercised by the functional cell, and phenotypic discrimination may be defined by this spectrum. Cell-surface molecules unique to a functional

subtype carry the advantage of enabling live cell purification using flow cytometry: intracellular markers generally require fixation and permeabilisation, which while quantifying a population, also results in cell death. Bonocchi and colleagues (1998) addressed this<sup>72</sup>, attempting to discriminate Th<sub>1</sub> and Th<sub>2</sub> cells by surface cytokine receptor profiling. This required a 'gold standard' reference population of Th<sub>1</sub> or Th<sub>2</sub> to ensure validity. Polyclonal 'Th<sub>2</sub>' cells were generated by stimulating density gradient separated human PBMC TCR-independently with phytohaemagglutinin (PHA), polarising with recombinant IL<sub>4</sub> and IL<sub>2</sub> along with neutralising anti-IL<sub>12</sub> antibodies for two weeks, and confirming phenotype using FACS analysis of intracellular cytokine staining with IL<sub>4</sub>. This has the advantage of enabling identification of individual cells, rather than broad populations of cells, expressing particular cytokine combinations<sup>165</sup>. Cells were purified using physical methods: plate-binding monocytes and nylon wool binding-out MHC-II (predominantly non-T) expressing cells. Using this polarisation/purification method, 25% of the resulting T cells expressed IL<sub>4</sub> (and 2% IFN- $\gamma$ ), compared to 2% of similarly prepared, Th<sub>1</sub> polarised cells (of which 60% produced IFN- $\gamma$ ). A number of antigen-specific T cell clones known to be cytokine profile polarised were also used, generated from *Lolium perenne* P<sub>1</sub>-allergic subject T cells by limiting dilution. Greater than 90% of the Th<sub>2</sub> cells in these cultures produced IL<sub>4</sub>. With these stringent definitions of Th<sub>2</sub> phenotype, RNA was extracted from purified T cells and probed using northern blot analysis for a variety of cytokines.

CCR<sub>4</sub> was over-expressed in Th<sub>2</sub> clones and polarisation cultures as well as in unpolarised, PHA-stimulated, purified T cells (T+PHA) compared to Th<sub>1</sub>, and expressed CCR<sub>3</sub> weakly, but more than in Th<sub>1</sub>. CXCR<sub>3</sub> was up-regulated in Th<sub>1</sub> and T+PHA compared to Th<sub>2</sub>, and CCR<sub>5</sub> in Th<sub>1</sub> and monocytes compared to Th<sub>2</sub>. CCR<sub>1</sub> was expressed at very low levels in Th<sub>1</sub> and Th<sub>2</sub>. The functional significance of these receptors was confirmed using a migration assay with known ligand for CCR<sub>4</sub>. Migration in response to CCR<sub>4</sub> ligand (MDC, now CCL<sub>22</sub>) and CCR<sub>3</sub> ligand (eotaxin, now CCL<sub>24</sub>) was superior in Th<sub>2</sub> cells, whereas Th<sub>1</sub> cells migrated preferentially towards CCR<sub>5</sub> and CXCR<sub>3</sub> ligands (MIP-1 $\beta$ , now CCL<sub>4</sub> and IP-10, now CXCL<sub>10</sub>).

This study established a functional chemokine receptor profile differential discriminating Th<sub>1</sub> from Th<sub>2</sub> in a relatively robust (using polarised antigen-specific clones) but nonetheless *in vitro* system. However, while relative expression of mRNA

and relative migrational capacity to their appropriate ligands had been shown, what could not be inferred was stability of expression of these receptors, importance *in vivo*, and uniqueness to Th2 or Th1 lymphoid cells. PBMCs, magnetic bead purified based on CCR4 expression alone<sup>166</sup> overexpress IL4 when stimulated compared to the unenriched fraction, with few expressing IFN- $\gamma$  as measured by intracellular cytokine FACS, however, the majority of cells remain uncommitted to IL4. The specificity of CCR4 (or indeed any alleged subset-defining 'signature' molecule) draws its usefulness as a functionally-defining marker into question. CCR4 is strongly up-regulated on regulatory T cells (Tregs)<sup>167</sup>, a functionally and otherwise phenotypically quite distinct T cell subset. Indeed, a growing murine literature exploring CCR4 function has failed to define it as either necessary or specific for Th2-like function. Undoubtedly, other surface molecules will emerge associating with various T cell subsets, most with key functional roles in target cell support or destruction, and tissue specific localisation. CRTH2, a prostaglandin receptor is one with a growing evidence base for Th2 specificity<sup>168, 169</sup>. However using surrogate markers without functional correlates is problematic.

### **1.6.5 A controversial subset: The regulatory T cell (Treg)**

#### 1.6.5.1 Defining the Treg as a distinct phenotypic cell type

The necessary potency and potential destructiveness of the immune response makes tolerance to self a vital capability. Tolerance arises partly through 'central' programming of the adaptive immune cells to ensure those reactive to self antigen are removed early in cell development: thymic and bone marrow mechanisms which delete immature T and B cells if they become activated within these central organs of production. Autoreactive cells that survive this and enter the secondary lymphoid organs are subject to peripheral mechanisms of tolerance: encounter of antigen in a 'benign' context implying no pathogen presence and hence without inflammatory triggering of co-stimulatory molecules provided by the innate and antigen presenting components of the immune system leads to inactivation of the cell: anergy. However, auto-reactive clones remain and may become pathological, such as in autoimmune disease or perhaps maintenance of lymphoid malignancies through ongoing antigen receptor signal-mediated survival<sup>170</sup>. A further layer of 'peripheral' protection has emerged more recently, arising from the longstanding knowledge that T cells not only promote, but also suppress the immune response.

The first evidence that T cells were essential not only in enhancing immunoglobulin production but also in immune tolerance was shown at a time when evidence demonstrating the T and B cell dichotomy was still in its infancy<sup>171</sup>. Irradiated, thymectomised mice rescued with syngeneic bone marrow then exposed to massive doses of foreign antigen (sheep red blood cells: SRBC) become tolerant to that antigen - unable to mount an immunoglobulin-secreting response to subsequent antigen challenge. Combining the antigen challenge with a thymocyte infusion could restore this response. However if the initial 'tolerising' event was preceded by an infusion of thymocytes, the animal's response to subsequent antigen challenge with thymocyte support was suppressed. Hence T cells tolerised by the initial antigen exposure appeared to be suppressing subsequent T cell help. While rudimentary in terms of purity of cell populations and using immunoglobulin synthesis as the sole measure of immune function, this provided first demonstration of a tolerance mechanism arising from the thymic component of the immune system. Discovery that mouse thymectomy could lead to autoimmunity as well as immunodeficiency if performed at particular stages of development in particular mouse strains<sup>172</sup> along with rescue from autoimmunity by reconstitution with spleen-derived lymphocytes<sup>173</sup>, specifically populations enriched for the Lyt-1 (CD5) antigen<sup>174</sup>, with reciprocal induction of autoimmunity by repopulation of Lyt-1 depleted splenocyte provided further evidence that there was a specific suppressive T cell subset. The early discovery of Lyt-1 as a lymphoid subset marker is particularly fortuitous for these experiments' findings: it happens to be highly expressed in the robustly investigated and widely accepted 'professional' suppressor T cell of contemporary studies - the regulatory T cell (Treg)<sup>175</sup> and may in fact be integral to these cells' survival and function<sup>176</sup>. However, failure to define effector mechanisms or unique phenotypic features for this proposed suppressor subset as had been robustly demonstrated for the Th<sub>1</sub>/Th<sub>2</sub> paradigm with their distinct cytokine and TF profiles, led to years of scepticism in this field<sup>177, 178</sup>.

This scepticism was convincingly overcome following the discovery that a subset of murine CD<sub>4</sub><sup>+</sup> cells constitutively expressing high levels of the IL-2R  $\alpha$  chain (CD25) specifically possessed suppressive activity<sup>179</sup>, then confirmed in humans<sup>180</sup>. A master TF (Forkhead Box Protein 3; FOXP<sub>3</sub>) was demonstrated first in mice, in which there was a mutation-associated disease phenotype: Scurfy<sup>181-183</sup>, then humans<sup>184</sup>, in which a disease

equivalent had already been described<sup>185, 186</sup>. This subset is generated in the thymic medulla, demonstrated by IHC thymus examination and functional studies of FACS-purified thymus-derived CD25<sup>hi</sup> CD4<sup>+</sup> cells<sup>187</sup>. The TCR affinity of this subset to self antigen is high, shown by the fact that protection against spontaneous EAE (experimental autoimmune encephalitis) requires the presence of MBP (myelin basic protein)-specific TCR  $\alpha/\beta$  expressing CD4<sup>+</sup> cells (but not B, CD8<sup>+</sup>, NK or  $\gamma/\delta$  T cells)<sup>188</sup> as well as evidence for thymic positive selection, rather than the expected deletion of CD4<sup>+</sup>CD25<sup>+</sup> cells possessing high affinity for this same self peptide<sup>189</sup>.

#### 1.6.5.2 Tregs defined by FOXP3

Although constitutive FOXP3 expression delineates a population of naïve T cells with self-antigen specificity and particularly potent suppressive activity (natural Tregs: nTregs), selected in the thymus and activated peripherally on recognizing autoimmunity promoting immunological cells, this TF is also expressed in other populations. Induced Tregs (iTregs), produced through activation of naïve T cells in the presence of TGF $\beta$ <sup>190</sup> may have some role in immunosuppression, perhaps potentiating the immunosuppressive capacity of nTregs, but their repertoire and potency of immunosuppression is likely much reduced, and in humans they may not possess immunosuppressive function at all<sup>191</sup>. Stability of FOXP3 expression of nTregs is superior to that seen in iTregs, and even expressed transiently following proinflammatory activation<sup>192</sup>, perhaps through differential chromatin modelling and DNA methylation<sup>193</sup>. Even nTregs show some plasticity of function and gene expression, perhaps explaining one mechanism of immune tolerance breakdown during dysfunctional, chronic inflammatory states<sup>194</sup>. This is a fundamental observation, a further illustration of the pitfalls of applying mouse models of immunity to humans, and in drawing conclusions about the significance of FOXP3 in the context of an active inflammatory or TGF $\beta$  rich microenvironment such as CHL.

#### 1.6.5.3 Tregs defined by surface protein expression

A functional assay of any T cell subset requires a purification technique that is not destructive to the cell, as discussed for Th2 above. No single surface-expressed nTreg marker has been determined, and the strategy of CD4<sup>+</sup>CD25<sup>-hi</sup> enriching human T cells does not yield equivalent cell purities as seen in the mouse, largely because of contamination by activated T cells, which also up-regulate CD25. A balance between

inadequate yield by over-stringent selection based on CD25 brightness, and impurity of the derived population must be struck. Combinations of markers have been investigated which eliminate these contaminating non-regulatory T cells while sustaining a reasonable yield, including IL7-receptor (CD127)<sup>195</sup>,  $\alpha$  chain of  $\alpha_4\beta_1$ -integrin/VLA4 (CD49d)<sup>196</sup>, both activated effector T cell associated and hence showing low expression in Tregs, while LAG-3 (CD223)<sup>197</sup> is associated with particularly high FOXP3 expression and suppressive capacity. None are entirely nTreg specific, and indeed there may not be any single unique marker of this, or any other subset.

#### 1.6.5.4 Mechanisms of Treg and immunosuppressive function

The mechanism of Treg action is still a being explored, with many candidate soluble and surface expressed molecules specifically, constitutively or over-expressed in purified Tregs. Treg-specific IL-10 gene knock out models develop spontaneous colitis and inflammatory reactions in skin and lung<sup>198</sup> while CTLA-4 knock out leads to fulminant lymphoproliferation, autoimmunity and death<sup>199</sup>. TGF- $\beta$  (an inducer of FOXP3 expression in CD25- T cells which may confer an 'induced' Treg phenotype in previously effector cells), IL35, a novel IL12 $\alpha$ -IL27 $\beta$  heterodimer with T cell antiproliferative effects<sup>200</sup> and galectin-1, a known inhibitor of T cell function<sup>201</sup> up-regulated in human Tregs<sup>202</sup> are synthesized by some subsets. Cytotoxic mechanisms through granzyme/perforin<sup>203</sup> or CD95/CD95-ligand interactions<sup>204</sup> are described. Other proposed mechanisms include suppression of ATP-mediated inflammatory signals through Treg expressed nucleotidase CD39<sup>205</sup> and blockade of MHC-II expression through the CD4 homolog LAG-3<sup>206</sup>. Multicellular models of immunosuppression more complex than the paradigm *in vitro* Treg-Tsuppressor functional assays<sup>207, 208</sup> have demonstrated the involvement of other immune cells in peripheral tolerance, such as antigen presentation by dendritic cells<sup>209</sup> or direct suppression of B cells<sup>210, 211</sup>. The dominant mechanism of suppression, along with the relative contributions of soluble and cell contact-dependent factors have yet to be determined and may in fact be conferred by tissue, effector mechanism and target cell specific subsets of Tregs, such as the proposed, but not universally accepted Tr1 subset (IL10-producing T cells<sup>212</sup>) and Th3 subset (gut-specific FOXP3+ TGF $\beta$ -expressing CD4+ T cells and hence perhaps a conglomerate of induced and natural Tregs<sup>213</sup>), and specific Th1 and Th2-type response-suppressing Tregs which coexpress Th subset-defining signalling molecules and TFs T-BET/Th1<sup>214</sup>, IRF4/Th2<sup>215</sup> and STAT3/Th17<sup>216</sup>.

Suppressor activity may lie in other non-CD4 expressing cells, including the CD8<sup>217</sup> and B cell<sup>218</sup> compartments, as well as in T cells not expressing FOXP3<sup>219</sup>.

It is now clear that Tregs represent an important, phenotypically distinct and functionally specific subset of CD4<sup>+</sup> T cells. There is accumulating evidence of their importance in the CHL microenvironment (see 1.7.2 and 1.9.2) but the relevance of this is not known: passive or induced bystander, suppressor of T cells, or direct suppressor of the B-cell derived HRS cells themselves.

#### 1.6.5.5 CTLA-4 and PD1: Immunosuppressive B/T interactions?

CTLA-4 was discovered as a T cell specific IGSF protein with structural homology to CD28<sup>220</sup>, expressed only on activated T cells and which more potently binds B7-1 but confers immunosuppressive function<sup>221</sup>. Discovery of a further ligand for both CD28 and CTLA4 arose when it was found that antibody blockade of the B7-1 pathways was insufficient to antagonise all of CTLA4's activity: there was another binding site for CTLA4: B7-2<sup>104</sup>, now confirmed to be closely related in the CD28/CD80/CD86 co-stimulatory system. Confirmation of its potent immunosuppressive role was found in murine gene knock-out experiments in which fatal lymphoproliferation occurred<sup>222</sup>.

A further unique structural homologue was discovered in apoptotic T cell lines<sup>223</sup> using subtractive hybridization during an analysis of the mechanisms of cell death, hence named Programmed Death 1 (PD1). Not a ligand for CD28 or CTLA4, its role as an immunosuppressive molecule was inferred from murine gene knock-out experiments<sup>224</sup> in which splenic enlargement and hypergammaglobulinaemia were noted in one early model, and multisystemic autoimmune disease in another<sup>225</sup>, both apparently attenuated forms of the CTLA4 knockouts. Further evidence for the immunosuppressive role of PD1 emerged using blocking antibodies in mouse models of immune-mediated disease, in which EAE<sup>226</sup>, diabetes<sup>227</sup> and graft-versus-host disease (GVHD)<sup>228</sup> were exaggerated. Its ligands, structural homologues of the B7 group (B7-H1/PD-L1/CD274 and B7-DC/PD-L2/CD273) were identified using structural homologue cloning techniques<sup>229</sup> and subtractive complementary DNA library screening in mouse<sup>230</sup> and found to possess suppressive activity via PD1 interactions, with a structural homologue in man<sup>231</sup>. Expression of PD-L1&2 is seen on a wide variety of immune cells: DCs, macrophages, T and B cells. The structural homology of receptor

and ligand, both possessing intracellular domains, suggests two-way interactions. The consequences of these remain to be fully elucidated. Evidence for alternative receptors for the ligands has been provided by experiments demonstrating that ligand exposure can also enhance T cell activity<sup>232</sup>. Overall the evidence suggests that cells expressing PD-L1&2, widespread amongst inflammatory tissue suppress the function of PD1-expressing T cells. However the role of PD1/PD-L1&2 signalling in the GC may be more complex, and potentially two-way, with T cells providing survival signals through PD1 back to the PD-L1 expressing B cell. Molecules in this system are over-represented in the CHL microenvironment but their function in this context is obscure<sup>18</sup>.

Further homology searches have gone on to reveal other members of the B7 family and respective receptors with probable inhibitory function. B7-H4/CD276<sup>233, 234</sup> was investigated with murine in-vivo antibody-mediated blocking experiments showing exaggeration of murine EAE; the molecule BTLA<sup>235</sup> may represent its receptor equivalent, although another IGSF candidate molecule, HVEM (herpes virus entry mediator) also binds BTLA with B/T cell functional consequences<sup>236</sup>. B7-H3<sup>237</sup> was found in a human DC-derived cDNA library and possesses both enhanced T cell activity<sup>237</sup> as well as inhibitory function<sup>238</sup>. Discrete definition of these molecules as co-stimulators or co-inhibitors appears overly simplistic, emphasizing that function varies by tissue, interacting cells, and activation states.

#### **1.6.6 A professional GCB cell-helping T cell: T follicular helper**

The most phenotypically suited T subset for normal B cell and by extension perhaps malignant B cell support, even with the limitations of subset definition and plasticity of differentiation described above appears to be the Th2 cell. With B cell stimulating and maturation-promoting IL4, IL5 and IL13 secretory activity, expression of a range of B cell activating surface proteins, along with decades of functional *in vitro* and *in vivo* evidence, this cell is theoretically best suited for activated B cell promotion, and could perhaps be the prime candidate microenvironment T cell conferring the B cell malignancy equivalent, the HRS cell, with its survival signals. The CHL microenvironment was once thought to be dominated by Th2 polarised cells, but this model has been substantially challenged, as will be discussed below. Additionally, there is another recently, robustly defined subset of T cells that may fill the role of a professional GC-specific B helper cell: the T follicular helper cell (Tfh). Understanding



this cell's function may provide candidate molecules of T cell-mediated HRS support.

#### 1.6.6.1 Evidence for a T follicular helper (Tfh) cell

Bowen and colleagues (1991)<sup>239</sup> first described the unique phenotype and localisation of a subset of T cells present in the GC, comprising around 10% of all cells. Their expression of the natural killer (NK) cell marker CD57 (Leu-7) and unique cytokine secreting profile<sup>240</sup> differentiated them from peripheral T cells and those T cells inhabiting the lymph node cortex. Follicular T cells present in tonsil were found to up-regulate membrane CD40-L more rapidly, suggesting that they possessed pre-synthesised intracellular protein<sup>240</sup>, and this, together with the knowledge of B cell help requiring CD40 signalling, provided further evidence that the T cells in the GC were not mere bystanders, but the providers of B cell help, and of a distinct phenotype to other T cells. Th1, Th2 and Tregs have convincing evidence of distinct surface protein, TF, cytokine secretion and functional profiles, and these Tfh cells have acquired their own evidence to support them as a further distinct subset. CXCR5 is up-regulated on their surface<sup>241</sup>, a receptor more characteristic of activated B cells and consistent with an ability to migrate into the CXCR5 ligand-rich (CXCL13) GC<sup>225</sup>. This surface factor is transiently expressed on most activated T cells, but appears to be retained on this subset<sup>242</sup>. Isolation based on CXCR5 expression enabled gene expression of this subset to be examined, revealing a distinct profile to those described for Th1, Th2, Th17 and Tregs<sup>243</sup>, and determining further characteristic surface proteins: CD200, PD1, ICOS, OX40 and Surface Lymphocyte Activated Molecule (SLAM) adaptor protein (SAP)<sup>243, 244</sup>. IL10 and IL21 secretion, along with expression of the GCB cell characteristic TF Bcl-6, unique in the context of T cells and distinct from other T cell subtypes<sup>244, 245</sup> as well as the Th2 associated c-Maf have been described. Mouse models deficient in IL4 and STAT 6 (essential for Th2 function), IFN- $\gamma$  and STAT4 (essential for Th1 function), IL17 and RORa/c (required for Th17 function) show evidence of an intact T follicular helper subset<sup>246</sup>. Hence, evidence supporting this CXCR5 expressing, GC localising T cell as a distinct entity is robust.

The mechanism of migration to the GC, implied by CXCR5 expression, was confirmed in mouse CXCR5<sup>-/-</sup> T cell adoptive transfer experiments in which the GC response was much impaired and T cell-rich light zones did not form<sup>247</sup>. CXCR5 expression also seems to depend upon intact signalling through other Tfh surface proteins - OX40 and

CD30<sup>248</sup> whose ligands are expressed in the T/B border zone in so-called lymphoid tissue inducer cells. These CD4<sup>+</sup> CD3<sup>-</sup> cells may provide the survival and migration signals for Tfh entry into the GC<sup>249</sup> by upregulation of CXCR5, overcoming the T cell characteristic CCR7 expression, which retains the cell in the cortex. Without sufficient expression of these Tfh over-expressed proteins, migration into the follicle is prevented, evidenced by the failure of CD30 and OX40 knockout mice to form robust GCs<sup>250</sup>.

The origin of the Tfh cell is not clear. Expression in the Tfh of Th1, Th2 and Th17 cytokines at low levels<sup>251</sup> implies conversion of naïve T cells, activated in a polarising context, but then switched to a GC homing, B cell helping phenotype rather than an effector T cell destined for target antigen expressing tissue. Alternatively, the context of antigen presentation to a naïve T cell may initially activate the Tfh program, which then acquires Th1, Th2 or Th17-like features, perhaps in order to bias the GCB cell response appropriately through influencing class switching. The location of this T cell's exposure to antigen also remains unclear. There is evidence for presence of these phenotypically similar cells in the interfollicular T zone, in close association with plasmablasts of extrafollicular primary B cell foci, as well as within the GC<sup>252, 253</sup> hence the cells may arise within or migrate towards their region of eventual function. Polarisation towards the Tfh phenotype seems to depend upon the nature of the initial antigen encounter, perhaps through the strength of TCR signalling: Tfh lineage cells induced in a competitive environment of T cell cognate antigen exposure were found to have the greatest affinity for antigen<sup>254</sup>, while polyclonally activated Tfh cells have a more restricted TCR repertoire compared to other T cell subsets effectors activated similarly. In addition, the strength of TCR signalling was directly proportional to the amount of Tfh-characterising cytokine, IL21 production. A co-stimulatory environment of antigen exposure is particularly important to avoid autoreactivity. Pathogen associated molecular patterns (PAMPs) are recognised by APCs, through toll like receptors (TLRs) and the like, leading to upregulation of CD28's agonist ligand CD80/86 (B7). This, along with MHC class II upregulation and hence more potent antigen presentation, leads to induction of CXCR5 and OX40 expression in the associated Tfh cell<sup>255</sup>, a mechanism essential to prevent the disastrous potential of an auto-reactive Tfh cell being permitted entry to a GC and providing help to auto-reactive B cell clones.

### 1.6.6.2 Tfh cell can be defined by BCL6 and C-MAF expression

Expression of the Tfh phenotypic programme, as with the other well-defined T helper subsets, requires coordination through TFs. The unique combination of BCL-6 and C-MAF expression is a candidate for this function. Over-expression of C-MAF is found in Tfh and is a dose-dependent enhancer of IL21<sup>245</sup>. Expression of C-MAF is impaired in ICOS null mice. Originally identified in B-cell lymphoma<sup>256</sup> BCL-6 is a sequence specific transcriptional repressor gene<sup>257</sup> expressed in GCB cells<sup>258</sup> enabling proliferation, affinity maturation, class switching and maturation to plasma cells<sup>259, 260</sup>. In T cells BCL-6 over-expression leads to CXCR5, PD1, ICOS and IL21R upregulation with CCR7 down-regulation, while T cell-specific knockout prevents GC formation as well as maturation into the full Tfh phenotype<sup>251, 261</sup>. Expression reciprocally inactivates expression of T-BET<sup>261, 262</sup> and GATA3<sup>263</sup>, preventing classical Th1/Th2 differentiation, and down-regulates the expression of their characteristic cytokines. In human tonsil-derived Tfh cells<sup>261, 262</sup> BCL-6 binds the promoters of T-BET and ROR- $\gamma$ t, implying suppression of Th1, Th2 and Th17 differentiation respectively. The mechanism of reprogramming the T cell phenotype may be through suppression of normal T cell microRNA signatures<sup>262, 264</sup>. Expression of BCL-6 may be induced through *in vitro* stimulation of naive T cells with supplementary IL21 and IL6<sup>246</sup>, although the physiological correlate of this in the initial activation context *in vivo* has yet to be confirmed.

### 1.6.6.3 Cell surface mechanisms of Tfh cell function

One mechanism by which the activated Tfh cell is able to enter the GC is through CD28-mediated ICOS expression. CD28-independent GC formation in response to antigen does not occur in CD28 knock-out mice<sup>255</sup>. However, if ICOS is aberrantly up-regulated (as is seen in the sanroque mouse strain with a Roquin gene point mutation leading to multisystemic autoimmunity) GCs are able to form without CD28 costimulation<sup>265</sup>. This was demonstrated in the *Roquin*<sup>san/san</sup> *Cd28*<sup>-/-</sup> mouse model, and could be blocked by genetic ablation of ICOS ligand signalling: the *Roquin*<sup>san/san</sup> *Cd28*<sup>-/-</sup> *Icos-L*<sup>-/-</sup> mouse. B cell specific ICOS-L knockout (via CD19-cre ICOS-L conditional flox allele-carrying mice) impaired GC formation but did not abrogate it, suggesting that this essential pathway for Tfh function may also be stimulated by non-B accessory cells<sup>246</sup>. Additionally, modulation of TCR signalling strength may occur through

SLAM/SAP signalling. Deficiencies in this pathway lead to reduced participation of the T cell in GC formation<sup>266, 267</sup>. SAP modulates TCR signalling strength through phosphorylation of proteins downstream of the receptor<sup>268</sup>. Hence the context of antigen encounter, with appropriate SLAM/SAP interactions with the antigen presenting cell, may induce Tfh polarisation and provide another regulator against autoimmunity by preventing further differentiation of a T cell encountering antigen outside the strict context of inflammatory stimulated APC or even cognate B cell in the T/B border. SLAM/SAP interactions appear essential for 'follicular' Tfh cell differentiation and function<sup>269</sup>, however knock-out models do show evidence of extra-follicular B cell proliferation and plasmablast interactions with T cells phenotypically similar to intrafollicular Tfh cells. These 'pre-follicular' Tfh cells over-express ICOS and BCL6, but not CXCR5 and PD1 and are found to interact with plasmablasts. Whether this represents an alternative fate for a naïve T cell in the early stages of Tfh commitment, or an entirely distinct Tfh-like lineage has yet to be determined (reviewed in Fazilleau 2009<sup>270</sup>).

The mechanism by which this T cell, following appropriate activation and polarisation and follicle entry, exerts its supportive function is beginning to be understood. Early expression of CD40-L and ICOS<sup>271, 272</sup> confirms their capacity to confer classic B cell help. IL4 production is likely to be important, since IL4 receptor deficient mice mount poor follicular humoral immunity, and GC CD4+ cells expressing a Tfh phenotype are seen particularly in the context of a parasite challenge<sup>273-275</sup> but this could also imply subtypes of the Tfh phenotype which are capable of skewing the eventual immunoglobulin isotype complement of the helped B cells. Tfh cells, through high FAS-L expression, may play a role in deleting suboptimal affinity or auto-reactive B cell clones. CD95 signalling is essential for this negative selection process, since B cell-specific CD95 knock out results in lymphoproliferation and increased spontaneous GC formation. B cells possessing a receptor most potently binding antigen and hence attracting most T cell support are therefore favoured<sup>130</sup> and the T cell reciprocates with survival signals. Further survival signals continue to emerge: IL21/IL21-R and, paradoxically, PD1/PD1-L, both of which may have functional importance in CHL.

#### 1.6.6.4 IL21: A Professional B cell-helping Cytokine

A relatively recently discovered cytokine, whose receptor was cloned before the ligand determined<sup>276</sup> has proved to be central to T cell / B cell interactions in the GC. IL-21 is an *in vitro* growth factor for B and T lymphocytes<sup>277</sup> acting via Blimp-1 and Bcl-6 upregulation<sup>278</sup>. However, its role *in vivo* seems more specific to maintaining GC reaction, as evidenced by the disease resulting from homozygous IL21 receptor mutation leading to hypogammaglobulinaemia with excess IgE: a failure of ordered class switching and plasma cell maturation, as well as some demonstration of a failure of Tfh cell maturation and GC formation in IL21 deficient mice<sup>246, 279</sup>. Tfh cells and GCB cells possess IL21-receptors (IL21-R), while Tfh cells secrete IL21<sup>278</sup> hence the contribution of this cytokine to GC survival may arise both through induction and autocrine maintenance of the Tfh cell, as well as promoting B cell survival. Further detail of the relative contributions of these pathways, as well as the precise contribution to the GC reaction came from work with chimeric mouse models possessing intact B cell complements, only their T cells being deficient in IL21-R or cytokine synthesis<sup>280</sup>. The IL21<sup>-/-</sup> or IL21-R<sup>-/-</sup> systems demonstrated impairment neither in Tfh cell differentiation nor initial GC establishment. However GC function was defective: plasma cells slower to form, reduced somatic hypermutation, reduced GC cell cycling, reduced affinity of eventual antibody production and premature termination of GC while relative contribution of memory cells to the B cell compartment was increased. The chimeric systems recapitulated these findings only when T cell synthesis of IL21 was impaired: T-cell specific loss of IL21-R led to only slight impairment in measures of GC function.

Hence IL21 activity seems to be mediated predominantly through T cell secretion enabling B cell survival, proliferation, hypermutation and selection via the B cell IL21-R. Mature memory B cells still manage to emerge from these systems, but with impaired antigen specificity and evidence of less rounds of proliferation. Clearly IL21 is an integral survival factor for the proliferating, maturing GCB cell. There is also evidence for its involvement in HRS survival. Both IL21 and IL21-R are expressed strongly by CHL cell lines and patient-derived samples, tumour infiltrating T cells express IL21, and IL21-treatment of CHL cell lines leads to activation of STAT5 survival/proliferation pathways: associated with NFκ-B pathway activation<sup>69, 281</sup>.

#### 1.6.6.5 PD1: A B Cell Promoting Role for a 'Suppressive' Molecule?

PD1/PD-L1&2, a classic immunosuppressive or 'exhausted' lymphocyte pathway described above, appears to play a novel role in the GC. Expression of PD1 by the Tfh subset may be fundamental to GCB cell survival. B cells (amongst many other cells) express PD1 as well as PD-L1, and once activated also express PD-L2<sup>282</sup>, the ligand constitutively expressed by accessory cells such as dendritic cells and macrophages<sup>231</sup>. A combination of mouse knock out and bone marrow chimeric models investigating PD1 and PD-L1&2 signalling through expression in both GCB cells and Tfh found an unexpected pro-survival role for this cell in the mouse GC<sup>283</sup>. During primary antigen response an upregulation of PD1, PD-L1 and PD-L2 was found in emerging memory B cells<sup>284</sup> which developed through the course of the GC reaction. Three mutant mice strains were developed, deficient either in PD-L2/PD1 signalling (by PD-L2 knock out), PD-L2 and PD-L1/PD1 signalling (by PD1 knock out), or deficient in PD-L1 and PD-L2 (abrogating all interactions with both PD1 and the structurally similar costimulator CD28). All were able to form normal GCs containing PD1+ T cells as readily as wild type C57BL/6 and early antibody response (defined by IgM and IgG1 titres at day 12), was unimpaired. At three months however, the knock-out mice proved to be deficient in long lived plasma cells.

Hence these signalling pathways appear to be important for a sustained GC reaction capable of generating an adequate complement of long-lived plasma cells. This was confirmed on analysis of antibody titres beyond day 15: PD1 pathway knockout mice were deficient. Analysis of the 'late' GCs (beyond day 12) revealed reduced B cell number and increased apoptosis, but numbers of emerging plasmablasts were equivalent. PD1 pathways were operating to maintain maturing germinal B cell survival during the affinity-maturing phase; 'escaped' plasmablasts no longer required the pathways for survival. Tfh numbers were not reduced: they were increased in number. However they were functionally abnormal: expressing less IL-4 and IL-21 mRNA. Generation of hybrid systems by either inter-organism transfer of lymphocytes, or mixed-bone marrow chimeras generated from lethally irradiated BALB/c recipients, enabling selective deletion of PD1 on either B or T cell only confirmed that the effect was as a result of B cell PD-L1 and PD-L2 interacting with PD1 on Tfh cells rather with PD1 on other B cells. Both signalling pathways (PD-L1&2) appeared to be important, with an additive role of loss of both pathways. This data highlights the complexity of

the PD1 system, a possible pro-survival role, and a T-to-B cell (PD1 to PD-L1/2) signal direction and identifies a further candidate cell contact mediated mechanism of T cell conferred B cell help.

### **1.6.7 Conclusions: Defining a T helper cell subset**

Defining a T cell merely by its complement of expressed genes and proteins, rather than directly observing an effector function will always be an oversimplification, and even confirming specific effector function artificially implies a stability of phenotype that may be influenced by the system in which it is being studied as well as by the inherent plasticity of a cell to enter another functional state. Phenotype stability seems to be conferred by increasing numbers of generations of cell divisions following antigen encounter and activation<sup>285, 286</sup> with chromatin modelling and epigenetic changes supporting this concept of progressive generational ‘imprinting’ of a phenotype<sup>287</sup>. Intracellular signalling pathways and TFs interact, mutually suppress or stimulate and are modulated by microenvironmental signals (chemokines, cytokines, growth factors and cell-cell interactions) with complex intracellular circuitry which ‘settle’ into a state of effector function (reviewed in Murphy & Stockinger 2010)<sup>288</sup>. Hence, while subsets may be defined by ‘master’ TFs which are mutually inhibitory and self promoting, (e.g. the T-BET Th1 vs GATA-3 Th2 paradigm) associated with well defined intracellular signalling events (STAT1 in Th1, STAT4/6 in Th2, STAT3 in Th17) there remains no gold standard of determination of a cell’s *in vivo* contribution. Measurable effector function (IL4 production in Th2, IFN- $\gamma$  production in Th1, effector T cell suppression in Treg) remains the most robust definition, with the caveats of plasticity and *in vitro* changes always present.

## **1.7 Current understanding of CD4+ T cells in the CHL microenvironment**

### **1.7.1 Evidence for a TH2-dominated infiltrate**

Burgeoning understanding of B cell/T cell cooperation led investigators to propose that the T cell infiltrate in CHL would likely represent a Th2 biased response. Evidence for this is largely based on one 1989 study in which Poppema’s group attempted to characterise the CHL-infiltrating T cells immunohistochemically<sup>47</sup>. They show that the majority of tumour-infiltrating cells are CD45RO+, CD45RA- and CD45RBlo. Understanding of CD45 isotypes at this stage was limited: the function of this surface protein remains fairly elusive even today, but apparently discriminates activated from

naive or memory T cells, and proliferative versus secretory/effector T cells (reviewed in Penninger 2001<sup>289</sup>). Poppema's study was based on only 10 cases of CHL and yet remains the much-cited basis of the assertion that the infiltrate in CHL is predominantly Th2. Drawing a functional conclusion based on a very limited panel of surface markers is erroneous, particularly in such a small and potentially non-representative sample of patients. Attributing Th2-like activity to CD4<sup>+</sup> CD45RO<sup>+</sup> CD45RA<sup>-</sup> CD45RB-low cells was itself based on a relatively primitive study by Morimoto<sup>290</sup> predating the seminal functional work of Mosmann and Coffmann's group<sup>149</sup>. Morimoto's work found that FACS-enriched human peripheral blood-derived CD45RA<sup>-</sup> cells were able to stimulate IgG production from autologous PWM (pokeweed mitogen)-stimulated B cells (hence termed T helper/inducer) whereas CD45RA<sup>+</sup> cells suppressed IgG production (termed T suppressor/inducer). Based on current understanding of CD45 isotypes, peripheral blood derived CD45RA<sup>+</sup> T cells would be enriched for an antigen naive or central/memory population while CD45RA<sup>-</sup> would contain more antigen experienced effector or effector/memory populations: clearly differing in their B cell helping capacity and in no way conferring a uniquely Th2 phenotype to the CD45RA<sup>neg</sup> cells.

More convincing functional work, favouring Poppema's group's definition of Th2 cells is available, but derived from a mouse model. In *Leishmania* exposed BALB/C mouse T cells, the CD45RB<sup>hi</sup> population secretes significant levels of IFN- $\gamma$  and little IL4 (hence perhaps Th1 enriched) while the CD45RB<sup>lo</sup> population is enriched for cells secreting significant IL4 and little IFN- $\gamma$  (hence perhaps Th2) on *in vitro* stimulation with *Leishmania* antigen and irradiated antigen-presenting cells (APCs)<sup>291</sup>. However, there was also significant IL10 secreting capacity in the CD45RB<sup>lo</sup> cells: a cytokine now attributed to Tregs rather than Th2. Congenic lymphocyte transfer experiments into functional T cell deficient mice (C.B-17scid) themselves incapable of eradicating *Leishmania*, led to restoration of an inflammatory response only on transfer of the CD45RB<sup>hi</sup> population, not on transfer of the CD45RB<sup>lo</sup> population. This experiment can only be used to define CD45RB<sup>hi</sup> as Th1 and CD45RB<sup>lo</sup> as Th2 in the BALB/c mouse model. An alternative explanation could be that while the BALB/c mouse is capable of mounting both Th1 and Th2 type responses it is already genetically predisposed (without *ex vivo* lymphocyte manipulation) to a Th2-dominated reaction<sup>157</sup>. Hence the CD45RB<sup>lo</sup>, effector and effector/memory subset may be



enriched for Th2 committed effector cells capable of reciprocally suppressing any potential Th1 response, while the CD45RBhi antigen naive subset would still have the capacity, if manipulated *ex vivo*, to produce a Th1-type response: CD45 isotype does not define polarisation, but rather capacity to be polarised. Hence the conclusion to be drawn from Poppema's study is that the majority of the T cells in the CHL microenvironment are antigen experienced, or activated T cells. No further functional sub-classification can be inferred.

Further immunohistological exploration of the T cell microenvironment has been carried out using expression of the 'master' transcription factors (TFs) for Th1 and Th2 to define subset representation<sup>46</sup>. Even assuming preserved expression with tissue fixation and staining procedures, this is another very small and potentially unrepresentative study: 16 cases of CHL showed considerable variability of expression of each factor, with nothing to support the hypothesis that the microenvironment was dominated by a Th2 response. GATA3 was expressed in <25% of all infiltrating cells, with the Th2-associated TF c-MAF weakly expressed in a similar proportion of cells. T-BET conversely was strongly expressed in over 50% of cells in more than half of cases. Little of functional significance can be concluded from this study except that these TFs are heterogeneously expressed from case to case, and certainly there is nothing to corroborate the assumption that the microenvironment is dominated by Th2 cells. NLPHL, not the subject of this discussion, conversely showed substantial expression of GATA3 and c-MAF in the microenvironment, with little T-BET expression, and more homogeneity between cases, further discriminating this as a quite distinct pathological entity. A further weakness of this study was the failure to correlate the Th1/Th2 TFs with EBV staining in the HRS. Substantial evidence exists that the immune infiltrate in EBV positive CHL is distinct to that in its EBV negative counterpart<sup>292</sup>, implying an ongoing active, if ineffective anti-EBV cytotoxic and perhaps Th1 dominated response, which might explain some of the heterogeneity of T-BET expression in this study.

### **1.7.2 Evidence for an anergic, suppressive CD4+ T cell infiltrate**

Evidence for antigen experience and hence activation status of T cells in the CHL microenvironment was confirmed in early IHC work showing expression of CD38, CD69, HLA-class II and CD28: co-stimulatory and homing molecules essential for effector function (Poppema 1995; unpublished observation; personal communication).

However, some expected activation factors are not expressed, and the T cells are clearly dysfunctional: failing to eradicate the tumour. CD26 (T<sub>H</sub>-1) is one such molecule remaining unexpressed by these otherwise 'activated' microenvironment T cells: a molecule expressed by normal activated T cells<sup>293, 294</sup> now understood to be an adenosine deaminase-anchoring protein involved, in cooperation with CD45RO, in mediating effective TCR signalling<sup>295</sup> perhaps more important in Th1-type responses<sup>296</sup>. This finding has led some to conclude that the T cell infiltrate is anergic, or regulatory in nature<sup>114</sup>. Isolated CD26- CHL-derived T cells were shown to have up-regulated genes typically associated with a regulatory phenotype – such as CTLA4 or CCR4, and failed on stimulation to up-regulate genes expected of an activated effector cell, such as IFN- $\gamma$ , IL2, IL4 and T-BET. However the control for these experiments (equivalent CD26- cells derived from tonsil) merely demonstrated that the phenotype of cells defined by absent CD26 was different between tonsil and HL-infiltrated lymph node, not that CD26 negativity conferred an anergic phenotype. Certainly no functional demonstration of suppressor activity was demonstrated in these cells.

NLPHL T cells show striking expression of CD57, a marker associated with clonal exhaustion: failure to respond to mitogenic stimuli despite preserved secretory capacity, with truncated telomeres, increased apoptosis susceptibility and down-regulation of the effector T cell markers CCR7 and CD28<sup>297</sup>. However this senescence marker is not seen in CHL<sup>46, 298</sup>. Anergy may well be a feature of many of the infiltrating T cells in CHL, and is evidenced by a failure of the infiltrate to eradicate or control tumour growth. However robust confirmation of this is lacking in the literature.

A functional attempt to demonstrate the anergic and suppressive nature of the lymphoid cell infiltrate was performed by Marshall's group in 2004<sup>299</sup>. They found that tumour infiltrating lymphocytes (TILs) failed to proliferate or secrete IFN- $\gamma$  or IL4 in response to mitogen, and suppressed proliferation of autologous lymphocytes in an IL-10 dependent manner (blocked by anti-IL10 antibody). The use of <sup>3</sup>H-thymidine in their suppression assay (hence failing to account for the comparative hypoproliferation of an anergic, but not frankly suppressive population of TILs), the use of unpurified node-derived cells rather than purified T cells (obtained by simple mechanical dissociation of lymph nodes) and inclusion of two 'control' nodes which

themselves containing malignant cells (breast and anaplastic lymphoma), along with a failure to examine for the more Treg-associated FOXP<sub>3</sub> expression (instead using CTLA<sub>4</sub> and CD25 as markers of Tregs - both up-regulated fairly non-selectively by activated T cells<sup>300, 301</sup>) limits the interpretation of these results and certainly does not convincingly demonstrate that the suppressive component of the tumour-derived cell preparation arose from the T cells. Regulatory T cells may well have a role to play in disease biology as evidenced by FOXP<sub>3</sub> expression in the microenvironment: discussed further below and in my own data. However there is little robust functional data of suppression in the CHL microenvironment.

## **1.8 Challenges in studying the function of the microenvironment in CHL**

### **1.8.1 Functional Studies**

To study the interaction between T cells and HRS usefully, in as robust an experimental way as that in which physiological B/T cell interactions have been studied, a representative model must be developed from which observations can be made and manipulations applied. The further such a model is from the *in vivo* pathophysiological state, the less valid any conclusions will be. CHL presents particular challenges in this respect.

### **1.8.2 In vitro culture systems**

Continuous cell lines are available, derived from patients with CHL, which can be maintained cheaply and simply in culture, and applied to standard *in vitro* assays. An extensive literature exists characterizing the most well recognized CHL derived cell lines, from gene expression and proteomics to pharmacological susceptibility<sup>302-315</sup>. The overwhelming disadvantage of continuous cell line use is the biological distance from the tumour of origin. Most patient-derived cancer cells will not reproduce *in vitro* for extended periods of time. This is particularly true of CHL, for which a continuous cell line was not established until 1980<sup>316</sup> compared to the first human tumour cell line established in 1951 (HeLa, by Gey<sup>317</sup>) and made more difficult by the rarity of the malignant cell compared to non-tumour infiltrate. The cells which sustain any long-term and continuous cell culture (the progenitor or stem cells) are likely a rare subpopulation of the malignant clone, with the bulk of the tumour comprised of terminally differentiated cells without the capacity to further reproduce. In addition, maintenance even of this progenitor cell will likely require interaction with the tumour

microenvironment: immune or stromal. In other haematological malignancies these problems are overcome by selecting for putative progenitor/stem populations using cell surface markers, enabling purification using immunological techniques (e.g. FACS or magnetic beads), and by developing coculture systems including supportive cells derived from a comparable niche to the cancer cell: such as autologous bone marrow-derived stroma or allogeneic continuous cell line equivalents. These confer the support required for growth without requiring up-front knowledge of the molecular basis for it. Once the molecular nature of support has been elucidated experimentally then supportive cells may be replaced by soluble or immobilized factors (as shown for B/T cell model systems described above), either plate-bound or (perhaps more physiologically) cell-sized bead-bound as has been achieved for antigen-presenting cell-free expansion of T cells using anti-CD3 and anti-CD28 antibodies<sup>318</sup>. However there will always be unknown *in vivo* factors that are absent from an *in vitro* culture system.

In CHL, while the terminally differentiated malignant cell is clearly identifiable histologically (the huge, multinucleate HRS) and hence fit for micro-dissection from fixed or frozen tissue for further study<sup>21</sup> and has a fairly unique signature of surface proteins (aberrant myeloid CD15+ and activated lymphoid TNFRSF member CD30+ in the absence of other B and T cell markers) enabling flow sorting of HRS<sup>319</sup>, it is well established that these cells have minimal proliferative capacity<sup>320</sup> to enable *in vitro* culture. The precursor cell remains a hypothetical concept which likely arises within the GCB cell compartment<sup>21</sup>, but being derived from a relatively mature cell unlike the acute leukaemias, may not express established markers of stem or progenitor cell. Expression of B cell markers has been found in some CHL cell lines which when flow sorted and cultured are capable of recapitulating the entire population with greater efficiency than culture of unsorted cells<sup>321, 322</sup> and with the capacity to persist over several replatings (a stem cell-like property). This, along with limited evidence that B cell marker positive cells with clonal relationship to the malignant cell can be isolated from the peripheral blood of patients lends weight to this argument<sup>322</sup> but remains methodologically flawed<sup>323</sup>. Definitive high-resolution genetic evidence of clonal relatedness, and subculture of these primary cells with generation of terminal HRS has yet to be achieved.

### **1.8.3 In vivo culture systems**

The animal model (usually murine) is an attempt to provide the 'unknown' systemic survival signals as well as a model more closely resembling that of the tumour *in situ*. Two approaches are possible. The first is really no more than using the mouse as a culture dish with accessory tissues: primary patient or continuous cell-line derived malignant cells are engrafted into the mouse. In order to prevent graft rejection the recipient must be profoundly immunocompromised (non-obese diabetic severe combined immunodeficient (NOD-SCID) or similar<sup>324</sup>) which intrinsically prohibits the study of any interaction of tumour with immune cells. Co-transfer of human immune cells is possible, but T cells in particular will often outcompete tumour cells and rapidly cause GVHD, engrafting in the bone marrow and leading to fatal haematopoietic failure<sup>325, 326</sup> with few conclusions possible regarding their interaction with tumour. Engraftment has relatively recently been achieved using CHL cell lines, showing contiguous lymphoid dissemination and subsequent multi-organ involvement resembling an accelerated form of human CHL<sup>327</sup>, but lacking the microenvironment of an immunocompetent host. In fact, a requirement of reliable engraftment is the use of the NOD/SCID/ $\gamma$ c<sup>null</sup> (NOG) mouse lacking B and T cells and possessing dysfunctional NK cells, macrophages and dendritic cells<sup>328</sup>. While essential in preventing graft destruction by innate immune system, the tumour is consequently devoid of the majority of the characteristic CHL microenvironment. Primary CHL samples tend to engraft poorly, or be rapidly overwhelmed by bystander EBV-immortalised B cell growth, a problem also encountered in early attempts to develop CHL cell lines<sup>329</sup>.

The second type of animal model exploits the technology of inducing targeted genetic lesions which lead to spontaneous (but autologous and hence species-specific) tumour development comparable to human disease, such as the E $\mu$ -myc mouse model of Burkitt lymphoma<sup>330</sup> or the E $\mu$ -TCL1 mouse model of CLL<sup>331</sup> where proteins known to be over-expressed or pathogenic in lymphoid malignancies are artificially up-regulated in murine B cells using the immunoglobulin promoter gene. This can be studied in the mouse of origin or following transfer into a syngeneic mouse lacking the mutation. Hence a malignancy can be observed in the presence of an intact immune system: integral to any study of immune/tumour interaction. However it is limited by the fact that the tumour is non-human derived, an oversimplification of most tumours arising

in man, being initiated by only a single or a few transforming events, and probably far more aggressive: itself a necessary function of finite experimental observation duration. In CHL, while recurrent genetic abnormalities have been observed now that purification of such a rare cell has been achieved to the extent that genetic interrogation can be performed, from the level of fluorescence hybridization-enhanced karyotyping<sup>332</sup> to that of comparative genomic hybridization (CGH)<sup>116, 333</sup> and whole transcriptome sequencing<sup>334</sup>, the highly aberrant multinucleated malignant cell possesses countless candidate mutations only a few of which are recurrent and none alone likely to recapitulate the disease if altered in an otherwise immunologically intact mouse model.

## **1.9 Descriptive and Correlative Studies of the CHL microenvironment**

### **1.9.1 The function / prognosis fallacy**

The importance of the immune infiltrate in defining prognosis and aggressiveness of a malignancy has long been recognized, with benefit apparently conferred by lymphoid cell infiltrate<sup>335</sup> and adverse outcome conferred by macrophage infiltrate<sup>336</sup>. However, prognostic markers have rarely led to a coherent explanation of molecular mechanisms of microenvironment interactions and functional models are lacking. Characterisation of the CHL microenvironment using biomarkers in an attempt to better understand the pathophysiology of the disease, and measuring patient to patient heterogeneity of biomarkers in an attempt to predict outcome are quite different approaches. While finding a favourable prognostic factor may provide some indication as to its importance in disease natural history, this is not robust confirmation of a biological mechanism. For example, correlating a high infiltrate of FOXP3 in the tumour microenvironment with a favourable clinical outcome (as will be shown) may lead to the conclusion that Tregs have a role in suppressing the tumour directly or through interactions with other microenvironment cells. However, even making the assumption that FOXP3 expression is indicative of an increased infiltrate of functional Tregs (rather than representative of transient FOXP3 expression following T cell activation induction of Treg from naïve T cell due to secretion of TGF $\beta$  by the tumour, passive chemotactic attraction of circulating natural Tregs, or a combination of these factors, as described above), there is no direct evidence that these cells are suppressing tumour growth. The presence of malignancy indicates failure of a successful tumour-suppressing immune response and CHL inevitably progresses without treatment.

Hence this 'favourable Treg response' could never have successfully eradicated the tumour. More importantly, anti-CHL therapy (cytotoxic chemotherapy or radiotherapy) eradicates the lymphoid microenvironment as much as the malignant cell itself and hence treatment success is unlikely a direct function of Treg presence. More likely, FOXP<sub>3</sub> expression is a surrogate marker of an intrinsic property of the malignant cell itself (for example increased TGFβ secretion, for which there has been no investigation of association with outcome) or of the host immune response (for example a marker of more robust anti-tumour immunity hence able to clear any residual disease failing to be removed by treatment). Both of these alternative explanations are entirely hypothetical with no evidence basis, however they highlight the limitations of any purely correlative, descriptive observations in drawing functional conclusions.

Despite the obvious logical fallacy of drawing mechanistic conclusions from such data, overzealous explanations of similar data are rife in the literature. Robust conclusions on disease mechanisms can only be drawn from functional experiments. Descriptive data may contribute, or stimulate hypothesis generation for functional work, but are not themselves a test of function. This is not to say that such biomarker data cannot be used in prognostic models or if validated for clinical decision-making; this is quite distinct from understanding the biology of a disease process. Prognostic and descriptive studies of the CHL microenvironment remain relatively primitive and are often crudely interpreted with inappropriate statistical methods and erroneous conclusions. Contradictory results between groups and failure to validate in independent datasets explains why few biomarkers translate into clinical practice. Without prospective studies and standardised methodology and statistical techniques, these studies will remain only hypothesis-generating.

## **1.9.2 Immunohistochemical Profiling of T cells in the CHL Microenvironment**

### **1.9.2.1 CD4+ Subset Markers**

One small study of Th<sub>1</sub>/Th<sub>2</sub> representation in the microenvironment has already been discussed<sup>46</sup>. A variety of other T cell-associated immunohistochemically-assessable markers have been applied in further studies. One used FOXP<sub>3</sub>, T-BET, C-MAF and Granzyme B (GrB) as markers of Treg, Th<sub>1</sub>, Th<sub>2</sub> and activated cytotoxic T cells respectively<sup>337</sup>. Validation of these markers as representative of T cell subsets (rather than expression in tumour or other infiltrating cell) was performed by co-staining a

small number of patient samples: FOXP<sub>3</sub>, C-MAF and GrB were confined to the T cell compartment but the analysis was complicated by T-BET expression in B cells and HRS cells in some cases. 87 CHL cases were examined, scored across entire sections using image analysis software and corrected to represent a 1mm<sup>2</sup> area. It was noted that FOXP<sub>3</sub> and C-MAF were represented in 'high numbers' and GrB and T-BET were 'rare' (contrast Atayar 2007 above<sup>46</sup>), this time consistent with the accepted model of a microenvironment being rich in Th<sub>2</sub>/suppressor phenotype T cells. However, variability of expression was considerable from patient to patient: range of FOXP<sub>3</sub> expression 40-1600 per mm<sup>2</sup>, C-MAF 100-1600: wide standard deviations. Mean values (the focus of discussion in this study) are a meaningless descriptor in the context of such wide variability, certainly when the aim of a study is to relate heterogeneity of outcome with heterogeneity of expression. Kaplan-Meier assessments of the data were performed which demonstrated an impact of GrB expression and C-MAF on survival outcomes, as well as a score based on C-MAF:FOXP<sub>3</sub> ratio. However different survival outcomes measures were used for each score, a method of 'optimal cut-point' between 'adverse' and 'good' outcome groups was applied, and an artificially derived measure (C-MAF/FOXP<sub>3</sub> ratio) used. All of this post-hoc analysis weakens any interpretation.

Optimal or multiple cut-point analysis is a commonly encountered pitfall of statistical analysis of novel biomarkers where normal ranges are unknown<sup>338</sup>. The availability of software that will determine by multiple comparisons the point at which statistically significant differences between groups is found (e.g. Xtile<sup>339</sup>) makes this statistical error more accessible. The consequence is a failure of many apparently significant biomarkers to be replicated by other investigators, and more important to find their way into clinical practice. Predetermination of cut-points or validation in independent datasets is the only robust method of confirming such findings: this is rarely done in the literature. Another significant problem lies in the method of data interpretation and generation of these raw data. Scoring by histopathologists ('manual scoring') was the original methodology, still used currently, tried and tested for decades, but long known to be hindered by interobserver (and day to day intraobserver) variability. In scoring large numbers of cells (a standard high powered field (HPF) of densely packed lymphoid cells comprises over 2,000 cells in a standard FFPE section) human error will invariably occur, and the limitations of human attention and perception will clearly render scoring large numbers of cases impossible. Even the introduction of



sophisticated image scanning and analysis software ('automated scoring') carries the limitation of interobserver variability where an initial training step is required to program the software to recognise 'positive' and 'negative' or varying degrees of intensity of staining. These problems only address the limitations of 'reading' the data: variability can occur at any point in data generation: acquisition of biopsy, quality of initial tissue preservation technique, selection of tissue area to analyse, staining technique and optimisation, and choice of image digitisation and analysis package.

The paper does confirm the wide variability of C-MAF and FOXP<sub>3</sub> expression and suggests sparse representation of T-BET (contrary to Atayar 2007<sup>46</sup>) and GrB. Its shortcomings are reflected in much of this field's literature.

#### 1.9.2.2 Cytotoxic T cell markers

A number of groups have looked at markers of the cell-mediated immune response to CHL and how they might be represented in the microenvironment. CD8 has not proved a prognostic marker, although the CD8<sup>+</sup> component of the CHL microenvironment is considered to be sizably less than its CD4<sup>+</sup> counterpart. Hence other markers of CD8 activation and activity have been investigated. GrB is required for some of the cytotoxic activity of T lymphocytes<sup>340</sup> while TIA-1 is a protein expressed in a subset of cytotoxic T cells, which may form part of their cytolytic function<sup>341</sup>. The earliest study in CHL, by Oudejans and colleagues (1997)<sup>342</sup> looked at CD8, GrB and TIA-1 in the microenvironment of CHL (n=80) and found that an infiltrate of GrB<sup>+</sup> cells greater than 15% of total lymphoid cells (determined manually and morphologically rather than by dual marker staining) was associated with adverse prognosis. However this was not significant on multivariate analysis, and the univariate analysis was performed using optimal cut-point analysis with its attendant statistical error. An association between GrB expression and EBV status was found. No survival associations were found with TIA1 or CD8 expression. Schreck (2009)<sup>337</sup>, as discussed above, confirmed this finding as well as the rarity of these cells also using an optimal cut-point technique but with different cut-point values. Alvaro (2005)<sup>343</sup> examined GrB and TIA-1 in a larger retrospective of 257 patients using TMA, found that high expression of TIA-1 was an adverse features, but found no impact of GrB. Cut-points were validly defined as quartiles with no 'optimal cut-point' strategy. Kelley (2007)<sup>344</sup> stained for GrB and FOXP<sub>3</sub> in a TMA comprising 98 patients with CHL,

counting 5 HPF manually and showed no impact on GrB expression unless combined with FOXP<sub>3</sub> as a ratio, where it improved the FOXP<sub>3</sub> only model (which had been significant for FFTF and OS). Cut-points were derived using an optimal cut-point strategy (recursive partitioning) hence limiting validity particular with a post-hoc derived score such as FOXP<sub>3</sub>:GrB ratio. Additionally, the absolute numbers of cells expressed per HPF were difficult to reconcile with other studies (possibly implying a different definition of HPF). Montalban (2004)<sup>345</sup> examined a very heterogeneous range of markers in a manually scored TMA, based on previously published IHC and GEP findings and found an association between TIA-1 and EFS (but no other outcome measure) in univariate analysis. The scoring system was oversimplified (as a simple 'positive' versus 'negative') leading to significant data loss (rather than reporting a continuous variable: the main problem of manual versus automated scoring) and no values for case-to-case variability of expression was reported. Canioni (2009)<sup>346</sup> found increased numbers of TIA-1 expressing cells in patients with refractory and early relapsed disease compared to long term responders (n=59) but performed no regression analysis using Kaplan Meier or multivariate which may have revealed confounding factors. Additionally scoring was manual, in limited numbers of fields, and the absolute numbers of cells was extremely small (42 vs 21 cells for the two prognostic groups amongst the thousands of cells in each HPF).

Taken together these studies, although flawed, perhaps show a correlation between increased infiltrate of GrB or TIA-1 and adverse outcome, but methods of scoring, cut-point and endpoint analysis and inconsistent use of multivariate analysis limits these findings and renders conclusions tenuous. It is clear that cytotoxic T cells as defined by these markers of activation represent a very minor component of the microenvironment; indeed any variability in such small numbers of cells may simply represent predominance of other cells. That such a small population is playing any functional part at all seems unlikely, unless these proteins are up and down-regulated throughout the course of the immune response in a manner that cannot be captured by assessment of this fixed non-vital tissue. The validity of these markers as indicators of T cell function is drawn into question by the fact that a significant proportion of the microenvironment is comprised of CD8+ cells, with no explanation as to what role they are playing and why they do not express effector proteins. It remains to be demonstrated whether these cells are suppressed and anergic, or active but ineffective.

### 1.9.2.3 Regulatory T cell markers

A number of TMA based IHC studies have found an association between expression of FOXP<sub>3</sub> and outcome. Studies in solid tumours have predominantly found an association between increased FOXP<sub>3</sub> infiltrate and adverse outcome<sup>347</sup> suggesting that their presence reflects an impaired immune response to tumour<sup>348, 349</sup>, and there is extensive mouse-model evidence that Treg depletion can lead to tumour regression (reviewed in Zou 2006<sup>350</sup>). However, in follicular lymphoma the converse has been found with increased infiltrate being associated with improved outcome<sup>351-353</sup> and as discussed this has also been shown in CHL<sup>343</sup>. This counterintuitive finding highlights the limitations of drawing mechanistic conclusions from descriptive data: suppression by large numbers of Tregs may be expected to reduce the antitumour immunity. However, interaction of FOXP<sub>3</sub> expression with treatment and primary tumour cell biology is likely far more complex. Evidence that FOXP<sub>3</sub> expression confers a superior prognosis in lymphoid malignancy has accumulated, with Kelley (2007)<sup>344</sup> finding an interaction with GrB in defining a favourable subgroup, IHC validation of GEP work by Chetaille 2009 (and see GEP discussion below)<sup>292</sup> confirming a beneficial impact of high FOXP<sub>3</sub> expression, although Schreck (2009)<sup>337</sup> failed to find an association. The considerable limitations of these studies have already been discussed. The most comprehensive IHC investigation of FOXP<sub>3</sub> in lymphoid malignancy was by Tzankov (2008)<sup>354</sup>, which including the largest CHL cohort (n=249) assessed with a manually scored TMA. Increased FOXP<sub>3</sub> infiltrate was associated with favourable prognosis: statistically significant using Kaplan-Meier survival analysis but applying a flawed optimal cut-point method (ROC curve analysis) and applying different cut-points to different outcome measures (statistically invalid). More of concern, numbers of FOXP<sub>3</sub><sup>+</sup> cells reported did not tally with our own experience, nor that in the wider literature, using '27.5' cells per mm<sup>2</sup> as a cut-point. Without a standard transparently reported measure of cell density, comparing data is difficult. To illustrate: a 1mm<sup>2</sup> core of a cell density suitable for immune microenvironment analysis contains 20-30,000 lymphoid sized cells, and between a few hundred and several thousand of these express FOXP<sub>3</sub> when counted using automated image analysis software.

### **1.9.3 Gene Expression Profiling of the CHL Microenvironment**

Gene expression profiling (GEP) has provided one means by which candidate markers for prognosis can be generated and validated in alternative datasets or using different techniques, for example IHC on 'discovered' proteins. Techniques in nucleic acid extraction have improved such that even FFPE tissue can be used to generate material of sufficient quality for analysis<sup>355</sup> with the potential to develop high throughput simple and relatively inexpensive gene expression techniques applicable to the clinic<sup>356</sup>.

GEP in lymphoma first gained prominence when it was shown that prognostic subgroups of DLBCL could be discriminated using the technique<sup>357</sup>. The importance of the microenvironment's gene signature (rather than the tumour cell itself) in contributing to prognosis was demonstrated in a later study which selected the most discriminatory genes for both poor and good prognosis in a large cohort of patients with follicular lymphoma (n=191) and found that these were expressed in a FACS sorted CD19- component, not in the CD19+, malignant cell enriched component<sup>358</sup>. The 'good prognosis' gene set was enriched for genes involved in T cell and some macrophage functional pathways, while the 'poor prognosis' gene set was enriched for pathways involved in dendritic cell and other macrophage functions. These were defined immune responses 1 and 2 and formed the basis of countless subsequent studies of the relative contribution of T cell and macrophage to tumour survival in lymphoma. While a substantial body of functional work strongly supports the concept of a tumour associated macrophage (TAM) conferring immunosuppressive and supportive roles in tumour progression (reviewed in Condeelis & Pollard 2006<sup>44</sup>), many conclusions derived from GEP of primary tissue: a merely descriptive and correlative technique, lack any robust corroborative functional basis. Three major groups have published on gene expression profiles in the CHL microenvironment: French, Spanish and Canadian.

#### **1.9.3.1 The French Group**

The first French investigation<sup>359</sup> was later expanded to involve GELA (Group d'Etude des Lymphomes de l'Adulte)<sup>292</sup>. The small initial study applied an in-house 1045 cDNA clone array to material derived from 21 patients with CHL. Using hierarchical cluster analysis<sup>360</sup>, CHL cases were found to segregate into two unsupervised clusters (n=6 and

n=15) in which the smaller cluster exclusively contained favourable outcome patients (however note the small numbers and the fact that 75% of the entire cohort had a favourable outcome). A second hierarchical analysis was then applied using only those genes that appeared to most successfully delineate these two unsupervised clusters in the first analysis, and three clusters were then discriminated. The poor outcome group remained distinct. This GEP (relative to the median expression across all samples) found 40 up-regulated genes and 19 down-regulated genes defining the favourable outcome group while the unfavourable group was distinguished by relative upregulation of the favourable group's down-regulated genes, and down-regulation of a further distinct cluster of 15 genes. Clear limitations of this study are low genome-representation of the microarray, very small patient numbers and failure to use gene set enrichment analysis (GSEA). GSEA in itself is a controversial methodology: a *post-hoc* bioinformatics method of integrating large GEP datasets into interrelated functional pathways, potentially conferring artificial biological plausibility to what are independently measured gene expression events, especially artificial when applied to the very heterogeneous mix of cells present in the immune microenvironment. The conclusion drawn from survival analysis in this study: that the GEP was superior to conventional prognostic scores in predicting outcome, was erroneous since it did not apply the hypothesis generating set of genes to an independent patient cohort. The gene set was also extremely restricted and hence unrepresentative: only around 1,000 of the 40-60,000 genes thought to be expressed in the human genome.

A similar method was applied to an expand pan-GELA cohort (n=63)<sup>292</sup> this time using a more comprehensive commercial platform (Affymatrix U133 A2.0) representing over 18,000 transcripts. Unsupervised hierarchical analysis successfully discriminated most (but not all) CHL cases from control samples of reactive lymph nodes and TCR/DLBCL (T cell-rich diffuse large B cell lymphoma, a histologically similar but clinically distinct disease) generating two clusters of patients in which unfavourable outcome patients were relatively overrepresented in one cluster. Supervised clustering (a statistically less robust *post-hoc* methodology) produced models with reasonable predictive value of EBV positivity and CHL histological subtype (although clearly the domination of EBV positivity in the mixed cellularity histological subtype known to have an overrepresentation of EBV positive cases will account for much of this difference) as well as a signature discriminating adverse from favourable outcomes. A number of

these genes were validated in an independent set of patients (n=146) by IHC read by histopathologists rather than automated image analysis. However, statistical robustness is again limited by the use of optimal cut-point analysis, and a categorizing, rather than continuous method of scoring (often the only feasible method when scoring manually). IHC was also performed on previously described prognostic markers including FOXP<sub>3</sub>, TIA<sub>1</sub> and CD20 all of which had failed to emerge as differentially expressed from the GEP data. Much of the IHC ‘validation’ was based on surrogate markers of biological pathways enriched for quite different genes (for example CD20, not differentially expressed in the GEP, justified on the basis of overrepresentation of other ‘B cell pathway genes’ such as BCL11A and CCL21) hence possibly not validation at all. FOXP<sub>3</sub> retained significance only in the EFS analysis, not in OS, while TIA<sub>1</sub> was significant for EFS and OS but not in the multivariate analysis (MVA), which incorporated numerous IHC markers and clinical features. The only microenvironment marker retaining significance on MVA was CD20 in the OS, but not EFS analysis. MVA using so many independent variables may be inappropriate in a cohort of this size, reducing the applicability of its findings<sup>361</sup>.

### 1.9.3.2 The Spanish Group

The Spanish Hodgkin Lymphoma Study Group applied this technique to its extensive tissue bank with a view to finding markers of poor risk disease<sup>362</sup>. An initial test set of 30 patients was determined, 50% with poor outcome (defined as first line treatment-refractory disease or relapse within 12 months of initial therapy) and 50% with good outcome. GEP was performed on this group using a commercial microarray chip representing over 9000 malignancy-associated genes (OncoChip v2) with a view to identifying candidate genes differentially expressed between the two groups. Unsupervised clustering failed to discriminate the groups, whereas a supervised approach dividing them by known good versus poor outcome revealed 145 differentially expressed genes, which clustered into 4 apparent signatures. The investigators chose to label these clusters based on over-representation of genes involved in various biological pathways: ‘microenvironment’ (T cell, macrophage, plasmacytoid dendritic cell), ‘adhesion/remodelling’ (fibroblast, matrix, antigen presenting cell), ‘apoptosis regulation’ and ‘cell-cycle regulatory’. This is a potentially misleading and artificial interpretation: *post-hoc* labelling of gene clusters based on a few convenient coincidences of expression, using labels as non-specific and unhelpful

as 'apoptosis/remodelling'. Why should extracellular matrix and APC be grouped together, while the antigen-presenting 'plasmacytoid dendritic cell' is segregated into a separate group with T cells and macrophages (as is done in this paper)? The 'adhesion/remodelling' signature was over-expressed in the favourable outcome group, while the other 3 signatures were over-expressed in the unfavourable group. Eight markers were selected for IHC on an independent series of 235 patients and analysed using tissue microarray and automated image analysis. Levels of expression were divided into quartiles and the patient cohort split in two, between the 'top' quartile and the rest. Using disease specific survival (DSS) as an endpoint a significant difference emerged between the groups using Kaplan-Meier and log-rank statistical tests. Cut-points were valid since quartiles, rather than optimal cut-points were used.

As already addressed, the major concern in GEP of material comprised of multiple tissue types: malignant cell, inflammatory cell, vasculature and stroma, is that interpretation will be rendered impossible without knowledge of the cell of origin, and that substantial data will be lost arising from biologically important cells that only comprise only a small amount of the tissue and hence contribute relatively little nucleic acid despite fundamental functional importance. The Spanish Group began to address this by categorising the candidate gene set generated in their first study into 'tumour-derived' and 'microenvironment-derived'<sup>363</sup>. They applied the same 9,000 gene chip as in their earlier study<sup>362</sup> to 5 CHL-derived cell lines and applied hierarchical clustering to examine differential gene expression between cell line (entirely tumour derived) and primary material (predominantly microenvironment). Unsupervised clustering failed to discriminate the groups, but supervised clustering identified cell-line over-expression in around half of differentially expressed genes, and primary sample over-expressed in the other half of differentially expressed genes. The limitations of this technique lie in using the cell line as representative of tumour cell since continuous cell lines are biologically extremely different to primary tumour cells, which are still embedded in their microenvironment. However, some validation of this technique came through IHC of a small subset of gene products in which microenvironment or tumour cell-specific expression was confirmed.

Another limitation is the use of 'over-expression' as the only discriminatory marker without normal control tissue as a comparator. If a gene is down-regulated pathologically, then apparent 'up-regulation' may simply represent expression at physiological levels. However, for the purposes of developing a set of prognostic markers (the primary aim of the paper) it is a reasonable, pragmatic approach.

With so many differentially expressed genes, and with the aim of producing a shortlist capable of being tested on a large scale for prognostic validation and potential clinical application, a number of statistical methods were applied which by their nature make very large assumptions about the data. Gene set enrichment analysis (GSEA) was performed on the 'poor prognosis' genes in each of the tumour and microenvironment gene lists, to identify genes clustering into purported biological pathways. This would have led to loss of data on 'isolated' genes that did not cluster into pathways on the GSEA database, but were nonetheless differentially expressed, as well as important 'good prognosis' genes, and assumes the validity of the method of tumour/microenvironment discrimination. The finding that 'tumour' pathways identified included 'drug resistance', 'cell cycling', 'MAP-kinase' and 'mitochondrial signalling' and that 'microenvironment' pathway included T cell subsets and macrophages is based on considerable *post-hoc* assumptions. Clearly other functional pathways will have been represented which are not reported in the paper since the microenvironment is full of cells actively dividing and intracellularly signalling (hence expressing genes in what might be considered the 'tumour' pathways) without themselves being malignant. From this short list, the investigators reduced the candidate gene list further to include only those genes best discriminating outcome (reasonable for a study aiming to predict outcome, and with a separate validation set available) and those with the greatest 'biological relevance' (another artificial criteria given the problems of GEP in heterogeneous cell populations). The final list contained 56 genes: 46 'tumour' and 10 'microenvironment'-specific. RT-PCR was applied to a validation set of 52 patients using a TaqMan low-density array (TLDA) to develop an 'integrative risk score' based on expression of all genes. The unfavourable group showed a significantly increased score, as expected by the methodology of gene selection. To further simplify the model and improve predictive capacity, genes with the best predictive capacity on ROC analysis were selected, giving a final shortlist of 14 genes.



Further enhancement of the score<sup>356</sup> was performed using another independent set of 262 patients, divided themselves into a test set (n=183) and a validation set (n=79) in which a 'modified' shortlist from the previous study (of 30 genes) was assessed by TLDA on the test set, a shortlist of 11 genes with best discrimination ability chosen, and logistic regression of overall expression scores for the various biological pathway gene clusters used to generate a model (the 'molecular risk score': MRS). Cutoffs were again defined using ROC analysis, and the resultant score applied to the validation set. Kaplan-Meier log-rank was significant with the outcome of FFTF. Except for stage IV disease, the MRS proved the only significant factor on a backward stepwise multivariate Cox proportional hazards model including each individual component of the IPSS, with FFTF as the dependent variable. Including both MRS and stage IV disease as criteria for patient stratification generated a cohort of patients of 'extremely poor risk' with median FFTF less than 6 months and 20% five year FFTF.

While an impressive prognostic model, even accounting for the potential limitations of GSEA and the subsequent statistical and biological assumptions in drawing up a shortlist of clinically applicable candidate genes, the model has virtually no capacity to indicate underlying disease mechanisms despite the assertions of the authors in their conclusions in the paper. The inclusion of IRF4 (MUM1) in the final 11 gene model gives one example of limitations: this gene was not picked out through shortlisting, but included due on prior studies showing its significance<sup>364</sup>. Similarly, FOXP3 expression on the level of gene expression did not emerge as important, despite growing IHC evidence.

### 1.9.3.3 The Canadian Group

The largest scale and most genome-representative GEP looking for prognostic factors was performed by a Canadian group<sup>116</sup>. GEP was carried out on 130 fresh frozen (not FFPE) specimens obtained at diagnosis using the GeneChip Human Genome U133 Plus 2.0 array (over 34,000 genes represented) and validated with IHC on an independent cohort of 166 patients. No discrimination of tumour versus microenvironment derived genetic material was attempted. A shortlist of candidate genes was determined following analysis of GEP data using sparse multinomial logistic regression (SMLR) and relative importance determined by cross-validation using a leave-one-out

regression technique. Classification accuracy of adverse versus favourable prognosis was measured using ROC curve analysis. Unsupervised clustering, as with previous studies, failed to identify the poor prognosis group. A shortlist of 271 differentially expressed genes were found in a supervised analysis to discriminate two clusters, and Ingenuity pathway analysis (one commercially available bioinformatics methodology) showed overrepresentation of 'cell-cell signalling', 'macrophage IL12-pathway signalling' and 'apoptosis' in the adverse outcome group, with underrepresentation of CTLA4 and G-protein coupled signalling. Globaltest (another commercial package) identified 'tumour-associated macrophage (TAM)', 'monocyte', 'angiogenesis', 'adipocyte' and 'HRS gene signature' over-expression, and 'GCB cell' signature under-expression. Further selection based on prognostic discriminability between the groups identified 27 genes superior in predictive ability to patient age, a well-documented clinical prognostic classifier, over-expressed in the adverse outcome group.

These genes were incorporated into a risk model. IHC confirmed one of these gene products: MMP11 (expressed in many elements of tumour and microenvironment including HRS, macrophages and endothelium) to be a prognostic marker on Kaplan Meier survival analysis (using manual, categorical scoring by histopathologists on duplicate cores in a TMA in the independent dataset, with cut-point determination method not clear from the paper). As a further validation and potential mechanistic correlate for this finding, staining for CD68 was carried out, which was also of prognostic significance (for DSS, PFS and outcome from secondary therapy). While providing further substantiation to the IHC data on the adverse impact of TAM in the microenvironment, the true mechanism of MMP11 over-expression conferring adverse outcome is not determined by this study: CD68 staining does not provide validation that macrophages' contribution to survival is represented by MMP11 gene over-expression.

#### 1.9.3.4 Conclusions: GEP in the CHL microenvironment

Overall, these studies have demonstrated that adverse risk disease can be discriminated from favourable risk using GEP and a real clinical benefit may indeed result from this work as long as cost effective, simple, reproducible techniques can be developed and prospective, independent dataset validity confirmed.

However the various studies have identified different candidate genes with few, if any commonalities (summarised in Table 1.2) This is unsurprising given the volume of data generated by such studies, different genome coverage in the initial analyses, and the attendant attrition arising from stripping huge datasets down to small numbers of manageable factors. The variety of statistical methods used, *post-hoc* and intrinsically biased gene selection methods based on ‘interesting pathway’ analysis, and variable patient cohorts and cohort size all contribute to these discrepancies. What these studies have not demonstrated, apart from the heterogeneity of the disease and the importance of the microenvironment, is the mechanisms by which this heterogeneity exerts its biological effect.

GEP has also failed to identify key mediators of prognosis that have been determined through IHC (such as FOXP3) highlighting another weakness. Finally, and perhaps most fundamentally, conclusions drawn from this technique which analyses the nucleic acid composition of a heterogeneous mixture of tissue and cell types without any prior purification steps, makes massive assumptions: that mRNA content correlates with functional protein content, and that simple snapshot expression levels relate to the magnitude of a biological response *in vivo* despite vast differences in relative potency and cascading consequences of such proteins.

Sanchez Esperidion			Steidl		Devillard	Chetaille	
2009	2010		2010		2002	2009	
ALDH1A1	HSP90AA1	ALDH1A1	ABAT	MDFIC	CDH5	A2M	LAMA4
AURKA	HSPA4	BCCIP	ACTR3	MID2	COL18A1	ADORA3	LMOD1
BCCIP	HSPA9B	BCL2	ANGPTL4	MINK1	COL18A1	AEBP1	LRP1
BCL2	IFI16	BCL2L1	ANKRD26	MMP11	COL6A1	AGRIN	LRRC32
BCL2L1	ITGA4	BUB3	ANKS1B	MORG1	CRABP1	AK1	MGC14376
BUB1B	LCP1	CASP3	ASCL1	MOSC1	ERHB2	ASGR2	MIER2
BUB3	LYZ	CCNA2	ATXN2L	MUC1	FAT	C10orf56	MKI67
CASP3	MAD2L1	CCNE2	B3GNT3	NCKIPSD	IGFBP4	CAMKK2	MYO10
CCNA2	MADPRE1	CD3D	BAIAP2	NCR1	MFAP2	CD34	NBL1
CCNE2	MAP3K7	CD8B1	C17ORF39	NCRNA00105	MKI67	CDKN1C	NFATC4
CCNH	MAPK6	CDC2	CCDC151	NDE1	MMP2	COL11A1	OLFML3
CD3D	MAPK9	CENPF	CD300C	NMNAT1	MMP3	COL18A1	PCDH12
CD8B1	MAPRE1	DNAJA2	CDYL	NT5C2	PDGFR	COL1A1	PCDHGC3
CDC2	MLH1	FOXP3	CENPO	PDE4D	PLA2G2A	COL4A1	PCDHGC3
CDC6	NBS1	GRB2	CIDEC	PERP	SELP	COL4A1	PCDHGC3
CDK7	NUMA1	GUSB	CLDN7	PERP	SFRP2	COL4A2	RAPGEF2
CDKN2C	RAMP	H2AFX	CLPS	PFDN6	TFAP2A	COL5A1	RASIP1
CENPE	RRM2	HIST1H3D	COL11A2	PIK3CB	TIMP1	COL5A1	TBC1D16
CENPF	RSN	HMBS	COMT	PKP1	TNF	CTDSPL	THBS1
CHEK1	SH2D1A	HMMR	CRCP	POLR2J4		EDNRA	THBS2
CSE1L	STAT1	HSPCA	DCUN1D3	PTRPF		EDNRA	TNS1
CTSL	TOP2Z	IFI16	DGCR8	RC3H2		FN1	TPST1
CYCS	TYMS	IRF4	EARS2	RIPPLY2		GDPD5	VWF
DCK		LYZ	EARS2	RIPPLY2		HRH1	
DNAJA2		MAD2L1	ELMO3	RNF144B		HSPG2	
GRB2		MAPK6	EMID2	RRAD		IDUA	
H1F0		RRM2	ERMAP	SAA1		ITGA7	
H2AFX		RSN	FAM166B	SHBG		ITGB5	
HIST1H3D		SH2D1A	FGFBP2	SHMT1		ITSN1	
HMMR		STAT1	FLJ40125	SLC22A14			
		TOP2A	FUZ	SLC47A1			
		TYMS	GOSR2	SLC4A11			
			GPT2	SLC6A2			
			GTF3C4	SLIT1			
			GTSF1L	SNAP47			
			HLA-DPB2	SNAPC2			
			HSDL1	STAP2			
			HUWE1	UBE3A			
			LOC751071	UTS2R			
			LPHN1	WBP4			
			LRRC14	WHSC2			
			LRRC20	ZMAT4			
			LYPD3	ZNF408			
				ZNF581			

**Table 1.2:** Genes up-regulated in unfavourable outcome CHL using methods applied by French (Devillard<sup>359</sup> and Chetaille<sup>292</sup>), Spanish (Sanchez-Esperidion<sup>356, 363</sup>) and Canadian (Steidl<sup>116</sup>) groups. Genes showing differential expression (up or down-regulation) in other prognostic subgroups are omitted. Key for the Spanish group (Sanchez-Esperidion<sup>356, 363</sup>) demonstrates lack of concordance even within the same group (although a different patient cohort): **black**: unique to the genelist demonstrated in the particular study shown, **blue**: common to both 2009 and 2010 studies, **red**: ‘additional’ genes not found through GEP but included due to pre-existing predominantly IHC data.

### 1.10 Aims and Objectives

Using patient-derived material available from the tissue bank of Barts Cancer Institute, applying immunohistochemistry (IHC) on formalin-fixed paraffin-embedded (FFPE) samples, flow cytometry (FACS) on frozen single cell suspensions (SCS) and *in vitro* cell culture models from fresh and frozen tissue I aimed to determine the key functional molecular markers represented on the CD4<sup>+</sup> T cells in the CHL microenvironment. In determining the molecular markers discriminating CHL-derived CD4<sup>+</sup> T cells from those present in non-malignant reactive and quiescent nodal tissue, along with those of tissue derived from other B cell malignancies, it may be possible to develop strategies to modify the interaction between HRS and CD4<sup>+</sup> T cells. This strategy will be investigated using an *in vitro* culture system derived from primary diagnostic tissue. Further, this approach will be used to investigate the impact of such markers on clinical outcome. The outline of this approach is as follows:

1. Construct a tissue microarray (TMA) of patients with known clinical outcome and adequate follow up.
2. Determine the heterogeneity of immunophenotype in CHL-infiltrating CD4<sup>+</sup> T cells based on normal and malignant B cell interactions and identify prognostic markers with potential for clinical translation by application of IHC and automated image analysis to a large extent of tissue, validation of markers correlated with patient outcomes established in the literature, and identification of new markers.
3. Develop *in vitro* culture strategies to determine the functional properties of malignancy-derived tissue, manipulating with selected growth factors known to influence T cell growth.
4. Analyse markers of T cell function, phenotype and proposed molecular mediators of interactions with CHL using multi-parameter flow cytometry.

## CHAPTER TWO:

### Materials and Methods

## 2. Materials and Methods

### 2.1 Patient Samples

#### **2.1.1: Formalin-Fixed Paraffin-Embedded Tissue**

Immunohistochemical analysis was carried out on formalin-fixed paraffin-embedded tissue which had been stored in paraffin blocks. Available blocks were determined by correlation of databases of the pathology and haemato-oncology departments in order to identify tissue stored for which there was data on clinical follow up (see 3.3.1). All samples were taken with full informed consent and ethical permission for use granted by the local regional ethics board and in accordance with the Declaration of Helsinki. Suitable blocks were retrieved, with sections made for staining with H&E and subsequent marking for tissue microarray.

#### **2.1.2: Frozen Single Cell Suspensions (SCSs)**

Ethics approval was obtained from the local regional ethics committee. Patient-derived samples were obtained with informed consent documented on a standard form and stored under conditions compliant with the Human Tissue Act 2008. SCSs derived from CHL, NHL, tonsil and reactive enlarged nodes were retrieved from archived samples in cell storage and subsequently as they became available from consented patients. Table 5.5 (in Chapter 5) shows the samples used in the subsequent immunophenotyping and cell culture experiments.

##### **2.1.2.1 Preparation of initial single cell suspensions for storage on liquid nitrogen**

Single cell suspensions were prepared from surplus material available after diagnostic biopsy or from tonsils removed for therapeutic purposes from which no diagnostic specimen was required. Surplus material was placed into a sterile specimen pot containing RPMI and transported to the cell storage suite. The specimens were disrupted using forceps and scalpel under sterile conditions on an ice-block and flushed using further RPMI injected via a needle and syringe. Resultant suspensions were filtered through a 70µm mesh under gravity to exclude undisrupted tissue and cell clumps and

the resulting suspensions washed twice in RPMI by centrifugation at 1500rpm for 6 minutes with the supernatant disposed of. The final suspension was assessed for cell concentration and viability using an automated cell counter by trypan blue exclusion (ViCell: Beckman Coulter) and resuspended at  $5 \times 10^6 - 5 \times 10^7$ /ml in 1 - 1.5ml freeze storage mix (10% DMSO in FCS) in Cryovials (NUNC). Cryovials were slow-frozen in adapted containers (CoolCell: BioCision) with temperature reduction of 1°C per minute in -80°C freezers for two hours before transfer to liquid nitrogen and long-term storage.

#### 2.1.2.2 Thawing and initial preparation of frozen SCS for immunophenotyping and cell culture

All SCS-derived culture systems and flow cytometry were performed on previously frozen and nitrogen stored samples in order to standardise all conditions since establishment of cultures and flow cytometric analysis of fresh SCSs would often not be feasible. SCSs were thawed in a water-bath at 37°C for 60 seconds, resuspended and washed twice in PBS by centrifugation at 1500rpm for 6 minutes with the supernatant disposed of and finally filtered through a 70µm mesh (BD Falcon) under gravity to exclude cell clumps. Viability and total cell count of the resulting suspension was estimated using manual haemocytometry.

## **2.2 Immunohistochemistry**

Samples used are as described in 2.1.1.

### **2.2.1 Tissue Microarray Construction**

Tissue microarray is a technology developed to enable immunohistochemical assessment of multiple markers across large patient cohorts<sup>365</sup>. The CHL microenvironment is widely heterogeneous, including areas of fibrosis and necrosis interspersed with dense infiltrates of malignant cells and immune infiltrate. As such careful selection of suitable representative areas containing sufficient cells to analyse microenvironment heterogeneity was necessary. Haematoxylin and Eosin-stained (H&E) sections were examined with an expert histopathologist (MC), and regions marked for array. Cores of tissue of 1mm<sup>2</sup> diameter were then using a sharpened steel tube from these selected regions of biopsy material from each 'donor' block (each derived from one patient) and



inserted into a defined array of 'recipient' paraffin blocks (Figure 2.1) interspersed with control samples (usually tonsil) as internal staining control and orientation controls (usually myocardium or gut) as a means of cross-checking the generated data. Several recipient blocks were necessary to accommodate each available patient in triplicate. The block was then sectioned and sections transferred onto microscope slides, enabling many cores to be represented on a single slide. Each slide was then available to be assessed for expression of the biomarker of interest (Figure 2.2).

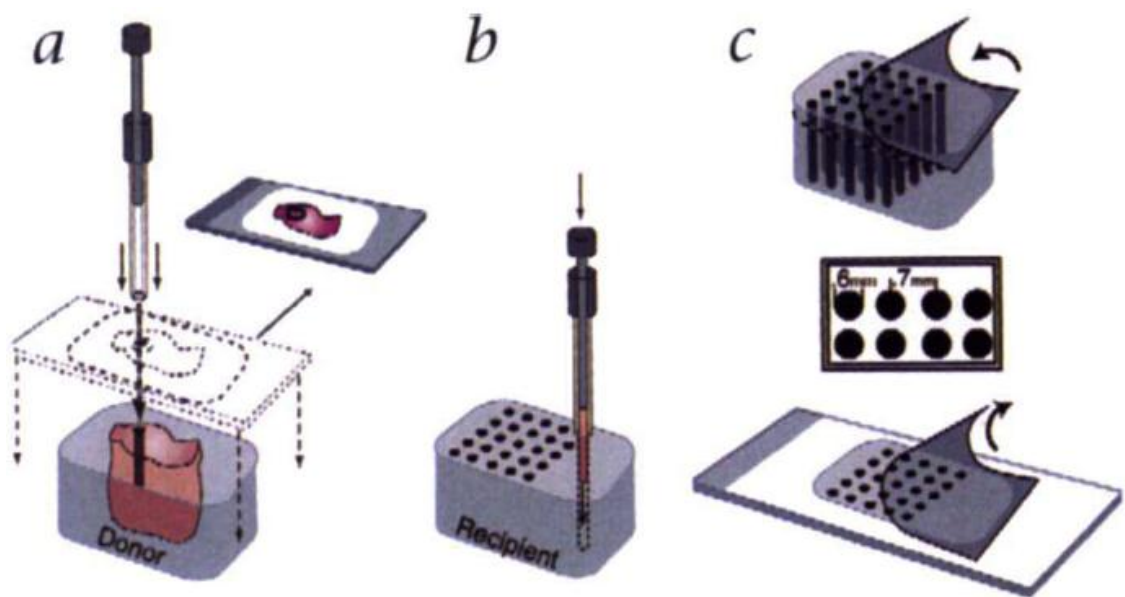


**Figure 2.1:** Tissue microarray construction<sup>365</sup>. Small tissue core biopsies are punched from selected regions of donor blocks using a thin-wall stainless steel tube sharpened like a cork-borer. HE-stained sections overlaid on the surface of the donor blocks guide sampling from morphologically representative sites on the tumour (a). A solid stainless steel stylet transfers tissue cores into defined array coordinates in the recipient block (b). An adhesive-coated tape sectioning system assists in cutting the tissue microarray block (c).

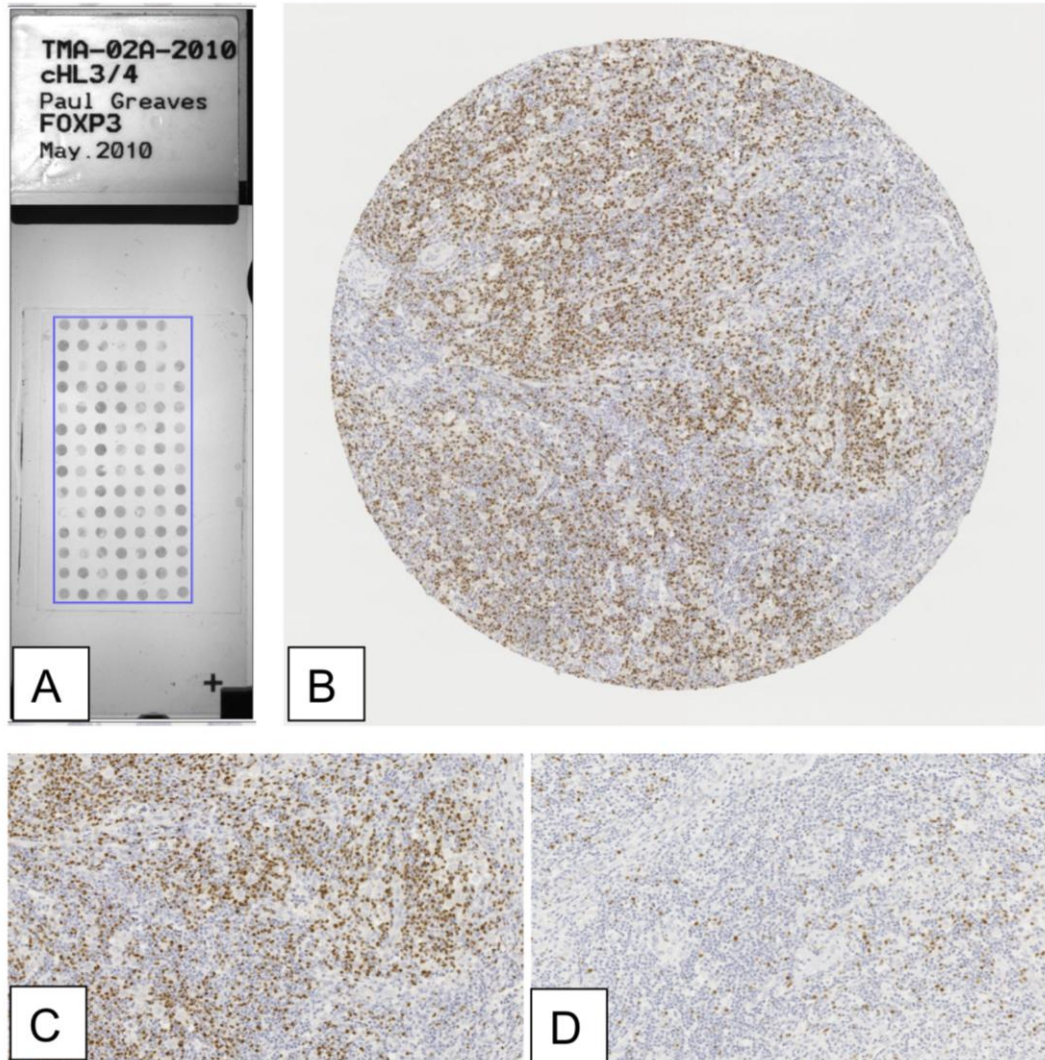


**Figure 2.2:** Example microarray slide showing slide (a), core at x5 (top) and x20 magnification stained for FOXP3 with high (c) and low (d) infiltration represented.

### **2.2.2 Principles of immunohistochemistry**

Antigen specific staining was carried out using commercial antibodies and optimised for the tissue under investigation, as described in experimental Chapters 3 & 4. All primary antibodies used are described in the experimental chapters, and were stained using the protocol detailed here. Modifications to this standard protocol, which was successful for the majority of stains, are detailed in the relevant chapter.

Immunohistochemistry relies on the specific binding of antibody to the target antigen for detection. This signal is amplified locally by subsequent binding of a multimeric compound capable of binding many molecules of a protein with enzymatic activity. Finally, the presence of the antibody – enzyme complex is determined by addition of a substance that both binds to, and is chemically altered by the enzyme such that a detectable colour change is observed. Unless stated in the specific methods of an experimental chapter, the chromogenic substrate was diaminobenzidine (DAB), which produces a dark brown/black colour when acted upon by peroxidase enzyme. The binding of the multimer–enzyme complex is achieved by addition of a secondary antibody with species and isotype specificity to the antigen-specific antibody (e.g. goat anti-mouse IgG<sub>2</sub>, if the primary is IgG<sub>2</sub> mouse-anti-antigen). Traditionally, the avidin-biotin complex (ABC) system has been used. Avidin, a glycoprotein egg-protein extract has particular avidity for the vitamin B complex member biotin, and can itself be conjugated with peroxidase. The secondary antibody is biotinylated (usually done commercially) and when avidin added, it binds many conjugated peroxidase molecules to each biotinylated antibody, thus providing a local amplification of the antigen signal. The non-specific binding properties of avidin, and the presence of endogeneous biotin in the tissue can lead to non-specific background staining, and as such the ABC method is being replaced by the dextran polymer method (Biogenix Supersensitive Polymer HRP), which was used for the staining in these experiments. In this case the multimeric compound is not avidin-biotin but another polymer (undisclosed by manufacturer, known as SuperEnhancer<sup>TM</sup> and PolymerHRP<sup>TM</sup>: BioGenix) conjugated with peroxidase and a secondary species-specific antibody (Figure 2.3).

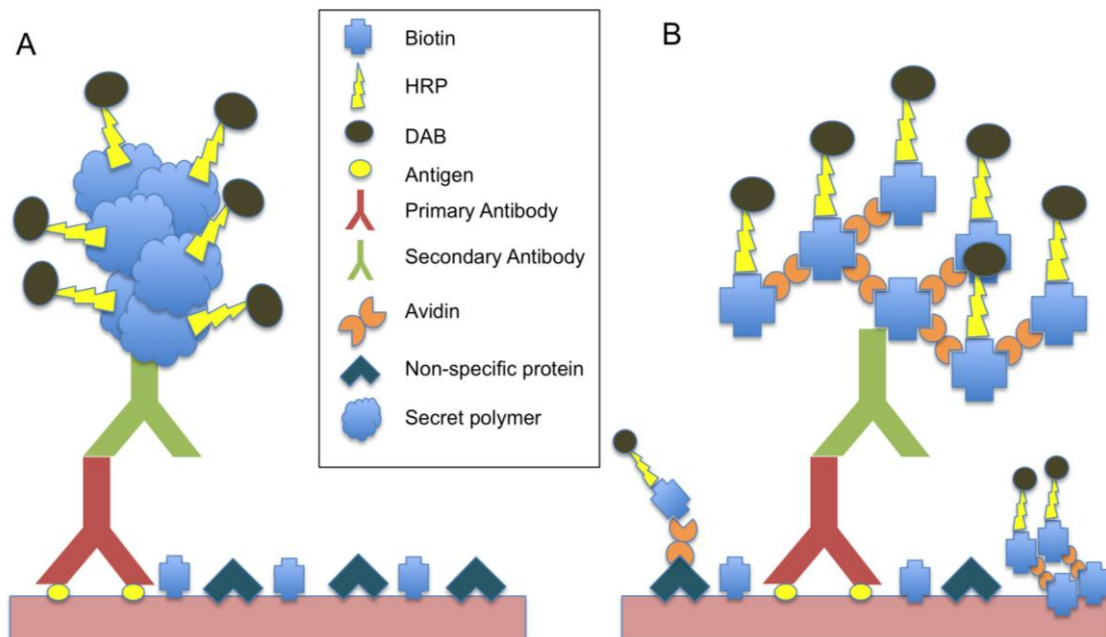


**Figure 2.3:** Primary Antibody (antigen-specific labelling) - Dextran polymer (signal amplification) - Horseradish peroxidase (enzymatic action) - DAB (staining readout) method of IHC (A) with more traditional Avidin-Biotin complex system for comparison (B) illustrating the non-specific signal that can result from avidin's promiscuous binding, and endogenous tissue biotin expression. HRP: Horse radish peroxidase; DAB: diaminobenzidine.

### **2.2.3 Batch Immunohistochemistry using the DAKO Autostainer System**

Staining was optimised for temperature, duration of reagent exposure and antibody concentration on a slide by slide basis, and subsequently larger numbers of slides were stained using an automatic staining system consisting of a slide rack, robot arm with nozzles to dispense reagents, pump system and reservoirs of bulk reagents and a dispensing rack for the various primary antibodies and secondary amplification / colourimetric reagents, controlled by an incorporated software package (Dako Autostainer Plus). As a counterstain, the potent arginine-rich-histone-binding blue/purple dye haematoxylin is used (fairly nucleus-specific). Industrial methylated spirits (IMS) at three concentrations (95%, 70% and 50%) provide a dehydrating and part hydrophobic part hydrophilic intermediate between the potent hydrophobic solvent xylene and subsequent water soluble staining steps. Xylene removes paraffin and improves clarity of image by dissolving hydrophobic residues. DPX (p-xylene-bis-

pyridinium promide) is a viscous mix of a polystyrene, plasticiser and xylene, which provides a durable mountant with refractive properties suitable for high-quality microscopy and photomicroscopy.

#### **2.2.4 Primary antibodies for immunohistochemistry**

Antigen specific staining was carried out using commercial antibodies and optimised for the tissue under investigation, as described in experimental Chapters 3 & 4. All primary antibodies used are described in the experimental chapters, and were stained using the protocol detailed here. Modifications to this standard protocol, which was successful for the majority of stains, are detailed in the relevant chapter.

#### **2.2.5 Protocol for Immunohistochemistry Staining using Autostainer**

##### **2.2.5.1 Paraffin Removal and dehydration**

1. Place TMA slides in oven overnight at 60°C in plastic racks
2. Prepare pots containing all reagents for dewaxing and dehydration as shown in Table 2.1
3. Remove paraffin using xylene in two stages: suspend slides in xylene pot for 5 minutes, shake off excess and transfer to second xylene pot
4. Transfer to industrial methylated spirits for 2 minutes
5. Transfer to hydrogen peroxide (2ml reagent grade) in 100ml IMS for 2 minutes. This further dehydrates tissue and increases specificity of the subsequent reaction which depends upon a colour change in a chromogenic chemical diaminobenzidine (DAB) following the action of antibody-conjugated horse radish peroxidase. Hence this step reduces non-specific staining arising from the action of endogeneous peroxidises on the chromogen. Transfer to a second IMS/H<sub>2</sub>O<sub>2</sub> pot for 2 minutes.
6. Transfer to a fresh IMS pot for 2 minutes (final dehydration step)

##### **2.2.5.2 Pressure Cooker Heat Antigen Retrieval<sup>366</sup>**

7. Heat 3000ml of a working solution of antigen unmasking solution (Vector Labs: See Table 2.1) in a pressure cooker on low heat setting (100-110°C).
8. Once solution is boiling immerse dewaxed, dehydrated slides in their plastic racks fully in the boiling solution.

9. Increase the heat setting to high setting (120-130°C) and leave for 10-15 minutes.
10. Remove from heat and cool pressure cooker under cold tap for 5-10 minutes.
11. Retrieve slides and rinse in wash buffer.
12. Ensure slides remain wet with wash buffer at all times during subsequent staining process.

#### 2.2.5.3 Antigen-specific staining using Dako Autostainer Plus

13. Mark slides using hydrophobic marker pen around the edge of the array field: this is to ensure uniformity of solution deposited on slide and hence of staining.
14. Program Autostainer control software specifying number of slides to be stained, reagents and incubation times, specifically the rinse steps, non-specific protein block steps (using casein-based commercial protein compound), primary antibodies to be used at optimal dilutions (in BSA/azide), polymer-conjugated secondary antibody (with species and antibody isotype specificity denoted by the primary antibody being used), and chromogenic substrate (DAB). The software package generates a reagent diagram illustrating the position in which all reagents are located within the automated stainer, and a slide map illustrating the position of all slides to be stained in the batch.
15. Top up wash buffer reservoirs, empty waste reservoirs, and fill appropriate bottles with reagents as dictated by the reagent diagram.
16. Start the Autostainer. The process takes 2-3 hours including incubation and wash steps.
17. Replace all slides in plastic racks ready for counterstaining and and mounting.

#### 2.2.5.4 Counterstaining, rehydration and mounting slides

18. Rinse in tap water for 5 minutes.
19. Suspend in haematoxylin solution for 5 minutes
20. Rinse for 2 minutes in tap water
21. Plunge into acid alcohol solution x5 quick plunges
22. Immediately into tap water wash for 2 minutes
23. Rehydrate tissue using three 2 minute suspensions in IMS.

24. Remove residue and clarify tissue by suspending in two xylene baths, then suspend in final bath prior to mounting.
25. Using DPX mountant apply cover slip removing trapped air bubbles. Air dry and label slide appropriately.

Reagent	Working Concentration	Supplier
Antigen unmasking solution	10ml/1000ml ddH <sub>2</sub> O	Vector Laboratories
Reagent Grade H <sub>2</sub> O <sub>2</sub>	Stock	VWR
Wash Buffer	1:10 ddH <sub>2</sub> O	DAKO
Xylene	Stock	Sigma
Industrial Methylated Spirits	Stock	VWR
Haematoxylin Gill 2	100ml filtered	Merck
Scotts Alkaline Tap Water Substitute	Stock	VWR
DPX Mountant	Stock	Sigma
Stable DAB Buffer	Ready to Use	Biogenix SuperSensitive
Liquid DAB	1 drop (38 µl) in 1ml DAB Buffer	Polymer-HRP IHC Detection System
SS Label Polymer HRP	Ready to Use	
SuperEnhancer	Ready to Use	

**Table 2.1:** Reagents used for the Polymer/HRP method of IHC.

### **2.2.6 Slide analysis, immunohistochemistry scoring and cell counting**

For IHC analysis, arrays can be scored either manually by histopathologists, or using automated image analysis software. The following details the general methodology used to enumerate infiltration with cells expressing markers investigated in experimental Chapters 3&4. Variations in methodology are presented where appropriate within these chapters.

#### **2.2.6.1 Automated Method for Cell Counting using the Ariol system**

The specimens were scanned using an Olympus BX 61 microscope with an automated platform (Prior). Absolute numbers of positive cells were counted across all intact cores by automated image analysis system (Ariol).

The image analysis system was trained to discriminate stained and unstained cells by colour and shape. Selected representative regions of tissue were used to determine specific hue, saturation and intensity, which were deemed to be positive (usually the brown/black resulting from DAB colour change) requiring sufficient contrast to background and counterstaining. This was achieved by the operator selecting individual pixels from positive events, which were then displayed by the Ariol software as a pixel mask. Once the resulting pixel mask obscured only positive events, with minimal pixel masking of negative events and non-specific staining, the algorithm generated by the software was saved. Finally, the algorithm was refined by limiting the size and shape of the areas deemed to be positive by the colour algorithm, which was particularly useful for staining of discrete and homogeneous sized events such as lymphoid nuclei.

Image analysis, while in itself automated, requires this extensive training step to define the algorithm, which introduces the possibility of inter-observer error. It arises from a need to compromise between sensitivity and specificity, with substantial signal/noise ratio due to variability of background staining. Automated image analysis has the major advantage of rapid assessment of very large numbers of events, consistency in application of predefined criteria defining events to be counted, and absence of fatigue, but is no better at discriminating positive or negative events than a human observer due to the need for a human-defined training step. It remains as influenced by technical variations in the quality and specificity of the stain applied. For these reasons results generated from nuclear staining of discrete cells such as FOXP3 or T-BET applied to lymphocytes are more reproducible than those generated from cytoplasmic or membrane stains applied to larger, more heterogeneous, interdigitating cells, such as CD68 or CD163 applied to macrophages.

#### 2.2.6.2 Manual Method for Cell Counting using the Hammamatsu system

In order to provide a validation of the automated counting system and the potential for translation to clinical application, a manual validation step needed to be carried out. This was done using digitised images acquired using the Hammamatsu Virtual Slide Scanner NanoZoomer 2.0 (Hammamatsu, Japan), which could subsequently be viewed



using NDP.scan software. For the manual validation steps two observers accessed the digitised slidemaps using the NDP.scan software. A random selection of 40 cores were selected from all available cores using random number generating software (<http://www.random.org/>) and the two observers selected x20 objective-equivalent fields viewed using the NDP.scan software and exported the files as compressed image files (Joint Photographic Expert Group: JPEG) into Photoshop (Adobe) which enabled a grid to be superimposed on the image (Figure 2.4). Superimposition of this guidance grid and visualisation on a standard computer screen facilitated counting of larger numbers of cells more easily than direct visualisation through a microscope eyepiece, without loss of image resolution. Total numbers of cells in the x20 exported image was then corrected to equivalent count across an entire  $1\text{mm}^2$  field by a multiplication factor determined by the area of the JPEG image exported, which could be calculated by the NDP.scan software.

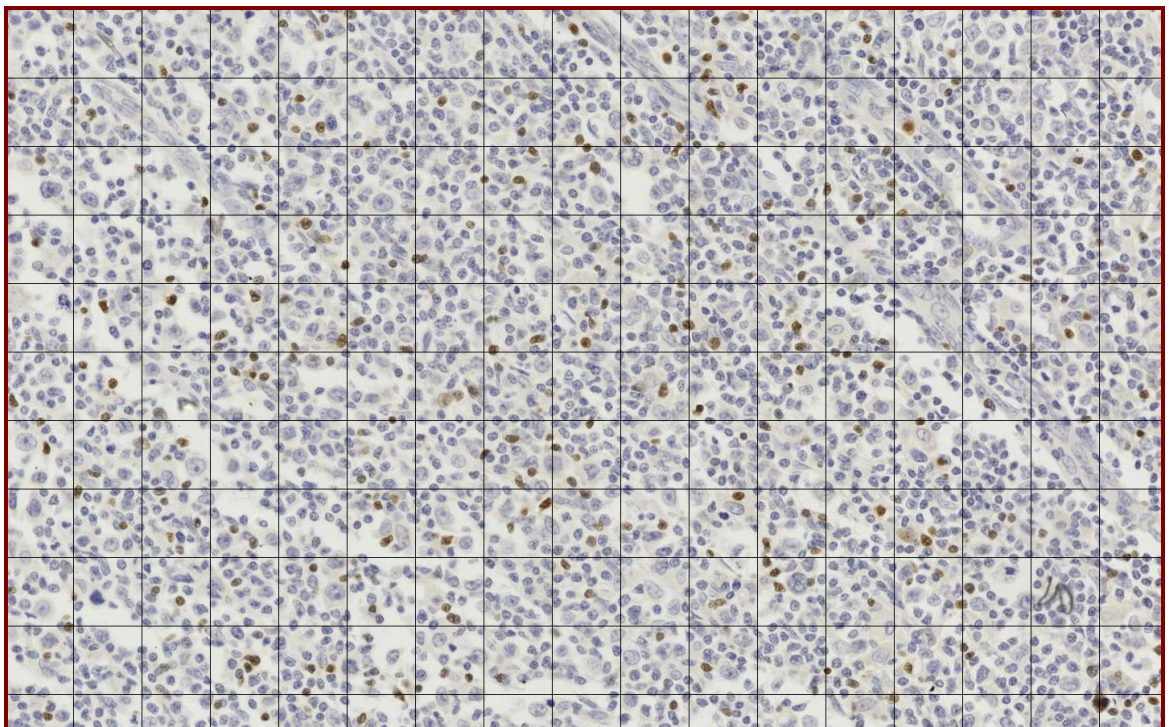


**Figure 2.4:** Grid superimposed in Adobe Photoshop from selected x20 region of tissue exported as a JPEG from NDP.scan software, acquired as a digital image from the Hammamatsu NanoZoomer 2.0. The example shown is CHL stained for FOXP3 representing an intermediate infiltrate of cells.

### 2.2.6.3 Method of Cut-point Determination and Survival Analysis

Optimal or multiple cut-point analysis is a commonly encountered pitfall of statistical analysis of novel biomarkers where normal ranges are unknown<sup>338</sup>. The availability of software that will determine by multiple comparisons the point at which statistically significant differences between groups is found (e.g. Xtile<sup>339</sup>) makes this statistical error more accessible. The consequence has been the failure of many apparently significant biomarkers to be confirmed or validated by other investigators, and more important to find their way into clinical practice. Predetermination of cut-points or validation in independent datasets is the only robust method of confirming such findings: this is rarely performed in the literature. Xtile (Yale University School of Medicine: (<http://medicine.yale.edu/labs/rimm/www/xtilesoftware.html>) is a software package providing a compromise method enabling novel marker cutpoints to be developed with statistical validity, by generating an optimal cut-point on only a subset of the cohort under investigation (the 'test set') and applying this as a 'predetermined' value to the remainder (the 'validation set'). The disadvantage of this method is that the resultant cohorts are smaller, and hence the statistical power to demonstrate differences impaired. However, should a difference be detected, the robustness of that finding, being generated from a smaller cohort (as long as that cohort was representative of the whole and unbiased in its selection) may be greater. However, the chance of erroneously accepting the null hypothesis is by definition increased.

The statistical significance of differences between groups segregated by these cut-points, according to outcome is assessed using the Kaplan Meier method<sup>367</sup> where censorship occurred at the date of last known contact with the patient at which the event under consideration had not occurred, or date at which the event occurred, with time to that event calculated from a specified point, usually the date of diagnosis or commencement of first therapy. The logrank test<sup>368</sup> was used to compare survival distributions. Xtile ranks the subjects in order of expression of the marker under investigation and divides into any number of groups using cut-points at every value generated for that marker. Using the Kaplan Meier method to generate variances for the estimated survival function and comparing functions using the logrank method, the probability of groups differing in terms of outcomes are generated for each of those cut-points. For one or two cut-

points, the most simple and hence clinically translatable system, this is displayed in the form of a heatmap whereby a green pixel represents a favourable outcome for higher expression of that marker and a red pixel unfavourable, with intensity of colour reflecting the level of significance, and black representing a p value  $>0.05$ . For division into two groups, each potential individual cut-point is represented as a coloured pixel on a line. For division into three groups, each cut-point combination is represented as a pixel on a two dimensional grid (Figure 2.5) The corresponding Kaplan Meier survival curves are generated concurrently. Should the data demonstrate consistency in colour (green vs red) the inference of a biologically meaningful relationship may be made, assuming that there was not a bimodal or more complex association between survival and the variable under investigation in which, for example, extremes of values were both disadvantageous while intermediate values advantageous.

## **2.3 Multicolour Flow Cytometry**

### **2.3.1 Principles**

Flow cytometry enables the simultaneous detection of different molecules present upon or within particles, in particular cells, using an integrated piece of equipment consisting of fluidic, optic, detector, computational and display components. The process depends on the particles being delivered as individually detected events in a uniform stream (fluidics), and requires the molecules to be tagged by different fluorescent markers (fluorochromes), whose emission spectra may be discriminated sufficiently from one another, by manipulation of incident laser wavelength and modulation of the emitted electromagnetic pulse through filters (optics), amplification of the wavelength-specific ('colour'-specific) signal resulting from incidence of that filtered pulse on detection photomultiplier tubes (detector), and application of a mathematical transformation of the absolute value of emitted pulse intensity (compensation: performed by the integrated computational and display components usually within a single software package). Advancement of flow cytometric technology, in particular numbers of lasers, novel fluorochromes, computational power and software design means that over 20 parameters can now be measured simultaneously.

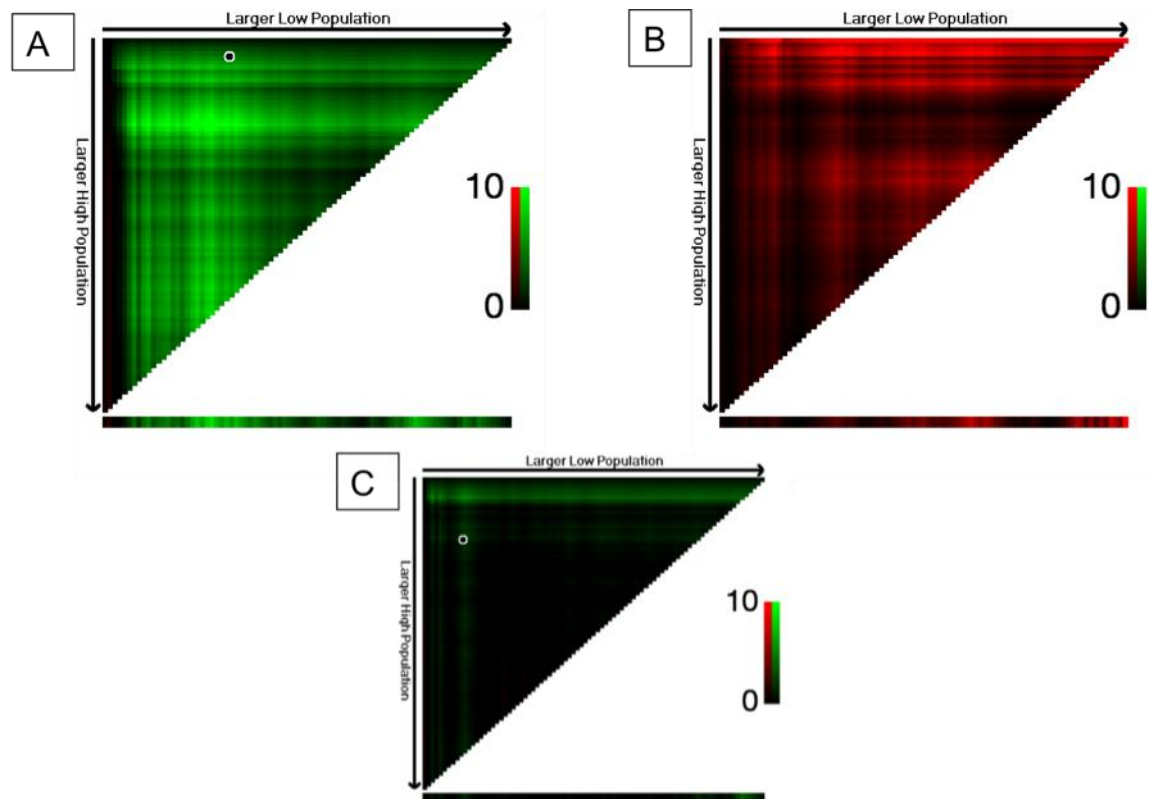


**Figure 2.5:** Cut-point uncorrected probability distribution figures. Each pixel on the matrix and horizontal bar represents every possible division of the data by cut-point. The colour of the pixel represents the effect of that marker on the group expressing it at the highest value when the cut-point is applied as indicated, where red indicates an adverse effect and green advantageous. The intensity of the colour indicates chi square probability level of group differences, with black indicating  $p > 0.05$  and bright green/red  $p < 0.0005$ . A: FOXP3: A beneficial prognostic effect at high levels, with most cut-points discriminating groups and indicating a probable dose-effect: the higher the expression, the better the outcome. B: CD68: Adverse prognostic effect at high levels, but fewer cut-points discriminate groups and hence dose relationship less likely. C: CD8: Minority of cut-points discriminate groups with  $p < 0.05$ . All plots are generated from the entire dataset, hence this visualisation represents optimal cut-point analysis and requires validation in an independent dataset. For A and B prognostic power was sustained in the validation set. This was not the case for CD8, although the consistency of the relationship (only green pixels, hence favourable prognosis with increased expression) suggests that there this marker should be explored in a larger, more highly powered dataset to detect differences. See Chapter 3 for further details.

Flow cytometry was carried out using a four laser LSR Fortessa (Becton Dickinson) with integrated fluidics and software package (BD FACSDiva™). This uses a pressure driven fluidics system to force sample cells through a flow cell cuvette as individual events passing through the focal point of the integrated laser beam. Fixed alignment of this system improves reproducibility, which is confirmed on a daily basis by a specialist technician (GR) according to the manufacturer's instructions.

The optical system consists of four lasers (Red emitting at 640nm wavelength, Yellow/Green emitting at 561nm, Blue emitting at 488nm, and Violet emitting at 405nm) with beam shaping lenses and pinholes focusing the combined laser light as a single beam into the cuvette. Emitted light is delivered through fibreoptics to detector arrays arranged to maximise the signal detection, using reflecting mirrors. Photomultiplier tubes (PMT) lie beyond bandpass filters (for Red lasers: 670+/-14nm, 730+/-45nm, 780+/-60nm, for Yellow/Green 585+/-15nm, 675+/-20nm and 780+/-60nm, for Blue 695+/-40nm and for violet 525+/-50nm and 450+/-50nm) enabling improved spectral resolution. These components were calibrated on a weekly basis using the FACS Comp software (BD) and Calibrite Beads (BD).

PMT voltages are adjusted for the purposes of each experiment to ensure maximum signal : noise ratio and minimise interference (spectral overlap) in competing channels (PMT detectors) and recorded as a matrix for each individual event, which can then be displayed graphically (see below). Apart from the wavelength-specific, bandpass-filtered fluorescence intensity arising from each fluorochrome as detected at the PMTs, data on light forward scatter (related to particle size) and side scatter (relating to internal complexity of the particle, such as granularity) are additionally collected.

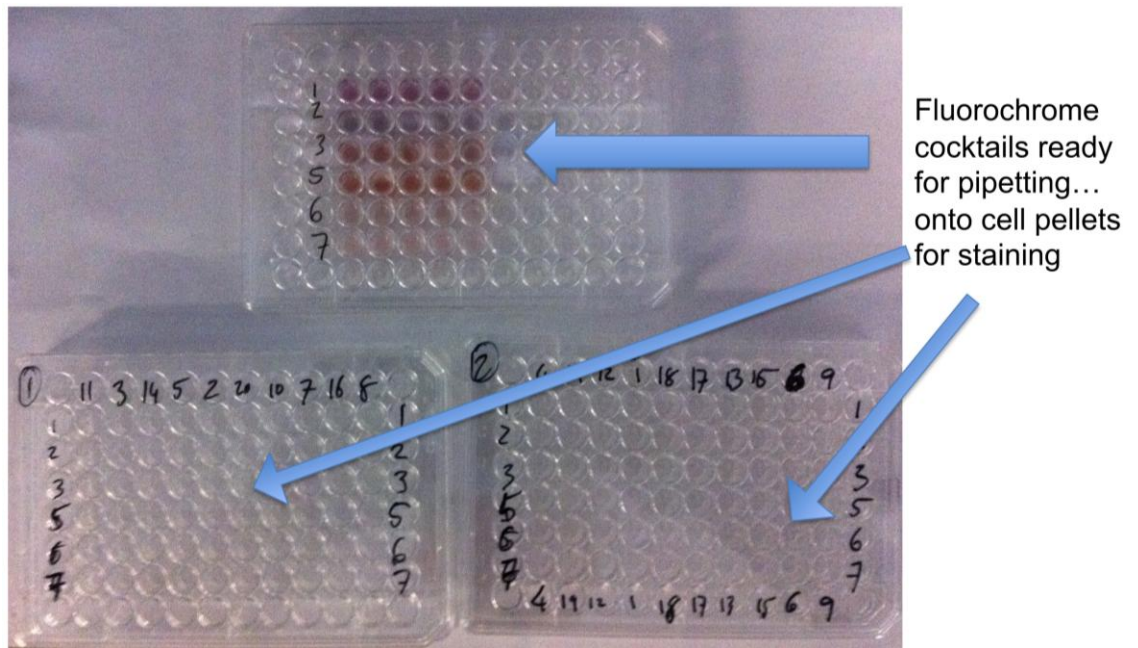
Data acquired is interrogated using a number of software packages capable of transforming (compensating) the PMT-derived values and displaying them either as one dimensional histograms showing frequency distributions of detected fluorescence intensity, or as two and three dimensional scatter plots, displaying multiple parameter intensities with each particle/event represented by the appropriately positioned dot. Multiple superimposed dots may be visualised by false colour or contour plots (e.g.

Figure 2.11) Definition of an event with which the fluorescing molecule in question is associated depends upon signal/noise ratio (including non-specific fluorescence and background signal as well as interference from other fluorochromes present) and requires careful determination of thresholds, known as gating, described below.

### **2.3.2 Fluorochromes and Staining Protocols**

Tagging of markers is usually achieved through conjugation of specific monoclonal antibodies to fluorochromes. For the experiments described here all such molecules were purchased from commercial laboratories which had themselves performed extensive quality control to ensure specificity and optimal dilutions. However, for each experiment, optimisation steps were carried out to determine the most appropriate concentrations of reagent for the samples under investigation. Fluorochrome combinations were also optimised for these experiments, as detailed in the experimental chapters, to maximise numbers of simultaneously assessable parameters while minimising spectral overlap or at least allowing for compensation of any overlap that occurred.

Markers capable of detection by specific monoclonal antibodies may be present in any cellular compartment (membrane, intracytoplasmic, intranuclear, etc.) with varying degrees of resistance of access to them. Flow cytometry is usually carried out on fresh or thawed, vital tissue in which lipid barriers are intact and hence the compartmentalisation of the cell remains, in contrast to work using fixed tissue. Most staining protocols documented here are modifications of those provided with commercially available reagents. Most staining procedures were not carried out in individual 5ml sample tubes, but in a 96 well round bottomed plate (Figure 2.6), in order to increase efficiency of protocols and reduce sample preparation time. The flow cytometer requires a 5ml tube from which samples are aspirated, and as such each well's contents were aspirated and transferred into 1ml polypropylene adaptor tubes which could be inserted consecutively into a standard tube for use on the flow cytometer (Figure 2.7). In the following staining protocols, in order to minimise sample to sample variations in staining when large numbers of conditions are being applied, cocktails of cytokines were pre-made and applied in batches using a multichannel pipette.



**Figure 2.6:** Illustration of 96 well plate staining technique

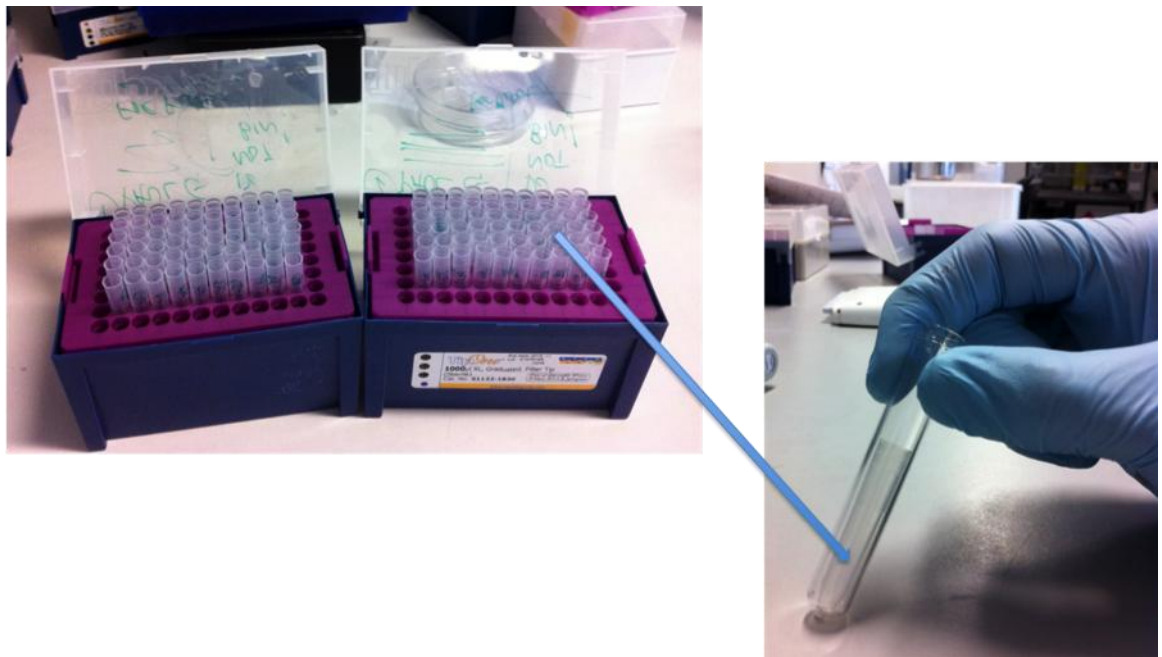


**Figure 2.7:** Final stage of 96 well plate staining technique: well contents harvested into receiver tubes arranged in pipette tip box; each tube analysed within standard 5ml FACS tube.

### **2.3.3 Surface Marker Staining**

Molecules present at the cell surface may be stained without any cellular disruption, following simple washing steps. This has the advantage of enabling cell viability to be maintained, as long as the preparation process is undertaken with care and in appropriate staining buffer. Subsequent functional studies may be carried out if the cells are analysed in strict sterile conditions and collected as they emerge in the waste stream from the flow cytometer.

### **2.3.4 Intracellular Marker Staining**

Molecules present within the cytoplasm may be stained following a chemical disruption step usually with a strong alcohol or aldehyde, which covalently bonds proteins, in particular cytoskeletal elements, physically immobilising them. Usually denaturation is minimal, however in some cases antibody-specific epitope is lost leading to alteration in binding of fluorochrome conjugates, and hence optimisation of any protocols is necessary. In some cases there is little alteration in binding properties, and surface and intracellular markers may be stained simultaneously. In other cases, an initial surface staining step is carried out prior to intracellular staining. In the experiments requiring fixation described within (cytokine staining), only well-characterised optimised surface antigens (CD3, CD4 and CD69) were stained for and their properties were such that only a single staining step was necessary, which is described in the protocol below. Some fixation reagents (e.g. methanol, 95% ethanol) are also capable of permeabilising the cells. Others (e.g. paraformaldehyde, formalin) require addition of a cell membrane permeabilising agent. This is usually a hydrophobic 'soap' such as triton or saponin. A standard commercially available fixation and permeabilisation kit was used (Ebioscience one-step fix/perm kit), which was found to be optimal for the cytokine staining experiments described in Chapter 6, which is described in the subsequent protocol.

### **2.3.5 Cytokine and secreted protein staining**

Some molecules, particularly those identifying functional pathways of cellular metabolism may only be released from cellular compartments, or fully assembled, following a stimulation step, and may subsequently be lost to the supernatant following secretion. As such, specific stimulation and protein secretion-blocking steps are required in order to artificially concentrate those molecules within the cytoplasm prior to



subsequent staining. While any such stimulation/secretion blocking step in itself represents a highly artificial system, careful control and optimisation of protocol enables at least between sample comparisons, even if conclusions regarding the *in vivo* equivalence of these markers should be drawn with caution. Various stimulants including phorbol-myristate acetate (PMA) and ionomycin, phytohemagglutinin (PHA), concanavalin (CCA), staphylococcal enterotoxin B (SEB) and bead-bound stimulatory anti-CD3 and anti-CD28 antibodies were used with various incubation times. The cytokines under investigation had differing 'optimal' stimulation times. Following optimisation, PMA/Ionomycin with a standardised time of 8 hours stimulation was decided upon. This enabled detection of the majority of cytokines with retained cellular viability. This incubation time was kept constant between experiments and within each batch between samples thus enabling comparisons to be made. Limitations of this relatively prolonged incubation (in particular for detecting cytokines associated with Th1 reactions) mean that comparisons with the literature are made more difficult. However the experiment compared various experimental and control sample groups exposed to the same conditions and as such it was deemed valid.

### **2.3.6 Viability**

Dying cells and debris have particularly high autofluorescent and non-specific binding properties and contribute to substantial noise in flow cytometry. As such, exclusion of these events using specific fluorescent markers improves the resolution of an assay. Most viability dyes depend upon the ability of live cells with intact cell membranes to actively exclude such a dye from their cytoplasm. These experiments used DAPI (4',6-diamidino-2-phenylindole), which is relatively excluded from live cells with intact cell membranes, compared to dying and dead cells with compromised membranes. Hence dead cells may be excluded by their fluorescence due to presence of DAPI. DAPI remains stably bound within the cell to Adenine/Thiamine-rich regions of DNA, absorbing in the UV and violet spectrum and emitting in the blue/violet spectrum. DAPI is also used for DNA quantification experiments, however staining and analysis protocols are different. Once plasma membrane integrity has been compromised by fixation or permeabilisation, the dye is no longer useful as a discriminant since all cells will take it up. New commercially available dyes are available which are actively excluded from live cells during the initial

staining step, and taken up by dead cells, but which remain excluded following cell permeabilisation steps, which is not the case with DAPI even if applied prior to a fixation / permeabilisation step. These dyes also have the advantage of being available with fluorescence properties across the detectable spectrum. The dye chosen for the cytokine staining experiments was compatible with the fluorochrome combinations already in use (Ebioscience Viability Dye).

### **2.3.7 Non-specific fluorochrome-conjugate binding-blocking step**

Non-specific binding of fluorochrome conjugates in particular to immunoglobulin Fc receptors, can interfere with signal/noise ratio within an experiment. Non-specific mixed protein suspensions (e.g. milk powder, serum, etc) can occupy immunoglobulin Fc receptors within an experimental system in preference to the subsequently added fluorochrome. However, the additional incubation and wash step required for this was found to lead to excess cell loss with the small numbers of cells used in these experiments, and did not contribute to determining thresholds and gating strategy described in Chapter 6, and as such no blocking step was performed.

### **2.3.8 Protocol for Staining: (Chapters 6&7; 96 Well Plate Method)**

Batch to batch variation in flow cytometry may be considerable due to differences in cell preparation, staining, flow cytometer calibration and other factors and as such comparisons should be made with internal standards on each run, and batched with as many concurrently run samples as is feasible. For clarity and reproducibility, the protocol combining surface and intracellular cytokine staining is detailed below. The entire protocol takes approximately 12 hours assuming PMT voltages pre-programmed on BDFortessa: 3-4 hours harvest, cytokine stimulation and surface staining, 4-5 hours surface stain data acquisition (assuming 120 tubes, 20 samples with 6 surface staining cocktails plus staining controls), 2 hours harvest, fix, permeabilise and stain stimulation step, 2 hours intracellular stain data acquisition (assuming 40+ tubes: 20 samples with 2 intracellular staining cocktails plus unstimulated and staining controls). Reagents used are shown in Table 2.2. For justification of reagents and controls used see 2.2.9. For details of fluorochromes used, and PMT voltages on BDFortessa see relevant experimental chapters (6 and 7). For compensation strategy see 2.2.10.

Reagent	Supplied Conc.	Stock Conc.	Experimental Conc.	Experimental Dilution	Supplier
DAPI	10mg dried	5mg/ml (dH <sub>2</sub> O)	2.5mcg/ml	1:2000	Invitrogen
Fix/Perm Concentrate (formaldehyde base)	4X	AS MANUFACTURER	AS MANUFACTURER	1:4 ddH <sub>2</sub> O	Ebioscience
Perm Buffer (Saponin base)	10X	-	-	1:10 ddH <sub>2</sub> O	Ebioscience
Fixable Viability Dye eFluor™ 780	USE AS SUPPLIED	USE AS SUPPLIED	DILUTED AS PROTOCOL	1mcl per condition in 1ml	Ebioscience
Ionomycin	1mg dried	1mg/ml DMSO	500ng/ml	1:2000	Sigma-Aldrich
Monensin	0.7ml	-	-	1:1000	BD
Phorbol- 12-myristate acetate (PMA)	1mg dried	50mcg/ml DMSO	50ng/ml	1:1000	Sigma-Aldrich

**Table 2.2** Reagents Used for Staining Protocol

### 2.3.8.1 Experimental Set up (to be done on day prior to main experiment)

1. Prepare staining cocktails (cocktails 1-8 as described in chapter 6) with adequate stain for the number of experimental and control conditions to be stained (+10% for pipetting errors) in advance, using optimised dilutions of fluorochrome conjugates. Ensure each cocktail is made up to equal total volumes with PBS to enable eventual dispensing of equal volumes across all samples using a multichannel pipette. For example, if the largest volume cocktail for each of 20 samples totals 60mcl, there will be a total of 60 x 20mcl = 1200mcl. All cocktails with a lesser volume should be 'topped up' to 1200mcl. The cocktails are stored at 4-8°C in opaque containers until use (<72 hours storage once made up). The cocktail is then dispensed for convenience into a 96 well 'dispensing' plate to enable the multichannel staining to proceed (Figure 2.6)

2. Identify the samples for analysis in the experiment and design a surface staining plate map where rows represent each of the six surface staining cocktails and columns each sample. Up to 20 samples in two 96 well plates may be run in one batch using this method and a single operator. Allocation of samples to each column should be randomised to prevent systematic errors of sample preparation, data acquisition and interpretation arising from unequal cell loss, staining cocktail dispensing or flow cytometry errors. Make a separate plate map for the 2 cytokine staining steps including 'stimulated' and 'unstimulated' controls, with randomised order of samples as for the surface staining.
3. Prepare '*stimulation mix*' from thawed aliquots before each experiments: 5ng/ml phorbol-myesterate-acetate (PMA) (1:1000 stock), inomycin (1:2000 stock) and Monensin (1:1000 stock) (Table 2.2).

#### 2.3.8.2 Harvest and Plate Samples for analysis:

4. Harvest cells and count using manual hemocytometry. Harvest may be from fresh growing cells within a 96 well plate, harvested from the plate using a multichannel pipette and into a petri dish and resuspended in tubes, or from frozen samples, thawed and washed as described, and filtered through a 70µm mesh filter if necessary. Fresh growing cells do not require the mesh filtration which removes dead cell clumps resulting from the freeze/thaw process.
5. Resuspend the cells at  $>1 \times 10^6$ /ml LCM during the final wash step which will enable an eight-cocktail staining experiment as described in chapter 6. Ten aliquots of each condition will be required: 6 surface stain, and 2 intracellular cytokine staining, for each of which a 'stimulated' and 'unstimulated' control is required. The unstimulated condition may be omitted in some cases to preserve cells / reagents but at least one unstimulated cytokine control is required for each experiment. 50-100,000 cells per aliquot are required optimally. This step should provide a cell suspension of around 1ml for each of the experimental and control conditions, containing at least 100,000 cells for each condition. Analysis is possible with fewer cells if a total of 1,000,000 cells are not available.

6. Divide the 1ml of each suspension into ten 100µl aliquots using a multichannel pipette across a 96 well plate according to the plate maps described in 2: six for surface staining and four for intracellular cytokine staining (a stimulated and unstimulated control for each of the two staining cocktails)
7. Split available cells into two aliquots: one for 'stimulated' condition and one for 'unstimulated' control. If insufficient cells are available a 'stimulated' only condition is adequate as long as there is an unstimulated control available from another experimental condition (one unstimulated condition per experiment).
8. Centrifuge 'Surface Stimulation' plate/s at 3000g in centrifuge for 5 minutes at room temperature. While centrifuging proceed with cytokine stimulation step:

2.3.8.3 Cytokine Stimulation:

9. Take 'Cytokine Stimulation' plate. Add 100µl of '*stimulation mix*' (See Step 3 of protocol) to each well according to plate map (resulting in 1:2 dilution).
10. Place Cytokine Stimulation plate in incubator at 37°C with 5% CO<sub>2</sub> for 8 hours, during which time staining and analysis of the surface markers is performed.

2.3.8.4 Surface Staining:

11. **WASH:** Flick off supernatant; resuspend all wells in 200µl PBS. Centrifuge at 3000g in centrifuge for 3 minutes at room temperature. Flick off supernatant.
12. **STAIN:** Apply staining cocktails (according to final total volumes calculated in 2., in this example 60µl per sample) simultaneously using multichannel pipette. Ensure on dispensing each 60µl aliquot, the cell pellet resulting from the previous centrifuge step is entirely resuspended with a partial volume aspirate/flush technique that itself does not introduce air bubbles into the sample. Air bubbles impair uniformity of staining and surface tension leads to problems with the 'flick' supernatant disposal technique.
13. **INCUBATE:** Place plates in dark for 30 minutes at room temperature.

14. Prepare single stain control samples using beads for all fluoro-chromes except DAPI and Horizon V500 conjugated-CD4, for which excess cell suspension from any condition (all of which assumed to contain CD4<sup>+</sup> cells and CD4<sup>-</sup> controls both viable and dead) may be used to provide internal controls.
15. **Compensation Beads:** Agitate all positive and negative control beads dispenser bottles; as described, each fluorochrome, but not each antigen, is represented in the control panel. Bead controls should be matched to the isotype specificity of the fluorochrome selected as the control (i.e. anti-mouse IgG or anti rat-IgG).
16. Label one FACS tube for each fluorochrome for compensation.
17. Dispense one drop each of positive and negative, or an aliquot of 100µl containing cells at  $1 \times 10^6$ /ml (DAPI and Horizon V500) into each tube.
18. Add preoptimised volume of selected fluorochrome/antibody conjugate to each tube.
19. Incubate for 15 minutes at room temperature (this is adequate for bead and CD4 controls). For the DAPI control, the DAPI may be added during the final step when DAPI is added to the experimental samples.

#### 2.3.8.5 Final Wash and Transfer to FACS Adaptor Tubes

20. Retrieve surface staining plates from dark.
21. Add 200µl PBS to each well as first wash and centrifuge as for (11)
22. **WASH:** Perform two further wash steps as per (11) using PBS.
23. During centrifuge steps label appropriate number of adaptor tubes to correspond with plate maps, one tube to receive the contents of one well. Load adaptor tubes into suitable racks as for the plate map (empty 100µl pipette tip dispenser is ideal: see Figure 2.7).

24. Resuspend final cell pellets in 200µl 1:2000 DAPI in PBS solution, and transfer in DAPI solution using multichannel pipette.
25. Top up receiver tubes with further 200µl PBS such that each contains 400µl stained cell suspension ready for analysis.
26. Ensure single stained control samples are exposed to similar washes, in 96 well plates or individual FACS tubes.

#### 2.3.8.6 Data Acquisition I using Fortessa

27. Acquire data using BDFortessa flow cytometer with pre-optimised settings as described in Table 2.3. Ensure data is acquired uncompensated, for subsequent compensation using beads.
28. Acquire optimally 5000 target events (in this case CD4<sup>+</sup> cells) gating on viable cells and CD3<sup>+</sup> CD4<sup>+</sup> cells (this is possible even prior to compensation). If 5000 CD3<sup>+</sup>CD4<sup>+</sup> events are acquired, the next sample may be run. If few cells are present, run until the sample is fully acquired. At least 500 CD3<sup>+</sup>CD4<sup>+</sup> cells should be acquired for subsequent inclusion in the analysis.

#### 2.3.8.7 Intracellular Cytokine staining

The acquisition of all samples (60-120 tubes plus compensation tubes) will take 4-6 hours, during which time cytokine stimulation will be completed.

29. Retrieve cytokine stimulation plate from incubator.
30. Remove viability staining dye from freezer and allow to equilibrate to room temperature.
31. **WASH:** Perform three wash steps as per (11) using PBS to ensure all stimulatory and Golgi-inhibiting reagents are removed.

32. Harvest stimulated and unstimulated cells for each sample into 5ml tubes (**'viability tubes'**). There will be two tubes generated for each sample. Harvest in 200µl PBS and pool both 'cocktail 4' and 'cocktail 8' samples for each sample and each of stimulated and unstimulated, giving a total of 400µl cell suspension x2 for each sample. Hence if there are 20 samples, there will be 40 resultant tubes each containing 400µl cell suspension, half stimulated, half unstimulated, requiring a total of 40µl of viability dye.
33. Add 1µl viability dye to each viability tube and resuspend fully using 1ml pipette.
34. Incubate in fridge (2-8°C) in dark for 30 minutes
35. Prepare fresh Fix/Perm working solution and Perm buffer as described in Table 5.2. There needs to be 100µl Fix/Perm working solution and 500µl Perm buffer per well (+10% for pipetting loss).
36. Harvest cells from viability dye tubes and replate into a 96 well plate as per the plate map, this time into two wells per sample, one well for 'Cocktail 4' and one well for 'Cocktail 8'. Hence if there are 20 samples there will be 40 wells, half stained with each of the cocktails.
37. **WASH:** Perform two wash steps as per (11) using PBS to ensure all viability dye is removed.
38. Resuspend all wells in 100µl Fix/Perm working solution. Incubate at room temperature for 45 minutes.
39. Spin Fix/Perm working solution-suspended cells at 3000g for 3 minutes.
40. **WASH:** Perform two wash steps as per (11) using Permeabilisation buffer working solution.
41. **STAIN:** Apply staining cocktails (according to final total volumes calculated in 2., in this example 60µl per sample) simultaneously using multichannel pipette.



Ensure on dispensing each 60µl aliquot, the cell pellet resulting from the previous centrifuge step is entirely resuspended with a partial volume aspirate/flush technique that itself does not introduce air bubbles into the sample. Air bubbles impair uniformity of staining and surface tension leads to problems with the 'flick' supernatant disposal technique.

42. **INCUBATE:** Place plates in dark for 30 minutes at room temperature.

#### 2.3.8.8 Final Wash and Transfer to FACS Adaptor Tubes

43. **WASH:** Perform one further wash steps as per (11) using Permeabilisation buffer.
44. During centrifuge steps label appropriate number of adaptor tubes to correspond with plate maps, one tube to receive the contents of one well. Load adaptor tubes into suitable racks as for the plate map (empty 1000µl pipette tip dispenser is ideal: Figure 2.7).
45. Resuspend final cell pellets in 200µl 1:2000 PBS, and transfer into receiver tubes.
46. Top up receiver tubes with further 200µl PBS such that each contains 400µl stained cell suspension ready for analysis.

#### 2.3.8.9 Data Acquisition II using Fortessa

47. Acquire data using BDFortessa flow cytometer with pre-optimised settings as described in Table 2.3. Ensure data is acquired uncompensated, for subsequent compensation using beads.
48. Acquire optimally 5000 target events (in this case CD4<sup>+</sup> cells) gating on viable cells and CD3<sup>+</sup> CD4<sup>+</sup> cells (this is possible even prior to compensation). If 5000 CD3<sup>+</sup>CD4<sup>+</sup> events are acquired, the next sample may be run. If few cells are present, run until the sample is fully acquired. At least 500 CD3<sup>+</sup>CD4<sup>+</sup> cells should be acquired for subsequent inclusion in the analysis.

### 2.3.9 Threshold Gating Strategy: Selection of Control Populations

#### 2.3.9.1 Unstained Controls

All particles possess intrinsic autofluorescence, biological particles such as cells particularly, and active or dying cells tend to autofluoresce more readily, in some wavelengths more than others. Hence to determine fluorescence of biological particles conferred by binding of a fluorochrome over and above the autofluorescent 'noise', unstained similar cells should have their fluorescence measured in all channels prior to acquiring stained cells in order to determine the difference. However, there will be non-specific binding of any fluorochrome-conjugated antibody in a system. This will lead to increased fluorescence of a cell without it possessing the cognate antigen (Figure 2.8).

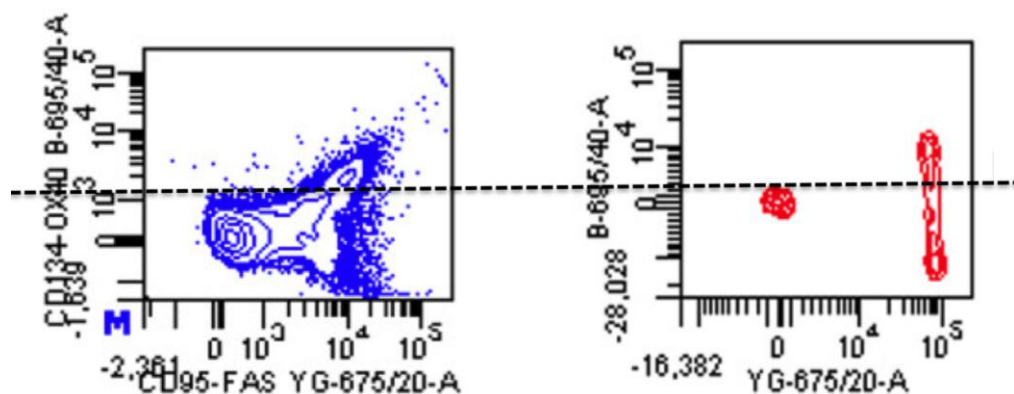


**Figure 2.8:** Threshold determination for gating: The problem of compensation. This figure is to illustrate the difficulty of determining gating thresholds in a multicolour system in which substantial compensation is required. On the left, a mixed cell population is stained with a 10 colour cocktail of antigens. It is known that a substantial proportion of the cells are CD95+ (the antibody conjugated to PE-Cy5, read from the YG-675/20 channel. However an unknown portion are stained with OX40+ PerCP-Cy5.5 (read from B695/50). Right: Setting the threshold as shown by the dotted line would be erroneous since for the single stained bead population shown here, only stained with PE-Cy5, the positive populations shows considerable overspill into the PerCP-Cy5.5 channel. Hence true expression of OX40 is difficult to establish in this population and FMO controls would be useful.

### 2.3.9.2 Isotype Controls

A simple control for this non-specific fluorescence present even in unstained cells is the isotype control. An isotype control possesses the immunoglobulin portion appropriate for the fluorochrome conjugate of interest, and as such the same non-specific binding properties, conjugated to that same fluorochrome, but without specificity for antigen within the sample under investigation. However, variability between isotypes, which are manufactured from a variety of hybridomas, may be considerable. Additionally, the non-specific binding and fluorescence conferred by isotype controls is often quite different to that encountered when a population negative for a particular antigen is exposed to a fluorochrome-antibody conjugate specific for that antigen. Additionally, compensation algorithms often distort negative populations with significant spectral overlap: a feature that cannot be accounted for by isotype fluorescence (Figure 2.9). Hence the isotype control is entirely inappropriate for definition of the negative/positive threshold in complex multicolour flow cytometry<sup>369, 370</sup>.

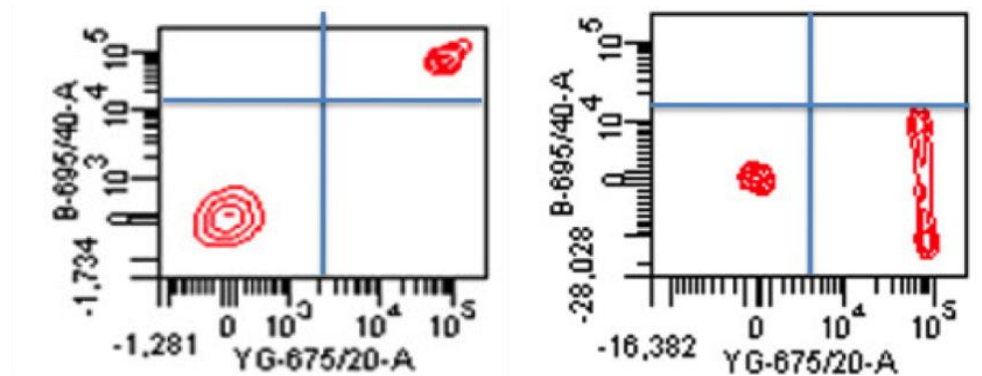


**Figure 2.9:** Compensation step 1: using beads. PE-Cy5 stained beads (read by the YG-675/20 output channel) with internal negative control beads shown as example, plotted against the PerCP-Cy5.5 output channel (B-695/40-A). LEFT: Prior to compensation, the beads stained only with PE-Cy5 appear brightly positive in the PerCP-Cy5.5 output channel due to spectral overlap. Applying a correction algorithm to the read-out in the YG-675-20 channel improves the discrimination. However this combination proved the most challenging to compensate, and it should be highlighted that fluorescence up to the 4<sup>th</sup> log decade is still apparent, despite the population being unstained for this fluorochrome, and substantial expansion of the y axis into negative log decades is necessary to illustrate the resulting mathematical distortion. These factors must be taken into account before attributing expression of antigen to a population apparently fluorescing in the channel in which there is this degree of interference and my require validation with alternative fluorochrome combinations.

#### 2.3.9.3 Fluorescence minus one (FMO) and blocking techniques

In order to discriminate non-specific fluorescence and apparent fluorescence arising from spectral overlap an antigen-specific blocking step could be carried out, or the fluorochrome conjugate for that antigen excluded in a control sample, with the difference in profile resulting from omission or blocking enabling a positive threshold to be set: the fluorescence uniquely conferred by addition of that fluorochrome. The major drawback of this technique is that in order to remove a single probe one at a time from a multicolour system, the number of resultant replicates required is multiplied enormously, and there will usually be insufficient sample for this, while reagent costs and data to be analysed also increase enormously. FMO is also unable to account for the combined contribution of a number of antibody/fluorochrome conjugates to the fluorescence detected in a channel, and would require fluorescence-minus-two, three and more for full exploration. This is unfeasible.

#### 2.3.9.4 The internal negative and positive controls (Figure 2.10)

The ideal control in a system will be a cell with similar biological properties of size, shape, internal complexity and viability, present within the same analysed sample or batch, but lacking any of the antigens under investigation (negative control), along with other cells in the same sample possessing one or more of the antigens (positive control), and discriminable from one another by staining for another known antigen (e.g. CD3 or CD20). The advantage of the panel of antigens analysed in this experiment is that they are all well described and in many cases differentially expressed by T and non-T populations in various activation states. A pilot experiment was performed to determine a 'common control' tube that could be run as part of every experimental batch in which populations of T and non-T cells both expressing and not expressing the antigens of interest were represented as comparator to the 'unknown' experiment samples. This optimisation experiment included tonsil, peripheral blood and CHL under resting and stimulated conditions. The stimulated condition was exposure to staphylococcal enterotoxin B for 72 hours since this stimulus was found to induce proliferation without significant apoptosis (unlike phytohaemagglutinin which induced significant apoptosis) in unfractionated lymphoid populations. It was found that unstimulated tonsil and

lymph node comprised the most diverse population of cells suitable for an internal negative/positive control for the greatest range of antigens of interest.

This method has been cited as the preferred threshold gating strategy by several groups<sup>369</sup>.

Any antigens whose expression remained ambiguous due to compensation problems or the absence of internal controls could then be analysed in separate experiments using alternative fluorochrome combinations containing less parameters, or validated using alternative methods of protein expression analysis.

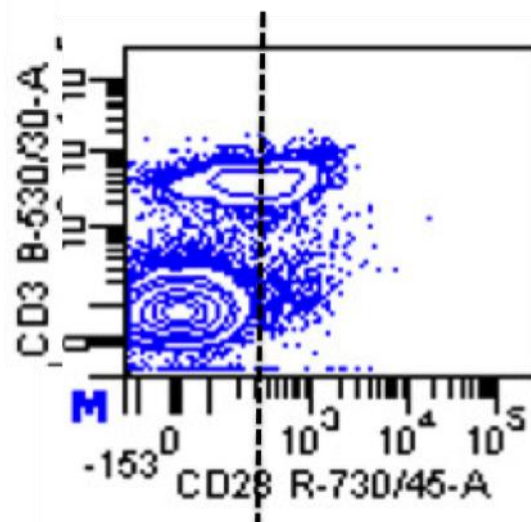


**Figure 2.10:** Threshold determination for gating: The internal control; The CD3 negative population should predominantly not express CD28, a T cell specific marker, which enables threshold to be set for this marker as shown. No isotype is necessary since the CD3neg fraction has been exposed to all other antibodies/flurochromes.

### **2.3.10 Data Acquisition and Analysis**

Multicolour flow cytometry requires a methodical strategy in order to robustly and reproducibly ensure maximum discrimination of populations expressing and not expressing the target antigen, expressed as a percentage of a defined parent population, and if possible discriminate degrees to which different populations express an antigen, by measuring median fluorescence intensity (MFI), which bears a non-linear relationship to actual number of molecules expressed on each cell. In order to examine CD4+ T cell-specific expression of each marker of interest, a common gating strategy was applied to

all samples as shown in Figure 2.11a&b. Each marker was reported as percentage of total viable CD3+ CD4+ cells which were positive, or in the case of ICOS and CD95, percentage positive and percentage bright, where clear defined populations could be discriminated.

In order to improve validity of comparisons of reported marker expression between samples derived from tissues of differing total cell viability and composition of the CD3+CD4+ cell of interest, sample data was rejected if the total number of analysed viable events was less than 1000 or the number of cells of interest (CD3+CD4+) less than 500. Figure 5.5 in Chapter 5 demonstrates the heterogeneity of viability by DAPI exclusion as determined using a uniform FSc/SSc gate across samples, where the limitations of this technique as an assessment of between sample viability is discussed.

#### 2.3.10.1 Data Acquisition using BD LSR Fortessa

Fluorescence data was acquired using the four laser BD LSR Fortessa (488 nm blue laser, 561 nm yellow green laser, 641 nm red laser, 405 nm violet laser). Voltages enabling maximal signal/noise discrimination with minimal spectral overlap using the fluorochrome conjugates and samples described in Chapters 6&7 are shown in Table 2.3.

Fluorochrome/Parameter	Excitation Laser	Filter	PMT Voltage
Forward Scatter/ Size	FSc		250
Side Scatter / Complexity	SSc		300
FITC (Fluorescein Isothiocyanate)	Blue (488nm)	530/30	450
PerCP-Cy 5.5 (Peridin-Chlorophyll A- Cyanine 5.5)	Blue (488nm)	695/40	576
Alexafluor 647	Red (641nm)	670/14	550
APC (Allophycocyanin)	Red (641nm)	670/14	550
Alexafluor 700	Red (641nm)	730/45	530
PerCP-Efluor710	Red (641nm)	730/45	530
APC-Cy 7 and Viability Dye Efluor 780	Red (641nm)	780/60	550
DAPI (4'-6-4'-6-Diamidino-2- phenylindole)	Violet (405nm)	450/50	400
Horizon V500	Violet (405nm)	525/50	475
PE (Phycoerythrin)	Yellow/Green (561nm)	585/15	415
PE-Cy5	Yellow/Green (561nm)	675/20	530
PE-Cy7	Yellow/Green (561nm)	780/60	550

**Table 2.3:** Final laser / filter and PMT voltages used for acquisition of data on LSRFortessa flow cytometer.

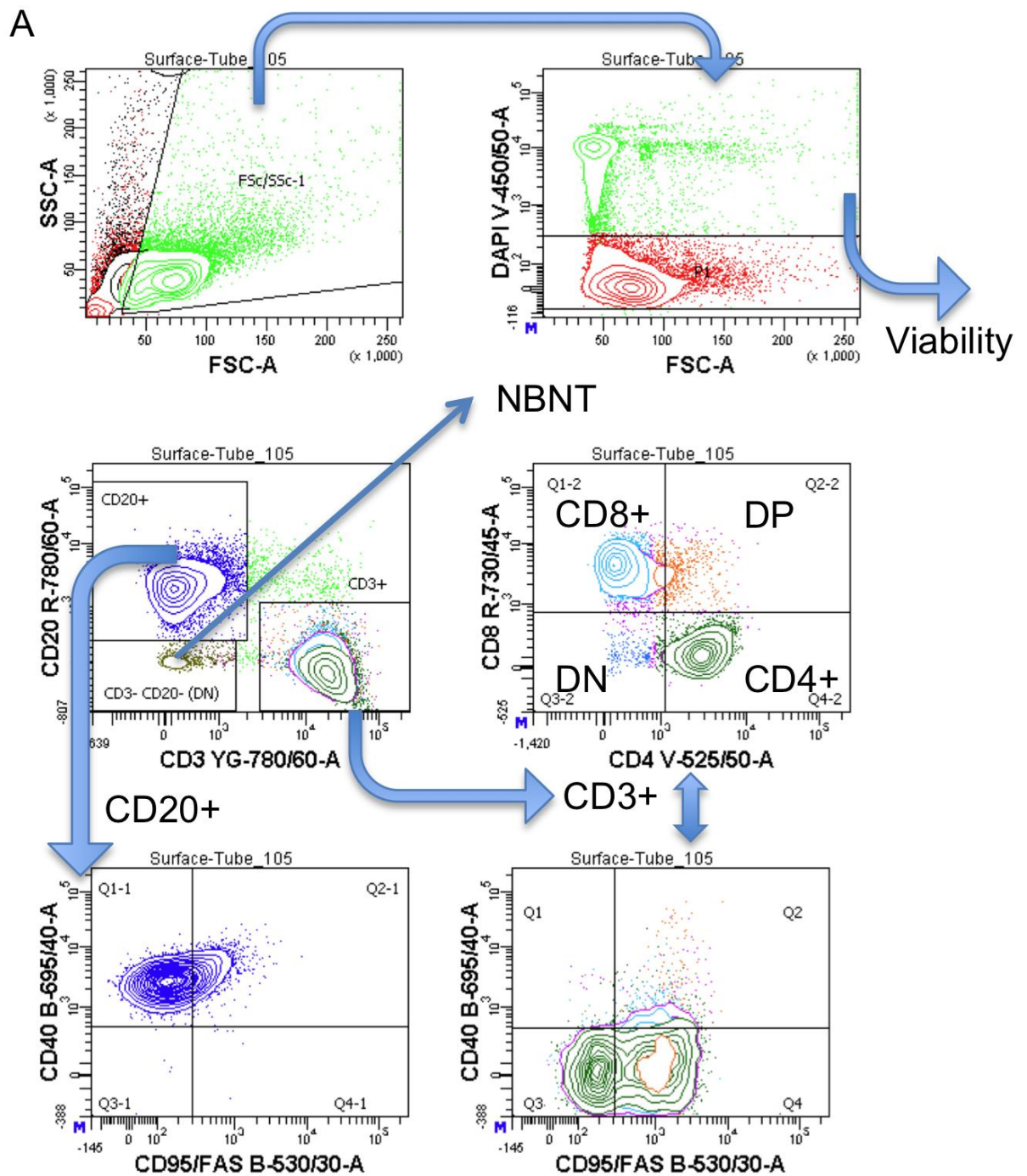
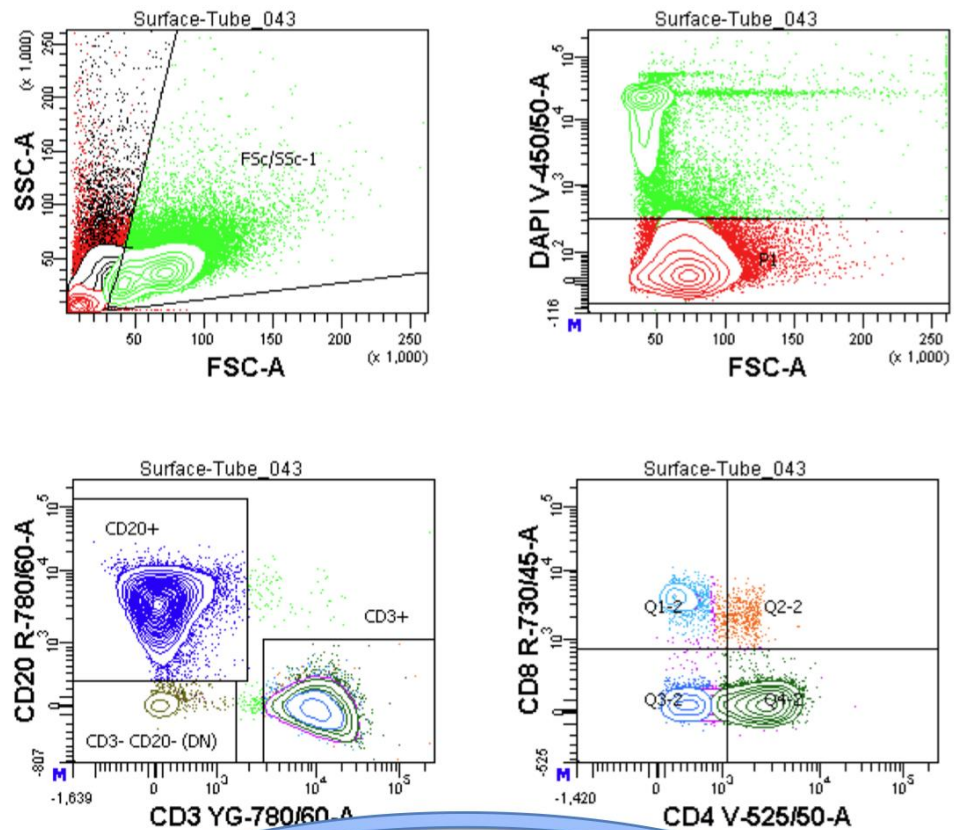


**Figure 2.11:** Gating strategy for analysis of SCS at baseline. A: SCS from CHL. Populations reported in subsequent analysis defined by gates as shown: Viable, CD3+, CD20+, NBNT, CD8+, CD4+. B (overleaf): SCS from tonsil. Validation of the multicolour compensation strategy and gating strategy is provided as indicated by the open circle – CD20+ gate are all CD40+ while CD3+ gate contains no CD40+ cells, as expected for this activated B cell-specific marker. CD95 expression analysis will be described in Chapters 6&7.



B



## Validation

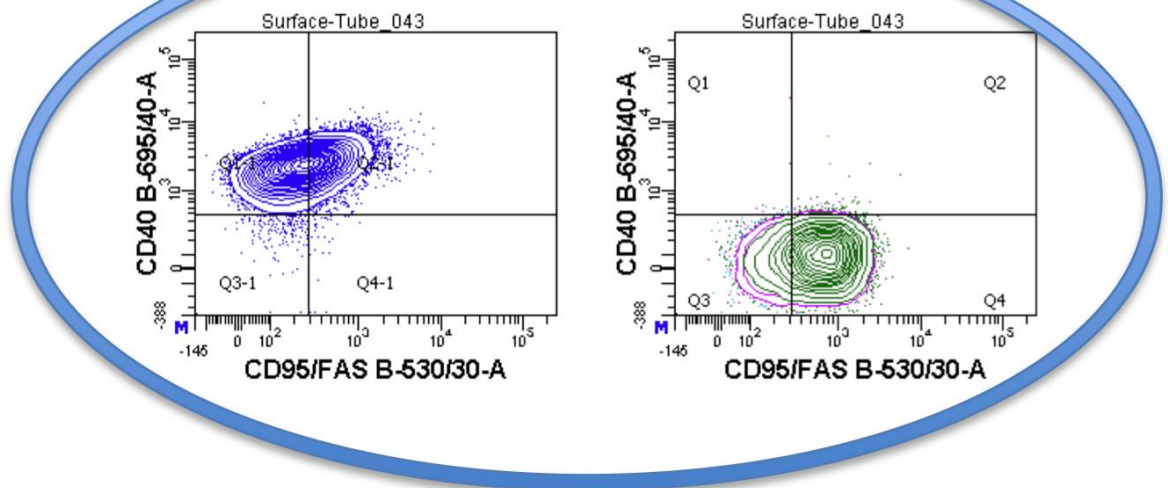


**Figure 2.11:** Gating strategy for analysis of SCS at baseline. A (previous page): SCS from CHL. Populations reported in subsequent analysis defined by gates as shown: Viable, CD3+, CD20+, NBNT, CD8+, CD4+. B: SCS from tonsil. Validation of the multicolour compensation strategy and gating strategy is provided as indicated by the open circle – CD20+ gate are all CD40+ while CD3+ gate contains no CD40+ cells, as expected for this activated B cell-specific marker. CD95 expression analysis will be described in Chapters 6&7.

### 2.3.10.2 Compensation Strategy

Compensation was carried out in two stages. No compensation was carried out at the time of data acquisition: this was all performed using the FACS Diva software after acquisition. Pre-optimisation experiments had been performed to determine the concentration of fluorochrome required to maximize signal to noise ratio without excess non-specific binding, and to determine the voltages required for amplification of signal in the photomultiplier tubes (shown in Table 2.3).

For the first stage, in order to guarantee maximum and uniform fluorescence and preserve cells within the 'unknown' experimental samples, in which expression of the corresponding antigen could not be guaranteed, beads coated with antibody recognizing the appropriate isotype for each fluorochrome represented in the panel were used in combination with uncoated beads as the internal negative control. These compensation tubes were run for each fluorochrome (6-10), but not for every conjugated antibody in order to reduce total number of tubes to be analysed and preserve reagent. Optimisation experiments had determined that for this stage of compensation, approximations for the algorithms required to correct for spectral overlap could be made using a representative fluorochrome and did not need to be replicated for every antibody in every tube. Scattergraphs were produced using FACS Diva software which plotted the appropriate output channel on the x axis, against all other output channels under investigation in turn on the y axis ('Compensation plots': Figures 2.12 and 2.13). Compensation was adjusted until the 'positive' stained beads aligned horizontally with the 'negative' stained beads by eye, and the final adjustment was made by calculating the MFI in the 'competing' channel (y axis) for positive and negative populations, and adjusting until these were equal. The two exceptions to using beads for the first compensation step were DAPI, for which a cellular population was used, and CD4-Horizon V500 since the beads themselves have substantial autofluorescence properties on exposure to the violet laser, and as such a T cell rich population was used to provide positive and negative controls: any frozen aliquot of the proliferating sample generated in Chapter 5 could be used.

**Figure 2.12 A&B** shows a composite of all such ‘compensation plots’ before (A) and after (B) applying the algorithm.

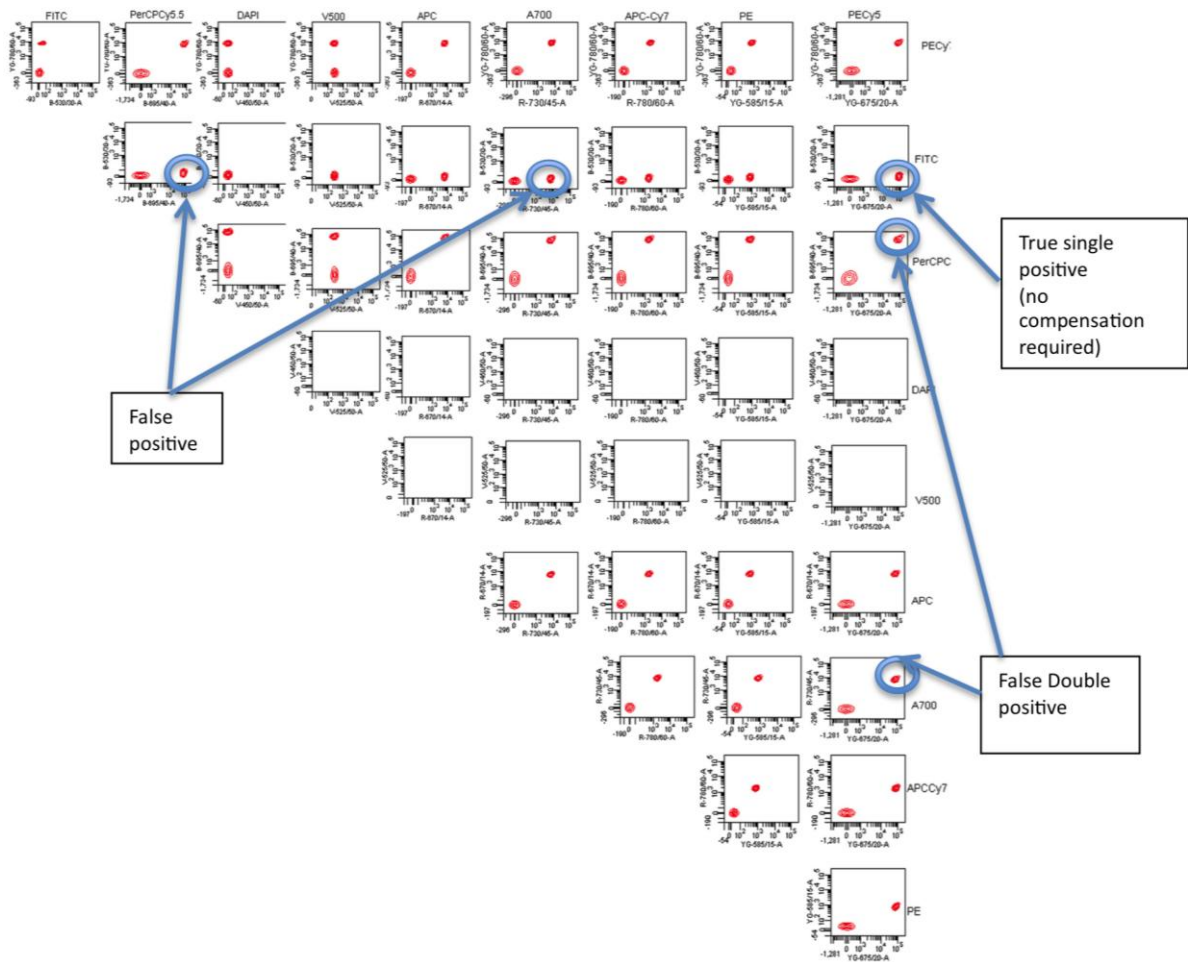


**Figure 2.12a:** Compensation step 1: using beads, pre-compensation. Composite of contour plots enabling all combinations of detector channel outputs (as summarised in Table 2.3) to be visualised. Gated on all bead F/SSc events. PE-Cy5 stained beads with internal negative control beads shown as example. Fluorochrome-equivalent channel outputs (log fluorescence intensity) are indicated by row headings (y axis) and column headings (x axis). Spectral overlap can be seen by detection of PE-Cy5 in inappropriate channels, either as a ‘false double positive’ population, or as a ‘false positive’ population. Two examples of each false population are shown, but many are present in this figure. V500 and DAPI are excluded from this plot since beads are unsuitable for single stained controls and cellular controls are necessary.

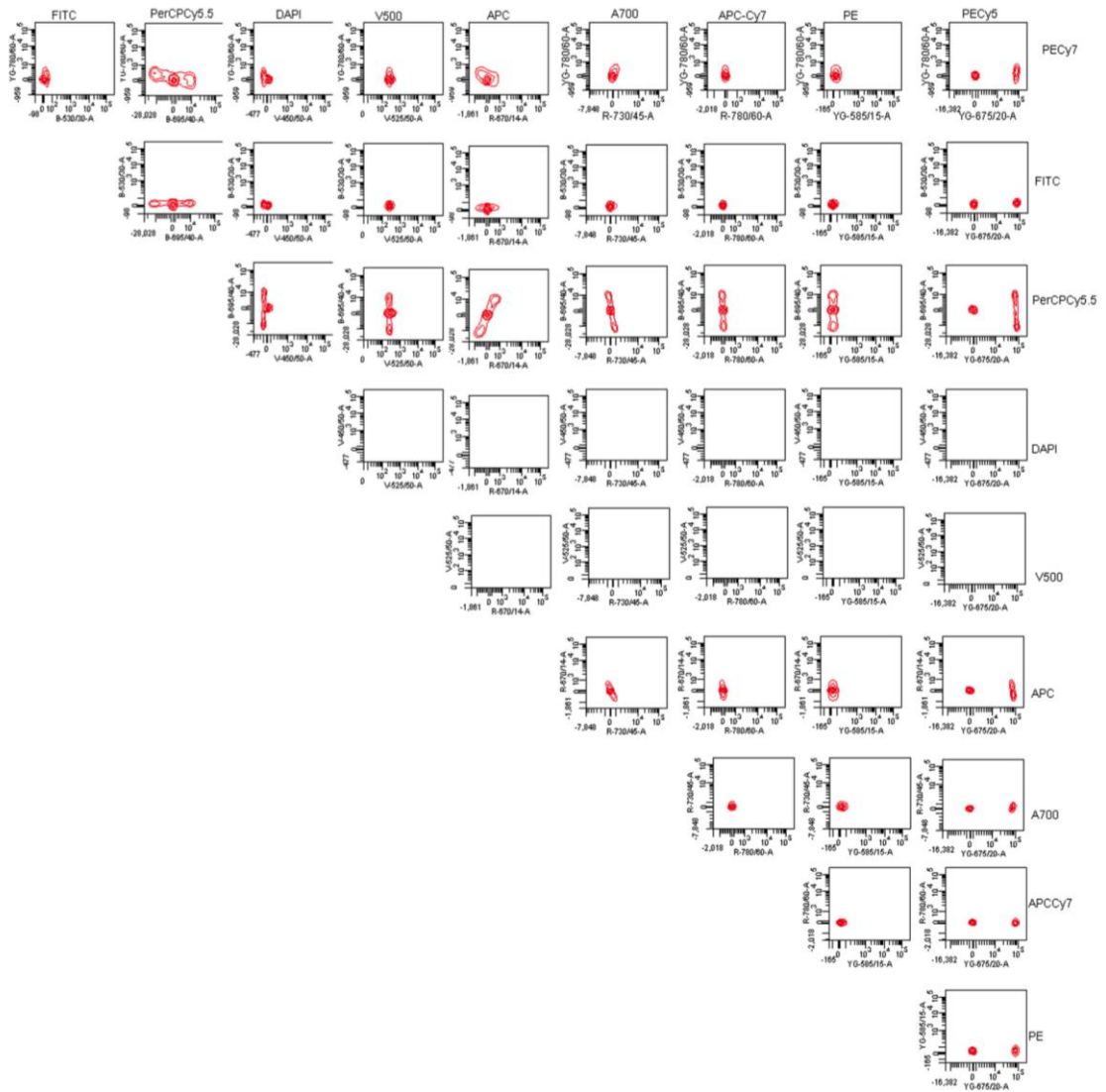


**Figure 2.12b:** Compensation step 1: using beads, post-compensation. Composite of contour plots enabling all combinations of detector channel outputs (as summarised in Table 2.3) to be visualised. Gated on all bead F/SSc events. PE-Cy5 stained beads with internal negative control beads shown as example. The compensation algorithm summarised in Table 2.4 has been applied resulting in the above fluorescence profile. Fluorochrome-equivalent channel outputs (log fluorescence intensity) are indicated by row headings (y axis) and column headings (x axis). V500 and DAPI are excluded from this plot since beads are unsuitable for single stained controls and cellular controls are necessary.

The second stage was to further augment these algorithms specifically for the cell populations being analysed, whose intrinsic spectral properties would interfere with fluorescence generated by attached markers and thus alter the compensation necessary. The bead-determined algorithm was applied to approximate the final algorithm. A cellular control was run in the same batch, in which positive and negative expression of the majority of antigens was known (see 'gating strategy' below). A figure was devised within FACS Diva plotting each sample's fluorescence in every channel for this sample, and the algorithm adjusted within FACS Diva until plots appeared appropriately compensated. Hence any inadequately or overcompensated sample could be readily visualised, and corrected, for each experimental tube, until the best compensation strategy had been applied for analysis. (Figures 2.13 A-C)

The final stage was to check every sample, using the composite compensation plots, individually, since sample to sample variation in autofluorescence was observed based on variable expression of antigens, and final adjustment of the algorithm was applied until a compromise reached which gave the clearest plots for every sample.

Table 2.4 shows the resultant algorithm used in the 10-colour experiment required for Cocktail 1 which would be modified slightly for each cocktail, but applied consistently across all samples within each cocktail's resultant analysis.

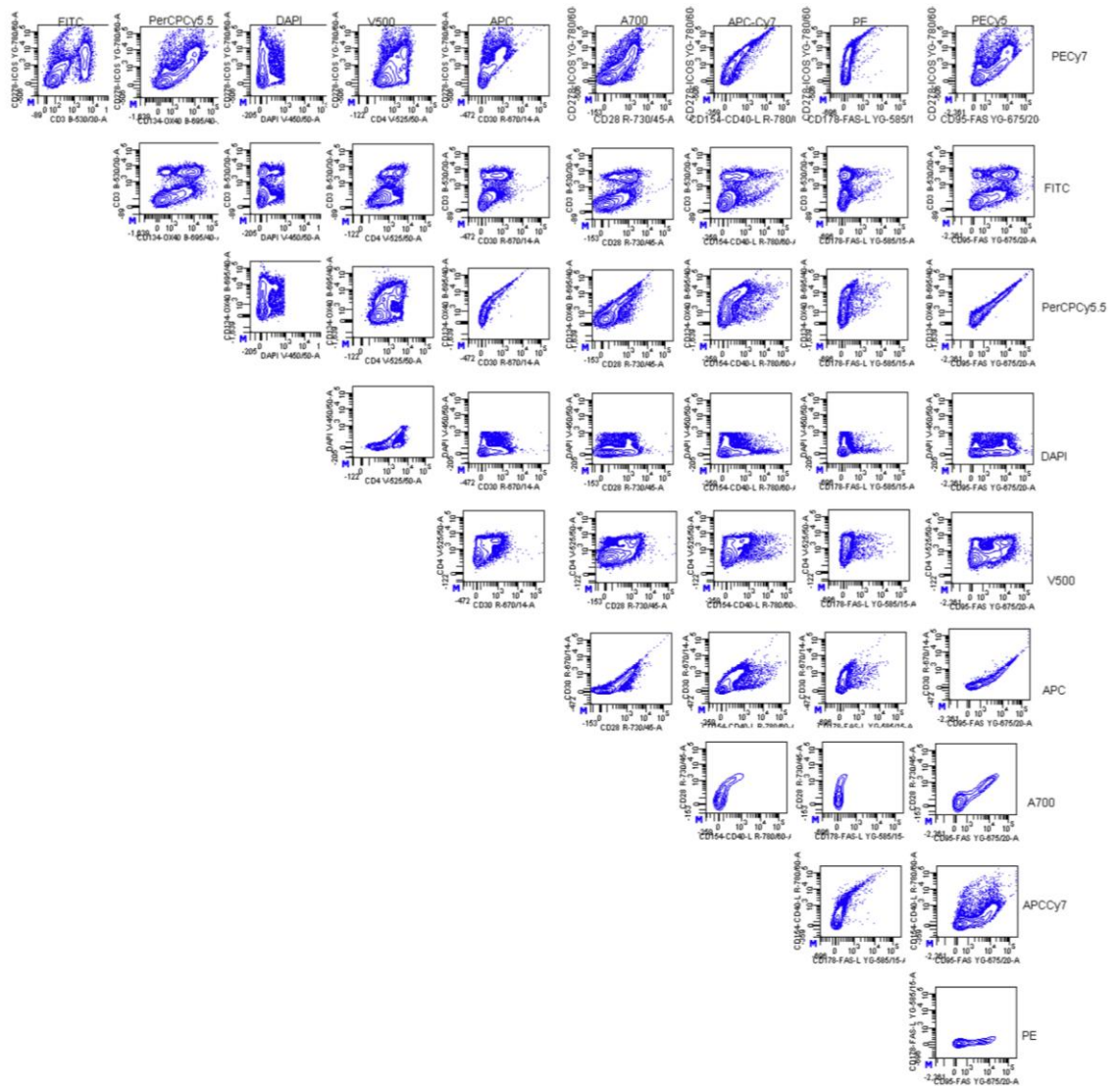


**Figure 2.13a:** Compensation step 2: sample by sample (pre-compensation). Cocktail 1 compensation, containing 9 colours, is used for illustration. Gated only on live cells (by DAPI exclusion). Substantial compensation required in many channels.

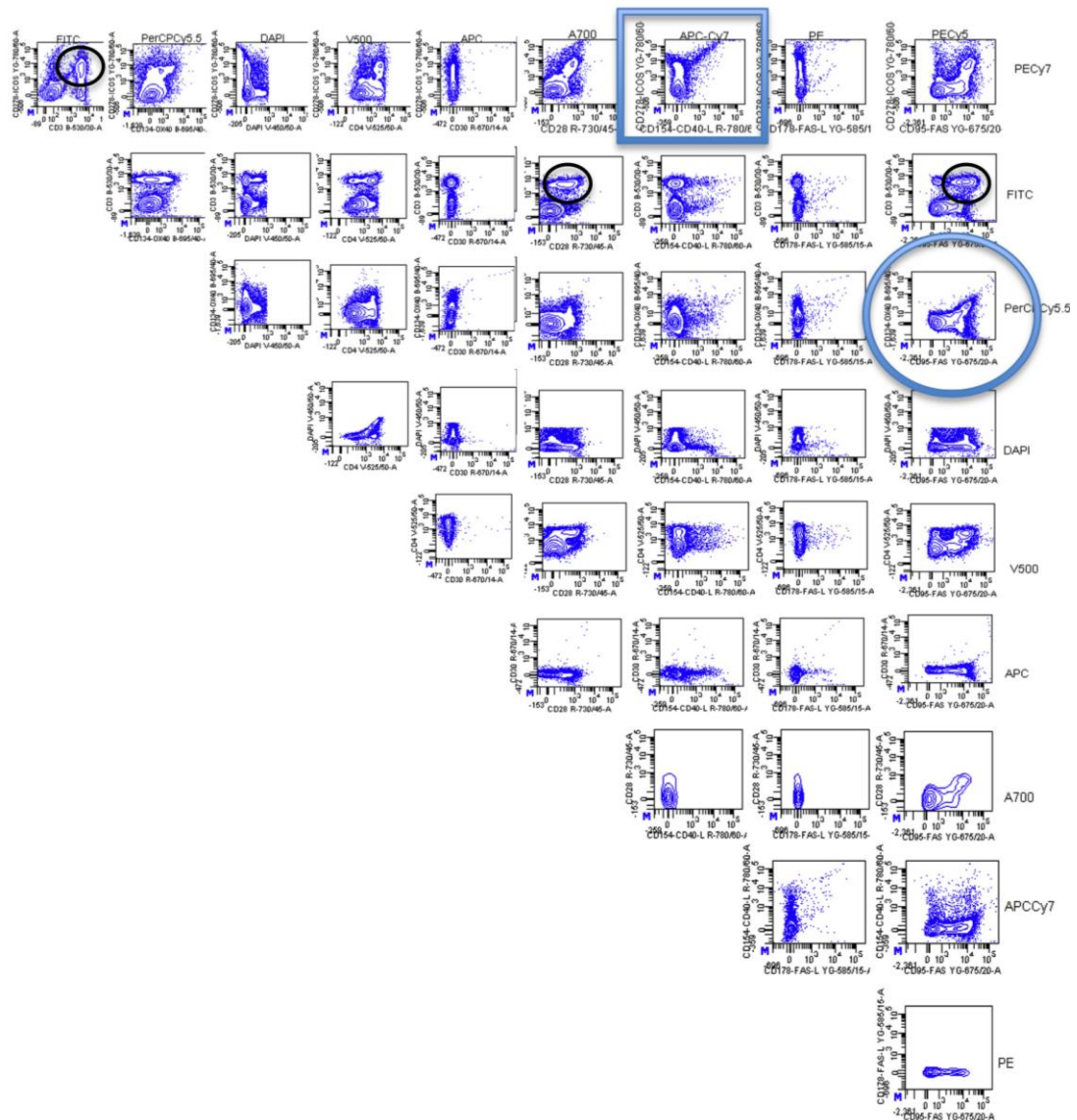


**Figure 2.13b:** Compensation step 2: sample by sample (post-compensation). Cocktail 1 compensation, containing 9 colours, is used for illustration. Gated only on live cells (by DAPI exclusion). Most plots look well compensated; the internal negative/positive controls (CD3<sup>+</sup> and CD3<sup>-</sup> differential expression of T cell specific or T cell over-expressed antigens: ICOS, CD28 & CD95 indicated for illustration with small black circles) provide valid gate positioning guides. However, spectral overlap of PE-Cy5 particularly into PerCP-Cy5.5 detecting channel (indicated by large blue circle) makes true OX40-PerCP-Cy5.5 difficult to determine. Additionally ICOS(bright) PE-Cy7 shows considerable overlap which cannot be compensated for into the APC-Cy7 detecting channel creating an artefact which is difficult to resolve (indicated by blue square).

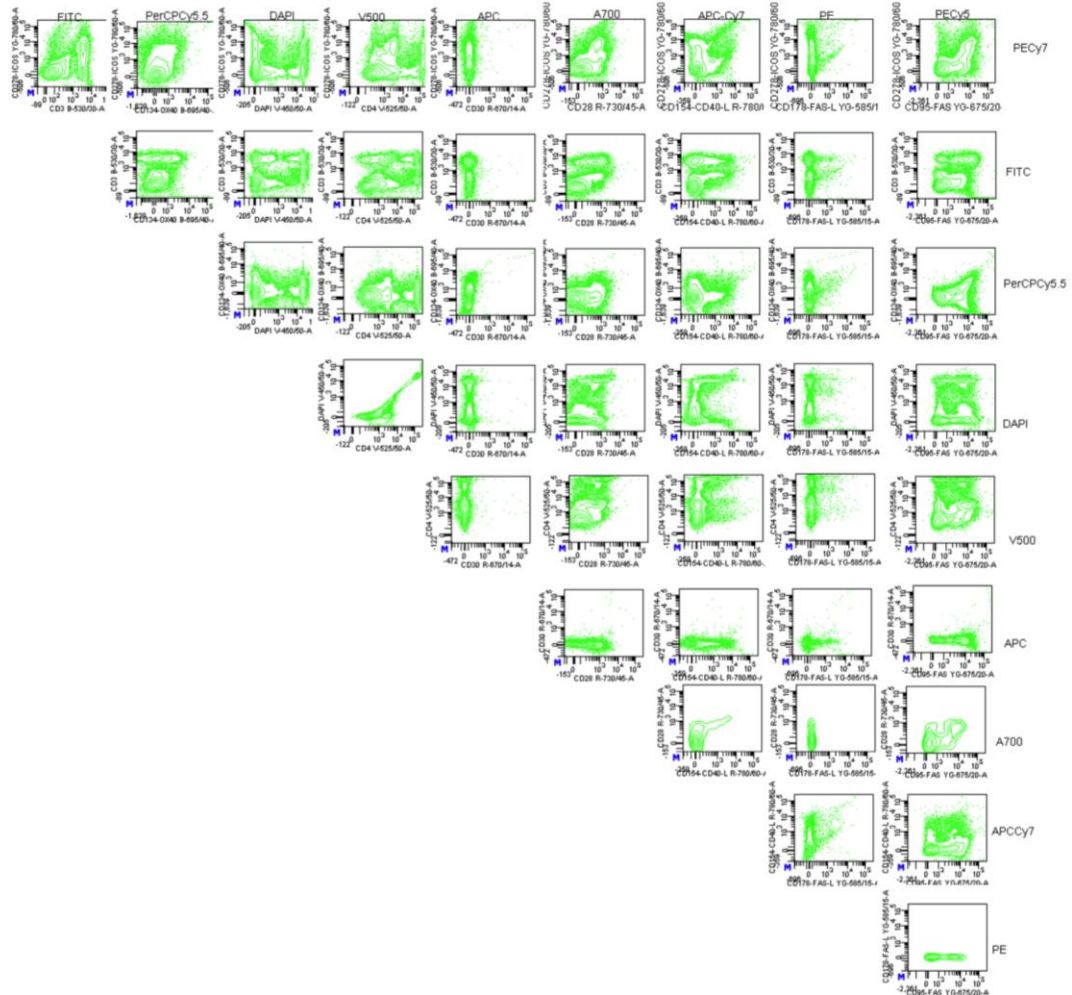


**Figure 2.13c:** Compensation step 2: sample by sample (post-compensation). Cocktail 1 compensation, containing 9 colours, is used for illustration. Importance of gating out DAPI positive events. Horizon V500 channel detects enormous spectral overlap from DAPI, hence all DAPI expressing events even at a low level must be excluded. DAPI-positive event exclusion creates a much cleaner plot (compare Figure 2.13b) with more clearly differentiated populations, since dying and dead cells autofluoresce, particularly in the red and violet spectra. This technique also enables valid comparisons to be made between samples of differing total cell viability, although the influence of proportion of viable cells within a total population on the immunophenotype of live cells live cells remains a potential confounding factor in data interpretation.



	FITC	PCP5.5	V500	APC	A700	APCCY7	PE	PECY5	PECY7	DAPI
FITC	X	2.3	9.25	0	0	0	0	0	0	X
PCP5.5	0	X	0	2.5	6.55	5	0	10.92	40	X
V500	2.6	1.45	X	2.9	0	0	0.5	0	1.55	X
APC	0	2.9	0	X	112.5	28.7	0	38.9	3.74	X
A700	0	3	0	0.5	X	23.2	0	0	5.1	X
APCCY7	0	0	0	3.15	12.6	X	0	3.9	30.78	X
PE	0.88	0	0	0	0	0.4	X	19.85	1.3	X
PECY5	0	275	0	7.36	7.88	0	0.85	X	165.3	X
PECY7	0.15	0.75	0	0	0	5.6	1.66	0.6	X	X
DAPI	X	X	X	X	X	X	X	X	X	X

**Table 2.4.** Compensation algorithm applied for Cocktail 1 analysis. The numerical values represent the percentage of fluorescence in competing channel (columns) which was accounted for by each fluorochrome (rows). Table 2.3 summarises the output channel (laser and filter applied) used for each fluorochrome. In yellow and red are values exceeding 20% and 50% compensation respectively. These values were achievable due to the presence of cross-beam compensation in the flow cytometer, enabling FACSDiva to calculate a ‘corrected’ fluorescence value based on spectral properties recorded in different output channels thus determining the likely contribution of the ‘appropriate’ fluorochrome to its own and competing channels. However in these cases, the resultant populations required careful definition of positive and negative gates, with an example of a difficult case shown in Figures 2.8 and 2.9.

### 2.3.10.3 Gating Strategy

Discrimination of positive and negative populations in flow cytometry requires the determination of arbitrary thresholds, which are specific for each experimental batch but must be applied consistency. When there are clearly defined populations, setting the threshold is not problematic. When there is a continuum of expression, this becomes more difficult, and the median or mean fluorescence intensity (MFI) may be reported as a surrogate for expression levels. However this value is more difficult to standardise from experiment to experiment, subject to more alteration by compensation algorithms, is non-linearly and non-predictably related to the actual underlying expression level of the antigen and as such is difficult to analyse particularly when applying comparative

statistics between groups. A statistically significant difference in MFI represents a difference in two values which have been considerably mathematically altered and hence abstracted from the underlying biological factor of concern. As such this statistical difference is difficult to robustly justify as a biologically relevant one, and is difficult to reproduce, being overall a relative term relevant just to that experimental batch. For this reason, MFI was not reported as a measure of expression for these experiments, but instead used to determine the gating thresholds for positive, negative, and in some cases 'bright', 'intermediate' and 'low/negative' expression of an antigen within each experimental batch. Differences in proportions of specifically defined cells falling within each threshold were then subject to statistical analysis. The object was to determine predominance or absence of populations of cells expressing the functional antigens of interest within the CD4+ compartment of CHL-lymph nodes, with normal and other malignant nodes as the comparator. Where possible, experiments were performed in batches, but where replicates or new batches were performed, new thresholds were set based on a common control used in every batch.

## **2.4 Other Statistical Analysis**

### **2.4.1 Comparison of Means and Medians of pooled samples**

For experiments in which the difference between means of pooled samples and various controls was to be determined, the distribution of the data was first analysed. If the data appeared Gaussian in distribution, an unpaired T test was performed. If the data were not Gaussian, the medians were compared using the technique of Mann and Whitney<sup>37</sup>. For groupwise comparisons, comparisons were made using ANOVA. Further discussion of the application of these tests appears in the relevant Experimental chapters. All calculations were carried out using the statistical software package Prism (Graphpad Software Inc).

### **2.4.2 Multivariate Analysis using the Cox Proportional Hazards Model**

Details of multivariate analysis applied to survival outcomes and predictive biomarkers is given within the relevant experimental chapters.

## CHAPTER THREE:

FOXP<sub>3</sub>, CD68 and CD20 expression  
in the classical Hodgkin lymphoma  
microenvironment  
are predictive of prognosis

### **3. FOXP3, CD68 AND CD20 expression in the classical Hodgkin lymphoma microenvironment are predictive of prognosis**

#### **3.1 Introduction**

As discussed in Chapter 1, classical Hodgkin lymphoma (CHL) is unique amongst the lymphomas in that the bulk of the infiltrate comprises not the malignant cells, Hodgkin and Reed Sternberg (HRS) cells, but inflammatory cells including macrophages, T cells, B cells, neutrophils, eosinophils, fibroblasts, plasma cells and mast cells<sup>1</sup>. Over 80% of patients are successfully treated to a long-term remission with conventional chemotherapy or radiotherapy-based protocols<sup>9-11</sup> but in those who are refractory to initial therapy or who relapse treatment is usually unsuccessful<sup>372, 373</sup>. In contrast, many long-term survivors suffer late effects of excessively toxic treatments, predominantly secondary malignancies and cardiovascular disease<sup>374</sup>. Established clinical prognostic indices for advanced stage disease<sup>17</sup>, such as those derived from the International Prognostic Factors Project (IPS)<sup>16</sup> are rarely used to modify treatment. Risk-adapted therapy would improve management of this disease, but this requires identification of reliable biomarkers for 'favourable' and 'unfavourable' risk patients. Such biomarkers could also provide insight into the molecular biology of the disease.

The malignant cell is probably at least as dependent on extracellular signals as from endogenous signals arising from its own mutated genome<sup>25</sup>. The macrophage appears to play a major role in tumour support<sup>44</sup> and previous studies have suggested an adverse effect of increased macrophage infiltration<sup>116, 336, 375, 376</sup>. As discussed in Chapter 1, the tumour-dominating CD4+ T cells are also important in pathophysiology, but functional data are lacking<sup>1</sup>. Studies of solid tumour immune infiltrates have found an association between adverse outcome and increased expression of FOXP3<sup>347</sup>, the marker of Tregs (Tregs), a subset responsible for suppression of aberrant immune responses. *In vivo* Treg depletion leads to tumour regression<sup>350</sup>, suggesting that their presence suppresses effective immune response to tumour<sup>348, 349</sup>. However, in follicular lymphoma and CHL

the converse is found, with increased infiltrate associated with improved outcome<sup>292, 343, 344, 351-354, 377</sup>. The role of 'bystander' B cells and other T cell subsets is more controversial, although there is evidence suggesting microenvironmental markers of B cell function are associated with favourable outcome<sup>292</sup>. The role of Epstein Barr virus (EBV) is poorly understood despite a clear association with this disease. EBV is present in the malignant cell in 20-30% of cases, associated with the mixed-cellularity subtype and disease presenting in immunosuppression and certain ethnic and age groups<sup>378</sup>. IHC and gene-expression profiling (GEP) data suggest that EBV may influence the microenvironment<sup>292, 378</sup>.

Translation of tissue microarray/immunohistochemistry (TMA/IHC) based studies to the clinic has been limited by experimental reproducibility and validity. This includes failure to apply consistent methodology, limited cohort sizes, inappropriate statistical methods (particularly optimal cut-point analysis), failure to validate findings in independent patient cohorts and the intrinsic fallibility of even expert histopathologists to count large numbers of cells across areas sufficiently large to draw conclusions regarding a heterogeneous microenvironment. Categorisation of the extent of infiltration as high, intermediate or low leads to substantial data loss and inter-observer discordance. Image analysis software can overcome some of these problems by counting huge numbers of events across larger regions, but has its own limitations.

### **3.2 Objectives**

This study set out to examine the immune microenvironment in CHL and in particular to validate three CHL microenvironment-expressed biomarkers with demonstrated prognostic significance in recent studies: the macrophage marker CD68<sup>116</sup>, the regulatory T cell marker FOXP3<sup>292, 343, 344, 354</sup> and the B cell marker CD20<sup>292</sup>. CD3, CD4 and CD8 - non-specific T, T helper and cytotoxic T cell markers - were also assessed. 10-20 HPF equivalents (2-3mm<sup>2</sup>) were assessed using image analysis software and reported as continuous variables. This approach addresses major limitations of previous IHC work, namely limited regions of tumour assessment, categorisation data loss, and inter-observer variability.

### 3.3 Methods

#### **3.3.1 Patients**

The patients for whom tissue and clinical data were available for array and subsequent analysis were identified from the St Bartholomew's Hospital (Bart's) database. This system was established in 1967 and documents clinical details of all patients presenting initially to, or referred from local hospitals to Bart's for treatment of haematological malignancy. Data on the extended follow up of patients presenting with Stage IIIA CHL has been published previously<sup>379, 380</sup>. This database is linked to a second database detailing stored tissue samples provided for research. First, patients were identified who had been treated for CHL at Bart's (n=1076). 219 patients were then excluded as having been treated initially at another centre and only subsequently referred for further treatment at Bart's. The database of FFPE tissue was then consulted and patients excluded if there was no record of stored tissue, or if this stored tissue could not be located (n=595). For the remaining 262 eligible patients FFPE tissue sections were cut, H&E-stained and examined by expert histopathologists (MC and HR) to confirm the diagnosis of CHL. A further 140 cases were identified as being non-CHL, laparotomy specimens containing only uninvolved splenic and nodal tissue, samples derived from patients following relapse or samples with inadequate tissue for TMA. This left 122 cases suitable for array. Outcome for patients comparing the initial Bart's treated cohort (n=857) and the cohort suitable for TMA and analysis (n=122) is presented for OS in Figure 3.1 and for freedom from first-line treatment failure (FFTF) in Figure 3.2, stratified by age and stage.

For the final analysis using all three biomarkers (CD20, CD68 and FOXP3) data from only 90 patients was available due to tissue loss and technical difficulties (see 3.3.2) however this final cohort had similar characteristics to the original 122. Characteristics of these patients are summarized in Table 3.1. Median follow up was 16.5 years (range 2-40 years). The final TMA cohort of 122, and the 90 analyzable for three biomarkers was found to be significantly enriched for advanced stage disease patients, with no representation by lymphocyte-rich disease, compared to the initial cohort of 857 (Fisher's exact test). This perhaps reflects the bulkier disease of advanced CHL providing

more tissue suitable for TMA. Enrichment for advanced stage disease, with its attendant poorer prognosis may increase the predictive power of the TMA given the increased numbers of events to then be applied to survival analysis. This technique of enrichment for advanced stage disease patients has been applied by other groups to improve the statistical power of a cohort in identifying new prognostic biomarkers<sup>16</sup>.

	% of TMA cohort (n=122)	% of patients analysed for all 3 biomarkers (n=90)	% initial cohort (n=857)	P (difference in TMA composition); Fisher
Male	65	66	62	0.66
Age>45	22	20	24	0.72
<b>Advanced (Stage IIB-IV)</b>	<b>71</b>	<b>71</b>	<b>59</b>	<b>0.019*</b>
Anthracycline-based chemotherapy	46	42	45	0.922
Alkylator-based chemotherapy	43	46	40	0.491
Radiotherapy only	11	12	15	0.454
Combined modality	39	34	35	0.364
<b>Histological Subtype</b>				
<b>Nodular Sclerosis</b>	<b>78</b>	<b>71</b>	<b>63</b>	<b>0.0011**</b>
Mixed Cellularity	20	27	21	0.897
<b>Classical Lymphocyte Rich</b>	-	-	<b>12</b>	<b>&lt;0.0001***</b>
Lymphocyte Deplete	2	2	3	0.56
EBV+ (EBER-ISH)	31	36	n/k	n/k

**Table 3.1:** Patient characteristics for the entire arrayed cohort (n=122) compared to those for which data on all biomarkers was available (n=90) and the original treated cohort of 857. The final TMAs were significantly enriched for advanced stage disease and NS subtype, at the expense of CLR compared to the total treated cohort, as determined using Fisher's exact test and highlighted in bold.

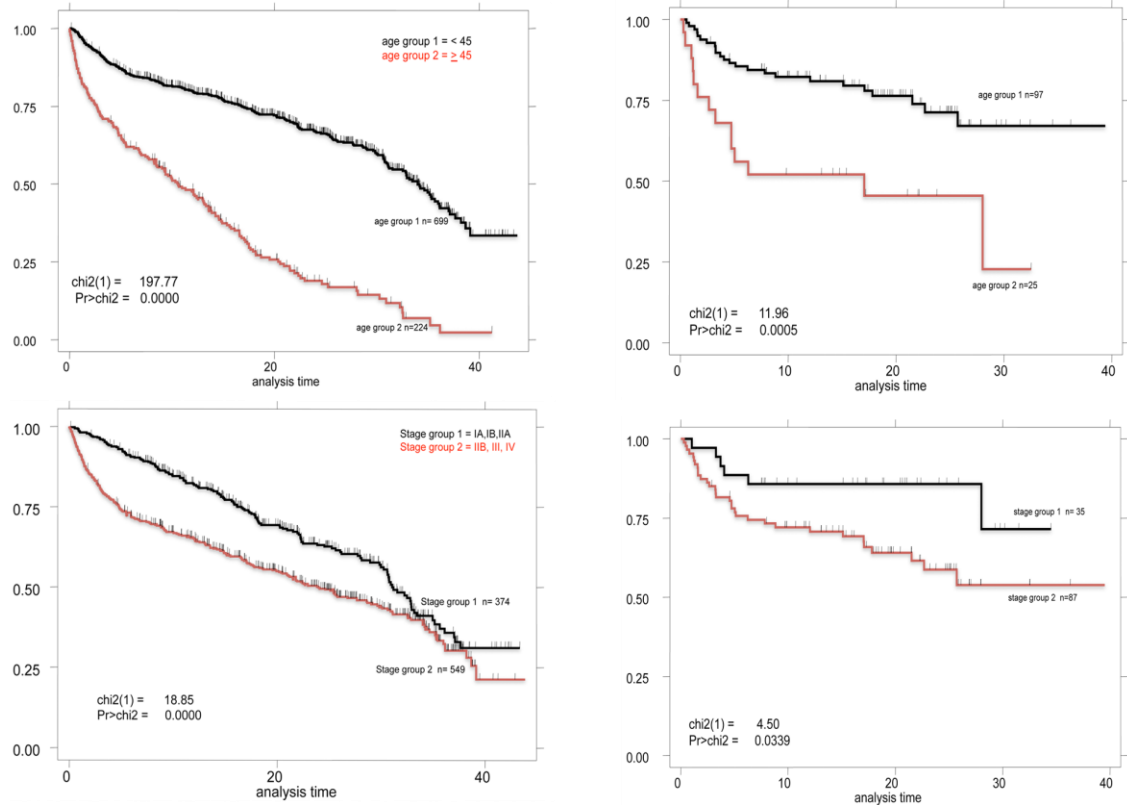


**Figure 3.1:** Kaplan Meier curves showing overall survival of all patients treated at Bart's (left) and those eligible for inclusion in the TMA analysis (right) stratified by age (top, according to international prognostic score cut-point of 45 years of age) or stage (bottom, early (stage group 1) versus advanced (stage group 2), with early stage disease being defined as stage I or IIA and advanced being defined as stage IIB, III or IV). Differences between groups were determined using the chi square method with significance defined as  $p < 0.05$ .



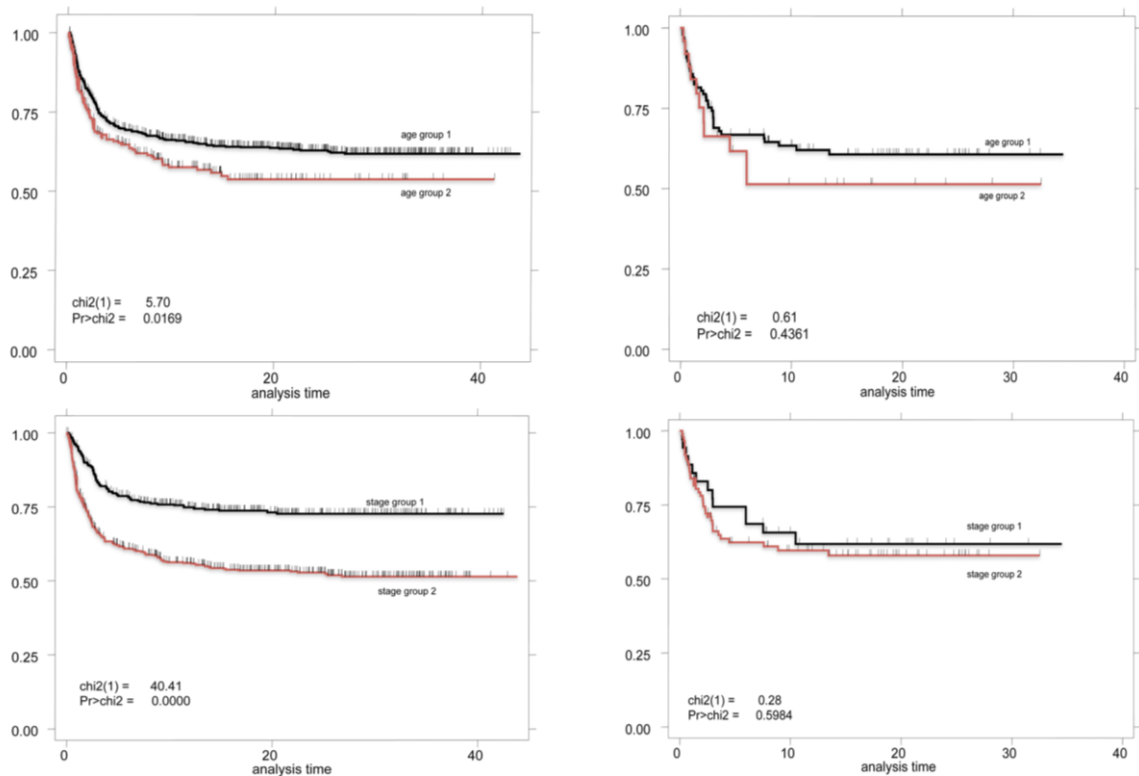


**Figure 3.2:** Kaplan Meier curves showing freedom from treatment failure of all patients treated at Bart's (left) and those eligible for inclusion in the TMA analysis (right) stratified by age (top, according to international prognostic score cut-point of 45 years of age) or stage (bottom, early (stage group 1) versus advanced (stage group 2), with early stage disease being defined as stage I or IIA and advanced being defined as IIB, III or IV). Differences between groups were determined using the chi square method with significance defined as  $p < 0.05$ .

### **3.3.2 TMA/IHC and IHC**

Triplicate  $1\text{mm}^2$  cores were taken from regions of biopsy material identified by an expert histopathologist (MC) on haematoxylin and eosin-stained sections, as being of high cellularity, containing malignant cells, avoiding fibrotic or acellular portions and confirmed to represent CHL. Sample collection followed informed, written consent in accordance with the Declaration of Helsinki. Ethical approval for this study was obtained from the local regional ethics board. Cores were arrayed into a recipient paraffin block, sectioned and transferred onto glass slides as described in 2.2.1. Staining for CD3, CD4, CD8, CD68 and FOXP3 following dewaxing and pressure-cooker antigen retrieval<sup>366</sup> as described in 2.2.5 was performed using primary antibodies and dilutions detailed in Table 3.2.

Antigen	Clone	Dilution	Supplier
CD3	SP7	1/500	Labvision
CD4	368	1/500	Novocastra Ltd
CD8	C8/144B	1/400	Dako
CD20	L26	1/2,000	Dako
CD21	2G9	1/130	Novocastra Ltd
CD68	KP1	1/8,000	Dako
FOXP3	263A/E7	1/100	Abcam
EBER ISH	Commercial kit	AS DIRECTED	Novocastra Labs

**Table 3.2:** Primary Antibodies or in-situ hybridization probes used for the experiment

To discriminate intact lymphoid follicle resident CD20+ cells from those in the malignant microenvironment (non-follicular CD20+ cells) dual-colour staining was employed, co-staining for CD21, a follicular dendritic cell-specific marker. Intact follicles were identified and with a dual-colour staining method, using a follicular dendritic cell-specific marker (CD21). Following antigen retrieval CD21 was stained using primary anti-CD21 antibody for 40 minutes, then gray SG peroxidase substrate (Vector Labs) for 10 minutes, Super-enhancer (Biogenix) for 20 minutes and SS-Label (Biogenix) for 20 minutes. After treatment with Mouse-on-mouse (MOM) block (Vector Labs) for 60 minutes, primary anti-CD20 antibody was added for 40 minutes and stained orange with AEC (3-amino-9-ethylcarbazole) peroxidase substrate (Vector Labs) for 20 minutes. Super-enhancer and SS-Label were added as for CD21. No counterstaining was applied to enhance contrast and image analysis. (Figure 3.3)

EBV status was determined using in-situ hybridization using a standard kit (Novocastra Laboratories).

### **3.3.3 Microscope slide scanning, Image Analysis and Cell Counting**

The specimens were scanned and analysed using the Ariol automated system as described in 2.2.6. For lymphoid markers, due to the homogeneous and discrete morphology of the cells, total number of positive cells was counted across each intact core. For the macrophage marker CD68 total area stained positive was determined using Ariol and expressed as a percentage of the total core area. This is due to the interdigitating, heterogeneous morphology of the cell and the fact that CD68 is a cytoplasmic marker. For CD20, images were initially 'censored' by excluding follicular regions with an intact FDC network (stained grey, as above) from the image analysis counting step, and total cell numbers in the remaining regions outside intact follicles defined as 'non-follicular'. The final counts for both total and non-follicular CD20 were then corrected for an equivalent area of  $1\text{mm}^2$ . Results were also reported per HPF enabling translation to manual histopathological techniques. Microscope technical variation means that there is no universal definition of HPF, however here it is defined as  $\times 400$  (assuming  $\times 10$  objective) with an area of  $0.143\text{mm}^2$ . The Ariol imaging system<sup>381</sup> (Genetix, San Jose, CA) was used to quantify antibody staining of the TMAs as described in 2.2.6. To standardize tumour area cellularity and enable valid comparisons, all cores were reviewed manually and the cell count accepted only if the core was intact, with  $<10\%$  total area fibrotic or acellular (Figure 3.4) Each case was entered into the subsequent analysis only if there were two or three high quality cores representing a total of  $2\text{-}3\text{mm}^2$  or  $10\text{-}20$  HPF. A mean count per  $1\text{mm}^2$  core for lymphoid markers and mean percentage area for CD68 was then calculated. From the original cohort there was further attrition of cases based on these quality criteria, but for all markers the total number of cases available was 90 or greater.

Manual validation of all counts was performed by two independent observers (RC and PG) using the method described in 2.2.6.2.

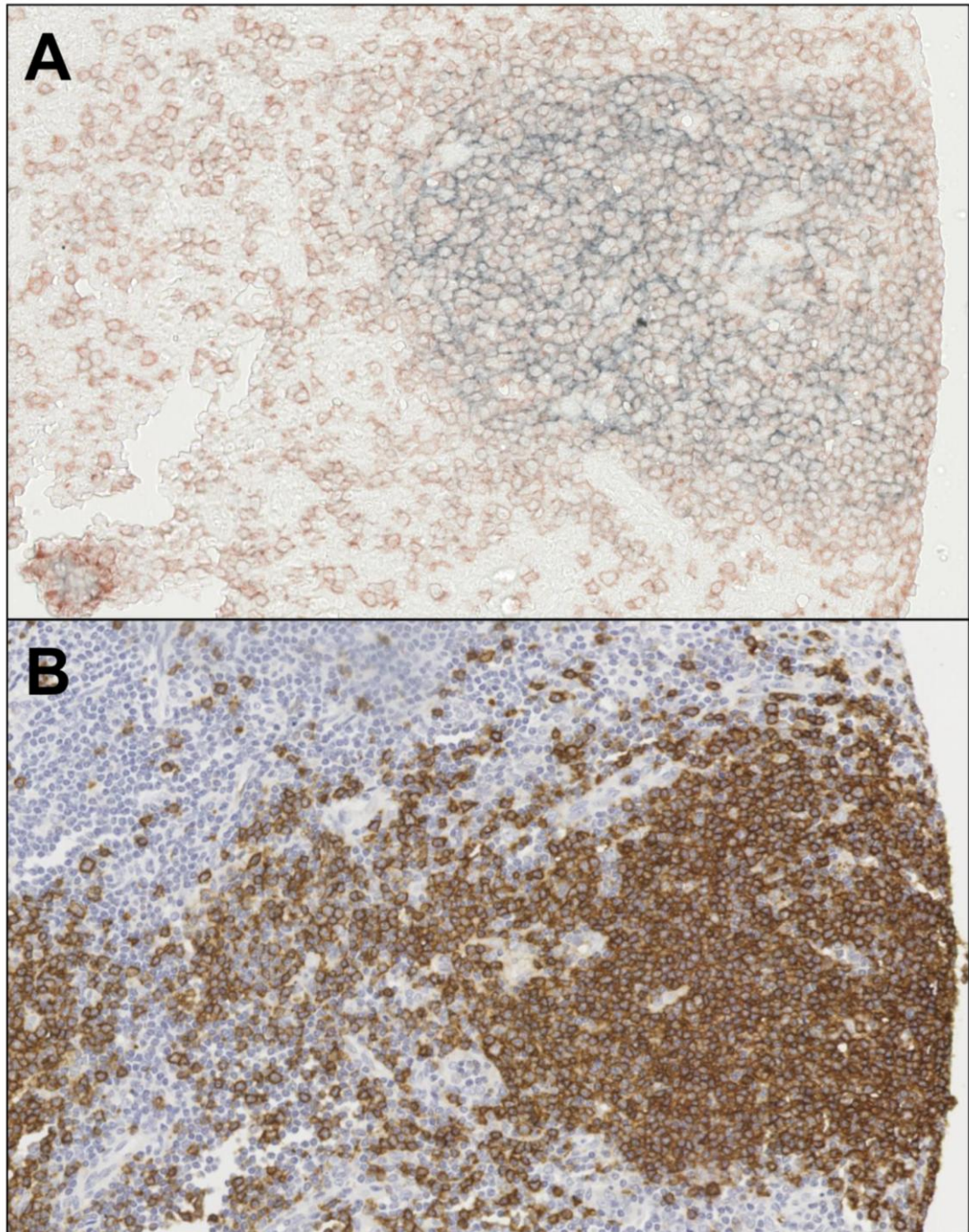


**Figure 3.3:** A: In order to discriminate follicular and non-follicular CD20+ cells, cores were co-stained for CD21 (grey) and CD20 (red) without haematoxylin counterstaining to improve contrast. B: Adjacent tissue section demonstrating standard DAB/HRP/Polymer method of staining for CD20 with haematoxylin counterstaining applied but without co-staining for CD21 preventing identification of intact follicular structures.

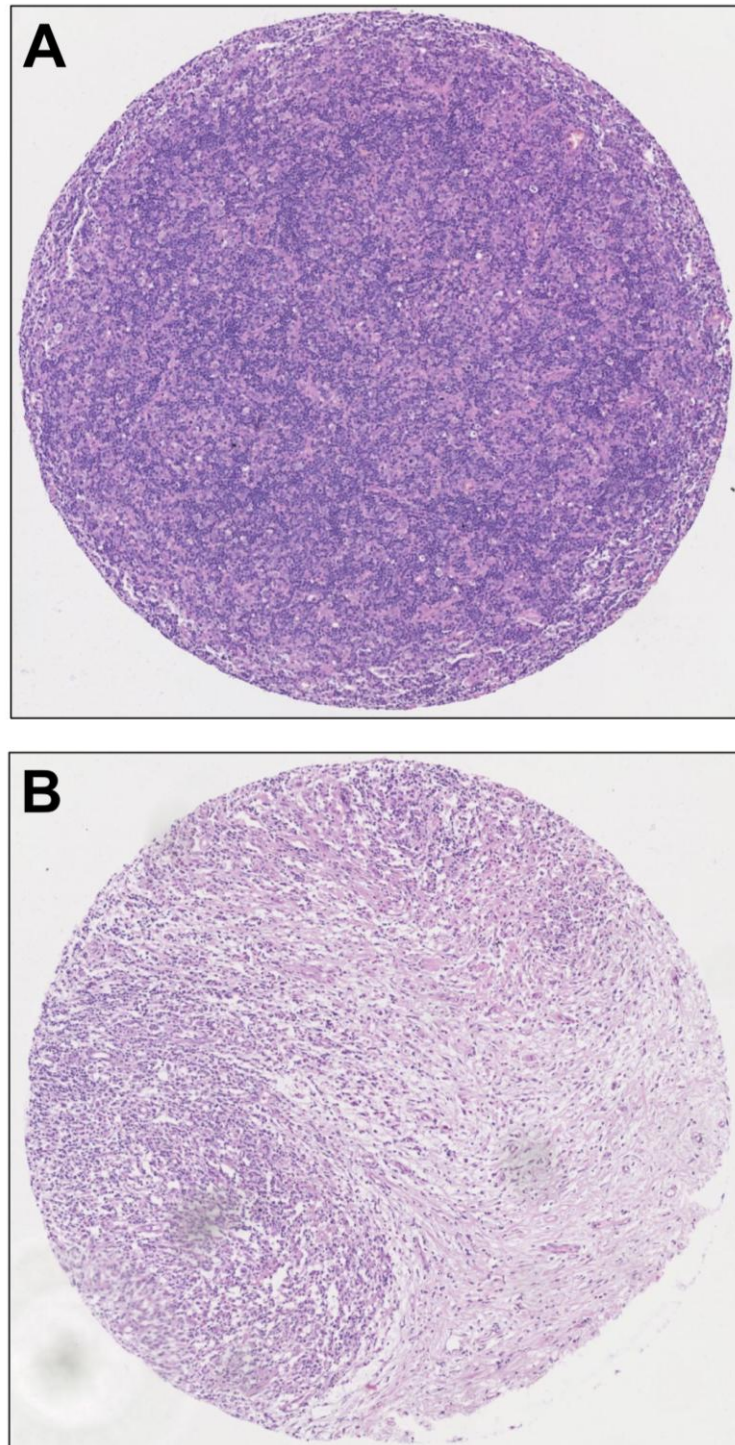


**Figure 3.4:** Example TMA cores to demonstrate quality control of samples. Only high quality, cellular cores containing HRS cells were included in analysis. Core A was deemed of acceptable quality, while core B was rejected due to excess representation of fibrous tissue.

### **3.3.4 Statistical Analysis**

To increase the robustness of statistical inferences, two independent analyses were performed; categorical and continuous data analysis. The first was a clinically applicable method, dividing patients categorically according to expression of each biomarker into cohorts based on levels of expression (high and low, or high, intermediate and low). The continuous data analysis analysed the prognostic effect of each of these biomarkers treated as continuous variables using Cox regression analysis. Outcomes, measured from date of diagnosis to occurrence of event or date of last follow-up, were overall survival (OS), the event being death from any cause, disease specific survival (DSS), the event being death from disease or complications of treatment for active disease, and freedom from first-line treatment failure (FFTF), the event being first relapse or progression of disease on first-line therapy, or therapy changed due to refractory disease.

#### **3.3.4.1 Categorical (Cut-point) Data Analysis**

Data analysis was performed using the Xtile statistical package<sup>339</sup> enabling cut-points to be determined for markers without validated 'normal ranges', as detailed in 2.2.6.3.

#### **3.3.4.2 Continuous Data Analysis**

Cox proportional hazards models were used for this analysis to obtain estimates of hazard ratios (HRs) along with 95% CIs for CD20, FOXP3, CD68 and for the clinical risk factors for each outcome. The aim was to develop a predictive prognostic score incorporating age for all patients and for patients with advanced stage disease; age, presence of stage IV disease at diagnosis, along with the clinical risk score (IPS) derived from the International Prognostic Project<sup>16</sup> (presence of >3 risk factors considered to represent high risk disease). There is no universally accepted prognostic score for early stage disease, and insufficient clinical information available to establish one for this cohort.

All patients with evaluable data were included. For the multivariate analysis the total number of cases with all biomarkers assessable was reduced to 90. We analysed the effect of all potential prognostic factors (biomarkers and clinical risk factors) for OS, FFTF and DSS using a Cox proportional hazards regression model. For each outcome,

models were formulated using forward selection procedure starting from the most significant clinical prognostic variable in the univariate analysis and adding factors, retaining only significant variables at each step. We used the backward selection method starting from a full model, to check that the prognostic factors maintained their significance in the final model<sup>382</sup>. For all analyses statistical significance was set at  $p < 0.05$ . For all patients, variables included in the backward and forward selection procedure comprised age, FOXP3, CD68 and CD20. For patients with advanced stage disease, variables included in the backward and forward selection procedure comprised age, stage IV disease (present/absent), IPS, FOXP3, CD68 and CD20. We assessed the interaction between FOXP3 and CD68 with respect to OS, FFTF or DSS. In this cohort there were 84/116 (72%) with advanced stage disease of which 77/84 (92%) had sufficient diagnostic clinical data to calculate an IPS. The proportional hazards assumption for each predictor in the final model was assessed by testing correlation between the ranked failure times and the scaled Schoenfeld residuals. The proportional hazards assumption was not rejected in any of the models. We used the final Cox regression model to derive a new prognostic index (PI).

The predictive performance of the final model was evaluated using measures of discrimination to distinguish patients with different prognostic factors. This was quantified using a Harrell's c (concordance) index, (probability of agreement between predicted and observed survival based on pairs of individuals). A value of 0.5 relates to no predictive ability to discriminate while a value of 1.0 relates to perfect discrimination of patients with different prognostic factors<sup>382</sup>. All statistical analyses were performed in STATA version 11.

#### 3.3.4.3 Manual validation of Automated Image Analysis

Comparisons of counts derived using the manual validation methods described in Chapter 2 (2.2.6.2), both between manual observers and between manual and automated methods, were carried out using the Spearman Rank correlation coefficient.

### 3.4 Results

#### 3.4.1 Categorical Data Analysis

Heterogeneity of expression of all biomarkers between patients is summarised in Figures 3.8 and 3.18. None of the biomarkers analysed were differentially expressed according to EBV status or histological subtype (Figure 3.5).

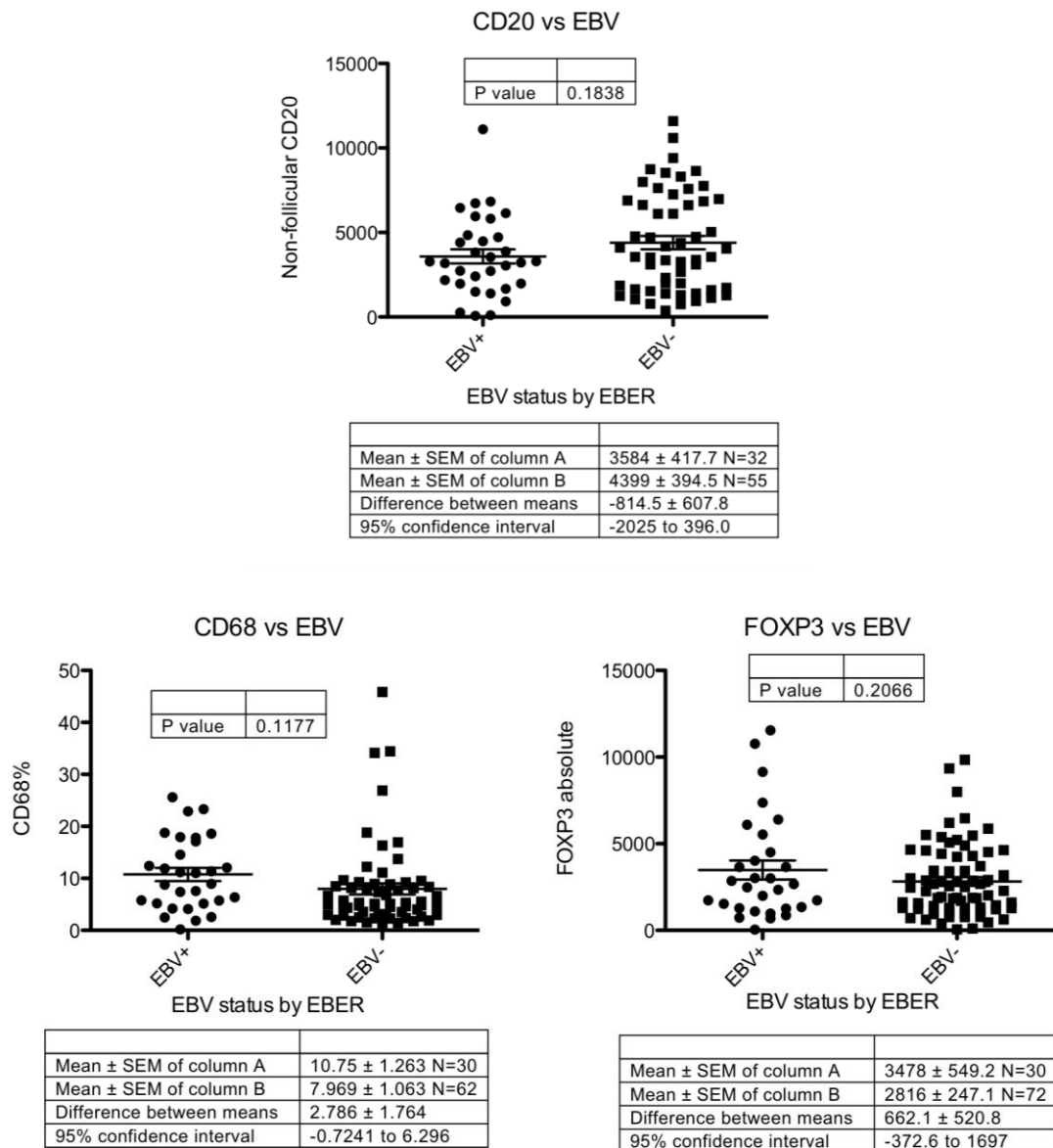


**Figure 3.5:** Mean expression of CD68, CD20 and FOXP3 was not significantly different between EBV+ and EBV- cases.



### 3.4.1.1 Prognostic significance of CD68 expression

Figure 3.6 shows the heterogeneity of expression of CD68 across the patient cohort for which 101 patients had adequate cores for assessment. Median expression of CD68 was 6.6% (Range 0.2%-45.9%). Three prognostic groups with low, intermediate and high CD68 density were defined with cut-points of <5%, 5-15% and >15% using the Xtile software, the favourable group having the lowest CD68+ density. OS was significantly different for low, intermediate and high groups ( $p=0.02$ ) with five year OS of 89%, 80% and 65% respectively. FFTF was also significantly different ( $p=0.001$ ) (Figure 3.7). The prognostic significance for FFTF was maintained in subgroups presenting with advanced (73%, 63% and 33%,  $p=0.03$ ) and early stage disease (92%, 70% and 20%,  $p=0.01$ ).

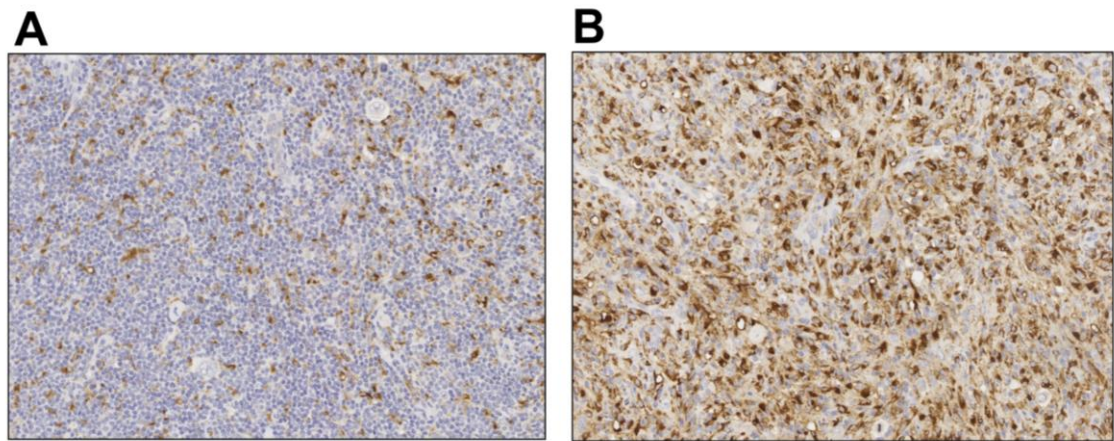


**Figure 3.6.** Variability of expression of CD68 between patients as illustrated by A: showing low infiltrate (<5% total area) and B: showing high infiltrate (>15%).

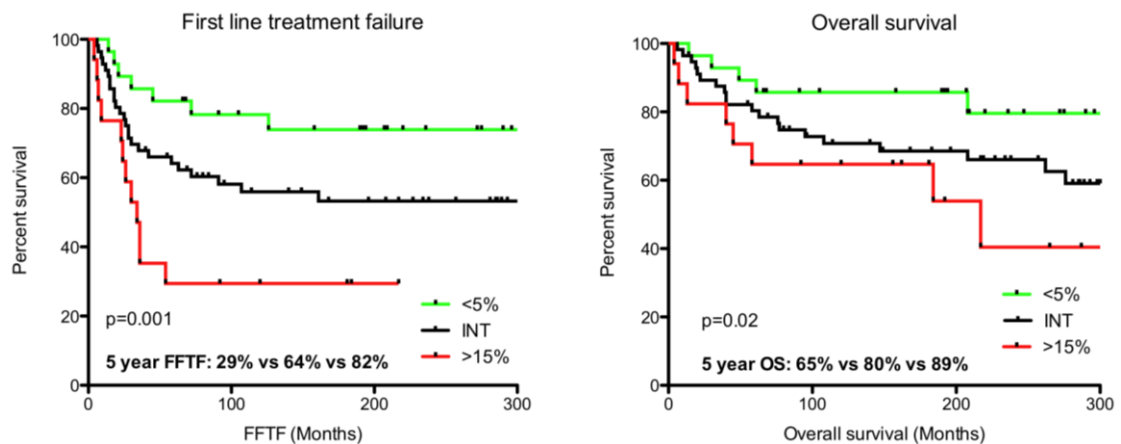


**Figure 3.7.** Level of expression of CD68 was associated with survival outcome, with increased expression associated with an adverse prognosis.

### 3.4.1.2 Prognostic significance of CD3+, CD4+ or CD8+ infiltrate

Expression levels of each of CD3, CD4 and CD8 varied considerably between patients as demonstrated for CD3 and CD8 in Figure 3.9. As expected, the median number of CD3+ cells (9080, range 1639-14136) approximated sums of the medians of CD4 (4105, range 1941-6560) and CD8 positive cells (5300, range 874-11363). Of interest, and in contrast to the literature to suggest that CD4+ cells predominate, there was a suggestion that CD8+ cells were more numerous (Mann Whitney  $p=0.015$ ), however while numbers of CD3+ cells were normally distributed, numbers of CD8+ cells were distributed bimodally and CD4+ positively skewed making valid statistical comparisons more difficult (Figure 3.8). Figure 3.10 shows optimal cut-point probability plots generated using the Xtile software for each of these markers (see 2.2.3.3 and Figure 2.5). It is apparent that very few cut-points generate patient groups for which there are significant differences in survival. This was confirmed on application of the test/validation set method.

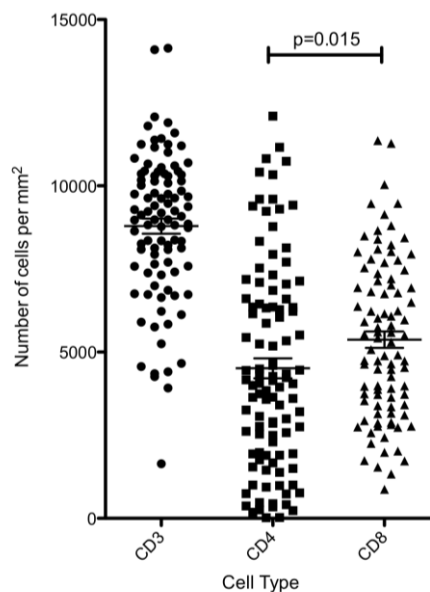


**Figure 3.8:** Heterogeneity of T cell infiltration between patients. The median number of CD3+ cells (9080, range 1639-14136) approximated sums of the medians of CD4 (4105, range 1941-6560) and CD8 positive cells (5300, range 874-11363) taken as a whole, as expected. Of interest, and in contrast to the literature to suggest that CD4+ cells predominate, there was a suggestion that CD8+ cells were more numerous (Mann Whitney  $p=0.015$ ), however while numbers of CD3+ cells was normally distributed, CD8+ cell numbers were bimodal in distribution and CD4+ positively skewed

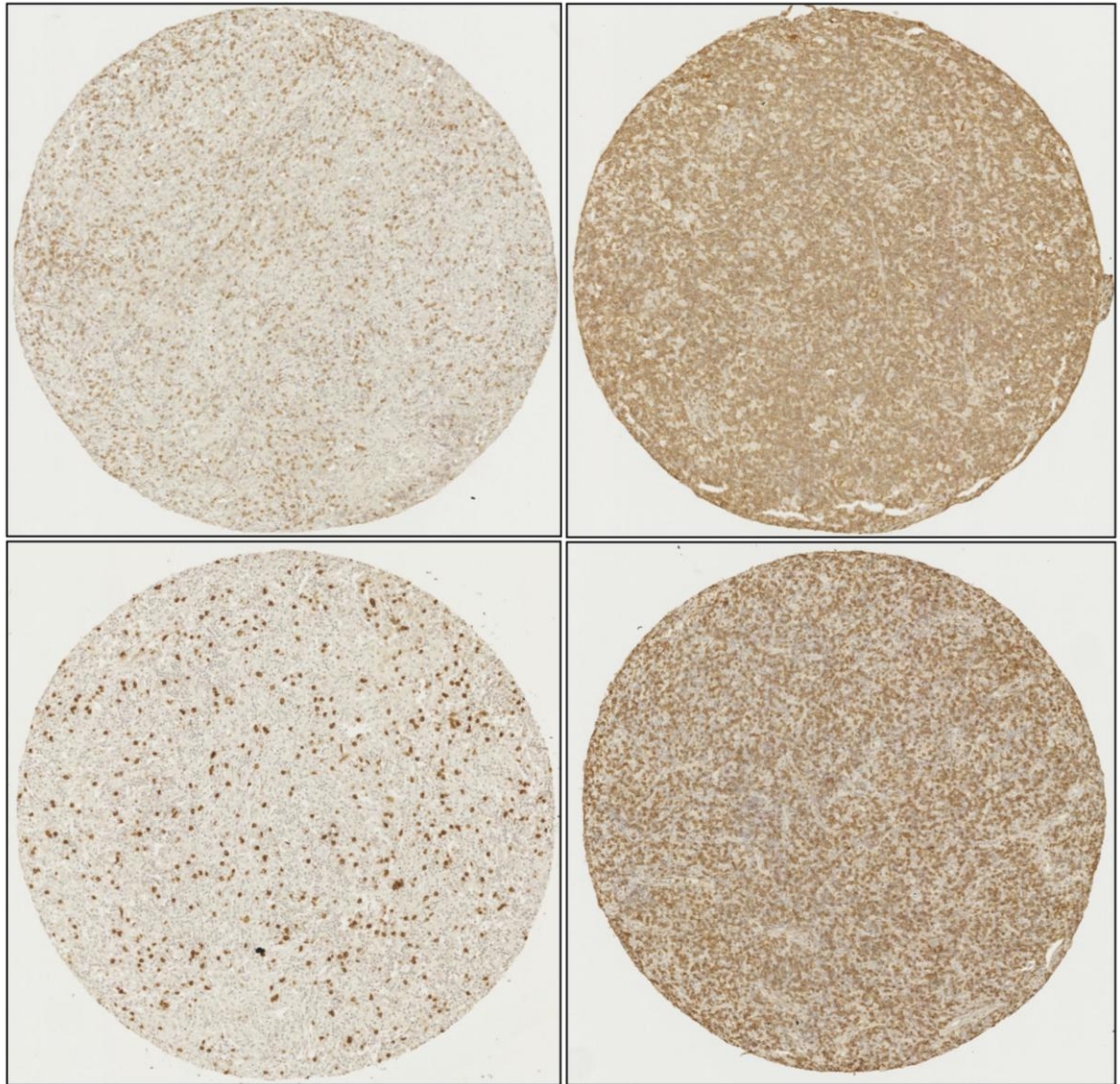


**Figure 3.9:** Heterogeneity of CD3 (top) and CD 8 (bottom) expression in the CHL microenvironment.

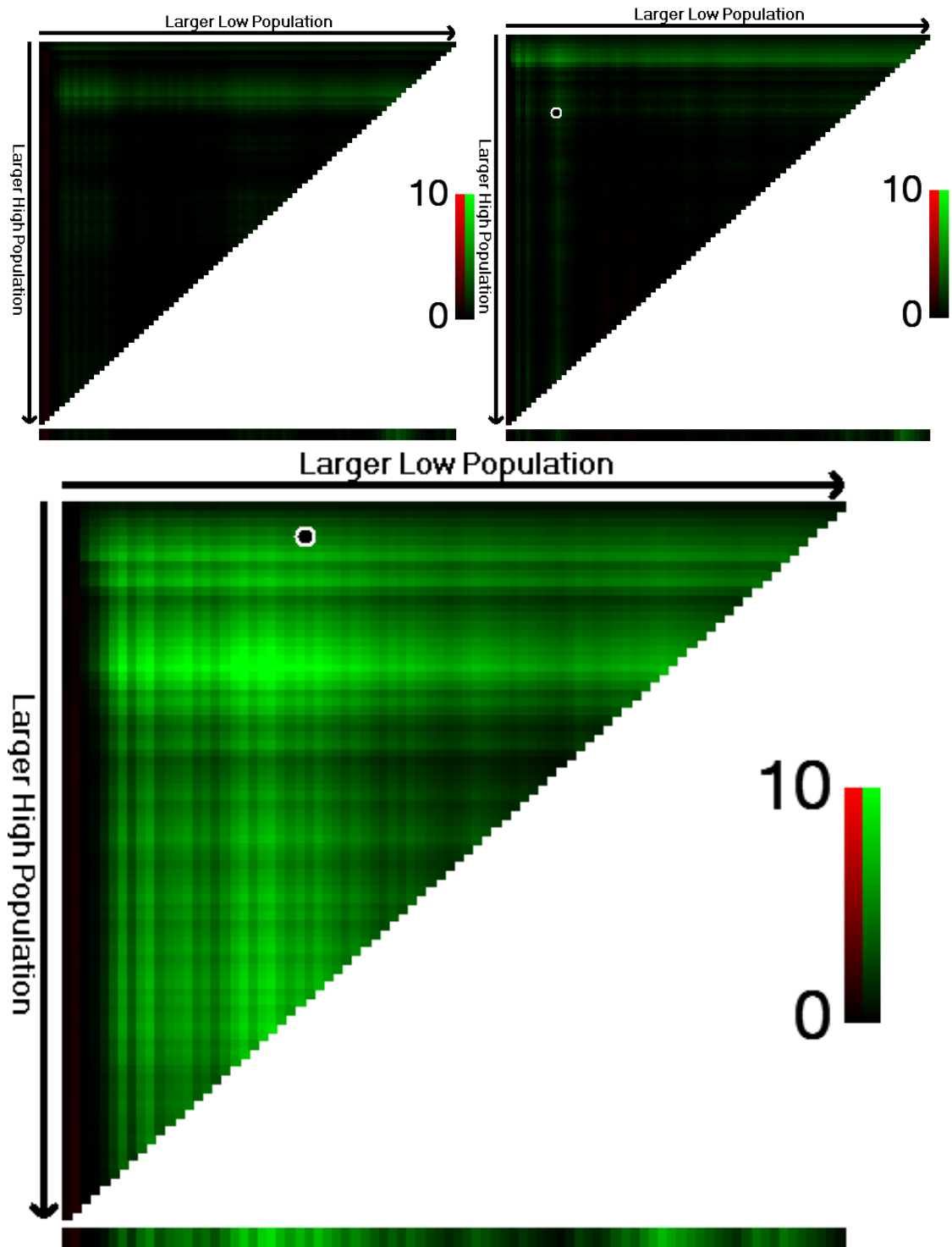


**Figure 3.10:** CD3 (top left) and CD8 (top right) optimal cut-point probability matrices showing a failure of expression level to predict outcome. Contrast the plot for FOXP3 (bottom), which has significant prognostic power. See also Figure 2.5.

### 3.4.1.3 Prognostic significance of FOXP3 expression

As described above, no significant association of overall CD3+, CD4+ or CD8+ cell infiltrate on prognosis was found. However FOXP3 cell density discriminated prognostic groups. 113 patients had adequate cores for assessment. Median expression of FOXP3 was 2346 cells/mm<sup>2</sup> or 335/hpf (range 46/mm<sup>2</sup> or 7/hpf to 11,540/mm<sup>2</sup> or 1650/hpf). Using Xtile-defined cut-points of <125, 125-500 and >500 nuclei/hpf, the favourable prognosis group had the highest FOXP3+ density (Figure 3.11). OS ( $p=0.006$ ) and FFTF ( $p=0.002$ ) were significantly different for low, intermediate and high groups, with five year OS of 68%, 80% and 94% respectively (Figure 3.12) The prognostic significance was maintained for both advanced (FFTF: 48%, 60% and 72%,  $p=0.04$ ) and early stage disease (FFTF: 57%, 67% and 100%,  $p=0.04$ ).

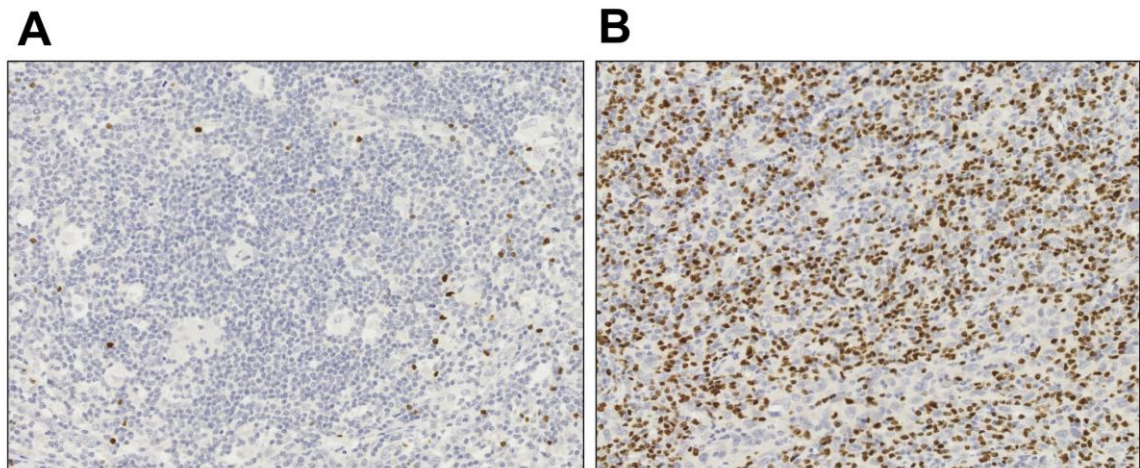


**Figure 3.11:** Variability of expression of FOXP3 between patients as illustrated by A: showing low infiltrate (<125 cells/mm<sup>2</sup>) and B: showing high infiltrate (>500 cells/mm<sup>2</sup>)

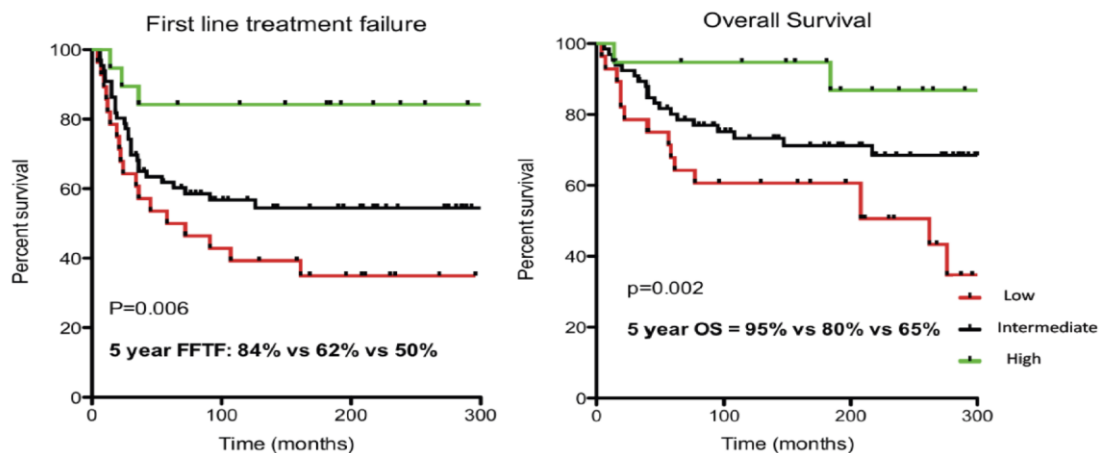


**Figure 3.12:** Level of expression of FOXP3 was associated with survival outcome, with increased expression associated with a favourable prognosis.

#### 3.4.1.4 Prognostic significance of CD20 expression

No prognostic significance was found for total CD20 expression. Non-follicular CD20 expression however was found to influence survival. 98 patients had adequate cores for assessment. Median expression of non-follicular CD20 was 3517 cells/mm<sup>2</sup> or 520/hpf (range 66/mm<sup>2</sup> or 9/hpf to 11,593/mm<sup>2</sup> or 1660/hpf). Using Xtile software a cut-point of 1700 cells/mm<sup>2</sup> (250 cells/hpf) defined two prognostic groups with low and high non-follicular CD20+ cell density (Figure 3.13). OS was improved for patients with high non-follicular CD20 expression (p=0.003), 87% versus 70% at 5 years, 84% versus 52% at 10 years and OS 76% versus 43% at 20 years (Figure 3.14). There was no significant difference by 5 year FFTF (64% vs 57%; p=0.27), or DSS (90% vs 74%; p= 0.09).

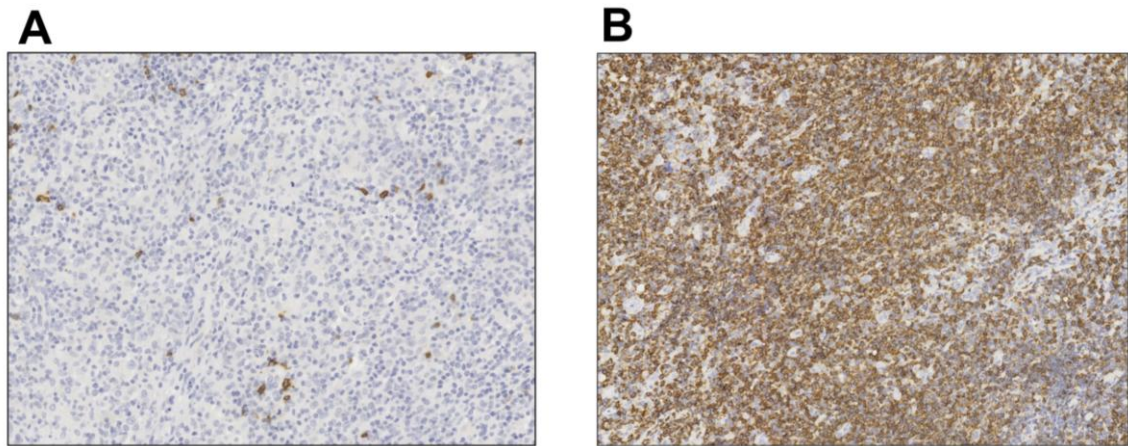


**Figure 3.13:** Variability of expression of CD20 between patients as illustrated by A: showing low infiltrate (<1700 cells/mm<sup>2</sup> / <250 cells/hpf) and B: showing high infiltrate (>1700 cells/mm<sup>2</sup>). Counting was carried out using the CD21/CD20 co-staining method but here DAB/HRP/polymer-stained samples are shown for clarity.

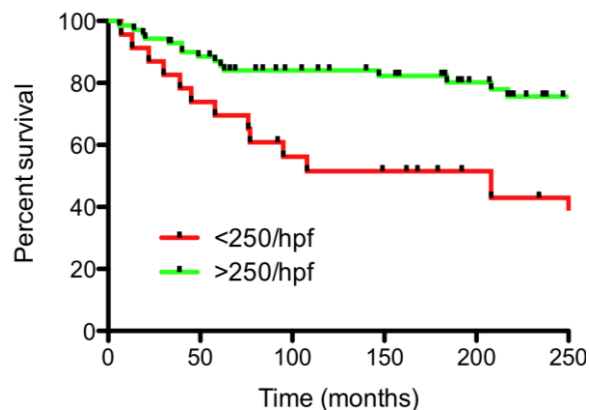


**Figure 3.14:** Level of expression of CD20 was associated with survival outcome, with increased expression associated with a favourable prognosis: overall survival was significantly improved with a greater infiltrate of CD20+ cells.

#### 3.4.1.5 A combined prognostic score comprising FOXP3 and CD68

We next sought to determine whether expression of CD68, FOXP3 and non-follicular CD20 were related, or independent variables. There was significant correlation between expression of non-follicular CD20 and FOXP3 while there was no significant correlation between FOXP3 and CD68 ( $p=0.684$ ) (Figure 3.15). We determined whether a combined score of these two markers provided additional prognostic information. Suitable cores were available for both FOXP3 and CD68 on 98 patients. Patients were allocated into a 'good', 'intermediate' or 'poor' risk combined FOXP3/CD68 score (Fox/Mac) according to the risk group for each marker individually, as described in Figure 3.16. Outcomes based on categorisation by Fox/Mac for 'good', intermediate' and 'poor' risk were significantly different for FFTF ( $p=0.0002$ ), with five year FFTF of 93%, 62% and 47%, DSS ( $p=0.03$ ), with 5 year DSS of 93%, 82% and 63% (data not shown) and OS ( $p=0.002$ ), with 5 year OS of 93%, 82% and 59% respectively (Figure 3.17) The statistical significance was maintained for both early and advanced stage patients with five year FFTF for patients with advanced stage 92%, 62% and 50% ( $p=0.03$ ) and early stage of 100%, 72% and 25% ( $p=0.03$ ).

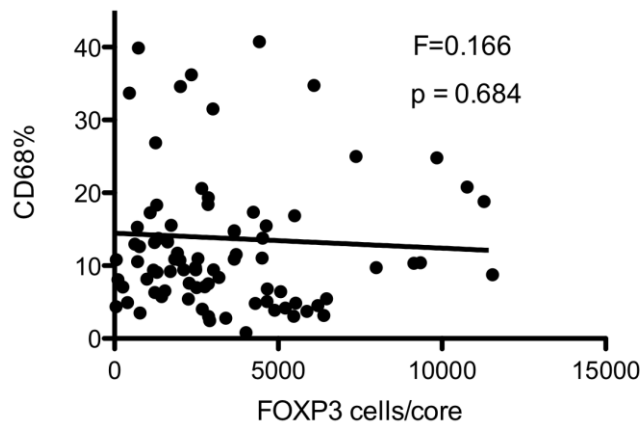


**Figure 3.15:** FOXP3 and CD68 expression show no correlation in CHL. Correlation assessed assuming non-Gaussian distribution of variables, using the Spearman Rank coefficient with significance in correlation set at the 0.05 level.

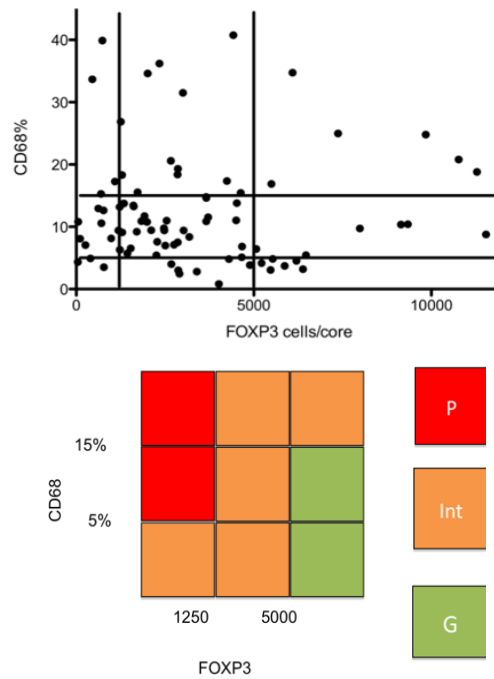


**Figure 3.16:** Illustration of method of assigning a combined FOXP3/CD68 score for each patient (bottom), showing the resulting distribution of patients between groups (top). P = Poor risk FOX/Mac, Int = Intermediate risk FOX/Mac, G = Good risk FOX/Mac.

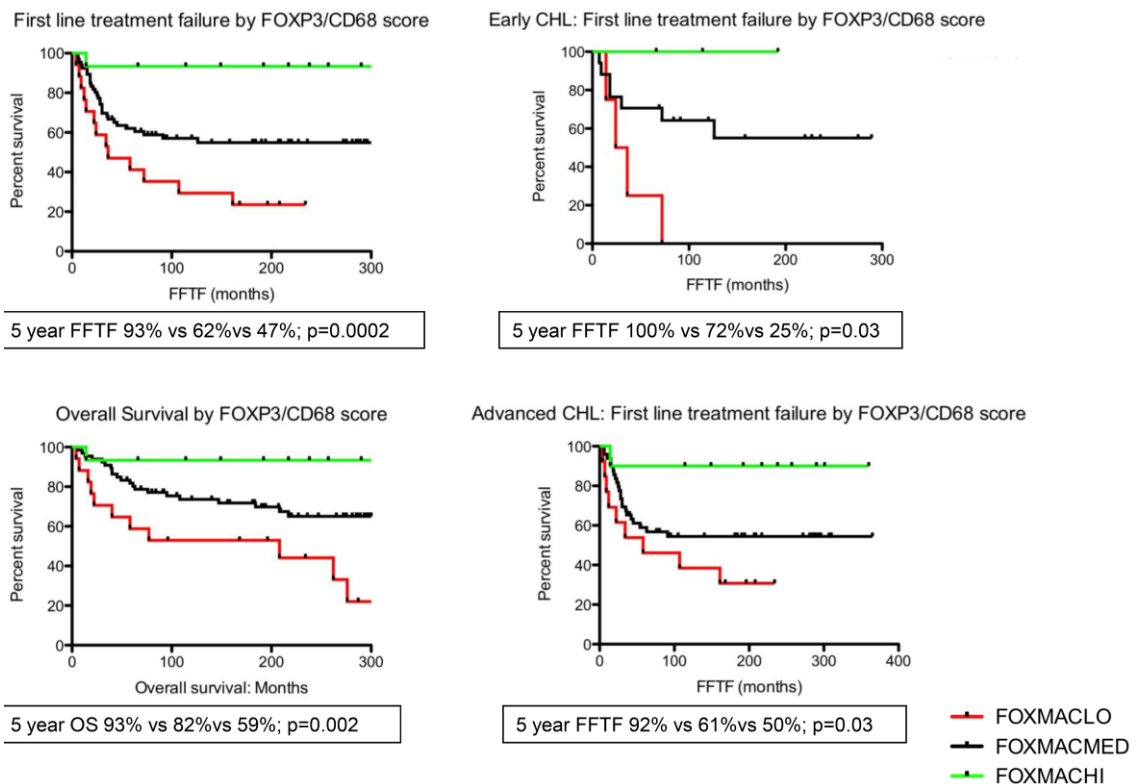


**Figure 3.17:** The combined FOXP3/CD68 score discriminates prognostic groups for patients with either early or advanced stage disease at diagnosis.



### 3.4.2 Continuous Data Analysis

The distribution of FOXP3, CD68 and CD20 was assessed using dot plot graphs and a transformation of each of the three markers using the log function was used to facilitate multivariate analysis (Figure 3.18). Summaries of probability levels for the univariate and multivariate analyses of the continuous data are summarized in Table 3.3.

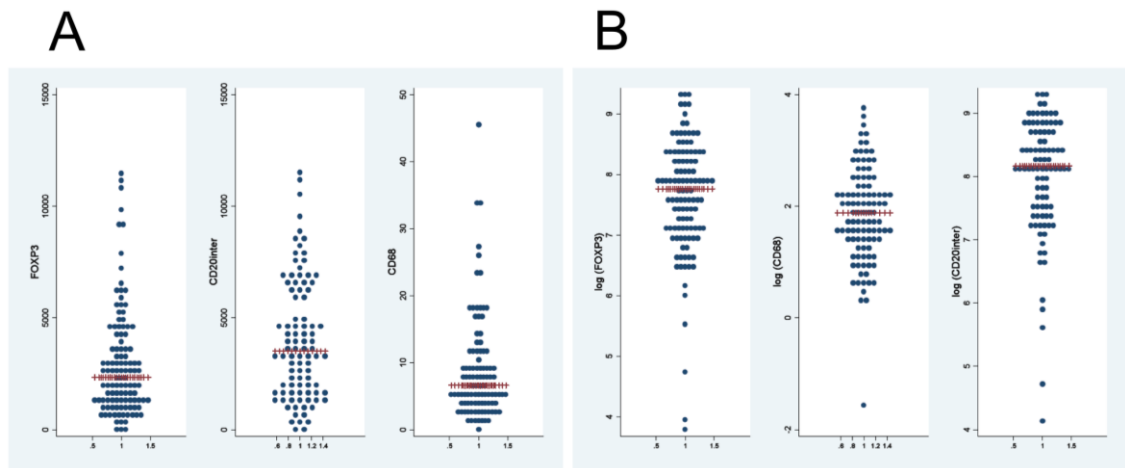


**Figure 3.18:** Applying a logarithmic transformation (B) to the raw data (A) for the three markers FOXP3, CD20 and CD68 generated a more Gaussian distribution of variables suitable for subsequent multivariate analysis.

#### 3.4.2.1 Overall Survival

In univariate analysis incorporating the biomarkers as continuous variables, only age, CD68 and FOXP3 were significant prognostic factors for OS. Multivariate analysis using a Cox proportional hazards model (based on 113 patients with available data and 37 observed deaths) included age and FOXP3. In this model there was no significant overall interaction term effect determined between FOXP3 and CD68 ( $p=0.475$ ). There was a significantly greater risk of mortality associated with older age and lower levels of FOXP3. The repeated multivariate analysis including clinical factors<sup>16</sup> in the model was based on 76 advanced-stage patients and 28 deaths. Only FOXP3 was an independent prognostic variable ( $p=0.005$ ). The model best explaining data variation included age and FOXP3 (PI =  $0.040 \times [\text{Age}] - 0.00017 \times [\text{FOXP3 absolute}]$ ) where Harrell's c-index was 0.709 indicating that both covariates in the model explain the variation in OS reasonably well.

### 3.4.2.2 Disease Specific Survival

In univariate analysis only age and FOXP3 were significant prognostic factors for DSS. Multivariate analysis (based on 113 patients with available data and 24 observed events) included age and FOXP3. There was no significant interaction between FOXP3 and CD68 ( $p=0.423$ ). The repeated multivariate analysis including clinical factors was based on 76 advanced-stage patients and 20 events. Only FOXP3 was an independent prognostic variable ( $p=0.015$ ) and the model best explaining variation in the data included age and FOXP3 ( $PI = 0.0293^{*}[Age>45:1/0] - 0.00028^{*}[FOXP3 \text{ absolute}]$ ) where Harrell's c-index was 0.719.

Prognostic factor	OS		DSS		FFTF	
	Uni-variate	Multi-variate	Uni-variate	Multi-variate	Uni-variate	Multi-variate
<b>FOXP3</b> (Based on 113 patients and 37 events)	<b>0.026</b>	<b>0.038</b>	<b>0.018</b>	<b>0.035</b>	<b>0.005</b>	<b>0.010</b>
<b>CD68 percent</b> (Based on 101 patients and 34 events)	<b>0.022</b>	NS	0.233	NA	<b>0.005</b>	NS
<b>CD20-non-follicular</b> (Based on 93 patients and 30 events)	0.255	NA	0.998	NA	0.191	NA
<b>Age</b> (Based on 116 patients and 37 events)	<b>&lt;0.005</b>	<b>&lt;0.005</b>	<b>0.004</b>	<b>0.012</b>	0.100	NA
<b>Advanced vs Early Stage</b> (Based on 116 patients and 37 events)	0.074	NA	0.083	NA	0.540	NA
<b>Stage IV vs not Stage IV</b> (Based on 116 patients and 37 events)	0.268	NA	0.272	NA	<b>0.005</b>	<b>0.043</b>
<b>IPS &gt;3</b> (Based on 77 patients and 28 events)	0.057	NA	0.309	NA	0.197	NA

**Table 3.3:** Probability values generated from the Cox regression analysis for survival factors based on each biomarker incorporated into the analysis as a continuous variable. Only factors significant in the univariate (Uni) analysis were incorporated into the multivariate (Multi) analysis. Effect of the variable on outcome was deemed significant for  $p<0.05$ . These significant values are highlighted in bold in this table.

### 3.4.2.3 Freedom From Treatment Failure

In univariate analysis only stage, CD68 and FOXP3 were significant prognostic factors for FFTF. Multivariate analysis (based on 113 patients with available data and 50 observed events) included presence of stage IV disease and FOXP3. There was no significant overall interaction effect between FOXP3 and CD68 ( $p=0.728$ ). The repeated multivariate analysis using prognostic score was based on 76 advanced-stage patients and 35 events. Only FOXP3 was an independent prognostic variable ( $p=0.03$ ) and the model best explaining variation in the data included FOXP3 and presence of stage IV disease ( $PI = 0.635*[\text{StageIV:1/0}] - 0.00021*[\text{FOXP3 absolute}]$ ) where Harrell's c-index was 0.656.

Hence for all outcomes, incorporating FOXP3 into the prognostic score improved the predictive value of the model above that derived from the significant clinical factor alone (Shown for age in Table 3.4).

Model	OS	FFTF	DSS
Age only	0.646	0.531	0.629
Age and FOXP3	0.709	0.624	0.719

**Table 3.4:** Improvement in the predictive value of the prognostic model derived from regression analysis when incorporating FOXP3 infiltrate as a continuous variable, compared to that derived using age alone.

## 3.5 Discussion

A biomarker signature that is validated robustly, powerfully predictive, and cost-effective for clinical implementation remains elusive in CHL. Few biomarkers have translated into clinical practice, as a result of flawed statistical analyses and failure to validate findings. This study validates three recently proposed prognostic biomarkers in a new patient cohort, and for the first time incorporates an automated system of image analysis to generate continuous variables applied to a multivariate analysis, eliminating the potential data loss of categorisation of data, and examining dose-effects of expression of each biomarker. The study includes a separate analysis of categorical data, comparable to the studies it set out to validate, and more applicable to manual scoring and clinical

translation. For each of the biomarkers CD68, FOXP<sub>3</sub> and CD20, the prognostic association suggested in previous studies is confirmed.

Non-follicular CD20 expression was predictive of superior OS in the categorical analysis without retaining a dose-effect in the continuous data analysis. High CD68 expression predicted adverse outcome by all survival measures in the categorical analysis but only showed a dose-effect for OS in the continuous variable analysis and was not significant in the multivariate analysis. High FOXP<sub>3</sub> expression emerged as the most robust predictor of superior outcome in both independent statistical analyses. As a continuous variable this marker showed a dose-effect significant in univariate and multivariate analyses. It retained predictive power as a categorised variable in a simplified scoring system applicable to manual scoring or clinical use (high, medium and low infiltration). A combined categorical score incorporating both FOXP<sub>3</sub> and CD68 was able to discriminate patients with particularly poor and good risk, in both early and advanced stage disease. A prognostic index based on absolute number of FOXP<sub>3</sub> infiltrating cells and the patient's age as continuous variables was able to predict OS and DSS better than one incorporating clinical factors alone.

### **3.6 Summary and Further Work**

TMA stained for various biomarkers can be used to characterise the CHL microenvironment and better understand disease pathophysiology, as well as measure patient heterogeneity to predict outcome. Much published IHC work is limited by experimental and statistical methodology and hence inadequate for translation into clinical practice. Conclusions drawn from gene expression profiling (GEP) of the microenvironment in CHL are limited by the heterogeneity of the tissue represented, and different groups have proposed quite different prognostic GEP patterns arising from different experimental and statistical methodologies<sup>116, 292, 356</sup>. Large-scale validation or clinical application of these findings is made difficult by the expense of the technology and lack of consistent findings. Finding that a biomarker is predictive of prognosis is merely a description of correlation, and suggests, but does not robustly confirm, a biological mechanism of functional importance. For example, the benefit of FOXP<sub>3</sub> expression could indicate that Tregs directly suppress the malignant B cell in CHL,

suppress tumour-supporting T cells in the microenvironment, reflect another aspect of tumour biology or host immune response beneficial in eradicating residual disease after treatment, or simply represent a non-specific T cell activation marker. The favourable impact of CD20 expression may indicate that normal B cells are contributing to anti-tumour response or represent malignant cell precursors that are more treatment responsive. Finding that CD20 expression confers an impact on OS but not FFTF suggests a complex role for normal B cells in CHL, including interactions with host immunity, therapeutic late effects, late relapse, salvage, and overall host fitness. The role of the macrophage in tumour promotion has been demonstrated far more robustly in biological models<sup>10,11</sup>, but further functional work is required to demonstrate the pathophysiological importance of individual biomarkers. The absence of representative *in vivo* or *in vitro* models of CHL remains problematic and is the focus of ongoing investigation.

Notwithstanding these limitations, correlative IHC biomarker data, generated appropriately, examined with statistical rigor and validated extensively could contribute to clinical decision-making in CHL. Functional imaging has shown considerable promise as a prognostic tool by demonstrating early treatment responsiveness<sup>383</sup>, but pre-treatment prognostic biomarkers are scarce, and none used routinely to guide treatment. This study has validated and confirmed recently proposed prognostic biomarkers by examining a greater extent of pre-treatment lymph node-derived tissue per patient than any published work in CHL to date, analysing using test/validation methodology for cut-point determination, and independently as continuous variables in a multivariate analysis, to demonstrate dose-responsiveness and avoiding categorisation data loss. We propose that by using only the widely available immunohistochemical markers CD68 and FOXP3, with cut-points as described, a simple prognostic score can be developed which may be clinically translatable. To further validate these findings, we have initiated an international collaborative effort in two further independent patient cohorts, using predefined cut-points and both automated and manual counting methods across three different laboratories.

## CHAPTER FOUR:

T-BET, GATA<sub>3</sub>, PD<sub>1</sub> and PD-L<sub>1</sub>  
expression in the classical Hodgkin  
lymphoma microenvironment

## 4. T-BET, GATA3, PD1 and PD-L1 expression in the classical Hodgkin lymphoma microenvironment

### 4.1 Introduction

The majority of the cellular CHL immune infiltrate is comprised of CD4<sup>+</sup> T cells, along with cytotoxic T cells, macrophages and non-malignant B cells, and cells of the innate immune system. The heterogeneity of function of CD4<sup>+</sup> T cells has made determining their role in the microenvironment more challenging. Data presented in Chapter 3 has highlighted the importance of one particular functional subset: Tregs, as having a potential fundamental role, although the limitations of defining a subset using only a single marker (in this case FOXP<sub>3</sub>) have also been introduced. There is very little functional work investigating the mechanism of interaction of the various components of the immune system with each other and with the malignant cell, and as presented in Chapter 5, the development of an experimental model capable of investigating such interactions is challenging. The approach introduced in Chapter 3 correlating clinical outcomes with immunohistochemical markers of immune function, enables mechanistic hypothesis generation, and additionally provides potential biomarkers for future clinical validation and translation.

The number of CD4<sup>+</sup> T cells in the microenvironment shows no correlation with patient outcome. The number of FOXP<sub>3</sub><sup>+</sup> cells shows a substantial correlation with outcome, tested using cut-points with appropriate validation methods, and independently as continuous variable, maintaining significance in multivariate analysis. Of all the markers tested in Chapter 3, FOXP<sub>3</sub> remains the most statistically robust, although clinical validation remains to be confirmed in an independent cohort. As such, and consistent with the heterogeneity of CD4<sup>+</sup> T cell function, it appears that the functional composition of this immune compartment is more important than the total number of CD4<sup>+</sup> cells.

Defining functional subsets in normal physiology has limitations, which have been outlined in the introduction. Defining them in pathological circumstances is even more challenging, particularly those in which a chronic inflammatory stimulus (in this case malignancy) fails to be resolved, and further complicated by the nature of the malignancy being a subversion of the normal immune response, B cell derived malignancy emulating many of the stimulatory, survival and suppressor mechanisms of normal B and T cell interactions. Some markers have proved more robust determinants of T cell function. Three subsets of CD4+ T cells have been proposed as important in CHL, and malignancy in general: Th1, Th2 and Tregs. Th17 represents a further functionally distinct subset whose contribution to anti-tumour immunity is evident<sup>384</sup> but whose contribution to CHL has not yet been adequately investigated<sup>114</sup>.

#### **4.1.1 TH1 and TH2 in malignancy**

It has been proposed that a cell-mediated, macrophage and cytotoxic T cell effector response orchestrated by Th1-polarised inflammation is as important to the elimination of cancer by the immune system as it is to the elimination of intracellular pathogens. Th1-promoting cytokine administration has been associated with murine tumour regression<sup>385</sup>. Murine models of melanoma have demonstrated enhanced tumour control and generation of cytotoxic T cells after suppression of a Th2 or Treg response by Th2-polarising signalling pathway knock-out<sup>386</sup> or administration of neutralizing anti-IL4, IL10 or TGF- $\beta$  antibodies<sup>387</sup>. Tumour-infiltrating or circulating lymphocytes derived from patients with progressive malignancy have demonstrated a Th2-biased phenotype<sup>388</sup>, while Th1-biased infiltrates are seen preferentially in regressing tumours<sup>389</sup>. Hence it is believed that a Th2 biased immune response is inferior in combating progressive tumour and may suppress the more potent Th1 response. However, there is evidence to suggest that a Th2 component to anti-tumour immunity is also important<sup>390, 391</sup>, and conflicting evidence on Th-polarisation in tumour-derived lymphocytes<sup>392</sup>. Evidence for a Th2 response bias in haematological malignancy is sparse and predominantly correlative rather than functional<sup>393-397</sup>. A Th2 bias in CHL has been suggested, but as was discussed in 1.7.1 is based on inadequately interpreted data.



#### **4.1.2 TH1 and T-BET**

There is a robust functional literature on the importance of T-BET in CD4<sup>+</sup> T cells in producing a stable functional phenotype: a T cell which produces IFN- $\gamma$ , TNF $\alpha$  and IL2, along with other pro-inflammatory cytokines. The presence of these Th1 cells stimulates the cell-mediated immune response: with activated macrophages and cytotoxic T cells providing the final effector mechanism, while Th1 cells predominantly augment their microenvironment to optimise the response.

In haematological malignancies, the differential expression of T-BET by the malignant component in contrast to the immune infiltrate is difficult to discriminate. Flow cytometry or multi-colour / fluorescence IHC could be used to discriminate the T-BET expressed by individual components, but there is no published work in the literature applying this method. The expression of T-BET, despite its original description in Th1 polarised T cells, is not restricted to T cells: B cells are known to express T-BET at the stage of class switching where it may have a role in augmenting the cell-mediated nature of an immune response by the production of the appropriate antibody class<sup>398</sup> (IgG2 and 3 rather than IgG1<sup>399</sup>). T-BET is expressed by cytotoxic T cells, with a possible role in promoting effector function rather than memory differentiation<sup>400</sup> and promotion of survival with repression of mediators of immunosuppression and exhaustion<sup>401</sup>. T-BET is notably restricted to the interfollicular T cell zone of reactive lymph nodes and underrepresented within follicles and germinal centres<sup>402</sup>. T-BET is expressed in a subset of B cell malignancies, with evidence to suggest that expression is not seen in the malignant cell of germinal centre B cell, pre-germinal centre B cell or plasma cell-derived malignancies, (mantle cell lymphoma, diffuse large B cell lymphoma (DLBCL), follicular lymphoma (FL), plasmacytoma) whereas it is highly expressed in some cases of post-germinal centre B cell malignancies (small lymphocytic lymphoma (SLL)/ chronic lymphocytic leukaemia (CLL), marginal zone lymphoma (MZL), hairy cell leukaemia (HCL) and Burkitt lymphoma (BL)) and unexpectedly in pre-B ALL<sup>403</sup>. As expected it has been found to be expressed at high levels in many peripheral T cell lymphomas (being derived from mature T cells) but not immature T cell-derived acute T cell leukaemias<sup>402</sup>. These studies had the disadvantage of failing to co-stain for B and T cell markers for the counting of T-BET positive cells. As such, and given that much of the infiltrate of the

lymphomas comprises immune infiltrate as well as neoplastic cells, unless the neoplastic cell is morphologically quite distinct (as in high grade lymphomas and CHL, but less so in lymphomas with small lymphocyte morphology), the true expression of T-BET by the malignant cells is uncertain. Rather it seems that T-BET (including B cell and cytotoxic T cell-expressed T-BET) is indicative of a substantial cell-mediated immune response present within the malignant microenvironment, unable to effectively discharge its function. This same group confirmed previous work<sup>404</sup> demonstrating that a subset of cases of CHL contained malignant cells (which can be easily discriminated from the immune microenvironment by their morphology) expressing T-BET at high levels. They similarly observed that a substantial component of the lymphoid infiltrate comprised T-BET positive cells. Co-staining with CD3 or CD20 was not undertaken, and as such the identity of these microenvironment cells was not clear. Any conclusions drawn regarding the importance of T-BET expression in HRS cells are speculative: e.g. denoting maturity of the B cell of origin (germinal centre vs post germinal centre) or importance in mediating malignant cell survival or suppression of the B cell program of differentiation<sup>405</sup> (e.g. Notch1 activation with Pax5 suppression<sup>406</sup>). Aberrant transcription factor expression may provide a marker for the putative precursors of terminally differentiated HRS cells present in the microenvironment, which are able to sustaining disease despite the poor proliferative capacity of HRS cells. However no such work has been carried out and these HRS progenitor cells remain only a theoretical concept with a limited evidence base<sup>323</sup>.

No clinical correlates of T-BET expression, expressed in HRS cell or microenvironment, are reported, and although an association with EBV expression in the malignant cell, in terms of viral induction of a Th1 response has been reported in one study other aspects of this study are inconsistent and apply flawed methodology<sup>407</sup>.

#### **4.1.3 TH2 and GATA3**

The CHL microenvironment has classically been described as comprising a large proportion of Th2 polarised cells, however evidence is sparse and justification based on citation of an early paper in which there was flawed interpretation of data<sup>47</sup> (See 1.7.1 and Chapter 6). In fact evidence is accumulating to indicate a relative absence of Th2-

defining markers in the microenvironment, with the exception of some less specific markers such as CCR4, whose expression is shared by other functional subsets. GATA3 and C-MAF have been described as the master regulators of Th2 polarisation. Th2 function is characterised by promotion of B cell development, maturation and class switch towards the humoral, extracellular pathogen eradication response, via production of cytokines IL4, IL5 and IL13. This response is coordinated by engagement of transcription factor programmes of GATA3<sup>463</sup> and C-MAF<sup>408, 409</sup>, through suppression of a Th1 response and differential activation of the intracellular pathways JAK1/JAK3 and STAT5<sup>410</sup>/STAT6<sup>411, 412</sup>. These factors have been robustly determined in functional mouse and human experiments and as such may be considered the best markers of such a response. However, as understanding of these pathways evolves it is clear that no marker has complete specificity for any cellular function, and as such can only provide supportive evidence as to the role of any expressing cell. A key example is the finding that GATA3 is essential in early T cell development<sup>413</sup>, before antigen encounter or lineage commitment, and may have a role in Treg function<sup>414</sup>.

A shift towards a Th2 response is often cited as being responsible for the failure of an immune response to eradicate tumour by the more effective cell-mediated mechanisms<sup>415</sup> with Th2-biased lymphocyte composition described in patients with a wide variety of cancers<sup>388, 416</sup>. Much of this literature has failed to explore the potential role of Tregs whose functional sub-classification has only relatively recently emerged. In these cells, functional markers including cytokines and chemokine receptors (e.g. IL10 and CCR4) are often overlapping and whose importance in failure of the immune response in cancer is now widely accepted (Reviewed in Curiel 2007<sup>417</sup>). Evidence for a Th2 dominated infiltrate in CHL is unconvincing with low expression of C-MAF and GATA3 in the immune infiltrate, in stark contrast to that derived from NLPHL<sup>46</sup>. There is little other direct evidence supporting the assumption that Th2 cells dominate the CHL microenvironment, as has already been discussed in 1.7.1.

#### **4.1.4 Immunosuppression and PD1**

The importance of Tregs in cancer and immunosuppression has been discussed, although the molecular mechanisms mediating this are still being established, including

secreted factors such as IL10, IL35 and TGF- $\beta$ , cell-surface associated proteins such as CTLA4, and competition for key inflammatory stimulators such as IL2. The PD1/PD-L1&2 axis is another potent immunosuppressive mechanism which appears to be important in malignancy, as has already been discussed in 1.6.5.1. Its importance in CHL has been suggested by the finding of amplification of the PD-L1 and PD-L2 genes by copy number changes occurring at the chromosomal region containing their genes (9p24.1) in CHL cell lines and 38% of 16 NS-CHL-derived HRS cells, microdissected from tumour specimens<sup>418</sup>. Over-expression of PD-L1 was confirmed at the protein level by IHC, along with members of JAK/STAT signalling pathways associated with PD-L1 & 2 signalling in CHL-derived cell lines and primary tissue. Further evidence was provided by a whole-transcriptome paired-end sequencing assay which for the first time showed evidence of a recurrent chromosomal translocation in CHL, in 15% of 55 cases analysed (along with 38% of cases of the pathophysiologically similar but clinically more aggressive primary mediastinal B-cell lymphoma (PMBCL) in which expression was associated with a poorer clinical outcome), resulting in the apparent upregulation of CIITA expression<sup>334</sup>. Two fusion partners for this translocated gene were found to be PD-L1 and PD-L2, resulting in unmodified translational reading frames beginning at the original gene transcriptional start site, and corroboration by RT-PCR that in tumours harbouring CIITA translocations there were 400-4000-fold changes in PD-L1/2 mRNA expression.

PD-L1 is expressed by a range of cell lines and tumours, which has been postulated as mediating part of the immuno-evasive strategy of cancer<sup>419, 420</sup>. However, it is a non-specific marker, and is up-regulated by a broad range of activated immune cells<sup>421</sup>. PD1 expression is similarly widely up-regulated by T cells following activation, on exposure to chronic inflammatory stimuli such as chronic viral infections or malignancy<sup>422</sup>. Signalling through the pathway, as has been discussed, may also be involved in augmenting the germinal centre reaction and conferring B cell help, although the mechanisms of this are only partly described. PD1 is highly expressed in the microenvironment of NLPHL, although its representation in the CHL microenvironment is at relatively low levels. One study has found it to confer adverse prognosis when expressed at higher levels in CHL<sup>423</sup>, contrary to a finding in FL<sup>353</sup>. Functional evidence for the importance of this axis in CHL is limited and contradictory to the IHC evidence of under-expression of PD1 in the

tumour infiltrating lymphocytes. Indeed the paper demonstrating adverse prognosis of PD1 used an upper cut-point of 23 PD1+ cells per mm<sup>2</sup> tissue to confer adverse prognosis. As has been shown in Chapter 3, the dense immune infiltrate of CHL comprises around 20,000 cells per mm<sup>2</sup>, and a dense FOXP3 infiltrate comprised over 2500 positive cells per mm<sup>2</sup>. Hence PD1 expressing cells are generally very sparse in CHL, consistent with the findings of other published work<sup>424-426</sup>. Although lymphocyte-rich CHL may itself contain a greater proportion of PD1-positive cells<sup>427</sup> it is a rarely described entity representing <1% of all CHL, and often misclassified<sup>428</sup>.

Yamamoto and colleagues reported a relatively high expression of PD1 in CD4+ T cells derived from CHL lymph nodes (54-76%), although this data was derived from only three patients, and the authors report this to be at similar levels to that seen in other non-Hodgkin lymphoma-derived tumour infiltrating lymphocytes<sup>18</sup>. Both of these findings are entirely at odds with published IHC data, and the limited number of samples examined fails to address any patient-to-patient heterogeneity of expression. Comparing expression of a marker by two contrasting techniques, such as IHC compared with flow cytometry, without well defined negative and positive internal controls (as reported in this paper), is open to misinterpretation. The functional experiment described in the paper, demonstrating PD1-dependent suppression of CD4+ T cell IFN- $\gamma$  production, was limited by very small number of primary tumour samples tested (n=2), the simplicity of the *in vitro* model used (lymph node derived cells cultured with or without PD-L1&2 pathway blocking antibodies, and subsequently depleted of CD4, CD8 and CD20-expressing cells respectively), and the limited number of measures of immunosuppression tested – performing only assays of IFN- $\gamma$  production and SHP-2 phosphorylation (a downstream mediator of PD1/PD-L1 signalling). Although there was clearly an effect of blocking antibodies, to conclude that this arose due to the overrepresentation of PD1 positive CD4+ cells interacting with the PD-L1 positive malignancy is an over-interpretation of rather minimal data. In fact, the addition of anti-PD-L1 antibodies may instead have mediated upregulation of IFN- $\gamma$  secretion directly, by acting on PD-L1 present on the surface of activated T cells themselves, not indirectly by removing inhibitory PD1/PD-L1 interactions. The authors remark that the IFN- $\gamma$  production of the CHL-derived culture system was markedly greater than that in any

NHL-derived sample, and present contradictory data regarding the amount of IFN- $\gamma$  produced with or without the blocking antibodies. Overall, the best conclusion that can be drawn from this data is that the CHL-microenvironment is more capable of producing IFN- $\gamma$  than NHL (in the very few primary samples tested here), and that this can be augmented by adding PD-L1-blocking antibodies. This is consistent with the finding that CHL contains few PD1 expressing lymphocytes, particularly compared to NLHPL or NHL.

The data are overall contradictory, and while it appears that the activation-induced molecule PD-L1 is indeed expressed by the malignant cell in CHL, there is no convincing IHC, flow cytometric or functional data that it exerts any effect through PD1 expressing T cells in the CHL microenvironment.

## **4.2 Objectives**

This study set out to determine the heterogeneity of expression of the T cell subset defining markers GATA3 and T-BET in the CHL microenvironment and determine its relationship to clinical outcome, along with the potent immunosuppressive PD1/PD-L1 axis, using IHC on the TMA described in Chapter 3. The markers were selected as being most representative of the subsets Th1 and Th2 (with FOXP3 already investigated for Tregs in Chapter 3), along with an immunosuppressive axis (PD1/PD-L1) whose importance in CHL has been suggested by functional and gene expression data but for which corroborative data is conflicting.

## **4.3 Materials and Methods**

### **4.3.1 Patient samples, TMA construction and Staining Methodology**

This was as described in Chapter 3 using the same patient cohort. Antibodies used for this experiment along with optimal dilutions are shown in Table 4.1. It was observed that in most cases with T-BET expression in the HRS cells, the majority of HRS cells expressed the marker. Hence a simple manual scoring system was applied which classified HRS cells based on their intensity of staining (Figure 4.1) Counting of positive cells was otherwise performed by the automated system, using the scanning and training

system described in 2.2.6.1. T-BET being a nuclear stain, was expressed as mean number of cells per mm<sup>2</sup>, which facilitated correlation with expression of FOXP3 whose nuclear staining characteristics are similar. Strategies for the assessment of the other markers are addressed in the results section due to difficulties relating to non-specific staining and low levels of expression.

Antibody	Isotype	Clone	Dilution	Supplier
PD1	Mouse IgG1	NAT	1:100	Abcam
PD-L1	Rabbit	Polyclonal	1:5	Abcam
GATA3	Rabbit	Polyclonal	1:1000	Abcam
T-BET	Mouse IgG1	4B10	1:100	Santa Cruz

**Table 4.1:** Optimal antibody dilutions and suppliers for the experiments reported in Chapter 4.

#### **4.3.2 Statistical Analysis**

Statistical methodology was restricted to univariate analysis using the Kaplan Meier method applied to the outcome measures as described in Chapter 3. A multivariate analysis was not applied because of difficulty enumerating PD-L1 and GATA3, and the very low expression of PD1 demonstrated for this patient cohort. T-BET expression was not applied to a multivariate analysis since correlation was significant for only one outcome measure, namely DSS. Expression levels appeared to correlate with FOXP3, and there was a bimodal distribution of outcomes (see results section). However, this would be an important future analysis once these findings have been validated in an expanded cohort as outlined in Chapter 3. Statistical significance of correlations between variables were assessed using Pearson's R test following log transformation to improve normal distribution of the data.

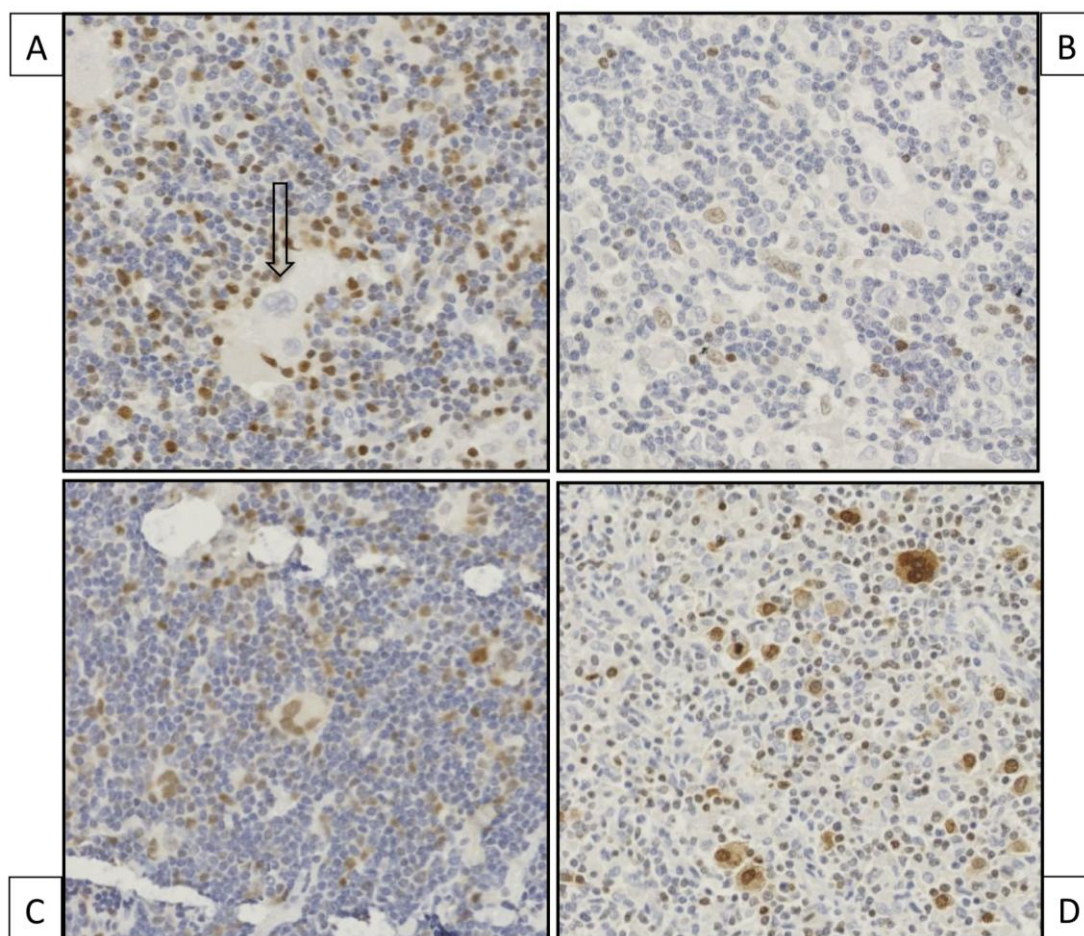


**Figure 4.1:** HRS cells were positive for T-BET in the majority of cases but at varying levels of expression. A manual scoring system was developed allocating each core a score: A: 'o' = no expression, HRS marked with arrow (although note substantial expression in the microenvironment) B: '+' = weak expression C: '++' = intermediate expression D: '+++ = strong expression. Mean levels were determined for each sample based on this score.

## 4.4 Results

### 4.4.1 T-BET expression in the microenvironment

T-BET staining in the tonsil was consistent with the literature and was confined predominantly to the interfollicular T cell zone with little expression in the germinal centres or follicles (Figure 4.2) The distribution in tonsil was notably similar to that seen for FOXP<sub>3</sub> (Figure 4.3) in keeping with the findings of Roncador et al<sup>429</sup>. T-BET expression was restricted to the nucleus, but was present in lymphoid cells in the



immune infiltrate as well as morphological HRS cells in a subset of patients. Staining appeared specific, with little non-cellular staining, with nuclear restriction and providing adequate contrast using the DAB chromogen to facilitate cell counting by manual or automated image analysis systems.

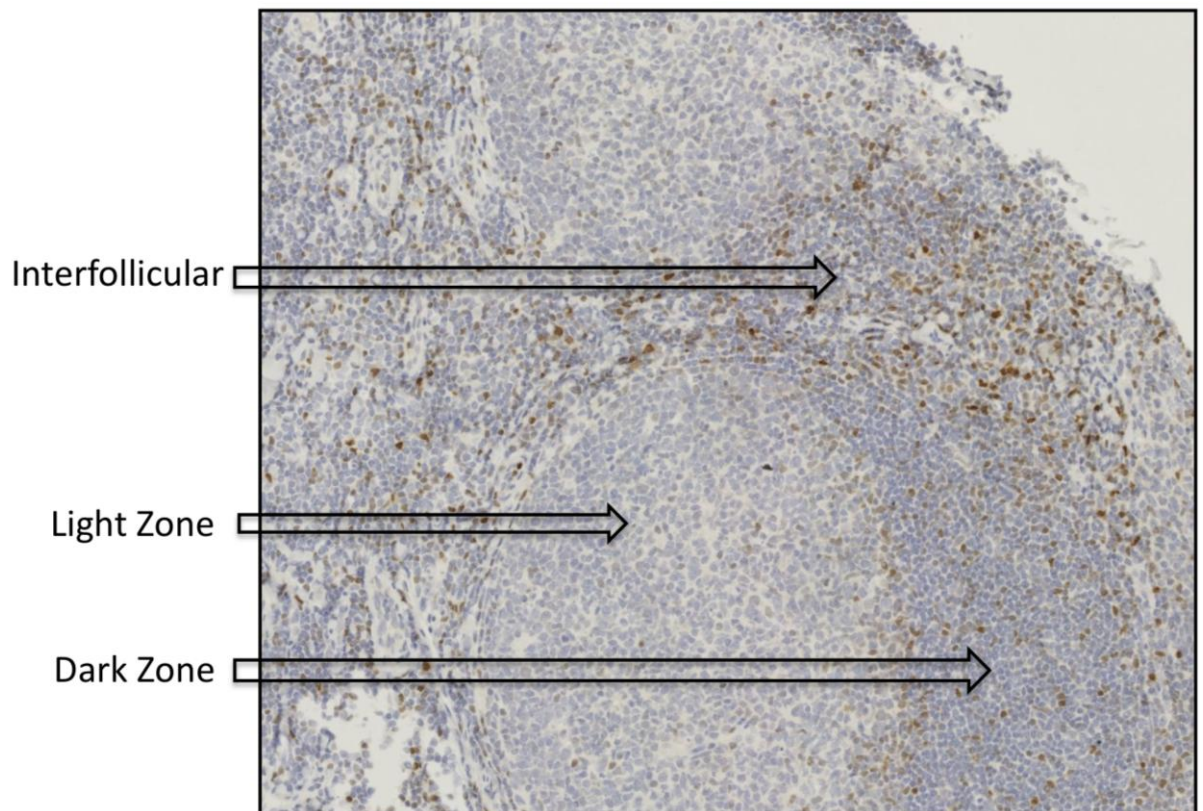


**Figure 4.2:** Expression of T-BET in TMA control tonsil: T-BET is represented in a substantial proportion of interfollicular T cells, far more so than in the germinal centre of the lymphoid follicle, in which expression is virtually absent in the light zone, and present at a lower level in the dark zone.

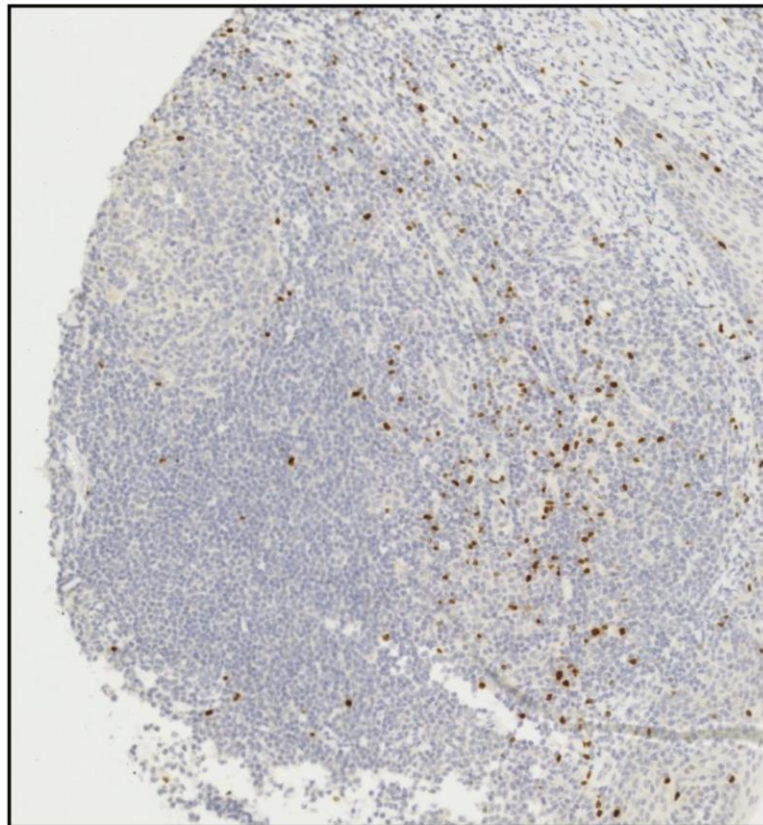
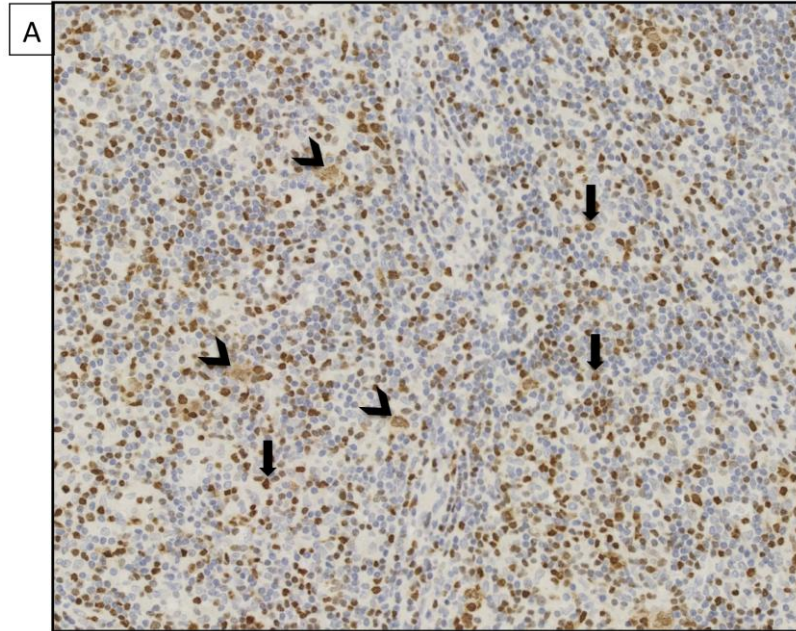


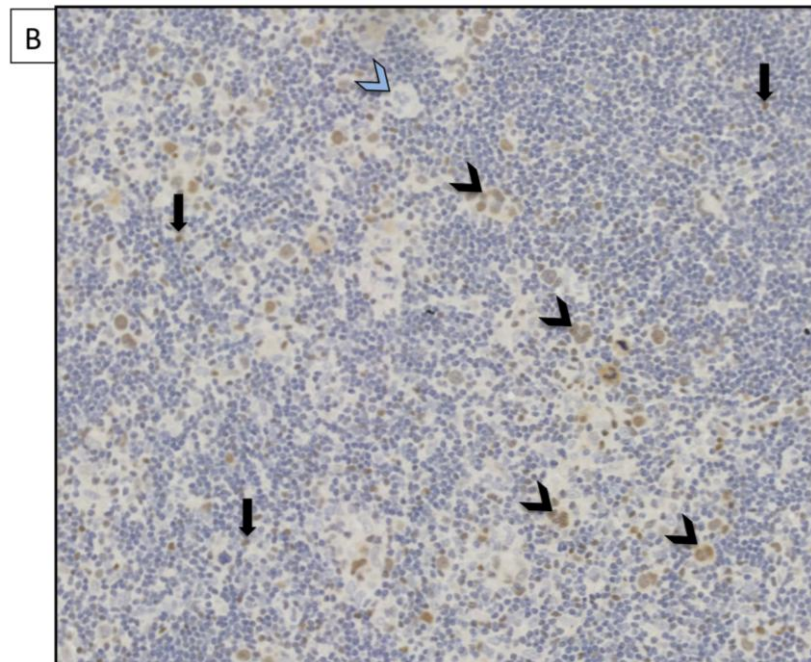
**Figure 4.3:** Expression of FOXP3 in TMA control tonsil: FOXP3 is represented in a substantial proportion of interfollicular T cells, far more so than in the follicular region.

The level of expression of T-BET was widely heterogeneous between samples (expressed in 14-5406 cells, mean 1285, median 879) but present in all cases (Figure 4.4a-d). Frequency distributions comparing variability of expression of T-BET to that of FOXP3 are shown in Figure 4.5. Distribution was positively skewed similarly to that of FOXP3, but was generally at lower levels than FOXP3. There was evidence of a statistically significant correlation between the two variables (Pearson's R applied to log transformed values = 0.225; 95% CI: 0.03-0.39;  $p=0.021$ ). The absolute counts of T-BET expressing cells, being generated using the Ariol automated image analysis software without counterstaining (e.g. CD4, CD8 or CD20), included all cells expressing the marker, discriminating neither immune cell type nor HRS cells expressing T-BET. Hence the total count is influenced in part by density of non-CD4+ cells in the tissue and expression of T-BET in the malignant cells. This further limits interpretation of the data. T-BET expression was found to be greater in cases which were EBV positive than in EBV negative CHL (Figure 4.6: mean expression 1750 vs 1055/mm<sup>2</sup>,  $p = 0.0027$ ).

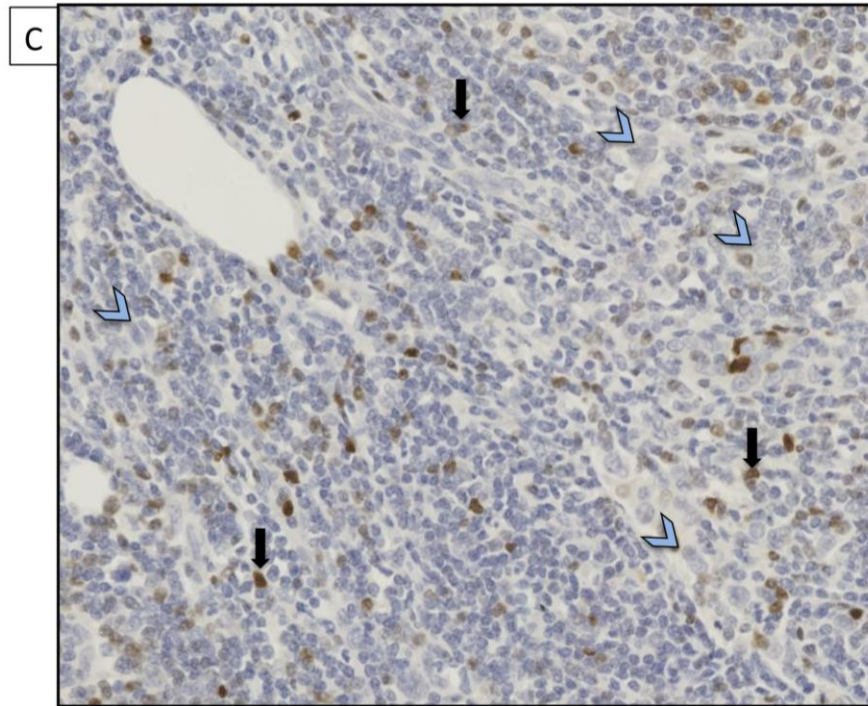
**Figure 4.4a-d:** Heterogeneity of expression of T-BET in the CHL microenvironment. Representative T-BET expressing HRS cells indicated with black arrowheads, T-BET negative HRS cells with blue arrowheads, and lymphoid microenvironment cells with black arrows.



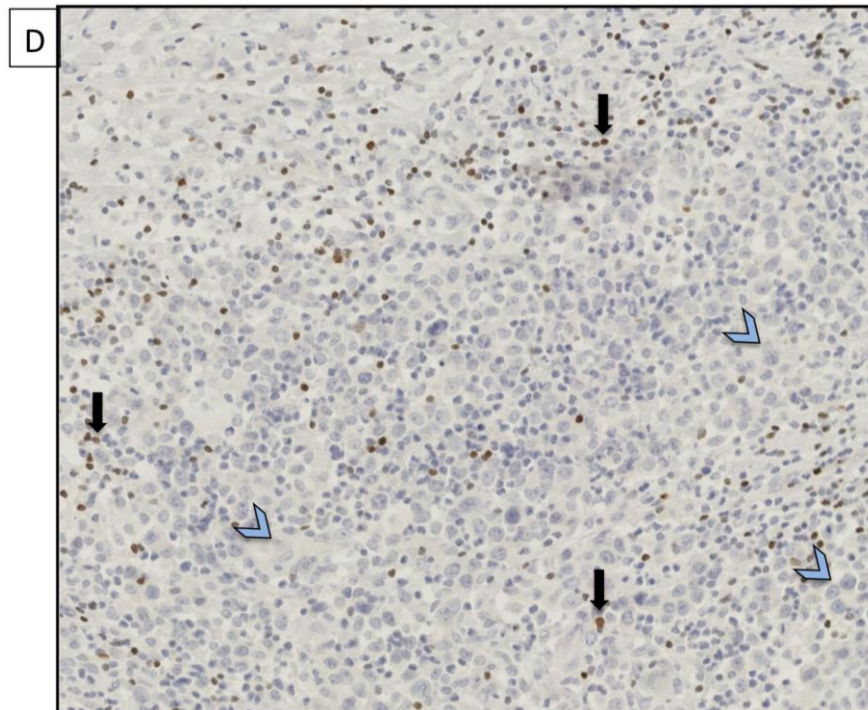
**4.4a** High microenvironment T-BET expression with HRS cells positive for T-BET.



**4.4b:** Low microenvironment T-BET expression with HRS cells positive for T-BET.



**4.4c:** High microenvironment T-BET expression with HRS cells negative for T-BET.



**4.4d:** Low microenvironment T-BET expression with HRS cells negative for T-BET.

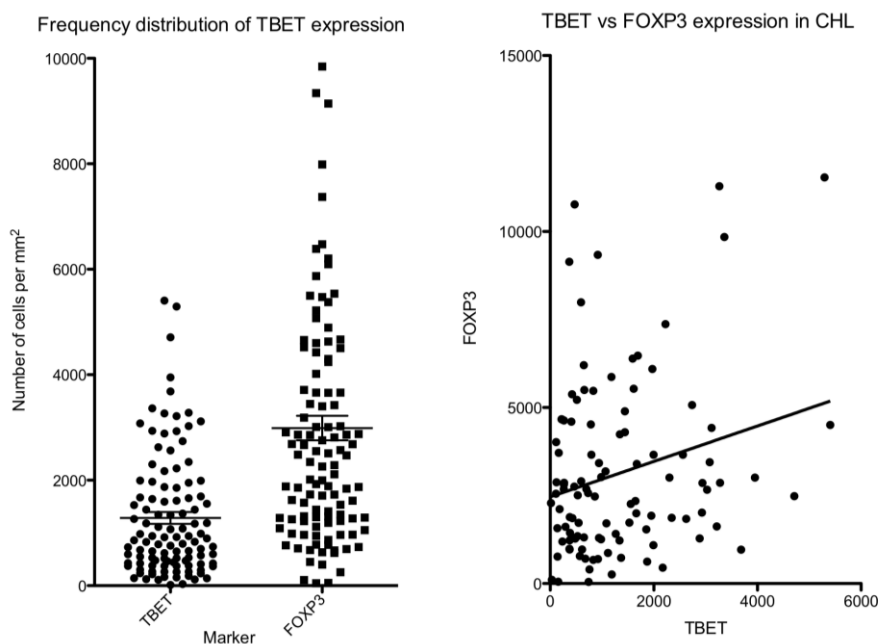


**Figure 4.5:** T-BET expression was widely heterogeneous between patients, positively skewed as for FOXP<sub>3</sub>, and expressed at lower levels than FOXP<sub>3</sub>. However there was a positive correlation between expression levels of the two markers.

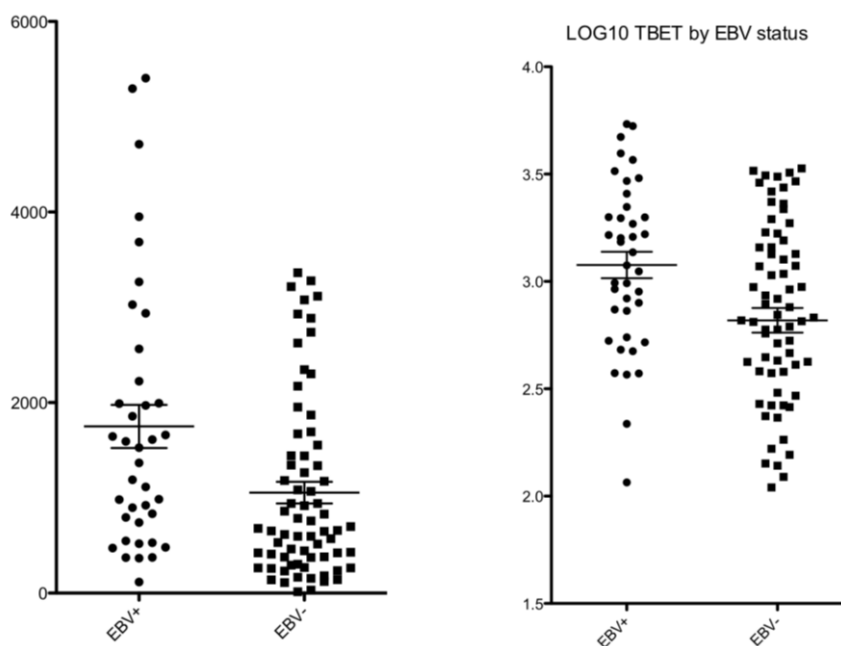


**Figure 4.6:** T-BET expression was significantly greater in EBV+ cases compared to EBV- cases (mean number of cells per mm<sup>2</sup> = 1750 vs 1055,  $p=0.0033$  comparing raw values using non-parametric Mann-Whitney U test (left), and  $p=0.0046$  using unpaired T test comparing log transformed values (right) where normal distribution is better approximated).

#### 4.4.1.1 T-BET density may influence survival outcomes

110 of the total 122 patient samples were deemed adequate for further analysis. Using the test/validation set methodology described in Chapter 3, the cohort could be divided into two groups (using a cut-point 1500 T-BET-expressing cells/mm<sup>2</sup>) or three groups (using cut-points of 500 and 1500 T-BET-expressing cells/mm<sup>2</sup>). Figure 4.7 shows Kaplan Meier survival curves for each of the outcome measures using these cut-points, with Table 4.2 summarising these findings. Using optimal cut-point analysis enables the data to be analysed for trends for which larger datasets may be adequately powered to demonstrate differences, although this may not be statistically robust (See 2.2.6.3). When optimal cut-point analysis fails to demonstrate a statistically significant difference, the test/validation method is not applied, since following this step levels of significance are invariably reduced. However if the 'uncorrected p' generated for optimal analysis falls below the 0.05 level, further validation work may be warranted. Numbers of T-BET-expressing cells failed to discriminate the groups using the outcomes of FFTF or OS, even using optimal cut-point analysis. However, numbers of T-BET-expressing cells did significantly influence DSS, both by optimal cut-point analysis, with an increased infiltrate conferring a superior outcome, and correcting this p value by applying the test/validation method (corrected p=0.045 using either two or three prognostic groups).

However, on dividing the cohort into three groups using two cutpoints, an intermediate-outcome group emerged in which T-BET infiltrate was lowest (<500 cells/mm<sup>2</sup>) yet in which DSS was superior compared to the group with intermediate infiltrate (500-1500 cells/mm<sup>2</sup>). The indication of a direct correlation of T-BET infiltrate with FOXP3 infiltrate, along with the known biological interactions between cells expressing these transcription factors<sup>430</sup> suggests that these findings need to be pursued using functional analysis.

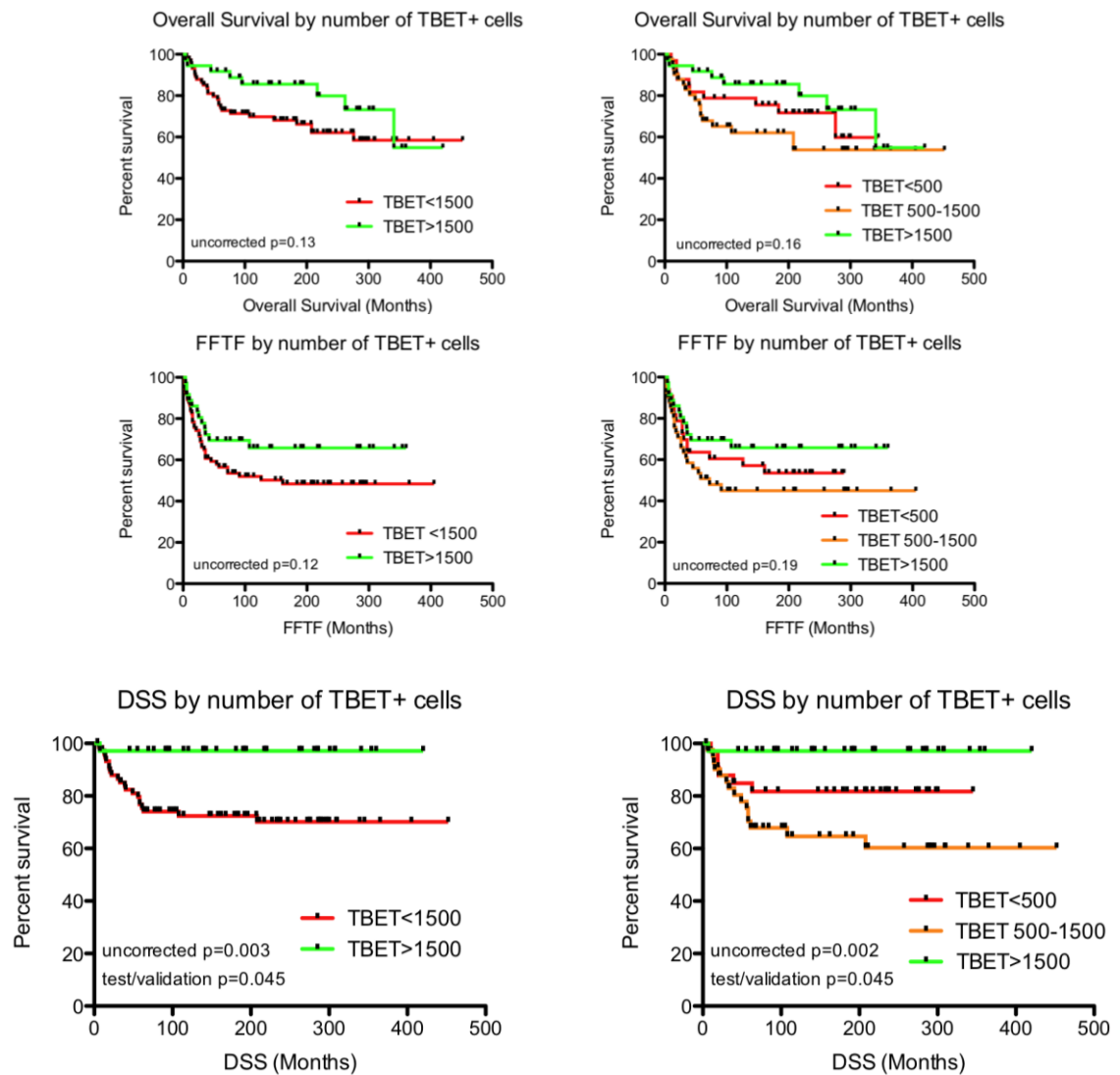


**Figure 4.7:** Survival Curves generated by Kaplan Meier analysis with patients stratified by expression of T-BET using either one (left) or two (right) cut-points. Outcome measures of OS, DSS and FFTF are included with only DSS proving statistically significant, as summarised in Table 4.2 (below).

Outcome measure	Hi vs Low 5 year % event	Hi/Med/Low 5 year % event	P (null); one cut-point	P (null); two cut-points
OS	92%/76%	92%/70%/82%	0.13	0.16
DSS	<b>97%/77%</b>	<b>97%/68%/85%</b>	<b>0.045</b>	<b>0.045</b>
FFTF	69%/56%	69%/51%/64%	0.12	0.19

**Table 4.2:** Summary of results of Kaplan Meier analysis based on T-BET expression using one cut-point (Hi=>1500/mm<sup>2</sup>, Low=<1500/mm<sup>2</sup>), or two cut-points (Hi=>1500/mm<sup>2</sup>, Med=500-1500/mm<sup>2</sup>, Low=<500/mm<sup>2</sup>) with p values reported for the uncorrected optimal cut-point analysis in the case of OS and FFTF (where no significant differences could be demonstrated in any analysis) and the corrected value (in bold) after test/validation set application for DSS.

#### 4.4.1.2 T-BET is expressed in malignant cells in the majority of cases

As has been previously reported, T-BET was found to be expressed in a majority of cases, with strong nuclear expression apparent. There was no apparent relationship between expression of T-BET in the HRS cell and degree of T-BET positive infiltrate, although in all cases T-BET was present in a substantial proportion of lymphoid microenvironment cells as reported above. Table 4.3 summarises the findings of T-BET expression in the HRS cells using the manual scoring system as described. Hence T-BET was expressed at any level in 82% of cases, strongly in 25%, and absent in only 18%. Stratifying by these groups did not reveal any survival differences by OS, DSS or FFTF (Figure 4.8).

HRS T-BET score	No cases	% cases
0	20	18.2
+	32	29.1
++	30	27.3
+++	28	25.5

**Table 4.3:** Summary of differential expression of T-BET in HRS nuclei using the scoring system described in Figure 4.1

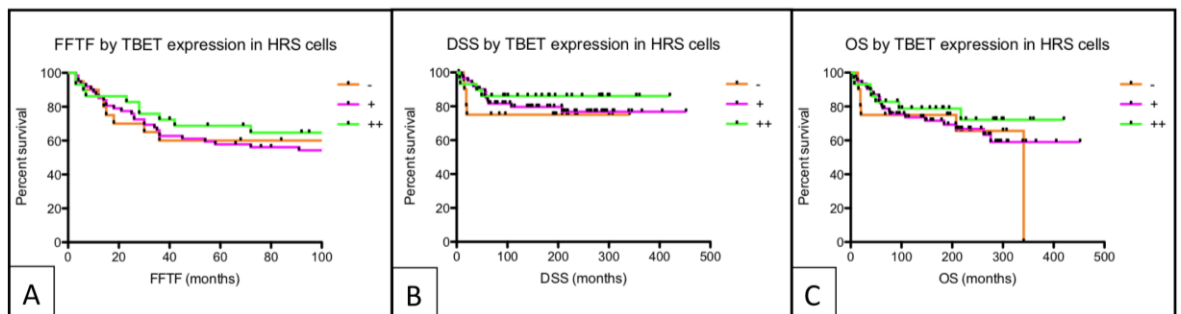


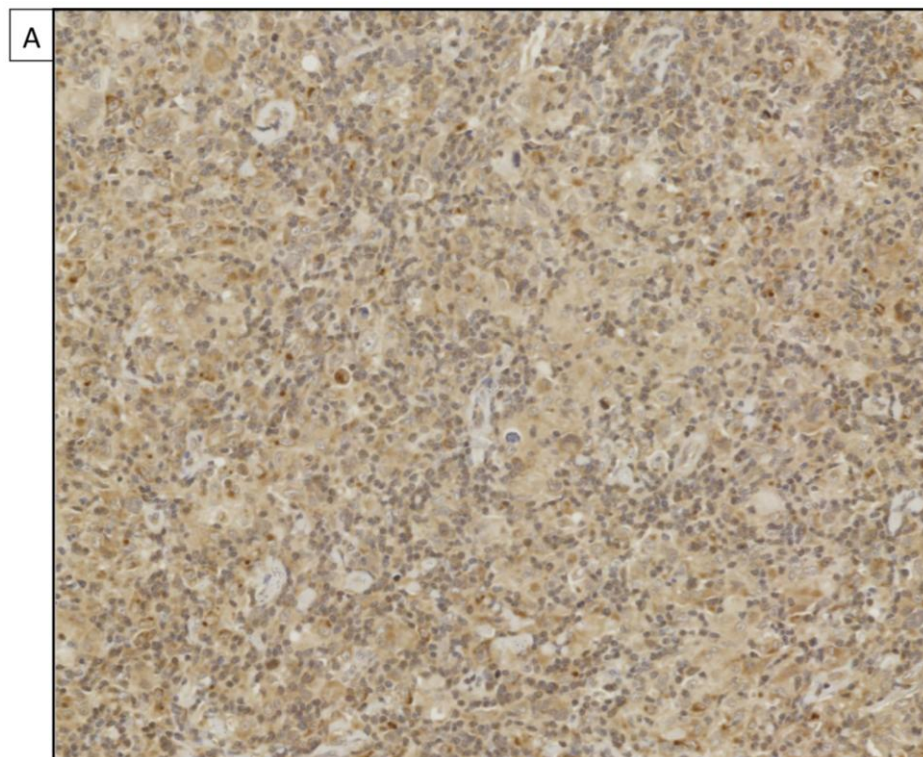
**Figure 4.8:** Expression of T-BET in HRS cells, while heterogeneous, did not enable stratification of patients by prognosis. In these figures for FFTF (A), DSS (B) and OS (C), degree of HRS staining as determined by the manual scoring system described, is stratified as ‘-’=absent, ‘++’=present at high levels (+++ in the manual system) and the intermediate group ‘+’ (+ / ++ in the manual system).



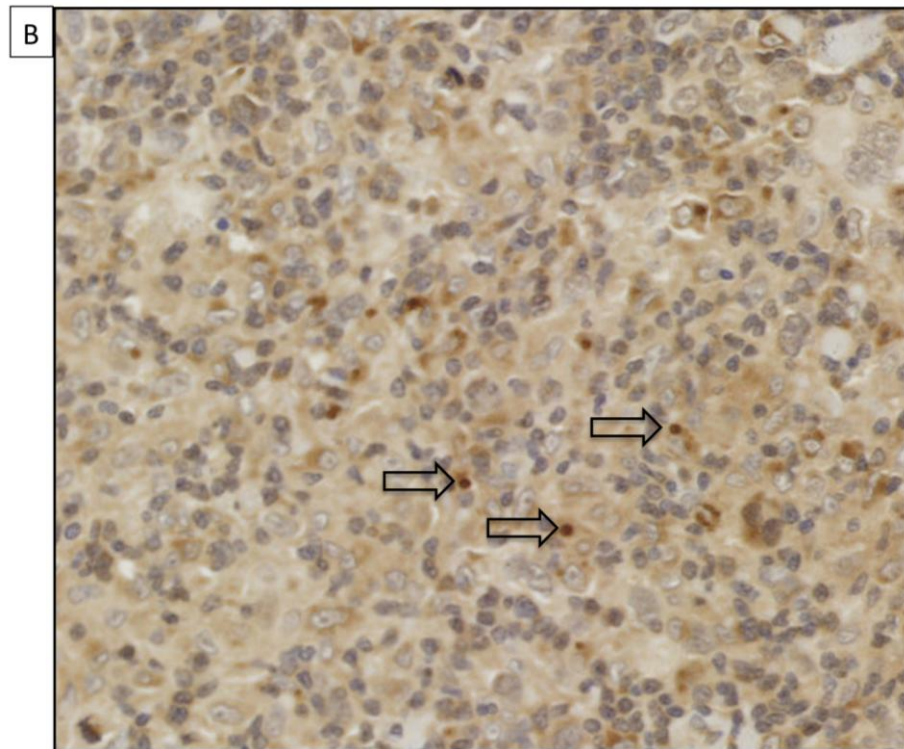
#### **4.4.2 GATA3 expression in the microenvironment**

GATA3 expression was difficult to analyse under the conditions applied for this study (Figure 4.9a-d) There was significant background staining in all cases, particularly dense in immunoglobulin-rich regions, consistent with non-specific binding, despite measures taken to attempt to reduce this. Strong expression was restricted to the cytoplasm, not the nucleus as was expected for a transcription factor. Those cells strongly taking up the marker included plasma cells and, consistent with the literature, morphological HRS cells in a proportion of cases, although this finding may also be an artefact. Due to the non-specificity of the staining, failure to stain the nuclei (unlike T-BET and FOXP3 for which potent and easily enumerable nuclear staining was apparent), no further analysis was carried out. Optimisation by alteration of the antibody concentration was carried out, but with no improvement in resolution, and no nuclear staining.

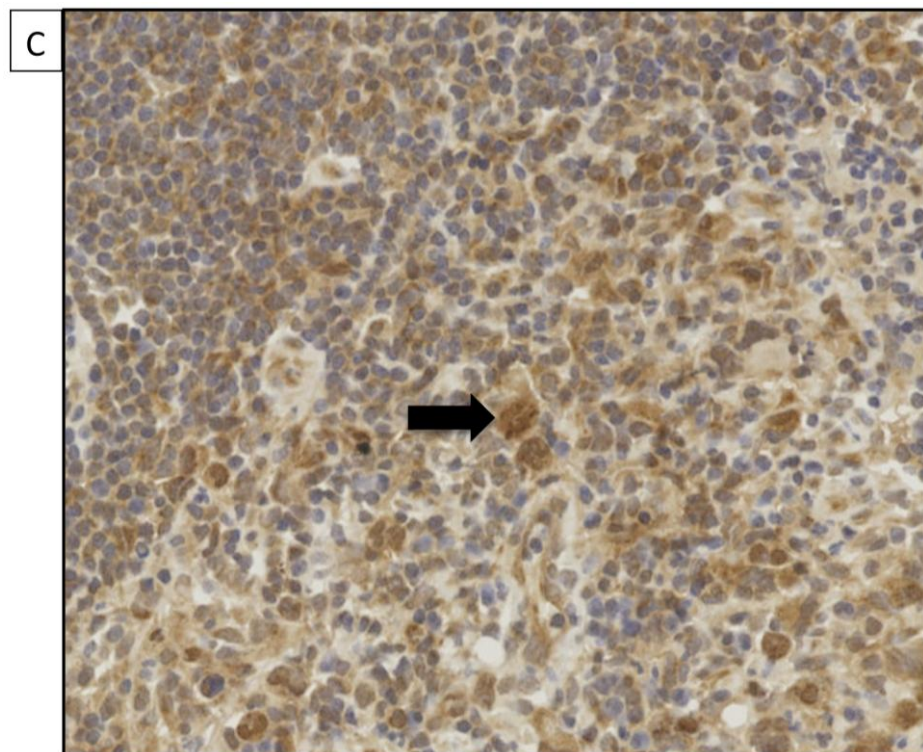
**Figure 4.9a-d:** GATA3 staining difficulties and observations:



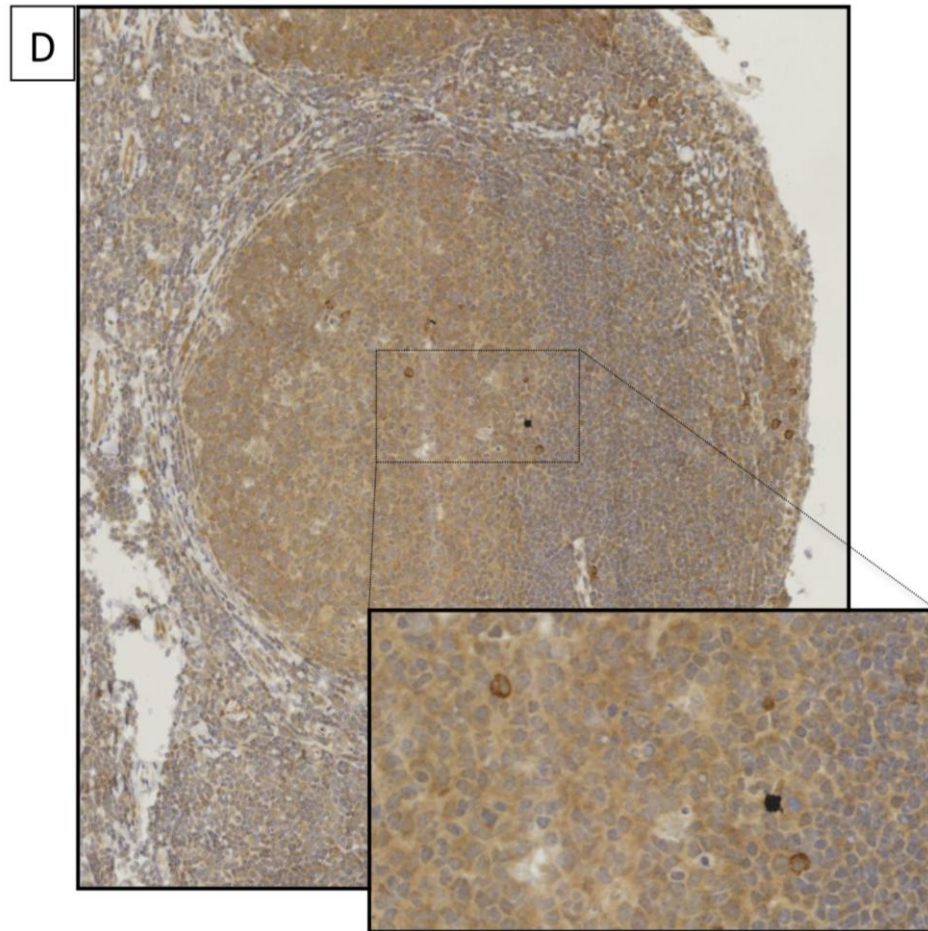
**4.9a:** Substantial non-specific background staining.



**4.9b:** Predominant expression in cytoplasm and only infrequently in nucleus (Arrow).



**4.9c:** Expression apparent in HRS cells including nuclear staining.



**4.9d:** Tonsil revealing differential non-specific uptake in follicle light zone compared to T cell zone and (inset) strong cytoplasmic staining apparently in plasma cells, indicative of nonspecific binding in immunoglobulin-rich regions.

As a pilot to these experiments, an alternative marker of Th<sub>2</sub> cells to GATA<sub>3</sub> - C-MAF - was also examined. However similar staining problems were encountered and this was not taken forward. The literature on IHC staining for GATA<sub>3</sub> has demonstrated similar problems, and concurs with these findings that very little of this TF is present in the microenvironment of CHL. Notably, it is also absent from NLPHL which, in contrast, has a striking over-expression of C-MAF<sup>46</sup>, perhaps indicating an over-representation of a Tfh component in NLPHL, rather than the presence of Th<sub>2</sub>-polarised cells (see Introduction 1.6.6.1). There is a limited literature on the assessment of GATA<sub>3</sub> expression using IHC, likely due to the same staining problems as those encountered during this study. Staining is predominantly cytoplasmic, not nuclear, except in the case of HRS cell nuclei in a subset of patients, while non-specific staining remains problematic. The cytoplasmic

localisation of GATA3 using antibodies designed for IHC has been previously described but not been explained in the literature, leading to inconsistencies in reporting of 'GATA3-positive' cells and immune infiltrates<sup>431</sup>. As such no further assessment using Th2-defining transcription factors was carried out, and a failure to find convincing evidence of Th2-defining cytokine profile cells using flow cytometry in subsequent experiments (Chapter 6) further justifies this.

#### **4.4.3 PD1 expression in the microenvironment**

PD1 expression was strikingly low or absent in the microenvironment of the majority of cases of CHL (Figure 4.10): <0.5% of cells in 80% of cases and <0.1% of cells in 42% (Median expression 0.14%, or 5 cells/hpf, 30 cells/mm<sup>2</sup>, range 0-8.9% (0-1700/mm<sup>2</sup> or 250/HPF: Figure 4.11) This was in stark contrast to tonsillar expression in which there was strong expression predominantly within the lymphoid follicles, as expected (Figure 4.10). The pattern of staining in CHL was at a lower level than in the tonsillar follicles, and predominantly as a low-level background infiltrate with frequent clusters/nodules of PD1 positive lymphoid cells aggregating around HRS cells (Figure 4.12). Based on this apparent biological separation of cases: virtually absent expression contrasting with a few patients with relatively higher expression, patients were divided by quartiles, in which the upper quartile had infiltration >0.5% all cells (15/hpf or 120/mm<sup>2</sup>). The group expressing PD1 had poorer outcome (Figure 4.13) measured by DSS (63% vs 86% at five years; p=0.012) while FFTF and OS outcomes were not significantly inferior, with 5 year OS 63% vs 84% (p=0.18) and 5 year FFTF 44% vs 66% (p=0.051). There was no apparent association with EBV status, with 11% of the EBER+ cases expressing PD1 at a high level and 15% of the EBER- cases.

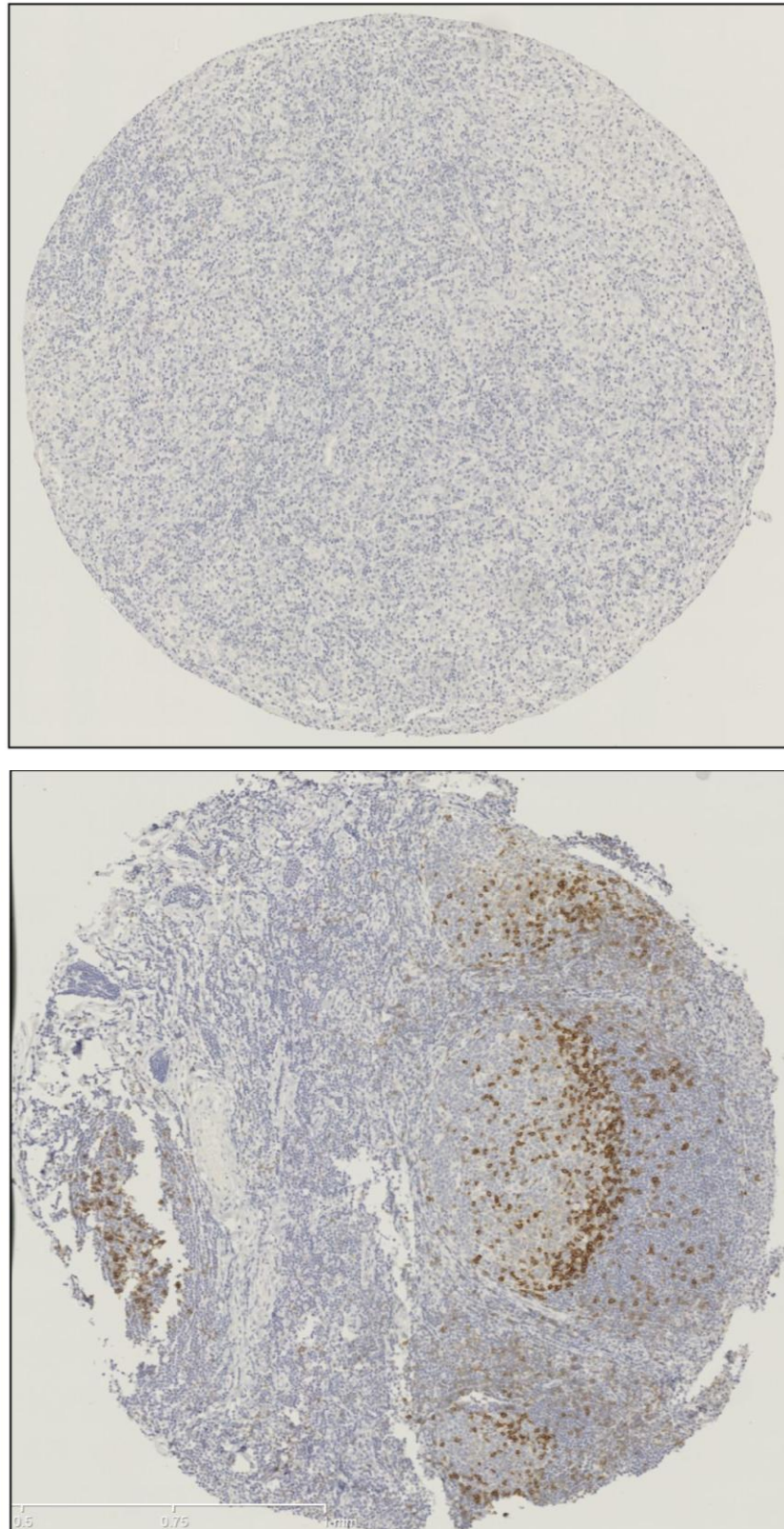


**Figure 4.10:** PD1 expression virtually absent in most CHL cases (top) in contrast to the striking expression in germinal centre of reactive lymph node (bottom).

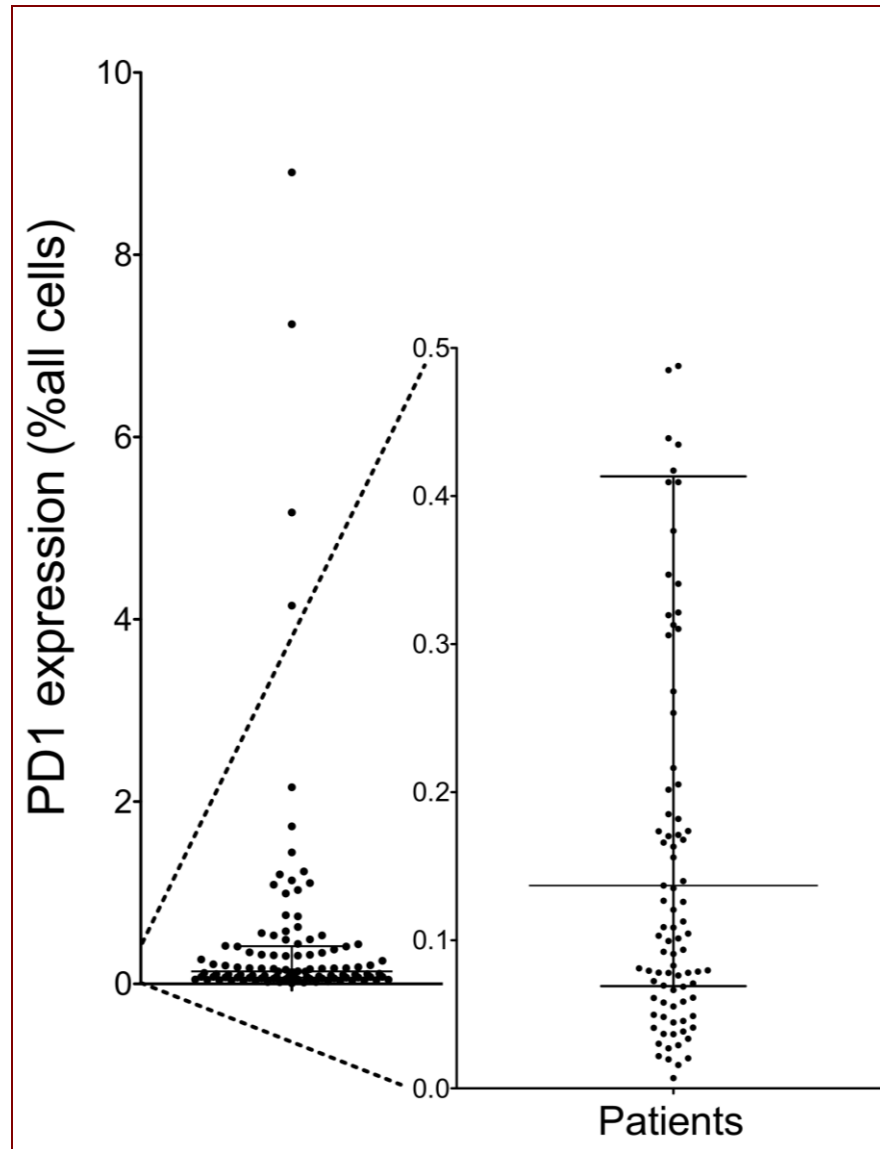


**Figure 4.11:** Heterogeneity of expression of PD1 showing predominance of extremely low levels (<0.5% level expanded to demonstrate clustering of the lower three quartiles and distinct nature of upper quartile)

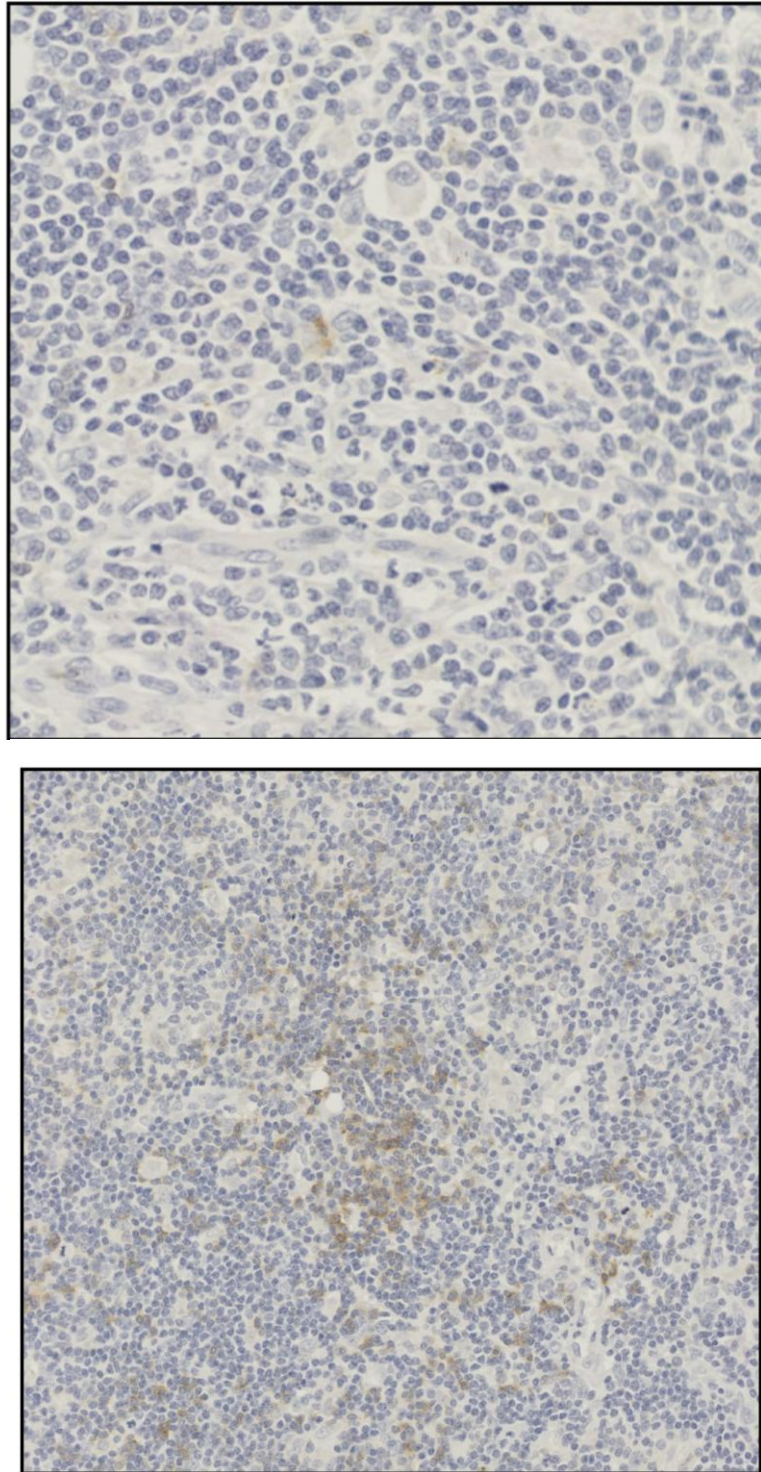


**Figure 4.12:** In most cases of CHL only a tiny minority of microenvironment cells weakly express PD<sub>1</sub> (top). In cases expressing PD<sub>1</sub> a nodular/clustering pattern of PD<sub>1</sub>+ lymphoid cell infiltration was apparent (bottom) but staining intensity was overall far weaker than in tonsillar follicles and germinal centres.

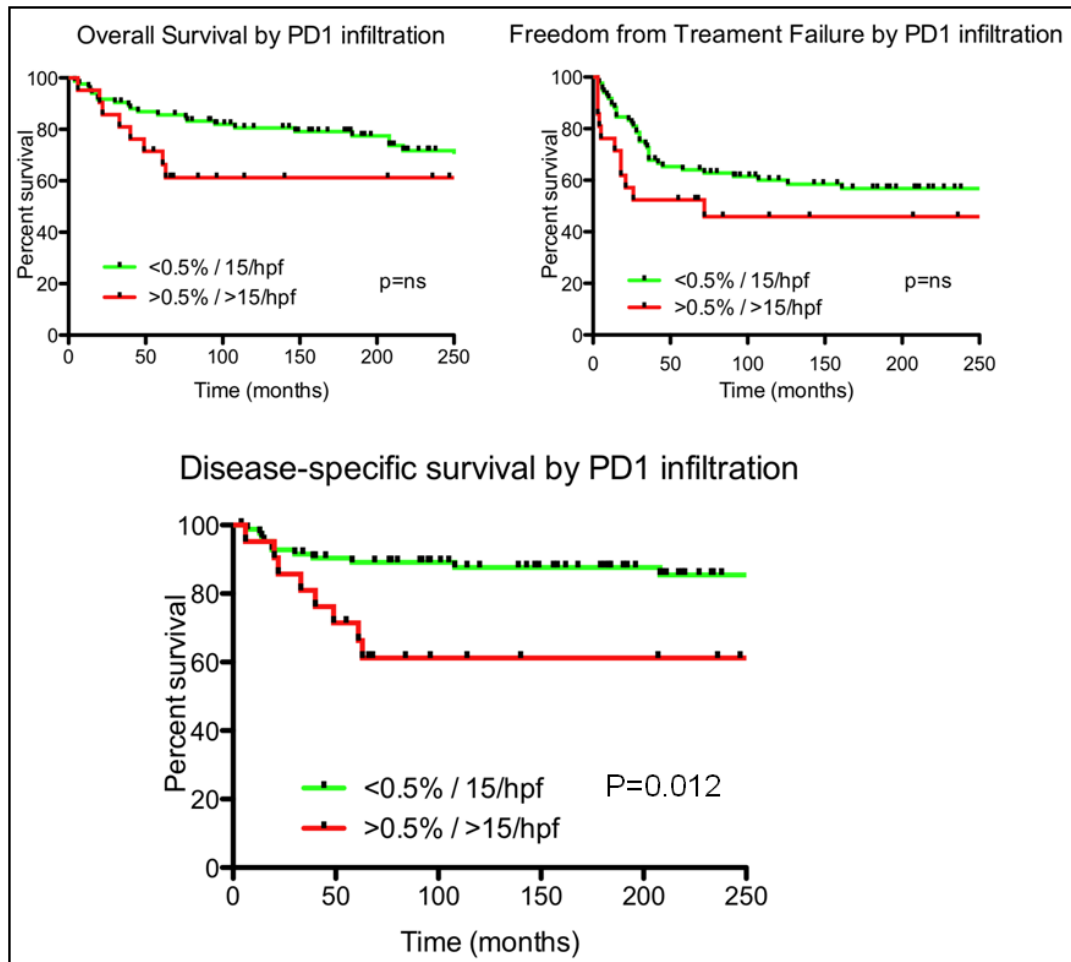


**Figure 4.13:** In the few patients in whom PD1 was expressed in >15 of cells/hpf ( $120/\text{mm}^2$ ), or 0.5% of all cells, DSS is inferior (at 5 years 63% vs 86%,  $p=0.012$ ). 5 year OS was 63% vs 84% ( $p=0.18$ ), and 5 year FFTF 44% vs 66% ( $p=0.051$ ).

#### 4.4.4 PD-L1 expression in the microenvironment

Expression of PD-L1 was marked across all samples. However staining pattern, consistent with the membrane and cytoplasmic expression of the protein, rather than the easily defined nuclear localisation of transcription factors, meant that enumeration was difficult, and raises the possibility of the contribution of non-specific staining (Figure 4.14). Intensity of staining varied from sample to sample, however the validity of IHC staining intensity as a reflection of biologically relevant relative amounts of antigen is questionable, with little validation against gold standards. Tonsillar staining was also relatively ubiquitous, but with denser staining apparent in the follicles (Figure 4.15)



Whether this was merely a reflection of cellular density and non-specific immunoglobulin binding, presence of a greater proportion of B cells, in which PD-L1 is more commonly expressed as an activation marker, or reflective of activated germinal centre reactions, in which PD-L1 plays a vital role, is not clear. However, difficulty in devising a consistent and reproducible enumeration strategy, despite apparent heterogeneity between samples, led this not to be pursued as a means of discriminating patient prognostic groups. PD-L1 clearly has importance in CHL as discussed, but IHC studies (and flow cytometry, as will be shown in Chapter 6), have not provided evidence that its expression is any different to that seen in other activated lymph nodes.

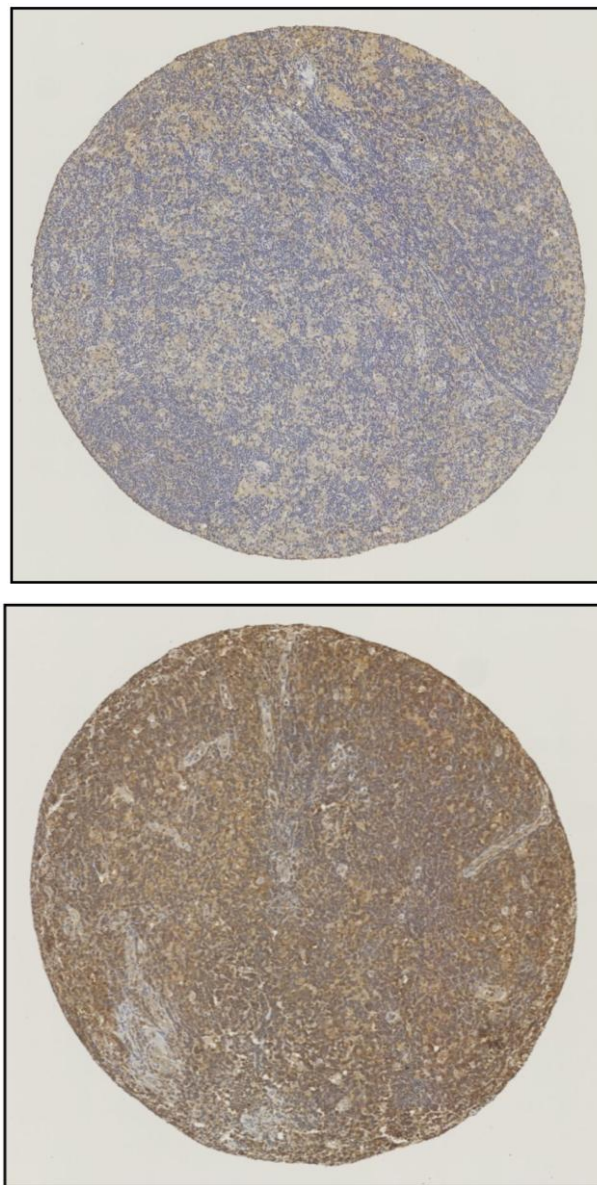


**Figure 4.14:** PD-L1 staining is heterogeneous between samples but difficult to quantify.

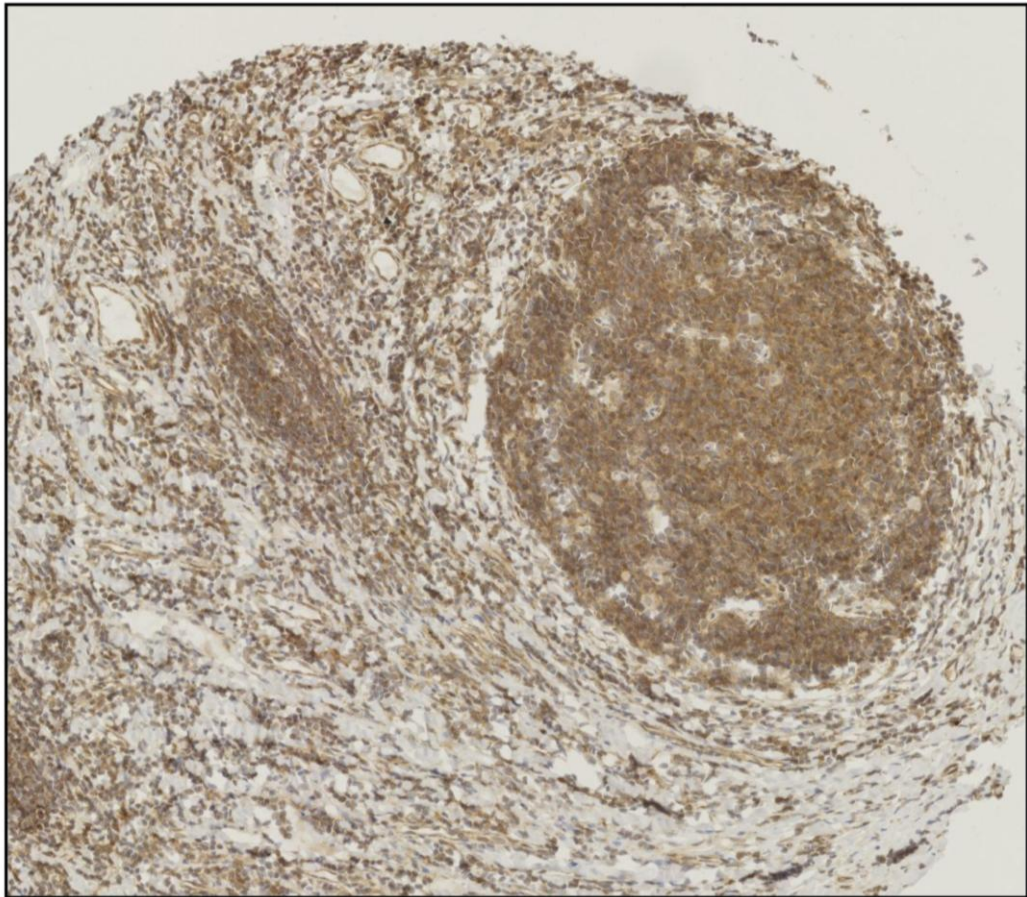


**Figure 4.15:** Tonsillar PD-L1 staining reveals apparent differential staining intensity between follicle and T-zone.

## **4.5 Discussion**

### **4.5.1 Limitations of IHC**

Single colour IHC is limited by its inability to determine the cell in which a marker is expressed unless it is morphologically quite distinct, along with difficulty in interpretation and the technical challenge of an alternative method - multicolour or fluorescence IHC. The problems of antigenic alteration by preparation and storage technique are another limitation. However analysis of FFPE tissue has the advantage of preserving tissue architecture thus enabling analysis of the spatial organisation of tissue components without the need for tissue disruption and cryopreservation steps, which favour the survival of some cell subsets over others and potentially introduce contamination from peripheral blood cells. While flow cytometry is able to identify the

cell subtype expressing an antigen of interest with a reproducible, robust and technically simple method, it requires tissue disruption and consequent loss of structural data. Therefore, these two approaches should be used in tandem. Discrepancies in interpretation of levels of expression arising from application of these two distinct techniques are well documented, and in the case of this study, comparing results in this chapter and Chapter 6, it is clear that for PD1 and PD-L1 results are inconsistent.

#### **4.5.2 Limitations of TMA**

Drawing conclusions about the nature of the microenvironment as a whole using only small, if apparently representative samples, may lead to significant interpretation bias, loss of data, and difficulty translating and validating the work of other laboratories. However, substantial work in solid tumour has established the validity of conclusions drawn using 1mm<sup>2</sup> cores analysed in duplicate or triplicate compared to whole section analysis<sup>432-435</sup>. There is only one validation study in CHL. This concluded that duplicate cores were sufficient to draw valid conclusions about the tissue as a whole, at least for B cell markers and LMP1<sup>65, 436</sup>. However problems arising from the fibrotic, heterogeneous nature of the disease remains, hence it is important to standardise optimal practice to determine regions representative of the overall microenvironment, hence suitable for reproducible, comparative analysis. Strategies could include standardisation by overall tissue cellularity, as has been described here, or standardising by numbers of HRS cells present. However, density of HRS cells varies widely between cases and may have independent effects on prognosis. This study adopted a pragmatic approach, selecting high quality regions of tissue with hypercellular infiltrate and presence of any number of HRS cells for array and analysis, with no further criteria of standardisation. This may well be a limitation, but has enabled a simple protocol to be developed and applied to validation cohorts in other laboratories.

#### **4.5.3 Th1 and Th2**

This study was not an exhaustive immunohistochemical study of Th1 and Th2-defining markers in the microenvironment. However, the markers were chosen for the robustness of their evidence base and the fact that they represent relatively specific determinants of function. T-BET showed consistent expression in the microenvironment at variable levels consistent with a Th1 polarised response, although the identity of the expressing cell was

not determined (CD4 vs CD8 vs CD20). GATA3 could not be demonstrated at any convincing level, although the staining was suboptimal as had already been encountered in the literature. Reporting of these findings is relatively neglected in reviews describing the CHL microenvironment. In fact, the major classical T subsets within the microenvironment based on this and preceding work, appear to be Tregs and Th<sub>1</sub> cells. Co-staining with both factors would establish this more convincingly. Whether FOXP<sub>3</sub> represents functional Tregs and T-BET functional Th<sub>1</sub> cells remains to be determined. This expression pattern is strikingly similar to that observed in the interfollicular T cell zones of normal lymph nodes, in contrast to follicles and germinal centres, from which T-BET<sup>+</sup> cells in particular, and to a large extent FOXP<sub>3</sub><sup>+</sup> cells, are excluded (Figures 4.2 and 4.3). It is also in contrast to the infiltrate of NLPHL in which the markers of Tfh cells: C-MAF<sup>46</sup>, BCL6, CD57<sup>437</sup> and PD1<sup>425</sup> in particular, have been described as over-expressed.

The infiltrate in CHL could be interpreted as a failed immune response, rich in Th<sub>1</sub> cells but also in Tregs, which are always found accompanying any acute inflammatory reaction. It could alternatively be interpreted as a massive expansion of the normal interfollicular T cell zone initiated by the presence of the malignant cells, causing it to fill with non-specific T cells recruited from the circulation. Any cell residing in the normal T cell zone is primed to encounter antigen, yet will only fully activate to proliferate and discharge its function when a cognate antigen-specific encounter has occurred. HRS cells meanwhile will be insulated from specific anti-tumour immune responses by the overwhelming numbers of non-specific T cells enveloping them. This model of CHL has already been alluded to in the literature<sup>438</sup>. However, the explanation coexists with an ongoing description of a Th<sub>2</sub>-polarised infiltrate in which Tregs mediate further immunosuppression leading to failed tumour clearance. In fact, since the FOXP<sub>3</sub><sup>+</sup> cells are associated with favourable prognosis, expression of this marker may simply reflect the robustness of the host immune response. Any inflammatory infiltrate is rich in FOXP<sub>3</sub><sup>+</sup> cells, part of normal immune homeostasis, and not necessarily reflective of these cells being the major mediators of pathological immunosuppression.

#### **4.5.4 PD1 and PD-L1**

This study confirmed that PD-L1 is ubiquitously expressed by tumour and microenvironment in CHL, but at levels indistinguishable from tonsil. While heterogeneity of expression between samples appears evident, IHC is inadequately sensitive to quantify this. PD1, on the other hand, is markedly underrepresented. The chapter introduction (4.1.3) has discussed some of the assertions made in the literature about the functional importance of the PD1/PD-L1 axis in mediating immunosuppression in CHL. However these studies have a weak functional basis. The profound absence of PD1 demonstrated here, and in previous studies suggests that this pathway is not important in the majority of cases, and cannot explain the failure of the immune response to eradicate tumour. Its apparently adverse prognostic significance in the small minority of cases in which it is expressed, along with its close association with the malignant cells in nodular configurations, suggests that perhaps it is important in these particular rare cases, but not in general.

#### **4.6 Summary and Further Work**

Chapters 3 and 4 have documented attempts to describe the heterogeneity of the CHL microenvironment based on the expression of non-specific immune cell markers (cytotoxic and helper T cells, B cells, macrophages), and T cell subset (Th1, Th2, Treg) and functional markers (PD1, PD-L1) already described in the literature, but examined for the first time here using automated image analysis. Clinically translatable prognostic models may emerge from this data as long as robust validation is carried out. However, associations of expression with patient outcome only allude to function and are in no way demonstrative of the importance of biological pathways in initiating, maintaining or suppressing the disease. This requires *in vitro* and *in vivo* model systems capable of manipulation. The development of these systems however, is problematic, as described in 1.8. An attempt to develop an *in vitro* co-culture system to specifically investigate the interaction between the HRS cell and CD4+ T cells will be described in Chapter 5.

## CHAPTER FIVE:

A culture system to sustain  
primary tissue-derived HRS cells and  
tumour-infiltrating CD4<sup>+</sup> T cells

## 5. A culture system to sustain primary tissue-derived HRS cells and tumour-infiltrating CD4<sup>+</sup> T cells

### 5.1 Introduction

#### **5.1.1 Clinical Trials without in vitro or in vivo models**

CD4<sup>+</sup> T cells are numerically dominant in CHL and correlative data are highly suggestive that these cells play a fundamental role in malignant cell survival comparable to the absolute dependence of B cell survival on CD4<sup>+</sup> T cells in normal physiology. However as described in 1.8, development of a model system beyond CHL-derived continuous cell lines and simplistic murine tumour transplant models, has eluded investigators. Hence, conclusions regarding the functional importance of micro-environmental cells in tumour survival are often derived from the success of pharmacological manipulation of survival pathways in clinical trials, not from data derived from basic science. Examples include the success of the anti-CD20 antibody rituximab in inducing remissions in relapsed patients despite the absence of expression of CD20 by the malignant cell<sup>439</sup>, anti-CD40 antibodies (SGN-40) administered for NHL and under investigation in CHL<sup>440</sup> which may antagonise key T cell-mediated B cell survival signals (described in 1.5.2), and the use of the T cell depleting antibody anti-CD52 (alemtuzumab) to treat refractory CHL, under investigation in a number of Phase II clinical trials as part of conventional chemotherapy as a single agent, or to improve outcomes following allogeneic transplantation<sup>441</sup>. The use of immunomodulatory drugs such as lenalidomide in CHL also has a hypothetical basis of action by manipulating the T cell microenvironment in particular<sup>442</sup>. The actual mechanism of action of these 'indirect' therapies has little evidence base since clinical trials have been performed without the usual preceding *in vitro* or *in vivo* model demonstration of action required of novel pharmacological agents, and are justified ethically due to a context of failed conventional therapies, and inevitability of tumour progression and death without treatment.

### **5.1.2 Maintaining the HRS cell indirectly using T cell supporting cytokines**

#### **5.1.2.1 IL2**

IL2 is a T cell growth and survival factor that signals via a receptor comprising three subunits. One subunit, the common gamma chain (CGC/CD132) is constitutively expressed by many immune cells including B cells and monocytes<sup>443</sup> and shared by a number of other interleukin receptors<sup>444</sup>. The receptor has two other cell type and activation status-specific components which determine affinity for ligand, namely IL2R $\beta$  (CD122), expressed preferentially by cytotoxic T cells and NK cells<sup>445</sup>, and IL2R $\alpha$  (CD25) constitutively expressed by nTregs<sup>179</sup> and up-regulated on activation of other lymphoid cells<sup>301</sup>. IL2 leads to activation, proliferation and enhanced function of lymphocytes<sup>446</sup>, but also induces apoptosis<sup>447</sup> (activation induced cell death) unless other survival pathways are induced: notably in Tregs whose survival and expansion are dependent upon prolonged exposure to IL2<sup>448</sup>. While many CHL-derived cell lines and primary tissues express IL2R $\alpha$ <sup>449, 450</sup> there is little convincing evidence that CHL itself produces IL2<sup>451</sup> nor that IL2 is a growth factor for the HRS cells themselves<sup>452</sup> although its role in the T cell rich microenvironment is not clear.

#### **5.1.2.2 IL4**

IL4 signals through its receptor, comprising the common  $\gamma$  chain as well as a unique subunit CD124 (IL4R $\alpha$ ), to stimulate growth and survival of B and T lymphocytes. In CD4+ T cells IL4 activates the Th2 differentiation pathway<sup>151</sup> via the transcription factors GATA3, C-MAF and STAT6 inducing further IL4 production as well as other Th2-defining cytokines such as IL5 and IL13<sup>453</sup>. IL2 and IL4 may act antagonistically, cooperatively or synergistically on T cell growth and activation depending upon the experimental conditions and responder cell populations<sup>454-458</sup>. There is evidence to suggest that IL4 is an autocrine stimulus of HRS derived cell line growth<sup>48</sup>. IL4-encoding mRNA is present in the reactive tumour microenvironment of biopsy material<sup>49</sup>, and HRS-derived cell lines strongly express the IL-4 receptor<sup>50</sup>, although contradictory evidence exists<sup>51-53</sup> and there are clear limitations to analysis of cytokine function in non-vital fixed tissue.



### 5.1.2.3 IL13

IL13 is more widely expressed in primary samples and HRS cell lines<sup>54-56</sup>, distinguishing CHL from NLPHL and another histologically similar malignancy, T cell-rich B cell lymphoma (TCRBCL)<sup>54</sup> with IL13R expressed in most CHL cell lines and primary CHL cases<sup>55, 56</sup>. While exogenous IL13 fails to augment cell line growth, some growth is inhibited by antibody-mediated IL13 receptor blockade<sup>54-56</sup>.

## 5.2 Aims and Objectives

A culture system was developed to test the hypothesis that the survival of the HRS cell in CHL is dependent upon signals derived from the microenvironment and that a significant contribution to these signals arises from CD4+ T cells. An attempt was made to prolong the survival of primary CHL-derived lymph node single cell suspensions (SCS) by enriching with cytokines known to sustain both T cell, specifically Th2, and HRS growth. Should survival of measurable cell populations be achieved, conditions of the culture system could be manipulated in order to determine the molecular mediators of survival and proliferation of HRS cells and tumour-sustaining T cells. Pathway and molecule-specific blocking methods could include monoclonal antibodies or gene knock-down. Candidate molecules participating in this interaction have been discussed in 1.5.2. In order to determine the effects of manipulating such a system the following conditions were required:

1. Development of an optimised culture system including media composition and plating techniques.
2. Identification of a technique to identify or isolate HRS cells within mixed cell populations at baseline and at subsequent time points in order to perform assays on this specific population.
3. Selection of a method to conclusively demonstrate that any population being assayed was derived from clonal B cells, consistent with it representing the malignant cell.
4. Selection of control cell populations, derived from benign and malignant nodal tissue.
5. Selection of quantitative assays of proliferation and growth in this population
6. Modifications of the system to identify mediators of proliferation and survival.

## 5.3 Materials and Methods

### 5.3.1 Single cell suspensions

Details on preparation of single cell suspensions is provided in Materials and Methods 2.1.2. Table 5.1 shows the samples used in the following immunophenotyping and cell culture experiments.

Sample	Source	Histology Immuno EBV status	SCS Classes	Biopsy Date	Date plated	% viable at baseline (Tryp Blue exclusion)	Total cells plated	Total no wells
C <sub>1</sub> (501)	Axillary LN	CHL: NS EBV- CD30+ CD3- CD20-	CHL/ Malig	19/06/09	11/05/2011	>90%	10x10 <sup>6</sup>	120
C <sub>2</sub> (302)	Cervical LN	CHL: NS EBV- CD30+ CD3- CD20-	CHL/ Malig	19/02/09	11/07/2011	>90%	5x10 <sup>6</sup>	60
C <sub>4</sub> (304)	Cervical LN	CHL: MC EBV+ CD30+	CHL/ Malig	17/09/99	11/07/2011	>90%	5x10 <sup>6</sup>	60
C <sub>5</sub> (305)	Cervical LN	CHL: NS EBV+ CD30+	CHL/ Malig	18/08/99	11/07/2011	>90%	5x10 <sup>6</sup>	60
C <sub>6</sub> (506)	Cervical LN	CHL: NS EBV- CD30+	CHL/ Malig	21/02/02	11/05/2011	>90%	10x10 <sup>6</sup>	120
F <sub>1</sub> (603C)	Cervical LN	Grade 2 FL	FL/ Malig	05/07/11	05/07/2011	>90%	10x10 <sup>6</sup>	120
F <sub>2</sub> (802)	Axillary LN	Grade 2 FL	FL/ Malig	02/08/10	15/08/2011	<60%	5x10 <sup>6</sup>	60
F <sub>4</sub> (805)	Cervical LN	Grade 3A FL	FL/ Malig	01/02/08	15/08/2011	<60%	5x10 <sup>6</sup>	60
L <sub>1</sub> (801)	Inguinal LN	NLPHL	NLPHL/ Malig	11/09/06	11/7/2011	<60%	5x10 <sup>6</sup>	60
P <sub>1</sub> (605)	Cervical LN	PTGC EBV-	Reactive / Benign	22/08/11	22/08/2011	>90%	5x10 <sup>6</sup>	60
R <sub>2</sub> (808)	Cervical LN	Follicular hyperplasia EBV-	Reactive / Benign	29/03/10	12/10/2011	>90%	5x10 <sup>6</sup>	60
T <sub>1</sub> (804)	Tonsil	Tonsil	Tonsil/ Benign	-	15/08/2011	<60%	5x10 <sup>6</sup>	60
T <sub>2</sub> (806)	Tonsil	Tonsil	Tonsil/ Benign	-	15/08/2011	<60%	5x10 <sup>6</sup>	60
T <sub>3</sub> (T <sub>3203</sub> )	Tonsil	Tonsil	Tonsil/ Benign	-	N/A	<60%	N/A	N/A
T <sub>4</sub> (T <sub>3121</sub> )	Tonsil	Tonsil	Tonsil/ Benign	-	N/A	<60%	N/A	N/A

**Table 5.1** Samples established in culture using the optimised cytokine enrichment systems. Note that T<sub>3</sub> and T<sub>4</sub> were not established in culture but instead used as control for subsequent immunophenotyping experiments. Key: NS: Nodular Sclerosis, MC: Mixed Cellularity.

### 5.3.2 Multicolour Flow Cytometry for identification of HRS cell population

Details on staining technique and analysis for flow cytometry are provided in Materials and Methods 2.3. Details specific for this experiment are provided below. Flow cytometry was performed on thawed single cell suspensions prepared as described.

#### 5.3.2.1 Selection of fluorochromes and antibodies

HRS can usually be identified not only by a unique immunophenotype distinct from other haematological, lymph node and bone marrow resident cells but also by their large size. They rarely express the characteristic cell surface markers of B cells (CD19 and CD20), T cells (CD3, 4 and 8) or cells of the monocyte/macrophage/dendritic cell lineage e.g. CD64<sup>39</sup>. They often express TNFRSF markers of activation such as CD40 and CD95 and are characterised by expression of the B and T cell activation and co-stimulatory TNFRSF molecule CD30, which was first discovered when a novel antibody was raised to a CHL-derived cell line<sup>12</sup>. These features have been used to develop an antibody panel and gating strategy which can identify HRS cells within a CHL-derived lymph-node population<sup>39</sup>. These studies did not demonstrate clonality by investigating the genome of the immunophenotype-defined purported HRS cell, and were validated only by first demonstrating that this cell had forward and side scatter properties consistent with being larger and more intracellularly complex than surrounding cells, second by examining the morphology of cells flow-cytometrically sorted using this panel, and finally by confirming the panel's ability to discriminate CHL from other lymph node-derived malignant and non-malignant tissue<sup>49</sup>. As such it should be considered only a promising pilot strategy. Based on the panel proposed by this group the fluorochrome and antibody panel shown in Table 5.2 was proposed:

	Eponym	Fluorochrome	Clone	Isotype	Supplier
CD3	-	PE-Cy7	UCHT1	Mouse IgG1-kappa	Biologend
CD4	-	Horizon V500	RPA-T4	Mouse IgG1-kappa	BD
CD8	-	Alexafluor 700	HIT8A	Mouse IgG1-kappa	Biologend
CD20	-	APC-H7	2H7	Mouse IgG2b-kappa	BD
CD30	TNFRSF8	PE	BY88	Mouse IgG1-kappa	Biologend
CD64	Fc-γ-R1	APC	10.1	Mouse IgG1-kappa	Biologend
CD40	TNFRSF5	PerCP-Cy5.5	5C3	Mouse IgG1-kappa	Biologend
CD95	FAS/TNFRSF6	Alexafluor 488	DX2	Mouse IgG1-kappa	Biologend

**Table 5.2:** Antibody panel to examine T cell, B cell and monocyte/macrophage lineage within experimental lymph nodes, and attempt to identify HRS cells by surface markers.

### 5.3.3 Culture of single cell suspensions derived from lymphoid tissue

#### 5.3.3.1 Lymphocyte Culture Media (LCM)

Enriched media, known as 'lymphocyte culture media' (LCM) was prepared as stock as described in Table 5.3 and discarded and replaced if unused within 28 days. This is based on the media used by various groups in order to proliferate and polarise human T cells<sup>191, 460</sup>.

Reagent	Supplier	Volume	Final concentration
RPMI with added glutamine	PAA Laboratories	500ml	-
Heat-inactivated human AB serum	Invitrogen	16ml	3%
Penicillin/streptomycin	Invitrogen	5.5ml	1%
1M HEPES	PAA Laboratories	5.5ml	10mM
Non-essential amino acids	PAA Laboratories	5.5ml	1%
Sodium pyruvate	PAA Laboratories	5.5ml	1%
2-mercapto-ethanol 14.3mM stock (dilute 14.3M stock 1:1000 in ddH <sub>2</sub> O)	PAA Laboratories	2ml	50mM

**Table 5.3:** Lymphocyte culture media enrichment reagents

#### 5.3.3.2 Cytokine Enrichment and Culture Establishment

Cytokines were added as required from frozen aliquots to LCM immediately prior to plating as shown in Table 5.4.

	Supplier	Aliquot	Culture condition			Biological activity		
			Dilute	Concentration		ED <sub>50</sub> (ng/ml)	Specific Activity (units/ng)	Responder Assay cells
				ng/ml	U/ml			
rh-IL2	Milteyi Biotec	50mcg in 5ml	1:1000	10	>50	<0.1	>5	HT-2 <sup>461</sup> CTLL-2 <sup>462</sup>
rhIL-4	Gibco	25mcg in 2.5ml	1:1000	10	25	0.05-0.4	2.5	TF-1 <sup>463</sup>
rh-IL13	eBio Science	200mcg in 2ml	1:2000	100	20-100	1-5	0.2-1	TF-1 <sup>463</sup>

**Table 5.4:** Cytokines used for cell culture, supplied as freeze-dried concentrate, made up in 0.1% HuABS/PBS aliquots as in Table 5.3 stored at -80°C. Specific activity was defined by the growth-stimulating activity of each cytokine on responder cells as indicated.

Thawed, washed SCS-derived cells were resuspended at  $0.25\text{-}0.4 \times 10^6/l$  in a total volume of LCM enriched with cytokines at the concentrations shown in Table 5.4 as determined by the experimental condition (no cytokine, single cytokine enrichment with IL4, IL13 or IL2 alone, and dual enrichment with IL4&IL13 or IL4&IL2). Cytokine concentrations were based on the literature on T cell stimulation, proliferation and expansion<sup>460</sup> and IL13 stimulation of HRS-derived cell lines<sup>54</sup>. Cell culture was carried out in round-bottom 96 well plates to maximise cell-cell contact and thereby emulate the close proximity of cells within the lymph node microenvironment. The number of wells established depended upon the availability of viable cells from the original SCS. No more than 60 wells were established for each sample and each culture condition. Based on a final LCM+/- cytokine suspension of  $0.25\text{-}0.4 \times 10^6$  cells per ml each well was filled with 200µl of cell suspension at plating, thus 50-80,000 cells per well. 96 well plates were placed into primary cell culture-designated incubator humidified at 35°C with 5% CO<sub>2</sub>.

At no point was any non-specific or specific activator of lymphoid cells nor any additional co-stimulatory factors added except the cytokines described and 2-mercaptoethanol. These may have included anti-CD3, anti-CD28, phorbol-myristate acetate (PMA), PHA (phytohaemagglutinin), concanavalin, or bacterial super-antigen. As such, for these experiments, any proliferative effects result only from the action of the LCM and supplementary cytokines on intrinsic properties of the cell suspensions derived from each lymph node.

### 5.3.3.3 Refinement of Cytokine Enrichment Conditions

In initial pilot experiments using tonsil and one CHL case exposed to media only, IL13 only, IL4 only and IL4&IL13 colony/cluster formation was only apparent in IL4-enriched conditions, with no apparent superiority of colony formation on further addition of IL13, and culture death within 2 weeks with no or little evidence of culture/cluster formation in IL13-only or media-only conditions. Therefore subsequent culture systems were established using IL2 only and IL2 & IL4. Figure 5.1 shows the growth resulting from a subsequent pilot experiment in which SCS-derived cells from tonsil and one case of CHL (C1) were established using media only, IL2 or IL4 only or both cytokines. For this pilot, all wells were harvested weekly in the first instance and fortnightly subsequently, and

total cells estimated by haemocytometry on the resulting cell suspension. Cells were then replated across the appropriate number of wells. This experiment was abandoned after 10 weeks once a clear differential in growth had been established. Subsequently, culture systems were limited to IL2 and IL2&4 only given that only these conditions enabled persistence or expansion of the culture. Additionally, the method of harvest, resuspensions, cell counting and replating as described for this pilot was abandoned at this stage in favour of the technique described below (estimating growth by viable vs non-viable well counting, Table 5.5) which enabled a larger number of different tissue-derived SCS to be cultured simultaneously with minimum disruption to the culture system at each assessment.

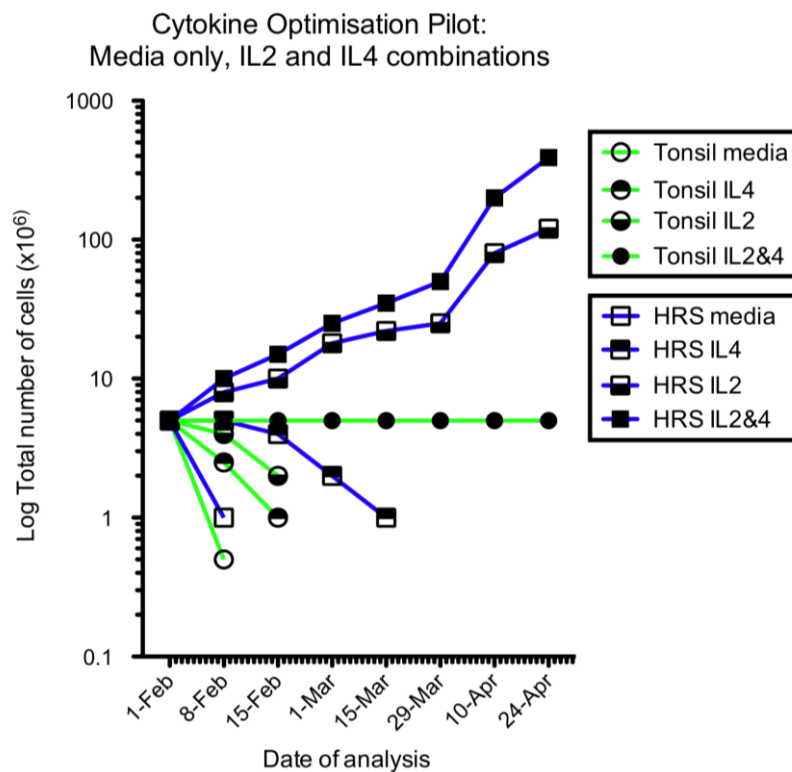


**Figure 5.1:** Cytokine Optimisation Pilot: Relative growth rates and survival of culture systems according to cytokine augmentation. HRS: CHL lymph node-derived SCS (C<sub>1</sub>). Blue lines/Squares: estimated growth rate of HRS, Green lines/Circles: estimated growth rate of tonsil-derived SCS. Filled figures: IL2&4, open figures: Media only, Top filled: IL4 only, Bottom filled: IL2 only. IL<sub>3</sub> was rejected since no growth was seen when used alone and no apparent augmentation of growth when used in conjunction with IL<sub>4</sub>.

Only a single CHL-derived SCS and single control tonsil were used for this pilot experiment. Hence IL13 may have a role to play in augmenting further the growth of other CHL-derived SCS. However it was decided to focus only on IL2 and IL4 given the relative redundancy of IL13 and IL4 in Th2 cell polarisation and growth augmentation well documented in the literature<sup>464</sup>. Therefore the influence of IL13 on residual HRS cells in the system has not been pursued any further.

#### 5.3.3.4 Culture plate inspection and splitting

Culture plate wells were examined every 3-5 days by the naked eye for media colour change indicating active cellular respiration and consequent pH change, and under an inverted microscope using a x5 and x10 objective (Figure 5.2). Using this technique, the majority of cells were a homogeneous lymphoid population and large HRS cells could not be identified. However, this was likely due to difficulty assessing cellular detail in cells in close contact or multiple layers within the round-bottom plate. However colonies and clusters of cells could be identified easily within and surrounding the main cell pellet and at the periphery of the pellet blastic cells and apoptotic debris were identifiable. Potential bacterial or fungal contamination could also be identified using this method. Individual culture wells were abandoned, split or media replaced depending upon an assessment of proliferation and viability in that well, using the method described in 5.3.3.6. Photomicrographs were acquired using an inverted microscope using a x5 objective lens and digital imaging software.

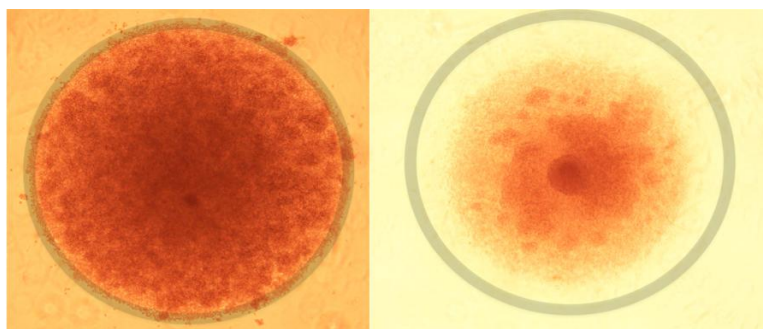


**Figure 5.2:** Cell number estimation by occupancy of x10 objective field on inverted microscope. The semi-transparent rings indicate the approximate extent of the x10 objective field. Left: Well appropriate for SPLITTING. Proliferating colony containing innumerable cell clusters occupying greater than the total x10 field. Right: Well appropriate for MEDIA CHANGE. A viable well containing a dense central colony/cluster with multiple less distinct surrounding colony/clusters.

#### 5.3.3.5 Initial LCM Change

One week after initiation of culture some systems showed clear formation of cell colonies/clusters on inspection of wells as above, while others showed minimal growth or evidence of cell death. However there was little evidence of media colour change, nor increase in overall cell numbers assessed by haemocytometry or by estimation of cell pellet size. Two weeks after initiation, there was substantial growth in the majority of wells in some systems with media colour change and increase in pellet size. Subsequent to this time period, growth tended to be sustained, with media colour change and increase in pellet size every 5-10 days. As such it was decided that the first media change should be to remove 50% of the media from each well and replace with fresh LCM with appropriate cytokine enrichment. Aspiration of media was easily achieved using a 200µl pipette (either well by well or using a multichannel pipette), removing 90µl of supernatant LCM (assuming some evaporation since the previous media change) without disruption of the cell pellet. Replacement was with 100µl of appropriately cytokine enriched LCM dispensed similarly through a 200µl pipette individually or using a multichannel pipette, the force of which led to a complete resuspension of all cells. Extreme care was taken on replacement of media that no well to well contamination occurred, by ejecting fresh LCM gently from a short distance above the plate.

#### 5.3.3.6 Assessment of Proliferation

Pilot experiments counting cells by haemocytometry determined that the number of cells per well when the cell pellet occupied the entirety of a  $\times 10$  objective field was between 100,000 and 150,000 (Figure 5.2) As such, in order to minimise time of culture systems spent outside the incubator due to multiple well sampling for haemocytometry, or the disruption of evacuating an entire plate into sample tubes in order to perform a cell count on total volumes followed by replating, a method to estimate overall culture system proliferation was devised. Each well was visually inspected under the inverted microscope and scored according to Table 5.5.

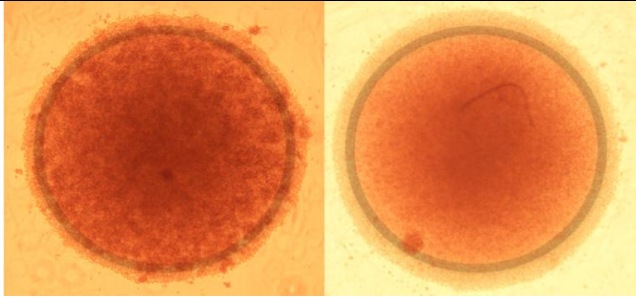
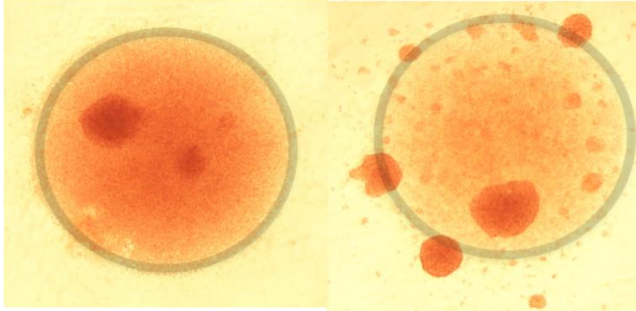
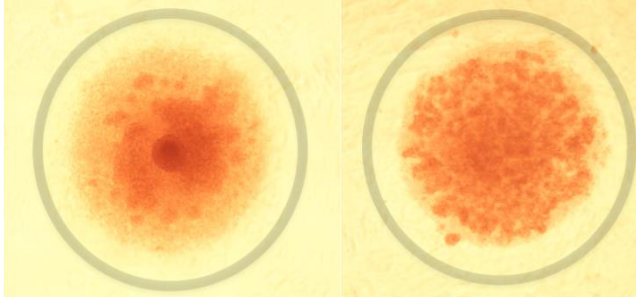
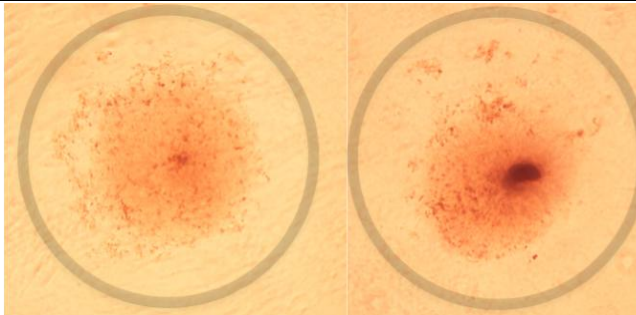
Any well appearing senescent was classified as 'dead' for counting purposes. All other growth was classified simply as 'live' for counting purposes, and media changed according to Table 5.5. Classification as 'live' or 'dead' was taken to reflect successful



plating on the previous media change. Hence from this inspection and scoring, the total number of live and dead wells on each media change was recorded. A total cell count could be estimated from this assuming that wells plated on the previous media change contained 50-80,000 cells. This relies on an estimate of total cells occupying a  $\times 10$  objective field. However, applying this methodology consistently across all conditions and being blinded to the source of each culture system during the counting process enabled valid comparison between systems and conditions to be made.

#### 5.3.3.7 Subsequent media change

Media was changed every 7-10 days according to the scoring system described in 5.3.3.6 and with appropriate cytokine enrichment on each occasion. Weekly cytokine enrichment was chosen since this is consistent with standard T cell proliferation and polarisation protocols<sup>460</sup>. Cytokine-enriched LCM for each media cycle was made up fresh at double the concentration of cytokine required (see Table 5.4). Media change constituted removal of 90ml supernatant and replacement with 100ml fresh LCM as for the initial media change one week after first plating. Splitting 1:2 required initial resuspension of each cell pellet, followed by aspiration of 50% of the volume of the well (75-90ml) and plating half in a fresh well, leaving half in the original well. Splitting 1:3 required resuspension of each cell pellet, followed by aspiration of two aliquots of 50-60ml of cell suspension and plating into new wells, leaving approximately one third in the original well. Each resultant well was topped up with fresh media as for media change, ensuring that a total of 200ml was present in each well. It is acknowledged that this strategy meant 1:3 splits led to a final concentration of fresh cytokine 150% that of 1:2 splits and 50:50 media changes (assuming that all cytokine from the previous cycle had been exhausted or degraded). The assumption was made that since cytokines were being used at the upper limit of biological activity as defined in Table 5.4, this would not lead to additional advantages for the cells within that well. Should there be any advantage, however, this would be applied consistently across all culture systems and should therefore not influence an analysis of differences between systems.

Description	Examples	Media change
Prolif++		SPLIT 1:3
Prolif+		SPLIT 1:2
Prolif+/-		REPLACE MEDIA
Senescent		DISCARD

**Table 5.5:** Scoring system for individual wells using visual inspection to determine media change technique.

5.3.3.8 Estimation of overall culture system proliferation

Assessment of numbers of viable wells using the technique described above enabled an estimation of overall proliferation of the culture system across all wells over a period of many weeks. Continual expansion of the more proliferative systems would not be practical or economically feasible, requiring many hundreds of culture plates and large amounts of media and cytokine. Hence, at each media change in the more proliferative systems, only a proportion of total proliferating wells were subsequently split and replated. Total number of wells maintained at any one time for each proliferating culture system was typically between 60 and 300. Less proliferative systems were maintained at the maximum possible number of viable wells.

At each media change, the number of viable wells and the proportion of viable wells in actively proliferating cultures that were then split was recorded, and an estimate calculated of the ‘theoretical potential maximum’ number of viable wells that could have been populated in the ideal situation of all viable wells having split at each cycle. This was documented as a ‘corrected’ number of total wells, using the equation overleaf applied using an Excel spreadsheet (Figure 5.3).

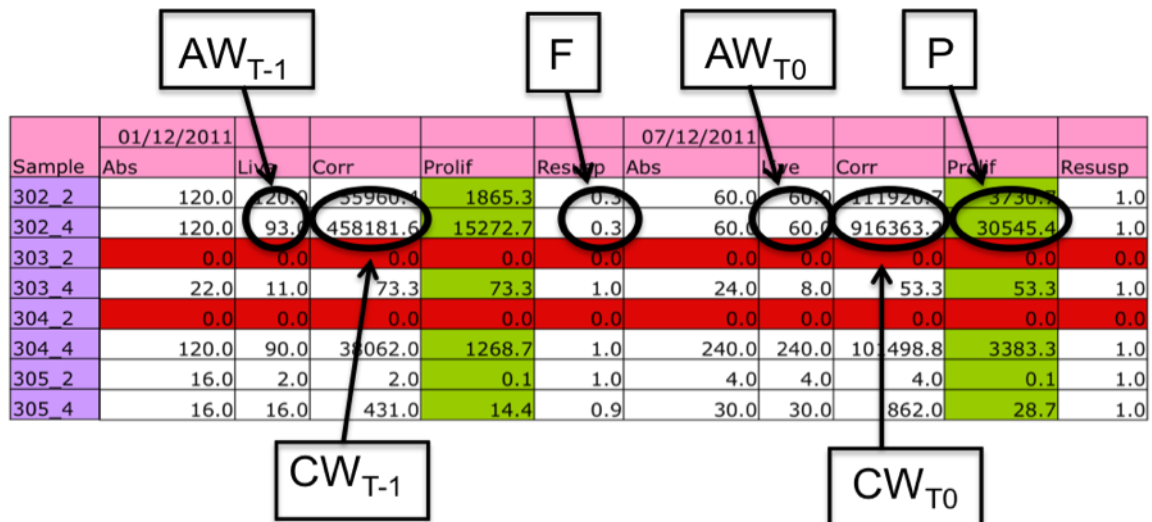


**Figure 5.3:** Portion of Excel spreadsheet demonstrating documentation of viable wells at each media change and application of formula to estimate theoretical maximum / corrected number of total wells at each point (CW). Estimated overall proliferation in each of the systems are highlighted in green. Cultures in which all cells have died are highlighted in red.

**Equation to calculate proliferation in cell culture system:**

$$CW_{T_0} = \frac{AW_{T_0} (CW_{T-1} / AW_{T-1})}{F}$$

Where:

$CW_{T_0}$  = Theoretical (corrected) number of viable wells at current media change

$AW_{T-1}$  = Actual number of viable wells present at current media change

$CW_{T-1}$  = Corrected number of viable wells at previous media change

$AW_{T_0}$  = Actual number of viable wells at previous media change

F = Fraction of total number of viable wells replated at previous media change (where F is a decimal  $\leq 1.0$ ).

And the overall proliferation (P) of the system at the time of the current media change was calculated thus:

$$P = \frac{CW_{T_0}}{CW_{TW_2}}$$

Where  $CW_{T_2}$  = Number of viable wells present at week 2.

This value is a crude estimate, likely overestimating the proliferative potential of each culture system. However the method was applied across all culture systems in a standard manner, enabling comparisons between groups. Absolute values generated should not be taken as representative of the actual total number of cells that would have been generated had all viable, proliferating wells been split at every opportunity, but rather as a comparative indicator of the proliferative potential of each culture system.

**5.3.3.9 Freezing down of cells for subsequent analysis**

Cells were stored down once they had proliferated in sufficient numbers to occupy individual freezing vials (approximately  $5-10 \times 10^6$  cells stored in 1-1.5ml of freeze mix.) Longevity of culture systems was longer than anticipated and in some cases exceeded 25 media changes and 200 days of culture. It was decided to discontinue further expansion at day 200 to preserve reagents, reduce costs, and enable further SCSs to be assessed for proliferative capacity. There were insufficient excess cells expanded for cryopreservation

in any system until beyond 4 weeks of expansion. As such, and ideally, excess cells were frozen down at baseline, day 30, day 60, day 100, day 150 and day 200 where the culture system was declared 'viable at day 200' and discontinued. In cases where proliferation was inadequate, freezing was carried out once sufficient numbers had been acquired. In some cases freezing down of samples was not possible beyond baseline. Cells were subsequently analysed for extended CD4+ cell phenotype as described in Chapter 7.

#### 5.3.3.10 Senescence of culture systems

Wells were declared senescent if after two media changes (and hence no splitting) there was no evidence of ongoing growth by the morphological criteria defined in Table 5.5. Culture systems were terminated if there were no viable wells remaining. However, even if a single viable well remained an attempt was made to support its growth using the media change technique described. A culture system was declared senescent if the theoretical maximum number of viable wells at any time point (CW) fell below 50% of the highest previous value of CW ( $CW_{max}$ ). As explained, an attempt to maintain even a few remaining viable wells was made in any case. However, in no case did a culture system recover once there was such a reduction below  $CW_{max}$ , although in some cases the CW remained static or fell marginally before recovering again.

### 5.3.4 Statistical Analysis

#### 5.3.4.1 Immunophenotyping

Composition of each cell subtype defined by surface antigen expression was expressed as a percentage of a parent population or of all viable cells (Figure 5.4), as described in the results. Means were calculated for each class of SCS derived cells (malignant, non-malignant, CHL, FL, Reactive and Tonsil) and medians compared between classes as non-Gaussian variables using the method of Mann & Whitney with significance values set at  $<0.05$ .

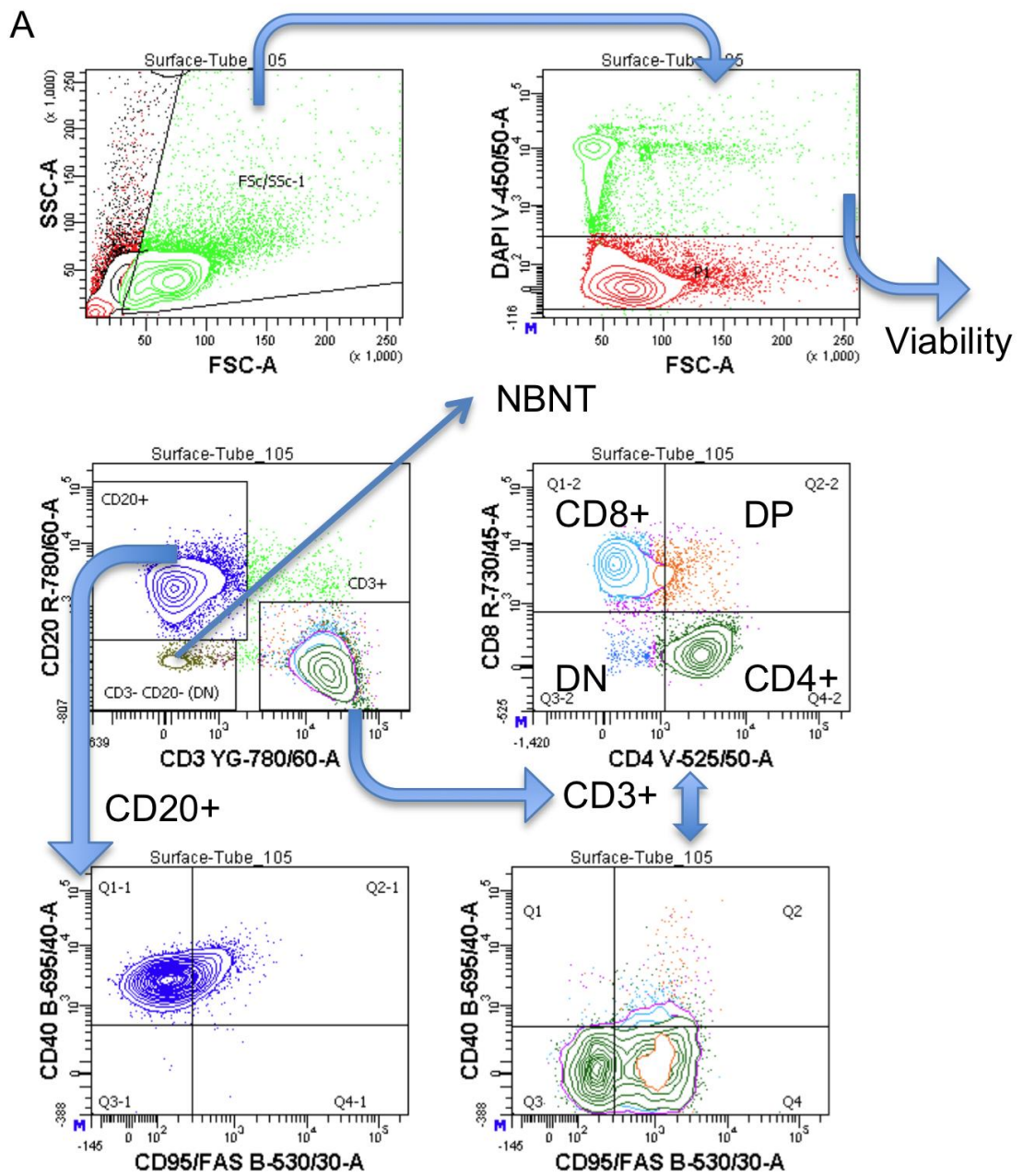


**Figure 5.4:** Gating strategy for analysis of SCS at baseline. SCS from CHL. Populations reported in subsequent analysis defined by gates as shown: Viable, CD3+, CD20+, NBNT, CD8+, CD4+.

#### 5.3.4.2 Proliferation

Survival of each culture system was determined by time to senescence as defined above. Data was pooled by class of SCS and survival duration compared between groups using Kaplan Meier analysis. Differences between survival of SCS classes was determined using the log rank method and deemed significant if the chi square value generated had an equivalent p value of  $<0.05$ . Proliferative capacity of each culture system was assessed at each media change point as described above, generating a CW value (See 5.3.3.8) at each time point. Differences in median proliferation (median CW) for each SCS class at each time point were compared assuming non-Gaussian distribution using the method of Mann and Whitney.

### **5.4 Results**

#### **5.4.1 Flow cytometry of single cell suspensions**

##### 5.4.1.1 Viability heterogeneity between SCSs

The viability of single cell suspensions as measured by DAPI exclusion in a population defined by FSc/SSc properties was highly variable between samples. There was no significant difference in total cellular viability comparing malignant with non-malignant conditions (Figure 5.5) although the numbers are small and influenced by the outliers which have been included. However, the suspensions with the highest viability ( $>70\%$ ) were all derived from malignant tissue and all but one of the non-malignant tissue samples (T<sub>1</sub>) had total cell viability  $<60\%$ . This finding may influence the validity of subsequent immunophenotyping findings.

##### 5.4.1.2 B cell, T helper and cytotoxic T cell composition

Representative plots for each sample type is shown in Figure 5.6. Tables 5.6 and 5.7, and Figures 5.7 & 5.8 summarise the findings of immunophenotyping of the SCSs at the time of culture plating. Only samples in which greater than 1000 viable events were recorded were analysed. With limited numbers of replicates this experiment was underpowered to demonstrate significant differences between the groups. The dominant lymphoid subset in all cases was CD<sub>3</sub><sup>+</sup> CD<sub>4</sub><sup>+</sup>, or T helper cells (Figure 5.8). There was no significant

difference in composition of CD3+ subsets (CD4+, CD8+, DP and DN) between samples. CHL-derived SCS were comprised of a significantly greater proportion of CD3+ cells than tonsil or reactive node with corresponding reductions in CD20+ cell numbers. However, of those CD3+ cells there was no significant difference in relative composition defined by CD4 and CD8 expression (Figure 5.8).

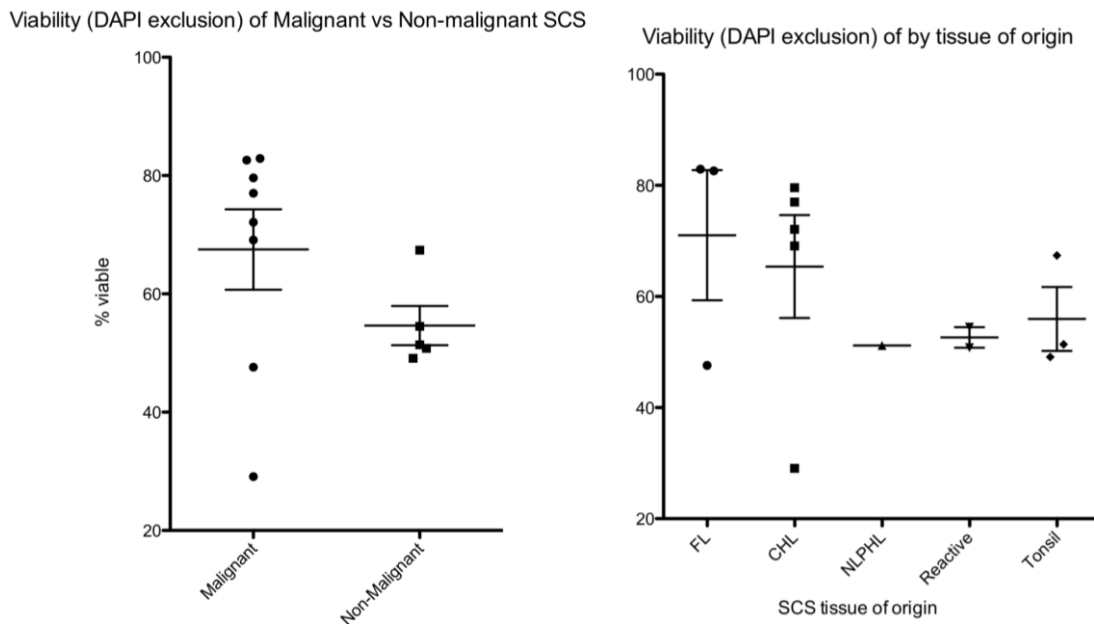


**Figure 5.5:** Viability of all SCS-derived cells at baseline. Left: Malignant-derived vs non-malignant. Right: By histological or tissue subtype (FL (n=3): Follicular Lymphoma, CHL: Classical Hodgkin lymphoma (n=5), NLPHL (n=1): Nodular Lymphocyte Predominant Hodgkin Lymphoma, Reactive (n=2): Progressive transformation of germinal centre and follicular hyperplasia, Tonsil (n=3)).



	No viable cells	% viable	% CD20	% CD3	Of CD3%				% NBNT
					% CD4	% CD8	% DP	% DN	
C1	14732	29.1	53	34.6	63.1	25.4	4.1	4.4	7.7
C2	42870	77	23.8	19.4	70.7	20.5	1.5	5.4	54.1
C4	23941	72.1	30.4	60.7	32.9	50.1	5.1	2.2	3.1
C5	20892	79.6	43.2	48.5	51	37.8	6.3	1.7	3.1
C6	10368	69.1	33.9	59.1	85.9	7.4	2.7	1.7	2.2
F1	42711	82.9	66.6	28.3	80.8	9.9	2.3	5.1	1.2
F2	4361	47.6	77.5	6.4	45.1	9.2	4.9	34.5	9.7
F4	70504	82.6	87.1	11.7	67.4	15.4	9.6	4.9	0.4
L1	8626	51.2	31.1	64.5	80.3	3.1	14.6	12.1	2.3
P1	6738	54.5	61	21.8	58.7	22.6	7.1	8	15
R2	5335	50.8	65.5	27.9	62.9	21.4	2.3	9.8	5.2
T1	39314	67.4	70.1	26.5	66.9	10.2	4.4	15.1	2.1
T2	18295	51.4	68.8	23.4	58.8	15.4	1.9	20.2	5.6
T3	68859	49.1	84.3	7.1	86.3	4.8	2.1	4.7	5.2
T4	459	3	35.4	6.8	62.1	10.3	10.3	0	5.9

**Table 5.6:** Composition of all viable cells at baseline in lymph node tissue derived frozen SCS. T4 was omitted from further analysis due to extremely poor viability and number of events recorded. DP = CD4+CD8+ (double positive), DN = double negative, NBNT = non-B non-T (CD3- CD20-).

	CHL Mean (SEM)	FL Mean (SEM)	Reactive Mean (SEM)	Tonsil Mean (SEM)
CD20%	33.6 (5.1)	77.1 (5.9)	63.3 (2.3)	74.4 (4.9)
CD3%	44.6 (7.8)	15.5 (6.6)	24.9 (3.1)	19.0 (6.0)
CD4%	60.7 (9.0)	64.4 (10.4)	60.8 (2.1)	70.7 (8.2)
CD8%	28.2 (7.3)	11.5 (2.0)	22.0 (0.6)	10.1 (3.1)
CD4% of all	26.2 (6.4)	11.2 (6.0)	15.2 (2.4)	12.5 (3.4)

**Table 5.7:** Summary of composition of viable cells at baseline by tissue of origin, as represented in Figure 5.8. SEM = Standard error of the mean.

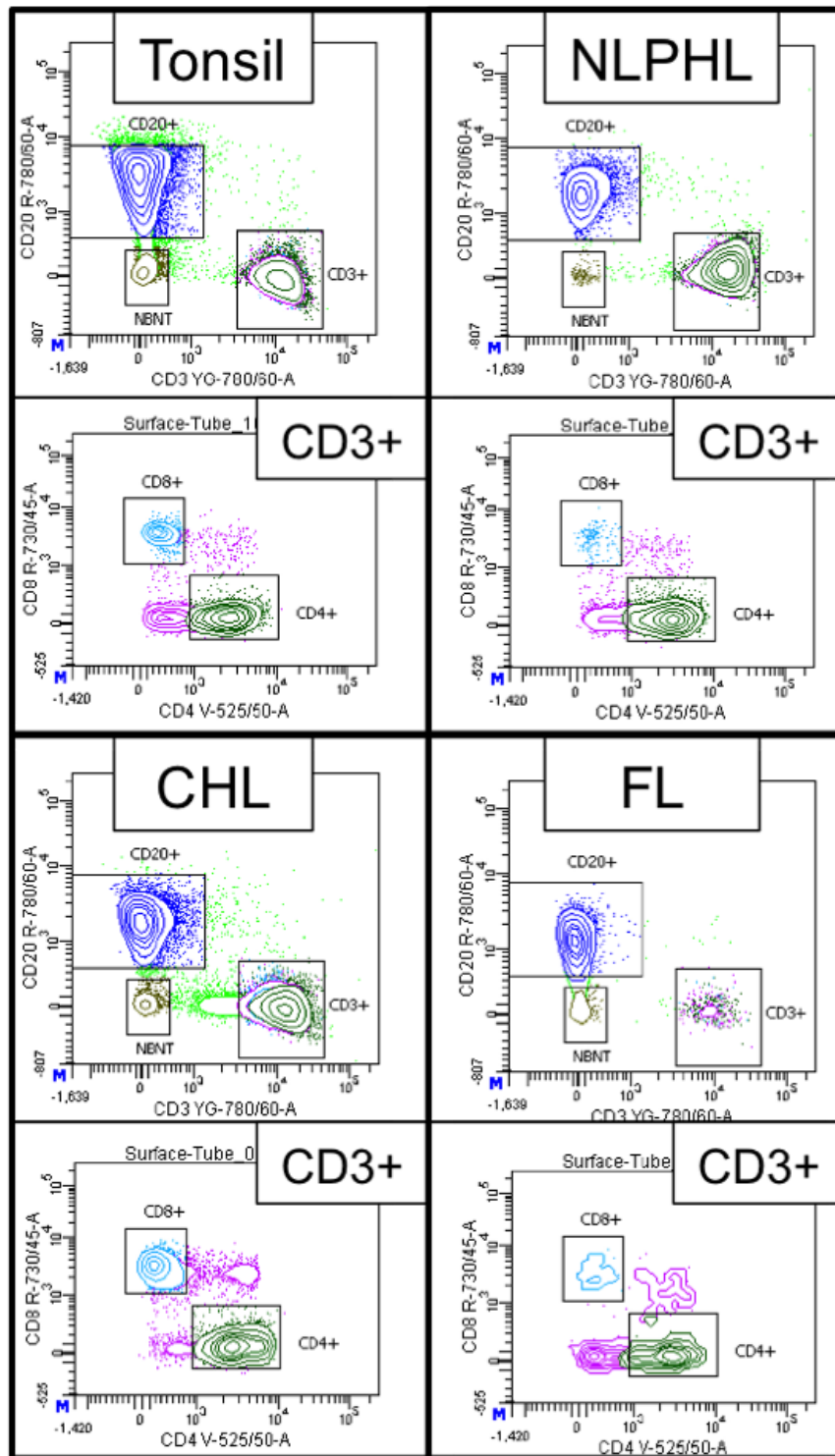


**Figure 5.6:** Representative FACS plots derived from each sample type showing variation in composition of lymphoid cell subsets gating on the CD3<sup>+</sup> population and as shown in figure 5.4.

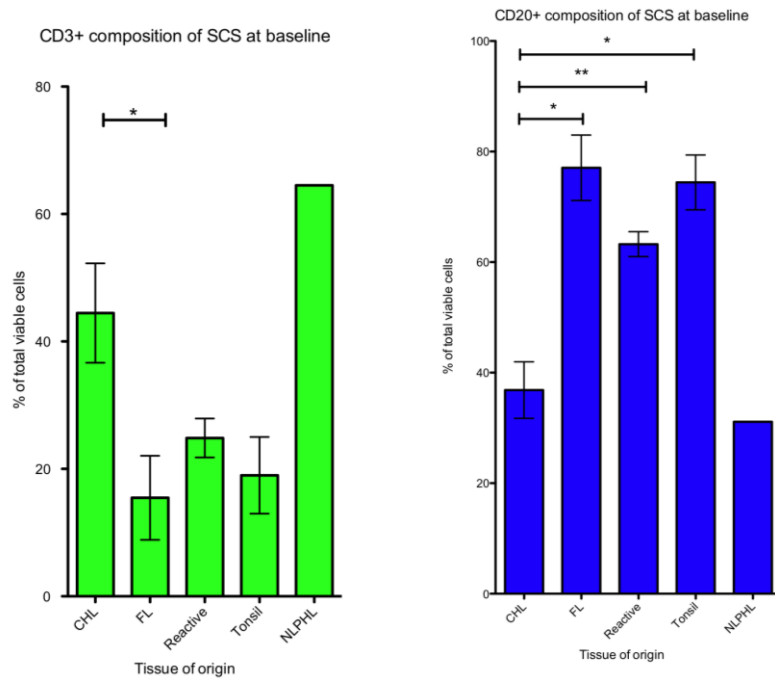


**Figure 5.7:** Lymphoid subset composition of SCS at baseline. Left: CD3+ cells represented a significantly greater proportion of total viable cells in SCS derived from CHL compared to those derived from FL. Right: CD20+ represented a significantly lesser proportion of total viable cells in SCS derived from CHL compared to those derived from FL, reactive nodes or tonsil.

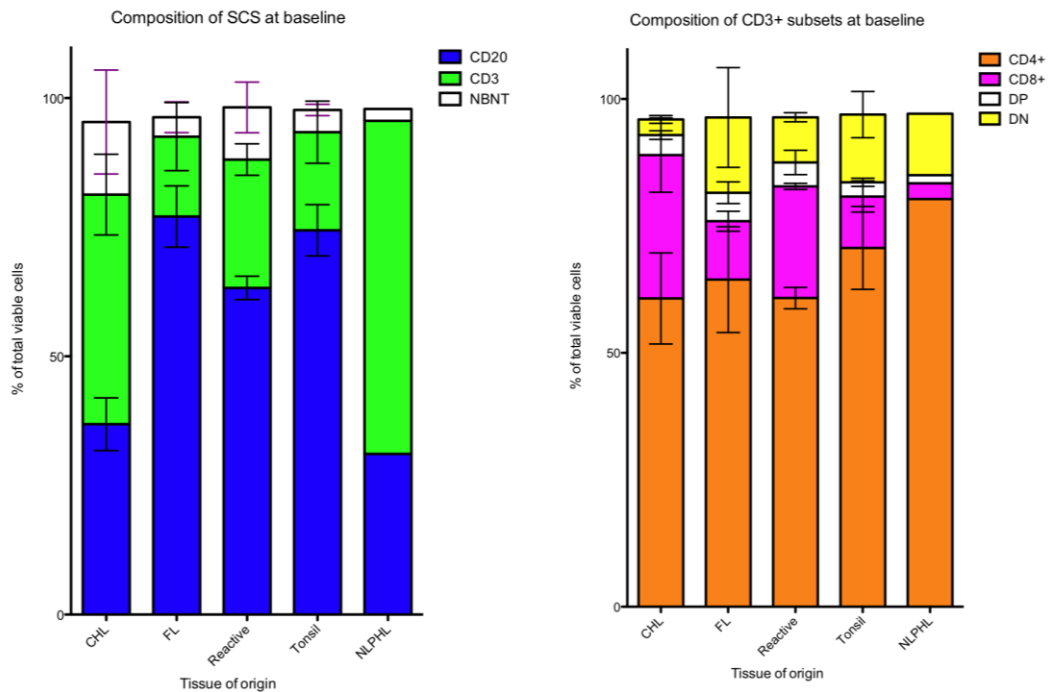


**Figure 5.8:** Composition of SCS at baseline. Left: B and T cells, Right: T subsets by CD4 and CD8 expression. Bars are subdivided by mean % of all viable cells with SEM indicated by bars, illustrating significant heterogeneity between samples obtained from each source.

#### 5.4.1.3 Identification of HRS cell population:

Using the gating strategy shown in Figure 5.9 (CD3<sup>-</sup>, CD20<sup>-</sup>, CD30, 40 & 95<sup>+</sup>) a small minority of cells fulfilling the immunophenotype criteria established by Fromm<sup>319</sup> were present (Table 5.8). However, this population was not unique to the CHL-derived samples, also being present in tonsil and reactive cells, although not in the FL or NLPHL derived samples. The population was also at such a low level that validation of this strategy using flow sorting or other purification techniques would not be feasible.

Sample	Absolute number of cells in 'HRS gate'	% of all viable cells
C <sub>1</sub>	2	0.0001
C <sub>2</sub>	1	0.00002
C <sub>4</sub>	0	0
C <sub>5</sub>	0	0
C <sub>6</sub>	0	0
F <sub>1</sub>	1	0.00002
F <sub>2</sub>	0	0
F <sub>4</sub>	0	0
L <sub>1</sub>	1	0.0001
P <sub>1</sub>	0	0
R <sub>2</sub>	0	0
T <sub>1</sub>	2	0.00005
T <sub>2</sub>	2	0.0001
T <sub>3</sub>	107	0.001

**Table 5.8:** Using the strategy proposed by Fromm et al<sup>319</sup> and illustrated in Figure 5.9, few cells, or none at all appeared in the proposed HRS gate for any sample, and this strategy was not specific for samples derived from CHL.

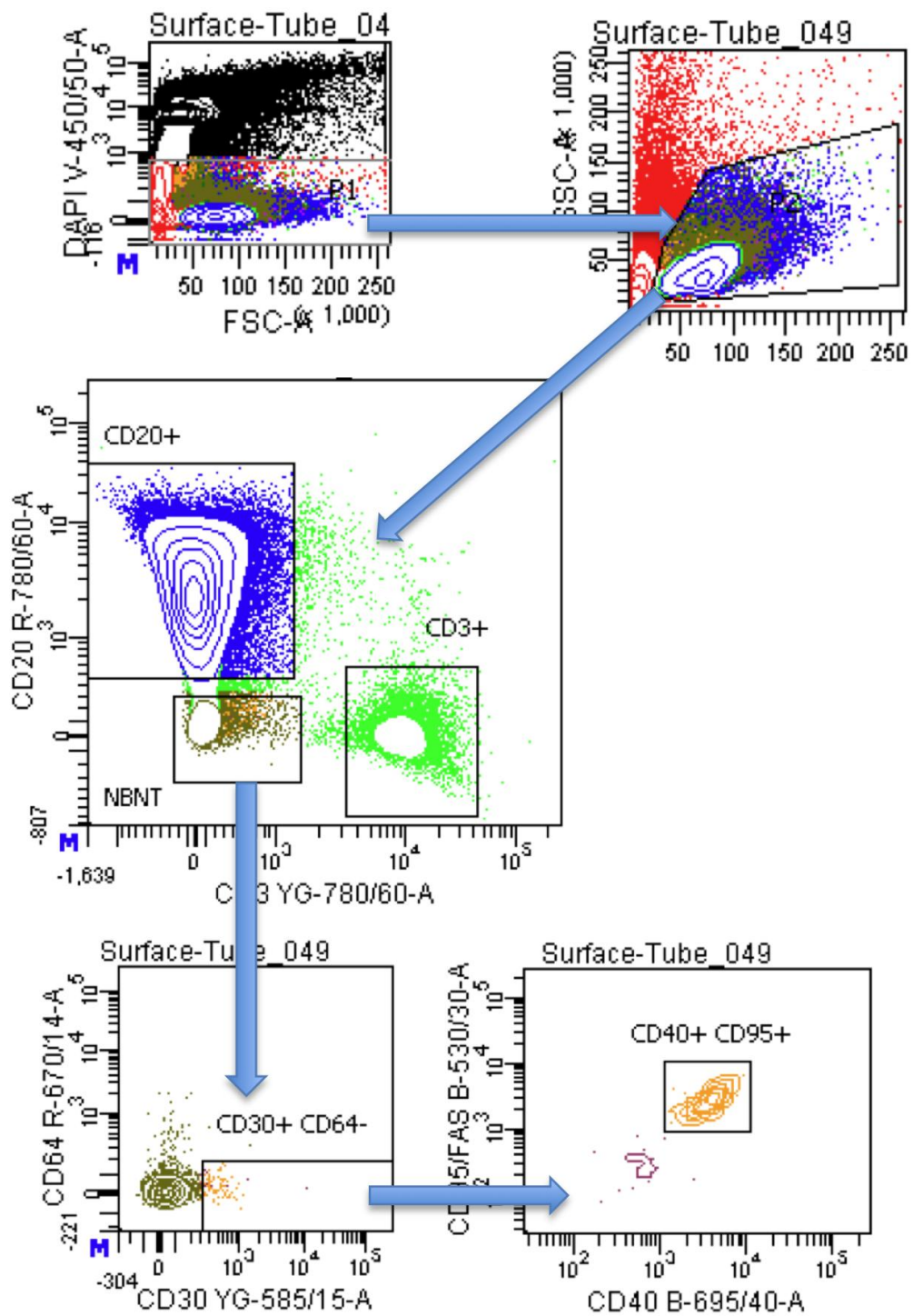


**Figure 5.9:** Gating strategy for analysis of identification of putative HRS population defined as CD3- CD20- CD30+ CD64- CD40+ CD95+.

### **5.4.2 Culture of SCS derived cells**

The results of initial pilot experiments to determine the optimal cytokine combination have been described in the methods. As such, all subsequent results are reported for IL2 and IL2 & IL4 augmented conditions only. Viability and absolute numbers of cells plated at baseline is summarised in Table 5.1. Viability of cells derived from malignant and reactive conditions, particularly CHL was often superior at baseline to that of tonsil which may influence the validity of subsequent assessments of proliferation (Figure 5.5).

#### **5.4.2.1 Proliferation in culture systems**

Using only the optimised cytokine enrichment techniques, proliferation was seen in the majority of culture systems for the first four weeks. There was significant heterogeneity from sample to sample and by class of SCS source, particularly malignant vs non-malignant.

#### **5.4.2.2 Identity of Proliferating Cells**

Immunophenotyping at day 30 and day 60 in two systems: one tonsil and one CHL-derived, revealed that the majority of cell classes were no longer present in the system and that >99% of viable cells were now T cells. In CHL >95% of T cells were CD4+. In tonsil >80% of cells were CD8+ (Figure 5.10). Further immunophenotyping of expanding cell populations was performed in the experiment described in Chapter 6. However the absence of any CD3- or B cell population meant that there was no evidence in any CHL-derived system of maintenance or expansion of a putative immunophenotypically-defined HRS cell. The extended immunophenotype of the CD3+ CD4+ population at baseline is the subject of Chapter 6 while that of the expanded T cells is described in Chapter 7.

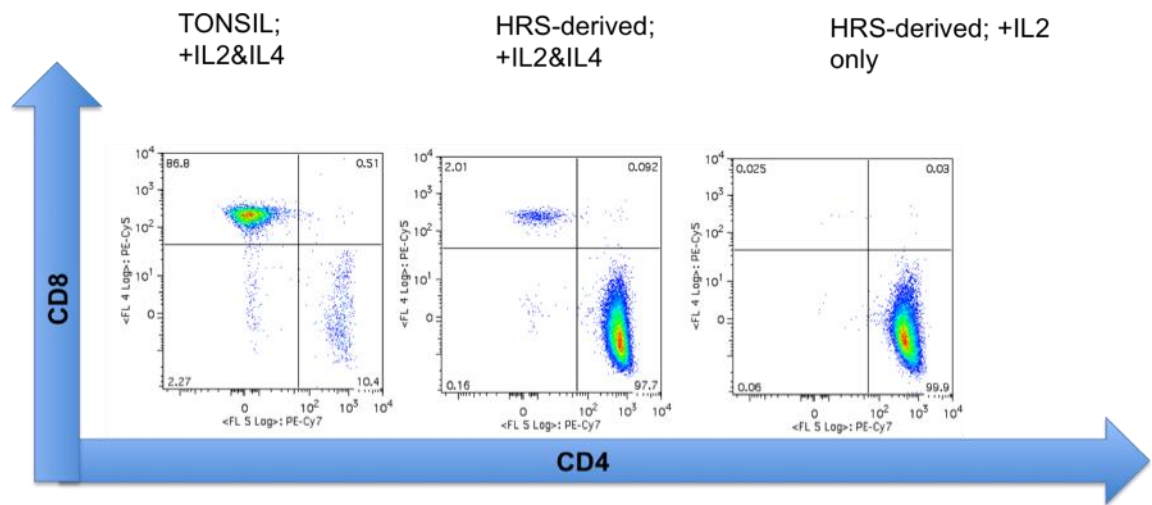


**Figure 5.10:** Composition of example cultures at day 60. Gating on all viable events there were no CD3 negative events at this stage. Tonsil derived cultures were comprised predominantly of CD8+ T cells, while CHL derived cultures comprised >97% CD4+ T cells, with almost complete absence of CD8+ T cells in the IL2 only condition.

#### 5.4.2.3 Time to Senescence

IL2&IL4-enriched culture systems had superior survival compared to those enriched with IL2 alone. Pooling all malignant and benign SCS-derived culture systems, median survival of IL2-enriched systems was only three media changes (approximately 30 days) whereas 75% of IL2&IL4-enriched systems survived to 200 days or approximately 25 media changes (Figure 5.11). The surviving IL2-only enriched systems were exclusively derived from CHL SCSs. No tonsil-derived cultures survived beyond 100 days or 10-12 media changes. All CHL-derived culture systems survived beyond 200 days. Two of three FL-derived culture systems enriched with IL2 and IL4 survived to 200 days. Pooling all benign culture systems and comparing to FL and CHL-derived systems there was no significant difference by Kaplan Meier analysis but the number of replicates were not powered to detect less extreme differences between groups (Figure 5.12).

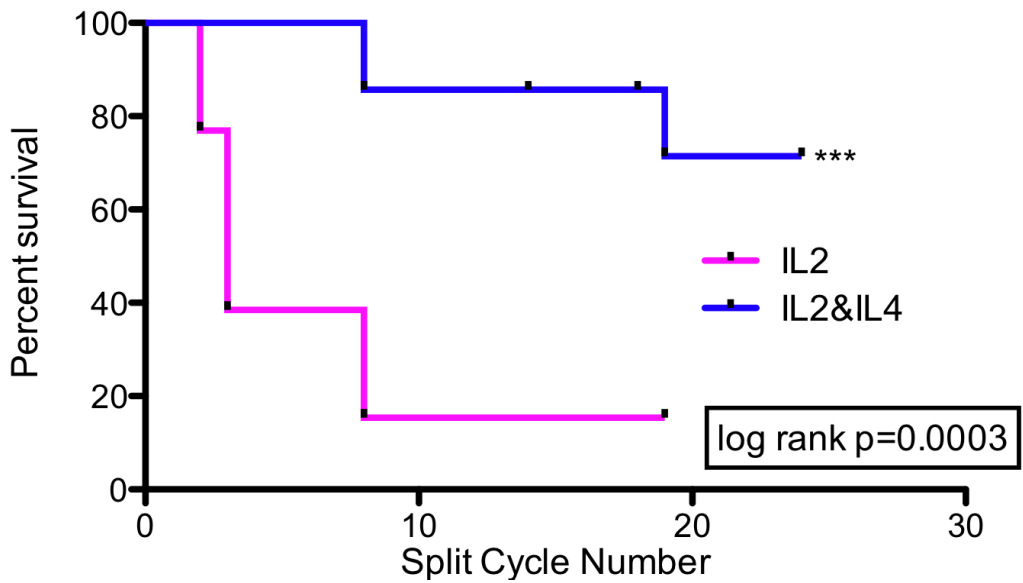


**Figure 5.11:** IL2&IL4-enriched culture conditions were longer lived than IL2-only enriched conditions; all samples pooled.

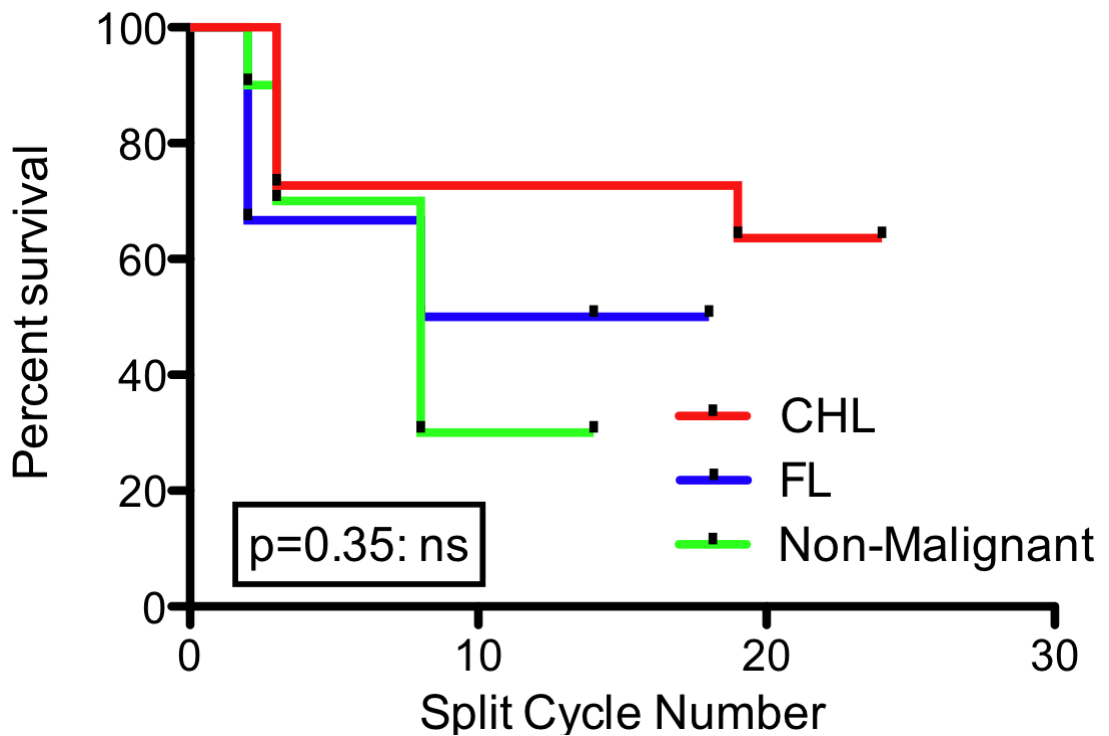


**Figure 5.12:** Longevity of T cell cultures may have been influenced by node of origin, but sample size is too small to demonstrate significant differences.



#### 5.4.2.4 Proliferative Capacity: IL2-only enrichment

Proliferation was not sustained beyond 5 media changes or around 40-50 days in any IL2-only enriched culture systems except those derived from CHL. Only two of five CHL-derived samples enriched with IL2 only survived beyond 5 cycles (40%) but in these cases the proliferation was sustained beyond 200 days (Figure 5.13). Due to the poor survival of the IL2-only enriched conditions, subsequent analysis will only examine the IL2&IL4 enriched conditions.

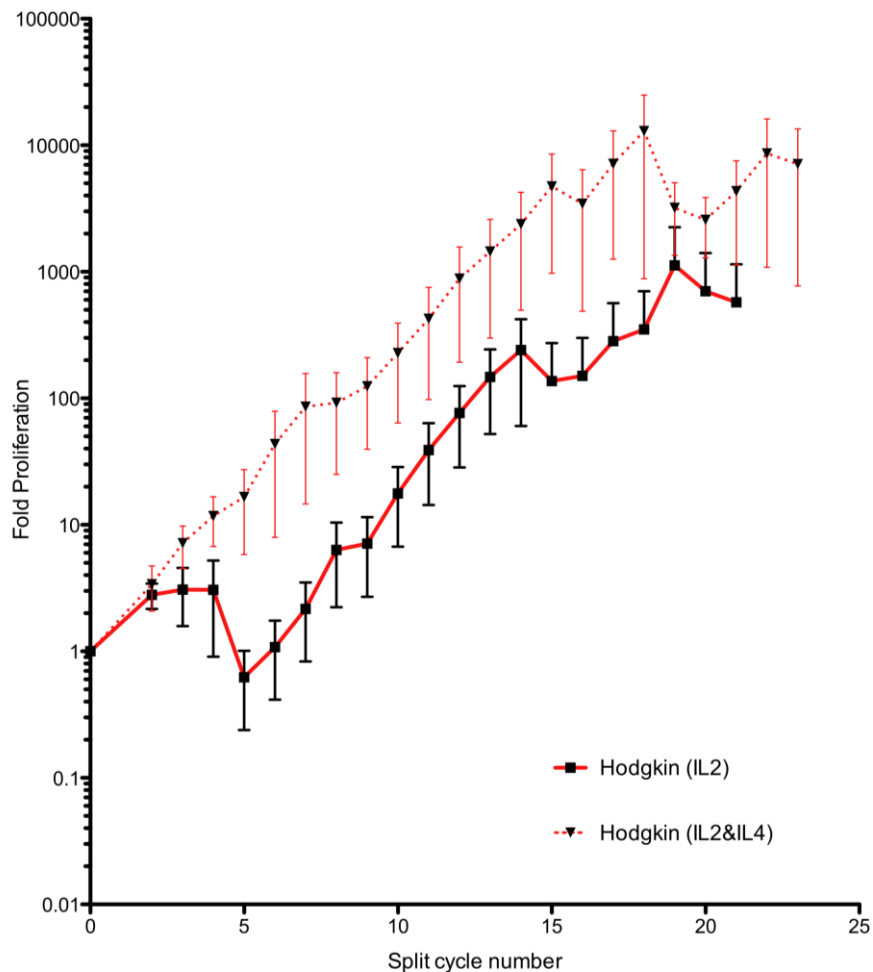


**Figure 5.13:** Graph to illustrate differences in proliferation in IL2-only and IL2&IL4-enriched conditions for cultures derived from CHL-infiltrated lymph nodes. Since only two of five samples in the IL2-only condition survived beyond 5 split cycles, comparison of proliferation rates between the IL2-only and IL2&IL4 enriched systems could not be determined. However in those IL2 only-enriched samples surviving beyond 5 split cycles, proliferation was comparable to the IL2&IL4 conditions and sustained to 200 days.

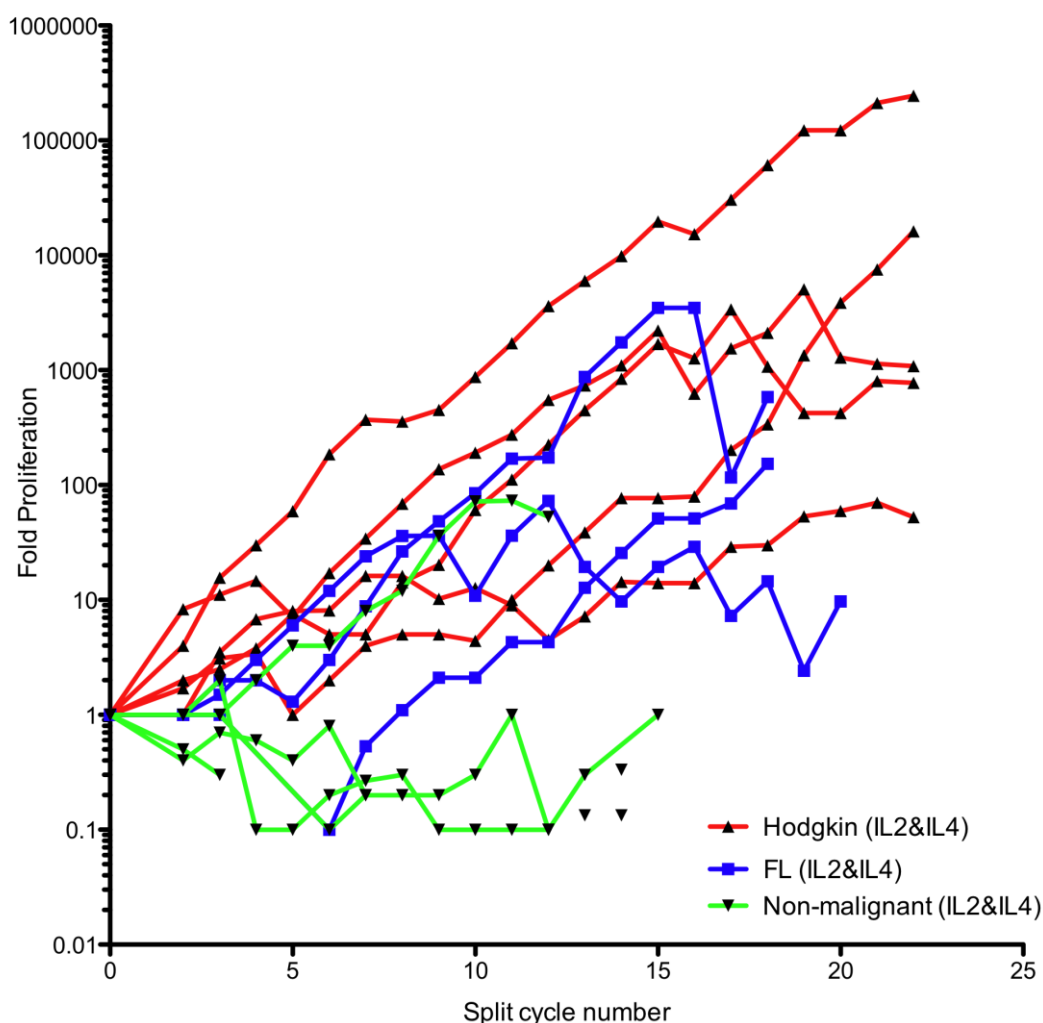


**Figure 5.14:** Relative proliferation of IL2&IL4-enriched culture systems colour coded by tissue of origin and plotted for each individual sample, showing apparent superiority of growth of the CHL-derived systems. Note that a single non-malignant sample, derived from a node containing follicular hyperplasia, continued to proliferate comparably to malignant samples while all other non-malignant samples have senesced.

#### 5.4.2.5 Proliferative Capacity: IL2&IL4 enrichment

Proliferation for each IL2&IL4-enriched culture system is shown in Figure 5.14, while Figure 5.15 shows mean proliferation for samples pooled by SCS class. Fold proliferation of pooled FL-derived samples compared to pooled CHL samples were 2.4 vs 16.6 at 5 splits, 32.6 vs 228.1 at 10 splits and 250 vs 13,000 at 20 splits (Figure 5.14). However, statistically significant differences were not demonstrated, due to small numbers of

replicates and wide heterogeneity of proliferation between samples, using either a T test on log-transformed data for improved Gaussian distribution, or the Mann-Whitney non-parametric test on the raw data. For similar reasons, a significant difference was not demonstrated between pooled malignant and pooled benign samples at 5 splits. However, only a single benign culture system continued to expand beyond 10 splits. This was derived from follicular hyperplasia (the granulomatous reactive node and PTGC were senescent within 5 splits) and proliferation of this sample was comparable to the expanding malignant culture systems (Figure 5.13).

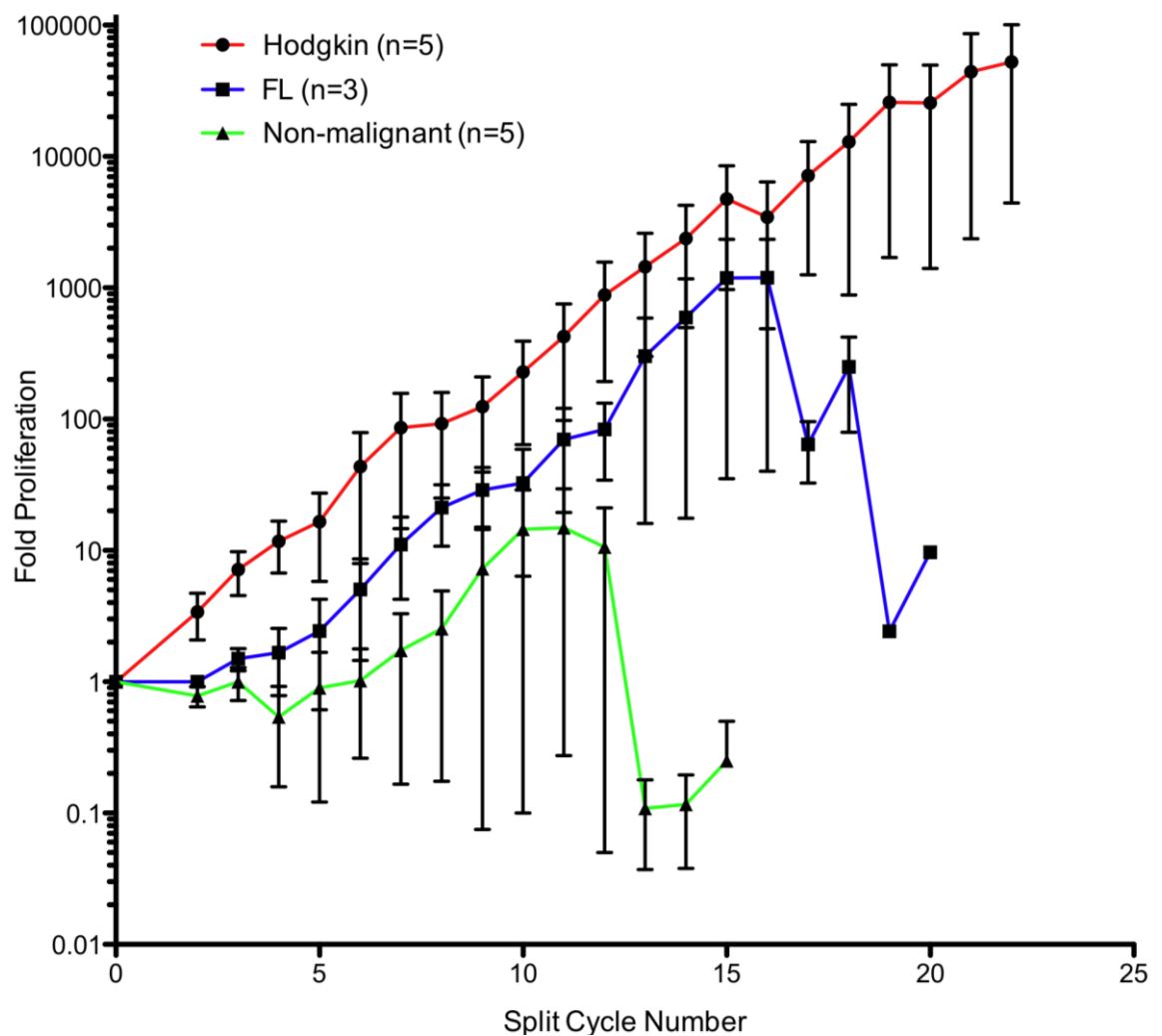


**Figure 5.15:** Mean relative proliferation of IL2&4-enriched culture systems by tissue of origin showing an apparent superior proliferation in CHL-derived systems compared to FL and non-malignant derived systems. This did not reach statistical significance owing to low replicate numbers and wide heterogeneity in proliferative capacity between samples.

## 5.5 Discussion

In order to study the functional relationship between HRS cells and a major component of the inflammatory infiltrate – CD4<sup>+</sup> T cells – in an *in vitro* co-culture system capable of further manipulation, an attempt was made to sustain lymph node-derived cells *ex vivo*. The B cell helping T cell phenotype, Th<sub>2</sub> is proposed in the literature to represent the majority of the T cell infiltrate although the functional evidence for this is scarce, and as such Th<sub>2</sub>-polarising cytokines were used to supplement the system.

Using a previously validated panel of antibodies in a flow cytometric assay, five frozen SCSs derived from CHL infiltrated lymph nodes were examined for the presence of the malignant HRS cell. However this strategy failed to identify a convincing population present at sufficiently high numbers, or which was absent in control lymph nodes. Additionally, there was no evidence for the presence of this population after 30 days in culture. However, there was significant proliferation in IL<sub>2</sub>&IL<sub>4</sub> augmented media, which was sustained for many weeks, up to and beyond 200 days or 25 media changes for all CHL-derived cultures and the majority of FL-derived cultures. Benign lymph nodes did not show the same longevity or proliferative capacity with the exception of a single case of follicular hyperplasia.

This culture system is unsuitable as a model system to manipulate trophic or antagonistic factors conferred by T cells on the malignant cell in CHL since no malignant cell population could be convincingly identified. The conflict with the results of Fromm's group, and other groups which have successfully isolated PCR-defined clonal HRS cells using magnetic bead sorting based on surface antigen phenotype<sup>465</sup> may be explained by differences in preparation technique, in particular the use of frozen samples in this case, in which only the most robust cells in the node survive the initial indeterminate period prior to SCS preparation, and then the subsequent freezing process. HRS cells in particular are known to be pre-apoptotic and replicatively senescent<sup>320</sup> with the exception of cell lines unable to survive *ex-vivo*, while lymphocytes, particularly T lymphocytes, are known to have remarkable proliferative capacity *ex-vivo*. Activated lymph nodes, such as those in a malignancy-infiltrated process or reactive process, as opposed to predominantly quiescent nodal tissue such as tonsil, are likely to have greater

proportions of viable cells capable of surviving this preparation and this was evidenced by the predominantly low viability at baseline in tonsillar, compared to malignancy-derived cells.

Long-lived non-malignant T cells (predominantly CD4+) have been generated from malignant and non-malignant inflammatory tissue by another group, using inflamed skin specimens<sup>466</sup>. All culture systems in this case were established as in this experiment without stimulatory TCR agonist, plant lectin or super-antigen exposure. The resultant cell lines were IL2-dependent in all cases and IL2 and IL4-dependent in some cases, with the dependence on IL4 being lost in some cases, as has been observed in this experiment. 7/12 atopic dermatitis derived T cell lines persisted beyond 40 to 50 population doublings, to 500 doublings in one case, retaining their requirement of cytokine augmentation. Details of culture conditions (e.g. culture plates and supplementation to the media) are not provided but it appears that doubling was occurring every 20-30 hours in these systems, far exceeding anything in the experiments described in this chapter. Further work arising from this finding is not published and further characterisation of the resultant T cells in terms of clonality, function or surface phenotype not performed or documented. T cell proliferation and expansion is easily achieved *in vitro* but requires combined 'signal one' stimulation via the TCR, either specifically and directly (antigen/APC or peptide tetramer), non-specifically and directly (anti-CD3 with co-stimulatory anti-CD28) or non-specifically and indirectly (super-antigen such as SEB, small molecules or plant lectins such as PMA, PHA and Concanavalin). Cytokines provide augmentation of the so-called 'signal two' stimulation (such as IL2), and altered intracellular signalling may alter the eventual proliferative capacity and phenotype of resulting cells (polarising conditions including IL4 and anti-IL12, or IL12 and anti-IL4 to produce Th2 or Th1 cells respectively). Supra-physiological doses of such cytokines can provide TCR-independent stimulus sufficient to induce activation and proliferation<sup>467</sup> although this phenomenon is reported more in CD8+ T cells than CD4+, which may simply reflect a publication or investigator bias than a true physiological distinction between the cell subtypes. Most T cell expansion protocols suggest restimulation through the TCR every 7-10 days. However there is *in vitro* and *in vivo*<sup>468</sup> evidence to suggest that once activated, a proliferating population of CD4+ T cells

can continue to expand without further antigen exposure, although augmentation of proliferation is achieved upon re-exposure to antigen. Conversely other studies have demonstrated a dependence on ongoing TCR stimulation<sup>469</sup>. IL2 is thought to be the major mediator of this process<sup>469</sup> although believed not to be important in proliferation of naïve T cells. It seems unlikely in the culture systems described in this experiment that any antigen persists and hence TCR-independent proliferation must be occurring. IL2 dependence of ongoing survival is confirmed. However there is no further investigation of the mechanism of such cytokine-dependent TCR-independent expansion in the literature, nor of the contribution of IL4 to such a system. The culture systems established here are extremely artificial, *in vitro* and as such likely unrepresentative of any *in vivo* process. At best the superior proliferation seen in some systems, particularly malignant over non-malignant and possibly CHL-derived over any other system, may be a functional read-out of activation status of a minority of T cells in the tissue of origin. However, it may represent a functional class of T cells lying dormant and non-functional in the context of the lymph node, but which is 'primed' for proliferation and function. The mediators of its suppression are unclear, but apparently overcome by removal of these cells from the node environment and exposure to large excesses of IL2 and IL4. The importance of other non-T and CD4- constituents of the cell suspension at this time in stimulating or suppressing T cell growth is not clear.

Further experiments to determine this would include purification of the CD4+ cells prior to plating and exposure to the same cytokine enriched media. Ongoing presence of a malignant cell providing antigen to be recognised by the proliferating CD4+ T cells is unlikely given the relative purity of the CD4+ component of the system after several weeks proliferation, and the virtual absence of HRS-phenotype cells at baseline. A HRS precursor, progenitor or stem cell of a different phenotype could be driving the process but there is no established phenotypic marker of this and it remains a hypothetical concept<sup>323</sup>. There is no evidence that the proliferating T cells are tumour antigen specific: priming or preactivation could in itself have been a result of exposure to the cytokine and chemokine products and cell-cell interactions within the malignant node, of tumour non-specific T cells that have been passively attracted into and retained within the node. Hence these cells could be derived from memory, rather than naïve T cell populations

whose TCR-independent, cytokine dependent proliferation and survival has been investigated previously<sup>468</sup>. Relatively slow overall proliferation compared to that achieved with TCR-stimulating expansion techniques implies that only a small minority of T cells are expanding even in the most proliferative system.

There is little or no information in the literature investigating the molecular mediators, nor the functional, gene or protein expressing phenotype of the T cells participating in this *in vitro* phenomenon, despite its being well described. Further experiments to characterise the expanding T cell populations arising from each SCS class, along with markers present at baseline and predictive of the T cells possessing such capabilities will be described in Chapter 6 and 7. A better understanding of this *in vitro* phenomenon may provide insight into why this apparently activated and expansile population is suppressed within the tumour microenvironment and may enable *in vivo* activation by pharmacological means.

## 5.6 Summary and Further Work

Taken together, these data suggest that the immune microenvironment of CHL may be investigated using frozen SCS prepared as described, that HRS cells may not be detected using a previously proposed panel of antibodies in frozen samples, nor can any putative malignant population be sustained in culture. However, the CD4<sup>+</sup> T cell component in CHL is not anergic or hypoproliferative as has been suggested and apparently demonstrated functionally<sup>299</sup>, but rather highly responsive to a cytokine-induced proliferation, most optimally with IL2 and IL4 augmentation. This phenomenon may also be a feature of other malignant and benign reactive tissue: certainly in some cases of FL and in one case of FH, but not in tonsil-derived tissue. The phenotype of this proliferating CD4<sup>+</sup> population, although an artificial *in vitro* phenomenon, and differential expression of CD4<sup>+</sup> markers at baseline should be assessed in order to determine the origin of this survival advantage, and potential implications for the pathophysiology of the disease.

## CHAPTER SIX:

Fluorescence immunophenotyping to  
functionally characterise and  
discriminate CHL-infiltrating CD4<sup>+</sup> T  
cells from other lymph node-infiltrating  
CD4<sup>+</sup> T cells



## **6. Fluorescence immunophenotyping to functionally characterise and discriminate CHL-infiltrating CD4+ T cells from other lymph node-infiltrating CD4+ T cells**

### **6.1 Introduction**

The introduction to this thesis (1.5) has described the genes and proteins through which T cells exert their influence on the HRS cell in CHL. Pharmacological manipulation of these factors may result in improved treatments, however as discussed in Chapter 5, basic functional data is lacking. Studies investigating the entire microenvironment have the disadvantage of failing to discriminate the contribution of individual cells, leading to a loss of information. However, investigation only of individual cellular components may fail to recognise the importance of complex coordinated systems and networks at work in the CHL microenvironment.

### **6.2 Aims and Objectives**

The aim of this study was to use multi-parameter flow cytometry to validate markers described in the literature as being important in CD4+ T cells in CHL, and in physiological B/T cell interactions, and use these to characterise the CD3+CD4+ infiltrate in CHL. By defining CHL-specific CD4+T cell-mediated functional pathways and contrasting them with those present in other haematological malignancies (using FL and NLPHL samples as controls), reactive nodes (PTGC, FH and bacterial reactive node), and tonsils potential mediators of the pathophysiology of the disease may be determined. In addition, identifying markers showing substantial heterogeneity of expression across CHL samples will allow application to a wider patient cohort using IHC in order to investigate for interactions with clinical factors, in particular prognosis. Hence an understanding of the disease-defining and pathophysiological heterogeneity-conferring molecular signature of the CD4+ T cell could be established for future functional experiments manipulating these factors. The drawbacks of analysis by IHC, or gene

expression profiling of unselected, heterogeneous cell populations have been discussed in the Introduction 1.9.2.2 and 1.9.2.3.

### **6.2.1 Selection of antigens for T cell panel**

Flow cytometry is limited by the number of factors assessable simultaneously and the expense of the reagents per factor analysed, in contrast for example to gene expression profiling. Multicolour flow is usually performed with a panel of 4-8 markers, although using newer techniques 20 and more may be assessed simultaneously. However the technique has the advantage of analysing on an individual cell basis and therefore expression of proteins is not 'averaged' across heterogeneous cell populations but instead determined for specific subpopulations. This property also enables cells to be analysed at relatively low numbers with minimal disruption prior to analysis (single cell suspension preparation, wash, stain, analyse) compared, for example, to nucleic acid extraction and gene expression profiling, or formalin fixation, paraffin embedding and IHC. For these reasons, and due to the extremely limited amount of tissue available as frozen SCSs, flow cytometry was selected as the method to analyse the properties of the CD4<sup>+</sup> T cells. Selection of this method meant that the number of function-defining antigens available for investigation was limited and as such stringent antigen-selection criteria were applied, as justified in the Introduction, and summarised in Table 6.1.

## **6.3 Materials and Methods**

### **6.3.1 Single cell suspensions**

Single cell suspensions used for extended phenotype analysis of the CD3<sup>+</sup> CD4<sup>+</sup> population were as used in chapter 5 and detailed in Table 5.1.

### **6.3.2 Selection of fluorochromes and antibodies**

The difficulty of attributing T cells to functional subsets, as well as the limited validity of subset-defining markers has been described. Therefore only antigens with a pre-existing evidence base for expression or functional importance in CHL were selected for further investigation. These have been described in detail in the introduction and are summarized in Table 6.1.

CD / Common name	Eponym	Class	Justification for inclusion
CD134	OX40	TNFRSF	?HRS promotion
CD154	CD40-L	TNFRSF	?HRS promotion
CD254	RANK-L	TNFRSF	?HRS promotion
CD278	ICOS	IGRSF	?HRS promotion
CD30	-	TNFRSF	?HRS promotion
CD40	-	TNFRSF	?HRS promotion
IL13	-	CK	?HRS promotion
IL21	-	CK	?HRS promotion
IL6	-	CK	?HRS promotion
TNF $\alpha$	-	CK	?HRS promotion
CD69	-	?	T cell activation
CD27	-	TNFRSF	T cell activation
CD28	-	IGRSF	T cell activation
CD122	IL2-Rb	CK receptor	T cell activation
CD124	IL4-Ra	CK receptor	T cell activation
CD132	CGC	CK receptor	T cell activation
CD25	IL2-Ra	CK receptor	T cell activation
IL2		CK	T cell activation
CD127	IL7-Ra	CKR	SUBSET: Memory T cell
CD197	CCR7	CKR	SUBSET: Naïve T cell / lymphoid homing
CD62L	L-selectin	Adhesion	SUBSET: Naïve T cell / lymphoid homing
CD45RO	-		SUBSET: Memory T cell
CD45RA	-		SUBSET: Naïve T cell / Late memory T cell
CD185	CXCR5	Chemokine receptor	SUBSET: Tfh
IFN- $\gamma$		CK	SUBSET: Th1
CD183	CXCR3	Chemokine receptor	SUBSET: Th1
IL4	-	CK	SUBSET: Th2
CD193	CCR3 / RANTES-receptor	Chemokine receptor	T CELL RECRUITMENT: Th2
CD194	CCR4 / TARC-receptor	Chemokine receptor	T CELL RECRUITMENT: Th2/Treg
CD195	CCR5 / MIP1a-receptor	Chemokine receptor	T CELL RECRUITMENT: Th1
CD196	CCR6/ MIP3-receptor	Chemokine receptor	T CELL RECRUITMENT: Treg/Th17
CD178	FAS-ligand	TNFRSF	Apoptosis/Activation
CD95	FAS	TNFRSF	Apoptosis/Activation
CD152	CTLA-4	IGRSF	Immunosuppression
CD274	PD-L1	IGRSF	Immunosuppression
CD279	PD1	IGRSF	Immunosuppression
CD57	-	?	Senescence

**Table 6.1:** Justification for selection of antigens for use in CD4+ characterising panel. Key: ?HRS Promoting: ligand for receptor expressed on Hodgkin-Reed-Sternberg cell with evidence for downstream pathway activation promoting survival, anti-apoptotic factors or proliferation.

**Table 6.2:** Details of fluorochromes for CD4+ T cell typing experiment

CD / Common name	Eponym	Clone	Isotype	Source	Fluoro-chrome	Tube
CD4	-	RPA-T4	Mouse IgG1-κ	BD	Horizon V500	1-8
CD69	Very Early Activation Antigen	FN50	Mouse IgG1-κ	Biolegend	PE/Cy7	4&5
CD3	-	UCHT1	Mouse IgG1-κ	BD	FITC	1-5, 7&8
CD134	OX40 / TNFRSF4	Ber-ACT35	Mouse IgG1-κ	Biolegend	PerCP/Cy5.5	1
CD154	CD40-L	24-31	Mouse IgG1-κ	Biolegend	APC/Cy7	1
CD178	FAS-ligand / CD95-L	NOK-1	Mouse IgG1-κ	BioLegend	PE	1
CD278	ICOS	C398.4A	Armenian Hamster IgG	Biolegend	PE/Cy7	1
CD28	T44/Tp44	CD28.2	Mouse IgG1-κ	BioLegend	Alexa Fluor® 700	1
CD30	TNFRSF8	BY88	Mouse IgG1-κ	Biolegend	APC	1
CD40	TNFRSF5	5C3	Mouse IgG1-κ	Biolegend	PerCP/Cy5.5	1
CD95	FAS / TNFRSF6	DX2	Mouse IgG1-κ	BioLegend	PE/Cy5	1
CD185	CXCR5	TG2/CXCR5	Mouse IgG2b-κ	BioLegend	PerCP/Cy5.5	2
CD193	CCR3 / RANTES-receptor	5E8	Mouse IgG2b-κ	BioLegend	PE	2
CD194	CCR4 / TARC-receptor	TG6/CCR4	Mouse IgG2b-κ	BioLegend	PE/Cy7	2
CD195	CCR5 / MIP1a-receptor / HIV-1 fusion co-receptor	HEK/1/85a	Rat IgG2a-κ	BioLegend	Alexa Fluor® 700	2
CD196	CCR6/ MIP3-receptor	TG7/CCR6	Mouse IgG2b-κ	BioLegend	Alexa Fluor® 647	2
CD127	IL7-Ra	A019D5	Mouse IgG1-κ	BioLegend	PerCP/Cy5.5	3
CD152	CTLA-4	L3D10	Mouse IgG1-κ	BioLegend	PE	3
CD183	CXCR3	1C6/CXCR3	Mouse IgG1-κ	BD	PE	3
CD197	CCR7	3D12	Rat IgG2a-κ	BD	PE/Cy7	3

CD / Common name	Eponym	Clone	Isotype	Source	Fluoro-chrome	Tube
CD274	PD-L1 / B7-H1	29E.2A3	Mouse IgG2b-κ	BioLegend	APC	3
CD279	PD1	EH12.2H7	Mouse IgG1-κ	BioLegend	APC/Cy7	3
CD62L	L-selectin	DREG-56	Mouse IgG1-κ	BioLegend	PE/Cy5	3
IFN-γ	-	4S.B3	Mouse IgG1-κ	BD	PE	4
IL2	TCGF	MQ1-17H12	Rat IgG2a, κ	BioLegend	Alexa Fluor® 700	4
IL6	-	MQ2-13A5	Rat IgG1, κ	Biolegend	APC	4
TNFα	-	MAB11	Mouse IgG1-κ	Biolegend	PerCP/Cy5.5	4
CD122	IL2-Rb	9A2-CD122	Mouse IgG2a, κ	Ebioscience	PerCP-eFluor 710	5
CD124	IL4-Ra	hIL4R-M57	Mouse IgG1-κ	BD	PE	5
CD132	CGC	TUGh4	Rat IgG2b-κ	BioLegend	APC	5
CD25	IL2-Ra	BC96	Mouse IgG1-κ	BioLegend	PE/Cy5	5
CD27	S152/T14	O323	Mouse IgG1-κ	Biolegend	PerCP/Cy5.5	5
CD20		2H7	Mouse IgG2b-κ	BD	APC-H7	6
CD3		UCHT1	Mouse IgG1-κ	Biolegend	PE-Cy7	6
CD30	TNFRSF8	BY88	Mouse IgG1-κ	Biolegend	PE	6
CD40	TNFRSF5	5C3	Mouse IgG1-κ	Biolegend	PerCP-Cy5.5	6
CD64	Fc-γ-R1	10.1	Mouse IgG1-κ	Biolegend	APC	6
CD8	-	HIT8A	Mouse IgG1-κ	Biolegend	Alexafluor 700	6
CD95	FAS / TNFRSF6	DX2	Mouse IgG1-κ	BD	APC	6
CD254	RANK-L / TRANCE	MIH24	Mouse IgG1-κ	Biolegend	PE	7
CD45RA	-	HI100	Mouse IgG2b-κ	BioLegend	APC/Cy7	7
CD45RO	-	UCHL1	Mouse IgG2a-κ	BioLegend	PE/Cy5	7
CD57	NK-1, / Leu-7	HCD57	Mouse IgM-κ	BioLegend	Alexa Fluor® 647	7
CD69	Very Early Activation Antigen	FN50	Mouse IgG1-κ	BD	Alexa Fluor® 700	8
IL4	BSF-1 / TCGF-2	8D4-8	Mouse IgG1-κ	BioLegend	PE	8
IL10	B-TCGF / TGIF	JES3-9D7	Rat IgG1-κ	BioLegend	PE-Cy7	8
IL13	-	JES10-5A2	Rat IgG1-κ	Biolegend	APC	8
IL21	-	3A3-N2	Mouse IgG1-κ	Biolegend	PE	8

Table 6.2: Details of fluorochromes for CD4+ T cell typing experiment

Final fluorochrome panels were based on optimisation experiments using combinations of fluorochromes with manageable spectral overlap, in order to minimise total number of tubes and hence cells used and enable processing of up to twenty samples in each batch. Combinations (cocktails) were based on availability of compatible conjugated antibodies and ‘class’ of target antigen as summarised in Table 6.3 with conjugate details in Table 6.2.

Cocktail number	Antigen Class
1	TNFRSF/IGSF
2	Chemokine receptor
3	Suppressor/Memory (homing)
4	CYTOKINE PANEL: Th <sub>1</sub> /proinflammatory
5	Cytokine receptor
6	Lymphocyte Subsets / TNFRSF
7	Activation/Senescence/Memory (CD45)
8	CYTOKINE PANEL: Th <sub>2</sub> /suppressor

**Table 6.3:** Summary of cocktails and major antigen class for analysis within each cocktail

### **6.3.3 Flow cytometric analysis, data acquisition, compensation and gating**

This has been described and justified in detail in Materials and Methods 2.3.

### **6.3.4 Statistical Analysis**

#### **6.3.4.1 Differences between sample classes / lymph node of origin**

Percentage expression of each marker within the CD<sub>3</sub><sup>+</sup> CD<sub>4</sub><sup>+</sup> population was pooled for each sample class and expressed as mean percentage for each sample class (CHL, FL, Reactive, Tonsil) and for a separate calculation of mean expression for all control samples (‘pooled controls’). Significance of differences of expression was compared between samples assuming non-Gaussian distribution of data using the Mann-Whitney U test with significance set at the <0.05 level. Only a single case of NLPHL was available for this experiment, the analysis of which is included in each figure for completeness.

#### 6.3.4.2 Hierarchical Cluster Analysis

Hierarchical cluster analysis was applied to these flow cytometry results in order to test the hypothesis that the composition of the CD4<sup>+</sup> component in CHL was unique to the disease and able to discriminate it from all other sample classes, and also in order to better visualise the combined flow cytometry data. The data was log transformed to remove skew and each marker was expressed as the number of SDs from the mean across all samples. Hierarchical clustering derived from this data was applied using complete linkage and Pearson correlation for the distance metric, based on a method applied in previous published literature using cluster analysis to discriminate lymphoid subsets from flow cytometric data, which found that the most stable clustering based on multiple replicates of randomised samples was derived from these statistical algorithms<sup>470</sup>. Analysis was performed using the Cluster 3.0 software package (eisen@rana.lbl.gov; copyright Stanford University) and presented using the Java Treeview (V1.1.6r2) package (alokito@users.sourceforge.net).

### **6.4 Results**

#### 6.4.1 Raw Flow Cytometry Data

Representative scatterplots from only four of the analysed cases are presented: in all cases for C<sub>1</sub>, C<sub>4</sub>, N<sub>4</sub> and P<sub>1</sub> representing two cases of CHL, one of FL and a PTGC. Comparative data for all markers are described below and shown in Tables 6.4-6.11 and Figures 6.1-6.9 grouped by functional class or staining cocktail from which they were derived. In all cases, the expression level of each marker is expressed as a percentage of all CD3<sup>+</sup> CD4<sup>+</sup> cells for each sample, and means derived from data pooled by sample class as described in 6.3.4.1 (lymph node of origin), or calculated from all control samples compared to mean expression in pooled CHL-derived samples, depicted in the figures with standard errors of the mean indicated. Any significant differences between mean expression is indicated on figures.

6.4.1.1 Cocktail 1: TNFRSF/IGSF (Table 6.4; Figures 6.1 & 6.2 a&b)

Data for RANK-L and CD69 are included due to functional grouping with TNFRSF/IGSF members, but were acquired from Cocktails 5&7 due to fluorochrome combination considerations. CD154/CD40L was significantly under-expressed by CD3+CD4+ cells derived from CHL SCSs compared to tonsillar controls (mean = 6.0% vs 17.9%; p=0.036), but not pooled controls. No other marker was represented at a statistically significant differential level in CHL samples compared to controls, either individually or pooled. Both CD27 and CD28 were expressed at high levels in all samples (mean CD27 = 57.4% of CHL-derived CD3+ CD4+ cells vs 60.6% controls, CD28 = 43.5% of CHL-derived CD3+ CD4+ cells vs 31.9% controls). CD95 was expressed in a mean of 79% of CHL-derived CD3+CD4+ cells vs 96% pooled controls and 90% of FL-derived CD3+CD4+ cells. CD95 was expressed in a mean of 79% of CHL-derived CD3+CD4+ cells vs 96% pooled controls and 90% of FL-derived CD3+CD4+ cells. OX40 was expressed in a mean of 34% of CHL-derived CD3+CD4+ cells vs 30% pooled controls and 35% of FL-derived CD3+CD4+ cells. ICOS was expressed in a mean of 49% of CHL-derived CD3+CD4+ cells (range 28%-77%) vs 58% pooled controls, 60% of FL-derived and 79% tonsil-derived CD3+CD4+ cells.

RANK-L was not expressed at a level exceeding 1.5% in any sample nor was there any appreciable difference for this marker between CHL-derived and any control SCS-derived CD3+CD4+ cells. CD69 is significantly under-expressed in the CD3+CD4+ component of CHL (mean=51.5%) compared to tonsils (mean=81.9%; p=0.04) but not reactive nodes (mean=50.2%; p=0.23) or pooled controls (mean=63.7%; p=0.23).



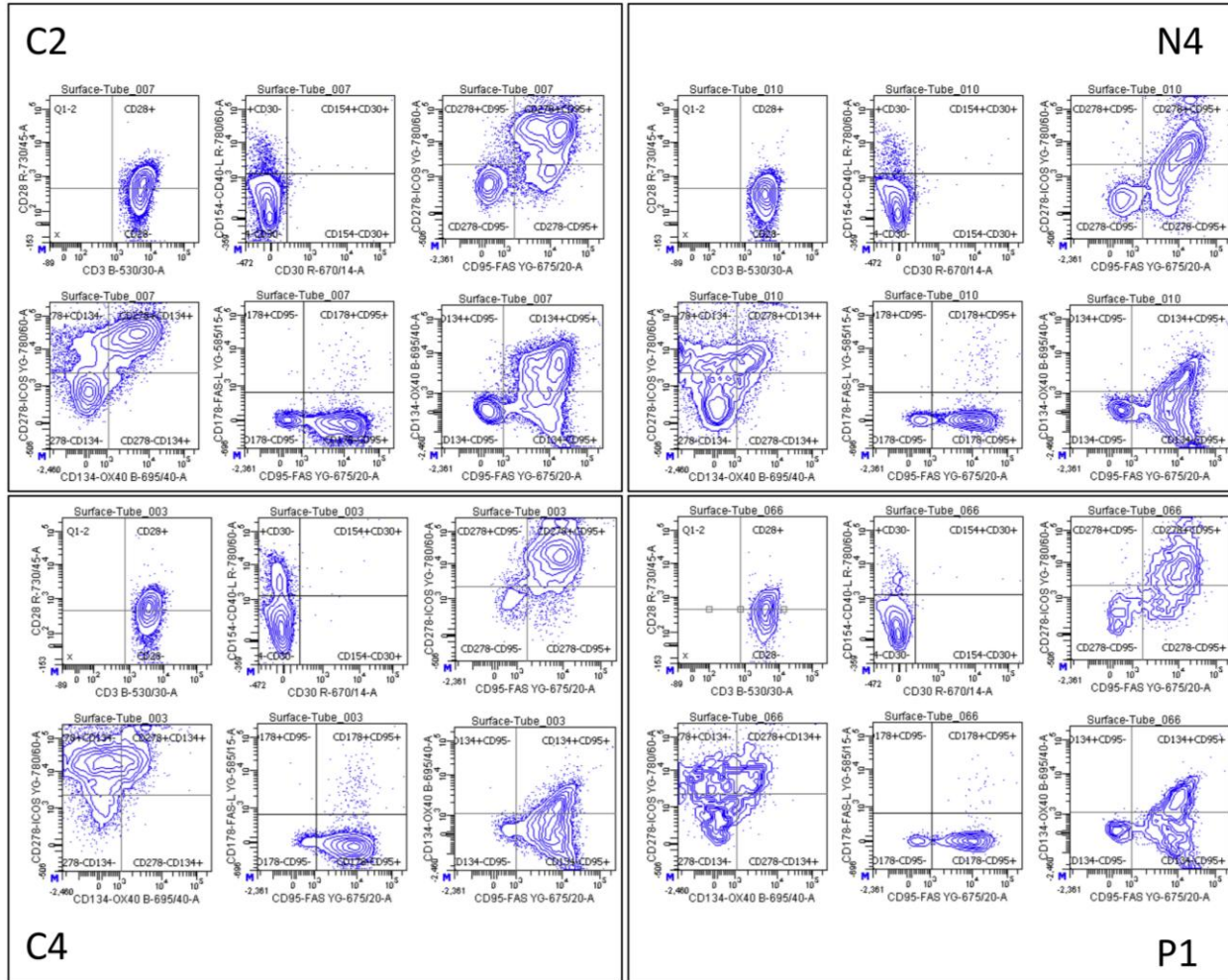


**Figure 6.1a:** Cocktail 1 Analysis: TNFRSF and IGSF member expression. Representative FACS plots for four samples showing variability of expression of markers in CD3+ CD4+ population. C2&C4: CHL; N4: FL; P1: PTGC. Results for all samples are summarised in Table 6.4.

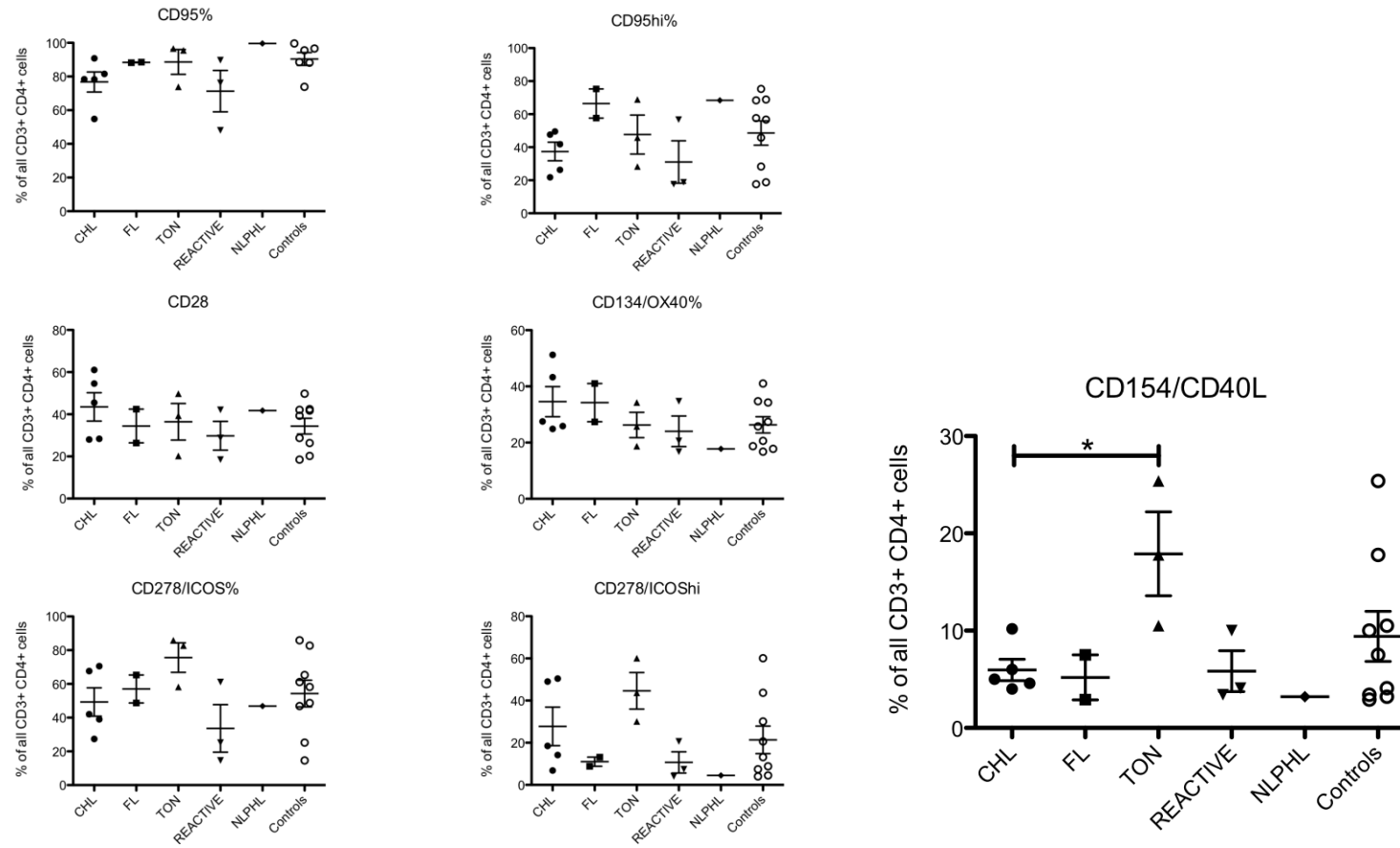


**Figure 6.1b:** Cocktail 1 Analysis: TNFRSF and IGSF member expression. : Summary of expression of cocktail 1 markers shown as a % of all viable CD3+CD4+ cells. Sample set is indicated on the x axis. 'Controls' indicates pooled control (not CHL) samples. Individual results are plotted, along with mean (horizontal line) and SEM (vertical bars). Medians were compared assuming non-Gaussian distribution of data using the Mann-Whitney U test.

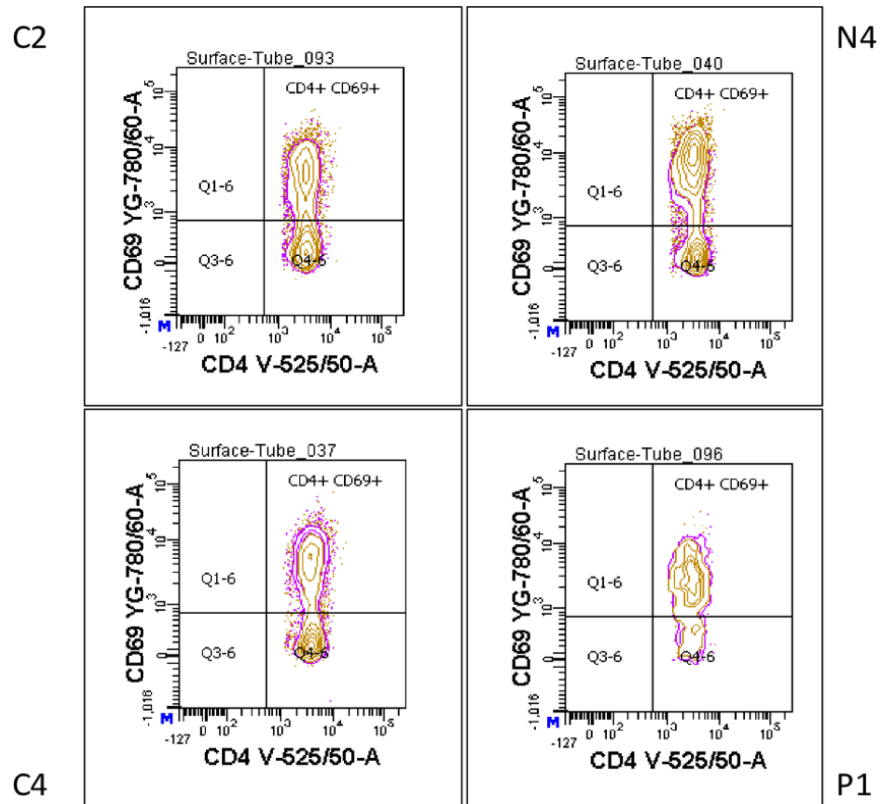


**Figure 6.2a:** CD69 analysis: Representative FACS plots for four samples showing variability of expression of CD69 in CD3+ CD4+ population. C2&C4: CHL; N4: FL; P1: PTGC. Results for all samples are summarised in Table 6.4.

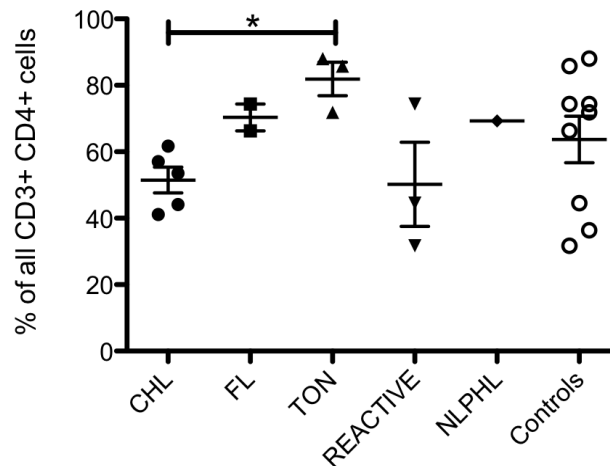


**Figure 6.2b:** CD69 Analysis: CD69 is significantly under-expressed in the CD3+CD4+ component of CHL (mean=51.5%) compared to tonsils (mean=81.9%; p=0.04) but not reactive nodes (mean=50.2%; p=0.23) or pooled controls (mean=63.7%; p=0.23).

ID	%CD3+	%CD4+	CD4	CD95+	CD95hi	CD28+	CD134+	RANK-L
C1	46.8	65.3	12314	78.4	26.3	45.5	24.9	2
C2	19.1	48.4	11464	81.5	49.5	54.6	51.2	0.2
C4	56.6	40.3	6307	54.8	21.8	28.4	27.5	0.7
C5	54.8	54.4	5849	78.3	41.8	28	25.9	0.8
C6	50	77.3	6073	90.8	47.6	61	43.3	0.5
L1	65	75.2	748	99.6	68.4	41.8	17.8	0.5
N1	31.4	83.4	12493	88.5	75.3	42.4	41	0.4
N2	6.5	52.8	174	98.8	31	9.8	33.3	0
N4	12.9	68.6	6734	88.2	57.6	26.4	27.4	0.4
P1	21.1	62	1719	89.7	56.7	42.1	34.7	0.6
R1	45	53.4	1033	76.2	18.8	28.8	16.8	0.7
R2	27.9	69.7	1115	48	17.6	18.5	20.6	0.6
T1	25.8	66.2	7282	95.5	45.8	49.8	25.8	0.5
T2	18.8	62.4	2084	73.9	28.3	20.2	18.7	1.1
T3	7.3	84	2304	96.6	68.9	39.3	34.3	1.4

ID	CD278+	CD278hi	CD154+	CD178+	CD30+	CD69+	CD27+
C1	27.4	6.8	4	4.4	0.6	41.1	59.9
C2	67.6	50.4	6	1.1	0.6	61.7	54.5
C4	39	14.2	5	0.7	0.9	44.1	73.8
C5	42	18.5	4.6	0.6	0.7	53.5	62.7
C6	70.5	49	10.2	1.2	0.9	57	35.9
L1	46.9	4.5	3.2	0.9	0.2	69.3	32.1
N1	65.3	8.8	2.9	0.5	1.4	74.4	62.7
N2	19	17	0.6	0	0.6	x	x
N4	48.7	13.2	7.5	1.8	0.8	66.3	73.7
P1	61.1	20.6	10	1.8	0.9	74.4	60.2
R1	14.6	4	3.4	1.4	0.7	31.7	28.8
R2	25.2	7.4	4.1	0.5	0.6	44.5	73
T1	82.7	60.1	17.8	2.9	0.3	85.8	69.3
T2	58.2	30.1	10.5	0.9	0.4	71.9	72.4
T3	85.9	43.7	25.4	8.7	0.7	88	74.3

**Table 6.4:** Expression of Cocktail 1 markers (TNFRSF/IGSF) expressed as % of all CD3+CD4+ events. Total number of CD4+ events is shown to illustrate wide heterogeneity between samples. A minimum of 500 viable CD4+ events was required for inclusion in the statistical analysis. %CD3 is expressed as % total viable events. %CD4 is expressed as % total CD3+ events.

*6.4.1.2 Cocktail 2: Chemokine Receptors (Table 6.5; Figures 6.3a&b)*

CXCR5 was under expressed in CHL CD4<sup>+</sup> T cells compared to pooled controls (mean=25.8% vs 48.7%, p=0.099/ns), significantly lower than tonsil (mean=65.2%, p=0.037). CCR3 and CCR6 were expressed at relatively low levels in all samples (<10%) but relatively over expressed in CHL CD4<sup>+</sup> T cells population compared to pooled controls (CCR3 mean=5.9% vs 2.2%, p=0.043; CCR6 mean=2.42% vs 0.85%, p=0.036). CCR4 and CCR5 were heterogeneously expressed across all samples without significant differences in mean expression levels.

ID	CD4	CCR3	CCR4+	CCR5+	CCR6+	CXCR5
C1	5196	12.3	42.9	15.4	2.9	13.7
C2	5411	2.9	66.2	33.5	1.2	6.8
C4	6052	2	15.4	12	3.4	30.4
C5	6131	7	22	24.2	2.7	30.5
C6	6150	4.3	77.2	10.1	1.9	47.5
L1	6478	1.9	33.4	29.2	0.3	53.2
N1	6221	1.4	14.5	6.5	0.4	73.4
N2	474	3	51	17.2	1.3	26.7
N4	5580	1.6	50.1	13.8	0.3	43.8
P1	2490	1.1	40.5	2.7	0.3	46.2
R1	938	4.3	57.1	41	3.4	22.6
R2	2157	1.2	16.7	1.1	0.2	25.2
T1	6892	2	53.1	2.7	0.5	66
T2	2567	1.2	25.7	5.2	0.2	56
T3	5682	4.7	27.1	12.5	1.6	73.5

**Table 6.5:** Expression of Cocktail 2 markers (Chemokine Receptors) expressed as % of all CD3<sup>+</sup>CD4<sup>+</sup> events. Total number of CD4<sup>+</sup> events is shown to illustrate wide heterogeneity between samples. A minimum of 500 viable CD4<sup>+</sup> events was required for inclusion in the statistical analysis.

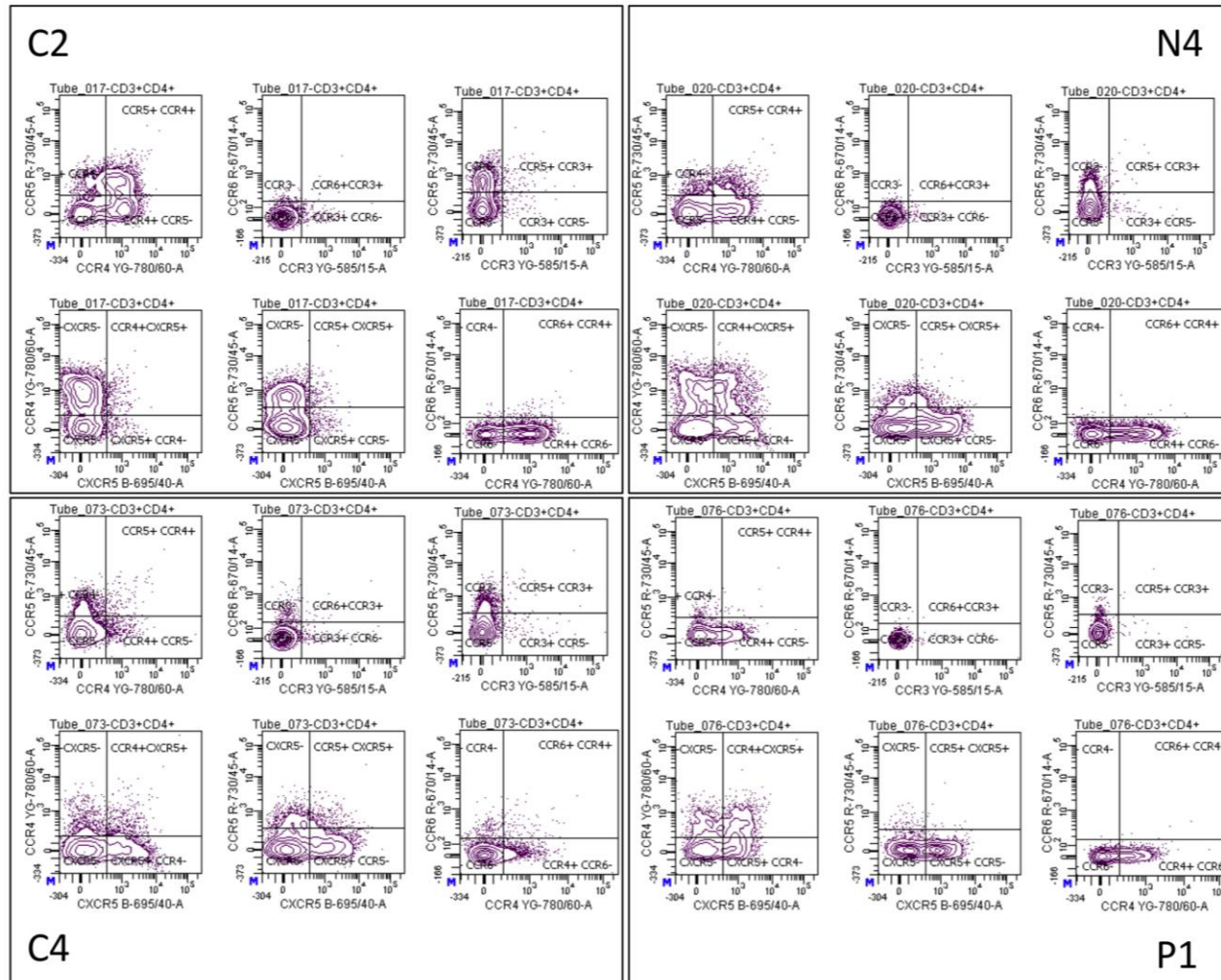


**Figure 6.3a:** Cocktail 2 Analysis: Chemokine receptor expression. Representative FACS plots for four samples showing variability of expression of markers in CD3+ CD4+ population. C2&C4: CHL; N4: FL; P1: PTGC. Results for all samples are summarised in Table 6.5.

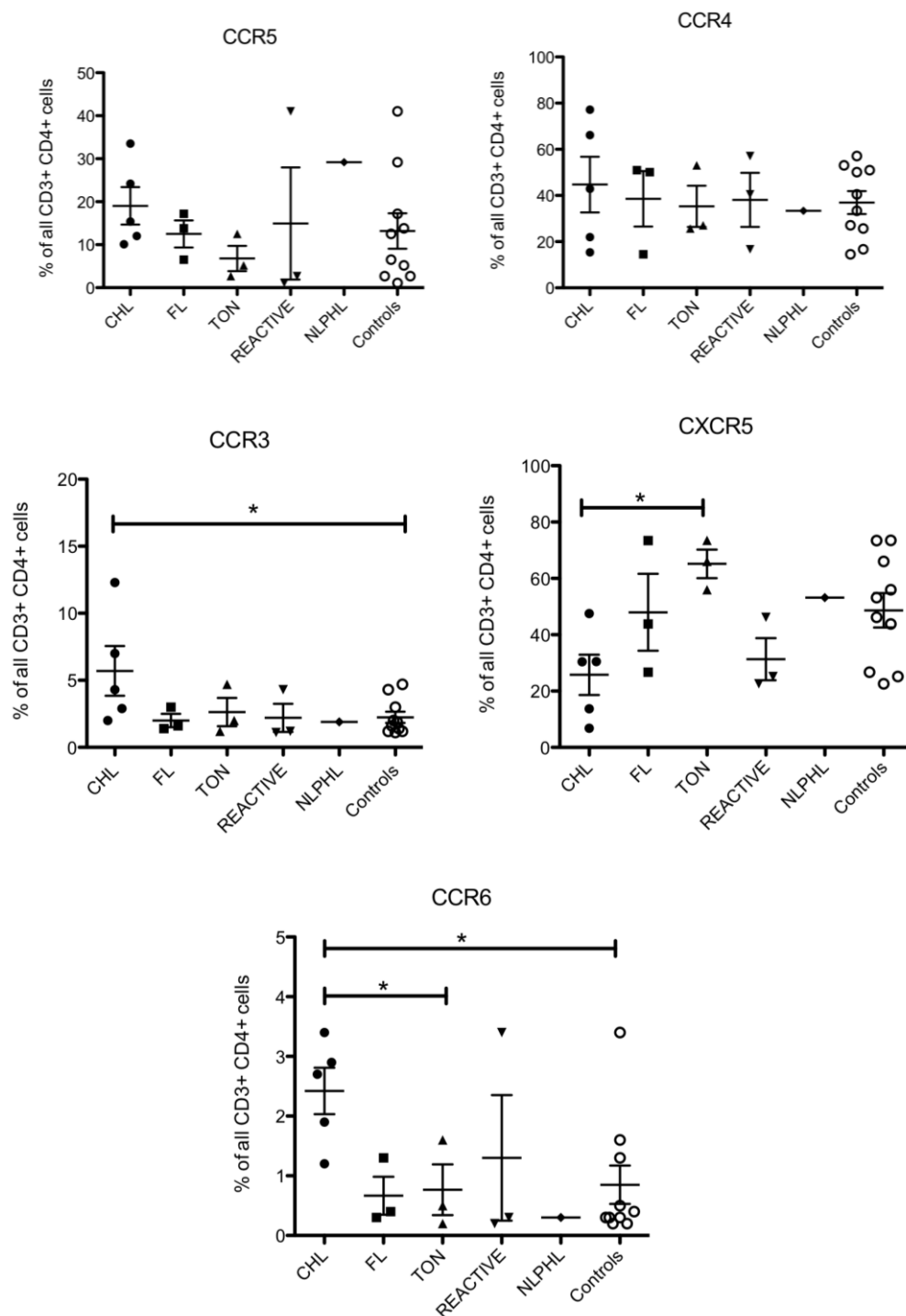


**Figure 6.3b:** Cocktail 2 Analysis: Chemokine receptor expression.

Overview of expression of cocktail 2 markers shown as a % of all viable CD3+CD4+ cells. Sample set is indicated on the x axis. 'Controls' indicates pooled control (not CHL) samples. Individual results are plotted, along with mean (horizontal line) and SEM (vertical bars). Medians were compared assuming non-Gaussian distribution of data using the Mann-Whitney U test.

6.4.1.3 Cocktail 3a: Naïve T cell markers / Lymphoid tissue homing markers (Table 6.6 and Figures 6.4a&b)

CCR7 and CD62L were both over-expressed in CHL compared to pooled control, with double positive cells particularly discriminatory (Mean % total CD3+CD4+ cells CCR7+CD62L+ in CHL 16.6% vs 4.8% pooled controls ( $p=0.001$ ), vs 4.3% tonsils ( $p=0.036$ ) and vs 4.8% reactive ( $p=0.036$ ). CD62L was expressed in 50.4% of CHL CD3+CD4+ T cells, compared to 18.2% pooled control ( $p=0.002$ ) and 14.5% tonsil ( $p=0.036$ ) CD3+CD4+ cells. CD127 was over-expressed in 23.3% CHL T cells, compared to 11.1% pooled controls ( $p=0.012$ ) using the arbitrary CD127hi gate determined as defined in Figure 6.4a. By MFI of all CD3+CD4+ cells there was also evidence of over-expression: MFI in CHL was 402 vs 248 in pooled control ( $p=0.05$ ), although the limitations of application of comparative statistics on arbitrary, compensated logarithmic values generated using flow cytometry in terms of validity and translatability have been discussed in 2.3.10.3.

ID	CD4	CD62L+	CCR7+	CD62L+ CCR7+	CD127+	CD127 MFI
C1	4699	32.6	22.7	8.1	36.1	658
C2	5419	71.2	13.2	10.7	16.5	195
C4	5156	48.9	31.5	19.9	26.5	468
C5	5315	58.5	42.5	31.9	24.6	413
C6	5040	40.7	21.9	12.2	12.8	277
L1	5114	4.5	4.8	1.8	6.4	239
N1	4885	18.7	13.5	6.1	7.5	148
N4	5399	27.3	17.2	7.5	14.1	187
P1	558	19.2	8	4.1	11.6	267
R1	1770	16.6	52.6	7.3	22.7	413
R2	526	33.6	7.8	3	14.6	384
T1	4766	15.8	11.8	3.7	8.5	245
T2	573	21	17.8	7.7	11	237
T3	4158	6.8	5.3	1.6	3.1	111

**Table 6.6:** Expression of Cocktail 3 naïve / homing T cell markers expressed as % of all CD3+CD4+ events. Total number of CD4+ events is shown to illustrate wide heterogeneity between samples. A minimum of 500 viable CD4+ events was required for inclusion in the statistical analysis. %CD3 is expressed as % total viable events.



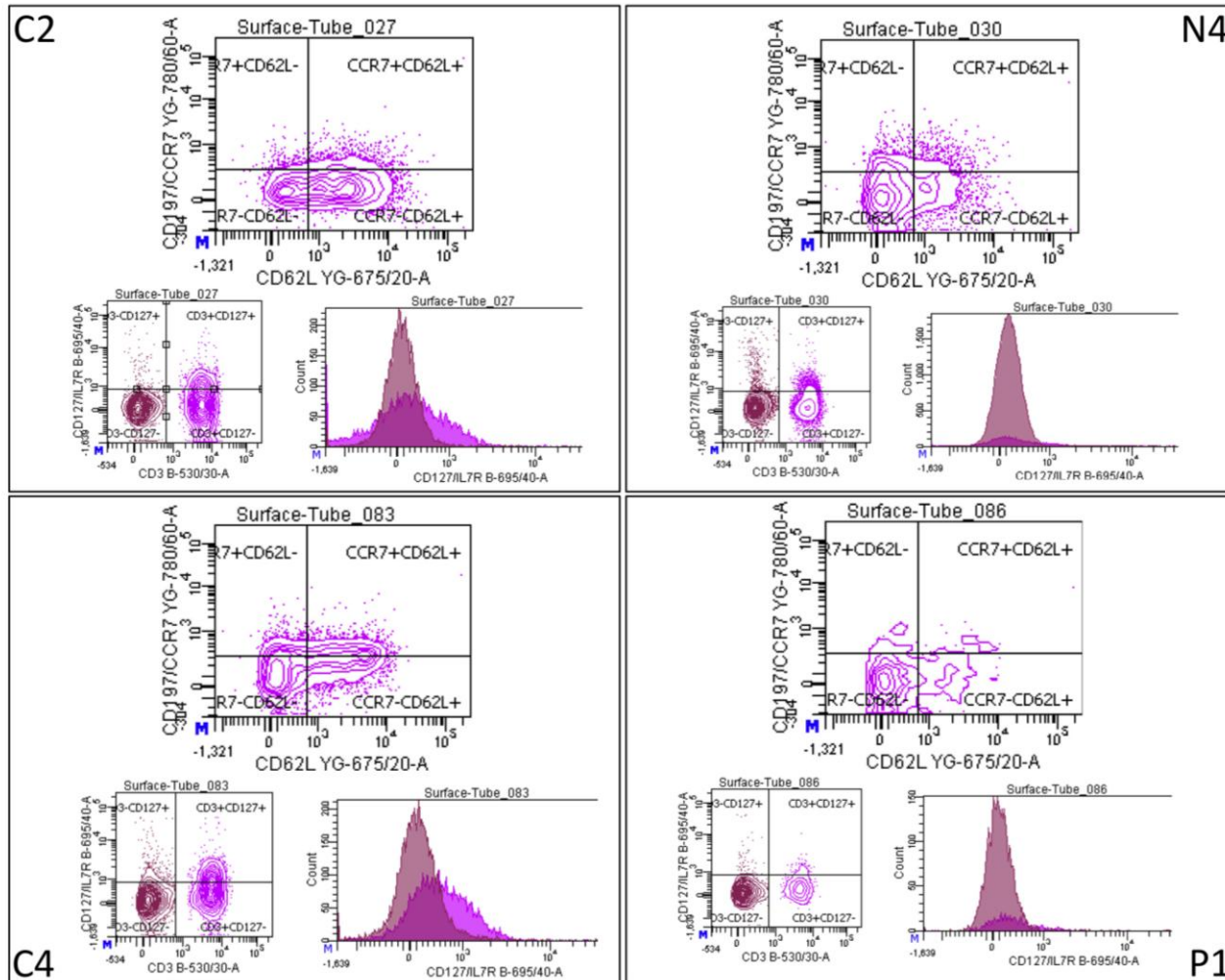


**Figure 6.4a:** Cocktail 3a Analysis: Naïve T cell / T cell homing markers. Representative FACS plots for four samples showing variability of expression of markers in CD3<sup>+</sup> CD4<sup>+</sup> population. C2&C4: CHL; N4: FL; P1: PTGC. Results for all samples are summarised in Table 6.6.

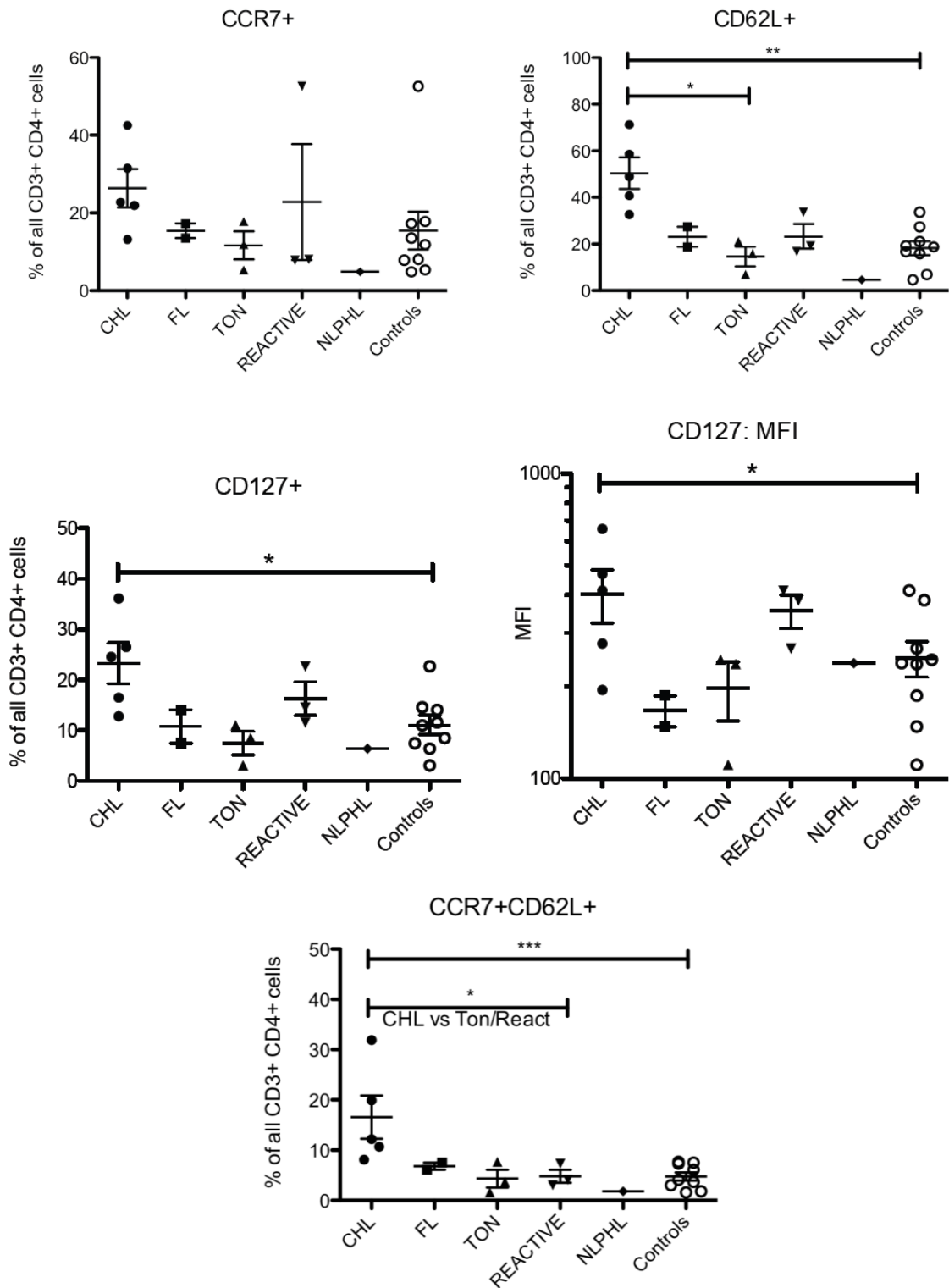


**Figure 6.4b:** Cocktail 3a Analysis: Naïve T cell / T cell homing markers. ‘Controls’ indicates pooled control (not CHL) samples. Individual results are plotted, along with mean (horizontal line) and SEM (vertical bars). Medians were compared assuming non-Gaussian distribution of data using the Mann-Whitney U test.

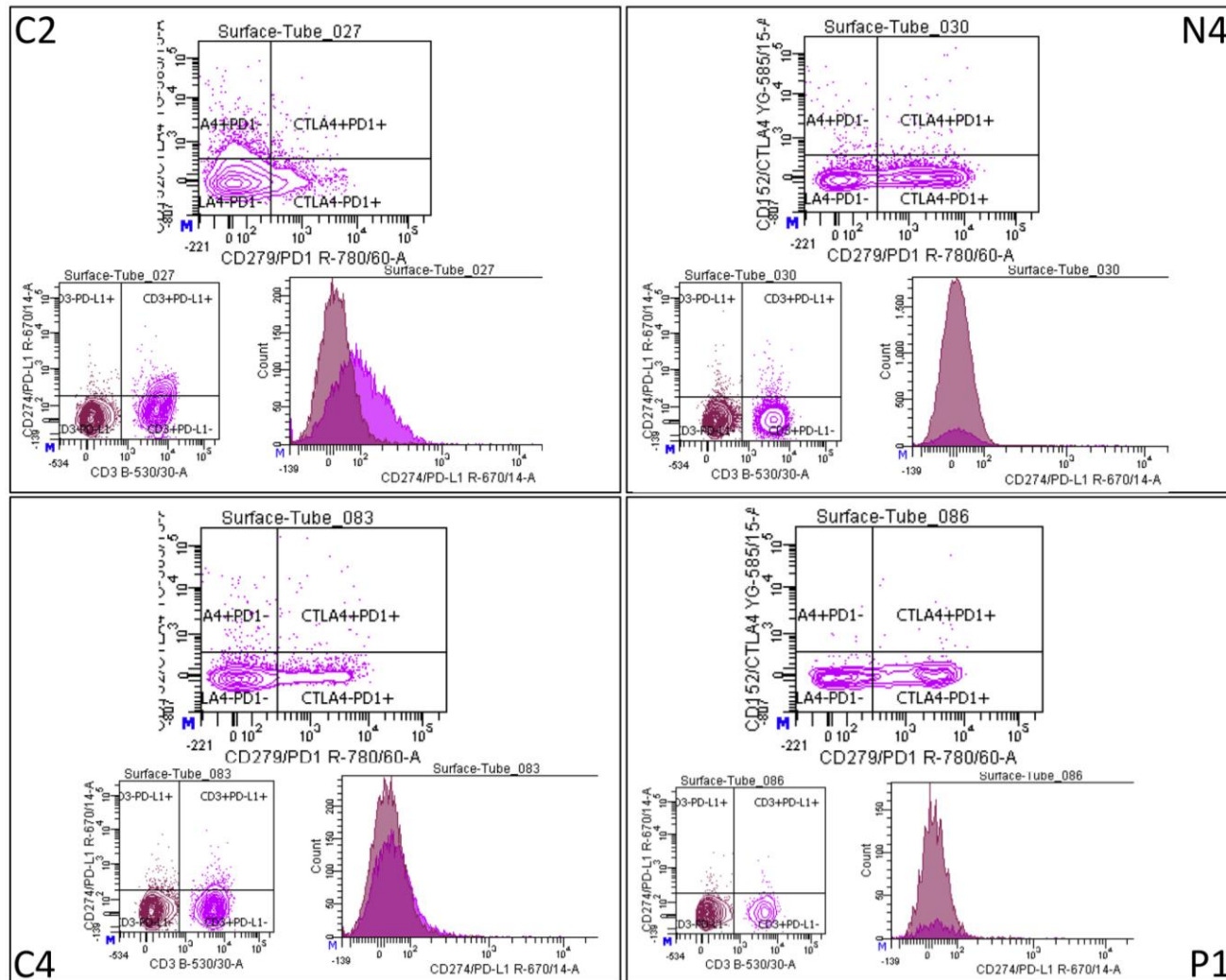


**Figure 6.5a:** Cocktail 3b Analysis: Immunosuppressor markers. Representative FACS plots for four samples showing variability of expression of markers in CD3+ CD4+ population. C2&C4: CHL; N4: FL; P1: PTGC. Results for all samples are summarised in table 6.7.

ID	CD4	PD1+	PD-L1+	PD-L1 MFI	CTLA4+	CD57+
C1	4699	7.3	9.9	86	4.4	5.2
C2	5419	16.2	17	85	10.9	3.1
C4	5156	18.3	3.2	34	2.5	6.8
C5	5315	16.9	5.9	50	4.6	4.7
C6	5040	51.4	1.7	23	12.8	5.7
L1	5114	86.9	3.2	14	3.9	54.5
N1	4885	76.7	1.3	1	4.2	28.3
N4	5399	54.1	1.6	12	2.6	32.6
P1	558	54.6	2.2	25	4.1	8.2
R1	1770	20.6	1.8	23	2.3	5.5
R2	526	21.3	1.3	18	2.7	7.5
T1	4766	79.4	5.4	21	5.8	21.1
T2	573	53.9	3.5	16	4.7	36.7
T3	4158	90.3	7.7	27	15.4	40.6

**Table 6.7:** Expression of Cocktail 3b immunosuppressive/senescence T cell markers expressed as % of all CD3+CD4+ events. Total number of CD4+ events is shown to illustrate wide heterogeneity between samples. A minimum of 500 viable CD4+ events was required for inclusion in the statistical analysis.

#### 6.4.1.4 Cocktail 3b: Suppressive / Senescence markers (Table 6.7 & Figures 6.5 & 6.6a&b)

Data for CD57 is included due to functional resemblance to suppressive markers, but was acquired from Cocktail 7 due to fluorochrome combination considerations. CTLA4 showed significant heterogeneity of expression although was never expressed in more than 15% of CD3+CD4+ cells (2.3%-15.4% across all samples). PD-L1 was apparently significantly over-expressed ( $p=0.009$ ) using MFI of all CD3+CD4+ cells in CHL (MFI=55.6) compared to pooled controls (MFI=17.4) although the limitations of application of comparative statistics on arbitrary, compensated logarithmic values generated using flow cytometry in terms of validity and translatability have been discussed and using this antibody/fluorochrome and data acquisition settings expression was not demonstrated at a high level despite contrasting IHC data (see chapter 4) There

was no significant over-expression by proportion of total CD3+CD4+ expressing PD-L1 at a level determined by the gating strategy shown in Figure 6.5a. CD57 is markedly suppressed in the CHL CD3+CD4+ population (mean expression: 5.1%) compared to pooled controls (mean expression: 26.1%;  $p=0.004$ ), tonsil (mean expression: 32.8%) or FL (mean: 30.5%, inadequate replicates for comparison) CD3+CD4+ cells, but at similar levels to all reactive nodes (mean expression 7.1%). CD57 is expressed by >50% CD3+CD4+ cells from NLPHL. PD1 was significantly under-expressed in the CHL CD3+CD4+ population (mean=22%) compared to other groups (mean=59.8% in pooled controls;  $p=0.004$ , 74.5% in tonsil;  $p=0.036$ ) but not compared to reactive benign nodes (mean=32.2%;  $p=0.14$ ). PD1 was markedly over-expressed in NLPHL (86.9%).

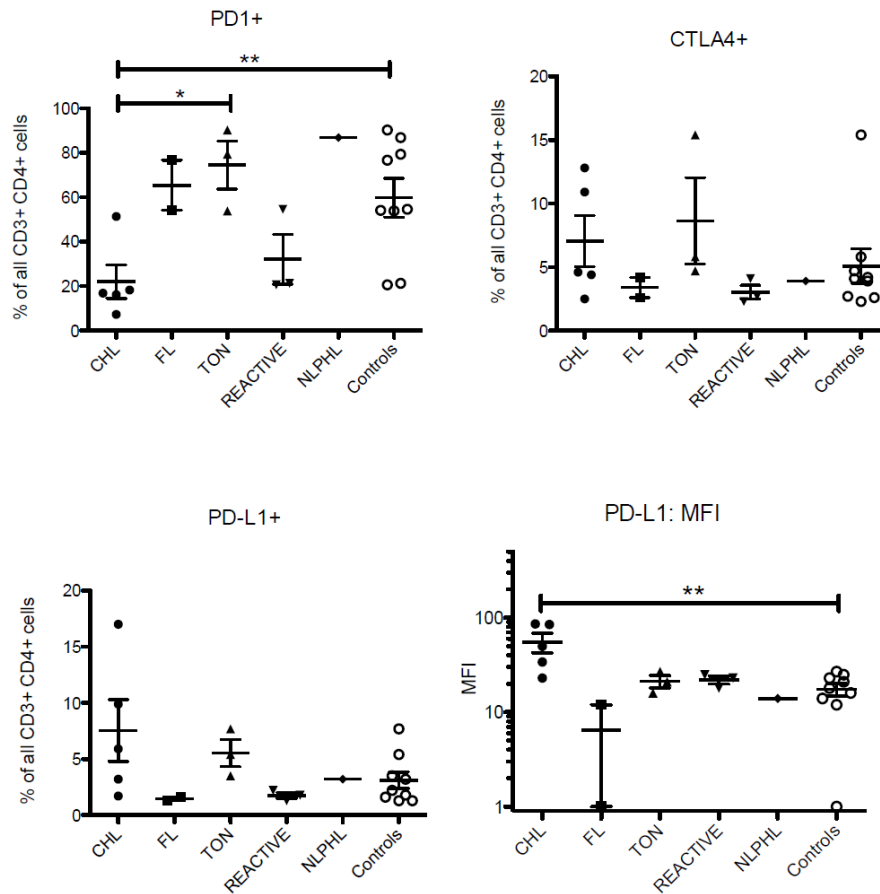


**Figure 6.5b:** Cocktail 3b Analysis: Immunosuppressor markers. ‘Controls’ indicates pooled control (not CHL) samples. Individual results are plotted, along with mean (horizontal line) and SEM (vertical bars). Medians were compared assuming non-Gaussian distribution of data using the Mann-Whitney U test.

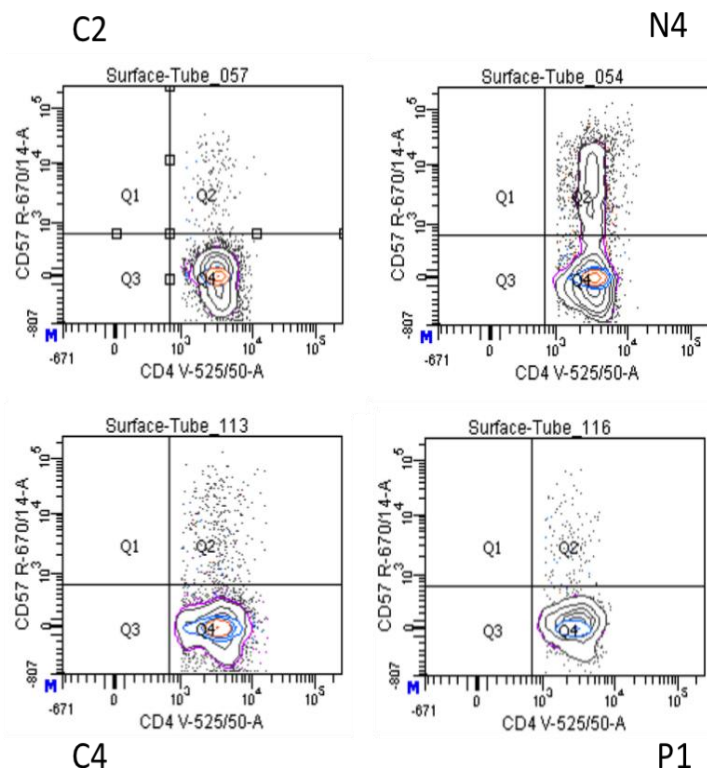


**Figure 6.6a:** CD57 expression. Representative FACS plots for four samples showing variability of expression of marker in CD3<sup>+</sup> CD4<sup>+</sup> population. C2&C4: CHL; N4: FL; P1: PTGC. Results for all samples are summarised in table 6.7.

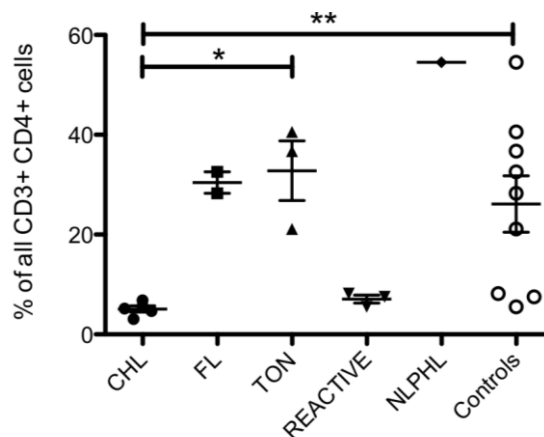


**Figure 6.6b:** CD57 Analysis: Summary of expression of cocktail 1 markers shown as a % of all viable CD3<sup>+</sup>CD4<sup>+</sup> cells. Only markers expressed in at least one sample at a level of >10% of all CD3<sup>+</sup>CD4<sup>+</sup> are shown. Sample set is indicated on the x axis. 'Controls' indicates pooled control (not CHL) samples. Individual results are plotted, along with mean (horizontal line) and SEM (vertical bars). Medians were compared assuming non-Gaussian distribution of data using the Mann-Whitney U test.

## 6.4.1.5 Cocktail 5: IL2 and IL4 receptor components (Table 6.8 and Figures 6.7a&amp;b)

IL2R $\beta$  was not appreciably expressed in CHL-derived samples and only rarely in control samples, with the exception of C<sub>1</sub>, an outlier whose expression was twenty-fold greater than other CHL-derived samples (11% vs 0.4-0.8%). As such no comparison with other groups was carried out. IL4R $\alpha$  was similarly expressed at a low level in all samples, with mean CHL-expression not significantly different from pooled controls (5.2% vs 3.3%) except for the same outlier, C<sub>1</sub>, with expression of 15.3%. CD25/IL2R $\alpha$  was heterogeneously expressed across CHL-derived samples (9.8-43.2% of all CD3+CD4+ cells), with mean expression significantly greater than pooled controls (23.9% vs 11.2%;  $p=0.045$ ). Similarly CD132/CGC was heterogeneously expressed across CHL-derived samples (27.5-53.3%) with mean expression in CHL derived CD3+CD4+ cells (40.0%) significantly greater than in pooled controls (mean=24.7%;  $p=0.016$ ) or tonsils (mean=22.6%;  $p=0.036$ ).

ID	CD4	CD25+	CGC+	IL2R $\beta$ +	IL4R $\alpha$ +
C <sub>1</sub>	7981	24.8	48.1	10.9	15.3
C <sub>2</sub>	5754	43.2	53.3	0.6	2.5
C <sub>4</sub>	6236	9.8	27.5	0.4	1.5
C <sub>5</sub>	9975	24	40	0.9	2.1
C <sub>6</sub>	4668	17.5	31.2	0.8	4.5
L <sub>1</sub>	9036	7.6	17.3	0.6	0.7
N <sub>1</sub>	5662	8.6	22.5	0.2	1.2
N <sub>4</sub>	6520	18.4	32.7	0.8	1.7
P <sub>1</sub>	1619	16	23.3	2	4.1
R <sub>1</sub>	2871	11.1	32.7	5.1	5.1
R <sub>2</sub>	1063	11.1	26.3	1.2	6
T <sub>1</sub>	6647	10.3	25.9	1.5	1.5
T <sub>2</sub>	1119	5.9	17.4	1.8	2.6
T <sub>3</sub>	5385	12.2	24.6	7.3	7

**Table 6.8:** Expression of Cocktail 5 IL2/IL4 receptor components expressed as % of all CD3+CD4+ events. Total number of CD4+ events is shown to illustrate wide heterogeneity between samples. A minimum of 500 viable CD4+ events was required for inclusion in the statistical analysis.

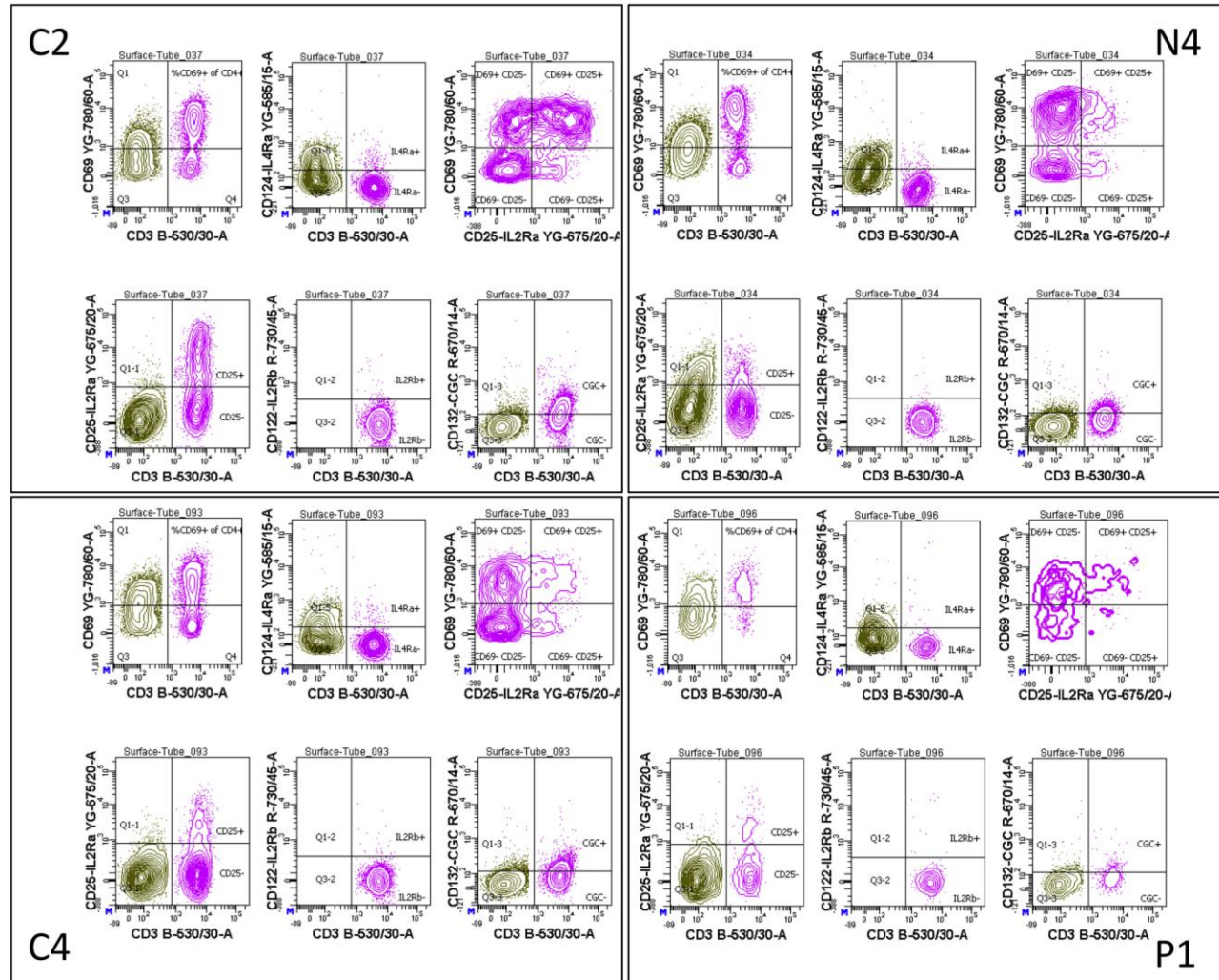


**Figure 6.7a:** Cocktail 5 Analysis: IL2 and IL4 receptor expression: Representative FACS plots for four samples showing variability of expression of markers in CD3+ CD4+ population. C2&C4: CHL; N4: FL; P1: PTGC. Results for all samples are summarised in table 6.8.



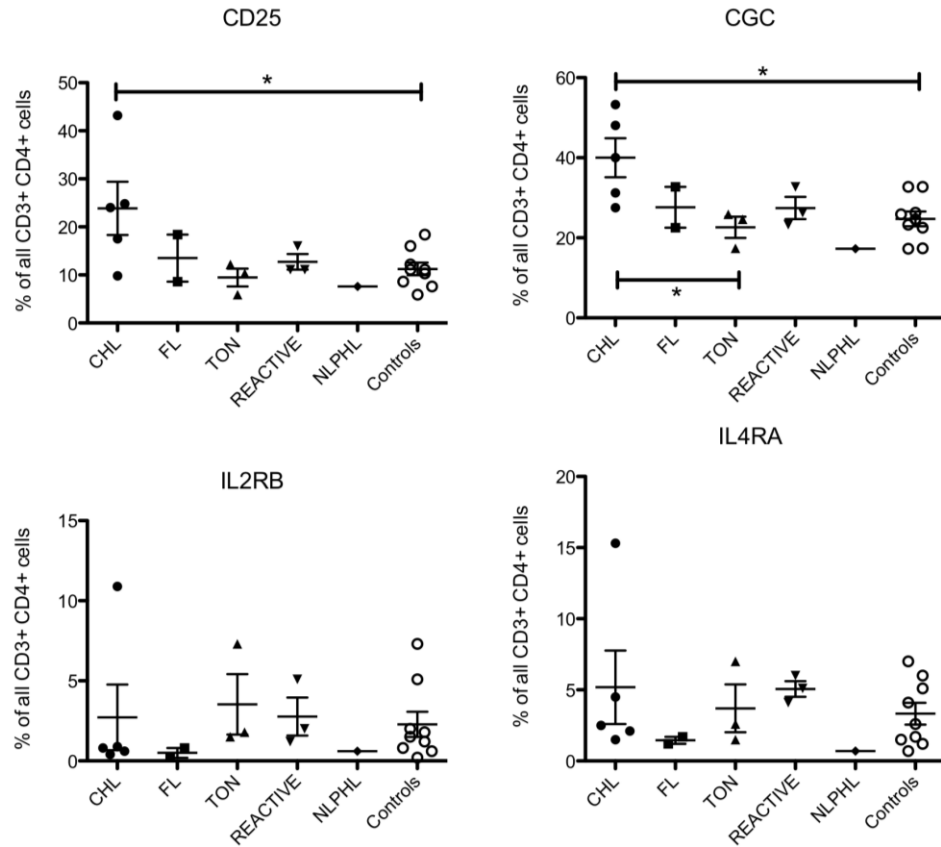


**Figure 6.7b:** Cocktail 5 Analysis: IL2 and IL4 receptor expression. Summary of expression of cocktail 5 markers shown as a % of all viable CD3+CD4+ cells. Sample set is indicated on the x axis. 'Controls' indicates pooled control (not CHL) samples. Individual results are plotted, along with mean (horizontal line) and SEM (vertical bars). Medians were compared assuming non-Gaussian distribution of data using the Mann-Whitney U test.

6.4.1.6 Cocktail 7: CD45 Isotype (Table 6.9 and Figures 6.8 a-c)

CD45 isotype expression defined by CD45RO and CD45RA assumed a characteristic phenotype for the CHL-derived population, with a substantial CD45RA+ population, and an ‘intermediate’ population less pronounced in other samples (Figure 6.8a). Analysis of gated populations showed a trend towards a greater expression of CD45RA and lesser CD45RO with increased ‘intermediate’ population for the CHL component compared to FL or tonsil, but was indistinguishable from reactive CD3+CD4+ cells, and only significant comparing the intermediate population in CHL (mean=6.2%) with tonsil (mean=1.8%; p=0.036).

ID	%CD45RO+	%CD45RA+	%CD45RORA
C1	59.8	28.1	9
C2	75.6	11.9	9.1
C4	58.2	25.2	4.8
C5	65.3	22	5.1
C6	89.2	5.8	3.2
L1	93.9	1.8	1.2
N1	80.1	10.9	5.6
N4	82.6	10.4	4.2
P1	88.8	7.5	1.8
R1	71.4	16.6	4.3
R2	57.1	32.6	7.8
T1	88.1	9.5	1.4
T2	83.3	13.4	1.5
T3	88.9	6.1	2.4

**Table 6.9:** Expression of Cocktail 5 CD45 isotype, expressed as % of all CD3+CD4+ events. A minimum of 500 viable CD4+ events was required for inclusion in the statistical analysis.

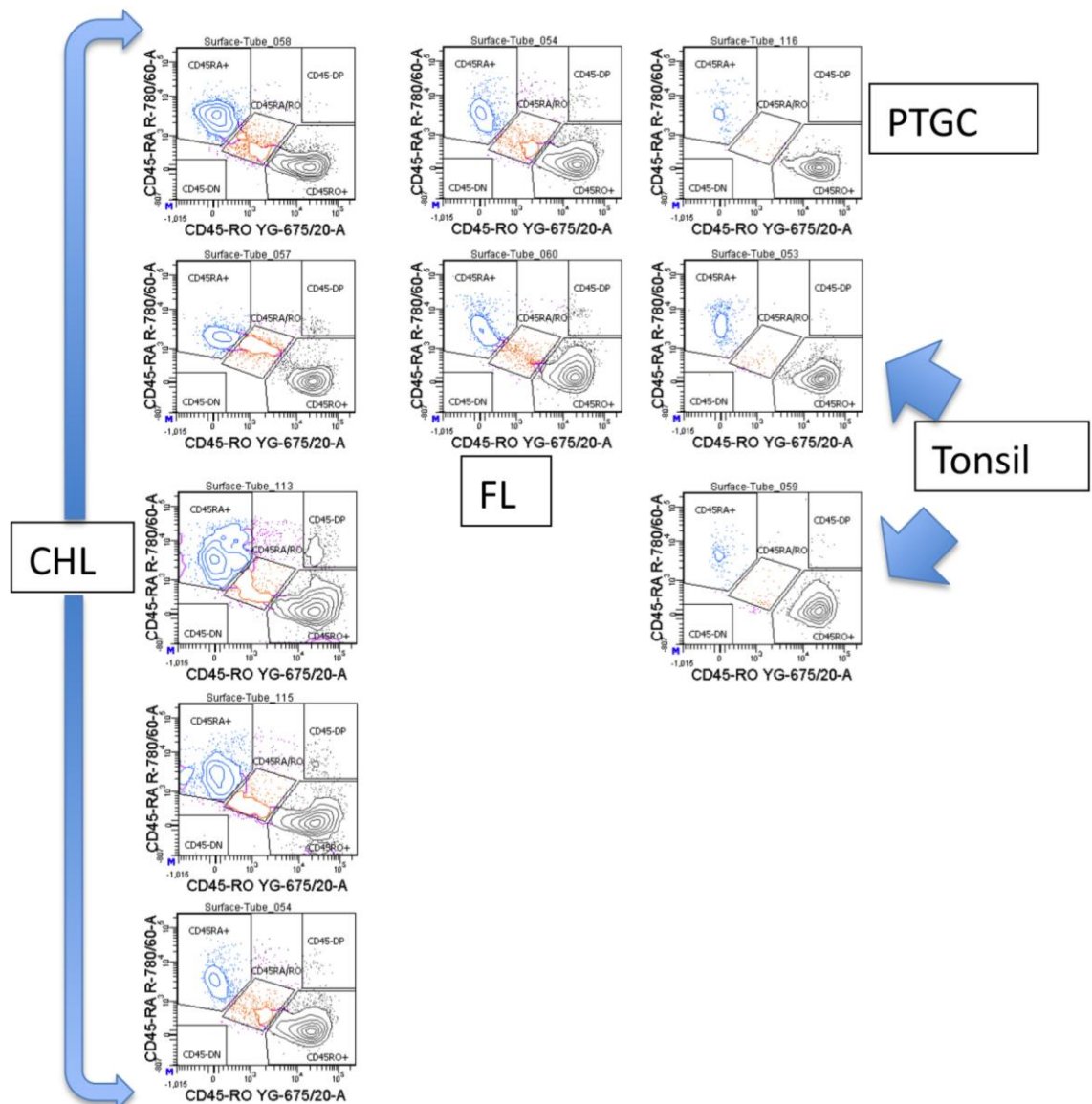


**Figure 6.8a:** Cocktail 7 analysis: CD45 isotype. Illustration of the distinctive CD45RO/RA isotype profile of the CD3+CD4+ component of the majority of CHL cases (left column) with a bias towards CD45RA and intermediate population, rather than the majority CD45RO expression seen in tonsil and PTGC (right column) or FL (central column).

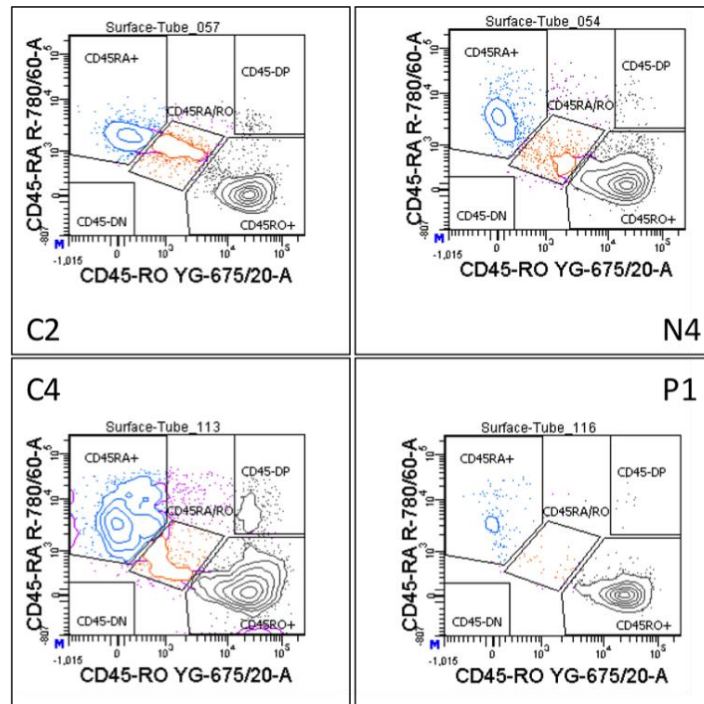


**Figure 6.8b:** Cocktail 7 Analysis: CD45 isotype. Representative FACS plots for four samples showing variability of expression of markers in CD3+ CD4+ population. C2&C4: CHL; N4: FL; P1: PTGC. Results for all samples are summarised in table 6.9.

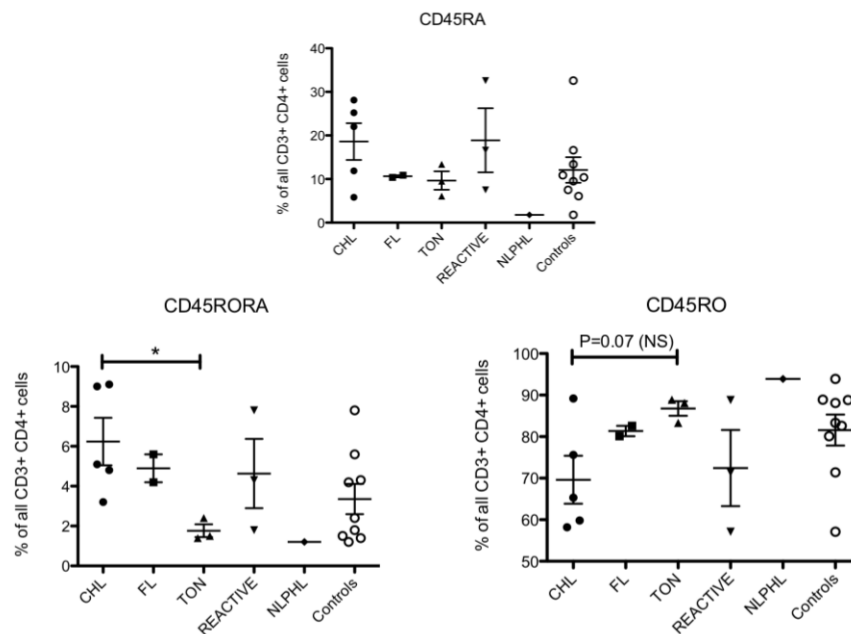


**Figure 6.8c** Cocktail 7 Analysis: CD45 isotype. Summary of expression of cocktail 6 markers shown as a % of all viable CD3+CD4+ cells. Sample set is indicated on the x axis. ‘Controls’ indicates pooled control (not CHL) samples. Individual results are plotted, along with mean (horizontal line) and SEM (vertical bars).

**6.4.1.7 Cocktail 4: Th1/inflammatory Cytokine Profile (Table 6.10 and Figures 6.9a & 6.10)**

Neither IL2 nor IL6 were expressed at any appreciable level. There was a wide heterogeneity of expression of both IFN- $\gamma$  (7.7%-89.8%) and TNF $\alpha$  expression (2.8%-20.3%). Only malignant-derived T cells expressed IFN- $\gamma$  in greater than 40% of cells (three samples, 2 CHL, one FL), and CHL-derived T cell expression was never less than 18%, while tonsillar samples expressed IFN- $\gamma$  in <18% of T cells in both samples. However there was no statistically significant difference between the means of any sample classes, nor between means of pooled malignant (35.1%) versus pooled benign (19.7%) samples ( $p=0.13$ ). Note that NLPHL expressed IFN- $\gamma$  at extremely high levels (89% of all T cells) however was excluded from comparative statistics due to its being an outlier and the only representative of its histological class. TNF $\alpha$  similarly showed no statistically significant difference in mean expression between sample classes, however there was a significantly greater expression in pooled malignant node-derived T cells than those derived from benign lymph nodes (14.2% vs 7.1%;  $p=0.030$ ).

ID	% viability	CD4	IL2	IL6	IFN- $\gamma$	TNF $\alpha$	IFN- $\gamma$ / TNF $\alpha$
C1	69.6	1252	0	0.1	30.6	18.2	8.1
C2	93.1	9211	0	0	21.7	7.6	5.5
C4	86.9	1449	0	0.1	65.6	15.9	14.6
C5	91.3	5184	0.1	0	58.2	20.3	17.8
C6	79	619	0.5	0.3	18.3	12.2	4.5
L1	73.4	2558	0.1	0.1	89.8	17.2	16.6
N1	92.7	5828	0	0.1	25.7	8.5	4.2
N2	94.4	1195	0.1	0	14.5	14.8	2.8
N4	75.2	5562	0	0.1	45.8	16.1	11.6
P1	81	1386	0	0.1	33	11.2	6.1
R1	68.6	810	1.5	1.5	27	13.2	10.2
R2	85.4	1923	0.1	0.1	7.7	3.8	1
T1	83.7	2125	0	0	13.7	4.6	1.5
T2	83.1	609	0	0	17.2	2.8	1

**Table 6.10:** Expression of Cocktail 4 Th1/inflammatory cytokines, expressed as % of all CD3+CD4+ events. Total number of CD4+ events is shown to illustrate wide heterogeneity between samples. A minimum of 500 viable CD4+ events was required for inclusion in the statistical analysis.

6.4.1.8 Cocktail 8: Th2/suppressor Cytokine Profile (Table 6.11 and Figures 6.9b & 6.10)

Neither IL10 nor IL13 were expressed at appreciable levels (<2.5% of CD3+ cells in all samples). There was an apparent over-expression of IL13 relative to pooled controls (1.62% vs 0.67%;  $p=0.0024$ ), however the expression as measured by MFI was at a low level and hence the gating strategy may have lead to overestimation of the population of cells expressing it (prior experiments on stimulated population have showed a distinct IL13 population in Th2 polarised cultures which was absent from all samples in this experiment). IL4 and IL21 were only expressed in the reactive nodes (FH and PTGC but not the granulomatous lymph node), but not in CHL (mean expression for IL4 in CHL 0.48% vs reactive 6.43%;  $p=ns$ , for IL21 CHL 1.6% vs reactive 7.57% of CD3+ cells;  $p=0.035$ ).

ID	% viability	CD4	IL13	IL21	IL10	IL4
C1	69.6	1252	2.4	2.8	0.1	1.3
C2	93.1	9211	1.9	0.6	0.9	0.2
C4	86.9	1449	1	2.2	0.4	0.1
C5	91.3	5184	1.6	2.2	1.3	0.2
C6	79	619	1.2	0.6	0	0.6
L1	73.4	2558	0.8	1.3	0.1	0.3
N1	92.7	5828	0.6	0.7	0.1	0.9
N2	94.4	1195	1.3	4	0.9	1.3
N4	75.2	5562	0.8	0.3	0.2	0.5
P1	81	1386	0.7	15.1	1.2	14.4
R1	68.6	810	0.5	3.1	0	0.3
R2	85.4	1923	0.3	4.5	1.2	4.6
T1	83.7	2125	1.1	0.8	0.1	0.5
T2	83.1	609	0.7	3	0.3	1.3

**Table 6.11:** Expression of Cocktail 4 Th2/suppressor cytokines, expressed as % of all CD3+CD4+ events. Total number of CD4+ events is shown to illustrate wide heterogeneity between samples. A minimum of 500 viable CD4+ events was required for inclusion in the statistical analysis.

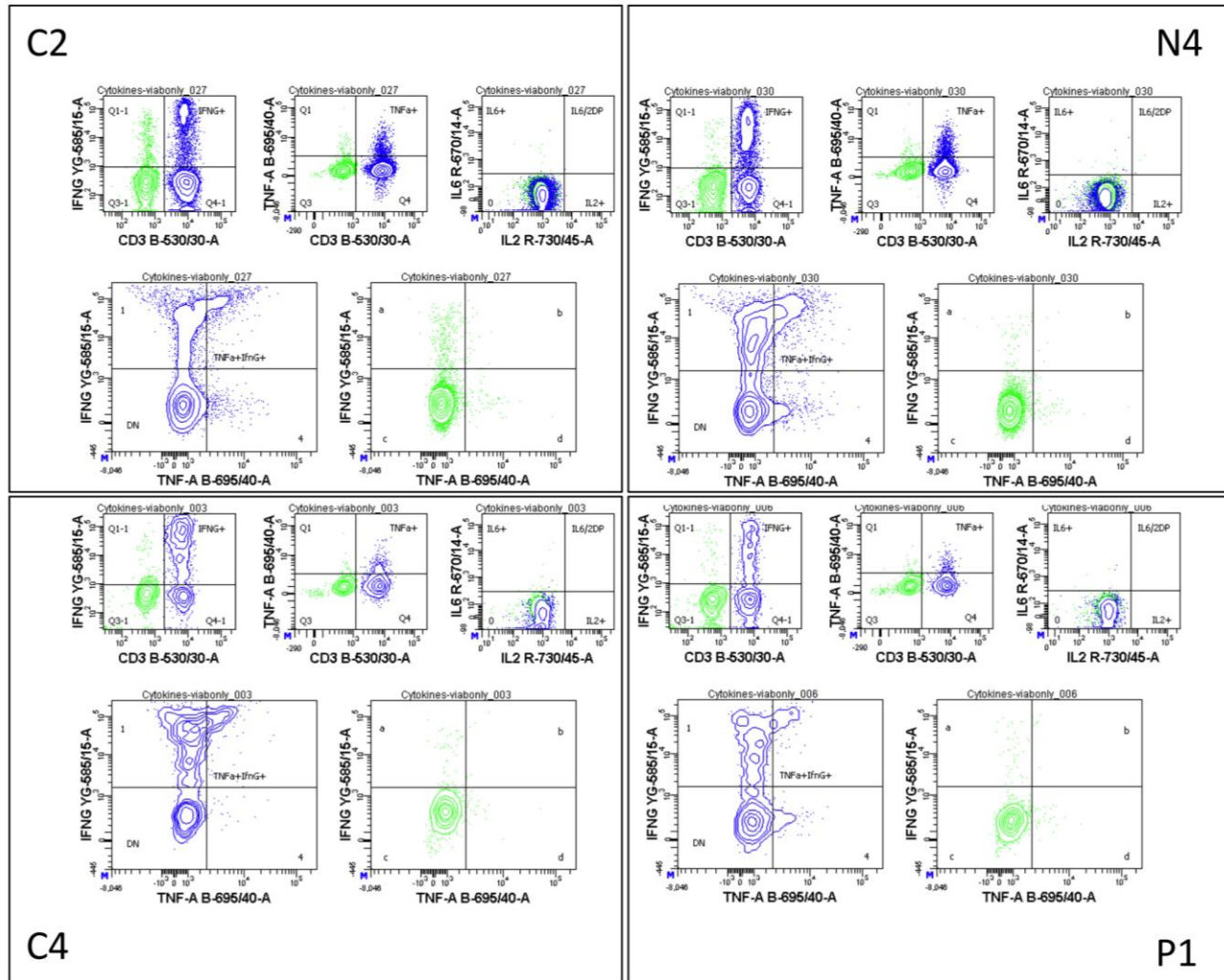
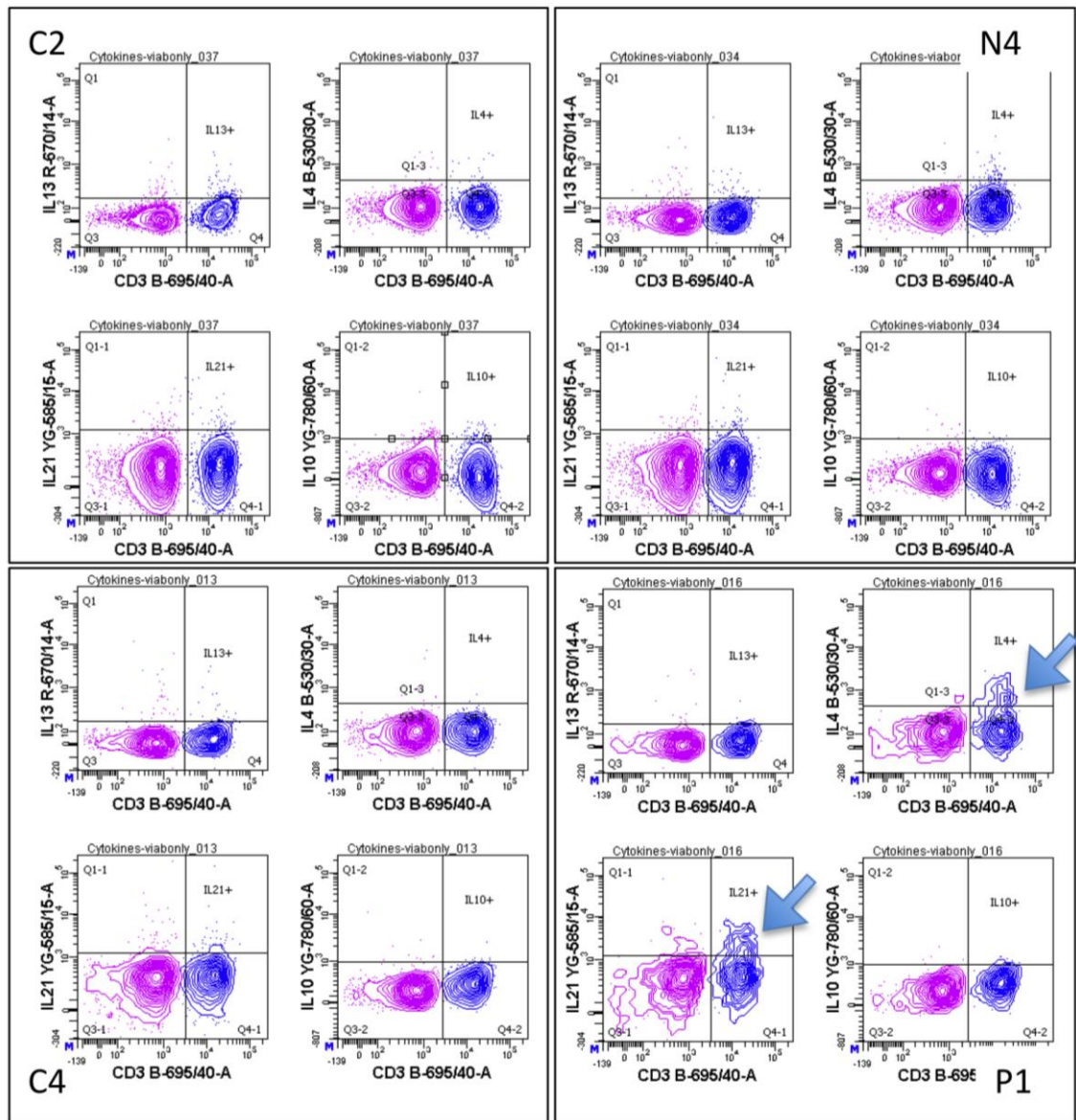
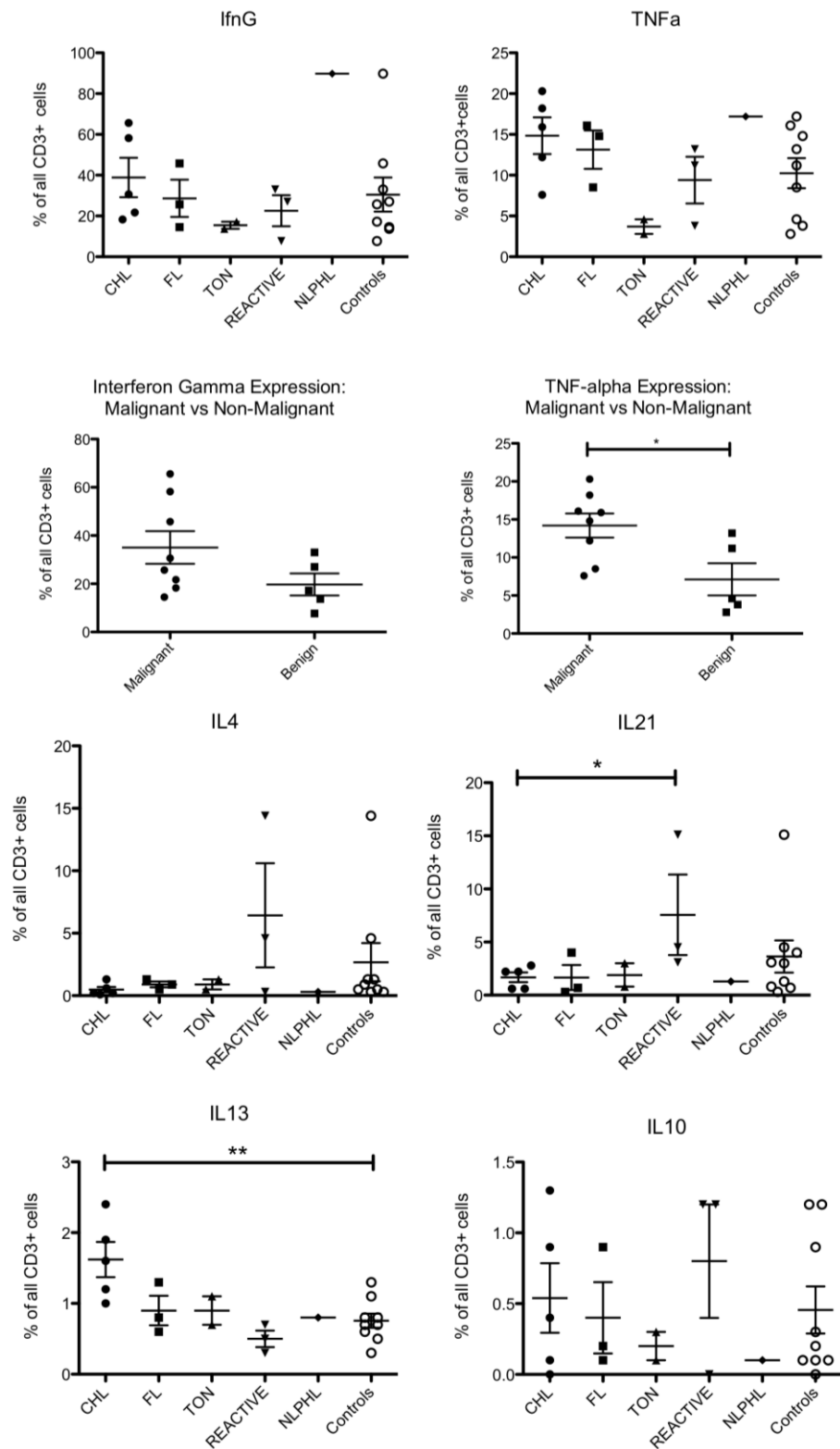


Figure 6.9a: Cocktail 4 Analysis: Th1 / inflammatory cytokines. Representative FACS plots for four samples showing variability of expression of markers in CD3<sup>+</sup> population.



**Figure 6.9b:** Cocktail 8 Analysis: Th2/T suppressor cytokines. Representative FACS plots for four samples showing variability of expression of markers in CD3+ population.





**Figure 6.10:** Overall Cytokine expression profile. Representative FACS plots for four samples showing variability of expression of markers in CD3+ population.

## 6.4.2 Summary of Flow Cytometry findings

### 6.4.2.1 Cluster Analysis

Figure 6.12 (overleaf) displays the result of unsupervised hierarchical clustering. Two main clusters emerge: one containing all CHL-derived T cell samples as well as one reactive node (granulomatous inflammation), the other segregating into two clusters: one containing both malignant samples with one of the tonsils, the other containing benign samples. Repeating the analysis without log transformation resulted in the same clustering. A second unsupervised hierarchical clustering analysis incorporating only those factors found to be most discriminatory in the marker by marker analysis described above (6.4.1) led to similar clustering despite the reduced number of available parameters to with which to form groups (Figure 6.11).

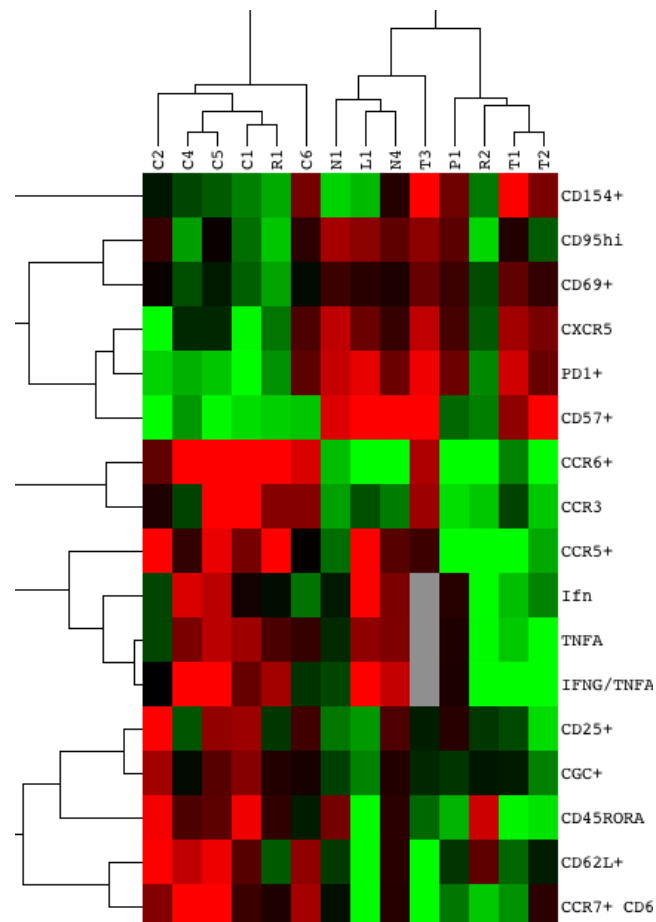


**Figure 6.11:** See figure overleaf for initial clustering. A second unsupervised hierarchical clustering analysis incorporating only those factors found to be most discriminatory using the marker by marker analysis led to similar clustering despite a reduced number of available parameters with which to form groups.

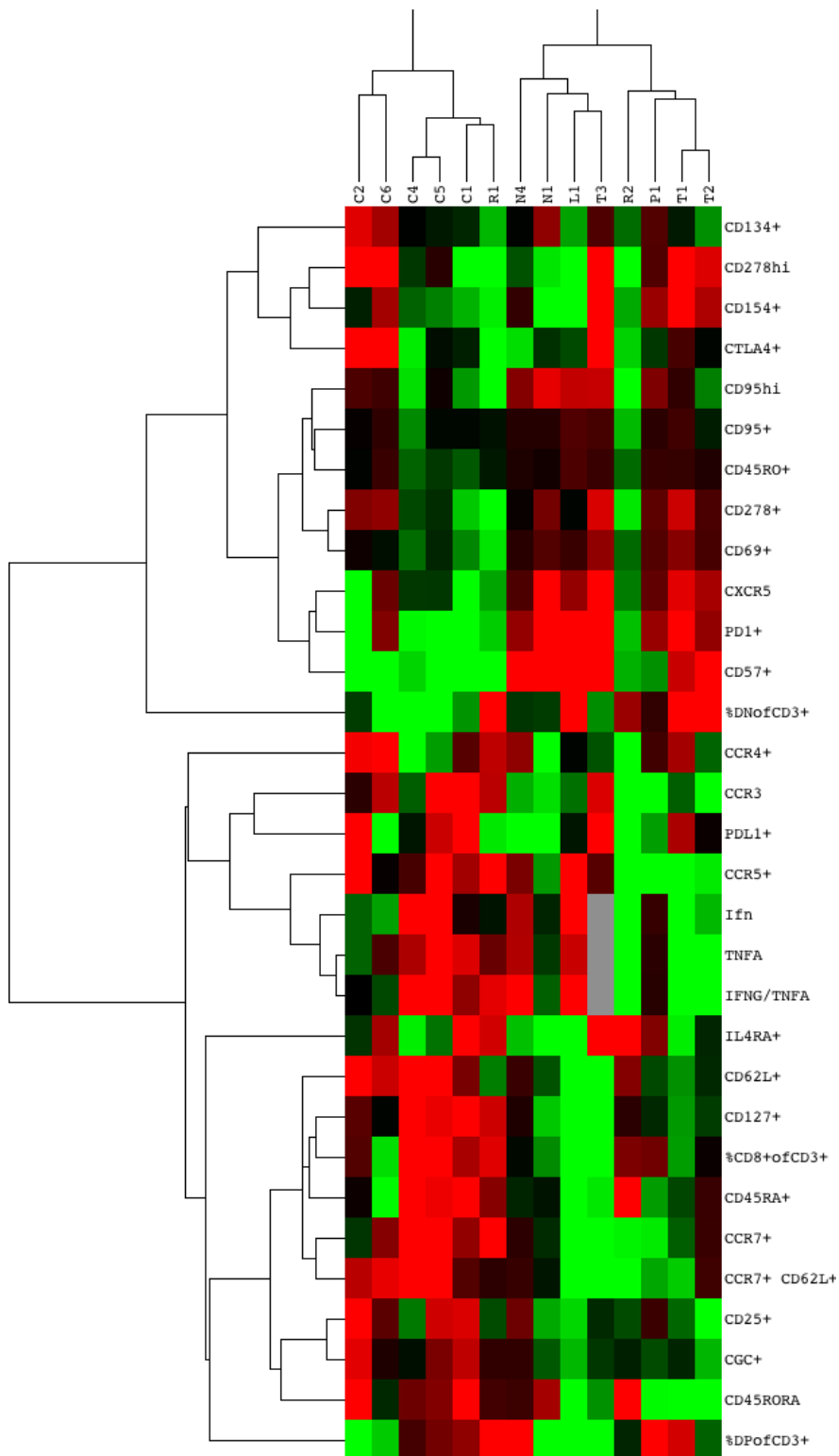


**Figure 6.12** Unsupervised hierarchical clustering using Pearson's correlation coefficient and complete linkage derived two major clusters, one containing all the CHL-derived CD<sub>3</sub>+CD<sub>4</sub>+ phenotypes, and the other containing a mixture of benign and non-CHL-derived tissue.

#### 6.4.2.2 Heterogeneity of CD4+ T cell markers

Figure 6.13 shows markers which are expressed in >5% of CHL-derived CD4+ T cells and with considerable variability of expression. This is summarised in Table 6.12. Those markers that are expressed as a discrete positive population (e.g. CCR4, CD278) and hence easily discriminated from a negative population are potentially applicable to assessment by IHC, as performed in Chapters 3 and 4. Those expressed as a continuum (e.g. CD25, CD28) would be more difficult to quantify using IHC since degrees of expression are less reproducible than in flow cytometry. Using IHC those markers expressed heterogeneously may be validated, and potentially applied to correlative studies of clinical outcome.

CD	Eponym	Min %	Max%	SD	Discrete or Continuous
CCR5	-	9	35	12	D
CCR4	-	15.4	77.2	26.9	D
CCR3	-	2	12.3	4.2	D
CXCR5	-	6.8	47.5	16.0	D
CD45RA	-	5.8	28.1	9.4	D
CD127	IL7RA	12.8	36.1	9.1	C
CD25	Il2RA	9.8	43.2	12.4	C
CD132	CGC	27.5	53.3	10.9	C
CD28	-	28	61	15.0	C
CD134	OX40	24.9	51.2	11.0	D
CD278	ICOS	27.4	70.5	18.9	D
CD278hi	ICOS	6.8	50.4	20.5	C
IFN- $\gamma$	-	18.3	65.6	21.7	D
TNF $\alpha$	-	7.6	20.3	5.0	D

**Table 6.12:** Most heterogeneously expressed CD4+ T cell markers. Final column indicates the potential for validation and further investigation using IHC, with those markers expressed in a discrete manner (D), that is more easily segregated into a positive and negative population, being more likely to be interpretable using IHC than those with a range of expression levels (continuous/C)

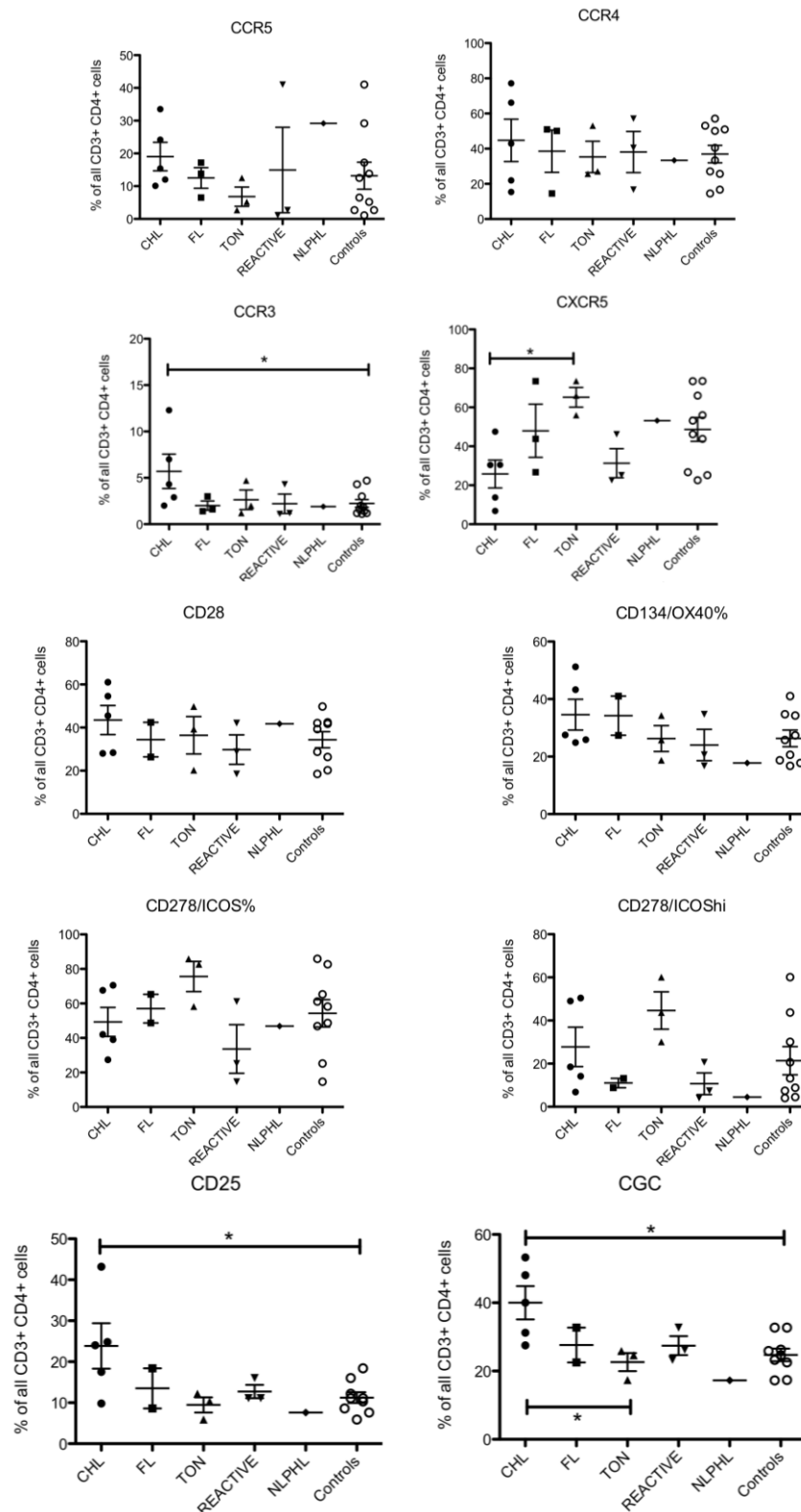


**Figure 6.13** Markers expressed in >5% of CHL-derived CD4+ T cells and with considerable variability of expression. This is summarised in Table 6.12.

## 6.4.2.3 Discriminatory Molecules

Table 6.13 and Figure 6.14 a&b summarises those markers whose mean expression was significantly different in CHL-derived CD4<sup>+</sup> T cells to those derived from other lymph nodes.

Marker	Eponym	Control Population	%CD4 <sup>+</sup> CHL	% CD4 <sup>+</sup> Control	P vs control
<b>CD154</b>	<b>CD40L</b>	<b>Tonsil</b>	<b>3.0</b>	<b>17.9</b>	<b>0.036</b>
<b>CCR3</b>	-	<b>Pooled</b>	<b>5.9</b>	<b>2.2</b>	<b>0.043</b>
<b>CCR6</b>	-	<b>Pooled</b>	<b>2.4</b>	<b>0.9</b>	<b>0.036</b>
<b>CXCR5</b>	-	<b>Tonsil</b>	<b>25.8</b>	<b>65.2</b>	<b>0.037</b>
CXCR5	-	<i>Pooled</i>	25.8	48.7	(ns=0.099)
<b>CD62L</b>	<b>L-selectin</b>	<b>Pooled</b>	<b>50.4</b>	<b>18.2</b>	<b>0.002</b>
<b>CD62L</b>	<b>L-selectin</b>	<b>Tonsil</b>	<b>50.4</b>	<b>14.5</b>	<b>0.036</b>
<b>CCR7</b> <b>CD62L</b>	-	<b>Pooled</b>	<b>16.6</b>	<b>4.8</b>	<b>0.001</b>
<b>CCR7</b> <b>CD62L</b>	-	<b>Tonsil</b>	<b>16.6</b>	<b>4.3</b>	<b>0.036</b>
<b>CCR7</b> <b>CD62L</b>	-	<b>Reactive</b>	<b>16.6</b>	<b>4.8</b>	<b>0.036</b>
<b>CD127</b>	<b>IL7R</b>	<b>Pooled</b>	<b>23.3</b>	<b>11.1</b>	<b>0.012</b>
<b>PD1</b>	-	<b>Pooled</b>	<b>22.0</b>	<b>59.8</b>	<b>0.004</b>
<b>PD1</b>	-	<b>Tonsil</b>	<b>22.0</b>	<b>74.5</b>	<b>0.036</b>
<b>CD25</b>	<b>IL2Ra</b>	<b>Pooled</b>	<b>23.9</b>	<b>11.2</b>	<b>0.045</b>
<b>CD132</b>	<b>CGC</b>	<b>Pooled</b>	<b>40.0</b>	<b>24.7</b>	<b>0.016</b>
<b>CD132</b>	<b>CGC</b>	<b>Tonsil</b>	<b>40.0</b>	<b>22.6</b>	<b>0.036</b>
<b>CD45RORA</b>	-	<b>Tonsil</b>	<b>6.2</b>	<b>1.8</b>	<b>0.036</b>
CD45RO	-	<i>Tonsil</i>	69.6	86.8	(ns=0.07)
<b>CD57</b>	-	<b>Pooled</b>	<b>5.1</b>	<b>26.1</b>	<b>0.004</b>
<b>CD57</b>	-	<b>Tonsil</b>	<b>5.1</b>	<b>32.8</b>	<b>0.004</b>
<b>CD69</b>	<b>VEA</b>	<b>Tonsil</b>	<b>51.5</b>	<b>81.9</b>	<b>0.04</b>
CD69	<i>VEA</i>	<i>Pooled</i>	51.5	63.7	(ns=0.23)

**Table 6.13:** Most discriminatory CD4<sup>+</sup> T cell markers showing mean in CHL and indicated control and p value by Mann-Whitney test. Those markers showing significant differences in expression level compared to the appropriate control as indicated, are highlighted in bold, non-significant trends are in italics

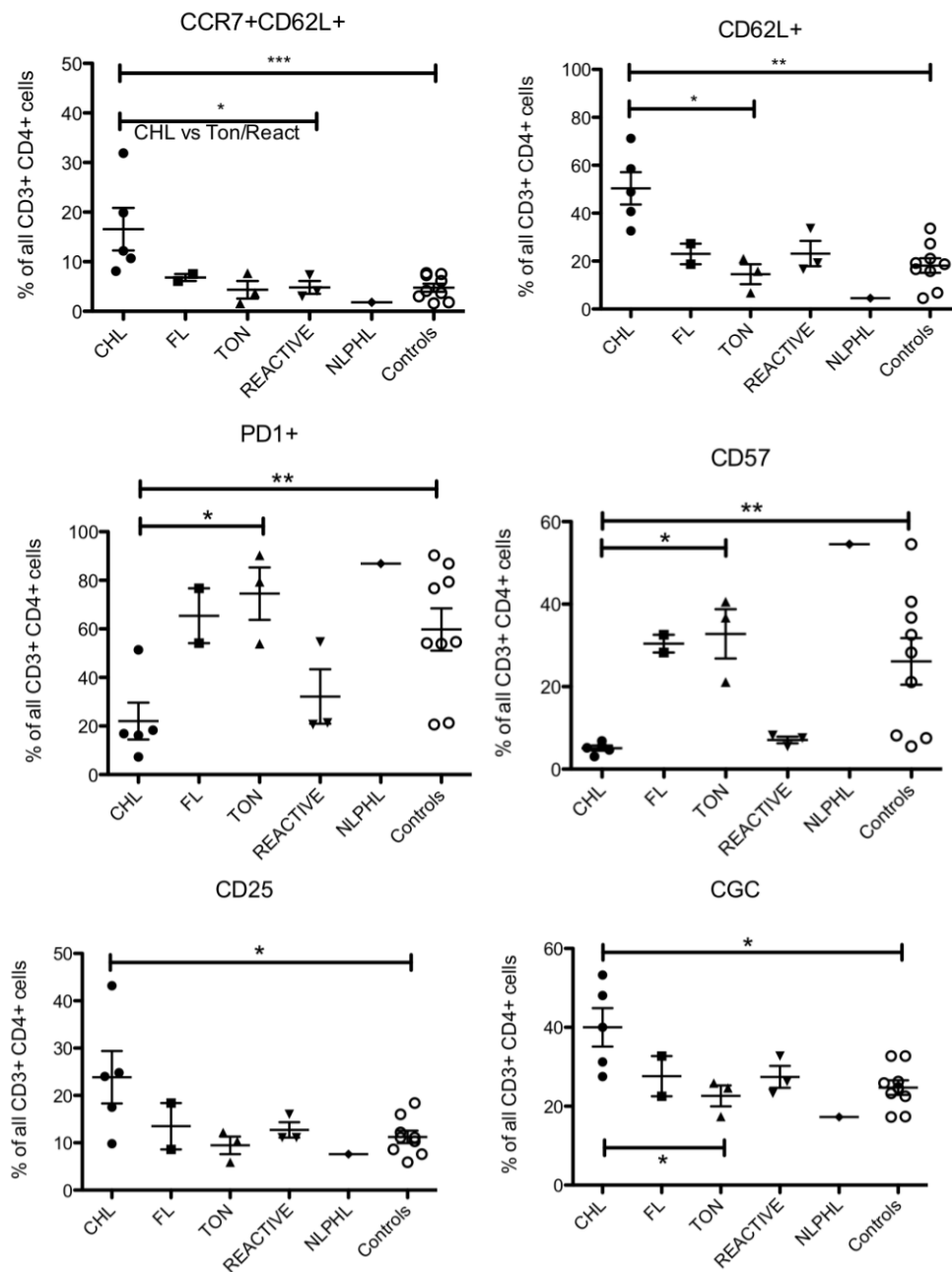


**Figure 6.14a** Markers whose mean expression was significantly different in CHL-derived CD4+ T cells compared to those derived from other lymph nodes. Summarised in Table 6.13. See also Figure 6.16b.

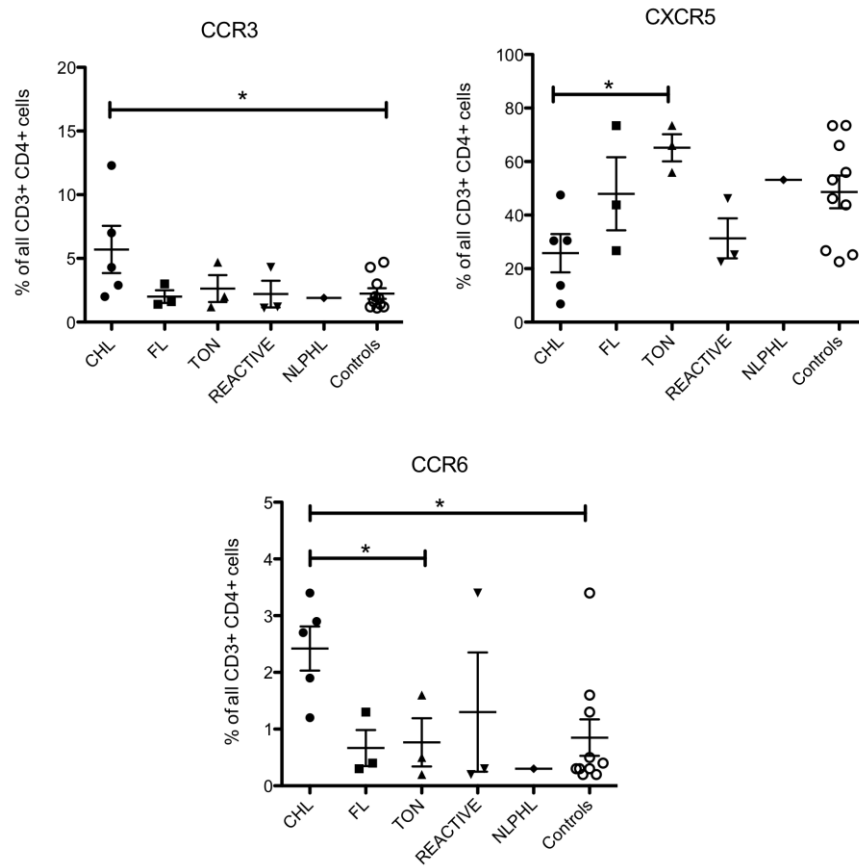


**Figure 6.14b** Further markers whose mean expression was significantly different in CHL-derived CD4+ T cells compared to those derived from other lymph nodes. Summarised in Table 6.13. See also Figure 6.16a.

#### 6.4.2.4 Homogeneity of CHL markers

Figure 6.15 shows the CD4+ T cell-expressed markers demonstrating the least variability in CHL as well as some ability to discriminate from other lymphoid tissue CD4+ T cells. CD62L over-expression (in particular when co-expressed with CCR7) and CD57 under-expression, are the most robust discriminators, with down-regulation of CD95 and CD69 compared to FL and tonsil, and of CD154/CD40-L compared to tonsil. Of the control groups, that which most frequently 'overlaps' with CHL in terms of marker expression is derived from reactive nodes, although these in themselves are clinically and histopathologically heterogeneous, with some markers showing wide heterogeneity of expression between samples. An expanded reactive control group would be important to



further validate these findings. Failure to discriminate reactive nodes was a feature of the cluster analysis described above. If only these three most discriminatory markers are incorporated into a CHL-defining CD4<sup>+</sup> T cell score as shown in Table 6.13, a ‘CHL score’ may be proposed. Scoring one point for each of the following features, defined as % of total viable CD3<sup>+</sup> CD4<sup>+</sup> cell populations the following is applied:

**CD3<sup>+</sup>CD4<sup>+</sup> population:**

CD62L<sup>+</sup> >30% - SCORE 1

CCR7+CD62L<sup>+</sup> >5% - SCORE 1

CD57 <10% - SCORE 1

A score of 3 defines CHL, 1/0 is unlikely to be CHL, and 2 an intermediate group which may represent reactive tissue. Table 6.14 shows the resulting score applying this method to all samples analysed for this experiment.

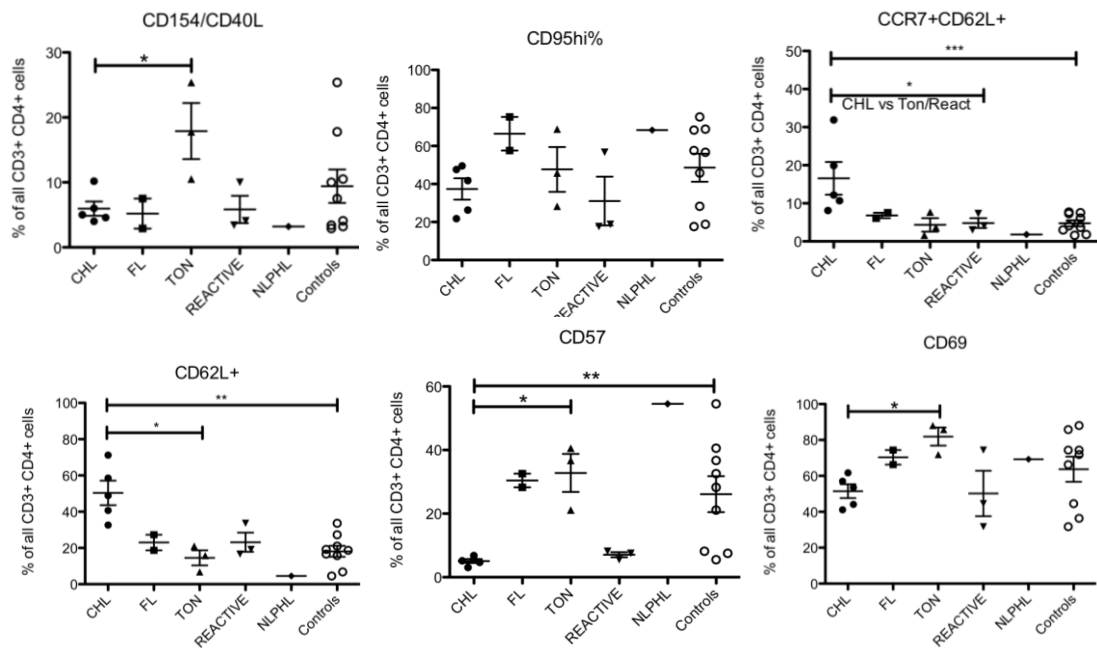


**Figure 6.15:** CD4<sup>+</sup> T cell-expressed markers demonstrating the least variability as well as an ability to discriminate between other lymphoid tissue CD4<sup>+</sup> T cells.

ID	CD62L +	CD57 +	CCR7+ CD62L+	>30% CD62L?	>5% CD62L+ CCR7+?	<10% CD57?	'CHL score'
C1	32.6	5.2	8.1	1	1	1	3
C2	71.2	3.1	10.7	1	1	1	3
C4	48.9	6.8	19.9	1	1	1	3
C5	58.5	4.7	31.9	1	1	1	3
C6	40.7	5.7	12.2	1	1	1	3
L1	4.5	54.5	1.8	0	0	0	0
N1	18.7	28.3	6.1	0	1	0	1
N4	27.3	32.6	7.5	0	1	0	1
P1	19.2	8.2	4.1	0	0	1	1
R1	16.6	5.5	7.3	0	1	1	2
R2	33.6	7.5	3	1	0	1	2
T1	15.8	21.1	3.7	0	0	0	0
T2	21	36.7	7.7	0	1	0	1
T3	6.8	40.6	1.6	0	0	0	0

**Table 6.14:** CHL score-defining markers demonstrating a classification system for further validation

## 6.5 Discussion

### 6.5.1 Limitations of interpretation

#### 6.5.1.1 Low replicate numbers and statistical underpowering

The data here presented are based on limited numbers of replicates, and are intended as an exploratory pilot experiment. As such, any conclusions to be drawn remain predominantly speculative, but provide the grounds for further validation.

#### 6.5.1.2 Limitations of using frozen tissue

Ideal experiments would be performed on fresh samples, disrupted, resuspended, stained and analysed within hours of collection. Practicality, disease rarity, and batch processing prevent this. As such, the 'standard method' used samples frozen soon after collection and tissue disruption, analysed within hours of thawing. Controlling for conditions prior to cell storage is difficult and data must be interpreted with caution particularly when comparing with previous reported work using "fresh" samples. This will be more important for some antigens and functional assays than for others.

#### 6.5.1.3 Limitations of control tissue

##### **6.5.1.3.1. Peripheral Blood**

Peripheral blood has the advantage of being in plentiful supply from normal donors and affected patients. However, the nature of the lymphoid component of peripheral blood is quite different to that within the lymph node. The blood is merely an organ of conveyance for T cells for which the majority of antigen encounter, proliferation and effector functions occur within the confines of primary lymphoid organs and immune infiltrates at sites of inflammation, infection and malignancy. Only 2-5% of total body lymphocytes are circulating at any one time, while >40% is within lymph nodes. Hence the effector status of circulating T cells cannot be considered a valid comparator.

Contrasting the characteristics of circulating T cells between unaffected controls and patients with active disease may be valid in determining the systemic impact of malignancy on immune status. However it is not a valid comparator for T cells derived from lymph nodes or malignancy-infiltrated tissues. Peripheral blood T cells are in an entirely different functional state from those arising within inflamed tissue or lymph nodes, expressing distinct complements of markers. Interpretation of data arising from peripheral blood T cells should hence be made with caution, bearing these factors in mind. For the purposes of this experiment specifically investigating the tumour-infiltrating T cell, peripheral blood was deemed unsuitable as a control.

#### 6.5.1.3.2. Tonsil

Overall, it is clear that even within a supposedly homogeneous tissue like tonsil, there is wide heterogeneity in expression of many functional T cell markers. This may be a result of the extreme variation in initial tissue handling at the point of surgical excision, despite uniformity of sample preparation once received by the cell storage laboratory. Other variables that are difficult to control for or even to quantify accurately include the characteristics of the patient from whom the tonsil was excised, particularly age and immune status in terms of prior infectious challenge, and inflammatory state of the tonsils at the time of excision. Excised tonsils, while normally in a relatively quiescent state at the time of operation, are by their definition pathological, or there would be no indication for excision. For these reasons it is erroneous for tonsillar control to be defined as 'normal' or 'homogeneous' in any way.

Tonsillar tissue is different to other lymph nodes being mucosa-associated-lymphoid tissue (MALT), a distinct immune compartment with function and anatomy more comparable to the gut's immune system, not that of other lymph nodes. Tonsils possess no afferent lymph vessel; antigen is encountered via direct contact through the epithelial surface which is essentially the only separation from the outside world. This is in contrast to lymph nodes existing in relatively sterile conditions within body cavities (tonsillar-derived culture systems frequently grow *candida*: a problem encountered during this project) and encountering antigen in a far more regulated way through delivery, as unaltered antigen, immune complex, or in association with migrating antigen-presenting cells entering via afferent vessels. As such immune cell trafficking is mediated by expression of a different spectrum of adhesion molecules and chemokines, and the immune response is biased in favour of a localised mucosal protective response (IgA-based) rather than systemic immune response (IgG-based). Hence, pathophysiological, physiological, donor characteristics and preparatory techniques make this a highly imperfect control for 'normal lymph node tissue'. Use as a control is simply a function of availability, not suitability.

### **6.5.1.3.3. Reactive nodes**

Ideally, an experiment designed to define CHL-specific T cells, in contrast to those activated in a physiological antigen-specific immune response (likely a substantial component of T cells found within any malignant microenvironment) would ideally use reactive lymph nodes derived from age-matched controls. Uninvolved lymph nodes from the same donor may be ideal but to be a useful control without the influence of systemic effects of CHL they would need to be derived from the same patient in remission who develops a reactive lymph node suitable for biopsy. Incidence of such an event is too rare to be of use, and would be influenced further by any germline-derived immune defect that may predispose to the development of the disease and for which evidence is accumulating<sup>471-473</sup>.

Approximately age-matched reactive lymph nodes are a more available control. Of clinical applicability, presentations resembling CHL in terms of patient characteristics and tissue of origin are Follicular Hyperplasia (FH) and Progressive Transformation of Germinal Centre (PTGC), as well as infection-reactive nodes with a clearly defined causative organism. PTGC is seen in around 10% of cases of FH, usually idiopathic in origin, with distinct histopathological characteristics<sup>474</sup>. The demographic and anatomical similarities of these conditions, as well as comparable immune-stimulating pathophysiology make these conditions the ideal benign correlates against which to compare the T cell constituent of lymphoid malignancies. Availability of this tissue is the major drawback.

### **6.5.2 Condition-defining CD3+CD4+ T cell subsets**

This experiment focussed only on the CD3+CD4+ compartment, being a dominant and heterogeneous component in CHL, in which classical functional definitions have failed to satisfactorily describe or explain its role in CHL, and a compartment which even in normal physiology, unlike B cells or cytotoxic T cells (CD8+) with well-defined function, has diverse and largely poorly understood roles.

6.5.2.1 NLPHL contains an entirely distinct population of cells unlike PTGC or CHL

Only a single case of NLPHL was available for this study. However the CD4<sup>+</sup> T cell component of this sample proved particularly distinct from all other samples. The rarity of this condition, along with its resemblance of CHL by classical histopathology and a favourable clinical course has led it to be classified as a related lymphoma. However there is evidence with which this study is in concordance, that the disease is quite different, even at the level of the tumour-infiltrating T cell. CD95, CD57, PD1, CD45RO and IFN- $\gamma$  were expressed at particularly high levels of CD4<sup>+</sup> T cells, while IL2 receptor components were virtually absent. These markers are well-described in NLPHL, with 'rosetting' CD57<sup>437</sup> and PD1-expressing T cells<sup>425, 475</sup> used to corroborate the diagnosis. High levels of the follicular-homing molecule CXCR5 along with under-expression of CCR7 in this sample were also found, additional characteristic features of Tfh cells. As seen in Chapter 5, T cells derived from this sample failed to proliferate in IL2 and IL4-enriched culture systems, perhaps more markedly even than those derived from benign tonsillar or reactive lymph nodes. Further validation is essential to ensure that the sample was not unrepresentative of the disease. However, most of the phenotypic features observed in this experiment are entirely consistent with the established IHC literature, in which the relative novelty of this experiment is the use of flow cytometry, which has confirmed that these markers arise in the CD4<sup>+</sup> T cell compartment.

Over-expression of markers of activation and senescence, with potent Th1-defining effector activity (IFN- $\gamma$ ), along with a failure to proliferate in vitro is suggestive of a terminally differentiated effector cell phenotype, existing alongside a Tfh-like immunophenotypic signature typical of germinal centre reactions. These two signatures may coexist within a single cell, since IFN- $\gamma$  expressing 'Th1-type' Tfh cells are proposed to be a functional subset. Alternatively the finding may indicate two separate CD4<sup>+</sup> T cell populations. However these results are interpreted, it would seem that the CD4<sup>+</sup> T cell in NLPHL is entirely distinct from that in CHL – representing an apparent expansion of a germinal centre or proliferating follicle reaction, with Th1-like functional capacity. These findings are consistent with the documented histology of the disease, which comprises large germinal centres and expanded mantle zones<sup>474</sup>. There is some description in the literature and anecdotally of transformation from PTGC to NLPHL or

DLBCL, with the suggestion that PTGC represents a precursor lesion. Indeed there are cases of PTGC in which chromosomal lesions characteristic of B cell malignancy have been described<sup>476</sup>. However evidence is limited and patho-physiological mechanisms speculative. This experiment demonstrated some overlap with the single PTGC sample in terms of high expression of CD95, PD1, CD57, CXCR5 and CD45RO, although CCR7, the T cell zone marker, was present at higher levels in PTGC. Further replicates are essential to corroborate these distinctions.

#### 6.5.2.2 Is the dominant CHL-infiltrating CD4+ T Th1, Th2, Treg or Tfh?

##### **6.5.2.2.1 Treg**

Substantial IHC evidence, including that presented in Chapter 3 exists to demonstrate that FOXP3 is expressed by a significant proportion of T cells in the CHL microenvironment<sup>344</sup>. Expression is heterogeneous between patients, with pathophysiological implications evidenced by the impact of this heterogeneity on survival. However, there is no functional evidence that these CHL-derived T cells are in fact Tregs. The only published study to have isolated a Treg population (based on CD25 and CD127 expression) from the immune infiltrate of a malignancy managed to demonstrate suppressive activity in a standard autologous T-responder cell / purported Treg coculture/stimulation assay<sup>377</sup>. The cells used in this suppressor assay were derived from colorectal carcinoma. This group demonstrated an equivalent CD25-hi, CD127-lo FOXP3-expressing population in CHL-derived lymph nodes, but could not isolate sufficient cells from these samples to perform functional suppressor assays (personal communication). Being the major interface between antigen, infectious organisms and the immune system of the body, the gastrointestinal tract requires particularly well-developed mechanisms of effector/regulatory immune homeostasis comprising abundant and various regulatory T cells. Mouse models demonstrate this, in that colitis severity is used as the quantitative readout of regulatory T cell dysfunction<sup>182</sup>. Hence, functional conclusions regarding cells derived from GI tract tissue, malignant or benign, may not be applicable to other lymphoid tissue.

The limited flow cytometric data presented in this chapter shows only a trend towards greater representation of CD4+CD25+ cells, with comparable heterogeneity of

representation to that seen for FOXP3 in the IHC experiment presented in Chapter 3 (10-45% cells) although co-staining was not carried out to confirm that these represented the same cells. Moreover, CD127 is heterogeneously expressed in these CHL-derived CD4+ T cells at comparable levels to reactive nodes, and at significantly higher levels than tonsil or FL-derived tissue. CTLA4, one potent effector of Treg function<sup>222</sup>, is expressed at a higher level than in the reactive or FL-derived samples, but at comparable levels to that seen in tonsillar CD4+ cells. Expression was observed in less than 15% of cells in all cases. However, only surface CTLA4 was stained. This molecule demonstrates rapid intracellular/extracellular trafficking, which is essential to its function<sup>477</sup>. As such evidence based only on surface, and not total cellular expression, should be interpreted with caution. This data is suggestive of a greater role for CTLA4 in CHL than in reactive nodes. It should also be noted, however, that CD25 and CTLA4 are non-specific markers of cell activation<sup>478</sup> and not entirely specific to Tregs.

IL10, a classically described immunosuppressive cytokine was not expressed at an appreciable level in any sample.

Overall, although there is evidence suggesting an overrepresentation of Treg-associated markers such as CD25 and CTLA4 by CD4+ cells in CHL compared to non-CHL-derived nodal tissue, this study does not provide evidence favouring the Treg as the numerically dominant cell. The functional role of a Treg component however, may be more profound than its cellular frequency suggests - as the IHC FOXP3 expression levels' correlation with survival implies.

#### **6.5.2.2.2 Th1**

As presented in Chapter 4 there is IHC evidence for substantial and heterogeneous expression of the transcription factor T-BET in the microenvironment, confirming previous reports<sup>46</sup>. However, co-staining with CD4 was not performed to confirm the identity of the cells expressing T-BET, important since this TF is also expressed by CD8+ T cells, B cells and malignant HRS cells. A proportion of samples showed expression of T-BET in the morphologically distinct HRS cells as previously reported<sup>404</sup>. Some impact on survival was demonstrated based on heterogeneity of expression although expression of



T-BET by the malignant cells was not related to survival. The dominance of the microenvironment by cells expressing a TF associated with the promotion of a Th1-skewed immune response is therefore likely to have functional significance. The cytokine flow immunophenotyping presented in this chapter has corroborated this evidence, with Th1-defining IFN- $\gamma$  (under the influence of pathways coordinated by T-BET) highly expressed in CHL, reactive, NLPHL and FL-derived CD4+ T cells, more so than in tonsil, along with TNF $\alpha$ , another Th1 defining factor. IL2 was notably not detectable. There is already a suggestion in the literature that CHL-derived T cells can be stimulated *in vitro* to produce IFN- $\gamma$  and TNF $\alpha$  (again, and intriguingly, not IL2), but apparently also IL4 (not demonstrated in these experiments<sup>479, 480</sup>). It has also been reported that the CHL-derived lymphoid cells are capable of co-expressing IL4 and IFN- $\gamma$  at high levels when stimulated with IL2 and anti-CD28 (without TCR stimulation, similar to experiments reported in Chapters 5 and 7). However these reports are anecdotal, give little methodological detail, and there is no formal presentation of results except in unreferenced literature reviews.

The Th1-associated cytokine CCR5<sup>72</sup> was expressed in a significant minority of CHL-derived CD4+ T cells (10-30%), and to a greater extent than in tonsillar and reactive tissue with the exception of the granulomatous-reactive lymph node (which if bacterially reactive would be expected to have a significant Th1 bias in response), with FL expressing to a similar extent, and NLPHL a larger extent. While no significant differences could be confirmed comparing nodes of origin, expression is at a lower level than that of CCR4, and greater than CCR3 (a less subtype-specific Th2 marker) or CCR6 (a possible memory T cell marker, whose ligands CCL20 and CCL19 MIP3- $\alpha$  and  $\beta$  are over-expressed in the CHL microenvironment (See introduction). Hence, using chemokine receptors to define functional subsets, a CCR3 expression-defined Th1 response is well represented in the CHL microenvironment, although at a lower level than the CCR4-expressing population.

Chemokine receptors, as discussed, are imperfect markers of functional phenotype of CD4+ T cells. The panel selected here included those whose expression has been detected at high levels in CHL-derived tissue or cell lines in previous experiments. Overall they were not found to be expressed at high levels in CHL-derived CD4+ T cells

with the exception of CCR4 and CCR5, whose ligands are the most well described CHL-associated chemokines: TARC and RANTES. Expression levels as defined in this experiment could have been influenced by preparation techniques. Importantly, incorporating a variety of control tissues into the experiment has revealed that expression of all receptors appears to be universal in nodal tissue regardless of source. While this does not imply a lack of importance in CHL, there is no suggestion that pathways mediated through these receptors are any more important than in normal inflammatory processes, and are certainly not relatively suppressed. Probably more functionally relevant are the cytokines produced by these cells, of which IFN- $\gamma$  and TNF $\alpha$  predominated for all tissues, although IL2 was absent. There was some evidence to suggest that expression of these Th1-associated cytokines was significantly greater in malignant tissues, particularly in NLPHL, compared to the benign controls.

Overall, the evidence gathered on the samples assessed in this experiment is in favour of a Th1-bias in the microenvironment, but one which is no different to that seen in reactive nodes, FL-derived nodes, and one which is substantially less than in NLPHL.

#### **6.5.2.2.3 Th2**

As presented in Chapter 4 there was no evidence by IHC assessment of the transcription factor GATA3 for an increased representation of Th2 cells in the microenvironment, consistent with a limited IHC literature, but contrasting with many investigators' current description of the CHL CD4+ T cell compartment. As discussed this is based on flawed interpretation of the data. While intracellular cytokine staining based on stimulation with PMA/Inomycin has its own limitations by intrinsically altering the system with profound activating stimuli via massive calcium release and TCR-independent mechanisms, there is an established evidence base for the method's validity<sup>165</sup>, and as will be described in chapter 7, it is capable of discriminating Th2 cytokine-producing cells in the expanded culture T cells. In this analysis there was no evidence of any Th2-defining cytokines (IL4, IL13 or IL21) except in the case of PTGC, and certainly not in the CHL-derived CD4+ T cells. IL13 has been found by IHC in HRS cells and is expressed by a number of CHL-derived cell lines, and IL13 receptor inhibition leads to growth suppression in HRS cells. However, the major source of this cytokine would not appear to be microenvironment Th2-polarised CD4+ cells.

Two early studies investigated the expression of Th subset defining cytokine mRNA arising from CHL but arrived at contradictory results. The first demonstrated no IL4, 5 or 9 mRNA expression in CHL-derived lymph node tissue, while IFN- $\gamma$  and TNF $\alpha$  were expressed, much as suggested at the protein level by the flow cytometry data reported here<sup>481</sup>. However a subsequent study found IL4 and IL5 as well as IFN- $\gamma$  mRNA transcript in all nodes tested (n=14) and at similar levels to reactive nodes<sup>482</sup>. This second study went on to culture T cell clones derived from CHL and predominantly derived cells expressing both IL4 and IFN- $\gamma$  again resembling clones derived from reactive nodes. These results are in line with the cytokine expression profiles for expanded T cells described in Chapters 7, under culture conditions described in Chapter 5. However, unlike experiments described here, these early experiments expanded clones using a mixed lymphocyte reaction (co-culture with irradiated allogeneic PBMCs with IL2 augmentation), and following separation of CD4+ cells using magnetic beads after lymph node dissociation and density gradient separation. To draw conclusions regarding the lineage-commitment of a founder clone, based on the cytokine mRNA profile of MLR-stimulated and expanded colonies, appears to be an over-interpretation of the data. These results may instead be explained as arising due to the expansion of multipotent or phenotypically plastic initiating cells, themselves without Th1 or Th2 bias, which were then polarised under these *in vitro* culture conditions. The heterogeneity of the clones produced may represent the relatively stochastic nature of lineage commitment<sup>483</sup> *in vitro* without robust Th1 or Th2 defining conditions (e.g. IL12, IFN- $\gamma$  or exogenous IL4 exposure). The presence of both IL4 and IFN- $\gamma$  in the supernatant despite the apparent mutual inhibition of synthetic pathways may mean that the clonal colonies remained phenotypically plastic<sup>288</sup>, with some resulting cells going on to develop a Th1-cytokine secreting phenotype and others Th2.

Alternatively, and in line with the results presented in Chapter 7, in which intracellular cytokine flow cytometry enables the origin of the cytokine production to be determined on a cellular basis, an intermediate phenotype may be present capable of producing both cytokines. This may be an *in vitro* artefact, or result from intracellular regulatory mechanisms not yet understood, which enable co-expression of Th1 and Th2-defining

cytokines by a single cell. However these results are interpreted, the contradiction in Th2-defining mRNA expression between studies, possibly arising from differential methodology, and limited by the small number of samples tested in this heterogeneous disease, cannot be explained. Level of mRNA transcript does not necessarily reflect eventual cytokine expression, for which no data is presented at baseline, and only for that derived from *in vitro* cloned, expanded and allogeneic PBMC-exposed cells.

CCR4, a non-specific Th2 and Treg expressed molecule which is the receptor for TARC, a chemokine produced at high levels in CHL and purported to be the mechanism of T cell chemo-attraction to the microenvironment, was not expressed at significantly different levels to control samples, although it was expressed at substantial levels (15-80% of CD4+ T cells). However, as a Th2 defining marker its specificity is limited and without corroborating evidence at the cytokine or transcription factor level, should be interpreted carefully. Another Th2 defining chemokine receptor, CCR3 is expressed at significantly greater levels in CHL than in control samples, but at <5% in most samples and <15% in all samples. Its ligand RANTES is well described in CHL but a substantial contribution of CCR3/RANTES interactions to the composition of the microenvironment is not supported by these results. CCR3 expression in CHL assessed by IHC and flow cytometry has been performed for a number of lymphoid subsets in a previous small IHC and fluorescence immunophenotyping (n=5) experiment<sup>484</sup>. This confirmed a relative over-expression of CCR3 in CHL-derived CD4+ T cells and to a greater extent than found in the data presented in this chapter, although no cytokine-based functional work was performed. This discrepancy may be explained by the use of fresh tissue (in the cited experiment) rather than frozen (as in this experiment), although it is clear that inter-patient heterogeneity exists, and sample numbers are small in both experiments. Additionally HRS-overexpressed RANTES is recognised by a number of other chemokine receptors, including Th1-expressed CCR1 and CCR5 and Treg/Th2-expressed CCR4, and hence an absence of CCR3 does not preclude a substantial role for RANTES in defining the microenvironment.

#### 6.5.2.2.4 Tfh

The Tfh-defining markers CXCR5, CD57 and PD1 are expressed at significantly lower levels in the CD4<sup>+</sup> T cells of CHL compared to pooled controls, and while ICOS, another Tfh-characteristic cell surface marker is present at substantial levels, expression is heterogeneous and comparable to controls. This study does not support the hypothesis that the HRS is being sustained through a dominating infiltrate of these professional-B cell supportive cells. PD1 and CD57, while expressed strongly in normal germinal centres and expressed by Tfh cells, have also been defined as markers of immunosuppression, chronic activation and senescence whose relative under-expression in CHL derived CD4<sup>+</sup> T cells is of interest particularly with respect to the longevity and proliferative capacity of these cells *in vitro* described in Chapter 5.

#### 6.5.2.3 Is the dominant CHL-infiltrating CD4<sup>+</sup> T cell naïve, activated or memory?

Notably, and consistent with the proliferation experiments described in Chapter 5, the senescence/immunosuppressor markers PD1 and CD57 were under-expressed in CHL-derived CD4<sup>+</sup> T cells compared to control samples, and starkly in contrast with the single NLPHL sample in which both markers were highly over-expressed.

Homing to the T cell zone requires expression of CD62L, L-selectin, whose ligands include endothelial cell proteins such as CD34 and GlyCAM-1<sup>485</sup> which enables entry to the node via the afferent high endothelial venules, and CCR7 which retains the T cell within the interfollicular T cell zone, within which it will encounter antigen-bearing APC and cognate B cell. CCR7 and CD62L are expressed preferentially by naïve and central memory cells<sup>445</sup>. These markers proved to be amongst the most discriminatory of CHL-derived T cells from control samples, suggesting an overrepresentation of these subsets. However, CD27, a TNFRSF member associated with memory cells and prolonged survival and proliferative capacity<sup>486</sup>, was expressed at similarly high levels of CD4<sup>+</sup> T cells in all samples.

CD45 isotype is an indicator of maturity of the T cell – with CD45RA being expressed in naïve T cells, lost to become CD45RO following activation, and subsequently re-expressed in a subset of memory cells which tend also to be hypoproliferative,

hyporesponsive and expressive of markers of senescence seen in chronic viral infections<sup>487, 488</sup>. CHL-derived CD4<sup>+</sup> T cells appeared in this study to express CD45RO<sup>+</sup> at lower levels, although CD45RA<sup>+</sup> cells were not seen at significantly greater levels, perhaps due to a large proportion being in an intermediate CD45RORA<sup>+</sup> state.

CD28 is highly expressed in naïve T cells, and down-regulated in response to stimulation despite its expression being cited in the literature as evidence that the CHL-infiltrating T cell is activated<sup>47</sup>. High levels of expression are confirmed in all samples, with no significant difference according to tissue of origin. CD69, the early activation marker, is transiently and rapidly up-regulated following stimulation in lymphoid cells, particularly T cells<sup>489</sup>, persisting for around 30 hours following removal of the stimulus<sup>490</sup> but whose function remains unclear since both proinflammatory<sup>491</sup> and immunosuppressive<sup>492</sup> actions have been demonstrated. In this study it was expressed at relatively homogeneous levels across all CHL samples, and at a lower level than that seen in all but reactive nodes. The transient nature of this molecule's expression means that this observation may either reflect an over-representation of naïve T cells in CHL, or instead chronically active cells in which CD69 has been down-regulated, and so is difficult to interpret.

Expression of other activation markers in CHL was heterogeneous, and not significantly different to other lymphoid tissue derived cells. CD95, a non-specific marker of activation in T cells, which triggers apoptosis on encountering its ligand<sup>493</sup>, shows a trend towards under-expression in CHL compared to control samples. ICOS and OX40, whose ligands are expressed by the HRS cell, were not expressed at significantly different levels in CHL compared to control tissue across all samples, although heterogeneity of expression was greater in CHL than in other tissues, which may be of biological relevance. CD40 is expressed by HRS cells and signals through similar pathways to those triggered by LMP1, the EBV-encoded protein, and is key to normal B cell survival. However these data show relative under-expression of its ligand CD154/CD40L in the CHL-derived CD4<sup>+</sup> T cells compared to tonsil, although CD40L was also underrepresented in other activated tissues. Expression of these activation markers in a snapshot experiment on frozen tissue may be unrepresentative of the situation *in vivo*,

where dynamic and transient changes in expression level may occur. However, overall there is no indication that CHL-derived CD4<sup>+</sup> T cells express ligands for receptors involved in HRS survival at any greater level than non-malignant lymphoid tissue. CD30L was not included in the panel for technical reasons but would be an important inclusion in future experiments. CD30 is the HRS-defining marker<sup>112</sup>, signalling through which in lymphocytes can trigger cell proliferation and survival via the NF-κB pathway, while reverse signalling from which can have diverse immunosuppressive or stimulatory effects<sup>494</sup>.

Taken together, and considering the pooled CHL samples in contrast to the pooled controls, there is evidence to suggest that the CD4<sup>+</sup> T cell compartment in CHL is comprised of fewer chronically stimulated, senescent cells (lower CD45RO, CD69, CD95, PD1 and CD57) particularly in contrast to those of FL and NLPHL. While activation markers such as CD95, ICOS and OX40 are confirmed to be expressed at a high level, this is only as much as seen in the control reactive nodes or tonsils, and is markedly heterogeneous between samples. The abundance of activated T cells is also evidenced by cytokine expression data presented here. The proliferative capacity of CHL-derived T cells demonstrated in Chapter 5 is a property to be expected of primed memory or naïve CD4<sup>+</sup> T cells, but not chronically activated or terminally differentiated effector cells. This, along with overexpression of CD62L and CCR7 in the CHL-derived samples, provides further evidence that coexisting with the activated, cytokine-secreting cells in the microenvironment there is a substantial CD4<sup>+</sup> T cell component, which is either naïve or derived from central memory cells.

#### 6.5.2.4 Does cytokine receptor expression explain the proliferative capacity of the T cells?

There is evidence that IL2-receptor components CD25 and CD132 (although not CD122, more characteristic of cytotoxic T cells) were relatively over expressed in CHL-derived CD4<sup>+</sup> T cells compared to control samples, providing some explanation for the superior IL2 responsiveness described in Chapter 5. However, there was no evidence for IL4-specific receptor component expression in any sample. Hence levels of receptor expression cannot explain the augmentation of growth observed with dual cytokine enrichment.

#### 6.5.2.5 Summary and Context

To classify a T cell infiltrate as predominantly one subset or another is inherently flawed, particularly given the relative artificiality of those subsets in the first place. However a description of the overall complement of function-defining markers unique to or showing heterogeneity within a disease is likely to enable a better understanding of the contribution of any microenvironment cells possessing those marker to disease pathophysiology. These results have been interpreted only on CD4+ T cells in isolation. Their numerical dominance implies primary importance, but clearly other functional classes: cytotoxic T cells, B cells and macrophages in particular, also interact in a complex network with the malignant cell. This study provides some insight into this and by focusing on a single subclass has the advantage over an integrated study of the entire microenvironment, which cannot discriminate between the relative contributions of the different cell types. This is the problem of gene expression profiling, which has failed to generate any reproducible, functional or clinically translatable conclusions<sup>116, 292, 356</sup>.

#### 6.5.3 A CD3+CD4+ signature for CHL with potential clinical application

A more clinically useful application of these findings, avoiding functional inferences, would be the capacity to discriminate a malignancy by its compliment of CD3+CD4+ cells. Since these cells provide the majority of infiltrate in reactive nodes, and a substantial minority in haematological malignancies, they may therefore be amenable to assessment using a minimally invasive strategy such as fine needle aspiration (FNA). Flow cytometric analysis of FNA samples has been shown to be sufficiently robust for use in diagnosis of many lymphoid malignancies, but due to the scarcity of the malignant cell has the technique has not been applied to CHL diagnosis. Although FNA has exceptional specificity in those rare cases in which HRS cells are detected by microscopy of the samples, it has poor sensitivity, and flow cytometry of the samples remains unsuitable at this stage for clinical diagnosis<sup>495-498</sup>. Whole fresh lymph node flow cytometry may be capable of discriminating phenotypic HRS cells<sup>459</sup> but this remains relatively untested clinically, is no less invasive than conventional histopathology, requiring whole nodes and could not be reproduced using the SCSs and techniques documented in Chapter 5.



Using only the most differentially and consistently expressed markers – CD57, CCR7 and CD62L, and cut-points at levels that could be easily and reasonably assessed as long as valid internal negative and positive controls are available (peripheral blood provides T cells with high expression of CCR7 and CD62L, and tonsils T cells with high expression of PD1), the strategy detailed in 6.4.2.4 above could be applied. Scoring 1 for each of the following expressed as a percentage of all CD3+CD4+ cells, CD57 < 5%, CD62L > 30%, CCR7+CD62L+ >10%, a score of 3 is proposed as a strong indicator of CHL being present, a score of 2 that the differential remains with a reactive node, and a score of <2 that the node is unlikely to be CHL. NLPHL may in itself have a far more unique profile, which needs to be taken forward into a larger scale validation exercise.

## 6.6 Summary and Further Work

The data presented here on the extended phenotype of CD4+ T cells may be interpreted as showing that CHL T cells represent an aberrant accumulation of naïve or memory cells attracted by the presence of malignant HRS (or precursor) cells arising within the lymph node, demonstrating under-expression of markers of senescence (PD1, CD57), over-expression of markers of priming prior to activation (CGC, CD28, both down-regulated after activation) and a substantial admix of activated IFN- $\gamma$  secreting, T-BET expressing Th1 cells, and CD25, CCR4, CTLA4 and FOXP3 expressing Tregs. The naïve/central memory component is primed for activation by cytokines, lineage uncommitted and hence capable of Th1 and Th2 polarisation (see Chapter 7) as well as prolonged survival and substantial proliferation.

*In vivo*, these cells are perhaps drawn into the microenvironment antigen non-specifically by chemotaxis, through secretion of chemokines by the HRS, and retained by ongoing expression of CD62L and CCR7. Potential HRS-clearing Th1 cells, and their attendant Tregs (whose presence is always a feature of inflammatory tissue) are attracted and capable of discharging their function, but rendered unable to reach their target cells due to being embedded within a primed but not activated, antigen non-specific mass of naïve and memory T cells. The sequestration of this compartment within the malignant

lymph node may further lead to systemic immunosuppression, particular cellular immunity.

These hypotheses are highly speculative. Further validation, with modified antibody combinations to demonstrate appropriate co-expression of markers, as well as increased sample and control numbers, is required to substantiate this hypothesis. The possibility of a clinical application of the HRS-infiltrating CD4<sup>+</sup> T cell in the form of diagnostic flow cytometry is one that requires substantial ongoing validation and optimisation but certainly shows potential.

## CHAPTER SEVEN:

Fluorescence immunophenotyping to  
characterise CHL-derived proliferative  
CD4<sup>+</sup> T cells

## 7. Fluorescence immunophenotyping to characterise CHL-derived proliferative CD4<sup>+</sup> T cells

### 7.1 Introduction

Chapter 5 described an attempt to develop an autologous co-culture system in which both microenvironment and malignant cells could be supported through addition of T cell supportive cytokines. While presence of the malignant cell could not be demonstrated convincingly at baseline or subsequently in the proliferating culture by flow cytometry, it was found that the system supported the growth of CD4<sup>+</sup> T cells derived from all CHL samples and most control samples derived from FL. There was substantially less or no significant CD4<sup>+</sup> T cell growth arising from benign lymph nodes. Chapter 6 investigated the extended phenotype of the CD4<sup>+</sup> T cells at baseline derived from the same frozen SCSs as those from which the proliferative cells were derived, along with benign and malignant controls. It was shown that the CHL-derived CD4<sup>+</sup> T cell has a distinctive phenotype, although there was still heterogeneity between cases. The distinctive aspects were the absence of markers of chronic immune activation and senescence (PD1 and CD57) and an overrepresentation of markers of central memory (CCR7, CD62L and CD127). The dominant cytokines produced on stimulation indicated a Th1 bias (IFN- $\gamma$  and TNF $\alpha$ ), likely to a greater extent than seen in benign nodes, and similar to that seen in the CD4<sup>+</sup> T cell component of the FL-infiltrate. The most potent cytokine combination for growth was found to be IL2 and IL4, at concentrations used for *in vitro* Th2 polarising experiments<sup>460</sup>. However Th2-specific markers were notably absent, as demonstrated using IHC in Chapter 4 and in the analysis of the SCS CD4<sup>+</sup> T cells presented in Chapter 6. Other groups have successfully sustained long-lived T cell culture systems using similar methods<sup>466, 467</sup>. However immunophenotypic and functional analysis of the expanding cultures has been limited in these studies to confirmation of CD3, CD4 and CD8 expression, along with a demonstration that the cells became oligoclonal and develop chromosomal aberrations. Characterising the long lived T cell, although an entirely *in vitro* phenomenon, may identify the originating cell

population within the original cell suspension along with molecular mechanisms that enable it to persist without TCR stimulation or antigen exposure. The hypothesis that the dominant cell in CHL is a central memory or naïve T cell as proposed from the results of the immunophenotype demonstrated in Chapters 6 and superior proliferative capacity shown in Chapter 5, may be further tested by investigating the functional diversity of the expanding progeny of these cells.

## **7.2 Aims and Objectives**

The aim of this experiment was to investigate the phenotype of the proliferative T cells derived as described in Chapter 5 applying the panel of antibodies used at baseline as described in Chapter 6. Hence the change in phenotype of the population over time could be determined along with comparisons between CHL, FL and any sufficiently expanded benign lymph node-derived sample.

## **7.3 Materials and Methods**

### **7.3.1 Single cell suspensions**

At various time points as the SCS-derived cultures expanded, aliquots of cells were frozen down. Ideally, aliquots were taken at days 30, 60, 100, 150 and 200. However, this was clearly dependent upon the proliferative capacity of the system. A representative selection of 20 frozen samples were chosen as shown in Table 7.1. These were chosen based on availability and to ensure adequate controls.

### **7.3.2 Freezing methodology**

For consistency, proliferative plates were frozen down as long as >50% of wells were 'live' as defined in Chapter 5. One 96 well plate was harvested into a 30ml sample tube using a multichannel pipette, centrifuged at 2000RPM for 8 minutes, the supernatant removed by aspiration and the resultant cell pellet resuspended in 1ml freeze mix comprising 90% heat-inactivated human AB serum as used for the culture medium and 10% dimethyl sulphoxide (DMSO) and frozen as described in 2.1.2.1 until ready for analysis. At this stage the samples were thawed and resuspended as described in 2.1.2.2.

Data Acquired	Source	Code	Day
6	CHL	302	0
6	CHL	304	0
6	CHL	305	0
6	FL	603	0
6	NLPHL	801	0
6	FL	802	0
6	TON	804	0
6	FL	805	0
6	FH	808	0

Data Acquired	Source	Code	Day
7	CHL	302	100
7	CHL	302	60
7	CHL	302	30
7	CHL	304	60
7	CHL	304	30
7	CHL	304	0
7	CHL	304	100
7	CHL	305	30
7	CHL	305	60
7	FL	603	60
7	FL	603	30
7	NLPHL	801	30
7	FL	802	30
7	FL	802	100
7	TON	804	30
7	FL	805	30
7	FL	805	100
7	FL	805	60
7	FH	808	100
7	FH	808	60

**Table 7.1:** Samples used for the experiment described in Chapter 7. The selection was made based on availability and in order to include sufficient and different time points of observation. The internal control (304 Day 0) was included to facilitate gating strategy, and provide a validation for reproducibility of results between batches. The remaining Day 0 results had been acquired for the experiment described in Chapter 6 and as such part of a separate experimental batch, with the potential problems of batch variation. However, they were included to provide a baseline for all samples.

### **7.3.3 Selection of fluorochromes and antibodies**

The same panel of antibodies was applied in this experiment as had been used in the extended phenotyping experiment as described in 6.3.2.

### **7.3.4 Flow cytometric analysis, data acquisition, compensation and gating**

This has been described and justified in detail in Materials and Methods 2.3. For the purposes of an internal 'known phenotype' control, as discussed in 2.3.9.4 an aliquot of baseline sample C4/304 was available which provided a sufficiently mixed population of cells, with a known phenotype based on the data acquired in Chapter 6, from which a gating strategy consistent with the previous experiment could be applied to the new experimental samples. This was of particular importance for antigens showing a global increase in representation without a clearly discriminant positive population (for example CD27, CD28, CD127 and PD-L1). By examining the MFIs derived from this new

experimental batch, some consistency between batches could be applied, although the limitations of between-batch comparison were taken into consideration in interpreting results.

### **7.3.5 Statistical Analysis**

Percentage expression of each marker within the CD3<sup>+</sup> CD4<sup>+</sup> population were analysed in a variety of ways given the limited numbers of samples available for each tissue type and each time point. First, the hypothesis was tested that the marker concerned would be expressed at a significantly different level at various time points compared to expression in the baseline sample. Hence data were pooled according to the time point at which the sample had been frozen (day zero, 30, 60 or 100) and the assumption was made that the proliferating population at each time point was comparable regardless of lymph node of origin. Second, the hypothesis was tested that the marker concerned would be expressed in the proliferating culture systems at differing levels according to the tissue of origin, but disregarding the time point at which the sample was analysed. Hence data were pooled according to the tissue of origin, but combining all samples across sampling time points (i.e. days 30, 60 and 100: day zero was not included since this was not derived from a proliferative culture system). Finally, for CHL and FL only, since there were adequate numbers of samples to draw preliminary conclusions on each tissue individually, these two factors (age of culture system and tissue of origin) were discriminated, and data pooled for each time point and for each tissue. Only those samples analysed at subsequent proliferative time points were included for the day zero analysis, as described in Table 7.1.

For each distribution of data: by age of culture system, by tissue of origin, and finally by age of culture system for each of CHL and FL individually, analysis of variance (ANOVA) was performed to determine differences between groups with statistically significant difference set at 0.05. Additionally, significance of differences between paired sample means were calculated using the method of Mann and Whitney<sup>371</sup>. Multivariate analysis combining the three variables: tissue of origin, time of sampling and expression level of marker requires more samples than were available for this experiment in order to be adequately powered and as such was not carried out.

## 7.4 Results

### **7.4.1 Limitations of Method and Data Interpretation**

In the interpretation of these results, it should be taken into account that changes in expression levels of any particular marker may represent either up-regulation or down-regulation of that marker on cells within the total CD3+CD4+ cell population, or a relative enrichment or depletion of subsets of cells expressing that marker at baseline. Without tracking individual cells and their progeny these explanations cannot be discriminated. In addition any comparisons between the day zero pooled samples and those derived from subsequent samples may be subject to batch variation. Additionally, inadequate viable cells were available for analysis from the single tonsil-derived sample that showed evidence of proliferation at day 30. This was in keeping with poor growth observed in all tonsil-derived culture systems. As such the pilot finding reported in Chapter 5, that the CD8+ cell dominated in a successful tonsil-derived system in contrast to the CD4+ cell in CHL, could not be replicated. All benign control samples available were therefore reactive nodes as detailed in table 5.1.

### **7.4.2 Individual marker analysis, ANOVA and pairwise comparisons**

For each class of marker described below, composite figures are divided into three. The first two columns indicate changing expression of the marker in the proliferating CD4+ T cells for each time point sampled. The leftmost column displays results pooled by malignant lymph node of origin: either CHL (red) or FL-derived (blue). The middle column pools all samples at each time point regardless of node of origin. The final column displays the mean expression across all proliferative time points (i.e. excluding baseline results) pooled by lymph node of origin to enable comparisons to be made between resultant CD4+ cells according to originating tissue.

While most CD4+ T cell markers showed a variation of expression level with time, variation in expression levels between samples, regardless of tissue of origin, was far less marked (See 7.4.3). Significance of differences between samples by time point or by tissue of origin are determined as described in 7.3.5, and levels of significance shown in the appropriate figures (Figures 7.1 – 7.12)

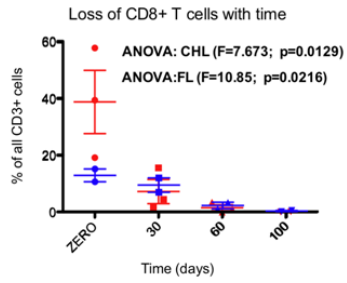


7.4.2.1 CD4<sup>+</sup> CD45RO<sup>+</sup> T cells are the dominant cell type in all culture systems.

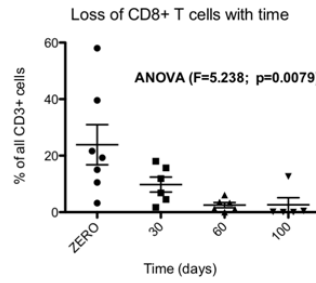
Figure 7.1 shows the loss of CD8 expression with time. By day 30 <10% (mean all pooled samples) T cells expressed CD8, and by day 60 <2%, with no recovery of cell numbers. There was no expression of CD20 in any system by day 30. Hence in all culture systems analysed at day 30 the CD4<sup>+</sup> T cell was the dominant or exclusive cell type. This is in contrast to the single analysis of a tonsil performed in the pilot experiment described in Chapter 5 where CD8<sup>+</sup> T cells dominated. However, poor growth in the subsequent tonsil-derived culture systems prevented any further analysis of proliferative tonsillar T cells.

CD45RO was present at high levels in all samples at baseline and persisted with time. The CD45RA component was present at widely heterogeneous levels at baseline (see Chapter 6) and was lost with time (mean all pooled samples: Day zero: 20%, Day 30: 8%, Day 60: 3%, Day 100: 2%). This was most pronounced for CHL (Baseline: 25%, Day 30: 12%, Day 60: 4%, Day 100: 2%) although this did not reach significance by ANOVA, probably reflecting under-powering for the small sample size.

**Variance of expression by time:  
CHL (red) vs FL (blue)**



**Variance of expression by time:  
all pooled samples**



**Variance of expression by tissue of origin:  
pooled proliferating cells from all timepoints**

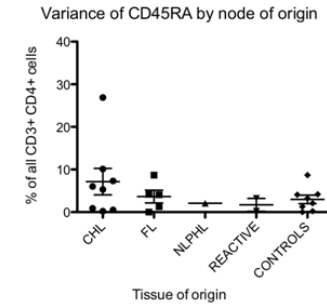
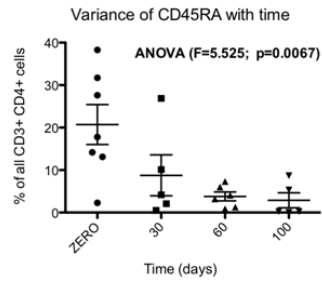
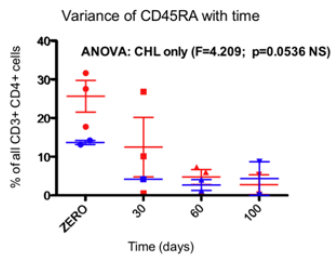
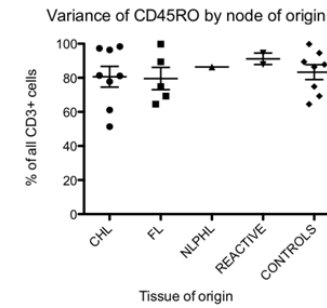
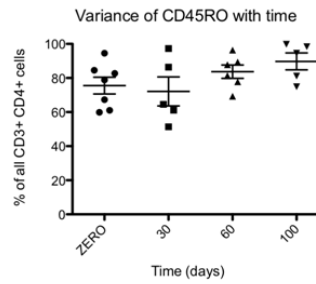
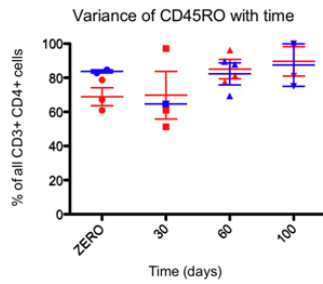


**Figure 7.1:** Loss of CD8 cells and CD45 isotype change with time.

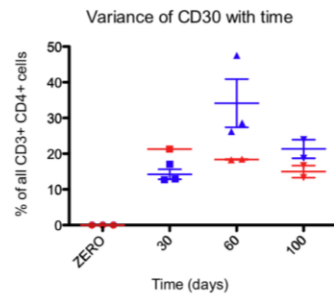
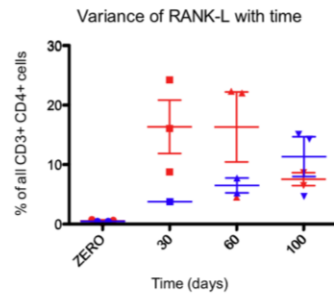
7.4.2.2 TNFRSF and IGSF members (Figures 7.2 and 7.3)

By day 30 cells in all culture systems universally expressed CD95 (Figure 7.2), having been expressed at widely variable levels at day zero (Chapter 6). This persisted at day 100.

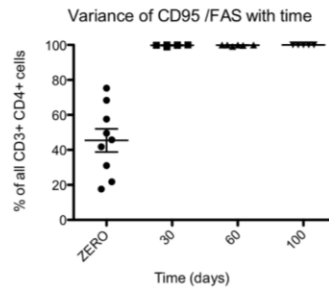
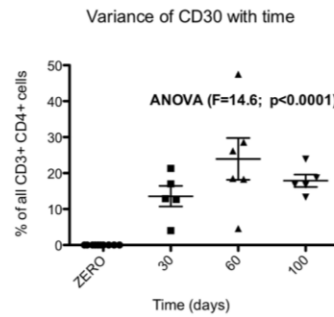
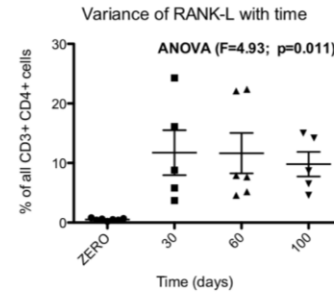
With time there was significant loss of expression of CD27 (means: Day zero vs Day 30 vs Day 60 vs Day 100 = 64% vs 18% vs 5% vs 2%) and CD28 (means: 33% vs 23% vs 16% vs 22%) and ICOS/CD278 (means: 48% vs 32% vs 18% vs 18%). For CD27 this loss was significant for both FL-derived and CHL-derived CD4<sup>+</sup> T cells. However no difference could be found according to node of origin except for CD27, where CHL derived cultures expressed the marker at mean level of 12%, compared to 2% in FL, predominantly due to persistence of expression at day 30. Most expression had been lost in all cultures by day 60 (Figure 7.3)

In contrast, there was a significant increase in expression of CD30, CD40-L and RANK-L expression with time in all culture systems (Figure 7.2) without any significant difference according to node of origin. At baseline, no marker was expressed at appreciable levels. However by day 30, CD40-L was expressed in 11% of cells (mean of all pooled samples), 23% at day 60, and 21% at day 100. RANK-L expression was seen in 11% of all cells at day 30, persisting at this level until day 100, while CD30 was expressed in 12% at day 30, 23% at day 60, and 18% at day 100. OX40 persisted in all culture systems derived from all lymph node types, with no significant variation by tissue type or time point (mean expression 30% at day zero, 15% at day 30, 27% at day 60 and 22% at day 100). Data not shown in Figures for OX40 or CD40-L; CD30 and RANK-L included for illustration.

**Variance of expression by time:  
CHL (red) vs FL (blue)**



**Variance of expression by time:  
all pooled samples**



**Variance of expression by tissue of origin:  
pooled proliferating cells from all timepoints**

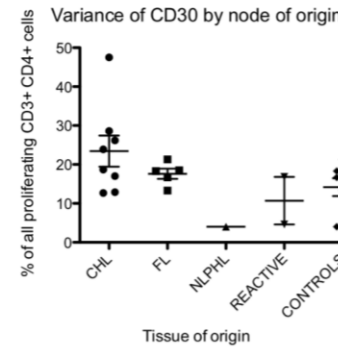
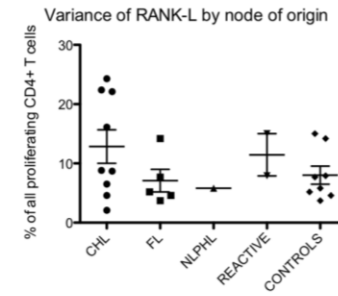
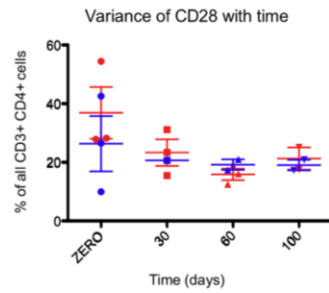
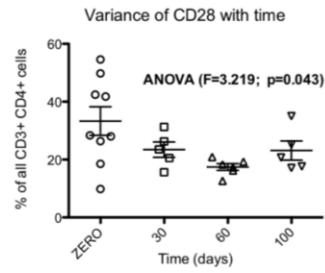


**Figure 7.2:** Gain of expression of TNFRSF and IGSF members by CD4+ T cells with time in culture

**Variance of expression by time:  
CHL (red) vs FL (blue)**



**Variance of expression by time:  
all pooled samples**



**Variance of expression by tissue of origin:  
pooled proliferating cells from all timepoints**

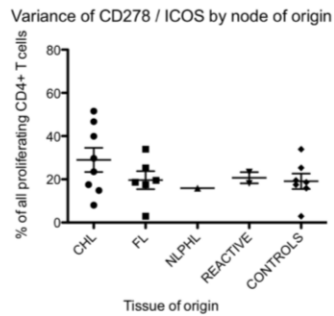
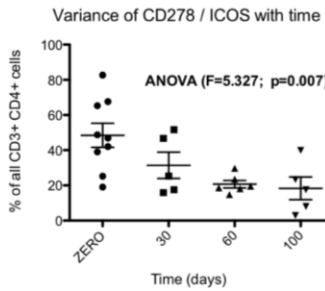
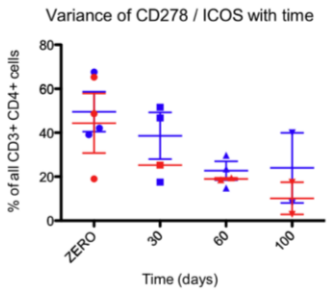
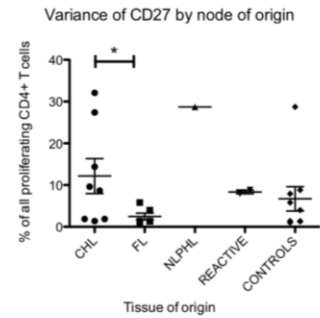
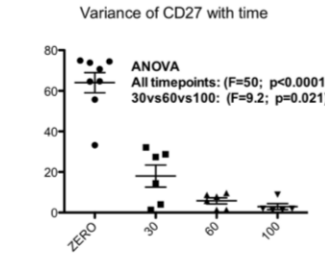
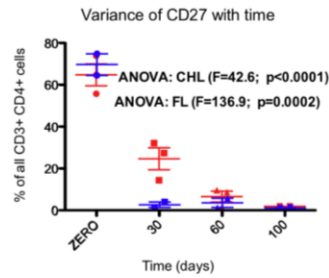
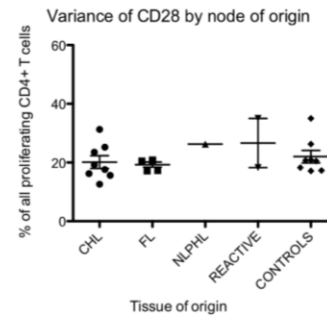


**Figure 7.3:** Loss of expression of TNFRSF and IGSF members by proliferating CD4+ T cells with time in culture

#### 7.4.2.3 Cytokine Receptors and Early Activation Marker (Figures 7.4 and 7.5)

All culture systems analysed were those derived from the IL2 and IL4 stimulated conditions, which had demonstrated best proliferation and longest duration of survival. Hence expression of these cytokine receptors was of interest. IL2R $\beta$  was not expressed at any time point in the CD4<sup>+</sup> T cell compartment. However IL2R $\gamma$  (CGC) was present in all systems, persisting at similar levels across all time points, although with greater heterogeneity at day zero, than by day 100. The range of expression of CGC had narrowed from 17% - 53% at day zero to 29% - 43% by day 100. Mean expression levels remained comparable at all time points. IL2R $\alpha$  (CD25), however was expressed by a greater proportion of cells as the culture system aged, largely accounted for by a substantial increase in FL-derived cultures. At day zero a significantly greater proportion of CHL-derived CD4<sup>+</sup> T cells expressed CD25 than those derived from FL (6.4.2.3) whereas in proliferating CD4<sup>+</sup> T cells, levels were similar regardless of nodal source, at day 30 and beyond (mean day 30: 28%, by day 100: 36%).

IL4R $\alpha$  was present at low levels in CD4<sup>+</sup> T cells of all SCSs at day zero, although its presence was confirmed as expected in the CD3<sup>-</sup> component comprising B cells, monocyte and macrophages. In the IL4-rich conditions of *in vitro* culture, IL4Ra was up-regulated to a similar extent regardless of tissue of origin (Figure 7.4) which persisted to day 100. Mean expression at day zero was 2% and 10% by day 30. However, only a minority of CD4<sup>+</sup> T cells (never >20%, and <10% in most cases) expressed this receptor, of interest since IL4 seems integral to the prolonged survival of the culture system.

The early activation marker CD69 was present at widely heterogeneous levels at baseline, with significantly lower expression in CHL-derived cells than control samples (6.4.2.3). This heterogeneity persisted with time, however for all pooled samples levels of expression were significantly reduced (mean day zero: 59%, day 30: 27%, day 60: 36%, day 100: 32%). However, this loss of expression was less marked for CHL with no significant change from baseline (mean expression 56% day zero vs 37% day 30, 51% day 60, 42% day 100), while for FL levels dropped significantly (69% to around 30%). Replicate numbers were few and require further validation. However, it appears that there is relative loss of this marker from the CD4<sup>+</sup> T cell component with prolonged

culture except in CHL in which it is retained at a consistent level, having been present at a lower level at baseline (Figure 7.5). This gives rise to a significant difference of expression by tissue of origin pooling all proliferating samples.

#### 7.4.2.4 Lymph node homing (Figure 7.6)

CD62L and CCR7 provided two of the best discriminating markers of CHL-derived CD4+ T cells compared to all controls at baseline (Chapter 6). However there was loss of expression of both markers in CHL-derived cells with time in culture, such that in proliferating cells there was no difference in expression of CD62L and CCR7 alone, or in combination, by tissue of origin. Expression of CD62L had reduced from mean 60% to 28% by day 60/100, CCR7 from 28% to 15% and combined expression from 20% to 3%.

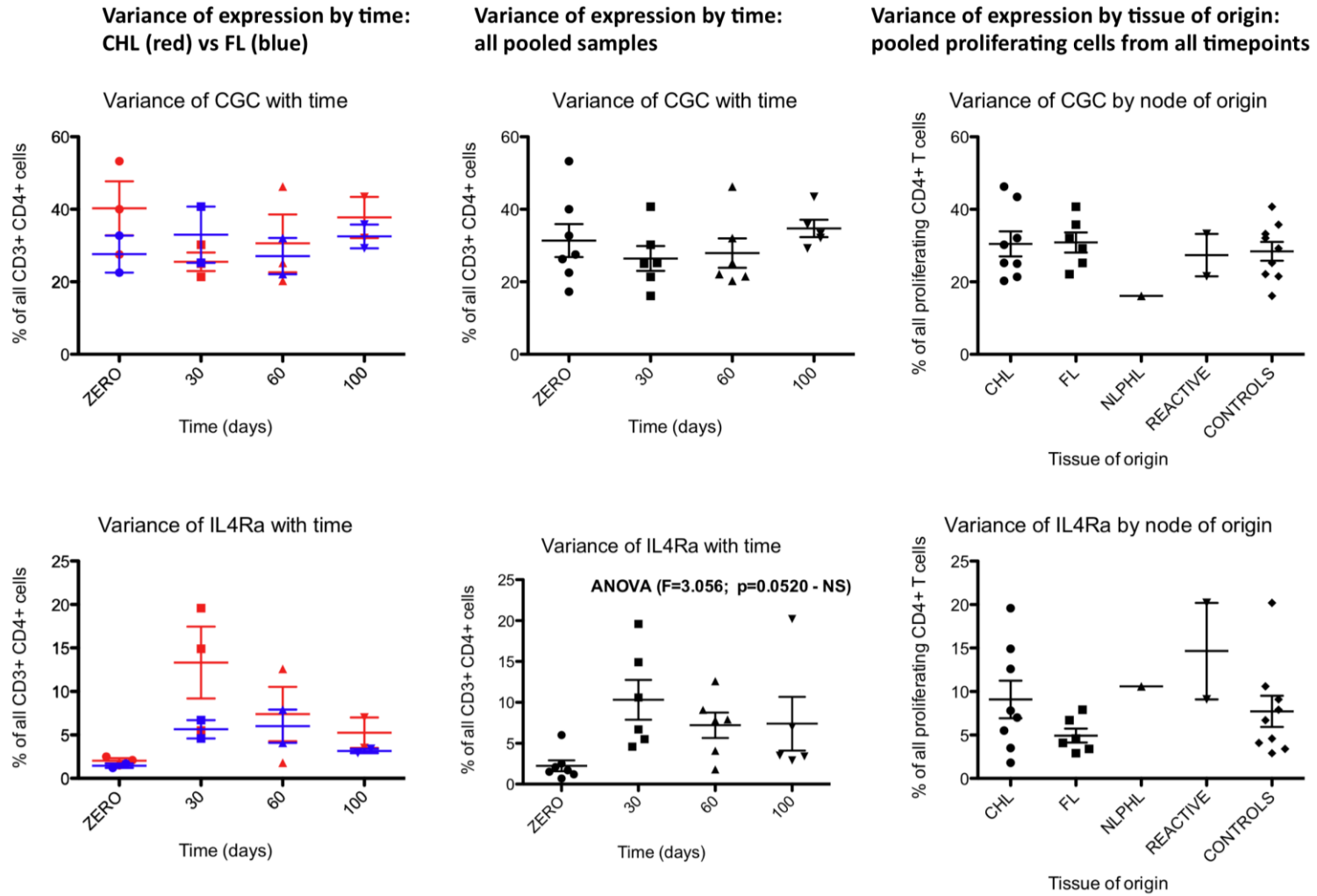
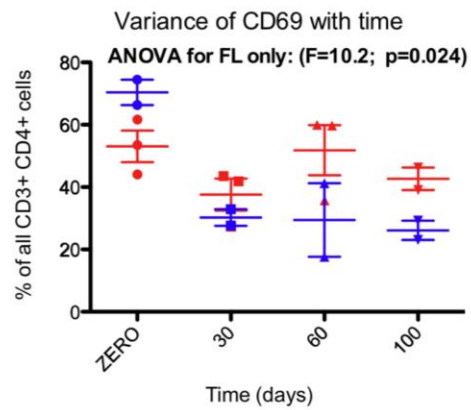


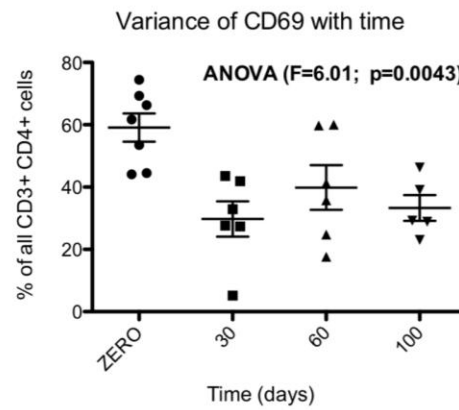
Figure 7.4: Variance of expression of IL4Ra and CGC on proliferating CD4+ T cells with time in culture.



Variance of expression by time:  
CHL (red) vs FL (blue)



Variance of expression by time:  
all pooled samples



Variance of expression by tissue of origin:  
pooled proliferating cells from all timepoints

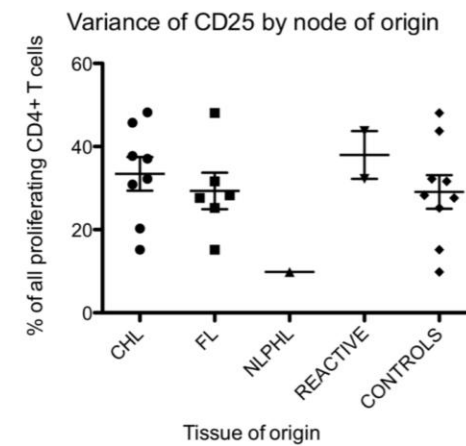
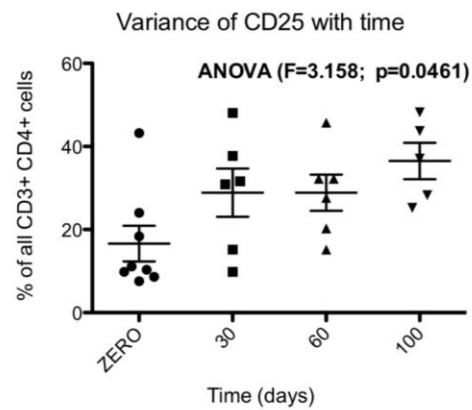
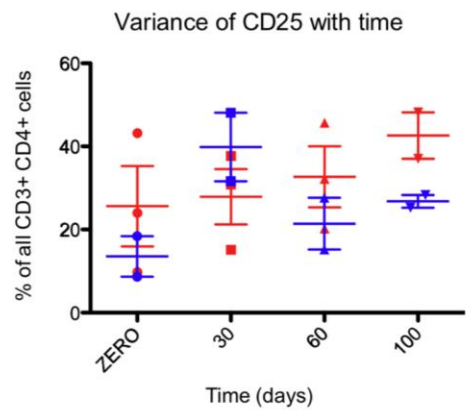
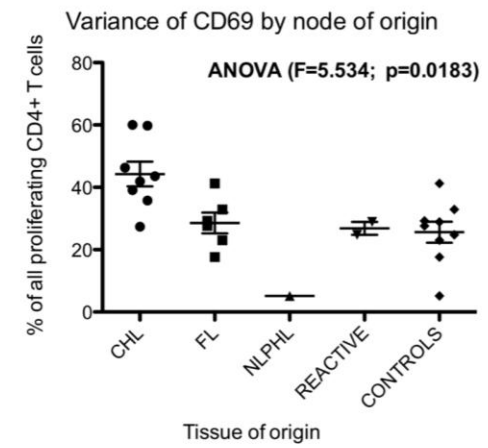


**Figure 7.5:** Variance of expression of CD25 and CD69 on proliferating CD4+ T cells with time in culture.

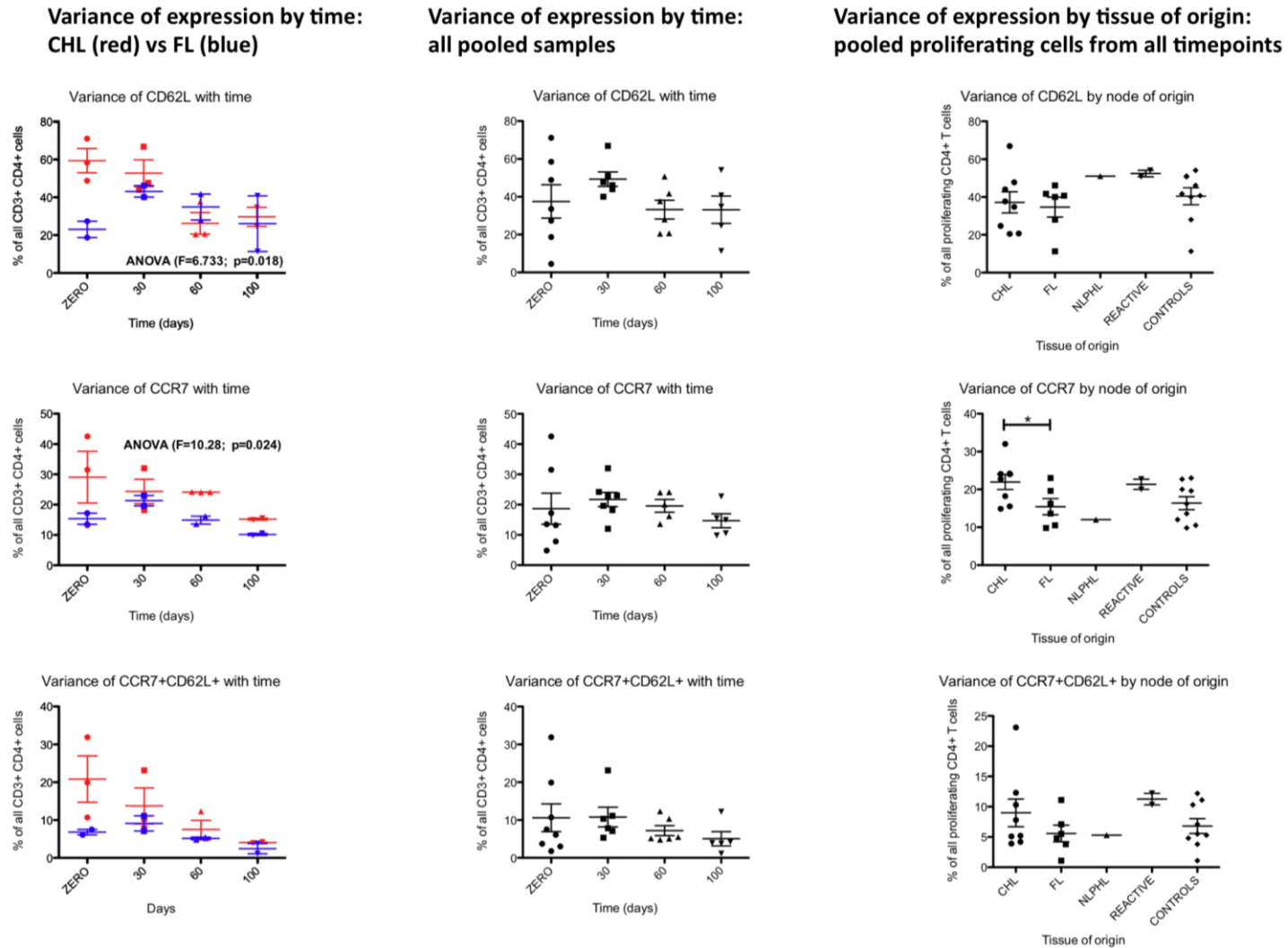


**Figure 7.6:** Variance of expression of lymph node homing molecules on proliferating CD4+ T cells with time in culture.

7.4.2.5 Persistence, Senescence and Immunosuppression (Figure 7.7 and 7.8)

CD57 and PD1, markers of senescence and immunosuppression respectively, provided two more of the best discriminating markers of CHL-derived CD4+ T cells compared to all controls at baseline (Chapter 6). CD57, as anticipated, was up-regulated with time in culture (Figure 7.7). This was most marked for CHL, with a significant increase by day 30 which persisted until day 100 (around 30%, having been <5% at baseline). This was similar to baseline levels for FL, although there were inadequate replicates to draw further conclusions regarding FL-derived cells. Overall there was no difference of expression levels in proliferating cells by tissue of origin. The main difference arose due to increased expression levels in CHL-derived samples. PD1 had a distinctive pattern of expression (Figure 7.8) being present at higher levels in FL-derived CD4+ T cells compared to CHL (Chapter 6). In contrast to CD57 expression of this marker was lost in proliferating cultures (baseline = 40% vs 20% at 30 days, 12% at 60 days and 8% at 100 days). Mean expression levels of both markers were comparable in proliferating cells regardless of tissue of origin.

PD-L1 and CTLA4 are both mediators of immunosuppression and expressed widely on activated lymphoid cells. Consistent with this activation-induced expression both markers were increased by day 30 (PD-L1 mean 4% at baseline, 22% at day 30, CTLA4 mean 4% at baseline, 11% by day 30), but subsequently reduced by day 100 (PD-L1: 7%, CTLA4: 9%). This was significant for FL-derived CD4+ T cells for both CTLA4 and PD-L1, but significant variation of only CTLA4 expression could only be demonstrated for CHL.

As discussed in the introduction, persistence of long-lived memory T cells is IL7 and hence IL7-receptor (CD127) dependent. This marker was present in a greater proportion of CHL-derived CD4+ T cells at baseline than control samples. With time, expression of this marker increased across all samples and persisted (Figure 7.7). Pooled mean expression level at baseline was 14%, compared to 23% by day 30 and 18% by day 100. Despite all samples showing an increase in CD127 expression with time, the receptor remained in a significantly greater proportion of CHL-derived proliferating CD4+ T cells compared to all other samples (CHL-derived T cell mean = 26%, pooled controls: 19%, FL-derived CD4+ T cells: 18%).

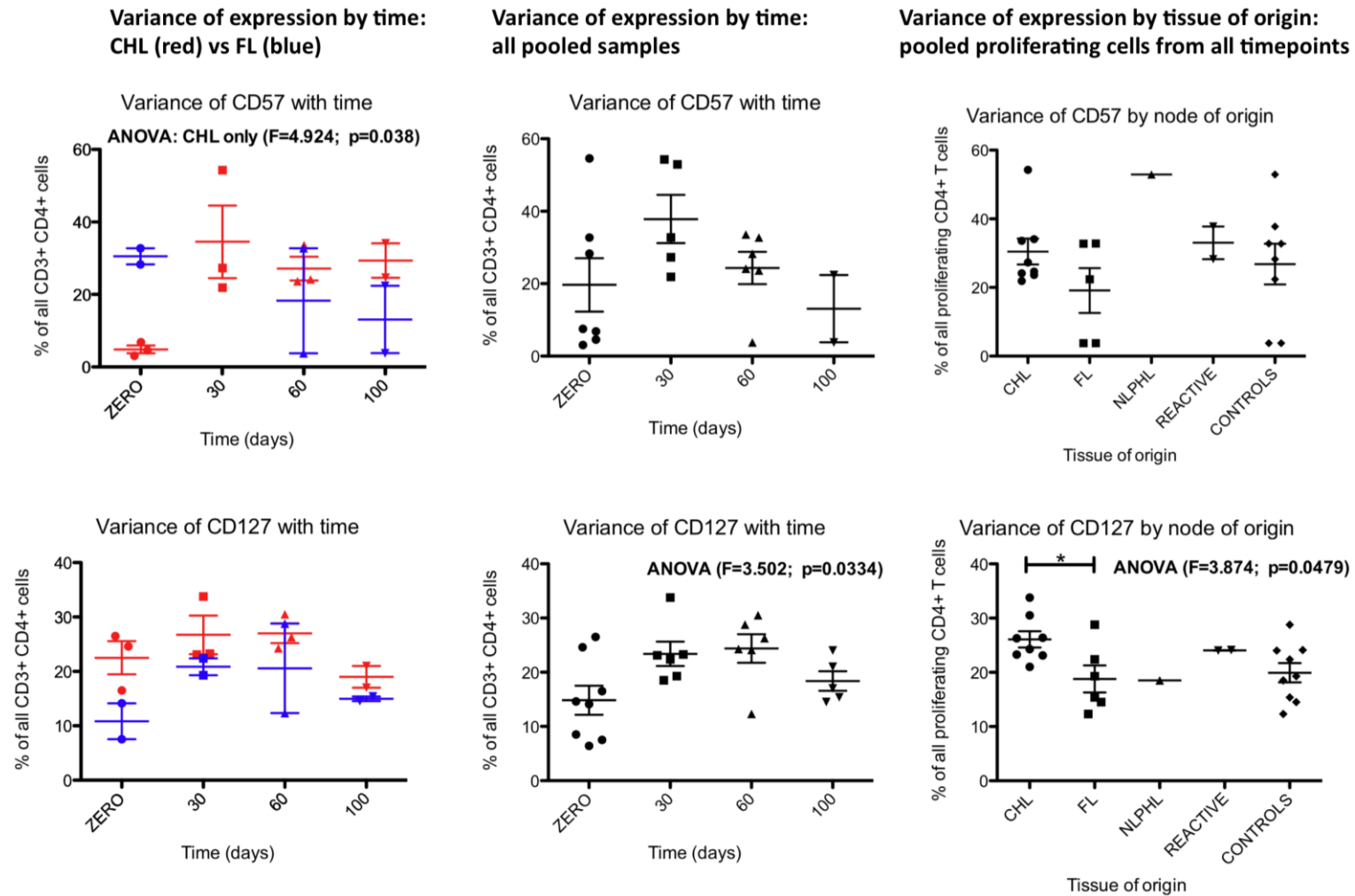


**Figure 7.7:** Variance of markers of persistence and senescence on proliferating CD4+ T cells with time in culture.

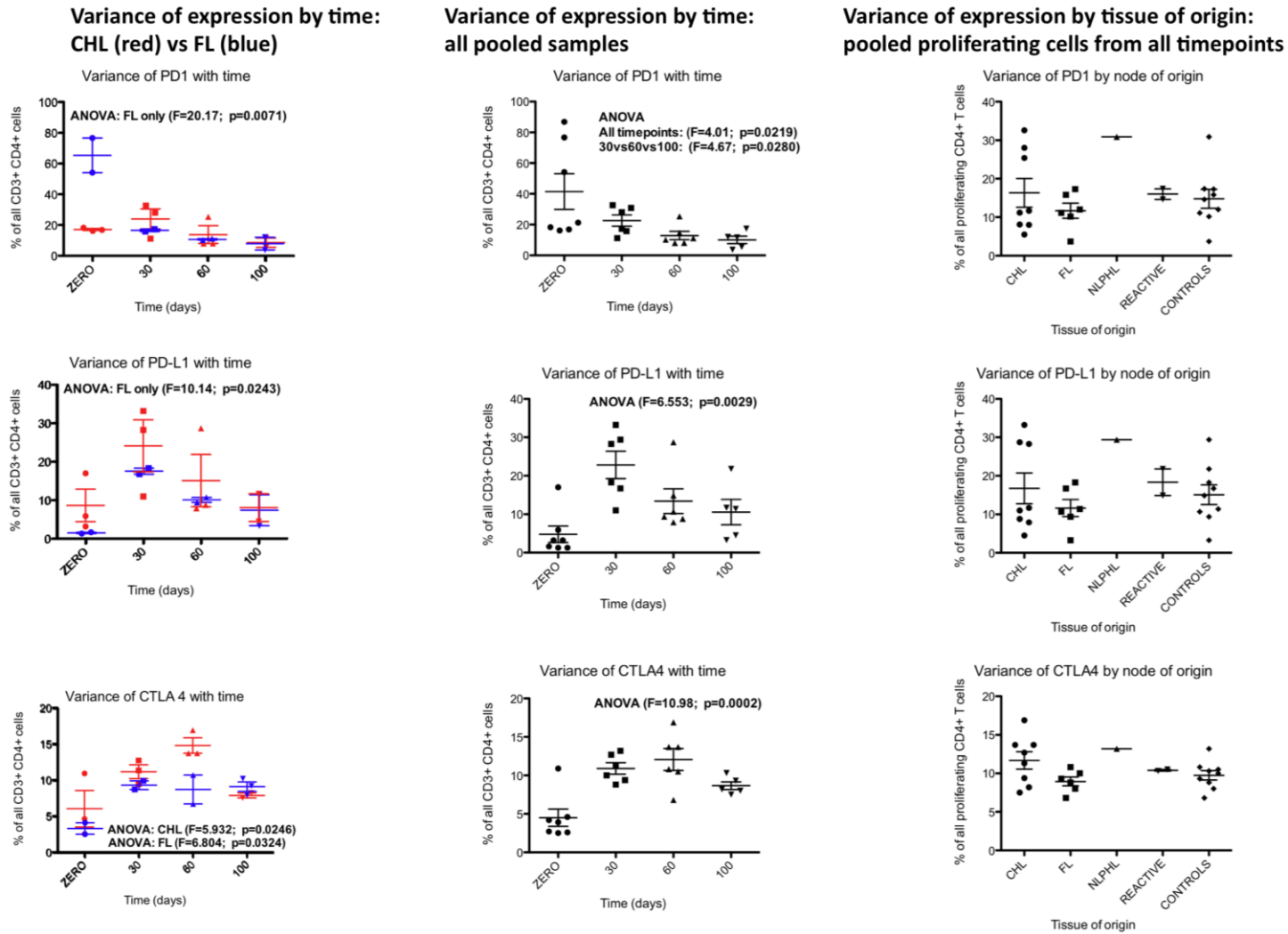


**Figure 7.8:** Variance of markers of immunosuppression on proliferating CD4+ T cells with time in culture.

#### 7.4.2.6 Cytokine expression (Figures 7.9 and 7.10)

Th<sub>1</sub>-defining pro-inflammatory cytokines (IFN- $\gamma$  and TNF $\alpha$ ) dominated all tissue samples at baseline (Chapter 6) with a greater expression in malignant-derived T cells than benign controls, although there was no measurable IL2 expression in any sample. In contrast little measurable Th<sub>2</sub>-defining or immunosuppressive IL10 could be detected in any SCS, except for some IL4 expression by PTGC-derived cells.

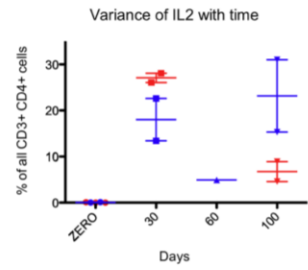
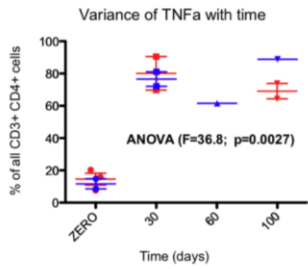
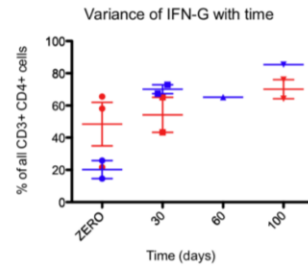
In contrast, proliferating cells showed a diverse cytokine expression repertoire, expressing both Th<sub>1</sub> and Th<sub>2</sub> cytokines simultaneously in some cases. There was no significant difference in expression of Th<sub>1</sub> cytokines IFN- $\gamma$ , TNF $\alpha$  or IL-2 by CD<sub>4</sub><sup>+</sup> T cells according to tissue of origin. IFN- $\gamma$  was expressed at comparable high levels of around 60% of CD<sub>4</sub><sup>+</sup> T cells at all time points. TNF $\alpha$  was significantly up-regulated compared to baseline in all tissues (baseline mean 12%, at day 30: 52%, day 60: 43%, day 100: 58%) and to a similar degree regardless of the origin of the proliferating CD<sub>4</sub><sup>+</sup> T cell. IL2, not detectable at baseline in any CD<sub>4</sub><sup>+</sup> T cells, was expressed in a substantial proportion of cells by day 30, which apparently persisted until day 100, although sample loss for this condition limited the number of replicates. Mean expression was similar regardless of tissue of origin, although the range of expression varied considerably (4%-30% of all CD<sub>4</sub><sup>+</sup> T cells).

Th<sub>2</sub>-defining cytokines were expressed in a substantial and increasing proportion of CD<sub>4</sub><sup>+</sup> T cells as time passed. By day 100 a mean of 58% of cells expressed IL4, 22% expressed IL13 and 9% expressed IL21. Fewer CHL-derived proliferating CD<sub>4</sub><sup>+</sup> T cells expressed IL4 than those derived from FL or reactive lymph nodes (mean 39% across all proliferating cells for CHL, compared to 59% for FL and 78% for reactive nodes), and fewer expressed IL13 than those derived from reactive nodes (20% vs 41%). Heterogeneity of expression for IL13 was substantial however. IL21 was expressed heterogeneously across all samples, with a suggestion of increasing expression with time that was not significant.

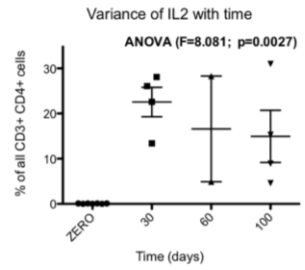
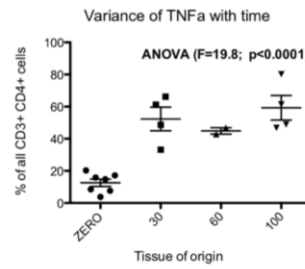
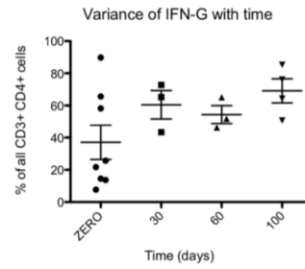
IL10 was not expressed at baseline or in any proliferating CD<sub>4</sub><sup>+</sup> T cell.

There was no single tube combining antibodies to concurrently detect both Th<sub>1</sub> and Th<sub>2</sub>-defining cytokines in this experiment, and hence there is no direct evidence for co-expression of these normally mutually exclusive cytokine systems. However, expression of both IFN- $\gamma$  and IL<sub>4</sub> in greater than 50% of cells demonstrates that at least a proportion of cells co-express both markers. It is possible that some proliferating cells are Th<sub>1</sub>-like IFN- $\gamma$  producing cells and others Th<sub>2</sub>-like IL<sub>4</sub> producing cells, with a proportion of cells co-expressing both cytokines and others expressing a wider range of Th<sub>1</sub> or Th<sub>2</sub>-defining cytokines (TNF $\alpha$ /IL<sub>2</sub> and IL<sub>13</sub>/IL<sub>21</sub> respectively). Expression of Th<sub>1</sub>-defining cytokines emerges rapidly and persists, while Th<sub>2</sub>-defining cytokine expression emerges more slowly and is most marked by day 100.

**Variance of expression by time:  
CHL (red) vs FL (blue)**



**Variance of expression by time:  
all pooled samples**



**Variance of expression by tissue of origin:  
pooled proliferating cells from all timepoints**

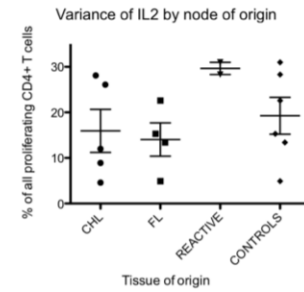
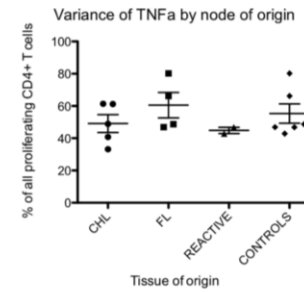
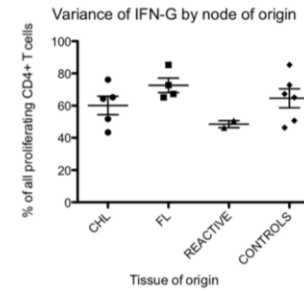
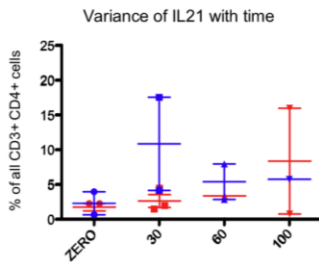
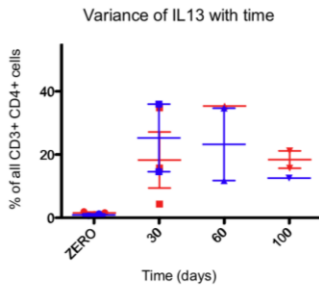
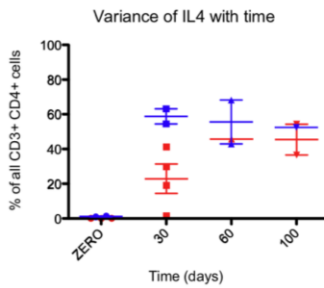


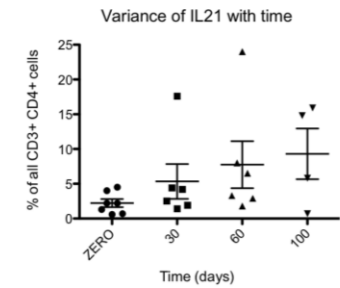
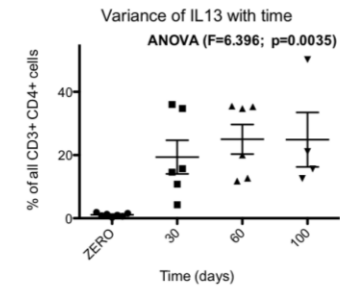
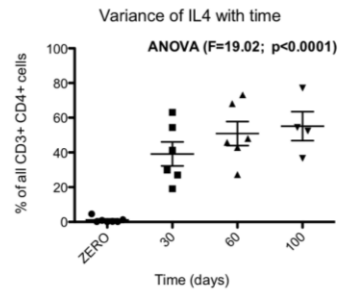
**Figure 7.9:** Variance of Th1 cytokine expression on proliferating CD4+ T cells with time in culture.



**Variance of expression by time:  
CHL (red) vs FL (blue)**



**Variance of expression by time:  
all pooled samples**



**Variance of expression by tissue of origin:  
pooled proliferating cells from all timepoints**

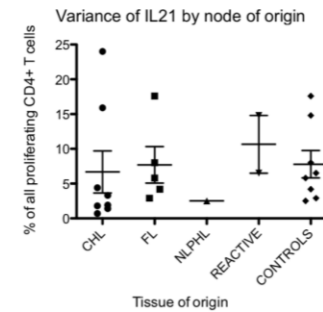
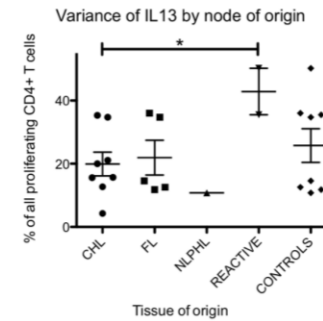
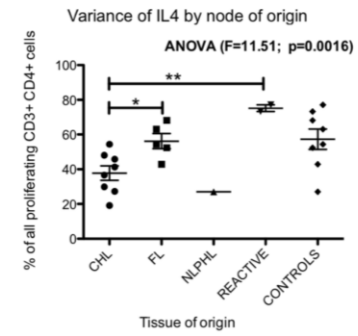


**Figure 7.10:** Variance of Th2 cytokine expression on proliferating CD4+ T cells with time in culture.

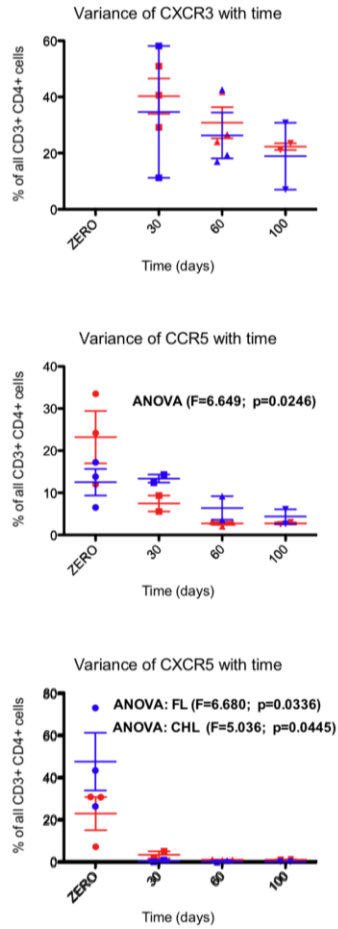
7.4.2.7 Chemokine Receptor Expression (Figures 7.11 and 7.12)

CCR4 is highly and heterogeneously expressed at baseline in CD4+ T cells derived from all tissues, particularly so for CHL (see Chapter 6). This expression persists with proliferation, although significant change with time, or tissue of origin could not be shown (Figure 7.11).

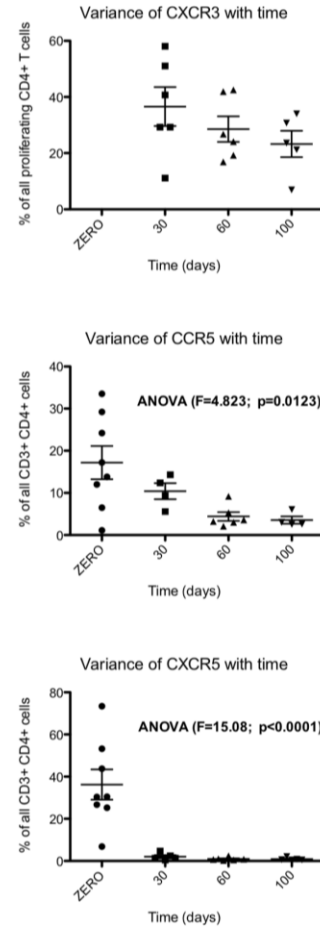
Neither CCR6 nor CCR3 (Figure 7.12) were expressed at high levels (<10%), at baseline, or in proliferating T cells although there was a significant reduction in CCR3 levels across all pooled samples with proliferation, from 2.5% at baseline to 0.8% by day 30, remaining below 2% in all samples. This difference was predominantly accounted for by expression in 7% of CD4+ T cells in a single case of CHL at baseline, and as such this outlier may be questioned as being truly representative, and would require validation in a larger cohort.

The Th1-associated cytokine CCR5 was present at considerable levels at baseline in all samples but with no significant difference between samples demonstrated (Chapter 6). Expression was significantly lost with time in all samples (Figure 7.10), with mean expression across all pooled samples being 18% at baseline, 10% at day 30, 4% at day 60 and 3% by day 100. This was in spite of the extremely high levels of expression of Th1-associated cytokines in all samples. In contrast, CXCR3, which was not included in the panel for the experiment described in Chapter 6, was expressed in a high proportion of CD4+ T cells at day 30, and while there was a reduction in the mean expression across all pooled samples at each time point (38% day 30, 30% day 60, 25% day 100) this was not significant. There was no difference in mean expression between samples, but overall expression levels were highly heterogeneous, ranging from 5% to 80% expression. This loss of Th1-defining chemokine receptors is in contrast to the high levels of expression of Th1-defining cytokines, highlighting the limitations of surface molecule expression as markers of the functional capacity of T cells, as well as the limitations of any longstanding *in vitro* culture system subject to unphysiological alterations of phenotype.

**Variance of expression by time:  
CHL (red) vs FL (blue)**



**Variance of expression by time:  
all pooled samples**



**Variance of expression by tissue of origin:  
pooled proliferating cells from all timepoints**

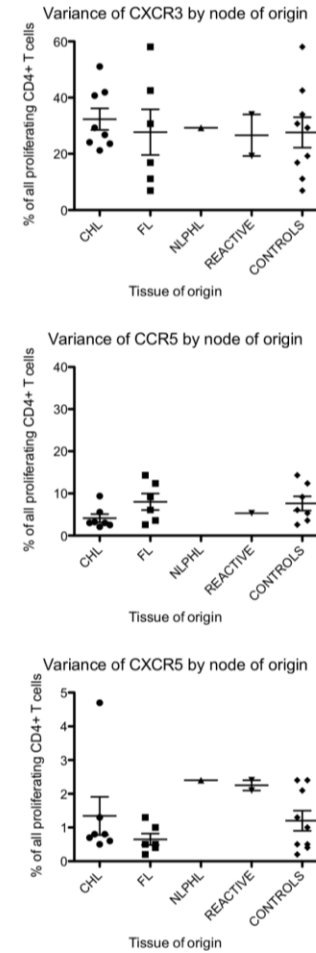
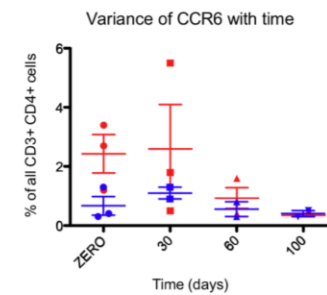
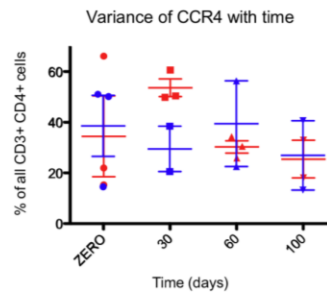
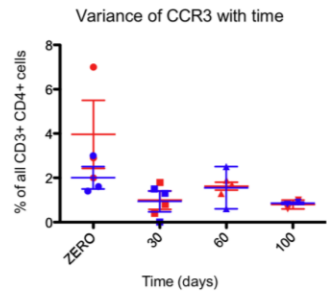
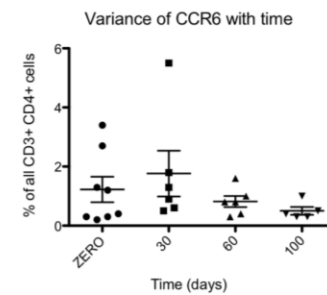
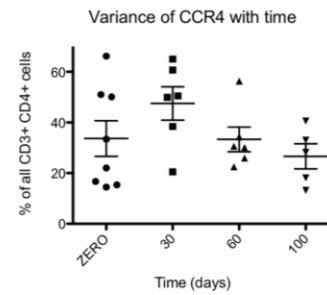
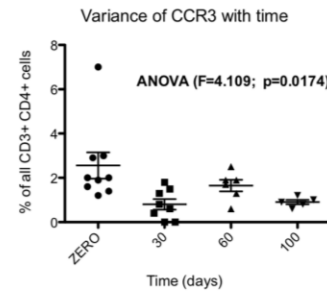


**Figure 7.11:** Variance of Th1 and Tfh associated chemokine receptors on proliferating CD4+ T cells with time in culture.

**Variance of expression by time:  
CHL (red) vs FL (blue)**



**Variance of expression by time:  
all pooled samples**



**Variance of expression by tissue of origin:  
pooled proliferating cells from all timepoints**

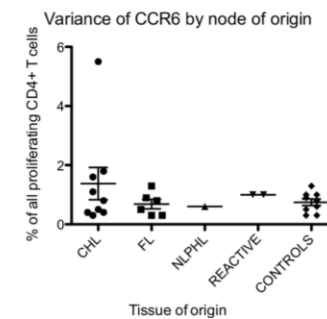
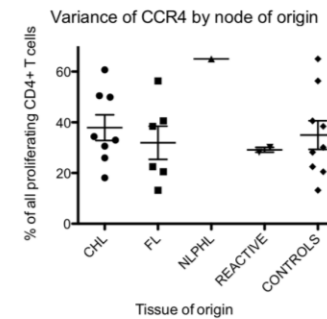
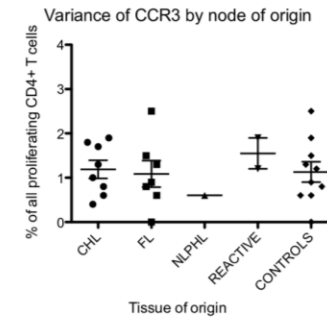


**Figure 7.12:** Variance of Th2 and regulatory associated chemokine receptors on proliferating CD4+ T cells with time in culture.

### 7.4.3 Discriminatory markers in proliferating cells

Combining all results, it is clear that the proliferating CD4<sup>+</sup> T cells express a distinct repertoire of markers compared to the unstimulated cells of the SCSs. However, the resulting proliferative T cells are remarkably similar, regardless of node of origin, despite markedly different proliferative properties dependent upon node of origin described in Chapter 5, and the distinct phenotypes of the CD4<sup>+</sup> compartment at baseline (Chapter 6). This is apparent in an unsupervised hierarchical cluster analysis using the same approach as applied at baseline (6.3.4.2 & 6.4.2.1), which this time fails to discriminate samples by tissue of origin or time point of sampling (Figure 7.13).

However, there are six markers whose expression appears discriminatory for CHL. CD69, CD27, CCR7 and CD127 remain expressed at higher levels in CHL-derived T cells, whereas IL4 and IL13 are expressed at lower levels, compared to control tissues.

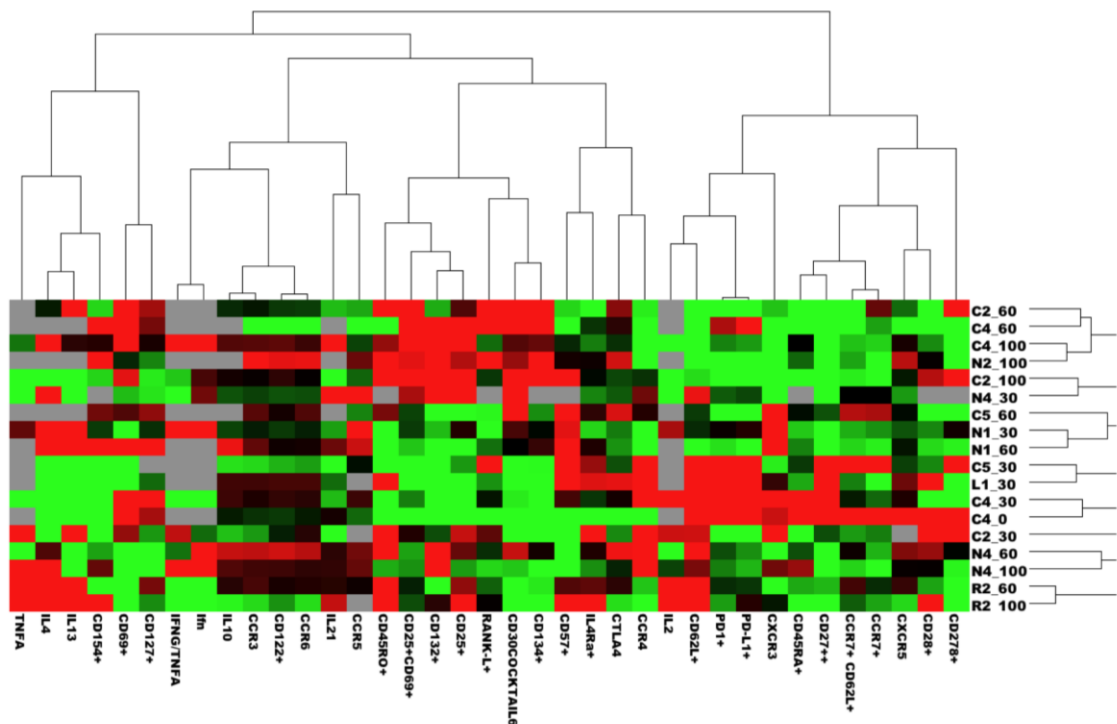


**Figure 7.13:** Hierarchical clustering fails to differentiate groups by tissue of origin when applied to proliferative CD4<sup>+</sup> T cells

## 7.5 Discussion

### **7.5.1 Limitations of this experiment**

The limitations of the sources of primary tissue and controls have been addressed in 6.5.1.3 and remain pertinent to this experiment. The culture systems are entirely artificial and the resultant cells unlikely to represent any *in vivo* phenotypic equivalent. The proliferation conditions selected, while avoiding any direct stimulation of the cells through TCR specific or super-antigenic stimuli, involved exposure to supraphysiological levels of cytokine which in themselves may have provided sufficient stimulation to induce antigen and MHC-independent proliferation.

Hence analysis of the resulting proliferating cells phenotype when exposed to such non-physiological stimulation and stress is unlikely to reveal the 'dominant' or 'founder' cell's phenotype that went on to populate the system. An increase in the representation of a marker in a population of cells as much indicates new expression of that marker by a proportion of those cells as it demonstrates proliferation in a specific subset of cells which expressed that marker at baseline and goes on to represent a greater proportion of the final population. Markers of activation and senescence in general were expressed as would be expected for any chronically stimulated system. However, despite these substantial limitations a number of conclusions may be drawn.

### **7.5.2 Markers of Activation**

First, it appears that any mixed lymph-node derived single cell suspension culture, when exposed to IL2 and IL4 at levels capable of sustaining T cell proliferation, will give rise to a virtually pure population of CD4<sup>+</sup> T cells, with few CD8<sup>+</sup> cells and no non-T cells surviving beyond 30 days. These cells are exclusively CD95<sup>+</sup> and despite this survive without undergoing CD95-mediated apoptosis perhaps due to the absence in the system of CD95/FAS-ligand. CD45RA expression is lost with ongoing stimulation, representing either loss of an unstimulated naïve cell population or TCR-independent stimulation of all CD45RA<sup>+</sup> naïve cells with consequent expression of CD45RO.

The cells are functionally competent in that a high proportion of cells express Th<sub>1</sub> and Th<sub>2</sub>-cytokines, and at least some express both concurrently. CD57 is expressed by an increasing proportion, as expected under conditions of chronic stimulation.

CD30 and RANK-L, not expressed by the T cells at baseline, are expressed in a minority of cells in the ongoing cultures. CD30 expression is induced by IL<sub>4</sub> and associated with IL<sub>4</sub>-responsiveness and a Th<sub>2</sub>-polarised phenotype<sup>499</sup>, so this finding is consistent with chronic IL<sub>4</sub> exposure. The functions of CD30 on interacting with CD30-L are numerous, with both receptor and ligand found on B cells, T cells and other immune cells, and functional data suggesting bidirectional signalling of both suppressive and stimulatory nature<sup>494</sup>. The receptor itself was discovered as a consequence of its characteristic expression first in CHL-derived cell lines and then in primary tissue in contrast to other B cell-derived malignancies, and in common with the mature T cell malignancy anaplastic large cell lymphoma (ALCL). However apart from its representing a distinctive marker of these malignancies, and downstream signalling pathways communicating with the NF- $\kappa$ B proliferative/survival networks suggesting a role in tumour maintenance and interaction with the microenvironment, no definitive evidence for the oncogenic or obligate role for this receptor have been defined. CD30-targetted monoclonal antibody therapy is relatively ineffective in either CHL or ALCL unless conjugated to toxins<sup>500</sup>, suggesting that the mediator of toxicity is neither interference with necessary survival signals, nor direction of immune cells towards the malignant cells, but simply tumour targeting by its expression of a unique marker.

RANK (receptor-activator of NF- $\kappa$ B) and its ligand are expressed by HRS cells<sup>119, 501</sup>, and signalling through this pathway is suggested to be of importance in its survival and interaction with the immune microenvironment. The molecule has sequence and potential functional homology with CD40, interacts with its own ligand, RANK-L and is essential in lymphoid cell development<sup>502</sup>. Expression on CD4<sup>+</sup> T cells was not found at baseline (Chapter 6), but it appears to be up-regulated in this in-vitro system for all samples including CHL and controls. Persistence of expression over time may reflect activation through the cytokine stimuli to which the cells were exposed<sup>503</sup>. This expression pattern is in contrast to the corresponding loss of another similar activation-

induced molecule, ICOS. Other markers of activation, PD-L1 and CTLA4, these with immunosuppressive function, are also found expressed by the expanding T cells. However without functional corroboration it is difficult to determine their significance except as nonspecific activation markers. CD28 is present at high levels in naïve T cells, and lost upon activation and stimulation in this culture system as expected.

### **7.5.3 The significance of chemokine receptors in the expanding cultures**

As discussed in the Introduction (1.4.3) the expression of chemokine receptors in CHL is complex and diverse, and comparisons within the heterogeneity of the disease and between diseases rarely performed. Associations with functional CD4+ T cell subsets are limited in their applicability and validity. CHL is distinguished by a high expression of the chemokines TARC/CCL17 and RANTES/CCL5, which predominantly attract CCR4 and CCR5-expressing cells respectively. This has been suggested to be a mechanism by which the microenvironment of CHL is enriched for T cells of particular function. CCR4 expression has been associated with Th2 and Tregs, while CCR5 has been described as a Th1-expressed receptor, as detailed in the Introduction 1.6.4.3. CXCR3 and CCR3 (ligand eotaxin/CCL11) are associated with Th1 and Th2 cells respectively and were also included in the phenotyping panel. CXCR3 was not included in the baseline experiment described in Chapter 6 for technical reasons, but was available for this experiment. In addition, CXCR5 was included which is a marker of germinal centre-associated T cells and B cells. There is limited literature to suggest that CCR6 expression is associated with a association with a suppressive or memory phenotype.<sup>504</sup>

Chemokine receptors are an essential component of T cell trafficking, compartmentalisation, intercellular communication and intracellular survival signalling. The *in vitro* system used in these experiments contains no survival mechanisms based on anatomical compartmentalisation, comprises only CD4+ T cells, and is dominated by the presence of excess specific cytokines. Hence the continuous signalling provided by supplementary cytokines *in vitro* subsumes the relative importance of chemokine receptors responsible for maintaining survival *in vivo*. This is most clearly demonstrated



by the fact that FAS/CD95, which *in vivo* indicates a cell destined for apoptosis, is universally expressed while the cells continue to survive and proliferate.

#### **7.5.4 The significance of TH2 cytokines in the expanding culture**

While Th2-specific cytokines are expressed at high levels in this system, the presence of IL4 predisposes uncommitted CD4+ T cells towards Th2 polarisation. The ongoing presence of a majority of Th1 cytokine-producing cells in spite of IL4 exposure does not support a predominance of Th2-determined cells in the initiating culture. Indeed, the balance of evidence of IHC (Chapter 4) and SCS flow phenotyping (Chapter 6) argue against any significant Th2 presence at baseline.

#### **7.5.5 The influence of a suppressor/regulatory T cell in the expanding cultures**

The growth of CHL-derived CD4+ cells despite an apparently significant infiltrate of Tregs, evidenced by IHC staining for FOXP3 and fluorescence immunostaining for CCR4 and CTLA4 is in contrast to the findings of Marshall et al detailed in the Introduction (1.7.2) describing a hypoproliferative, IL10-secreting, suppressive phenotype for the tumour-derived SCSs<sup>299</sup>. Once again, the large cytokine doses to which the system described in this experiment is exposed, in contrast to TCR-bypassing / super-antigen stimulus of the system of Marshall et al means that direct comparisons are impossible. However, neither system could be deemed more physiological representations of the *in vivo* lymph node microenvironment so these differences are another indicator of the problems of *in vitro* modelling. The experiment described in this chapter did not set out to functionally demonstrate the presence of Tregs, so ongoing presence of Tregs in the expanding cultures cannot be ruled out, and may be essential in maintaining the systems. However an alternative explanation, that the hypoproliferative Tregs are simply outcompeted and outgrown by a more proliferative component, is just as feasible.

#### **7.5.6 Markers of Longevity and Senescence**

CD27 expression may be indicative of cells with a greater capacity for prolonged survival and proliferation, with *in vitro* experiments showing that its expression in association with CCR7, the lymph node T cell zone-homing receptor, marks a functional subset with longer telomeres, better proliferative capacity and lesser cytokine-producing capacity<sup>505</sup>. In contrast, CD57 is associated with chronically stimulated, terminally differentiated

cells. Most functional work on CD57 is derived from models of chronic viral infection such as HIV<sup>297</sup>.

The loss of PD1, another marker of chronic immune stimulation, in spite of the emergence of CD57 is of interest and difficult to explain. Its disappearance coincides with the loss of CXCR5. Both markers are expressed on Tfh cells (See 1.6.6) and while co-staining for both markers was not carried out to confirm this, the loss of both these markers along with another marker of Tfh cells – ICOS, may indicate that Tfh cells within the system are lost.

Cytokine expression, in particular Th1-defining cytokines, is often an indication of terminal differentiation of a cell. Activation-induced apoptosis will usually follow once the cell has discharged its function in order to maintain immune homeostasis and prevent excess, aberrant inflammation – the effector T cell ‘contraction phase’<sup>44</sup>. While these cells may be capable, once committed to cytokine secretion, of further proliferation, it is more likely that the system is being sustained by another subpopulation of cells with a greater capacity for self renewal and proliferation rather than a terminally differentiated cytokine-secreting cell. Hence the longest-lived system may be that which possesses the greatest number of, or the most robust progenitor / stem cell-like T cells at baseline. These proliferating cells may be relatively multipotent, in line with some models of T cell development in which only activation, proliferation and exposure to particular inflammatory environments commits the T cell to a phenotype (which may eventually itself be relatively plastic) while in the early stages of proliferation it remains relatively uncommitted<sup>506</sup>.

#### **7.5.7 A distinctive phenotype for the proliferating CHL-derived CD4+ T cell?**

Unlike the immunophenotype of the CD4+ T cell at baseline, few markers in this panel distinguish expanded CHL-derived T cells from those derived from non-malignant or FL-infiltrated nodes. However, there is clearly a difference in functional phenotype evidenced by the longevity of malignant cultures over benign cultures, and the greater proliferative capacity and longevity of CHL-derived over FL-derived CD4+ T cells.

The few distinguishing markers that do exist provide some insight into the nature of this population as a whole, and as such the basis for further phenotyping and functional work. All findings require validation in a larger cohort of CHL and control node-derived SCSs.

CCR7 and CD27 are lost with culture age, but retained to a greater extent in the CHL-derived system. CD127 is retained, not lost with time, despite the absence of supplementary IL7, its ligand, implying either autocrine production of the cytokine, or that it is up-regulated in any cell population that has longer survival. CD69, while present at lower levels at baseline (indicating perhaps a lesser proportion of CD4<sup>+</sup> cells in CHL are in an early activated state, or alternatively more are chronically activated than in control node-derived cells), is sustained at similar levels through time, in comparison to expanding control nodes in which it is lost. The loss of CD62L as a distinguishing marker: one of the most discriminant at baseline, may simply reflect the loss of importance of the adhesion molecule interaction which is essential to transporting a T cell into a lymph node. While the same may be said for CCR7, which homes the T cell to the CCL19 and 21-rich paracortical T cell zone, perhaps this again has other functions, is being sustained by autocrine production of CCL19 and CCL21 (although predominantly these are thought to be secreted by stromal cells<sup>120</sup>) or is another non-specific activation marker.

One model explaining all of these findings would be that the CHL-derived node contains a CD4<sup>+</sup> subpopulation with self-renewal and proliferative capacity capable of generating terminally differentiating, functional, cytokine-secreting cells. The progeny of these cells are detected by activation markers (e.g. CD69, and other TNFRSF members) and probably have a short lifespan, limited proliferative capacity and die off. However, the self-renewal capacity of the originating subpopulation sustains the overall expansion of the culture system. Such cells resemble the central memory cell phenotype in their expression of CD27, CCR7, and CD127<sup>505</sup>, may be resistant to FAS-mediated apoptosis (or in this system perhaps simply not encountering FAS-ligand), remain IL2 and IL4 dependent, and are capable of producing progeny with both Th1 and Th2-like cytokine secretion profiles. In this model, any terminally differentiated cells rapidly die off,

including the CXCR5+PD1+CD57+ICOS++ Tfh cells apparently dominant in NLPHL, and present to a greater extent in FL and tonsillar tissue, as well as T-BET-expressing effector cells, and perhaps hypoproliferative FOXP3 cells. The maintained expression of CCR4, from baseline and throughout culture is intriguing, but may represent the replacement of native baseline CCR4-expressing Th2 cells and Tregs, with cells expressing CCR4 induced by IL4 exposure. These cells may or may not have other features of Th2 cells or Tregs, and represent two of several phenotypically distinct lineages arising from the progenitor central memory-like cell. As these central memory-like cells become exhausted, they express CD57 and lose CD27, perhaps a precursor to senescence of the culture system as a whole.

### **7.6 Summary and Further Work**

Proliferating CD4+ T cells derived from CHL and control nodes are indistinguishable using this immunophenotyping panel. They retain effector function in their production of Th1- and Th2-defining cytokines throughout. However, the CHL-derived (and to an extent FL-derived, more so than benign node-derived) culture may contain a greater proportion of central memory-like cells expressing CD27, CCR7 and CD127 at higher levels and hence capable of sustaining ongoing growth for longer, through self-renewal, while continuing to produce Th1 and Th2-determined terminally differentiated effector cells. Validation of this model requires a further extension of the central memory cell phenotype which would involve combining markers spread across different tubes in this panel into a single tube (e.g. CD27, CD127, CD45 isotype as well as CCR7 and CD62L). A larger number of replicates are required to increase the robustness of findings, and this should include a validation of the long-term cell culture as well as the phenotyping work. Cell labelling studies may enable multiple lineages to be followed from individual central memory-phenotype progenitors, and provide evidence of self-renewal. Clinical translatability of this finding is essential to justify pursuing any further work. This will be addressed in Chapter 8.

## CHAPTER EIGHT:

### Discussion

## 8. Discussion

This thesis set out to investigate interactions of the tumour-dominating CD4<sup>+</sup> T cell with the malignant HRS cell in CHL through IHC, flow cytometry and *in vitro* cell culture and as such determine the molecular mechanisms through which these interactions support growth and progression of the malignancy. By applying some of these markers to tissue microarray, it set out not only to validate prognostic factors already in the literature but also to investigate new factors, in order to develop a clinically translatable system to identify patients for whom outcome would be poorest and in whom treatment could be modified.

This project has provided evidence to set against a well-established yet often misrepresented literature on the nature of the microenvironment, arising from over-interpretation and superficial presentation of data.

### 8.1 A model for the CHL pathogenesis based on the CD4<sup>+</sup> T cell infiltrate

The immunophenotyping data presented in Chapter 6 have shown that the CHL-infiltrating CD4<sup>+</sup> T cell appears to have a unique signature, distinguishing it from similar cells derived from benign or FL infiltrated lymph nodes. Based on this phenotype, a model could be proposed for the T cell infiltrate in CHL.

#### **8.1.1 The CHL microenvironment sequesters naïve and memory T cells from the physiological lymphoid pool**

A B cell, which has likely encountered antigen, but not yet engaged its cognate T cell, or at least entered a germinal centre reaction, develops a malignant transformation, perhaps arising through the genetic instability intrinsic to B cell receptor rearrangement. This mechanism of early oncogenesis remains obscure and was not investigated in this project. However, while the molecular genetic mechanism of transformation may be spontaneous or virally induced, a surrounding infiltrate of supportive cells is required for

survival. The malignant HRS cell, or its hypothetical progenitor induces a generalised activation state in its lymph node surroundings through cytokine and chemokine release. This in turn activates high endothelial vessels of the lymph node, stimulates upregulation of adhesion and chemotactic molecules and encourages further lymphoid homing to that node, emulating the physiological response to foreign antigen load arriving at a draining lymph node. T cells expressing the highest levels of receptors for those adhesion molecules and chemotactic stimuli are preferentially recruited from the circulation and accumulate within the affected node. A key adhesion molecule initiating entry to the lymph node, L-selectin (CD62-L), is essential to this recruitment<sup>120</sup>. This molecule is particularly enriched on naïve and central memory T cells<sup>145</sup>. The activation state of the node leads to inhibition of lymphoid egress and ongoing recruitment of cells of the immune response, while other cells are polarised towards a phenotype determined by the inflammatory state of the node.

HRS-cells orchestrate this chronic aberrant production of a cytokine and chemokine milieu favourable to the survival of these arriving lymphocytes. However the impaired recognition of the HRS cell as foreign through poor antigen presentation, and the ongoing non-specific recruitment of lymphocytes reduce the opportunity for HRS-antigen specific interactions to occur. As the malignant cell divides, deriving growth and stimulatory stimuli from its own uncoupled intracellular survival and anti-apoptotic pathways and from interactions with surrounding immune cells and their secreted inflammatory mediators, further recruitment of non-specific lymphocytes occurs. The naïve central memory cells thus recruited are arrested in a primed state, with potential for proliferation and population of multiple effector compartments, but unable to realise this function due to isolation from their cognate antigen and possible suppressive signals within the microenvironment.

The cytokine milieu, including IFN- $\gamma$  and TNF $\alpha$  produced by the malignant cell and by other cells of the microenvironment polarises many infiltrating lymphocytes towards a Th1 phenotype. Some of these cells will have appropriately recognised aberrant intracellular antigen presented directly by the HRS cell or by other APCs in the node but are unable to mediate a coordinated response in the face of an overwhelming continuing

non-specific recruitment of uncommitted naïve and memory T cells, consuming cytokine and occupying space. Many of these cells secrete or express B cell helping molecules on their cell membrane capable of maintaining malignant cell survival. Other cells, including Tregs, Th1-polarised cells and memory cells, are attracted to the infiltrated lymph node more non-specifically through secretion of TARC and RANTES and other chemokines by malignant cells and the activated microenvironment, interacting with receptors such as CCR4 and CCR5. Their influence on the malignant cell, the potency of any residual immune response, and on the non-specific infiltrate may influence growth of the malignant cells. However, without cognate antigen presentation any anti-tumour effect is likely to be non-specific and overwhelmed by pro-tumour non-specific interactions.

#### **8.1.2 The immune infiltrate is an indicator of immunological health of the host hence predicting outcome**

The general potency of the immune response reflected by the efficiency of recruitment of various T cell subsets to the node, even if ineffective at eradicating the malignancy, may be a surrogate marker for overall immune competence and fitness of the host. Once treatment is commenced this may be reflected in ability to tolerate toxic therapy, speed of regeneration of immunity following immunosuppressive treatment, and efficiency of eradication of residual malignant cells once the bulk of disease is removed by treatment. This provides one explanation for the positive prognostic impact of expression of FOXP3, CD20 and T-BET in the immune infiltrate at baseline on eventual disease outcome.

#### **8.1.3 Sequestration of the central memory compartment leads to profound cell-mediated immune defect**

Malignant cells egress initially via normal channels of lymphoid circulation, into contiguous nodes, and later disseminate haematogenously leading to widespread aberrant recruitment of lymphocytes into the tumour microenvironment. This disturbs normal lymphoid circulation. Memory cell pools and lymphoid progenitors would initially compensate by proliferating to replace cell loss but eventually the capacity to replace sequestered cells would be overwhelmed, or homeostatic feedback from the sequestered populations negatively feed back to suppress further production. The preferential sequestration of the cells with most potent recall antigen response and



proliferative capacity as well as naïve cells would result in a profound functional defect of cell mediated immunity. This is well described in CHL<sup>42, 507</sup> manifesting as lymphopenia, impaired vaccine response<sup>41</sup>, predisposition to infection, transfusion-related GVHD<sup>508</sup> and is also consistent with the reported drop in CD4 count in patients with HIV in the months preceding development of overt clinical CHL<sup>120</sup>.

## **8.2 Potential Clinical Translation of this work**

Describing a single component of the heterogeneous multi-cellular microenvironment of CHL, with its complex, interacting networks and dynamism not apparent in fixed, dead tissue, nor convincingly modelled *in vitro* or *in vivo* may seem to be an exercise in abstract reductionism without any potential for translation to the clinic. However selection of the CD4+ T cell as the focus of this thesis was based on its numerical dominance in the tumour mass and the biological plausibility of it being most capable of providing support, as a T helper cell, to a B cell derived malignancy. This work has therefore hence yielded a number of specific and important hypotheses with potential for clinical translation.

### **8.2.1 A clinically applicable prognostic score may be derived based only on the expression of FOXP3 and CD68 at diagnosis.**

Several factors were found in the IHC panel applied to the TMA described in Chapters 3 and 4, which were associated with clinical outcome. While FOXP3 stood up to the greatest extent of statistical analysis, discriminating groups of significantly different outcome by test/validation optimal cut-point methodology, as a continuous variable in a dose-dependent manner, and in combination with elements of the clinical prognostic score in a multivariate analysis, with CD68 being the next most statistically robust, confirmation in independent patient datasets is the most important validation exercise to be carried out. CD20, PD1 and T-BET also provided prognostic information as single variables but were not included in any multivariate analysis. Multivariate analysis is often underpowered to detect significant differences between groups. When applying a Cox Proportional Hazards model to survival analysis, there must be sufficient numbers of events, for which each variable represents a hazard. Mathematical modelling has determined that there must be at least ten events for each variable under

consideration<sup>361</sup>. Relatively few patients die of CHL, and even using an outcome measure such as freedom from first line treatment failure (FFTF) for which there are more events, a very large patient cohort is required for there to be sufficient events to include more than a handful of markers as variables in such an analysis.

### **8.2.2 CHL can be discriminated from normal and other malignant tissue based only on the phenotype of the non-malignant CD4+ cell**

Chapter 6 demonstrated that CD4+ T cells derived from CHL-infiltrated lymph nodes could be discriminated from other reactive and malignant nodes by unsupervised hierarchical cluster analysis. *Post-hoc* analysis identified a subset of markers that are most discriminatory. While the freeze/thaw process undoubtedly alters cellular phenotype it is possible that this finding could be translated into a diagnostic test for CHL using a small number of fresh cells aspirated by FNA from a pathological lymph node<sup>498</sup>. This hypothesis remaining to be tested against a blinded sample of cells derived from fresh aspirated lymph nodes but a validation study could easily be carried out.

### **8.2.3 Appropriate T cell trafficking is essential to anti-CHL-immunity**

The major hypothesis arising from the model of T cell accumulation in CHL described in 8.1, is that non-specific naïve and central memory cells dominate the CHL microenvironment and may provide the cytokine, chemokine and cell membrane conveyed signals essential HRS survival. Should the accumulation of such T cells be prevented, by blocking key molecular mediators of trafficking to affected lymph nodes, then relapsed disease arising from the residual malignant precursor cells surviving primary therapy could be prevented. This could take the form of maintenance therapy in patients at high risk of relapse, using specific pharmacological blocking agents. Should the mediators of T cell trafficking be secreted systemically, as is likely, they may also provide early clinical indicators of relapse that may be detected at a stage where early therapeutic intervention could alter outcomes, or as an early assessment of treatment response at a point where intensification of therapy may be possible, as already explored clinically for TARC<sup>63</sup>.

Bioengineering tumour-specific cytotoxic T cells to encourage trafficking to affected nodes has already been proposed in the context of the TARC/CCR4 interaction, where

anti-CD30-specific cytotoxic T cells have been induced to express CCR4 and hence home preferentially to diseased nodes<sup>64</sup>. The relatively poor graft versus lymphoma response seen after most cases of allogeneic stem cell transplant for relapsed CHL<sup>509</sup> may be explained by failed T cell trafficking although newer approaches using T cell depletion and early donor lymphocyte infusion show promise<sup>441</sup>. *Ex vivo* expanded therapeutic T cells lose expression of CD62L and CCR7<sup>510</sup> hence if these markers are key to CHL-involved lymph node homing and are lost, donor effector T cells will fail to engage with their target. However, enhancement of expression of such molecules may come at the price of worsened GVHD<sup>511</sup>.

### **8.3 Th2 polarised cells are not an important part of the microenvironment**

The data presented in Chapter 6 failed to demonstrate any Th2-defining cytokine expression at baseline and only expression of both Th1 and Th2 defining cytokines once cells are activated and proliferated *in vitro*. This is consistent with the proliferating cells arising from a population of Th lineage-uncommitted naïve or memory T cells, which only express cytokine at meaningful levels once exposed to an *in vitro* stimulus. The absence of Th2-defining transcription factor expression by IHC demonstrated in Chapter 4 confirms a wider literature, in contrast to robust data supporting the presence of Th1-defining T-BET and IFN- $\gamma$  producing T cells in the microenvironment further supported by the experiments in Chapters 3, 6 and 7. Taken together, these data contest the hypothesis that the microenvironment is Th2-polarised. Hence this cannot be evoked as an explanation for its failure to eradicate the tumour.

### **8.4 Hypoproliferation, anergy and senescence are not characteristic of the microenvironment CD4+ T cell**

The experiments described in Chapter 5 demonstrated that CHL-derived CD4+ T cells proliferate well when exposed to IL2 and IL4 *in vitro*, better than benign node-derived cells, and probably than FL-derived cells, although there is also a highly proliferative component arising from the CD4+ T cell microenvironment of FL that warrants similar investigation. Increased sample number and possibly culture duration beyond 6 months is required to confirm this. Although these findings cannot directly refute the often cited

functional demonstration of hypoproliferation and anergy of Marshall et al<sup>299</sup> due to methodological differences, they certainly do not support it.

FOXP<sub>3</sub> and CCR<sub>4</sub> are indeed expressed at high levels in the microenvironment of CHL, confirmed here through IHC and flow cytometry respectively. However that these markers represent Tregs has neither been confirmed here nor in the literature and functional experiments using conventional suppressor assays are necessary, although other groups have found this technically challenging due to the small numbers of cells available<sup>377</sup>.

PD-L1 is certainly upregulated in the HRS<sup>334</sup> and its expression may be important to downstream survival pathways, with immunological evidence accumulating that PD1 to PD-L1 directional signalling promotes B cell survival<sup>283</sup>. However, the virtual absence of PD1 expression in the microenvironment, including the CD4+ component, argues against its importance in failed tumour clearance by mediating immunosuppression through PD-L1 to PD1 signalling.

## 8.5 Summary

Overall this work has contributed to the understanding of the role of the CD4+ T cell in the CHL microenvironment as a multipotential, central memory-like cell, arrested in function in the malignant lymph node yet capable of effector function and proliferation *in vitro*. Much validation work remains to be done, for the clinically translatable biomarkers, as well as the phenotyping and proliferation assays with increased sample numbers and refined fluorescent marker panels. There remains no satisfactory functional *ex vivo* or animal model of CHL in the context of its microenvironment available for pharmacological manipulation outside Phase 1 clinical trials in humans. There may well never be such a model, however progress will still be made as long as molecular mechanisms and networks of interactions can be measured, described, manipulated and interpreted with caution, scepticism and without preconceptions.

---

## Chapter 9: References

1. Steidl C, Connors JM, Gascoyne RD. Molecular Pathogenesis of Hodgkin's Lymphoma: Increasing Evidence of the Importance of the Microenvironment. *J Clin Oncol.* 2011 May 10;29(14):1812-26.
2. Rosenberg SA, Kaplan HS. Evidence for an orderly progression in the spread of Hodgkin's disease. *Cancer Res.* 1966 Jun;26(6):1225-31.
3. Mauch PM, Kalish LA, Kadin M, Coleman CN, Osteen R, Hellman S. Patterns of presentation of Hodgkin disease. Implications for etiology and pathogenesis. *Cancer.* 1993 Mar 15;71(6):2062-71.
4. SEER\*Stat Database. National Cancer Institute D, Surveillance Research Program, Cancer Statistics Branch. Surveillance, Epidemiology and End Results (SEER) Program. 2006.
5. Hu E, Hufford S, Lukes R, Bernstein-Singer M, Sobel G, Gill P, et al. Third-World Hodgkin's disease at Los Angeles County-University of Southern California Medical Center. *J Clin Oncol.* 1988 Aug;6(8):1285-92.
6. Macmahon B. Epidemiological evidence of the nature of Hodgkin's disease. *Cancer.* 1957 Sep-Oct;10(5):1045-54.
7. Hodgkin T. On some morbid appearances of the absorbent glands and spleen. *Med Chir Trans.* 1832(17):68.
8. Ziegler K. Die Hodgkinsche Krankheit. Jena: Gustav Fischer. 1911.
9. Viviani S, Zinzani PL, Rambaldi A, Brusamolino E, Levis A, Bonfante V, et al. ABVD versus BEACOPP for Hodgkin's lymphoma when high-dose salvage is planned. *N Engl J Med.* 2011 Jul 21;365(3):203-12.
10. Engert A, Diehl V, Franklin J, Lohri A, Dorken B, Ludwig WD, et al. Escalated-dose BEACOPP in the treatment of patients with advanced-stage Hodgkin's lymphoma: 10 years of follow-up of the GHSG HD9 study. *J Clin Oncol.* 2009 Sep 20;27(27):4548-54.
11. Engert A, Plutschow A, Eich HT, Lohri A, Dorken B, Borchmann P, et al. Reduced treatment intensity in patients with early-stage Hodgkin's lymphoma. *N Engl J Med.* 2010 Aug 12;363(7):640-52.
12. Greaves P, Wilson A, Matthews J, Brown DL, Auer R, Montoto S, et al. Early relapse and refractory disease remain risk factors in the anthracycline and autologous transplant era for patients with relapsed/refractory classical Hodgkin lymphoma: a single centre intention-to-treat analysis. *British journal of haematology.* 2012 Apr;157(2):201-4.
13. Jona A, Younes A. Novel treatment strategies for patients with relapsed classical Hodgkin lymphoma. *Blood Rev.* 2010 Nov;24(6):233-8.
14. Swerdlow AJ, Higgins CD, Smith P, Cunningham D, Hancock BW, Horwich A, et al. Second cancer risk after chemotherapy for Hodgkin's lymphoma: a collaborative British cohort study. *J Clin Oncol.* Nov 1;29(31):4096-104.
15. Ng AK, LaCasce A, Travis LB. Long-term complications of lymphoma and its treatment. *J Clin Oncol.* 2011 May 10;29(14):1885-92.
16. Hasenclever D, Diehl V. A prognostic score for advanced Hodgkin's disease. International Prognostic Factors Project on Advanced Hodgkin's Disease. *N Engl J Med.* 1998 Nov 19;339(21):1506-14.
17. Lister TA, Crowther D, Sutcliffe SB, Glatstein E, Canellos GP, Young RC, et al. Report of a committee convened to discuss the evaluation and staging of patients with Hodgkin's disease: Cotswolds meeting. *J Clin Oncol.* 1989 Nov;7(11):1630-6.
18. Pinkus GS, Said JW. Hodgkin's disease, lymphocyte predominance type, nodular--a distinct entity? Unique staining profile for L&H variants of Reed-Sternberg cells defined by monoclonal antibodies to leukocyte common antigen, granulocyte-specific antigen, and B-cell-specific antigen. *Am J Pathol.* 1985 Jan;118(1):1-6.
19. Brune V, Tiacci E, Pfeil I, Doring C, Eckerle S, van Noesel CJ, et al. Origin and pathogenesis of nodular lymphocyte-predominant Hodgkin lymphoma as revealed by global gene expression analysis. *J Exp Med.* 2008 Sep 29;205(10):2251-68.

- 
20. Orlandi E, Lazzarino M, Brusamolino E, Paulli M, Astori C, Magrini U, et al. Nodular lymphocyte predominance Hodgkin's disease: long-term observation reveals a continuous pattern of recurrence. *Leuk Lymphoma*. 1997 Jul;26(3-4):359-68.
  21. Küppers R, Rajewsky K, Zhao M, Simons G, Laumann R, Fischer R, et al. Hodgkin disease: Hodgkin and Reed-Sternberg cells picked from histological sections show clonal immunoglobulin gene rearrangements and appear to be derived from B cells at various stages of development. *Proc Natl Acad Sci USA*. 1994 Nov 8;91(23):10962-6.
  22. Stein H, Marafioti T, Foss HD, Laumen H, Hummel M, Anagnostopoulos I, et al. Down-regulation of BOB.1/OBF.1 and Oct2 in classical Hodgkin disease but not in lymphocyte predominant Hodgkin disease correlates with immunoglobulin transcription. *Blood*. 2001 Jan 15;97(2):496-501.
  23. Ushmorov A, Leithäuser F, Sakk O, Weinhäusel A, Popov SW, Möller P, et al. Epigenetic processes play a major role in B-cell-specific gene silencing in classical Hodgkin lymphoma. *Blood*. 2006 Mar 15;107(6):2493-500.
  24. Schwering I, Bräuninger A, Klein U, Jungnickel B, Tinguely M, Diehl V, et al. Loss of the B-lineage-specific gene expression program in Hodgkin and Reed-Sternberg cells of Hodgkin lymphoma. *Blood*. 2003 Feb 15;101(4):1505-12.
  25. Küppers R. The biology of Hodgkin's lymphoma. *Nat Rev Cancer*. 2009 Jan 1;9(1):15-27.
  26. Küpper M, Joos S, von Bonin F, Daus H, Pfreundschuh M, Lichter P, et al. MDM2 gene amplification and lack of p53 point mutations in Hodgkin and Reed-Sternberg cells: results from single-cell polymerase chain reaction and molecular cytogenetic studies. *Br J Haematol*. 2001 Mar 1;112(3):768-75.
  27. Montesinos-Rongen M, Roers A, Küppers R, Rajewsky K, Hansmann ML. Mutation of the p53 gene is not a typical feature of Hodgkin and Reed-Sternberg cells in Hodgkin's disease. *Blood*. 1999 Sep 1;94(5):1755-60.
  28. Feuerborn A, Möritz C, Von Bonin F, Döbelstein M, Trümper L, Stürzenhofecker B, et al. Dysfunctional p53 deletion mutants in cell lines derived from Hodgkin's lymphoma. *Leuk Lymphoma*. 2006 Sep 1;47(9):1932-40.
  29. Martín-Subero JI, Gesk S, Harder L, Sonoki T, Tucker PW, Schlegelberger B, et al. Recurrent involvement of the REL and BCL11A loci in classical Hodgkin lymphoma. *Blood*. 2002 Feb 15;99(4):1474-7.
  30. Emmerich F, Meiser M, Hummel M, Demel G, Foss HD, Jundt F, et al. Overexpression of I kappa B alpha without inhibition of NF-kappaB activity and mutations in the I kappa B alpha gene in Reed-Sternberg cells. *Blood*. 1999 Nov 1;94(9):3129-34.
  31. Emmerich F, Theurich S, Hummel M, Haeffker A, Vry MS, Döhner K, et al. Inactivating I kappa B epsilon mutations in Hodgkin/Reed-Sternberg cells. *J Pathol*. 2003 Nov 1;201(3):413-20.
  32. Martín-Subero JI, Włodarska I, Bastard C, Picquenot J-M, Höppner J, Giefing M, et al. Chromosomal rearrangements involving the BCL3 locus are recurrent in classical Hodgkin and peripheral T-cell lymphoma. *Blood*. 2006 Jul 1;108(1):401-2; author reply 2-3.
  33. Joos S, Küpper M, Ohl S, von Bonin F, Mechttersheimer G, Bentz M, et al. Genomic imbalances including amplification of the tyrosine kinase gene JAK2 in CD30+ Hodgkin cells. *Cancer Research*. 2000 Feb 1;60(3):549-52.
  34. Weniger MA, Melzner I, Menz CK, Wegener S, Bucur AJ, Dorsch K, et al. Mutations of the tumor suppressor gene SOCS-1 in classical Hodgkin lymphoma are frequent and associated with nuclear phospho-STAT5 accumulation. *Oncogene*. 2006 Apr 27;25(18):2679-84.
  35. Kilger E, Kieser A, Baumann M, Hammerschmidt W. Epstein-Barr virus-mediated B-cell proliferation is dependent upon latent membrane protein 1, which simulates an activated CD40 receptor. *EMBO J*. 1998 Mar 16;17(6):1700-9.
  36. Prehn RT, Main JM. Immunity to methylcholanthrene-induced sarcomas. *J Natl Cancer Inst*. 1957 Jun 1;18(6):769-78.
  37. Klein G, Sjogren HO, Klein E, Hellstrom KE. Demonstration of resistance against methylcholanthrene-induced sarcomas in the primary autochthonous host. *Cancer Research*. 1960 Dec 1;20:1561-72.
-

- 
38. Van Pel A, Vessière F, Boon T. Protection against two spontaneous mouse leukemias conferred by immunogenic variants obtained by mutagenesis. *J Exp Med.* 1983 Jun 1;157(6):1992-2001.
  39. van der Bruggen P, Traversari C, Chomez P, Lurquin C, De Plaen E, Van den Eynde B, et al. A gene encoding an antigen recognized by cytolytic T lymphocytes on a human melanoma. *Science.* 1991 Dec 13;254(5038):1643-7.
  40. Dunn GP, Bruce AT, Ikeda H, Old LJ, Schreiber RD. Cancer immunoediting: from immunosurveillance to tumor escape. *Nat Immunol.* 2002 Nov 1;3(11):991-8.
  41. Sartoris S, Cavallero P, Pegoraro L, Vergnano F, Fazio M. The absence of lymphocyte response in vitro to tuberculin challenge in Hodgkin's disease. *Panminerva medica.* 1965 Oct 1;7(10):370-2.
  42. Han T, Sokal JE. Lymphocyte response to phytohemagglutinin in Hodgkin's disease. *Am J Med.* 1970 Jun 1;48(6):728-34.
  43. Case DC, Hansen JA, Corrales E, Young CW, Dupont B, Pinsky CM, et al. Depressed in vitro lymphocyte responses to PHA in patients with Hodgkin disease in continuous long remissions. *Blood.* 1977 May 1;49(5):771-8.
  44. Condeelis J, Pollard JW. Macrophages: obligate partners for tumor cell migration, invasion, and metastasis. *Cell.* 2006 Jan 27;124(2):263-6.
  45. Willenbrock K, Roers A, Blohbaum B, Rajewsky K, Hansmann ML. CD8(+) T cells in Hodgkin's disease tumor tissue are a polyclonal population with limited clonal expansion but little evidence of selection by antigen. *Am J Pathol.* 2000 Jul;157(1):171-5.
  46. Atayar C, van den Berg A, Blokzijl T, Boot M, Gascoyne RD, Visser L, et al. Hodgkin's lymphoma associated T-cells exhibit a transcription factor profile consistent with distinct lymphoid compartments. *Journal of Clinical Pathology.* 2007 Oct 1;60(10):1092-7.
  47. Poppema S. The nature of the lymphocytes surrounding Reed-Sternberg cells in nodular lymphocyte predominance and in other types of Hodgkin's disease. *Am J Pathol.* 1989 Aug;135(2):351-7.
  48. Newcom SR, Ansari AA, Gu L. Interleukin-4 is an autocrine growth factor secreted by the L-428 Reed-Sternberg cell. *Blood.* 1992 Jan 1;79(1):191-7.
  49. Merz H, Flidner A, Orscheschek K, Binder T, Sebald W, Müller-Hermelink HK, et al. Cytokine expression in T-cell lymphomas and Hodgkin's disease. Its possible implication in autocrine or paracrine production as a potential basis for neoplastic growth. *Am J Pathol.* 1991 Nov 1;139(5):1173-80.
  50. Kawakami M, Kawakami K, Kioi M, Leland P, Puri RK. Hodgkin lymphoma therapy with interleukin-4 receptor-directed cytotoxin in an infiltrating animal model. *Blood.* 2005 May 1;105(9):3707-13.
  51. Hsu SM, Xie SS, Hsu PL, Waldron JA. Interleukin-6, but not interleukin-4, is expressed by Reed-Sternberg cells in Hodgkin's disease with or without histologic features of Castleman's disease. *Am J Pathol.* 1992 Jul 1;141(1):129-38.
  52. Herbst H, Foss HD, Samol J, Araujo I, Klotzbach H, Krause H, et al. Frequent expression of interleukin-10 by Epstein-Barr virus-harboring tumor cells of Hodgkin's disease. *Blood.* 1996 Apr 1;87(7):2918-29.
  53. Skinnider BF, Elia AJ, Gascoyne RD, Patterson B, Trümper L, Kapp U, et al. Signal transducer and activator of transcription 6 is frequently activated in Hodgkin and Reed-Sternberg cells of Hodgkin lymphoma. *Blood.* 2002 Jan 15;99(2):618-26.
  54. Kapp U, Yeh WC, Patterson B, Elia AJ, Kägi D, Ho A, et al. Interleukin 13 is secreted by and stimulates the growth of Hodgkin and Reed-Sternberg cells. *J Exp Med.* 1999 Jun 21;189(12):1939-46.
  55. Skinnider BF, Elia AJ, Gascoyne RD, Trümper LH, von Bonin F, Kapp U, et al. Interleukin 13 and interleukin 13 receptor are frequently expressed by Hodgkin and Reed-Sternberg cells of Hodgkin lymphoma. *Blood.* 2001 Jan 1;97(1):250-5.
  56. Ohshima K, Akaiwa M, Umeshita R, Suzumiya J, Izuhara K, Kikuchi M. Interleukin-13 and interleukin-13 receptor in Hodgkin's disease: possible autocrine mechanism and involvement in fibrosis. *Histopathology.* 2001 Apr 1;38(4):368-75.
-

- 
57. Samoszuk M, Nansen L. Detection of interleukin-5 messenger RNA in Reed-Sternberg cells of Hodgkin's disease with eosinophilia. *Blood*. 1990 Jan 1;75(1):13-6.
  58. Jücker M, Abts H, Li W, Schindler R, Merz H, Günther A, et al. Expression of interleukin-6 and interleukin-6 receptor in Hodgkin's disease. *Blood*. 1991 Jun 1;77(11):2413-8.
  59. Klein S, Jücker M, Diehl V, Tesch H. Production of multiple cytokines by Hodgkin's disease derived cell lines. *Hematol Oncol*. 1992 Jan 1;10(6):319-29.
  60. Skinnider BF. The role of cytokines in classical Hodgkin lymphoma. *Blood*. 2002 May 29;99(12):4283-97.
  61. Van Den Berg A, Visser L, Poppema S. High expression of the CC chemokine TARC in Reed-Sternberg cells. A possible explanation for the characteristic T-cell infiltrate in Hodgkin's lymphoma. *Am J Pathol*. 1999 Jun 1;154(6):1685-91.
  62. Imai T, Baba M, Nishimura M, Kakizaki M, Takagi S, Yoshie O. The T cell-directed CC chemokine TARC is a highly specific biological ligand for CC chemokine receptor 4. *J Biol Chem*. 1997 Jun 6;272(23):15036-42.
  63. Weihrauch MR, Manzke O, Beyer M, Haverkamp H, Diehl V, Bohlen H, et al. Elevated serum levels of CC thymus and activation-related chemokine (TARC) in primary Hodgkin's disease: potential for a prognostic factor. *Cancer Research*. 2005 Jul 1;65(13):5516-9.
  64. Di Stasi A, De Angelis B, Rooney CM, Zhang L, Mahendravada A, Foster AE, et al. T lymphocytes coexpressing CCR4 and a chimeric antigen receptor targeting CD30 have improved homing and antitumor activity in a Hodgkin tumor model. *Blood*. 2009 Jun 18;113(25):6392-402.
  65. Hedvat CV, Jaffe ES, Qin J, Filippa DA, Cordon-Cardo C, Tosato G, et al. Macrophage-derived chemokine expression in classical Hodgkin's lymphoma: application of tissue microarrays. *Mod Pathol*. 2001 Dec 1;14(12):1270-6.
  66. Maggio EM, Van Den Berg A, Visser L, Diepstra A, Kluiver J, Emmens R, et al. Common and differential chemokine expression patterns in rs cells of NLP, EBV positive and negative classical Hodgkin lymphomas. *Int J Cancer*. 2002 Jun 10;99(5):665-72.
  67. Sallusto F, Mackay CR, Lanzavecchia A. Selective expression of the eotaxin receptor CCR3 by human T helper 2 cells. *Science*. 1997 Sep 26;277(5334):2005-7.
  68. Ponath PD, Qin S, Post TW, Wang J, Wu L, Gerard NP, et al. Molecular cloning and characterization of a human eotaxin receptor expressed selectively on eosinophils. *J Exp Med*. 1996 Jun 1;183(6):2437-48.
  69. Lamprecht B, Kreher S, Anagnostopoulos I, Johrens K, Monteleone G, Jundt F, et al. Aberrant expression of the Th2 cytokine IL-21 in Hodgkin lymphoma cells regulates STAT3 signaling and attracts Treg cells via regulation of MIP-3alpha. *Blood*. 2008 Oct 15;112(8):3339-47.
  70. Kleinewietfeld M, Puentes F, Borsellino G, Battistini L, Röttschke O, Falk K. CCR6 expression defines regulatory effector/memory-like cells within the CD25(+)CD4+ T-cell subset. *Blood*. 2005 Apr 1;105(7):2877-86.
  71. Anderson MW, Zhao S, Ai WZ, Tibshirani R, Levy R, Lossos IS, et al. C-C chemokine receptor 1 expression in human hematolymphoid neoplasia. *Am J Clin Pathol*. 2010 Mar;133(3):473-83.
  72. Bonecchi R, Bianchi G, Bordignon PP, D'Ambrosio D, Lang R, Borsatti A, et al. Differential expression of chemokine receptors and chemotactic responsiveness of type 1 T helper cells (Th1s) and Th2s. *J Exp Med*. 1998 Jan 5;187(1):129-34.
  73. Hopken UE. Up-regulation of the chemokine receptor CCR7 in classical but not in lymphocyte-predominant Hodgkin disease correlates with distinct dissemination of neoplastic cells in lymphoid organs. *Blood*. 2002 Feb 15;99(4):1109-16.
  74. Mitchell GF, Miller JF. Cell to cell interaction in the immune response. II. The source of hemolysin-forming cells in irradiated mice given bone marrow and thymus or thoracic duct lymphocytes. *J Exp Med*. 1968 Oct 1;128(4):821-37.
  75. Schimpl A, Wecker E. Replacement of T-cell function by a T-cell product. *Nature New Biol*. 1972 May 3;237(70):15-7.
  76. Noelle RJ, Daum J, Bartlett WC, McCann J, Shepherd DM. Cognate interactions between helper T cells and B cells. V. Reconstitution of T helper cell function using purified plasma membranes from activated Th1 and Th2 T helper cells and lymphokines. *J Immunol*. 1991 Feb 15;146(4):1118-24.
-



- 
77. DeFranco AL, Ashwell JD, Schwartz RH, Paul WE. Polyclonal stimulation of resting B lymphocytes by antigen-specific T lymphocytes. *J Exp Med*. 1984 Mar 1;159(3):861-80.
78. Tse HY, Mond JJ, Paul WE. T lymphocyte-dependent B lymphocyte proliferative response to antigen. I Genetic restriction of the stimulation of B lymphocyte proliferation. *J Exp Med*. 1981 Apr 1;153(4):871-82.
79. Bartlett WC, McCann J, Shepherd DM, Roy M, Noelle RJ. Cognate interactions between helper T cells and B cells. IV. Requirements for the expression of effector phase activity by helper T cells. *J Immunol*. 1990 Dec 15;145(12):3956-62.
80. Ohara J, Paul WE. Receptors for B-cell stimulatory factor-1 expressed on cells of haematopoietic lineage. *Nature*. 1987 Jan 1;325(6104):537-40.
81. Prakash S, Robb RJ, Stout RD, Parker DC. Induction of high affinity IL 2 receptors on B cells responding to anti-Ig and T cell-derived helper factors. *J Immunol*. 1985 Jul 1;135(1):117-22.
82. Mond JJ, Seghal E, Kung J, Finkelman FD. Increased expression of I-region-associated antigen (Ia) on B cells after cross-linking of surface immunoglobulin. *J Immunol*. 1981 Sep 1;127(3):881-8.
83. Weaver CT, Hawrylowicz CM, Unanue ER. T helper cell subsets require the expression of distinct costimulatory signals by antigen-presenting cells. *Proc Natl Acad Sci USA*. 1988 Nov 1;85(21):8181-5.
84. Clark EA, Ledbetter JA, Holly RC, Dinndorf PA, Shu G. Polypeptides on human B lymphocytes associated with cell activation. *Hum Immunol*. 1986 May 1;16(1):100-13.
85. Green I, Paul WE, Benacerraf B. Genetic control of immunological responsiveness in guinea pigs to 2,4-dinitrophenyl conjugates of poly-L-arginine, protamine, and poly-L-ornithine. *Proc Natl Acad Sci USA*. 1969 Nov 1;64(3):1095-102.
86. Paul WE, Benacerraf B. Functional specificity of thymus- dependent lymphocytes. *Science*. 1977 Mar 25;195(4284):1293-300.
87. Hünig T, Schimpl A. Studies on the generation and expression of H-2-controlled T helper function in chimeric mice: evidence for two levels of H-2 restriction. *Eur J Immunol*. 1979 Sep 1;9(9):730-6.
88. Jones B, Janeway CA. Cooperative interaction of B lymphocytes with antigen-specific helper T lymphocytes is MHC restricted. *Nature*. 1981 Aug 6;292(5823):547-9.
89. Pierce CW, Kapp JA, Benacerraf B. Regulation by the H-2 gene complex of macrophage-lymphoid cell interactions in secondary antibody responses in vitro. *J Exp Med*. 1976 Aug 1;144(2):371-81.
90. Leclercq L, Cambier JC, Mishal Z, Julius MH, Theze J. Supernatant from a cloned helper T cell stimulates most small resting B cells to undergo increased I-A expression, blastogenesis, and progression through cell cycle. *J Immunol*. 1986 Jan;136(2):539-45.
91. Coffman RL, Seymour BW, Leberman DA, Hiraki DD, Christiansen JA, Shrader B, et al. The role of helper T cell products in mouse B cell differentiation and isotype regulation. *Immunol Rev*. 1988 Feb;102:5-28.
92. Rizzo LV, DeKruyff RH, Umetsu DT. Generation of B cell memory and affinity maturation. Induction with Th1 and Th2 T cell clones. *J Immunol*. 1992 Jun 15;148(12):3733-9.
93. Chartash EK, Imai A, Gershengorn MC, Crow MK, Friedman SM. Direct human T helper cell-induced B cell activation is not mediated by inositol lipid hydrolysis. *J Immunol*. 1988 Mar 15;140(6):1974-81.
94. Ledbetter JA, Shu G, Gallagher M, Clark EA. Augmentation of normal and malignant B cell proliferation by monoclonal antibody to the B cell-specific antigen BP50 (CDW40). *J Immunol*. 1987 Feb 1;138(3):788-94.
95. Armitage RJ, Fanslow WC, Strockbine L, Sato TA, Clifford KN, Macduff BM, et al. Molecular and biological characterization of a murine ligand for CD40. *Nature*. 1992 May 7;357(6373):80-2.
96. Noelle RJ, Roy M, Shepherd DM, Stamenkovic I, Ledbetter JA, Aruffo A. A 39-kDa protein on activated helper T cells binds CD40 and transduces the signal for cognate activation of B cells. *Proc Natl Acad Sci USA*. 1992 Jul 15;89(14):6550-4.
97. Spriggs MK, Armitage RJ, Strockbine L, Clifford KN, Macduff BM, Sato TA, et al. Recombinant human CD40 ligand stimulates B cell proliferation and immunoglobulin E secretion. *J Exp Med*. 1992 Dec 1;176(6):1543-50.
-

- 
98. Martin PJ, Ledbetter JA, Morishita Y, June CH, Beatty PG, Hansen JA. A 44 kilodalton cell surface homodimer regulates interleukin 2 production by activated human T lymphocytes. *J Immunol.* 1986 May 1;136(9):3282-7.
  99. Freedman AS, Freeman G, Horowitz JC, Daley J, Nadler LM. B7, a B-cell-restricted antigen that identifies preactivated B cells. *J Immunol.* 1987 Nov 15;139(10):3260-7.
  100. Yokochi T, Holly RD, Clark EA. B lymphoblast antigen (BB-1) expressed on Epstein-Barr virus-activated B cell blasts, B lymphoblastoid cell lines, and Burkitt's lymphomas. *J Immunol.* 1982 Feb 1;128(2):823-7.
  101. Linsley PS, Clark EA, Ledbetter JA. T-cell antigen CD28 mediates adhesion with B cells by interacting with activation antigen B7/BB-1. *Proc Natl Acad Sci USA.* 1990 Jul 1;87(13):5031-5.
  102. Gimmi CD, Freeman GJ, Gribben JG, Sugita K, Freedman AS, Morimoto C, et al. B-cell surface antigen B7 provides a costimulatory signal that induces T cells to proliferate and secrete interleukin 2. *Proc Natl Acad Sci USA.* 1991 Aug 1;88(15):6575-9.
  103. Freeman GJ, Gribben JG, Bousiotis VA, Ng JW, Restivo VA, Jr., Lombard LA, et al. Cloning of B7-2: a CTLA-4 counter-receptor that costimulates human T cell proliferation. *Science.* 1993 Nov 5;262(5135):909-11.
  104. Lenschow DJ, Su GH, Zuckerman LA, Nabavi N, Jellis CL, Gray GS, et al. Expression and functional significance of an additional ligand for CTLA-4. *Proc Natl Acad Sci USA.* 1993 Dec 1;90(23):11054-8.
  105. Hutloff A, Dittrich AM, Beier KC, Eljaschewitsch B, Kraft R, Anagnostopoulos I, et al. ICOS is an inducible T-cell co-stimulator structurally and functionally related to CD28. *Nature.* 1999 Jan 21;397(6716):263-6.
  106. Wang S, Zhu G, Chapoval AI, Dong H, Tamada K, Ni J, et al. Costimulation of T cells by B7-H2, a B7-like molecule that binds ICOS. *Blood.* 2000 Oct 15;96(8):2808-13.
  107. Ling V, Wu PW, Finnerty HF, Bean KM, Spaulding V, Fouser LA, et al. Cutting edge: identification of GL50, a novel B7-like protein that functionally binds to ICOS receptor. *J Immunol.* 2000 Feb 15;164(4):1653-7.
  108. Tafuri A, Shahinian A, Bladt F, Yoshinaga SK, Jordana M, Wakeham A, et al. ICOS is essential for effective T-helper-cell responses. *Nature.* 2001 Jan 4;409(6816):105-9.
  109. Mak TW, Shahinian A, Yoshinaga SK, Wakeham A, Boucher L-M, Pintilie M, et al. Costimulation through the inducible costimulator ligand is essential for both T helper and B cell functions in T cell-dependent B cell responses. *Nat Immunol.* 2003 Aug 1;4(8):765-72.
  110. Van Gool SW, Delabie J, Vandenberghe P, Coorevits L, De Wolf-Peeters C, Ceuppens JL. Expression of B7-2 (CD86) molecules by Reed-Sternberg cells of Hodgkin's disease. *Leukemia.* 1997 Jun 1;11(6):846-51.
  111. Stein H, Gerdes J, Schwab U, Lemke H, Diehl V, Mason DY, et al. Evidence for the detection of the normal counterpart of Hodgkin and Sternberg-Reed cells. *Hematol Oncol.* 1983 Jan 1;1(1):21-9.
  112. Schwab U, Stein H, Gerdes J, Lemke H, Kirchner H, Schaadt M, et al. Production of a monoclonal antibody specific for Hodgkin and Sternberg-Reed cells of Hodgkin's disease and a subset of normal lymphoid cells. *Nature.* 1982 Sep 2;299(5878):65-7.
  113. Carbone A, Ghoghini A, Gattei V, Aldinucci D, Degan M, De Paoli P, et al. Expression of functional CD40 antigen on Reed-Sternberg cells and Hodgkin's disease cell lines. *Blood.* 1995 Feb 1;85(3):780-9.
  114. Ma Y, Visser L, Blokzijl T, Harms G, Atayar C, Poppema S, et al. The CD4+CD26- T-cell population in classical Hodgkin's lymphoma displays a distinctive regulatory T-cell profile. *Lab Invest.* 2008 May;88(5):482-90.
  115. Xerri L, Carbuca N, Parc P, Hassoun J, Birg F. Frequent expression of FAS/APO-1 in Hodgkin's disease and anaplastic large cell lymphomas. *Histopathology.* 1995 Sep 1;27(3):235-41.
  116. Steidl C, Lee T, Shah SP, Farinha P, Han G, Nayar T, et al. Tumor-associated macrophages and survival in classic Hodgkin's lymphoma. *N Engl J Med.* 2010 Mar 11;362(10):875-85.
  117. Buglio D, Khaskhely NM, Voo KS, Martinez-Valdez H, Liu Y-J, Younes A. HDAC11 plays an essential role in regulating OX40 ligand expression in Hodgkin lymphoma. *Blood.* 2011 Mar 10;117(10):2910-7.
-

- 
118. Yamamoto R, Nishikori M, Kitawaki T, Sakai T, Hishizawa M, Tashima M, et al. PD-1-PD-1 ligand interaction contributes to immunosuppressive microenvironment of Hodgkin lymphoma. *Blood*. 2008 Mar 15;111(6):3220-4.
119. Fiumara P, Snell V, Li Y, Mukhopadhyay A, Younes M, Gillenwater AM, et al. Functional expression of receptor activator of nuclear factor kappaB in Hodgkin disease cell lines. *Blood*. 2001 Nov 1;98(9):2784-90.
120. von Andrian UH, Mempel TR. Homing and cellular traffic in lymph nodes. *Nat Rev Immunol*. 2003 Nov;3(11):867-78.
121. Kelsoe G. Life and death in germinal centers (redux). *Immunity*. 1996 Feb 1;4(2):107-11.
122. Garside P, Ingulli E, Merica RR, Johnson JG, Noelle RJ, Jenkins MK. Visualization of specific B and T lymphocyte interactions in the lymph node. *Science*. 1998 Jul 3;281(5373):96-9.
123. Reif K, Ekland EH, Ohl L, Nakano H, Lipp M, Förster R, et al. Balanced responsiveness to chemoattractants from adjacent zones determines B-cell position. *Nature*. 2002 Mar 7;416(6876):94-9.
124. Förster R, Schubel A, Breitfeld D, Kremmer E, Renner-Müller I, Wolf E, et al. CCR7 coordinates the primary immune response by establishing functional microenvironments in secondary lymphoid organs. *Cell*. 1999 Oct 1;99(1):23-33.
125. Förster R, Mattis AE, Kremmer E, Wolf E, Brem G, Lipp M. A putative chemokine receptor, BLR1, directs B cell migration to defined lymphoid organs and specific anatomic compartments of the spleen. *Cell*. 1996 Dec 13;87(6):1037-47.
126. EISEN HN, SISKIND GW. VARIATIONS IN AFFINITIES OF ANTIBODIES DURING THE IMMUNE RESPONSE. *Biochemistry*. 1964 Jul 1;3:996-1008.
127. Bernard O, Hozumi N, Tonegawa S. Sequences of mouse immunoglobulin light chain genes before and after somatic changes. *Cell*. 1978 Dec 1;15(4):1133-44.
128. Jacob J, Kelsoe G, Rajewsky K, Weiss U. Intracloonal generation of antibody mutants in germinal centres. *Nature*. 1991 Dec 5;354(6352):389-92.
129. Wang Y, Huang G, Wang J, Molina H, Chaplin DD, Fu YX. Antigen persistence is required for somatic mutation and affinity maturation of immunoglobulin. *Eur J Immunol*. 2000 Aug 1;30(8):2226-34.
130. Allen CDC, Okada T, Tang HL, Cyster JG. Imaging of germinal center selection events during affinity maturation. *Science*. 2007 Jan 26;315(5811):528-31.
131. MacLennan IC. Germinal centers. *Annu Rev Immunol*. 1994;12:117-39.
132. Hannum LG, Haberman AM, Anderson SM, Shlomchik MJ. Germinal center initiation, variable gene region hypermutation, and mutant B cell selection without detectable immune complexes on follicular dendritic cells. *J Exp Med*. 2000 Oct 2;192(7):931-42.
133. Hauser AE, Junt T, Mempel TR, Sneddon MW, Kleinstein SH, Henrickson SE, et al. Definition of germinal-center B cell migration in vivo reveals predominant intrazonal circulation patterns. *Immunity*. 2007 May;26(5):655-67.
134. MacLennan IC, Gulbranson-Judge A, Toellner KM, Casamayor-Palleja M, Chan E, Sze DM, et al. The changing preference of T and B cells for partners as T-dependent antibody responses develop. *Immunol Rev*. 1997 Apr 1;156:53-66.
135. Okada T, Miller MJ, Parker I, Krummel MF, Neighbors M, Hartley SB, et al. Antigen-engaged B cells undergo chemotaxis toward the T zone and form motile conjugates with helper T cells. *PLoS Biol*. 2005 Jun 1;3(6):e150.
136. Iezzi G, Karjalainen K, Lanzavecchia A. The duration of antigenic stimulation determines the fate of naive and effector T cells. *Immunity*. 1998 Jan 1;8(1):89-95.
137. Gaspal FMC, McConnell FM, Kim M-Y, Gray D, Kosco-Vilbois MH, Raykundalia CR, et al. The generation of thymus-independent germinal centers depends on CD40 but not on CD154, the T cell-derived CD40-ligand. *Eur J Immunol*. 2006 Jul 1;36(7):1665-73.
138. Basso K, Klein U, Niu H, Stolovitzky GA, Tu Y, Califano A, et al. Tracking CD40 signaling during germinal center development. *Blood*. 2004 Dec 15;104(13):4088-96.
139. Shiku H, Kisielow P, Bean MA, Takahashi T, Boyse EA, Oettgen HF, et al. Expression of T-cell differentiation antigens on effector cells in cell-mediated cytotoxicity in vitro. Evidence for functional heterogeneity related to the surface phenotype of T cells. *J Exp Med*. 1975 Jan 1;141(1):227-41.
-

- 
140. Constant S, Pfeiffer C, Woodard A, Pasqualini T, Bottomly K. Extent of T cell receptor ligation can determine the functional differentiation of naive CD4+ T cells. *J Exp Med*. 1995 Nov 1;182(5):1591-6.
141. Yang J, Zhu H, Murphy TL, Ouyang W, Murphy KM. IL-18-stimulated GADD45 beta required in cytokine-induced, but not TCR-induced, IFN-gamma production. *Nat Immunol*. 2001 Feb 1;2(2):157-64.
142. Amsen D, Blander JM, Lee GR, Tanigaki K, Honjo T, Flavell RA. Instruction of distinct CD4 T helper cell fates by different notch ligands on antigen-presenting cells. *Cell*. 2004 May 14;117(4):515-26.
143. Berard M, Tough DF. Qualitative differences between naive and memory T cells. *Immunology*. 2002 Jun;106(2):127-38.
144. McKinstry KK, Strutt TM, Swain SL. Regulation of CD4+ T-cell contraction during pathogen challenge. *Immunol Rev*. 2010 Jul;236:110-24.
145. Sallusto F, Lenig D, Forster R, Lipp M, Lanzavecchia A. Two subsets of memory T lymphocytes with distinct homing potentials and effector functions. *Nature*. 1999 Oct 14;401(6754):708-12.
146. Ahmed R, Bevan MJ, Reiner SL, Fearon DT. The precursors of memory: models and controversies. *Nat Rev Immunol*. 2009 Sep;9(9):662-8.
147. Tada T, Takemori T, Okumura K, Nonaka M, Tokuhisa T. Two distinct types of helper T cells involved in the secondary antibody response: independent and synergistic effects of Ia- and Ia+ helper T cells. *J Exp Med*. 1978 Feb 1;147(2):446-58.
148. Holling TM, Schooten E, van Den Elsen PJ. Function and regulation of MHC class II molecules in T-lymphocytes: of mice and men. *Hum Immunol*. 2004 Apr 1;65(4):282-90.
149. Mosmann TR, Cherwinski H, Bond MW, Giedlin MA, Coffman RL. Two types of murine helper T cell clone. I. Definition according to profiles of lymphokine activities and secreted proteins. *J Immunol*. 1986 Apr 1;136(7):2348-57.
150. Noma Y, Sideras P, Naito T, Bergstedt-Lindquist S, Azuma C, Severinson E, et al. Cloning of cDNA encoding the murine IgG1 induction factor by a novel strategy using SP6 promoter. *Nature*. 1986 Jan 1;319(6055):640-6.
151. Swain SL, Weinberg AD, English M, Huston G. IL-4 directs the development of Th2-like helper effectors. *J Immunol*. 1990 Dec 1;145(11):3796-806.
152. Le Gros G, Ben-Sasson SZ, Seder R, Finkelman FD, Paul WE. Generation of interleukin 4 (IL-4)-producing cells in vivo and in vitro: IL-2 and IL-4 are required for in vitro generation of IL-4-producing cells. *J Exp Med*. 1990 Sep 1;172(3):921-9.
153. Seder RA, Gazzinelli R, Sher A, Paul WE. Interleukin 12 acts directly on CD4+ T cells to enhance priming for interferon gamma production and diminishes interleukin 4 inhibition of such priming. *Proc Natl Acad Sci USA*. 1993 Nov 1;90(21):10188-92.
154. Chan SH, Perussia B, Gupta JW, Kobayashi M, Pospisil M, Young HA, et al. Induction of interferon gamma production by natural killer cell stimulatory factor: characterization of the responder cells and synergy with other inducers. *J Exp Med*. 1991 Apr 1;173(4):869-79.
155. Wolf SF, Temple PA, Kobayashi M, Young D, Dicig M, Lowe L, et al. Cloning of cDNA for natural killer cell stimulatory factor, a heterodimeric cytokine with multiple biologic effects on T and natural killer cells. *J Immunol*. 1991 May 1;146(9):3074-81.
156. Behin R, Mauel J, Sordat B. *Leishmania tropica*: pathogenicity and in vitro macrophage function in strains of inbred mice. *Exp Parasitol*. 1979 Aug 1;48(1):81-91.
157. Heinzel FP, Sadick MD, Holaday BJ, Coffman RL, Locksley RM. Reciprocal expression of interferon gamma or interleukin 4 during the resolution or progression of murine leishmaniasis. Evidence for expansion of distinct helper T cell subsets. *J Exp Med*. 1989 Jan 1;169(1):59-72.
158. Holaday BJ, Sadick MD, Wang ZE, Reiner SL, Heinzel FP, Parslow TG, et al. Reconstitution of *Leishmania* immunity in severe combined immunodeficient mice using Th1- and Th2-like cell lines. *J Immunol*. 1991 Sep 1;147(5):1653-8.
159. Jacobson NG, Szabo SJ, Weber-Nordt RM, Zhong Z, Schreiber RD, Darnell JE, et al. Interleukin 12 signaling in T helper type 1 (Th1) cells involves tyrosine phosphorylation of signal transducer and activator of transcription (Stat)3 and Stat4. *J Exp Med*. 1995 May 1;181(5):1755-62.
-

- 
160. Hou J, Schindler U, Henzel WJ, Ho TC, Brasseur M, McKnight SL. An interleukin-4-induced transcription factor: IL-4 Stat. *Science*. 1994 Sep 16;265(5179):1701-6.
161. Kaplan MH, Sun YL, Hoey T, Grusby MJ. Impaired IL-12 responses and enhanced development of Th2 cells in Stat4-deficient mice. *Nature*. 1996 Jul 11;382(6587):174-7.
162. Thierfelder WE, van Deursen JM, Yamamoto K, Tripp RA, Sarawar SR, Carson RT, et al. Requirement for Stat4 in interleukin-12-mediated responses of natural killer and T cells. *Nature*. 1996 Jul 11;382(6587):171-4.
163. Zheng W, Flavell RA. The transcription factor GATA-3 is necessary and sufficient for Th2 cytokine gene expression in CD4 T cells. *Cell*. 1997 May 16;89(4):587-96.
164. Szabo SJ, Kim ST, Costa GL, Zhang X, Fathman CG, Glimcher LH. A novel transcription factor, T-bet, directs Th1 lineage commitment. *Cell*. 2000 Mar 17;100(6):655-69.
165. Jung T, Schauer U, Heusser C, Neumann C, Rieger C. Detection of intracellular cytokines by flow cytometry. *J Immunol Methods*. 1993 Feb 26;159(1-2):197-207.
166. Pappas J, Quan N, Ghildyal N. A single-step enrichment of Th2 lymphocytes using CCR4 microbeads. *Immunol Lett*. 2006 Jan 15;102(1):110-4.
167. Iellem A, Mariani M, Lang R, Recalde H, Panina-Bordignon P, Sinigaglia F, et al. Unique chemotactic response profile and specific expression of chemokine receptors CCR4 and CCR8 by CD4(+)CD25(+) regulatory T cells. *J Exp Med*. 2001 Sep 17;194(6):847-53.
168. Nagata K, Tanaka K, Ogawa K, Kemmotsu K, Imai T, Yoshie O, et al. Selective expression of a novel surface molecule by human Th2 cells in vivo. *J Immunol*. 1999 Feb 1;162(3):1278-86.
169. Cosmi L, Annunziato F, Galli MIG, Maggi RME, Nagata K, Romagnani S. CRTH2 is the most reliable marker for the detection of circulating human type 2 Th and type 2 T cytotoxic cells in health and disease. *Eur J Immunol*. 2000 Oct;30(10):2972-9.
170. Mackay IR, Rose NR. Autoimmunity and lymphoma: tribulations of B cells. *Nat Immunol*. 2001 Sep 1;2(9):793-5.
171. Gershon RK, Kondo K. Cell interactions in the induction of tolerance: the role of thymic lymphocytes. *Immunology*. 1970 May 1;18(5):723-37.
172. Allison AC, Denman AM, Barnes RD. Cooperating and controlling functions of thymus-derived lymphocytes in relation to autoimmunity. *Lancet*. 1971 Jul 17;2(7716):135-40.
173. Penhale WJ, Irvine WJ, Inglis JR, Farmer A. Thyroiditis in T cell-depleted rats: suppression of the autoallergic response by reconstitution with normal lymphoid cells. *Clin Exp Immunol*. 1976 Jul 1;25(1):6-16.
174. Sakaguchi S, Takahashi T, Nishizuka Y. Study on cellular events in post-thymectomy autoimmune oophoritis in mice. II. Requirement of Lyt-1 cells in normal female mice for the prevention of oophoritis. *J Exp Med*. 1982 Dec 1;156(6):1577-86.
175. Suri-Payer E, Amar AZ, Thornton AM, Shevach EM. CD4+CD25+ T cells inhibit both the induction and effector function of autoreactive T cells and represent a unique lineage of immunoregulatory cells. *J Immunol*. 1998 Feb 1;160(3):1212-8.
176. Ordoñez-Rueda D, Lozano F, Sarukhan A, Raman C, Garcia-Zepeda EA, Soldevila G. Increased numbers of thymic and peripheral CD4+ CD25+Foxp3+ cells in the absence of CD5 signaling. *Eur J Immunol*. 2009 Aug 1;39(8):2233-47.
177. Bloom BR, Modlin RL, Salgame P. Stigma variations: observations on suppressor T cells and leprosy. *Annu Rev Immunol*. 1992 Jan 1;10:453-88.
178. Green DR, Webb DR. Saying the 'S' word in public. *Immunol Today*. 1993 Nov 1;14(11):523-5.
179. Sakaguchi S, Sakaguchi N, Asano M, Itoh M, Toda M. Immunologic self-tolerance maintained by activated T cells expressing IL-2 receptor alpha-chains (CD25). Breakdown of a single mechanism of self-tolerance causes various autoimmune diseases. *J Immunol*. 1995 Aug 1;155(3):1151-64.
180. Baecher-Allan C, Brown JA, Freeman GJ, Hafler DA. CD4+CD25high regulatory cells in human peripheral blood. *J Immunol*. 2001 Aug 1;167(3):1245-53.
181. Khattri R, Cox T, Yasayko S-A, Ramsdell F. An essential role for Scurfin in CD4+CD25+ T regulatory cells. *Nat Immunol*. 2003 Apr 1;4(4):337-42.
182. Fontenot JD, Gavin MA, Rudensky AY. Foxp3 programs the development and function of CD4+CD25+ regulatory T cells. *Nat Immunol*. 2003 Apr 1;4(4):330-6.
-

- 
183. Hori S, Nomura T, Sakaguchi S. Control of regulatory T cell development by the transcription factor Foxp3. *Science*. 2003 Feb 14;299(5609):1057-61.
184. Roncador G, Brown PJ, Maestre L, Hue S, Martínez-Torrecuadrada JL, Ling K-L, et al. Analysis of FOXP3 protein expression in human CD4+CD25+ regulatory T cells at the single-cell level. *Eur J Immunol*. 2005 Jun 1;35(6):1681-91.
185. Wildin RS, Ramsdell F, Peake J, Faravelli F, Casanova JL, Buist N, et al. X-linked neonatal diabetes mellitus, enteropathy and endocrinopathy syndrome is the human equivalent of mouse scurfy. *Nat Genet*. 2001 Jan 1;27(1):18-20.
186. Bennett CL, Christie J, Ramsdell F, Brunkow ME, Ferguson PJ, Whitesell L, et al. The immune dysregulation, polyendocrinopathy, enteropathy, X-linked syndrome (IPEX) is caused by mutations of FOXP3. *Nat Genet*. 2001 Jan 1;27(1):20-1.
187. Itoh M, Takahashi T, Sakaguchi N, Kuniyasu Y, Shimizu J, Otsuka F, et al. Thymus and autoimmunity: production of CD25+CD4+ naturally anergic and suppressive T cells as a key function of the thymus in maintaining immunologic self-tolerance. *J Immunol*. 1999 May 1;162(9):5317-26.
188. Olivares-Villagómez D, Wang Y, Lafaille JJ. Regulatory CD4(+) T cells expressing endogenous T cell receptor chains protect myelin basic protein-specific transgenic mice from spontaneous autoimmune encephalomyelitis. *J Exp Med*. 1998 Nov 16;188(10):1883-94.
189. Jordan MS, Boesteanu A, Reed AJ, Petrone AL, Hohenbeck AE, Lerman MA, et al. Thymic selection of CD4+CD25+ regulatory T cells induced by an agonist self-peptide. *Nat Immunol*. 2001 Apr 1;2(4):301-6.
190. Chen W, Jin W, Hardegen N, Lei K-J, Li L, Marinos N, et al. Conversion of peripheral CD4+CD25- naive T cells to CD4+CD25+ regulatory T cells by TGF-beta induction of transcription factor Foxp3. *J Exp Med*. 2003 Dec 15;198(12):1875-86.
191. Tran DQ, Ramsey H, Shevach EM. Induction of FOXP3 expression in naive human CD4+FOXP3 T cells by T-cell receptor stimulation is transforming growth factor-beta dependent but does not confer a regulatory phenotype. *Blood*. 2007 Oct 15;110(8):2983-90.
192. Gavin MA, Torgerson TR, Houston E, DeRoos P, Ho WY, Stray-Pedersen A, et al. Single-cell analysis of normal and FOXP3-mutant human T cells: FOXP3 expression without regulatory T cell development. *Proc Natl Acad Sci USA*. 2006 Apr 25;103(17):6659-64.
193. Miyara M, Yoshioka Y, Kitoh A, Shima T, Wing K, Niwa A, et al. Functional delineation and differentiation dynamics of human CD4+ T cells expressing the FoxP3 transcription factor. *Immunity*. 2009 Jun 19;30(6):899-911.
194. Wan YY, Flavell RA. Regulatory T-cell functions are subverted and converted owing to attenuated Foxp3 expression. *Nature*. 2007 Feb 15;445(7129):766-70.
195. Liu W, Putnam AL, Xu-Yu Z, Szot GL, Lee MR, Zhu S, et al. CD127 expression inversely correlates with FoxP3 and suppressive function of human CD4+ T reg cells. *J Exp Med*. 2006 Jul 10;203(7):1701-11.
196. Kleinewietfeld M, Starke M, Di Mitri D, Borsellino G, Battistini L, Rötzschke O, et al. CD49d provides access to "untouched" human Foxp3+ Treg free of contaminating effector cells. *Blood*. 2009 Jan 22;113(4):827-36.
197. Camisaschi C, Casati C, Rini F, Perego M, De Filippo A, Triebel F, et al. LAG-3 Expression Defines a Subset of CD4+CD25highFoxp3+ Regulatory T Cells That Are Expanded at Tumor Sites. *J Immunol*. 2010 Apr 26.
198. Rubtsov YP, Rasmussen JP, Chi EY, Fontenot J, Castelli L, Ye X, et al. Regulatory T cell-derived interleukin-10 limits inflammation at environmental interfaces. *Immunity*. 2008 Apr 1;28(4):546-58.
199. Wing K, Onishi Y, Prieto-Martin P, Yamaguchi T, Miyara M, Fehervari Z, et al. CTLA-4 control over Foxp3+ regulatory T cell function. *Science*. 2008 Oct 10;322(5899):271-5.
200. Collison LW, Workman CJ, Kuo TT, Boyd K, Wang Y, Vignali KM, et al. The inhibitory cytokine IL-35 contributes to regulatory T-cell function. *Nature*. 2007 Nov 22;450(7169):566-9.
201. Perillo NL, Pace KE, Seilhamer JJ, Baum LG. Apoptosis of T cells mediated by galectin-1. *Nature*. 1995 Dec 14;378(6558):736-9.
202. Garín MI, Chu C-C, Golshayan D, Cernuda-Morollón E, Wait R, Lechler RI. Galectin-1: a key effector of regulation mediated by CD4+CD25+ T cells. *Blood*. 2007 Mar 1;109(5):2058-65.
-

- 
203. Gondek DC, Lu L-F, Quezada SA, Sakaguchi S, Noelle RJ. Cutting edge: contact-mediated suppression by CD4+CD25+ regulatory cells involves a granzyme B-dependent, perforin-independent mechanism. *J Immunol.* 2005 Jan 15;174(4):1783-6.
204. Strauss L, Czystowska M, Szajnik M, Mandapathil M, Whiteside TL. Differential responses of human regulatory T cells (Treg) and effector T cells to rapamycin. *PLoS ONE.* 2009 Jan 1;4(6):e5994.
205. Deaglio S, Dwyer KM, Gao W, Friedman D, Usheva A, Erat A, et al. Adenosine generation catalyzed by CD39 and CD73 expressed on regulatory T cells mediates immune suppression. *J Exp Med.* 2007 Jun 11;204(6):1257-65.
206. Huang C-T, Workman CJ, Flies D, Pan X, Marson AL, Zhou G, et al. Role of LAG-3 in regulatory T cells. *Immunity.* 2004 Oct 1;21(4):503-13.
207. Shevach EM, McHugh RS, Piccirillo CA, Thornton AM. Control of T-cell activation by CD4+CD25+ suppressor T cells. *Immunol Rev.* 2001 Aug 1;182:58-67.
208. Venken K, Thewissen M, Hellings N, Somers V, Hensen K, Rummens J-L, et al. A CFSE based assay for measuring CD4+CD25+ regulatory T cell mediated suppression of auto-antigen specific and polyclonal T cell responses. *J Immunol Methods.* 2007 Apr 30;322(1-2):1-11.
209. Onishi Y, Fehervari Z, Yamaguchi T, Sakaguchi S. Foxp3+ natural regulatory T cells preferentially form aggregates on dendritic cells in vitro and actively inhibit their maturation. *Proc Natl Acad Sci USA.* 2008 Jul 22;105(29):10113-8.
210. Zhao D-M, Thornton AM, DiPaolo RJ, Shevach EM. Activated CD4+CD25+ T cells selectively kill B lymphocytes. *Blood.* 2006 May 15;107(10):3925-32.
211. Iikuni N, Lourenço EV, Hahn BH, La Cava A. Cutting edge: Regulatory T cells directly suppress B cells in systemic lupus erythematosus. *J Immunol.* 2009 Aug 1;183(3):1518-22.
212. Levings MK, Sangregorio R, Sartirana C, Moschin AL, Battaglia M, Orban PC, et al. Human CD25+CD4+ T suppressor cell clones produce transforming growth factor beta, but not interleukin 10, and are distinct from type 1 T regulatory cells. *J Exp Med.* 2002 Nov 18;196(10):1335-46.
213. Chen Y, Kuchroo VK, Inobe J, Hafler DA, Weiner HL. Regulatory T cell clones induced by oral tolerance: suppression of autoimmune encephalomyelitis. *Science.* 1994 Aug 26;265(5176):1237-40.
214. Koch MA, Tucker-Heard Gs, Perdue NR, Killebrew JR, Urdahl KB, Campbell DJ. The transcription factor T-bet controls regulatory T cell homeostasis and function during type 1 inflammation. *Nat Immunol.* 2009 Jun 1;10(6):595-602.
215. Zheng Y, Chaudhry A, Kas A, DeRoos P, Kim JM, Chu T-T, et al. Regulatory T-cell suppressor program co-opts transcription factor IRF4 to control T(H)2 responses. *Nature.* 2009 Mar 19;458(7236):351-6.
216. Chaudhry A, Rudra D, Treuting P, Samstein RM, Liang Y, Kas A, et al. CD4+ regulatory T cells control TH17 responses in a Stat3-dependent manner. *Science.* 2009 Nov 13;326(5955):986-91.
217. Liu Z, Tugulea S, Cortesini R, Suci-Foca N. Specific suppression of T helper alloreactivity by allo-MHC class I-restricted CD8+CD28- T cells. *Int Immunol.* 1998 Jun 1;10(6):775-83.
218. Mizoguchi A, Mizoguchi E, Smith RN, Preffer FI, Bhan AK. Suppressive role of B cells in chronic colitis of T cell receptor alpha mutant mice. *J Exp Med.* 1997 Nov 17;186(10):1749-56.
219. Rifa'i M, Kawamoto Y, Nakashima I, Suzuki H. Essential roles of CD8+CD122+ regulatory T cells in the maintenance of T cell homeostasis. *J Exp Med.* 2004 Nov 1;200(9):1123-34.
220. Brunet JF, Denizot F, Luciani MF, Roux-Dosseto M, Suzan M, Mattei MG, et al. A new member of the immunoglobulin superfamily--CTLA-4. *Nature.* 1987 Jan 1;328(6127):267-70.
221. Linsley PS, Brady W, Urnes M, Grosmaire LS, Damle NK, Ledbetter JA. CTLA-4 is a second receptor for the B cell activation antigen B7. *J Exp Med.* 1991 Sep 1;174(3):561-9.
222. Waterhouse P, Penninger JM, Timms E, Wakeham A, Shahinian A, Lee KP, et al. Lymphoproliferative disorders with early lethality in mice deficient in Ctl4. *Science.* 1995 Nov 10;270(5238):985-8.
223. Ishida Y, Agata Y, Shibahara K, Honjo T. Induced expression of PD-1, a novel member of the immunoglobulin gene superfamily, upon programmed cell death. *EMBO J.* 1992 Nov 1;11(11):3887-95.
-

- 
224. Nishimura H, Minato N, Nakano T, Honjo T. Immunological studies on PD-1 deficient mice: implication of PD-1 as a negative regulator for B cell responses. *Int Immunol*. 1998 Oct 1;10(10):1563-72.
225. Nishimura H, Nose M, Hiai H, Minato N, Honjo T. Development of lupus-like autoimmune diseases by disruption of the PD-1 gene encoding an ITIM motif-carrying immunoreceptor. *Immunity*. 1999 Aug 1;11(2):141-51.
226. Salama AD, Chitnis T, Imitola J, Ansari MJI, Akiba H, Tushima F, et al. Critical role of the programmed death-1 (PD-1) pathway in regulation of experimental autoimmune encephalomyelitis. *J Exp Med*. 2003 Jul 7;198(1):71-8.
227. Ansari MJI, Salama AD, Chitnis T, Smith RN, Yagita H, Akiba H, et al. The programmed death-1 (PD-1) pathway regulates autoimmune diabetes in nonobese diabetic (NOD) mice. *J Exp Med*. 2003 Jul 7;198(1):63-9.
228. Blazar BR, Carreno BM, Panoskaltsis-Mortari A, Carter L, Iwai Y, Yagita H, et al. Blockade of programmed death-1 engagement accelerates graft-versus-host disease lethality by an IFN-gamma-dependent mechanism. *J Immunol*. 2003 Aug 1;171(3):1272-7.
229. Dong H, Zhu G, Tamada K, Chen L. B7-H1, a third member of the B7 family, co-stimulates T-cell proliferation and interleukin-10 secretion. *Nat Med*. 1999 Dec;5(12):1365-9.
230. Tseng SY, Otsuji M, Gorski K, Huang X, Slansky JE, Pai SI, et al. B7-DC, a new dendritic cell molecule with potent costimulatory properties for T cells. *J Exp Med*. 2001 Apr 2;193(7):839-46.
231. Latchman Y, Wood CR, Chernova T, Chaudhary D, Borde M, Chernova I, et al. PD-L2 is a second ligand for PD-1 and inhibits T cell activation. *Nat Immunol*. 2001 Mar 1;2(3):261-8.
232. Liu X, Gao JX, Wen J, Yin L, Li O, Zuo T, et al. B7DC/PDL2 promotes tumor immunity by a PD-1-independent mechanism. *J Exp Med*. 2003 Jun 16;197(12):1721-30.
233. Sica GL, Choi IH, Zhu G, Tamada K, Wang SD, Tamura H, et al. B7-H4, a molecule of the B7 family, negatively regulates T cell immunity. *Immunity*. 2003 Jun 1;18(6):849-61.
234. Prasad DVR, Richards S, Mai XM, Dong C. B7S1, a novel B7 family member that negatively regulates T cell activation. *Immunity*. 2003 Jun 1;18(6):863-73.
235. Watanabe N, Gavrieli M, Sedy JR, Yang J, Fallarino F, Loftin SK, et al. BTLA is a lymphocyte inhibitory receptor with similarities to CTLA-4 and PD-1. *Nat Immunol*. 2003 Jul;4(7):670-9.
236. Sedy JR, Gavrieli M, Potter KG, Hurchla MA, Lindsley RC, Hildner K, et al. B and T lymphocyte attenuator regulates T cell activation through interaction with herpesvirus entry mediator. *Nat Immunol*. 2005 Jan;6(1):90-8.
237. Chapoval AI, Ni J, Lau JS, Wilcox RA, Flies DB, Liu D, et al. B7-H3: a costimulatory molecule for T cell activation and IFN-gamma production. *Nat Immunol*. 2001 Mar 1;2(3):269-74.
238. Suh W-K, Gajewska BU, Okada H, Gronski MA, Bertram EM, Dawicki W, et al. The B7 family member B7-H3 preferentially down-regulates T helper type 1-mediated immune responses. *Nat Immunol*. 2003 Sep 1;4(9):899-906.
239. Bowen MB, Butch AW, Parvin CA, Levine A, Nahm MH. Germinal center T cells are distinct helper-inducer T cells. *Hum Immunol*. 1991 May 1;31(1):67-75.
240. Velardi A, Mingari MC, Moretta L, Grossi CE. Functional analysis of cloned germinal center CD4+ cells with natural killer cell-related features. Divergence from typical T helper cells. *J Immunol*. 1986 Nov 1;137(9):2808-13.
241. Schaerli P, Willmann K, Lang AB, Lipp M, Loetscher P, Moser B. CXC chemokine receptor 5 expression defines follicular homing T cells with B cell helper function. *J Exp Med*. 2000 Dec 4;192(11):1553-62.
242. Ansel KM, McHeyzer-Williams LJ, Ngo VN, McHeyzer-Williams MG, Cyster JG. In vivo-activated CD4 T cells upregulate CXC chemokine receptor 5 and reprogram their response to lymphoid chemokines. *J Exp Med*. 1999 Oct 18;190(8):1123-34.
243. Kim CH, Lim HW, Kim JR, Rott L, Hillsamer P, Butcher EC. Unique gene expression program of human germinal center T helper cells. *Blood*. 2004 Oct 1;104(7):1952-60.
244. Chtanova T, Tangye SG, Newton R, Frank N, Hodge MR, Rolph MS, et al. T follicular helper cells express a distinctive transcriptional profile, reflecting their role as non-Th1/Th2 effector cells that provide help for B cells. *J Immunol*. 2004 Jul 1;173(1):68-78.
-



- 
245. Bauquet AT, Jin H, Paterson AM, Mitsdoerffer M, Ho I-C, Sharpe AH, et al. The costimulatory molecule ICOS regulates the expression of c-Maf and IL-21 in the development of follicular T helper cells and TH-17 cells. *Nat Immunol.* 2009 Feb 1;10(2):167-75.
246. Nurieva RI, Chung Y, Hwang D, Yang XO, Kang HS, Ma L, et al. Generation of T follicular helper cells is mediated by interleukin-21 but independent of T helper 1, 2, or 17 cell lineages. *Immunity.* 2008 Jul 18;29(1):138-49.
247. Haynes NM, Allen CDC, Lesley R, Ansel KM, Killeen N, Cyster JG. Role of CXCR5 and CCR7 in follicular Th cell positioning and appearance of a programmed cell death gene-1high germinal center-associated subpopulation. *J Immunol.* 2007 Oct 15;179(8):5099-108.
248. Gaspal FMC, Kim M-Y, McConnell FM, Raykundalia C, Bekiaris V, Lane PJL. Mice deficient in OX40 and CD30 signals lack memory antibody responses because of deficient CD4 T cell memory. *J Immunol.* 2005 Apr 1;174(7):3891-6.
249. Lane PJ, Gaspal FM, Kim MY. Two sides of a cellular coin: CD4(+)CD3- cells regulate memory responses and lymph-node organization. *Nat Rev Immunol.* 2005 Aug;5(8):655-60.
250. Gaspal FM, Kim MY, McConnell FM, Raykundalia C, Bekiaris V, Lane PJ. Mice deficient in OX40 and CD30 signals lack memory antibody responses because of deficient CD4 T cell memory. *J Immunol.* 2005 Apr 1;174(7):3891-6.
251. Johnston RJ, Poholek AC, DiToro D, Yusuf I, Eto D, Barnett B, et al. Bcl6 and Blimp-1 are reciprocal and antagonistic regulators of T follicular helper cell differentiation. *Science.* 2009 Aug 21;325(5943):1006-10.
252. Odegard JM, Marks BR, DiPlacido LD, Poholek AC, Kono DH, Dong C, et al. ICOS-dependent extrafollicular helper T cells elicit IgG production via IL-21 in systemic autoimmunity. *J Exp Med.* 2008 Nov 24;205(12):2873-86.
253. Chan TD, Gatto D, Wood K, Camidge T, Basten A, Brink R. Antigen affinity controls rapid T-dependent antibody production by driving the expansion rather than the differentiation or extrafollicular migration of early plasmablasts. *J Immunol.* 2009 Sep 1;183(5):3139-49.
254. McHeyzer-Williams LJ, Pelletier N, Mark L, Fazilleau N, McHeyzer-Williams MG. Follicular helper T cells as cognate regulators of B cell immunity. *Curr Opin Immunol.* 2009 Jun;21(3):266-73.
255. Walker LS, Gulbranson-Judge A, Flynn S, Brocker T, Raykundalia C, Goodall M, et al. Compromised OX40 function in CD28-deficient mice is linked with failure to develop CXC chemokine receptor 5-positive CD4 cells and germinal centers. *J Exp Med.* 1999 Oct 18;190(8):1115-22.
256. Ye BH, Lista F, Lo Coco F, Knowles DM, Offit K, Chaganti RS, et al. Alterations of a zinc finger-encoding gene, BCL-6, in diffuse large-cell lymphoma. *Science.* 1993 Oct 29;262(5134):747-50.
257. Baron BW, Stanger RR, Hume E, Sadhu A, Mick R, Kerckaert JP, et al. BCL6 encodes a sequence-specific DNA-binding protein. *Genes Chromosomes Cancer.* 1995 Jul 1;13(3):221-4.
258. Cattoretti G, Chang CC, Cechova K, Zhang J, Ye BH, Falini B, et al. BCL-6 protein is expressed in germinal-center B cells. *Blood.* 1995 Jul 1;86(1):45-53.
259. Dent AL, Shaffer AL, Yu X, Allman D, Staudt LM. Control of inflammation, cytokine expression, and germinal center formation by BCL-6. *Science.* 1997 Apr 25;276(5312):589-92.
260. Ye BH, Cattoretti G, Shen Q, Zhang J, Hawe N, de Waard R, et al. The BCL-6 proto-oncogene controls germinal-centre formation and Th2-type inflammation. *Nat Genet.* 1997 Jun 1;16(2):161-70.
261. Nurieva RI, Chung Y, Martinez GJ, Yang XO, Tanaka S, Matskevitch TD, et al. Bcl6 mediates the development of T follicular helper cells. *Science.* 2009 Aug 21;325(5943):1001-5.
262. Yu D, Rao S, Tsai LM, Lee SK, He Y, Sutcliffe EL, et al. The transcriptional repressor Bcl-6 directs T follicular helper cell lineage commitment. *Immunity.* 2009 Sep 18;31(3):457-68.
263. Kusam S, Toney LM, Sato H, Dent AL. Inhibition of Th2 differentiation and GATA-3 expression by BCL-6. *J Immunol.* 2003 Mar 1;170(5):2435-41.
264. Yu D, Tan AH-M, Hu X, Athanasopoulos V, Simpson N, Silva DG, et al. Roquin represses autoimmunity by limiting inducible T-cell co-stimulator messenger RNA. *Nature.* 2007 Nov 8;450(7167):299-303.
-

- 
265. Linterman MA, Rigby RJ, Wong R, Silva D, Withers D, Anderson G, et al. Roquin differentiates the specialized functions of duplicated T cell costimulatory receptor genes CD28 and ICOS. *Immunity*. 2009 Feb 20;30(2):228-41.
266. Crotty S, Kersh EN, Cannons J, Schwartzberg PL, Ahmed R. SAP is required for generating long-term humoral immunity. *Nature*. 2003 Jan 16;421(6920):282-7.
267. Cannons JL, Yu LJ, Jankovic D, Crotty S, Horai R, Kirby M, et al. SAP regulates T cell-mediated help for humoral immunity by a mechanism distinct from cytokine regulation. *J Exp Med*. 2006 Jun 12;203(6):1551-65.
268. Latour S, Gish G, Helgason CD, Humphries RK, Pawson T, Veillette A. Regulation of SLAM-mediated signal transduction by SAP, the X-linked lymphoproliferative gene product. *Nat Immunol*. 2001 Aug 1;2(8):681-90.
269. Linterman MA, Rigby RJ, Wong RK, Yu D, Brink R, Cannons JL, et al. Follicular helper T cells are required for systemic autoimmunity. *J Exp Med*. 2009 Mar 16;206(3):561-76.
270. Fazilleau N, Mark L, Mcheyzer-Williams LJ, Mcheyzer-Williams MG. Follicular Helper T Cells: Lineage and Location. *Immunity*. 2009 Mar 20;30(3):324-35.
271. Casamayor-Palleja M, Khan M, MacLennan IC. A subset of CD4+ memory T cells contains preformed CD40 ligand that is rapidly but transiently expressed on their surface after activation through the T cell receptor complex. *J Exp Med*. 1995 Apr 1;181(4):1293-301.
272. Campbell DJ, Kim CH, Butcher EC. Separable effector T cell populations specialized for B cell help or tissue inflammation. *Nat Immunol*. 2001 Sep 1;2(9):876-81.
273. Zaretsky AG, Taylor JJ, King IL, Marshall FA, Mohrs M, Pearce EJ. T follicular helper cells differentiate from Th2 cells in response to helminth antigens. *J Exp Med*. 2009 May 11;206(5):991-9.
274. King IL, Mohrs M. IL-4-producing CD4+ T cells in reactive lymph nodes during helminth infection are T follicular helper cells. *J Exp Med*. 2009 May 11;206(5):1001-7.
275. Reinhardt RL, Liang H-E, Locksley RM. Cytokine-secreting follicular T cells shape the antibody repertoire. *Nat Immunol*. 2009 Apr 1;10(4):385-93.
276. Parrish-Novak J, Dillon SR, Nelson A, Hammond A, Sprecher C, Gross JA, et al. Interleukin 21 and its receptor are involved in NK cell expansion and regulation of lymphocyte function. *Nature*. 2000 Nov 2;408(6808):57-63.
277. Ettinger R, Kuchen S, Lipsky PE. The role of IL-21 in regulating B-cell function in health and disease. *Immunol Rev*. 2008 Jun;223:60-86.
278. Ozaki K, Spolski R, Feng CG, Qi C-F, Cheng J, Sher A, et al. A critical role for IL-21 in regulating immunoglobulin production. *Science*. 2002 Nov 22;298(5598):1630-4.
279. Vogelzang A, McGuire HM, Yu D, Sprent J, Mackay CR, King C. A fundamental role for interleukin-21 in the generation of T follicular helper cells. *Immunity*. 2008 Jul 18;29(1):127-37.
280. Zotos D, Coquet JM, Zhang Y, Light A, D'Costa K, Kallies A, et al. IL-21 regulates germinal center B cell differentiation and proliferation through a B cell-intrinsic mechanism. *J Exp Med*. 2010 Feb 15;207(2):365-78.
281. Scheeren FA, Diehl SA, Smit LA, Beaumont T, Naspetti M, Bende RJ, et al. IL-21 is expressed in Hodgkin lymphoma and activates STAT5: evidence that activated STAT5 is required for Hodgkin lymphomagenesis. *Blood*. 2008 May 1;111(9):4706-15.
282. Zhong X, Tumang JR, Gao W, Bai C, Rothstein TL. PD-L2 expression extends beyond dendritic cells/macrophages to B1 cells enriched for V(H)11/V(H)12 and phosphatidylcholine binding. *Eur J Immunol*. 2007 Sep 1;37(9):2405-10.
283. Good-Jacobson KL, Szumilas CG, Chen L, Sharpe AH, Tomayko MM, Shlomchik MJ. PD-1 regulates germinal center B cell survival and the formation and affinity of long-lived plasma cells. *Nat Immunol*. 2010 Jun 1;11(6):535-42.
284. Tomayko MM, Anderson SM, Brayton CE, Sadanand S, Steinel NC, Behrens TW, et al. Systematic comparison of gene expression between murine memory and naive B cells demonstrates that memory B cells have unique signaling capabilities. *J Immunol*. 2008 Jul 1;181(1):27-38.
285. Murphy E, Shibuya K, Hosken N, Openshaw P, Maino V, Davis K, et al. Reversibility of T helper 1 and 2 populations is lost after long-term stimulation. *J Exp Med*. 1996 Mar 1;183(3):901-13.
-

- 
286. Bird JJ, Brown DR, Mullen AC, Moskowitz NH, Mahowald MA, Sider JR, et al. Helper T cell differentiation is controlled by the cell cycle. *Immunity*. 1998 Aug;9(2):229-37.
287. Wilson CB, Rowell E, Sekimata M. Epigenetic control of T-helper-cell differentiation. *Nat Rev Immunol*. 2009 Feb;9(2):91-105.
288. Murphy KM, Stockinger B. Effector T cell plasticity: flexibility in the face of changing circumstances. *Nat Immunol*. 2010 Aug;11(8):674-80.
289. Penninger JM, Irie-Sasaki J, Sasaki T, Oliveira-dos-Santos AJ. CD45: new jobs for an old acquaintance. *Nat Immunol*. 2001 May 1;2(5):389-96.
290. Morimoto C, Letvin NL, Distaso JA, Aldrich WR, Schlossman SF. The isolation and characterization of the human suppressor inducer T cell subset. *J Immunol*. 1985 Mar 1;134(3):1508-15.
291. Powrie F, Correa-Oliveira R, Mauze S, Coffman RL. Regulatory interactions between CD45RB<sup>high</sup> and CD45RB<sup>low</sup> CD4<sup>+</sup> T cells are important for the balance between protective and pathogenic cell-mediated immunity. *J Exp Med*. 1994 Feb 1;179(2):589-600.
292. Chetaille B, Bertucci F, Finetti P, Esterni B, Stamatoullas A, Picquenot JM, et al. Molecular profiling of classical Hodgkin lymphoma tissues uncovers variations in the tumor microenvironment and correlations with EBV infection and outcome. *Blood*. 2009 Jan 23;113(12):2765-3775.
293. Fox DA, Hussey RE, Fitzgerald KA, Acuto O, Poole C, Palley L, et al. Ta1, a novel 105 KD human T cell activation antigen defined by a monoclonal antibody. *J Immunol*. 1984 Sep 1;133(3):1250-6.
294. Mattern T, Scholz W, Feller AC, Flad HD, Ulmer AJ. Expression of CD26 (dipeptidyl peptidase IV) on resting and activated human T-lymphocytes. *Scand J Immunol*. 1991 Jun 1;33(6):737-48.
295. Martín M, Huguet J, Centelles JJ, Franco R. Expression of ecto-adenosine deaminase and CD26 in human T cells triggered by the TCR-CD3 complex. Possible role of adenosine deaminase as costimulatory molecule. *J Immunol*. 1995 Nov 15;155(10):4630-43.
296. Pacheco R, Martinez-Navio JM, Lejeune M, Climent N, Oliva H, Gatell JM, et al. CD26, adenosine deaminase, and adenosine receptors mediate costimulatory signals in the immunological synapse. *Proc Natl Acad Sci USA*. 2005 Jul 5;102(27):9583-8.
297. Brenchley JM, Karandikar NJ, Betts MR, Ambrozak DR, Hill BJ, Crotty LE, et al. Expression of CD57 defines replicative senescence and antigen-induced apoptotic death of CD8(+) T cells. *Blood*. 2003 Apr 1;101(7):2711-20.
298. Atayar C, Poppema S, Visser L, van den Berg A. Cytokine gene expression profile distinguishes CD4<sup>+</sup>/CD57<sup>+</sup> T cells of the nodular lymphocyte predominance type of Hodgkin's lymphoma from their tonsillar counterparts. *J Pathol*. 2006 Feb 1;208(3):423-30.
299. Marshall NA, Christie LE, Munro LR, Culligan DJ, Johnston PW, Barker RN, et al. Immunosuppressive regulatory T cells are abundant in the reactive lymphocytes of Hodgkin lymphoma. *Blood*. 2004 Mar 1;103(5):1755-62.
300. Freeman GJ, Lombard DB, Gimmi CD, Brod SA, Lee K, Laning JC, et al. CTLA-4 and CD28 mRNA are coexpressed in most T cells after activation. Expression of CTLA-4 and CD28 mRNA does not correlate with the pattern of lymphokine production. *J Immunol*. 1992 Dec 15;149(12):3795-801.
301. Robb RJ, Munck A, Smith KA. T cell growth factor receptors. Quantitation, specificity, and biological relevance. *J Exp Med*. 1981 Nov 1;154(5):1455-74.
302. Schaadt M, Fonatsch C, Kirchner H, Diehl V. Establishment of a malignant, Epstein-Barr-virus (EBV)-negative cell-line from the pleura effusion of a patient with Hodgkin's disease. *Blut*. 1979 Feb 19;38(2):185-90.
303. Bargou RC, Mapara MY, Zugck C, Daniel PT, Pawlita M, Dohner H, et al. Characterization of a novel Hodgkin cell line, HD-MyZ, with myelomonocytic features mimicking Hodgkin's disease in severe combined immunodeficient mice. *J Exp Med*. 1993 May 1;177(5):1257-68.
304. Wolf J, Kapp U, Bohlen H, Kornacker M, Schoch C, Stahl B, et al. Peripheral blood mononuclear cells of a patient with advanced Hodgkin's lymphoma give rise to permanently growing Hodgkin-Reed Sternberg cells. *Blood*. 1996 Apr 15;87(8):3418-28.

- 
305. Diehl V, Kirchner HH, Burcher H, Stein H, Fonatsch C, Gerdes J, et al. Characteristics of Hodgkin's disease-derived cell lines. *Cancer Treat Rep.* 1982 Apr;66(4):615-32.
306. Kamesaki H, Fukuhara S, Tatsumi E, Uchino H, Yamabe H, Miwa H, et al. Cytochemical, immunologic, chromosomal, and molecular genetic analysis of a novel cell line derived from Hodgkin's disease. *Blood.* 1986 Jul;68(1):285-92.
307. Diehl V, Kirchner HH, Schaadt M, Fonatsch C, Stein H, Gerdes J, et al. Hodgkin's disease: establishment and characterization of four in vitro cell lines. *J Cancer Res Clin Oncol.* 1981;101(1):111-24.
308. Jones DB, Furley AJ, Gerdes J, Greaves MF, Stein H, Wright DH. Phenotypic and genotypic analysis of two cell lines derived from Hodgkin's disease tissue biopsies. *Recent Results Cancer Res.* 1989;117:62-6.
309. Drexler HG, Gaedicke G, Lok MS, Diehl V, Minowada J. Hodgkin's disease derived cell lines HDLM-2 and L-428: comparison of morphology, immunological and isoenzyme profiles. *Leuk Res.* 1986;10(5):487-500.
310. Drexler HG, Gignac SM, Hoffbrand AV, Leber BF, Norton J, Lok MS, et al. Characterization of Hodgkin's disease derived cell line HDLM-2. *Recent Results Cancer Res.* 1989;117:75-82.
311. Poppema S, Visser L, de Jong B, Brinker M, Atmosoerodjo J, Timens W. The typical Reed-Sternberg phenotype and Ig gene rearrangement of Hodgkin's disease derived cell line ZO indicating a B-cell origin. *Recent Results Cancer Res.* 1989;117:67-74.
312. Poppema S, De Jong B, Atmosoerodjo J, Idenburg V, Visser L, De Ley L. Morphologic, immunologic, enzymehistochemical and chromosomal analysis of a cell line derived from Hodgkin's disease. Evidence for a B-cell origin of Sternberg-Reed cells. *Cancer.* 1985 Feb 15;55(4):683-90.
313. Kanzaki T, Kubonishi I, Eguchi T, Yano S, Sonobe H, Ohyashiki JH, et al. Establishment of a new Hodgkin's cell line (HD-70) of B-cell origin. *Cancer.* 1992 Feb 15;69(4):1034-41.
314. Naumovski L, Utz PJ, Bergstrom SK, Morgan R, Molina A, Toole JJ, et al. SUP-HD1: a new Hodgkin's disease-derived cell line with lymphoid features produces interferon-gamma. *Blood.* 1989 Dec;74(8):2733-42.
315. Wagner HJ, Klintworth F, Jabs W, Lange K, Schlegelberger B, Harder L, et al. Characterization of the novel, pediatric Hodgkin disease-derived cell line HKB-1. *Med Pediatr Oncol.* 1998 Sep;31(3):138-43.
316. Schaadt M, Diehl V, Stein H, Fonatsch C, Kirchner HH. Two neoplastic cell lines with unique features derived from Hodgkin's disease. *Int J Cancer.* 1980 Dec 15;26(6):723-31.
317. Scherer WF, Syverton JT, Gey GO. Studies on the propagation in vitro of poliomyelitis viruses. IV. Viral multiplication in a stable strain of human malignant epithelial cells (strain HeLa) derived from an epidermoid carcinoma of the cervix. *J Exp Med.* 1953 May 1;97(5):695-710.
318. Trickett A, Kwan YL. T cell stimulation and expansion using anti-CD3/CD28 beads. *J Immunol Methods.* 2003 Apr 1;275(1-2):251-5.
319. Fromm JR, Kussick SJ, Wood BL. Identification and purification of classical Hodgkin cells from lymph nodes by flow cytometry and flow cytometric cell sorting. *Am J Clin Pathol.* 2006 Nov 1;126(5):764-80.
320. Hsu SM, Zhao X, Chakraborty S, Liu YF, Whang-Peng J, Lok MS, et al. Reed-Sternberg cells in Hodgkin's cell lines HDLM, L-428, and KM-H2 are not actively replicating: lack of bromodeoxyuridine uptake by multinuclear cells in culture. *Blood.* 1988 May 1;71(5):1382-9.
321. Newcom SR, Kadin ME, Phillips C. L-428 Reed-Sternberg cells and mononuclear Hodgkin's cells arise from a single cloned mononuclear cell. *Int J Cell Cloning.* 1988 Nov 1;6(6):417-31.
322. Jones RJ, Gocke CD, Kasamon YL, Miller CB, Perkins B, Barber JP, et al. Circulating clonotypic B cells in classic Hodgkin lymphoma. *Blood.* 2009 Jun 4;113(23):5920-6.
323. Kupperts R. Clonotypic B cells in classic Hodgkin lymphoma. *Blood.* 2009 Oct 29;114(18):3970-1; author reply 1-2.
324. Zietman AL, Sugiyama E, Ramsay JR, Silobrcic V, Yeh ET, Sedlacek RS, et al. A comparative study on the xenotransplantability of human solid tumors into mice with different genetic immune deficiencies. *Int J Cancer.* 1991 Mar 12;47(5):755-9.
325. Rodt H, Kolb HJ, Netzel B, Rieder I, Janka G, Belohradsky B, et al. GVHD suppression by incubation of bone marrow grafts with anti-T-cell globulin: effect in the canine model and application to clinical bone marrow transplantation. *Transplant Proc.* 1979 Mar 1;11(1):962-6.
-

- 
326. Kernan NA, Collins NH, Juliano L, Cartagena T, Dupont B, O'Reilly RJ. Clonable T lymphocytes in T cell-depleted bone marrow transplants correlate with development of graft-versus-host disease. *Blood*. 1986 Sep 1;68(3):770-3.
327. Dewan MZ, Watanabe M, Ahmed S, Terashima K, Horiuchi S, Sata T, et al. Hodgkin's lymphoma cells are efficiently engrafted and tumor marker CD30 is expressed with constitutive nuclear factor-kappaB activity in unconditioned NOD/SCID/gammac(null) mice. *Cancer Sci*. 2005 Aug 1;96(8):466-73.
328. Ito M, Hiramatsu H, Kobayashi K, Suzue K, Kawahata M, Hioki K, et al. NOD/SCID/gamma(c)(null) mouse: an excellent recipient mouse model for engraftment of human cells. *Blood*. 2002 Nov 1;100(9):3175-82.
329. Kapp U, Wolf J, Hummel M, Pawlita M, von Kalle C, Dallenbach F, et al. Hodgkin's lymphoma-derived tissue serially transplanted into severe combined immunodeficient mice. *Blood*. 1993 Aug 15;82(4):1247-56.
330. Adams JM, Harris AW, Pinkert CA, Corcoran LM, Alexander WS, Cory S, et al. The c-myc oncogene driven by immunoglobulin enhancers induces lymphoid malignancy in transgenic mice. *Nature*. 1985 Jan 1;318(6046):533-8.
331. Bichi R, Shinton SA, Martin ES, Koval A, Calin GA, Cesari R, et al. Human chronic lymphocytic leukemia modeled in mouse by targeted TCL1 expression. *Proc Natl Acad Sci USA*. 2002 May 14;99(10):6955-60.
332. Weber-Matthiesen K, Deerberg J, Poetsch M, Grote W, Schlegelberger B. Numerical chromosome aberrations are present within the CD30+ Hodgkin and Reed-Sternberg cells in 100% of analyzed cases of Hodgkin's disease. *Blood*. 1995 Aug 15;86(4):1464-8.
333. Steidl C, Telenius A, Shah SP, Farinha P, Barclay L, Boyle M, et al. Genome-wide copy number analysis of Hodgkin Reed-Sternberg cells identifies recurrent imbalances with correlations to treatment outcome. *Blood*. 2010 Jul 22;116(3):418-27.
334. Steidl C, Shah SP, Woolcock BW, Rui L, Kawahara M, Farinha P, et al. MHC class II transactivator CIITA is a recurrent gene fusion partner in lymphoid cancers. *Nature*. 2011 2011;471(7338):377-81.
335. Clark WH, Elder DE, Guerry D, Braitman LE, Trock BJ, Schultz D, et al. Model predicting survival in stage I melanoma based on tumor progression. *J Natl Cancer Inst*. 1989 Dec 20;81(24):1893-904.
336. Normann SJ. Macrophage infiltration and tumor progression. *Cancer Metastasis Rev*. 1985 Jan 1;4(4):277-91.
337. Schreck S, Friebel D, Buettner M, Distel L, Grabenbauer G, Young LS, et al. Prognostic impact of tumour-infiltrating Th2 and regulatory T cells in classical Hodgkin lymphoma. *Hematol Oncol*. 2009 Mar;27(1):31-9.
338. Altman DG, Lausen B, Sauerbrei W, Schumacher M. Dangers of using "optimal" cutpoints in the evaluation of prognostic factors. *J Natl Cancer Inst*. 1994 Jun 1;86(11):829-35.
339. Camp RL, Dolled-Filhart M, Rimm DL. X-tile: a new bio-informatics tool for biomarker assessment and outcome-based cut-point optimization. *Clin Cancer Res*. 2004 Nov 1;10(21):7252-9.
340. Heusel JW, Wesselschmidt RL, Shresta S, Russell JH, Ley TJ. Cytotoxic lymphocytes require granzyme B for the rapid induction of DNA fragmentation and apoptosis in allogeneic target cells. *Cell*. 1994 Mar 25;76(6):977-87.
341. Tian Q, Streuli M, Saito H, Schlossman SF, Anderson P. A polyadenylate binding protein localized to the granules of cytolytic lymphocytes induces DNA fragmentation in target cells. *Cell*. 1991 Nov 1;67(3):629-39.
342. Oudejans JJ, Jiwa NM, Kummer JA, Ossenkoppele GJ, van Heerde P, Baars JW, et al. Activated cytotoxic T cells as prognostic marker in Hodgkin's disease. *Blood*. 1997 Feb 15;89(4):1376-82.
343. Alvaro T, Lejeune M, Salvadó MT, Bosch R, García JF, Jaén J, et al. Outcome in Hodgkin's lymphoma can be predicted from the presence of accompanying cytotoxic and regulatory T cells. *Clin Cancer Res*. 2005 Feb 15;11(4):1467-73.
344. Kelley TW, Pohlman B, Elson P, Hsi ED. The ratio of FOXP3+ regulatory T cells to granzyme B+ cytotoxic T/NK cells predicts prognosis in classical Hodgkin lymphoma and is independent of bcl-2 and MAL expression. *Am J Clin Pathol*. 2007 Dec 1;128(6):958-65.
-

- 
345. Montalban C. Influence of Biologic Markers on the Outcome of Hodgkin's Lymphoma: A Study by the Spanish Hodgkin's Lymphoma Study Group. *Journal of Clinical Oncology*. 2004 Mar 29;22(9):1664-73.
346. Canioni D, Deau-Fischer B, Taupin P, Ribrag V, Delarue R, Bosq J, et al. Prognostic Significance of New Immunohistochemical Markers in Refractory Classical Hodgkin Lymphoma: A Study of 59 Cases. *PLoS ONE*. 2009 Jul 22;4(7):e6341.
347. Curiel TJ, Coukos G, Zou L, Alvarez X, Cheng P, Mottram P, et al. Specific recruitment of regulatory T cells in ovarian carcinoma fosters immune privilege and predicts reduced survival. *Nat Med*. 2004 Sep 1;10(9):942-9.
348. Woo EY, Chu CS, Goletz TJ, Schlienger K, Yeh H, Coukos G, et al. Regulatory CD4(+)CD25(+) T cells in tumors from patients with early-stage non-small cell lung cancer and late-stage ovarian cancer. *Cancer Research*. 2001 Jun 15;61(12):4766-72.
349. Woo EY, Yeh H, Chu CS, Schlienger K, Carroll RG, Riley JL, et al. Cutting edge: Regulatory T cells from lung cancer patients directly inhibit autologous T cell proliferation. *J Immunol*. 2002 May 1;168(9):4272-6.
350. Zou W. Regulatory T cells, tumour immunity and immunotherapy. *Nat Rev Immunol*. 2006 Apr;6(4):295-307.
351. Lee AM, Clear AJ, Calaminici M, Davies AJ, Jordan S, Macdougall F, et al. Number of CD4+ Cells and Location of Forkhead Box Protein P3-Positive Cells in Diagnostic Follicular Lymphoma Tissue Microarrays Correlates With Outcome. *Journal of Clinical Oncology*. 2006 Nov 1;24(31):5052-9.
352. Yang Z-Z, Novak AJ, Stenson MJ, Witzig TE, Ansell SM. Intratumoral CD4+CD25+ regulatory T-cell-mediated suppression of infiltrating CD4+ T cells in B-cell non-Hodgkin lymphoma. *Blood*. 2006 May 1;107(9):3639-46.
353. Carreras J, Lopez-Guillermo A, Fox BC, Colomo L, Martinez A, Roncador G, et al. High numbers of tumor-infiltrating FOXP3-positive regulatory T cells are associated with improved overall survival in follicular lymphoma. *Blood*. 2006 Nov 1;108(9):2957-64.
354. Tzankov A, Meier C, Hirschmann P, Went P, Pileri SA, Dirnhofer S. Correlation of high numbers of intratumoral FOXP3+ regulatory T cells with improved survival in germinal center-like diffuse large B-cell lymphoma, follicular lymphoma and classical Hodgkin's lymphoma. *Haematologica*. 2008 Feb;93(2):193-200.
355. Koch I, Slotta-Huspenina J, Hollweck R, Anastasov N, Hofler H, Quintanilla-Martinez L, et al. Real-time quantitative RT-PCR shows variable, assay-dependent sensitivity to formalin fixation: implications for direct comparison of transcript levels in paraffin-embedded tissues. *Diagn Mol Pathol*. 2006 Sep 1;15(3):149-56.
356. Sánchez-Espiridión B, Montalbán C, López A, Menárguez J, Sabín P, Ruiz-Marcellán C, et al. A molecular risk score based on 4 functional pathways for advanced classical Hodgkin lymphoma. *Blood*. 2010 Aug 26;116(8):e12-7.
357. Rosenwald A, Wright G, Chan WC, Connors JM, Campo E, Fisher RI, et al. The use of molecular profiling to predict survival after chemotherapy for diffuse large-B-cell lymphoma. *N Engl J Med*. 2002 Jun 20;346(25):1937-47.
358. Dave SS, Wright G, Tan B, Rosenwald A, Gascoyne RD, Chan WC, et al. Prediction of survival in follicular lymphoma based on molecular features of tumor-infiltrating immune cells. *N Engl J Med*. 2004 Nov 18;351(21):2159-69.
359. Devillard E, Bertucci F, Trempat P, Bouabdallah R, Loricod B, Giaconia A, et al. Gene expression profiling defines molecular subtypes of classical Hodgkin's disease. *Oncogene*. 2002 May 2;21(19):3095-102.
360. Herrero J, Valencia A, Dopazo J. A hierarchical unsupervised growing neural network for clustering gene expression patterns. *Bioinformatics*. 2001 Feb 1;17(2):126-36.
361. Peduzzi P, Concato J, Feinstein AR, Holford TR. Importance of events per independent variable in proportional hazards regression analysis. II. Accuracy and precision of regression estimates. *J Clin Epidemiol*. 1995 Dec;48(12):1503-10.
362. Sanchez-Aguilera A. Tumor microenvironment and mitotic checkpoint are key factors in the outcome of classic Hodgkin lymphoma. *Blood*. 2006 Jul 15;108(2):662-8.

- 
363. Sánchez-Espiridión B, Sánchez-Aguilera A, Montalbán C, Martín C, Martínez R, González-Carrero J, et al. A TaqMan low-density array to predict outcome in advanced Hodgkin's lymphoma using paraffin-embedded samples. *Clin Cancer Res*. 2009 Feb 15;15(4):1367-75.
364. Valsami S, Pappa V, Rontogianni D, Kotsioti F, Papageorgiou E, Dervenoulas J, et al. A clinicopathological study of B-cell differentiation markers and transcription factors in classical Hodgkin's lymphoma: a potential prognostic role of MUM1/IRF4. *Haematologica*. 2007 Oct 1;92(10):1343-50.
365. Kononen J, Bubendorf L, Kallioniemi A, Bärklund M, Schraml P, Leighton S, et al. Tissue microarrays for high-throughput molecular profiling of tumor specimens. *Nat Med*. 1998 Jul 1;4(7):844-7.
366. Norton AJ, Jordan S, Yeomans P. Brief, high-temperature heat denaturation (pressure cooking): a simple and effective method of antigen retrieval for routinely processed tissues. *J Pathol*. 1994 Aug;173(4):371-9.
367. Kaplan ELM, P. Non parametric estimation from incomplete observations. *Journal of the American Statistical Association*. 1958 1958;53:457-81.
368. Mantel N. Evaluation of survival data and two new rank order statistics arising in its consideration. *Cancer Chemother Rep*. 1966 Mar;50(3):163-70.
369. Keeney M, Gratama JW, Chin-Yee IH, Sutherland DR. Isotype controls in the analysis of lymphocytes and CD34+ stem and progenitor cells by flow cytometry--time to let go! *Cytometry*. 1998 Dec 15;34(6):280-3.
370. Herzenberg LA, Tung J, Moore WA, Parks DR. Interpreting flow cytometry data: a guide for the perplexed. *Nat Immunol*. 2006 Jul;7(7):681-5.
371. Mann HBaW, D.R. On a Test of Whether One of Two Random Variables is Stochastically Larger Than the Other. *Annals of Mathematical Statistics*. *The Annals of Mathematical Statistics*. 1947;18:50-60.
372. Varterasian M, Ratanatharathorn V, Uberti JP, Karanes C, Abella E, Momin F, et al. Clinical course and outcome of patients with Hodgkin's disease who progress after autologous transplantation. *Leuk Lymphoma*. 1995 Dec;20(1-2):59-65.
373. Shamash J, Lee SM, Radford JA, Rohatiner AZ, Chang J, Morgenstern GR, et al. Patterns of relapse and subsequent management following high-dose chemotherapy with autologous haematopoietic support in relapsed or refractory Hodgkin's lymphoma: a two centre study. *Ann Oncol*. 2000 Jun;11(6):715-9.
374. Castellino SM, Geiger AM, Mertens AC, Leisenring WM, Tooze JA, Goodman P, et al. Morbidity and mortality in long-term survivors of Hodgkin lymphoma: a report from the Childhood Cancer Survivor Study. *Blood*. 2011 Feb 10;117(6):1806-16.
375. Tzankov A, Matter MS, Dirnhofer S. Refined prognostic role of CD68-positive tumor macrophages in the context of the cellular micromilieu of classical Hodgkin lymphoma. *Pathobiology*. 2010;77(6):301-8.
376. Kamper P, Bendix K, Hamilton-Dutoit S, Honore B, Nyengaard JR, d'Amore F. Tumor-infiltrating macrophages correlate with adverse prognosis and Epstein-Barr virus status in classical Hodgkin's lymphoma. *Haematologica*. 2011 Feb;96(2):269-76.
377. Beyer M, Classen S, Endl E, Kochanek M, Weihrauch MR, Debey-Pascher S, et al. Comparative approach to define increased regulatory T cells in different cancer subtypes by combined assessment of CD127 and FOXP3. *Clin Dev Immunol*. 2011;2011:734036.
378. Flavell KJ, Murray PG. Hodgkin's disease and the Epstein-Barr virus. *Mol Pathol*. 2000 Oct;53(5):262-9.
379. Lister TA, Dorreen MS, Faux M, Jones AE, Wrigley PF. The treatment of stage IIIA Hodgkin's disease. *J Clin Oncol*. 1983 Dec;1(12):745-9.
380. Lister TA. Treatment of Stage IIIa Hodgkin's disease: long follow-up perspective. *J Clin Oncol*. 2008 Nov 10;26(32):5144-6.
381. Kleiner HE, Krishnan P, Tubbs J, Smith M, Meschonat C, Shi R, et al. Tissue microarray analysis of eIF4E and its downstream effector proteins in human breast cancer. *J Exp Clin Cancer Res*. 2009;28:5.
-

- 
382. Harrell FE, Jr., Lee KL, Mark DB. Multivariable prognostic models: issues in developing models, evaluating assumptions and adequacy, and measuring and reducing errors. *Stat Med*. 1996 Feb 28;15(4):361-87.
383. Hutchings M, Loft A, Hansen M, Pedersen LM, Buhl T, Jurlander J, et al. FDG-PET after two cycles of chemotherapy predicts treatment failure and progression-free survival in Hodgkin lymphoma. *Blood*. 2006 Jan 1;107(1):52-9.
384. Muranski P, Boni A, Antony PA, Cassard L, Irvine KR, Kaiser A, et al. Tumor-specific Th17-polarized cells eradicate large established melanoma. *Blood*. 2008 Jul 15;112(2):362-73.
385. Nastala CL, Edington HD, McKinney TG, Tahara H, Nalesnik MA, Brunda MJ, et al. Recombinant IL-12 administration induces tumor regression in association with IFN-gamma production. *J Immunol*. 1994 Aug 15;153(4):1697-706.
386. Kacha AK, Fallarino F, Markiewicz MA, Gajewski TF. Cutting edge: spontaneous rejection of poorly immunogenic P1.HTR tumors by Stat6-deficient mice. *J Immunol*. 2000 Dec 1;165(11):6024-8.
387. Seo N, Hayakawa S, Takigawa M, Tokura Y. Interleukin-10 expressed at early tumour sites induces subsequent generation of CD4(+) T-regulatory cells and systemic collapse of antitumour immunity. *Immunology*. 2001 Aug;103(4):449-57.
388. Pellegrini P, Berghella AM, Del Beato T, Cicia S, Adorno D, Casciani CU. Disregulation in TH1 and TH2 subsets of CD4+ T cells in peripheral blood of colorectal cancer patients and involvement in cancer establishment and progression. *Cancer Immunol Immunother*. 1996 Jan;42(1):1-8.
389. Lowes MA, Bishop GA, Crotty K, Barnetson RS, Halliday GM. T helper 1 cytokine mRNA is increased in spontaneously regressing primary melanomas. *J Invest Dermatol*. 1997 Jun;108(6):914-9.
390. Tepper RI, Pattengale PK, Leder P. Murine interleukin-4 displays potent anti-tumor activity in vivo. *Cell*. 1989 May 5;57(3):503-12.
391. Shen Y, Fujimoto S. A tumor-specific Th2 clone initiating tumor rejection via primed CD8+ cytotoxic T-lymphocyte activation in mice. *Cancer Res*. 1996 Nov 1;56(21):5005-11.
392. Aoki Y, Tsuneki I, Sasaki M, Watanabe M, Sato T, Aida H, et al. Analysis of TH1 and TH2 cells by intracellular cytokine detection with flow cytometry in patients with ovarian cancer. *Gynecol Obstet Invest*. 2000;50(3):207-11.
393. Mori T, Takada R, Watanabe R, Okamoto S, Ikeda Y. T-helper (Th)1/Th2 imbalance in patients with previously untreated B-cell diffuse large cell lymphoma. *Cancer Immunol Immunother*. 2001 Dec;50(10):566-8.
394. Zhang XL, Komada Y, Chipeta J, Li QS, Inaba H, Azuma E, et al. Intracellular cytokine profile of T cells from children with acute lymphoblastic leukemia. *Cancer Immunol Immunother*. 2000 Jun;49(3):165-72.
395. Yotnda P, Mintz P, Grigoriadou K, Lemonnier F, Vilmer E, Langlade-Demoyen P. Analysis of T-cell defects in the specific immune response against acute lymphoblastic leukemia cells. *Exp Hematol*. 1999 Sep;27(9):1375-83.
396. de Toter D, Reato G, Mauro F, Cignetti A, Ferrini S, Guarini A, et al. IL4 production and increased CD30 expression by a unique CD8+ T-cell subset in B-cell chronic lymphocytic leukaemia. *Br J Haematol*. 1999 Mar;104(3):589-99.
397. Hamdi W, Ogawara H, Handa H, Tsukamoto N, Murakami H. Clinical significance of Th1/Th2 ratio in patients with myelodysplastic syndrome. *Int J Lab Hematol*. 2009 Dec;31(6):630-8.
398. Peng SL, Szabo SJ, Glimcher LH. T-bet regulates IgG class switching and pathogenic autoantibody production. *Proc Natl Acad Sci U S A*. 2002 Apr 16;99(8):5545-50.
399. Germann T, Bongartz M, Dlugonska H, Hess H, Schmitt E, Kolbe L, et al. Interleukin-12 profoundly up-regulates the synthesis of antigen-specific complement-fixing IgG2a, IgG2b and IgG3 antibody subclasses in vivo. *Eur J Immunol*. 1995 Mar;25(3):823-9.
400. Joshi NS, Cui W, Chandele A, Lee HK, Urso DR, Hagman J, et al. Inflammation directs memory precursor and short-lived effector CD8(+) T cell fates via the graded expression of T-bet transcription factor. *Immunity*. 2007 Aug;27(2):281-95.
-



- 
401. Kao C, Oestreich KJ, Paley MA, Crawford A, Angelosanto JM, Ali MA, et al. Transcription factor T-bet represses expression of the inhibitory receptor PD-1 and sustains virus-specific CD8+ T cell responses during chronic infection. *Nat Immunol*. 2011 Jul;12(7):663-71.
402. Dorfman DM, van den Elzen P, Weng AP, Shahsafaei A, Glimcher LH. Differential expression of T-bet, a T-box transcription factor required for Th1 T-cell development, in peripheral T-cell lymphomas. *Am J Clin Pathol*. 2003 Dec;120(6):866-73.
403. Dorfman DM, Hwang ES, Shahsafaei A, Glimcher LH. T-bet, a T-cell-associated transcription factor, is expressed in a subset of B-cell lymphoproliferative disorders. *Am J Clin Pathol*. 2004 Aug;122(2):292-7.
404. Atayar C, Poppema S, Blokzijl T, Harms G, Boot M, van den Berg A. Expression of the T-cell transcription factors, GATA-3 and T-bet, in the neoplastic cells of Hodgkin lymphomas. *Am J Pathol*. 2005 Jan;166(1):127-34.
405. Jundt F, Anagnostopoulos I, Forster R, Mathas S, Stein H, Dorken B. Activated Notch1 signaling promotes tumor cell proliferation and survival in Hodgkin and anaplastic large cell lymphoma. *Blood*. 2002 May 1;99(9):3398-403.
406. Pui JC, Allman D, Xu L, DeRocco S, Karnell FG, Bakkour S, et al. Notch1 expression in early lymphopoiesis influences B versus T lineage determination. *Immunity*. 1999 Sep;11(3):299-308.
407. Barros MH, Vera-Lozada G, Soares FA, Niedobitek G, Hassan R. Tumor microenvironment composition in pediatric classical Hodgkin lymphoma is modulated by age and Epstein-Barr virus infection. *Int J Cancer*. 2011 Oct 25.
408. Ho IC, Hodge MR, Rooney JW, Glimcher LH. The proto-oncogene c-maf is responsible for tissue-specific expression of interleukin-4. *Cell*. 1996 Jun 28;85(7):973-83.
409. Ho IC, Lo D, Glimcher LH. c-maf promotes T helper cell type 2 (Th2) and attenuates Th1 differentiation by both interleukin 4-dependent and -independent mechanisms. *J Exp Med*. 1998 Nov 16;188(10):1859-66.
410. Ouyang W, Lohning M, Gao Z, Assenmacher M, Ranganath S, Radbruch A, et al. Stat6-independent GATA-3 autoactivation directs IL-4-independent Th2 development and commitment. *Immunity*. 2000 Jan;12(1):27-37.
411. Shimoda K, van Deursen J, Sangster MY, Sarawar SR, Carson RT, Tripp RA, et al. Lack of IL-4-induced Th2 response and IgE class switching in mice with disrupted Stat6 gene. *Nature*. 1996 Apr 18;380(6575):630-3.
412. Takeda K, Tanaka T, Shi W, Matsumoto M, Minami M, Kashiwamura S, et al. Essential role of Stat6 in IL-4 signalling. *Nature*. 1996 Apr 18;380(6575):627-30.
413. Ho IC, Tai TS, Pai SY. GATA3 and the T-cell lineage: essential functions before and after T-helper-2-cell differentiation. *Nat Rev Immunol*. 2009 Feb;9(2):125-35.
414. Wang Y, Su MA, Wan YY. An essential role of the transcription factor GATA-3 for the function of regulatory T cells. *Immunity*. 2011 Sep 23;35(3):337-48.
415. Lee PP, Zeng D, McCaulay AE, Chen YF, Geiler C, Umetsu DT, et al. T helper 2-dominant antilymphoma immune response is associated with fatal outcome. *Blood*. 1997 Aug 15;90(4):1611-7.
416. Maeda H, Shiraishi A. TGF-beta contributes to the shift toward Th2-type responses through direct and IL-10-mediated pathways in tumor-bearing mice. *J Immunol*. 1996 Jan 1;156(1):73-8.
417. Curiel TJ. Tregs and rethinking cancer immunotherapy. *J Clin Invest*. 2007 May;117(5):1167-74.
418. Green MR, Monti S, Rodig SJ, Juszczynski P, Currie T, O'Donnell E, et al. Integrative analysis reveals selective 9p24.1 amplification, increased PD-1 ligand expression, and further induction via JAK2 in nodular sclerosing Hodgkin lymphoma and primary mediastinal large B-cell lymphoma. *Blood*. 2010 Oct 28;116(17):3268-77.
419. Iwai Y, Ishida M, Tanaka Y, Okazaki T, Honjo T, Minato N. Involvement of PD-L1 on tumor cells in the escape from host immune system and tumor immunotherapy by PD-L1 blockade. *Proc Natl Acad Sci U S A*. 2002 Sep 17;99(19):12293-7.
420. Dong H, Strome SE, Salomao DR, Tamura H, Hirano F, Flies DB, et al. Tumor-associated B7-H1 promotes T-cell apoptosis: a potential mechanism of immune evasion. *Nat Med*. 2002 Aug;8(8):793-800.
-

- 
421. Ishida M, Iwai Y, Tanaka Y, Okazaki T, Freeman GJ, Minato N, et al. Differential expression of PD-L1 and PD-L2, ligands for an inhibitory receptor PD-1, in the cells of lymphohematopoietic tissues. *Immunol Lett*. 2002 Oct 21;84(1):57-62.
422. Barber DL, Wherry EJ, Masopust D, Zhu B, Allison JP, Sharpe AH, et al. Restoring function in exhausted CD8 T cells during chronic viral infection. *Nature*. 2006 Feb 9;439(7077):682-7.
423. Muenst S, Hoeller S, Dirnhofer S, Tzankov A. Increased programmed death-1+ tumor-infiltrating lymphocytes in classical Hodgkin lymphoma substantiate reduced overall survival. *Hum Pathol*. 2009 Dec;40(12):1715-22.
424. Dorfman DM, Brown JA, Shahsafaei A, Freeman GJ. Programmed death-1 (PD-1) is a marker of germinal center-associated T cells and angioimmunoblastic T-cell lymphoma. *Am J Surg Pathol*. 2006 Jul;30(7):802-10.
425. Nam-Cha SH, Roncador G, Sanchez-Verde L, Montes-Moreno S, Acevedo A, Dominguez-Franjo P, et al. PD-1, a follicular T-cell marker useful for recognizing nodular lymphocyte-predominant Hodgkin lymphoma. *Am J Surg Pathol*. 2008 Aug;32(8):1252-7.
426. Carbone A, Gloghini A, Cabras A, Elia G. Differentiating germinal center-derived lymphomas through their cellular microenvironment. *Am J Hematol*. 2009 Jul;84(7):435-8.
427. Nam-Cha SH, Montes-Moreno S, Salcedo MT, Sanjuan J, Garcia JF, Piris MA. Lymphocyte-rich classical Hodgkin's lymphoma: distinctive tumor and microenvironment markers. *Mod Pathol*. 2009 Aug;22(8):1006-15.
428. de Jong D, Bosq J, MacLennan KA, Diebold J, Audouin J, Chasle J, et al. Lymphocyte-rich classical Hodgkin lymphoma (LRCHL): clinico-pathological characteristics and outcome of a rare entity. *Ann Oncol*. 2006 Jan;17(1):141-5.
429. Roncador G, Garcia JF, Maestre L, Lucas E, Menarguez J, Ohshima K, et al. FOXP3, a selective marker for a subset of adult T-cell leukaemia/lymphoma. *Leukemia*. 2005 Dec;19(12):2247-53.
430. Tian L, Altin JA, Makaroff LE, Franckaert D, Cook MC, Goodnow CC, et al. Foxp3(+) regulatory T cells exert asymmetric control over murine helper responses by inducing Th2 cell apoptosis. *Blood*. 2011 Aug 18;118(7):1845-53.
431. Stanelle J, Doring C, Hansmann ML, Kuppers R. Mechanisms of aberrant GATA3 expression in classical Hodgkin lymphoma and its consequences for the cytokine profile of Hodgkin and Reed/Sternberg cells. *Blood*. 2010 Nov 18;116(20):4202-11.
432. Gillett CE, Springall RJ, Barnes DM, Hanby AM. Multiple tissue core arrays in histopathology research: a validation study. *J Pathol*. 2000 Dec;192(4):549-53.
433. Camp RL, Charette LA, Rimm DL. Validation of tissue microarray technology in breast carcinoma. *Lab Invest*. 2000 Dec;80(12):1943-9.
434. Mucci NR, Akdas G, Manely S, Rubin MA. Neuroendocrine expression in metastatic prostate cancer: evaluation of high throughput tissue microarrays to detect heterogeneous protein expression. *Hum Pathol*. 2000 Apr;31(4):406-14.
435. Sallinen SL, Sallinen PK, Haapasalo HK, Helin HJ, Helen PT, Schraml P, et al. Identification of differentially expressed genes in human gliomas by DNA microarray and tissue chip techniques. *Cancer Res*. 2000 Dec 1;60(23):6617-22.
436. Hedvat CV, Hegde A, Chaganti RS, Chen B, Qin J, Filippa DA, et al. Application of tissue microarray technology to the study of non-Hodgkin's and Hodgkin's lymphoma. *Hum Pathol*. 2002 Oct;33(10):968-74.
437. Kraus MD, Haley J. Lymphocyte predominance Hodgkin's disease: the use of bcl-6 and CD57 in diagnosis and differential diagnosis. *Am J Surg Pathol*. 2000 Aug;24(8):1068-78.
438. Fozza C, Longinotti M. T-Cell Traffic Jam in Hodgkin's Lymphoma: Pathogenetic and Therapeutic Implications. *Adv Hematol*. 2011;2011:501659.
439. Younes A, Romaguera J, Hagemester F, McLaughlin P, Rodriguez MA, Fiumara P, et al. A pilot study of rituximab in patients with recurrent, classic Hodgkin disease. *Cancer*. 2003 Jul 15;98(2):310-4.
440. Advani R, Forero-Torres A, Furman RR, Rosenblatt JD, Younes A, Ren H, et al. Phase I study of the humanized anti-CD40 monoclonal antibody dacetuzumab in refractory or recurrent non-Hodgkin's lymphoma. *J Clin Oncol*. 2009 Sep 10;27(26):4371-7.
441. Peggs KS, Kayani I, Edwards N, Kottaridis P, Goldstone AH, Linch DC, et al. Donor lymphocyte infusions modulate relapse risk in mixed chimeras and induce durable salvage in

- relapsed patients after T-cell-depleted allogeneic transplantation for Hodgkin's lymphoma. *J Clin Oncol*. 2011 Mar 10;29(8):971-8.
442. Corazzelli G, De Filippi R, Capobianco G, Frigeri F, De Rosa V, Iaccarino G, et al. Tumor flare reactions and response to lenalidomide in patients with refractory classic Hodgkin lymphoma. *Am J Hematol*. 2010 Jan;85(1):87-90.
443. Ishii N, Takeshita T, Kimura Y, Tada K, Kondo M, Nakamura M, et al. Expression of the IL-2 receptor gamma chain on various populations in human peripheral blood. *Int Immunol*. 1994 Aug;6(8):1273-7.
444. Lin JX, Migone TS, Tsang M, Friedmann M, Weatherbee JA, Zhou L, et al. The role of shared receptor motifs and common Stat proteins in the generation of cytokine pleiotropy and redundancy by IL-2, IL-4, IL-7, IL-13, and IL-15. *Immunity*. 1995 Apr;2(4):331-9.
445. Ohashi Y, Takeshita T, Nagata K, Mori S, Sugamura K. Differential expression of the IL-2 receptor subunits, p55 and p75 on various populations of primary peripheral blood mononuclear cells. *J Immunol*. 1989 Dec 1;143(11):3548-55.
446. Swain SL. Lymphokines and the immune response: the central role of interleukin-2. *Curr Opin Immunol*. 1991 Jun;3(3):304-10.
447. Lenardo MJ. Interleukin-2 programs mouse alpha beta T lymphocytes for apoptosis. *Nature*. 1991 Oct 31;353(6347):858-61.
448. Fontenot JD, Rasmussen JP, Gavin MA, Rudensky AY. A function for interleukin 2 in Foxp3-expressing regulatory T cells. *Nat Immunol*. 2005 Nov;6(11):1142-51.
449. Schwarting R, Gerdes J, Ziegler A, Stein H. Immunoprecipitation of the interleukin-2 receptor from Hodgkin's disease derived cell lines by monoclonal antibodies. *Hematol Oncol*. 1987 Jan-Mar;5(1):57-64.
450. Agnarsson BA, Kadin ME. The immunophenotype of Reed-Sternberg cells. A study of 50 cases of Hodgkin's disease using fixed frozen tissues. *Cancer*. 1989 Jun 1;63(11):2083-7.
451. Hsu SM, Tseng CTK, Hsu PL. Expression of P55 (Tac) Interleukin-2 Receptor (IL-2r), but Not P75 IL-2r, in Cultured H-Rs Cells and H-Rs Cells in Tissues. *American Journal of Pathology*. 1990 Apr;136(4):735-44.
452. Hsu SM, Hsu PL. Lack of Effect of Colony-Stimulating Factors, Interleukins, Interferons, and Tumor Necrosis Factor on the Growth and Differentiation of Cultured Reed-Sternberg Cells - Comparison with Effects of Phorbol Ester and Retinoic Acid. *American Journal of Pathology*. 1990 Jan;136(1):181-9.
453. Ansel KM, Djuretic I, Tanasa B, Rao A. Regulation of Th2 differentiation and Il4 locus accessibility. *Annu Rev Immunol*. 2006;24:607-56.
454. Barcena A, Toribio ML, Gutierrez-Ramos JC, Kroemer G, Martinez C. Interplay between IL-2 and IL-4 in human thymocyte differentiation: antagonism or agonism. *Int Immunol*. 1991 May;3(5):419-25.
455. Noble A, Kemeny DM. Interleukin-4 enhances interferon-gamma synthesis but inhibits development of interferon-gamma-producing cells. *Immunology*. 1995 Jul;85(3):357-63.
456. Bream JH, Curiel RE, Yu CR, Egwuagu CE, Grusby MJ, Aune TM, et al. IL-4 synergistically enhances both IL-2- and IL-12-induced IFN-gamma expression in murine NK cells. *Blood*. 2003 Jul 1;102(1):207-14.
457. Ebner S, Ratzinger G, Krosbacher B, Schmuth M, Weiss A, Reider D, et al. Production of IL-12 by human monocyte-derived dendritic cells is optimal when the stimulus is given at the onset of maturation, and is further enhanced by IL-4. *J Immunol*. 2001 Jan 1;166(1):633-41.
458. Bello-Fernandez C, Oblakowski P, Meager A, Duncombe AS, Rill DM, Hoffbrand AV, et al. IL-4 acts as a homeostatic regulator of IL-2-induced TNF and IFN-gamma. *Immunology*. 1991 Feb;72(2):161-6.
459. Fromm JR, Thomas A, Wood BL. Flow cytometry can diagnose classical hodgkin lymphoma in lymph nodes with high sensitivity and specificity. *Am J Clin Pathol*. 2009 Mar;131(3):322-32.
460. Cousins DJ, Lee TH, Staynov DZ. Cytokine coexpression during human Th1/Th2 cell differentiation: direct evidence for coordinated expression of Th2 cytokines. *J Immunol*. 2002 Sep 1;169(5):2498-506.

- 
461. Kaye J, Porcelli S, Tite J, Jones B, Janeway CA, Jr. Both a monoclonal antibody and antisera specific for determinants unique to individual cloned helper T cell lines can substitute for antigen and antigen-presenting cells in the activation of T cells. *J Exp Med.* 1983 Sep 1;158(3):836-56.
462. Weston L, Geczy A, Farrell C. A convenient and reliable IL-2 bioassay using frozen CTLL-2 to improve the detection of helper T lymphocyte precursors. *Immunol Cell Biol.* 1998 Apr;76(2):190-2.
463. Kitamura T, Takaku F, Miyajima A. IL-1 up-regulates the expression of cytokine receptors on a factor-dependent human hemopoietic cell line, TF-1. *Int Immunol.* 1991 Jun;3(6):571-7.
464. Webb DC, McKenzie AN, Koskinen AM, Yang M, Mattes J, Foster PS. Integrated signals between IL-13, IL-4, and IL-5 regulate airways hyperreactivity. *J Immunol.* 2000 Jul 1;165(1):108-13.
465. Irsch J, Nitsch S, Hansmann ML, Rajewsky K, Tesch H, Diehl V, et al. Isolation of viable Hodgkin and Reed-Sternberg cells from Hodgkin disease tissues. *Proc Natl Acad Sci U S A.* 1998 Aug 18;95(17):10117-22.
466. Kaltoft K, Hansen BH, Pedersen CB, Pedersen S, Thestrup-Pedersen K. Common clonal chromosome aberrations in cytokine-dependent continuous human T-lymphocyte cell lines. *Cancer Genet Cytogenet.* 1995 Nov;85(1):68-71.
467. Geginat J, Campagnaro S, Sallusto F, Lanzavecchia A. TCR-independent proliferation and differentiation of human CD4+ T cell subsets induced by cytokines. *Adv Exp Med Biol.* 2002;512:107-12.
468. Lee WT, Pasos G, Cecchini L, Mittler JN. Continued antigen stimulation is not required during CD4(+) T cell clonal expansion. *J Immunol.* 2002 Feb 15;168(4):1682-9.
469. Yarke CA, Dalheimer SL, Zhang N, Catron DM, Jenkins MK, Mueller DL. Proliferating CD4+ T cells undergo immediate growth arrest upon cessation of TCR signaling in vivo. *J Immunol.* 2008 Jan 1;180(1):156-62.
470. Habib LK, Finn WG. Unsupervised immunophenotypic profiling of chronic lymphocytic leukemia. *Cytometry B Clin Cytom.* 2006 May;70(3):124-35.
471. Enciso-Mora V, Broderick P, Ma Y, Jarrett RF, Hjalgrim H, Hemminki K, et al. A genome-wide association study of Hodgkin's lymphoma identifies new susceptibility loci at 2p16.1 (REL), 8q24.21 and 10p14 (GATA3). *Nat Genet.* 2010 Dec;42(12):1126-30.
472. Cozen W, Gill PS, Ingles SA, Masood R, Martinez-Maza O, Cockburn MG, et al. IL-6 levels and genotype are associated with risk of young adult Hodgkin lymphoma. *Blood.* 2004 Apr 15;103(8):3216-21.
473. Cozen W, Gill PS, Salam MT, Nieters A, Masood R, Cockburn MG, et al. Interleukin-2, interleukin-12, and interferon-gamma levels and risk of young adult Hodgkin lymphoma. *Blood.* 2008 Apr 1;111(7):3377-82.
474. Hicks J, Flaitz C. Progressive transformation of germinal centers: review of histopathologic and clinical features. *Int J Pediatr Otorhinolaryngol.* 2002 Sep 24;65(3):195-202.
475. Churchill HR, Roncador G, Warnke RA, Natkunam Y. Programmed death 1 expression in variant immunoarchitectural patterns of nodular lymphocyte predominant Hodgkin lymphoma: comparison with CD57 and lymphomas in the differential diagnosis. *Hum Pathol.* 2010 Dec;41(12):1726-34.
476. Bouron-Dal Soglio D, Truong F, Fetni R, Hazourli S, Champagne J, Oligny LL, et al. A B-cell lymphoma-associated chromosomal translocation in a progressive transformation of germinal center. *Hum Pathol.* 2008 Feb;39(2):292-7.
477. Walker LS, Sansom DM. The emerging role of CTLA4 as a cell-extrinsic regulator of T cell responses. *Nat Rev Immunol.* 2011 Dec;11(12):852-63.
478. Depper JM, Leonard WJ, Kronke M, Noguchi PD, Cunningham RE, Waldmann TA, et al. Regulation of interleukin 2 receptor expression: effects of phorbol diester, phospholipase C, and reexposure to lectin or antigen. *J Immunol.* 1984 Dec;133(6):3054-61.
479. Poppema S, Potters M, Visser L, van den Berg AM. Immune escape mechanisms in Hodgkin's disease. *Ann Oncol.* 1998;9 Suppl 5:S21-4.
480. Gruss HJ, Pinto A, Duyster J, Poppema S, Herrmann F. Hodgkin's disease: a tumor with disturbed immunological pathways. *Immunol Today.* 1997 Apr;18(4):156-63.

- 
481. Frisan T, Sjoberg J, Dolcetti R, Boiocchi M, De Re V, Carbone A, et al. Local suppression of Epstein-Barr virus (EBV)-specific cytotoxicity in biopsies of EBV-positive Hodgkin's disease. *Blood*. 1995 Aug 15;86(4):1493-501.
482. Serrano D, Ghiotto F, Roncella S, Airoidi I, Cutrona G, Truini M, et al. The patterns of IL2, IFN-gamma, IL4 and IL5 gene expression in Hodgkin's disease and reactive lymph nodes are similar. *Haematologica*. 1997 Sep-Oct;82(5):542-9.
483. Schumacher TN, Gerlach C, van Heijst JW. Mapping the life histories of T cells. *Nat Rev Immunol*. 2010 Sep;10(9):621-31.
484. Buri C, Korner M, Scharli P, Cefai D, Uguccioni M, Mueller C, et al. CC chemokines and the receptors CCR3 and CCR5 are differentially expressed in the nonneoplastic leukocytic infiltrates of Hodgkin disease. *Blood*. 2001 Mar 15;97(6):1543-8.
485. Lasky LA, Singer MS, Dowbenko D, Imai Y, Henzel WJ, Grimley C, et al. An endothelial ligand for L-selectin is a novel mucin-like molecule. *Cell*. 1992 Jun 12;69(6):927-38.
486. Hendriks J, Gravestien LA, Tesselaar K, van Lier RA, Schumacher TN, Borst J. CD27 is required for generation and long-term maintenance of T cell immunity. *Nat Immunol*. 2000 Nov;1(5):433-40.
487. Pilling D, Akbar AN, Bacon PA, Salmon M. CD4+ CD45RA+ T cells from adults respond to recall antigens after CD28 ligation. *Int Immunol*. 1996 Nov;8(11):1737-42.
488. Di Mitri D, Azevedo RI, Henson SM, Libri V, Riddell NE, Macaulay R, et al. Reversible senescence in human CD4+CD45RA+CD27- memory T cells. *J Immunol*. 2011 Sep 1;187(5):2093-100.
489. Hara T, Jung LK, Bjorndahl JM, Fu SM. Human T cell activation. III. Rapid induction of a phosphorylated 28 kD/32 kD disulfide-linked early activation antigen (EA 1) by 12-o-tetradecanoyl phorbol-13-acetate, mitogens, and antigens. *J Exp Med*. 1986 Dec 1;164(6):1988-2005.
490. Testi R, Phillips JH, Lanier LL. Constitutive expression of a phosphorylated activation antigen (Leu 23) by CD3bright human thymocytes. *J Immunol*. 1988 Oct 15;141(8):2557-63.
491. Santis AG, Campanero MR, Alonso JL, Tugores A, Alonso MA, Yague E, et al. Tumor necrosis factor-alpha production induced in T lymphocytes through the AIM/CD69 activation pathway. *Eur J Immunol*. 1992 May;22(5):1253-9.
492. Sancho D, Gomez M, Viedma F, Esplugues E, Gordon-Alonso M, Garcia-Lopez MA, et al. CD69 downregulates autoimmune reactivity through active transforming growth factor-beta production in collagen-induced arthritis. *J Clin Invest*. 2003 Sep;112(6):872-82.
493. Nagata S, Golstein P. The Fas death factor. *Science*. 1995 Mar 10;267(5203):1449-56.
494. Kennedy MK, Willis CR, Armitage RJ. Deciphering CD30 ligand biology and its role in humoral immunity. *Immunology*. 2006 Jun;118(2):143-52.
495. Zeppa P, Marino G, Troncone G, Fulciniti F, De Renzo A, Picardi M, et al. Fine-needle cytology and flow cytometry immunophenotyping and subclassification of non-Hodgkin lymphoma: a critical review of 307 cases with technical suggestions. *Cancer*. 2004 Feb 25;102(1):55-65.
496. Jorgensen JL. State of the Art Symposium: flow cytometry in the diagnosis of lymphoproliferative disorders by fine-needle aspiration. *Cancer*. 2005 Dec 25;105(6):443-51.
497. Kaleem Z. Flow cytometric analysis of lymphomas: current status and usefulness. *Arch Pathol Lab Med*. 2006 Dec;130(12):1850-8.
498. Savage EC, Vanderheyden AD, Bell AM, Syrbu SI, Jensen CS. Independent diagnostic accuracy of flow cytometry obtained from fine-needle aspirates: a 10-year experience with 451 cases. *Am J Clin Pathol*. 2011 Feb;135(2):304-9.
499. Nakamura T, Lee RK, Nam SY, Al-Ramadi BK, Koni PA, Bottomly K, et al. Reciprocal regulation of CD30 expression on CD4+ T cells by IL-4 and IFN-gamma. *J Immunol*. 1997 Mar 1;158(5):2090-8.
500. Younes A, Bartlett NL, Leonard JP, Kennedy DA, Lynch CM, Sievers EL, et al. Brentuximab vedotin (SGN-35) for relapsed CD30-positive lymphomas. *N Engl J Med*. 2010 Nov 4;363(19):1812-21.
501. Zheng B, Fiumara P, Li YV, Georgakis G, Snell V, Younes M, et al. MEK/ERK pathway is aberrantly active in Hodgkin disease: a signaling pathway shared by CD30, CD40, and RANK that regulates cell proliferation and survival. *Blood*. 2003 Aug 1;102(3):1019-27.
-

- 
502. Kong YY, Yoshida H, Sarosi I, Tan HL, Timms E, Capparelli C, et al. OPGL is a key regulator of osteoclastogenesis, lymphocyte development and lymph-node organogenesis. *Nature*. 1999 Jan 28;397(6717):315-23.
503. Green EA, Flavell RA. TRANCE-RANK, a new signal pathway involved in lymphocyte development and T cell activation. *J Exp Med*. 1999 Apr 5;189(7):1017-20.
504. Rivino L, Gruarin P, Haringer B, Steinfeld S, Lozza L, Steckel B, et al. CCR6 is expressed on an IL-10-producing, autoreactive memory T cell population with context-dependent regulatory function. *J Exp Med*. 2010 Mar 15;207(3):565-77.
505. Fritsch RD, Shen X, Sims GP, Hathcock KS, Hodes RJ, Lipsky PE. Stepwise differentiation of CD4 memory T cells defined by expression of CCR7 and CD27. *J Immunol*. 2005 Nov 15;175(10):6489-97.
506. Lefrancois L, Masopust D. The road not taken: memory T cell fate 'decisions'. *Nat Immunol*. 2009 Apr;10(4):369-70.
507. Levy R, Kaplan HS. Impaired lymphocyte function in untreated Hodgkin's disease. *N Engl J Med*. 1974 Jan 24;290(4):181-6.
508. Twomey JJ, Laughter AH, Rice L, Ford R. Spectrum of immunodeficiencies with Hodgkin's disease. *J Clin Invest*. 1980 Oct;66(4):629-37.
509. Corradini P, Sarina B, Farina L. Allogeneic transplantation for Hodgkin's lymphoma. *Br J Haematol*. 2011 Feb;152(3):261-72.
510. Powell DJ, Jr., Dudley ME, Robbins PF, Rosenberg SA. Transition of late-stage effector T cells to CD27+ CD28+ tumor-reactive effector memory T cells in humans after adoptive cell transfer therapy. *Blood*. 2005 Jan 1;105(1):241-50.
511. Chen BJ, Cui X, Sempowski GD, Liu C, Chao NJ. Transfer of allogeneic CD62L- memory T cells without graft-versus-host disease. *Blood*. 2004 Feb 15;103(4):1534-41.